BUILDING APPROXIMATE STELLAR MODELS IN GENERAL RELATIVITY

by
Francisco Javier Egido Cuchí

A Dissertation Presented in Partial Fulfilment
of the Requirements for the Degree
Doctor of Philosophy

INSTITUTO DE FÍSICA FUNDAMENTAL Y MATEMÁTICAS
de la
UNIVERSIDAD DE SALAMANCA

February 2014

CONSTRUYENDO MODELOS ESTELARES APROXIMADOS EN RELATIVIDAD GENERAL

por

Francisco Javier Egido Cuchí

ha sido realizada y aprobada para su presentación oral
bajo la dirección de

Eduardo Ruiz Carrero, Profesor de la Universidad de Salamanca y miembro del Instituto de Física Fundamental y Matemáticas
y
Alfred Molina Compte, Profesor emérito del Departament de Física Fonamental de la Universidad de Barcelona y miembro del Institut de Ciències del Cosmos

El Director de la tesis,	El Director de la tesis,	El Doctorando,
		
Fdo.: Eduardo Ruiz	Fdo.: Alfred Molina	Fdo.: Fco. Javier E. Cuchí

Abstract

We build and study rotating and time-independent stellar models in General Relativity using analytical approximations (post-Minkowskian and slow rotation) for a perfect fluid with linear equation of state and some of its subcases, including in particular uniform density, the one of the Wahlquist's and Whitakker's solutions fluid and MIT bag model strange matter. We obtain a global spacetime matching the interior solution (inside the source) to an asymptotically flat exterior using both Lichnerowicz and Darmois-Israel matching conditions. Concerning the interior, we find its possible Petrov types and cast it into the same form a certain perturbative expansion of Wahlquist's solution has. We also use the AKM numerical code to obtain equivalent models to compare both the metric components and the results for many physical properties of the source we obtain from analytical formulae, getting good results from the comparison. Finally, we increase the complexity and adaptability of the interior adding an additional layer of linear EOS matter.

Agradecimientos

Supongo que cuando te excedes ligeramente en el tiempo dedicado a doctorarte y las épocas previas parecen infancia, tiene sentido empezar por el principio de todo. Ese lugar corresponde a mis padres y a las eternas cintas de Betamax que se encargaron de llenar de documentales. Así aparecen arriba sin excusas ñoñas para lo que no se agradece con palabras. Que en el sistema educativo de lo poco no insufrible sean las Ciencias puede ser subjetivo, pero parte del mérito está en gente joven como Manolo o ya mayor como Alberto Revuelta que no se erosiona riada tras riada de 35 chavales. Y hablando de amor por enseñar, probablemente debería saltar a la universidad hasta Chus Martín. Eso pueden decirlo muchos alumnos y esto debería ser más personal así que mencionaré el placer de compartir cervezas con él. Algo que también saben muchos pero menos. Gracias por la presencia y sonrisa constantes. Y si hay algo más conveniente que incluir a un miembro del tribunal en los agradecimientos es incluir a dos. Porque la Relatividad General es preciosa pero fue Marc Mars el que nos la presentó. "Nos" porque la mitad de la clase (¡5!) decidió intentar un doctorado en el tema. El resto gana dinero. A Eduardo le agradezco, siguiendo la tradición, la libertad para hacer lo que me apeteciera, y a Alfred los tacos, profesionalidad y la impagable corrección final.

Y si esta es la gente que te motiva para seguir adelante, también está la que te acompaña en el camino. Silvia, Alfonso, Víctor, Helena, Lucía, Fer, Jeni y Toni hicieron de los años de licenciatura lo que deben ser. El último todavía colabora entre sesiones de *anime* y facturas impagadas. El camaleón de Marta hizo que nos perdiéramos algunas clases de Nuclear, gracias también. Y la última etapa corresponde a las Marsopas. A la tropa clásica, Séneca, Jou y Álvaro; a los que fueron llegando, Álvaro 2.0 y Diego y al relevo que casi me adelanta, Cris, Soria y Edu. Años de Caja Negras, raptors, Pipers, mala comida y patos pekineses, cerveza, absenta y sake mientras uno y su tesis se encuentran. Sin querer han salido 9. La mayor parte está lejos. Ya nos veremos.

Terminando, un hueco especial para la gente que ha estado siempre y crece conmigo, Abu, los Carlos, David, JT, Joseal, Nano, Pablo y las nuevas, Raquel y Sandra, la cual comparte premio con mis padres por número de preguntas sobre cuándo defiendo. Y para Pilar, que probablemente se ha llevado lo peor de la incertidumbre vital del doctorando.

Al abuelo Paco, que se fue antes de tiempo

People assume that time is a strict progression of cause to effect, but actually from a non-linear, non-subjective viewpoint, it's more like a big ball of wibbly wobbly, timey wimey... stuff.

Steven Moffat, *Doctor Who, "Blink"*

Truth is a matter of the imagination.

Ursula K. Le Guin, *The Left Hand of Darkness*

Contents

List of Figures

List of Tables

Acronyms

1PN	first post-Newtonian approximation 3
AKM	the machine-accuracy numerical code introduced in Ansorg *et al.* (2002) 75
BGSM	the spectral numerical code by Bonazzola *et al.* (1993) 75
CGMR	the CMMR solution corresponding to a linear equation of state 56
CMMR	the double approximation scheme introduced in Cabezas *et al.* (2007) 13
EOS	equation of state 4
GR	General Relativity 1
ISCO	innermost stable circular orbit 3
LP	Lewis–Papapetrou 78
MR	mass-radius 6
PPN	parametrized post-Newtonian formalism 3
QCD	Quantum ChromoDynamics 80
QI	quasi-isotropic 84
QPO	quasi-periodic oscillation 4
rhs	right hand side 18

SQM strange quark matter 4

Symbols

$\tilde{A}_l$	gauge constant of the exterior solution 27
$\tilde{a}_l$	constant of the solution of the interior homogeneous system 27
α	one of the 4 free functions of the line-element in Lewis–Papapetrou coordinates 78
b	value of the 4-velocity normalization factor of Wahlquist's solution on the zero pressure surface (Chapter 4) 61
$\hat{B}$	one of the 4 free functions of the line-element in Lewis–Papapetrou coordinates 78
$\hat{\omega}$	one of the 4 free functions of the line-element in Lewis–Papapetrou coordinates 78
$\hat{u}$	one of the 4 free functions of the line-element in Lewis–Papapetrou coordinates 78
β	mass-shed parameter 112
$\tilde{B}_l$	gauge constant of the exterior solution 27
$\tilde{b}_l$	constant of the solution of the interior homogeneous system 27
C	custom EOS constant 77
c	a constant of the Wahlquist metric (Chapter 4) speed of light (elsewhere) 60
$C^{\alpha}_{\beta\gamma\delta}$	Weyl tensor 47
$\mathcal{C}_{\mathrm{eq}}$	length of the source equator 99
χ	angular Kepler coordinate 62
χ_+	embedding of Σ into $\mathcal{V}^+$ 38
χ_-	embedding of Σ into $\mathcal{V}^-$ 38

$\Box_\partial$	first—partial derivatives—term of the d'Alembertian operator 19
$\Box_\eta$	flat d'Alembertian 21
$\Box$	d'Alembertian operator 18
ϵ	energy density 22
ϵ_1	energy density of the inner spacetime of the bilayer stellar model 144
ϵ_2	energy density of the outer spacetime of the bilayer stellar model 145
ϵ^{ab}	bidimensional Levi–Civita symbol 86
ε_c	relative error at the source centre 116
ε	relative error 116
$\varepsilon_{2\varrho_{eq}}$	relative error at two times the equatorial coordinate radius 116
η	r/r_s 36
$\hat{\eta}_0$	value of $\hat{\eta}$ on the symmetry axis of Wahlquist's solution 60
$\eta_{\alpha\beta}$	Minkowski's metric 20
$\hat{\eta}$	one of the spatial Wahlquist coordinates 60
f	4-velocity normalization factor of Wahlquist's solution (Chapter 4) specific Helmholtz's free energy (Chapter 5) 60, 79
$g^+_{\alpha\beta}$	exterior metric in a stellar model 24
$g^-_{\alpha\beta}$	interior metric in a stellar model 24
$G_{\alpha\beta}$	Einstein tensor 19
$g_{\alpha\beta}$	metric of a spacetime 20
γ	polytropic exponent 77
$\gamma_{\alpha\beta}$	metric components in the orthonormal spherical-like cobasis 56
$\Gamma^\lambda_{\mu\nu}$	Christoffel symbol 18
h	specific enthalpy 77
h_1	one of the functions of the Wahlquist metric 60
h_2	one of the functions of the Wahlquist metric 60

H_α	quadratic part of the covariant harmonic condition 21
$h_{\alpha\beta}$	metric deviation 20
$\hat{\Omega}$	grand potential 79
$\hat{R}$	ratio R/r_0 88
$\boldsymbol{h}^{\pm}_{\text{hom}}$	general solution of the homogeneous harmonic post-Minkowskian equations 26
$\boldsymbol{h}^{i}_{\text{hom}}$	solution of the homogeneous PM system in inner layer of the bilayer stellar model 146
$\boldsymbol{h}^{\pm}_{\text{part}}$	particular solution of the post-Minkowskian equations 26
$\boldsymbol{h}^{s}_{\text{hom}}$	solution of the homogeneous PM system in outer layer of the bilayer stellar model 146
j^{α}_{b}	baryon 4-current 92
$\tilde{J}_l$	angular multipole moment 27
$\tilde{j}_l$	constant of the solution of the interior homogeneous system 27
K	polytropic constant 77
k	a constant of the Wahlquist metric 60
$k^{\alpha\beta}$	inverse metric deviation 20
κ	proportionality factor between Wahlquist's r_0 and ω 67
κ^{+}_{ab}	second fundamental form of Σ^+ 38
κ^{-}_{ab}	second fundamental form of Σ^- 38
L_α	linear part of the covariant harmonic condition 21
λ	post-Minkowskian approximation parameter 21
m	Newtonian mass of the source 28
M_{b}	baryon rest mass 92
m_{b}	rest mass per baryon 77
$\tilde{M}_l$	mass multipole moment 27
$\tilde{m}_l$	constant of the solution of the interior homogeneous system 27
M_{p}	proper mass 95

μ	mass density 56
μ_0	rest mass density at the centre of the source 55
μ_b	baryon mass density 77
μ_bc	central baryon rest mass density 114
$\hat{\mu}_i$	chemical potential 79
n_1	linear EOS parameter of the inner spacetime of the bilayer stellar model 144
n_2	linear EOS parameter of the outer spacetime of the bilayer stellar model 145
n_i	number density of particles of type i 79
$N_{\alpha\beta}$	Ricci terms which are at least quadratic in the metric deviation 21
N_b	total number of baryons in the source 92
n_b	baryon density 92
Ω	slow rotation approximation parameter 28
ω	angular velocity 25
ω_orb	orbital frequency 109
$\boldsymbol{\varpi}^\mathrm{W}$	twist vector of the Wahlquist metric 61
p	pressure 22
p_i	custom EOS coefficients 77
p_c	pressure at the centre of the source 45
p_g	point in the numerical grid from AKM 90
Φ	exterior latitudinal Papapetrou coordinate 37
ϕ	latitudinal Papapetrou coordinate 25
φ	one of the coordinates of Σ 40
$P_l^m(\cos\theta)$	associated Legendre polynomial of degree l and order m 26
$P_l(\cos\theta)$	Legendre polynomial of degree l 26
ψ	normalization factor of the 4-velocity 25
ψ_Σ	value of ψ on the surface Σ 25
q	ratio of energy density parameters of the linear EOS in the bilayer stellar model 146
q^+_{ab}	first fundamental form of Σ^+ 38
q^-_{ab}	first fundamental form of Σ^- 38

R	scalar curvature (Chapter 2), exterior spherical-like radial coordinate (Chapter 3), radial Kepler coordinate (Chapter 4), , quasi-isotropic radial coordinate (Chapter 5) 19, 37, 62, 78
r	spherical radial Papapetrou coordinate 25
r_0	a constant of the Wahlquist metric 60
$\mathcal{R}_{\text{circ}}$	circumpherential radius 99
R_{eq}	equatorial QI radial coordinate 98
$\mathcal{R}_{\text{eq}}$	proper equatorial radius 99
$R_{\alpha\beta}$	Ricci tensor 18
r_o	characteristic length in the bilayer stellar model 146
R_{p}	polar QI radial coordinate 98
$\mathcal{R}_{\text{p}}$	proper polar radius 100
r_s	coordinate radius ot the static source 28
r_Σ	explicit equation of the surface Σ 31
r_{Σ_i}	coordinate radius of the surface of the inner layer of the bilayer stellar model 144
r_{Σ_s}	coordinate radius of the surface of the outer layer of the bilayer stellar model 145
S	first order part of ψ_Σ 36
s	specific entropy 79
Σ^+	exterior embedding of the surface manifold Σ 38
Σ^-	interior embedding of the surface manifold Σ 38
σ_1	one of the constants of the μ_0 expansion of b 64
σ_2	one of the constants of the μ_0 expansion of b 64
ς_i	ansatz parameter of the surface of the inner layer of the bilayer stellar model 144
ς_n	free coefficients in the surface ansatz 31
ς_s	ansatz parameter of the surface of the inner layer of the bilayer stellar model 145
T	rotational energy, also exterior spherical-like temporal coordinate 37, 79, 97

t	temporal Papapetrou coordinate 25
$T_{\alpha\beta}$	stress-energy tensor 19
τ	one of the coordinates of Σ 40
Θ	exterior longitudinal Papapetrou coordinate, quasi-isotropic angular coordinate (Chapter 5) 37, 78
θ	spherical longitudinal Papetrou coordinate 25
ϑ	one of the coordinates of Σ 40
u^α	4-velocity 22
$\mathcal{V}^+$	exterior manifold in a stellar model 24
$\mathcal{V}^-$	interior manifold in a stellar model 24
ϱ	Lewis–Papapetrou radial coordinate 78
ξ	one of the spatial Wahlquist coordinates 60
$\boldsymbol{\xi}^-$	interior timelike Killing vector 24
$\bar{X}_l$	constants in the terms of negative powers of the radius in the solution for the outer layer of the bilayer stellar model 147
$\bar{x}_l$	constants in the terms of positive powers of the radius in the solution for the outer layer of the bilayer stellar model 147
$x^{(\mu)}$	harmonic or Cartesian-like coordinates 18
z_{eq}	equatorial redshift 105
ζ	Lewis–Papapetrou height coordinate 78
$\boldsymbol{\zeta}^-$	interior axisymmetry Killing vector 24
z_{p}	polar redshift 104

Chapter One

Introduction

Astrophysical observations have frequently been the source of unexpected experimental data for those societies which understand their importance and put the necessary economical effort to carry them out. Recent observations have made us broaden the spectrum of theories to levels probably never attained before, although in many aspects we are still developing the paradigm change of the beginning of the 20th century. Among the observations that led to it are the effects of mass and energy concentrations of objects of astrophysical size. These effects—mainly the gravitational redshift of photons and the bending of their trajectories, as well as the evolution of planetary orbits—had no explanation inside the Newtonian theory for gravity and have led to several different gravity theories, the most successful—and one of the oldest—of them being Einstein's General Relativity.

1. Using General Relativy

In General Relativity (GR), gravity does not act on particles as a traditional force. Seen as a traditional force, it was rather striking that the inertial mass that dictates how much a particle accelerates in response to any force was equal to the gravitational mass, the property of particles that generates gravitational fields. This implies that every object behaves in the same way in the presence of gravity, and this behaviour depends only on its initial velocity and position. It also lead Einstein to consider that the results of experiments made locally in different freely falling frames could only differ if they were subject to different gravitational fields and hence, most naturally, to consider that gravity is described by 4-dimensional manifolds with a geometry—and therefore curvature—described by a Lorentzian metric to ensure that physics are invariant under Lorentz transformations. Particles move along the geodesics of this curved manifold, with trajectories that depend only on their initial velocity and position.

The three odd effects already mentioned are, together with Shapiro's time delay (Shapiro, 1964), the classic tests successfully passed by the theory, but there have been more. In particular, the Nobel prize of 1993 was awarded to Hulse and

Taylor (1975) for the discovery of a pulsar that lead to an indirect confirmation of the existence of gravitational waves (Taylor and Weisberg, 1989), one of the predictions of GR.

Many other alternative theories of gravitation have appeared, and most of them do not pass the different experimental tests (see Will, 2006, for a review). GR has yet to fail a test and is currently part of the ΛCDM cosmological model, which despite possessing several worrying points like dark matter and dark energy, is still the mainly accepted model. Some new gravity theories have appeared in the last years trying to overcome these issues, though. Dark matter was introduced to explain the discrepancies between theory and observations of the galactic rotation curves (Rubin *et al.*, 1980), although it was promptly noticed these curves could be also explained modifying the description of gravity, what accomplishes the Modified Newtonian Dynamics (MOND) (Milgrom, 1983) and its relativistic generalisation, the Tensor-Vector-Scalar theory (TeVeS) (Bekenstein, 2004), which seems able to deal with other cosmological needs of dark matter (Dodelson and Liguori, 2006). A lot of attention has been put lately on $f(R)$ modifications of GR (Sotiriou and Faraoni, 2010) and braneworlds to deal with the observed accelerated expansion of the universe solved that in ΛCDM is solved with the introduction of the dark energy (Copeland *et al.*, 2006). Nevertheless, these theories focus on explaining cosmological behaviour, some times in different cosmological epochs, and they have to match the predictions of GR at least at solar system scales, where it has been successfully tested. In this thesis we will focus in the study of stellar models and GR will be our gravitational theory.

2. Relevance of stellar models in GR

The understanding of the physics of even common stars is of paramount importance in a field where any information from out of the solar system must be inferred from signals originated light years away. One could argue, though, that the corrections expected by relativistic effects in these objects are too small to care about them. We will now discuss how, beyond the initial simple impulse of seeking more precise models, one can

- improve the testing and keep on discarding theories that may imply big consequences in cosmology,
- gain in essential knowledge about the vast population of compact objects and
- help to discard some hypothesis about the ground state of matter

studying stellar models in GR.

2.1. Quadrupole moment and rotation

Astrometric observations have reached a precision of 1 microarcsecond (μas). This makes possible to observe several relativistic effects, in particular some associated with the quadrupole moment $\tilde{M}_2$ of gravity sources. In particular, its effect on the deflection of light (Klioner, 2003) can be measured and used to test several different gravity theories (Crosta and Mignard, 2006)[1] with the data from the ESA astrometric survey mission Gaia (2012-2018). It has also been claimed that this precision can measure orbital effects of $\tilde{M}_2$ with the Juno mission (2016-2017) (Iorio, 2013). The calculations in these works involve first post-Newtonian approximation (1PN) approximations of the orbits, which require the value of $\tilde{M}_2$ as input. Its value is inferred from observations of satellite flybys (Bagenal *et al.*, 2007), but one must rely on stellar models that can predict it from easier to measure parameters when no spacecraft is or has been around.[2]

A GR stellar model allows as well to know how the rotation of a source modifies the spacetime around it. The effect on deflection for a grazing ray of this rotational motion amounts to 0.7 μas and 0.2 μas in the Sun and Jupiter, respectively. These are not yet observable but only one order of magnitude above current precision (Klioner, 2003).

2.2. ISCO and kHz QPO

The innermost stable circular orbit (ISCO)—a orbit beyond which it is not possible to remain in a circular geodesic—is already present in Newtonian gravity (for non-massless particles) if the source deviates enough from sphericity, but GR predicts a higher effect of mass and quadrupole moment on its radii, making that for a given source this last stable orbit is (when present) further apart from the surface (Zdunik *et al.*, 2000; Gourgoulhon, 2010). Both the surface and ISCO radii depend on the mass, composition and spin rate of the source. In order to have an ISCO, quite strong gravitational fields are required and this is expected to happen in compact stars. Since the ISCO position carries information about the source, one needs GR stellar models to extract it from any ISCO-related observational data. Currently, it is of great interest in the study of neutron stars, as we show in what follows. Nevertheless, since we will use some terminology along this work, it is

[1] This is done using the parametrized post-Newtonian formalism (PPN) scheme.

[2] Of course we have the error introduced by composition and any approximation in the method to obtain the stellar model.

worth reviewing the current concept of neutron—and more generally—compact stars.

The kind of composition of the core is what allows us to classify a compact star. The lower level of compatification corresponds to atomic matter in a degenerate Fermi gas of electrons that is sustained by their degeneracy pressure, reaching densities of up to $\sim 10^9$ g cm^{-3}. Beyond this point, a core is unstable until it reaches densities of $\sim 10^{14}$ g cm^{-3}, where it is sustained by the degeneracy pressure of the neutrons of a fluid of neutron-rich β-stable nuclear matter (n , p, e, μ). As pressure increases, it is energetically favoured to occupy states with new particles and hyperons and baryon resonances appear (Λ, $\Sigma^{\pm}$, Σ^0, Ξ^-, Ξ^0, Δ). Also boson condensates of π^- or K^- and even u, d, s quark matter can appear in the inner part of the star. This last deconfined phase must first co-exist with the hadronic matter (Glendenning, 1992; Müller and Serot, 1995), but can eventually lead to a pure quark matter core. If strange quark matter (SQM) exists, then the whole core can be composed of strange matter. It would not necessarily be incompatible with the existence of non-strange compact stars (Bombaci *et al.*, 2004), though. Hence, due to its core composition, a compact star can be:

- a white dwarf, with a core of atomic matter with degenerate electrons;
- a neutron star, that encloses
  - "traditional" neutron stars with only n , p, e, and μ,
  - hyperon stars,
  - nucleon stars (those with kaon condensation),
  - neutron stars with pion-condensate and
  - hybrid stars, if there is some fraction of quark matter;
- a strange star, if it is composed of strange matter.

Black holes are also considered compact stars, but being its source totally structureless from the GR point of view, we will exclude them from now on from the *compact star* term.

Among compact stars, neutron stars are particularly interesting and hard to deal with because their equation of state (EOS), begin dominated by the strong interaction, is plagued with uncertainties. Some of these stars are source of X-ray bursts, whose intensity show a quasi-periodic oscillation (QPO) usually around a frequency of 200-400 Hz that is thought to be the spin rate of the source (Strohmayer *et al.*, 1996). But prior to the burst, the X-ray spectrum shows two kHz QPO

peaks. Currently, there is wide consensus in that the higher frequency one corresponds to the orbital frequency at the inner edge of the accretion disk around the source (Barret *et al.*, 2006; Lattimer and Prakash, 2007; Miller, 2010), for which the ISCO is the lower limit. If it were known to be at the ISCO, a stellar model could give the mass of the star. If it is out of the ISCO, the orbital frequency can then give an upper limit to the mass since for the same rotation rate, bigger mass implies further ISCO. Since whether or not a certain neutron star can hold up these masses depend on the EOS of its components, it can constrain the EOS of matter at supranuclear densities (Kaaret *et al.*, 1997; Kluźniak, 1998; Zhang *et al.*, 1998; Miller *et al.*, 1998; Thampan *et al.*, 1999; Schaab and Weigel, 1999; Zdunik *et al.*, 2000). This mass upper limit is near $2M_\odot$, which as upper limit is not restrictive, but the detection of Demorest *et al.* (2010) of a $1.97 \pm 0.04\,M_\odot$ pulsar in a binary system has been claimed to discard some compositions. Newer EOS have reintroduced them again into the possibilities (Lattimer and Prakash, 2010; Lattimer, 2012), though.

2.3. *The strange quark matter hypothesis*

Among the possible constituents of compact stars, one of the most intriguing candidates is the so-called *strange quark matter*. It is an hypothetical ground state of matter and as such, its possible existence has fundamental importance in laboratory physics, early and modern age universe cosmology, astrophysics and strong interactions. SQM was popularised by Witten (1984), who recovered the idea of Bodmer (1971) that strange quark matter could be more stable than nuclear matter and used a simple MIT bag model (Chodos *et al.*, 1974) to make some estimations, hinting to the possible existence of stable quark stars of large strangeness.

The main ideas behind stable SQM are the following. When nuclear matter is put under enough pressure, the quarks in its hadrons start to deconfine, expanding their wave functions all through the lump of matter. Eventually hadrons are no more and we get *quark matter*. Quarks of a flavor can be converted to another flavor through weak interaction, and as long as the mass of the new flavor is lower than the Fermi energy, this weak conversion will actually decrease the total energy of the system and thus will be favoured. The chemical potentials involved are around 300 MeV, so in practice only u, d, s quark matter will be favoured over u, d quark matter. Nevertheless, as Witten (1984) pointed out, there is no empirical or theoretical evidence ruling out the possibility of quark matter with large strangeness more tightly bounded than nuclear matter *at zero pressure and temperature*. All what is known in this regard is that nuclear matter with strangeness is heavier and will eventually decay into non-strange hadrons, and that two-flavour

quark matter has a higher energy per baryon than two-flavour nuclear matter. Witten (1984) and later Farhi and Jaffe (1984) used a simple MIT bag model to show that, within the uncertainties associated with strong interactions, strange matter (u, d, s quark matter with electrons to ensure charge neutrality) was a reasonable hypothesis as ground state of matter.

If this were true, although the absorption of nucleons by strange matter would be prevented by Coulomb barriers, neutrons could be absorbed and once a little quark matter is formed by the pressure inside a neutron star, it would rapidly grow and the entire star (except perhaps a thin outer crust without free neutrons) could be transformed into a *strange star* (Witten, 1984).

SQM hypothesis is quite old now but despite its interest it has not been confirmed or refuted yet. The most immediate test of the validity of the SQM hypothesis and the true nature(s) of compact stars (although a universe of coexisting neutron, hybrid and strange stars is possible [Weber, 2005]) is a comparison of the mass-radius (MR) relation for strange stars, neutron stars and hybrid stars.

The easiest scenario would have different maximum masses for each composition to contrast with the mass of heaviest (confidently measured) pulsar, $M = 1.97 \pm 0.4\,M_\odot$ (Demorest *et al.*, 2010), but it turns out that their behaviour in the high mass regime is quite similar (Haensel *et al.*, 1986; Alcock *et al.*, 1986) and very little information has come from this direction so far (Lattimer and Prakash, 2010; Lattimer, 2011).

The situation is different in the low-mass spectrum. A distinctive feature of SQM is that since it is absolutely stable, there is no need of gravitation to hold it together. Gravitation just makes strange stars more compact and accordingly, there is no lower mass limit for them, making the low-mass part of their MR relation radically different from the rest of compositions. Taking this into account, there are five measures (Weber, 2005) of objects with semiempirical MR relations conflicting with most theoretical models for compositions other than SQM:

- SAX J1808.4-3658 (Li *et al.*, 1999a),
- 4U 1728-34 ($M < 1.0 M_\odot, R < 9$km) (Li *et al.*, 1999b),
- RX J1856.5-3754 (see also Turolla *et al.*, 2008 and references therein) and
- 4U 1820-30 and Her X-1 (Dey *et al.*, 1998).

All these objects have MR relations overlapping in an area where only the strange star model of Dey *et al.* (1998), labeled "ss1" in Fig. 1.1, can get. Nevertheless, this model has a lower maximum mass than the very confidently measured minimum masses of Ter 5I and PSR J1903+0327. Other strange star models (Li *et al.*, 2011;

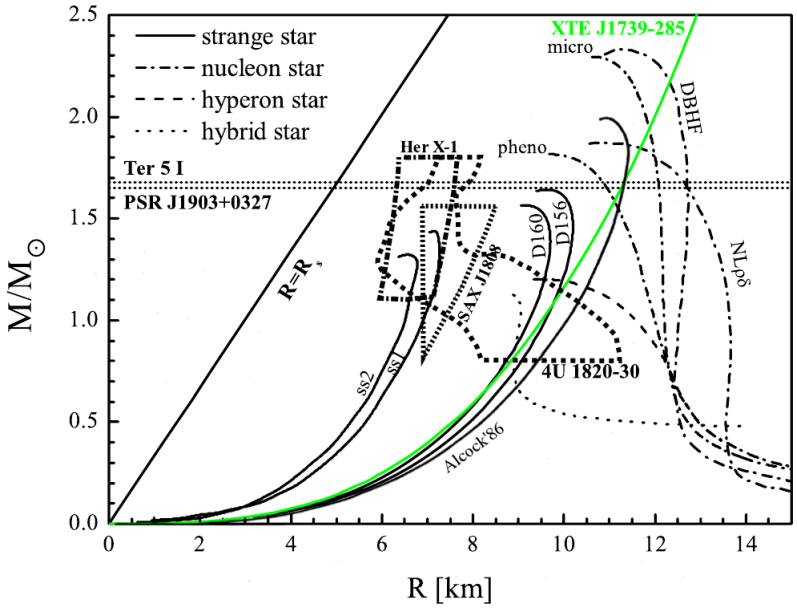

Figure 1.1: Regions of allowed mass-radius (MR) configurations for several pulsars and their relation with some known theoretical models with different compositions. The line $R = R_S$ marks the Schwarzschild radius depending on the mass; the green line gives the maximum radius of XTE J1739-285 as a function of its mass from observational data. The closed areas give the allowed configurations from semiempirical considerations for SAX J1808, 4U 1820-30 and Her X-1. Lines tagged Ter 5 I and PSR J1903+0327 give the minimum masses for these objects with at least a 95% confidence level. See Li *et al.* (2011) for details on the labels of the different MR curves. This figure is adapted from that work and Alcock *et al.* (1986).

Alcock *et al.*, 1986) and different kinds of star give masses compatible with these measurements but fail to reach the MR areas of most of the candidates. One could fine-tune at least some models to get to the MR areas. In the MIT bag model of Alcock *et al.* (1986), this happens for a bag constant $B \simeq 110\,\mathrm{MeV\ fm^{-3}}$ but it is quite far from the value used to fit light hadron masses ($B = 56\,\mathrm{MeV\ fm^{-3}}$) and also above the upper limit for stability of SQM of massless non-interacting quarks ($B \simeq 91.5\,\mathrm{MeV\ fm^{-3}}$)(Weber, 2005; Dey *et al.*, 1998).

Briefly, there is still much to know about about the behaviour of quark matter, although a simple MIT bag model gives the right qualitative MR behaviour for strange stars and, with some caveats, it can mimic more complete descriptions. Leaving the simple MIT bag model and allowing for more freedom, a linear EOS actually gives good approximations even for modern SQM EOS (Zdunik, 2000; Gondek-Rosinska *et al.*, 2000).

3. Obtaining stellar models in GR

Here we start making a more precise definition of the main characteristics of stellar models. As we will see, calculating them is not a trivial task at all and involves several simplifications. Some of them are necessarily assumptions, but in most of the cases they are proven consequences of GR for wide classes of stellar compositions, can be physically related to proven results or at least are expectable.

3.1. Main characteristics of stellar models and common simplifications

By stellar model we mean a solution of the self-gravitating fluid equations that can represent an isolated body. In the context of GR it means that the exterior spacetime of the source is asymptotically flat, and the whole model should be free of singularities. We refer implicitly to *equilibrium* stellar models, so we seek time-independent solutions. They should also have the angular velocity as a parameter and include a solution corresponding to staticity—no rotation at all.

This static state is generally assumed to be spherical, and though it is very reasonable on physical grounds it has been hard to prove even in Newtonian gravity (Carleman, 1919). In GR, the proof still is composition dependent. First, Avez (1964), Künzle (1971) and Lindblom (1978, 1980, 1981) established a base for the subsequent development using barotropic perfect fluids, with the work by Künzle and Savage (1980) proving that there are no almost spherical static stars in GR as the main consequence. The key point for the final proof came from Masood-ul Alam (1987). He showed that under some unphysical conditions, the spatial geometry of the static stellar model is conformal to a metric with non-negative scalar curvature and zero mass. Then, it must be conformally flat as a consequence of the rigidity part of the positive mass theorem (Schoen and Yau, 1979) and, applying a result developed in Avez (1964); Künzle and Savage (1980); Lindblom (1980), the conformally flat static spacetime is spherically symmetric. Along the next fifteen years these restrictions where relaxed and made more physical with the work of Lindblom (1988), Masood-ul Alam (1988) and Beig and Simon (1991, 1992), eventually reducing to inequalities of the adiabatic index of the fluid in Lindblom and Masood-ul Alam (1994); Simon (1993). Only recently these important restrictions were removed. Following his previous line of work, Masood-ul Alam (2007) gave a proof for general barotropic C^1 piecewise EOS, allowing a finite number of discontinuities inside the fluid (see the text for some extra conditions). Recently Pfister (2011) has lowered the original requirement on the energy density-pressure relation $\epsilon(p) \in C^1$ to be just Lipschitz continuous in the body of the source and to more general functions near the surface, including many polytropic equations of

state.

Regarding axisymmetry in rotating sources, there are time independent non-axisymmetric solutions already in Newtonian, such as Dedekind ellipsoids, and even non-axisymmetric solutions that are time dependent in the inertial frame but time independent in a rotating frame (Jacobi ellipsoids, see Chandrasekhar, 1969), so one could expect that axisymmetry is actually an assumption in GR. But this kind of Newtonian solutions have either shear—so viscous fluids would tend to depart from this configurations—or emit gravitational waves, so we eventually arrive at axisymmetric ones (Lindblom, 1976, 1992) even in GR. There are no proofs of reflection symmetry around the equatorial plane in GR, although in Newtonian gravity Lindblom (1977) proved it for the case of barotropic ideal fluids in stratified flow. Hence, it will be an assumption in GR stellar models.

We focus now in the kind on stress-energy tensor to use. Despite its interest in solar system experiments, the main field of application of GR stellar models is the study of compact stars, and in particular neutron stars. In current neutron star models, a solid nuclear matter crust surrounds a core of superfluid and superconducting material at supranuclear densities with several different possible compositions (see Weber, 2005, for a summary), although the interaction between the superfluid nuclear phase and the electrons gives them an effective viscosity (Flowers and Itoh, 1976). This fluid also sustains strong magnetic fields. The intensity of the currently observed magnetic fields on the surface of most of them is $\sim 10^{12}$ G, with values ranging mainly from 10^8 G to 10^{13} G, although in some of them—the so-called magnetars—it can reach 10^{15} G, (see Fig. 1.2). This scenario seems to lead to a very complex and difficult problem but it can be greatly simplified as we see in what follows.

- Neutron stars are expected to acquire differential rotation during the collapse phase from which they are born, but the increased magnetic fields of that phase causes a very efficient magnetic braking that acts on Alfvén timescales, which are $\lesssim 30$ ms for the average neutron star. The remaining differential rotation profile will be damped by viscosity typically in 100 years (Cutler and Lindblom, 1987; Shapiro, 2000; Shibata *et al.*, 2006). Hence, very soon after their birth they are at uniform rotation. Actually, Bonazzola *et al.* (1993) have shown that without convective motions and assuming infinite conductivity, the presence of magnetic fields imposes rigid rotation.

- Magnetic fields affect the structure of the star and are a source of anisotropy in the stress-energy tensor. They give rise to Lorentz forces that tend to flatten the fluid, but assuming only poloidal fields Bocquet *et al.* (1995) have

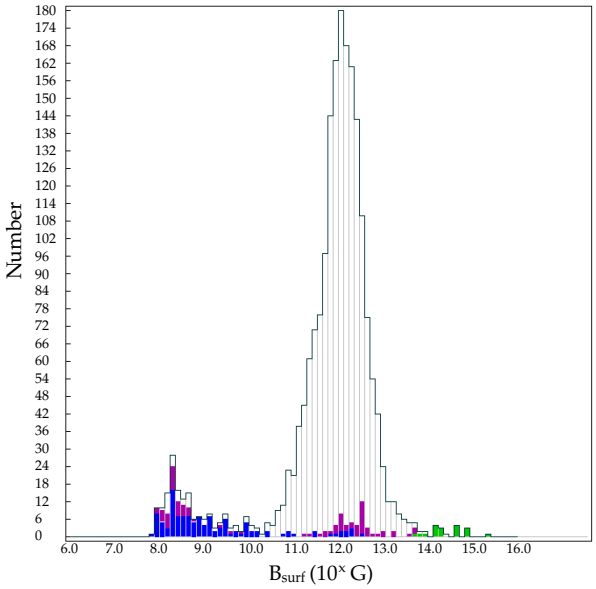

Figure 1.2: Number of known pulsars with a certain intensity of magnetic field on their surface. Units are Gauss and the scale on the X axis logarithmic. Color codes the kind of source; blue are pulsars in binary systems, green are anomalous X-ray pulsars or soft gamma-ray repeaters and purple are high energy sources. Obtained from `http://www.atnf.csiro.au` (Manchester *et al.*, 2005)

shown that in static and slowly rotating cases the deformation is appreciable only for magnetic field intensities $> 10^{15}$ G, and the ratio of magnetic central pressure vs. fluid central pressure is in general lower at typical rotation rates, so these fields would only affect the equilibrium structure of magnetars.

- The presence of the solid crust causes departures from perfect fluid behaviour of order 10^{-5}, and although the superfluid phase will be comprised of vortices, on scales above 1 cm it is well approximated using an averaged velocity field of uniform rotation, implying errors close to 10^{-11} computing the metric (see Friedman and Ipser (1992) and references therein).

Hence, in their equilibrium phase, neutron stars are rigidly rotating, so their viscosity does not play a dynamical part anymore, and their magnetic fields have negligible effect on their structure, so they can be very accurately described by a perfect fluid. Additionally, since the thermal energy associated to their typical temperature (10^{10} K $\approx$ 1 MeV) is much lower than the Fermi energies of the nu-

clear degenerate matter ($\sim$ 60 MeV), one can disregard the effect of temperature and use a barotropic EOS $\epsilon(p)$ (Stergioulas, 2003).

3.2. *Approaches to the problem*

One of the regrettable facts about General Relativity is that, by now, despite the numerous exact solutions and modern methods to generate them (see e.g. Senovilla, 1993; Stephani *et al.*, 2003), it has not been able to provide an exact solution describing a rotating stellar model other than the rotating disc of dust described by Neugebauer and Meinel (1995) and its generalisation for counter-rotating discs (Klein, 2001). Although this infinitesimally thin disc solutions are useful models for galaxies and accretion discs, they are quite far from describing sources of spheroidal shape which are the most common astrophysical objects.

Stellar models are built matching through its zero-pressure surface an interior spacetime describing the source and the exterior spacetime that encloses it. While the Einstein equations for stationary and axisymmetric exteriors form a completely integrable system (Maison, 1978, 1979) and then can be dealt with using solution generation methods to get general solutions, interiors are far more complicated. The only case we know to form a completely integrable system is the disc of dust so in any other case one can only try to get particular solutions. In spite of the effort and interest put in the problem, it has proved difficult to obtain non-singular solutions of this kind. Until now—and this includes the recent works of Davidson (2008, 2009)—, to our knowledge, the only candidates have been for a long time the Wahlquist metric (Wahlquist, 1968, 1992) and the differentially rotating solution by Chinea and González-Romero (1990). The zero-pressure surface of the latter has finite area but can not enclose the symmetry axis, and while numerical relativity predicts stationary toroidal sources (Ansorg *et al.*, 2009) that can be obtained starting from a spheroidal topology for a sufficiently strong degree of differential rotation, in the case of rigid rotation they are unreachable (Ansorg *et al.*, 2004). Here our focus is on rigidly rotating and—since we are interested also in the static limit of our stellar models—spheroidal sources. Accordingly, the only exact interior candidates are the singularity-free members of the Wahlquist family of metrics.

Summing to the difficulties of finding suitable exact interiors, there are the ones arising from the matching with the asymptotically flat exterior. For stellar models it is an overdetermined problem (Mars and Senovilla, 1998) so in general—and importantly, not only in the exact problem—we can not find an exterior that matches a given interior. Such seems to be the case for Wahlquist, where the derivations of the impossibility of matching it with an asymptotically flat exte-

rior (Wahlquist, 1968; Bradley *et al.*, 2000; Sarnobat and Hoenselaers, 2006) come from the analysis of the shape of its surface and involve approximations. This situation leads, if one is to extract information about spheroidal stellar models to purely numerical computations, analytical approximations or a mixture of both.

It is possible to obtain stellar models without any approximation, losing any analyticity and taking the fully numerical approach. The seminal works in GR are due to Bonazzola and Maschio (1971) and Bardeen and Wagoner (1971), using the *self-consistent field* scheme applied to Newtonian sources by Ostriker and Mark (1968). The most recent applications of this idea are the `rotstar` code (Bonazzola *et al.*, 1998; Gourgoulhon *et al.*, 1999b), based on BGSM (Bonazzola *et al.*, 1993), the `rotstar-dirac`, working in Dirac gauge (Lin and Novak, 2006), and last AKM (Ansorg *et al.*, 2002, 2003), which was the first to achieve machine accuracy, 16 meaningful digits when working with double precision programs.

Looking for some analyticity of the results one is far more limitated and must make approximations. Probably the main approximation schemes in GR are the post-Newtonian approximation—where the equations of motion are expanded in $1/c^n$ powers—and the post-Minkowskian one—that allows to linearize and solve iteratively the Einstein equations with a parameter related with the strength of the gravitational field—. Nevertheless, they have been more concerned by the exterior field of the sources, involving trajectories near sources, mass, angular momemtum and radiation of gravitational waves. Wide reviews can be found in Futamase and Itoh (2007) and Blanchet (2006). It is really hard to find analytical approximations for the interior of equilibrium stellar models.

Some pieces of information can be extracted using variational principles. Shapiro and Lightman (1976) used the variational principle of Zel'dovich and Novikov (1971) to obtain approximate formulas for a non-relativistic Fermi gas in fast rotation in the context of PPN, giving equations for the maximum density and mass, which are solved numerically. They also gave the kinetic/gravitational energy and mass/radius ratios for such configurations. Closely in time, Abramowicz and Wagoner (1976, 1977) generalised the variational principle of Nauenberg and Chapline (1973) from static to rotating sources and gave analytic expressions for the mass, angular momentum and baryon number of rigidly slowly rotating uniform interiors using the work of Hartle (1967). Later, using the variational principle of Bardeen (1970), they found expressions for the moment of inertia and angular velocity of the dragging of inertial frames.

Nevertheless, if one is to obtain analytic information about the global metric of the stellar model in full GR, the main option is, despite having to make numeric integrations to get the final metric, the approximate scheme of Hartle (1967). It shows how to build a global metric for a uniformly but slowly rotating perfect

fluid with barotropic EOS. Perturbations are made on the static initial solution of Einstein's equations, making expansions of the metric functions in Legendre polynomials and using the quotient of the Newtonian gravitational and centrifugal energies as expansion parameter. In this paper and also at least in it first applications (Hartle and Thorne, 1968; Chandrasekhar and Miller, 1974), the metric is explicitly assumed to be C^1 on the coordinates chosen. This is not the most general way of matching interior and exterior spacetimes (Darmois, 1927; Israel, 1966; Bonnor and Vickers, 1981), though. Recent applications of the method have improved this and use Darmois-Israel conditions. In the work by Bradley *et al.* (2000) the Hartle formalism is used to obtain an interior for Whittaker's metric fluid, reproducing the results obtained from a series expansion of Wahlquist's metric, and is later matched using Darmois-Israel conditions with an approximate exterior by Hartle and Thorne (1968) which depends on the mass, quadrupole moment and angular momentum of the source. In Bradley *et al.* (2007), a Hartle interior is matched with both asymptotically and non-asymptotically flat exteriors to investigate the possible Petrov types of physically realistic sources. Again, Bradley and Fodor (2009) match a Hartle interior for a quite general EOS with the Hartle-Thorne exterior to investigate possible sources of the Kerr metric. They also calculate a slowly rotating post-Minkowskian source for Newtonian polytropes, recovering some results from Martín *et al.* (2008).

To our knowledge, the only completely analytical stellar models in GR are the ones of Cabezas *et al.* (2007), (CMMR from now on) which is based on the previous work of Cabezas and Ruiz (2006) and deals with a constant density source, and a later application to polytropes (Martín *et al.*, 2008). The key for the complete analyticity is that it is mainly a post-Minkowskian approximation. The equations for the interior can be completely integrated in general, although in the polytropic case the final metric depends on the zeros of the Lane-Emden function. With the post-Minkowskian approximation one can solve iteratively a linearized version of the Einstein equations, but the general solution involves an infinite multipole expansion that must be truncated. They introduced a further approximation—slow rotation—in order to deal with this. The dependence of the multipole moments on the approximation parameters is obtained from the MacLaurin spheroids of Newtonian gravity. This dependence is later assigned to the interior constant that multiplies the same spherical harmonic tensor of the multipolar expansion, and the matching of the exterior and interior spacetimes enforces the metric to be C^1 on the surface. All this is done in harmonic gauge, with both metrics including terms that could be omitted but that parametrize coordinate changes. This last flexibility is key during the matching process.

In this work we will develop further this fully analytical scheme, CMMR, to un-

derstand better its characteristics and limitations, check its validity and the quality of its results. In particular, we intend to

- develop a systematic way of obtaining new metrics in the CMMR scheme, creating software as automatic as possible to help during the calculations and allow for going further in the approximation without heavy hours of work and attention;
- expand the range of applicability with a more general EOS, if possible containing several cases of exact known solutions to check the behaviour of the approximation, as well as physically relevancy;
- improve the quality of the matching from imposing C^1 to using Darmois-Israel conditions to see whether previous results are totally general or only partially;
- check the conditions for the interior to be matchable with an exterior, ruling out classes of solutions as candidate interiors of stellar models;
- check the behaviour with exact solutions to ensure that the theoretical predictions are meaningful and the hypothesis on the interior are well justified. At the same time, since the physical characteristics of our model are clear confirm or gain insight about the exact solution itself;
- check the results with an accurate numeric code, going to further orders of approximation to see the behaviour of the convergence of our results and the goodness of the global character of the solution;
- extract from our most precise solution analytic expressions for quantities of observational interest and
- increase the complexity of the interior allowing for two-layer compositions to identify possible issues and allow a wider span of applicability.

This task is organised in chapters in the following way. In Chapter 2 we start giving the theoretical background for taking the Einstein equations in harmonic gauge beyond the commonly used form of linearized gravity to deal with subsequent iterations. This is the base on which CMMR works. Then, we give a summarised but sufficient view of this approximate scheme, focusing on the main issues of each step. This chapter is supplemented by

1. Appendix A, which contains a more precise definition of perturbation theory in GR and summarise the work of Bruni *et al.* (1997) on gauge behaviour in non-linear approximation schemes.

2. Appendix B, where we give the full derivation of the general solution of the homogeneous part of the Einstein equations in harmonic gauge using as many simplifications as possible and a decomposition of the tensor spherical harmonics due to Martín (2006).

In Chapter 3 we build the stellar model corresponding to an interior with EOS $\epsilon + (1-n)p = \epsilon_0$, where ϵ and p are energy density and pressure, respectively, and n, ϵ_0 constants, going to second order in the post-Minkowskian approximation. In this model, we use Darmois-Israel matching conditions and make an analysis of the generality of our ansatz for the surface and the way we work with the exterior and interior coordinates. We also show the way to change the post-Minkowskian parameter to involve only invariant quantities and compare the Darmois-Israel results with the ones obtained directly from imposing a C^1 metric on the surface. Finally, we look for the possible Petrov types of this interior in order to find correspondences with exact solutions and point towards the possible futility of searching exact solutions for stellar models within the Petrov type II class. Some extra material concerning this chapter appears in

1. Appendix C, where we write the linear EOS metric components after performing Lichnerowicz matching,

2. Appendix D, with a summary of the Petrov classification of spacetimes and

3. Appendix E, that contains the expressions of the $\boldsymbol{Q}$ matrix of the interior spacetime, which is needed to find its Petrov type.

In Chapter 4 we compare one of the interior metrics contained in the solution from Chapter 3 with an exact solution, the Wahlquist metric. To do so, we make a post-Minkowskian and slow rotation expansion on Wahlquist's solution, and manage, through coordinate changes and identification of parameters, to transform our solution into this approximate Wahlquist metric. We make verifications of this procedure using the Petrov conditions derived in the previous chapter.

Chapter 5 faces the comparison with the numerical code. We make a wider review of the available choices and their characteristics to finally choose the AKM code. We find the way to make the approximate coordinate change from ours to the quasi-isotropic ones this code—and many others—use. Then we select a physically interesting subcase of the EOS of Chapter 3 and build several numerical stellar models to compare with an improved—fourth post-Minkowskian order—version of the Chapter 3 metric. The results are compared at each approximation order to check improvement and quality of the results in two ways,

- direct comparison of metric coefficients at *every point* inside and near the source and
- comparison of the value of physical quantities obtained through analytical formulae and the AKM ones.

Several other physical quantities of interest are computed, including ISCO radii and their orbital frequencies. The full matched fourth post-Minkowskian metric appears in Appendix F

Finally, Chapter 6 covers the possibility of building more complex interiors, calculating explicitly the solution for an interior containing two different layers $i = 1, 2$ with EOS $\epsilon + (1 - n_i)p = \epsilon_i$, opening the way to the study of more realistic sources. The full metric appears in Appendix G.

The original research fills Chapters 3 to 6, which include final summary sections. In Conclusions we summarise the main findings, contextualise them and hint at future developments.

Chapter Two

Stellar models in the post-Minkowskian approximation

This chapter sets the main theoretical background for the analytical calculations involved in the obtention of stellar models in the CMMR scheme, summarising the main points of the work of Cabezas *et al.* (2007) and adding some extra material for completeness. We start with a general vision of its fundamental ground, the post-Minkowskian approximation. We keep the discussion and equations as general as possible in the first part. Then we focus on the task at hand, i.e. , dealing with stellar models. We give the precise definition of this term, that will be used throughout the thesis, and use the simplifications it allows to ease the solution of the post-Minkowskian equations. In the process, we introduce an additional approximation, the slow-rotation or small deformation one, what forces us to guess the expansion of the free constants of the post-Minkowskian solution, what constitutes the main hypothesis of the method. The final sketch of the steps required is also given. It will guide the building of the solution for a linear equation of state in Chapter 3

1. The post-Minkowskian approximation in harmonic coordinates

In this section we will write Einstein's equations in a general way that can be iteratively solved. To allow this, the key is the post-Minkowskian approximation, but the harmonic gauge gives the equations a particularly simple structure that we will take advantage of. Hence, we start defining these harmonic coordinates and finding the expression Einstein's equations take when using them. Later we will define and use the post-Minkowskian approximation to get a simpler iterable form.

1.1. The relaxed Einstein Equations in harmonic coordinates

A certain function f is said *harmonic* if it satisfies

$$\Box f = 0, \tag{2.1}$$

where $\Box = g^{\alpha\beta}\nabla_\alpha\nabla_\beta$ is the d'Alembertian operator. If we look for a set of four harmonic functions $x^{(\mu)}$

$$\Box x^{(\alpha)} = g^{\mu\nu}\partial_\mu\partial_\nu x^{(\alpha)} - g^{\mu\nu}\Gamma^\lambda_{\mu\nu}\partial_\lambda x^{(\alpha)} = 0 \tag{2.2}$$

to use them as coordinates, $\partial_\nu x^{(\alpha)} = \delta^\alpha_\nu$ and hence the harmonic condition reduces to

$$\Gamma^\alpha := g^{\mu\nu}\Gamma^\alpha_{\mu\nu} = 0. \tag{2.3}$$

We can also find a different useful expression for it. Since $\partial_\alpha\left(g^{\mu\nu}g_{\sigma\nu}\right) = \partial_\alpha(\delta^\mu_\sigma) = 0$

$$g^{\mu\nu}\partial_\alpha g_{\sigma\nu} = -g_{\sigma\nu}\partial_\alpha g^{\mu\nu}. \tag{2.4}$$

Using it in the first two terms of

$$\Gamma^\alpha = \frac{1}{2}g^{\mu\nu}g^{\alpha\lambda}\left(\partial_\mu g_{\nu\lambda} + \partial_\nu g_{\lambda\mu} - \partial_\lambda g_{\mu\nu}\right) \tag{2.5}$$

and rewriting the last one as $-\frac{1}{2}g^{\mu\nu}g^{\alpha\lambda}\partial_\lambda g_{\mu\nu} = -g^{\alpha\lambda}\Gamma^\mu_{\lambda\mu}$ we get

$$\Gamma^\alpha = -\partial_\mu g^{\mu\alpha} - g^{\alpha\lambda}\Gamma^\mu_{\lambda\mu}, \tag{2.6}$$

which we will need below.

The harmonic condition notably simplifies the expression of the Ricci tensor

$$R_{\alpha\beta} = \partial_\lambda\Gamma^\lambda_{\alpha\beta} - \partial_\beta\Gamma^\lambda_{\alpha\lambda} + \Gamma^\lambda_{\rho\lambda}\Gamma^\rho_{\alpha\beta} - \Gamma^\lambda_{\rho\beta}\Gamma^\rho_{\alpha\lambda}. \tag{2.7}$$

To see it, we define

$$\Gamma_\alpha := g_{\alpha\lambda}\Gamma^\lambda = -g_{\alpha\lambda}\partial_\mu g^{\mu\lambda} - \Gamma^\mu_{\alpha\mu} \tag{2.8}$$

which, besides being zero in harmonic coordinates as well, is also, in terms of the covariant Christoffel symbol $\Gamma_{\alpha,\mu\nu} = g_{\alpha\lambda}\Gamma^\lambda_{\mu\nu}$,

$$\Gamma_\alpha = g^{\mu\nu}\Gamma_{\alpha,\mu\nu}. \tag{2.9}$$

Then, the first term in the right hand side (rhs) of (2.7)

$$\partial_\lambda\Gamma^\lambda_{\alpha\beta} = \partial_\lambda\left(g^{\lambda\mu}\Gamma_{\mu,\alpha\beta}\right) = g^{\lambda\mu}\partial_\lambda\Gamma_{\mu,\alpha\beta} + \partial_\lambda g^{\lambda\mu}\Gamma_{\mu,\alpha\beta} \tag{2.10}$$

turns into, using (2.6),

$$\partial_\lambda \Gamma^\lambda_{\alpha\beta} = g^{\lambda\mu}\partial_\lambda \Gamma_{\mu,\alpha\beta} - \Gamma^\mu \Gamma_{\mu,\alpha\beta} - \Gamma^\lambda_{\alpha\beta}\Gamma^\rho_{\lambda\rho} \tag{2.11}$$

leaving the Ricci tensor as

$$R_{\alpha\beta} = g^{\lambda\mu}\partial_\lambda \Gamma_{\mu,\alpha\beta} - \Gamma_\mu \Gamma^\mu_{\alpha\beta} - \partial_\beta \Gamma^\lambda_{\alpha\lambda} - \Gamma^\lambda_{\alpha\rho}\Gamma^\rho_{\beta\lambda}. \tag{2.12}$$

where the second term would vanish if harmonic coordinates are used. Now, from eq. (2.8), since

$$\begin{aligned} \partial_\beta \Gamma_\alpha &= \partial_\beta \left(g^{\mu\lambda}\partial_\mu g_{\alpha\lambda} \right) - \partial_\beta \Gamma^\lambda_{\alpha\lambda} \\ &= \partial_\beta g^{\mu\lambda}\partial_\mu g_{\alpha\lambda} + g^{\mu\lambda}\partial_\beta\partial_\mu g_{\alpha\lambda} - \partial_\beta \Gamma^\lambda_{\alpha\lambda}, \end{aligned} \tag{2.13}$$

we can combine the first term of eq. (2.12)

$$\begin{aligned} g^{\lambda\mu}\partial_\lambda \Gamma_{\mu,\alpha\beta} &= \frac{1}{2} g^{\lambda\mu}\partial_\lambda \left(\partial_\alpha g_{\beta\mu} + \partial_\beta g_{\mu\alpha} - \partial_\mu g_{\alpha\beta} \right) \\ &= \frac{1}{2}\left[-g^{\lambda\mu}\partial_\lambda\partial_\mu g_{\alpha\beta} + g^{\lambda\mu}\left(\partial_\lambda\partial_\alpha g_{\beta\mu} + \partial_\lambda\partial_\beta g_{\mu\alpha} \right) \right] \end{aligned} \tag{2.14}$$

with the third and get

$$g^{\lambda\mu}\partial_\lambda \Gamma_{\mu,\alpha\beta} - \partial_\beta \Gamma^\lambda_{\alpha\lambda} = -\frac{1}{2} g^{\lambda\mu}\partial_\lambda\partial_\mu g_{\alpha\beta} + \partial_{(\alpha}\Gamma_{\beta)} - \partial_{(\alpha} g^{\mu\lambda}\partial_\mu g_{\beta)\lambda}, \tag{2.15}$$

where the round brackets around indices stand for the corresponding symmetric part $\partial_{(\alpha}\Gamma_{\beta)} := \frac{1}{2}\left(\partial_\alpha \Gamma_\beta + \partial_\beta \Gamma_\alpha \right)$, rendering the Ricci tensor into

$$R_{\alpha\beta} = -\frac{1}{2}\Box_\partial g_{\alpha\beta} + \partial_{(\alpha}\Gamma_{\beta)} - \partial_{(\alpha} g^{\mu\lambda}\partial_\mu g_{\beta)\lambda} - \Gamma_\mu \Gamma^\mu_{\alpha\beta} - \Gamma^\lambda_{\alpha\rho}\Gamma^\rho_{\beta\lambda}, \tag{2.16}$$

where we have introduced $\Box_\partial := g^{\lambda\mu}\partial_\lambda\partial_\mu$. This expression of $R_{\alpha\beta}$ is important because the Einstein equations

$$G_{\alpha\beta} := R_{\alpha\beta} - \frac{1}{2} g_{\alpha\beta} R = 8\pi T_{\alpha\beta}, \tag{2.17}$$

—where $R = R^\alpha_\alpha$ is the scalar curvature and $T_{\alpha\beta}$ the stress-energy tensor—in its equivalent form ($R = -8\pi T^\lambda_\lambda$)

$$R_{\alpha\beta} = 8\pi \left(T_{\alpha\beta} - \frac{1}{2} T^\lambda_\lambda g_{\alpha\beta} \right), \tag{2.18}$$

are then written in harmonic coordinates as

$$\begin{cases} \frac{1}{2}\Box_{\partial} g_{\alpha\beta} = -\partial_{(\alpha} g^{\mu\lambda} \partial_{\mu} g_{\beta)\lambda} - \Gamma^{\lambda}_{\alpha\rho}\Gamma^{\rho}_{\beta\lambda} - 8\pi\left(T_{\alpha\beta} - \frac{1}{2}T^{\lambda}_{\lambda} g_{\alpha\beta}\right), \\ \Gamma^{\alpha} = 0 \end{cases} \tag{2.19}$$

where now the only second derivatives are those in $\Box_{\partial} g_{\alpha\beta}$, turning the Einstein equations into more easy to deal with Poisson equations.

In eq. (2.19) we write the so-called *relaxed* form of the Einstein equations together with the harmonic condition for a reason. Every solution of the full Einstein equations, if written in harmonic coordinates, satisfies the relaxed equation while not every solution of the relaxed equations is a solution of Einstein's equations though. Actually the contracted Bianchi identities

$$\nabla_{\mu} G^{\mu\nu} = 0 \tag{2.20}$$

do not hold for a Ricci tensor eq. (2.16) without the $\partial_{(\alpha}\Gamma_{\beta)} - \Gamma_{\mu}\Gamma^{\mu}_{\alpha\beta}$ terms. Instead, they lead to an expression that is only zero if $\Gamma^{\mu} = 0$. Hence, whenever using the relaxed Einstein equations, one must ensure the harmonic condition verifies as well if one is to get a solution of Einstein equations.

It is also thanks to the structure of 2.19 that the well-posedness of the Cauchy problem in General Relativity was proved, i.e. , that in a general spacetime sliced using spatial sections with $x^0 = \text{const.}$, imposing the harmonic condition in a $\Sigma := x^0 = 0$ slice and giving the value of $(g_{\alpha\beta}, \partial_{\nu} g_{\alpha\beta})|_{\Sigma}$ on it—a Cauchy data—one can evolve this data and get a metric that verifies the harmonic condition in any other $x^0 = \text{const.}$ slice of the spacetime (Foures-Bruhat, 1952; Choquet-Bruhat, 1962).

1.2. *The post-Minkowskian decomposition*

Now we introduce the main approximation in CMMR. In the post-Minkowskian approximation, we consider the exact metric of a spacetime $g_{\alpha\beta}$ to be expressible as Minkowski's metric $\eta_{\alpha\beta}$ plus the metric deviation

$$h_{\alpha\beta} := g_{\alpha\beta} - \eta_{\alpha\beta} \tag{2.21}$$

or, for the inverse metric,

$$k^{\alpha\beta} := g^{\alpha\beta} - \eta^{\alpha\beta}. \tag{2.22}$$

With these decompositions and taking into account that the harmonic coordinates of the flat metric are Cartesian, we can simplify and transform eq. (2.16) into the

form it has in CMMR as follows. Splitting the covariant harmonic condition into its linear (L_α) and quadratic parts (H_α)

$$\begin{aligned}\Gamma_\alpha &= -g_{\alpha\lambda}\partial_\mu g^{\mu\lambda} - \Gamma^\mu_{\alpha\mu} = g^{\mu\lambda}\partial_\mu g_{\alpha\lambda} - \frac{1}{2}g^{\mu\lambda}\partial_\alpha g_{\mu\lambda} \\ &= \underbrace{\partial^\lambda h_{\alpha\lambda} - \frac{1}{2}\partial_\alpha h}_{L_\alpha} + \underbrace{k^{\mu\lambda}\left(\partial_\mu h_{\alpha\lambda} - \frac{1}{2}\partial_\alpha h_{\mu\lambda}\right)}_{H_\alpha},\end{aligned} \tag{2.23}$$

we can group all the terms of $R_{\alpha\beta}$ which are at least quadratic in the deviation into[1]

$$N_{\alpha\beta} := -\frac{1}{2}k^{\lambda\mu}\partial_\lambda\partial_\mu h_{\alpha\beta} + \partial_{(\alpha}H_{\beta)} - \partial_{(\alpha}k^{\mu\lambda}\partial_\mu h_{\beta)\lambda} - \Gamma_\mu\Gamma^\mu_{\alpha\beta} - \Gamma^\lambda_{\alpha\rho}\Gamma^\rho_{\beta\lambda}\,, \tag{2.24}$$

where $\partial^\lambda := \eta^{\lambda\mu}\partial_\mu$ and $h := \eta^{\mu\lambda}h_{\mu\lambda}$. Then, we get

$$R_{\alpha\beta} = -\frac{1}{2}\Box_\eta h_{\alpha\beta} + \partial_{(\alpha}L_{\beta)} + N_{\alpha\beta} \tag{2.25}$$

with $\Box_\eta := \eta^{\lambda\mu}\partial_\lambda\partial_\mu$ the flat d'Alembertian, and making the usual definition $t_{\alpha\beta} := \left(T_{\alpha\beta} - \frac{1}{2}g_{\alpha\beta}T\right)$ we arrive finally at the expression of the relaxed Einstein equations in a post-Minkowskian decomposition and harmonic coordinates

$$\begin{cases}\Box_\eta h_{\alpha\beta} = -16\pi t_{\alpha\beta} + 2\left[N_{\alpha\beta} - \partial_{(\alpha}H_{\beta)}\right], \\ \partial^\rho\left(h_{\rho\alpha} - \frac{1}{2}\eta_{\rho\alpha}h\right) = -H_\alpha\,,\end{cases} \tag{2.26}$$

that groups all quadratic terms of the Ricci and harmonic condition in the right hand sides.

1.3. The iterative solution of the post-Minkowskian equations

This is still a system of non-linear differential equations. Going further in the post-Minkowskian approach, we can now introduce a dimensionless parameter λ related with the amount of deviation from flat spacetime such that

$$h_{\alpha\beta} = \lambda h^{(1)}_{\alpha\beta} + \lambda^2 h^{(2)}_{\alpha\beta} + \cdots \lambda^i h^{(i)}_{\alpha\beta} + \mathcal{O}(\lambda^{i+1}). \tag{2.27}$$

[1] Actually, one could write the relaxed equations without any reference to H_α just not including it in $N_{\alpha\beta}$. It may lead to some faster computations, but have sticked to the original formulation.

Introducing this expression into eq. (2.26) the non-linear system splits into infinite systems according to the $\lambda-$power involved. In the first of them

$$\begin{cases} \Box_\eta h^{(1)}_{\alpha\beta} = -16\pi t^{(1)}_{\alpha\beta}\,, \\ \partial^\rho \left[h^{(1)}_{\rho\alpha} - \dfrac{1}{2} h^{(1)} \eta_{\rho\alpha} \right] = 0\,, \end{cases} \tag{2.28}$$

the relaxed Einstein equations are reduced to Laplace equations in exterior (vacuum) spacetimes. In interior (source) spacetimes, the kind of equation depends on the type of stress-energy tensor. For perfect fluids of 4-velocity u^α we have

$$T^{\alpha\beta} = \left(\epsilon + p\right) u^\alpha u^\beta + p g^{\alpha\beta}, \tag{2.29}$$

with ϵ, p energy density and pressure, respectively, and hence, since one should only expect $g_{\alpha\beta} = \eta_{\alpha\beta}$ in an empty interior, the minimum dependence of the energy density ϵ and pressure p with λ is

$$\epsilon = \mathcal{O}(\lambda) \tag{2.30}$$

$$p = \mathcal{O}(\lambda) \tag{2.31}$$

what allows us to construct $t^{(1)}_{\alpha\beta}$ using only $\eta_{\alpha\beta}$. Thus, in a perfect fluid interior the first order relaxed equations are Poisson equations.

Hence, using this kind of source and because $N_{\alpha\beta}$ and H_α are nonlinear in $h_{\alpha\beta}$, in the i-th λ-order system

$$\begin{cases} \Box_\eta h^{(i)}_{\alpha\beta} = -16\pi t^{(i)}_{\alpha\beta} + 2N^{(i)}_{\alpha\beta} - \partial_\alpha H^{(i)}_\beta - \partial_\beta H^{(i)}_\alpha \\ \partial^\rho \left[h^{(i)}_{\rho\alpha} - \dfrac{1}{2} h^{(i)}\, \eta_{\rho\alpha} \right] = -H^{(i)}_\alpha \end{cases} \tag{2.32}$$

we can obtain the metric dependent rhs terms—ϵ and p may remain undetermined[2]—in both sets of equations using

$$g^{[i-1]}_{\alpha\beta} := \eta_{\alpha\beta} + \sum_{j=1}^{i-1} \lambda^j h^{(j)}_{\alpha\beta}\,. \tag{2.33}$$

The relaxed Einstein equations and harmonic condition are then transformed into a infinite set of differential equations systems like eq. (2.32) which are linear in $h^{(i)}_{\alpha\beta}$ and must be solved iteratively.

[2] This indeterminacy of ϵ and p depends on the EOS. In the one that will concern us later, unlike for polytropes, they are totally fixed.

It may be worth noting a difference regarding the use of harmonic condition between these post-Minkowskian equations and numerical codes that solve the Cauchy problem one slice at a time. They start from initial data that verify the harmonic condition, and thanks to the well-posedness of the relaxed equations in this gauge, they do not need to re-impose harmonic constraints at each step. Actually, sometimes the deviation from harmonic condition is used to measure the quality of the method. In the post-Minkowskian approach we start from $g_{\alpha\beta} = \eta_{\alpha\beta}$, and at after each iteration of the process we get a totally different metric. Hence, one can never drop the harmonic constraint. The iterative property of the method ensures that the condition up to $\mathcal{O}(\lambda^i)$ differs only in $\sim \lambda^i$ terms from the $\mathcal{O}(\lambda^{i-1})$ one, but it must be calculated.

1.4. Computing non-linear terms

Last, we focus now on easing the calculation of the quadratic terms $N_{\alpha\beta}$ and H_α. Regarding the first one, if we build the Ricci tensor corresponding to the metric up to order λ^{i-1}, $R_{\alpha\beta}(\boldsymbol{h}^{[i-1]})$, it must verify also

$$R_{\alpha\beta}\left(\boldsymbol{h}^{[i-1]}\right) = -\frac{1}{2}\Box_\eta h^{[i-1]}_{\alpha\beta} + \partial_{(\alpha}L_{\beta)}\left(\boldsymbol{h}^{[i-1]}\right) + N_{\alpha\beta}\left(\boldsymbol{h}^{[i-1]}\right). \tag{2.34}$$

Note that because of the non-linear terms this expression will differ from $R^{[i-1]}_{\alpha\beta}$. Now, L_α is linear in $h_{\alpha\beta}$, so if we built it using $h^{[i-1]}_{\alpha\beta}$, we obtain its full expression up to λ^{i-1}

$$L_\alpha\left(\boldsymbol{h}^{[i-1]}\right) = L^{[i-1]}_\alpha. \tag{2.35}$$

Conversely, $N_{\alpha\beta}$ is purely non-linear in $h_{\alpha\beta}$, so its terms containing λ^i verify

$$N^{(i)}_{\alpha\beta}\left(\boldsymbol{h}^{[i-1]}\right) = N^{(i)}_{\alpha\beta} \tag{2.36}$$

Thus, if we keep only the λ^i terms in eq. (2.34), we get

$$\begin{aligned} R^{(i)}_{\alpha\beta}\left(\boldsymbol{h}^{[i-1]}\right) &= N^{(i)}_{\alpha\beta}\left(\boldsymbol{h}^{[i-1]}\right) \\ &= N^{(i)}_{\alpha\beta}, \end{aligned} \tag{2.37}$$

what allows us to obtain $N_{\alpha\beta}$ directly from the Ricci tensor. This is useful because there are several algebraic codes for tensor calculus that compute the Ricci tensor straightaway.

Something similar happens with H_α. Since it is purely non-linear, we can do

$$H^{(i)}_\alpha = H^{(i)}_\alpha\left(\boldsymbol{h}^{[i-1]}\right) = \Gamma^{(i)}_\alpha\left(\boldsymbol{h}^{[i-1]}\right). \tag{2.38}$$

In this case, Γ_α is particularly easy to compute in a convenient set of coordinates as follows. It is known that the difference of connections is a tensor and on the other hand that the Levi-Civita connection associated to the flat metric in Cartesian coordinates is the trivial one. Hence we can write

$$\Gamma_\alpha = g^{\lambda\mu}(\Gamma_{\alpha,\lambda\mu} - \gamma_{\alpha,\lambda\mu}) \tag{2.39}$$

where $\gamma^\alpha_{\lambda\mu}$ is the flat connection in arbitrary coordinates. It is a tensor equality and also easy to compute from tensor calculus codes.

2. Solving stellar models with the post-Minkowskian approximation

By now we have discussed the post-Minkowskian equations with a focus on vacuum and perfect fluid spacetimes. This was in order to serve our main goal, the construction within General Relativity of *stellar models* in the sense of Lindblom (1992), i.e. , a global spacetime $(\mathcal{M}, g_{\alpha\beta})$, where $\mathcal{M}$ is a differentiable manifold and $g_{\alpha\beta}$ a Lorentzian metric that

- satisfies the Einstein equations,
- is stationary and axisymmetric,
- contains a compact and rotating perfect fluid surrounded by vacuum and
- describes an isolated self-gravitating source, and hence is asymptotically flat.

In practice this global solution is built up from two different spacetimes that one must obtain separately. The *interior*, that contains the perfect fluid source $(\mathcal{V}^-, g^-_{\alpha\beta})$, and the *exterior* asymptotically flat vacuum solution $(\mathcal{V}^+, g^+_{\alpha\beta})$. The special characteristics of stellar models allow for some important simplifications regarding structure and coordinate dependence of both metrics, as we see in what follows.

2.1. Papapetrou's structure

In the interior $(\mathcal{V}^-, g^-_{\alpha\beta})$, the condition of stationarity implies the existence of a timelike Killing vector field ξ^-. The axisymmetry of the spacetime is given by another Killing vector ζ^- with closed orbits and vanishing module on the symmetry axis. Carter (1970) showed that these two vector fields commute, i.e.

$$[\xi^-, \zeta^-] = 0, \tag{2.40}$$

so that we can choose two coordinates of $\mathcal{V}^-$ to be adapted to the symmetries. Calling them $\{t, \phi\}$, we have

$$\xi^- = \partial_t \qquad \text{and} \qquad \zeta^- = \partial_\phi. \tag{2.41}$$

When the fluid flows along the 2-surfaces spanned by the Killing vector fields, its 4-velocity is

$$\boldsymbol{u} = \psi \left(\partial_t + \omega \partial_\phi \right), \tag{2.42}$$

where ψ is a normalization function and

$$\omega := \frac{u^\phi}{u^t} \tag{2.43}$$

is the angular velocity as seen by an observer at infinity[3].

If, in addition to this, the fluid lacks of any energy flux, then there is no convective motion inside the source (Carter, 1969). This also implies the verification of the so-called *circularity condition* (Papapetrou, 1966; Carter, 1973) and then a theorem by Kundt and Trümper (1966) grants the integrability of 2-planes everywhere orthogonal to the transitivity surfaces of the isometry group. Choosing $\{r, \theta\}$ to be coordinates spanning these 2-surfaces, the metric becomes block diagonal (*Papapetrou's structure*)

$$g^-_{\alpha\beta} = \begin{pmatrix} g_{tt} & g_{t\phi} & 0 & 0 \\ g_{\phi t} & g_{\phi\phi} & 0 & 0 \\ 0 & 0 & g_{rr} & g_{r\theta} \\ 0 & 0 & g_{\theta r} & g_{\theta\theta} \end{pmatrix} \tag{2.44}$$

what is a great simplification of the problem. Hence, we assume these properties for the fluid and add a new one, that the function $\omega = \text{const.}$; rotation is then rigid and thus free of expansion and shear. Note that in this case $\psi = \text{const.}$ defines isobaric surfaces, so in particular the $p = 0$ surface Σ, the outer boundary of the interior, is implicitly defined $\psi = \psi_\Sigma$, with $\psi_\Sigma = \psi(p = 0)$.

This theorem holds as well for stationary and axisymmetric vacuum spacetimes, allowing us to use Papapetrou's structure in the exterior $\boldsymbol{g}^+$, too.

Besides, having our temporal coordinate adapted to a Killing, (2.32) gets the simpler form

$$\begin{cases} \triangle h^{(i)}_{\alpha\beta} = -16\pi t^{(i)}_{\alpha\beta} + 2N^{(i)}_{\alpha\beta} - \partial_\alpha H^{(i)}_\beta - \partial_\beta H^{(i)}_\alpha \,, \\ \partial^k \left[h^{(i)}_{k\alpha} - \dfrac{1}{2} h^{(i)} \eta_{k\alpha} \right] = -H^{(i)}_\alpha \,. \end{cases} \tag{2.45}$$

[3]This common use of ω in relation with a distant observer may hide some subtleties. We will discuss them in a later chapter.

2.2. *Solving the homogeneous system*

The linear structure of the equations in (2.45) for vacuum and perfect fluids allows us to solve the i-th order system in two steps, finding the general solution of the homogeneous equations, $\boldsymbol{h}^{+}_{\text{hom}}$, and adding a particular one of the full equations, $\boldsymbol{h}^{+}_{\text{part}}$ so that

$$\boldsymbol{h}^{\pm} = \boldsymbol{h}^{\pm}_{\text{hom}} + \boldsymbol{h}^{\pm}_{\text{part}}. \tag{2.46}$$

The homogeneous system has the same structure at any λ-order and it is formally equivalent to find its general solution at each order and finding its exact general solution. The latter is more convenient here.

In the exterior case, the general solution to the homogeneous system is, once we introduce all the simplifications allowed by the symmetries and Papapetrou's structure,

$$\boldsymbol{h}^{+}_{\text{hom}} = 2\sum_{l=0}^{\infty}\frac{\tilde{M}_l}{r^{l+1}}\left(\boldsymbol{T}_l + \boldsymbol{D}_l\right) + 2\sum_{l=1,3}^{\infty}\frac{\tilde{J}_l}{r^{l+1}}\boldsymbol{Z}_l + \sum_{l=0,2}^{\infty}\frac{1}{r^{l+3}}\left(\tilde{A}_l\boldsymbol{E}_{l+2} + \tilde{B}_{l+2}\boldsymbol{F}_{l+2}\right) \tag{2.47}$$

—the full derivation of this solution appears in Appendix B—where we have introduced the definitions for the spherical harmonic tensors

$$\begin{aligned}
\boldsymbol{T}_l &:= P_l(\cos\theta)\,\boldsymbol{\omega}^t\otimes\boldsymbol{\omega}^t \quad (l\geq 0),\\
\boldsymbol{D}_l &:= P_l(\cos\theta)\,\delta_{ij}dx^i\otimes dx^j \quad (l\geq 0),\\
\boldsymbol{Z}_l &:= P^1_l(\cos\theta)\,(\boldsymbol{\omega}^t\otimes\boldsymbol{\omega}^\phi + \boldsymbol{\omega}^\phi\otimes\boldsymbol{\omega}^t) \quad (l\geq 1),
\end{aligned} \tag{2.48}$$

and

$$\boldsymbol{\omega}^t = dt, \quad \boldsymbol{\omega}^r = dr, \quad \boldsymbol{\omega}^\theta = r\,d\theta, \quad \boldsymbol{\omega}^\phi = r\sin\theta\,d\phi \tag{2.49}$$

is the Euclidean orthonormal cobasis corresponding to the spherical-like coordinates $\{t,\phi,r,\theta\}$. They are called spherical-like in the sense that they are associated through the usual relations

$$x = r\sin\theta\cos\phi, \quad y = x = r\sin\theta\sin\phi, \quad z = \cos\theta \tag{2.50}$$

to a set $x^\alpha = \{t, x, y, z\}$ of harmonic coordinates which are in turn called Cartesian-like because they correspond to Cartesian coordinates when the spacetime is flat. Eventually, we will use cylindrical-like coordinates in the same way. $P_l(\cos\theta)$, $P^m_l(\cos\theta)$ are associated Legendre polynomials. The remaining spherical harmonic tensors

$$\begin{aligned}
\boldsymbol{H}_l &:= P_l(\cos\theta)\,(\delta_{ij} - 3e_ie_j)dx^i\otimes dx^j \quad (l\geq 0),\\
\boldsymbol{H}^1_l &:= P^1_l(\cos\theta)\,(k_ie_j + k_je_i)dx^i\otimes dx^j \quad (l\geq 1),\\
\boldsymbol{H}^2_l &:= P^2_l(\cos\theta)\,(k_ik_j - m_im_j)dx^i\otimes dx^j \quad (l\geq 2),
\end{aligned} \tag{2.51}$$

—where k_i, e_i and m_i stand for Euclidean unit vectors of the standard cylindrical coordinates, $d\rho = k_i dx^i$, $dz = e_i dx^i$, $\rho\, d\phi = m_i dx^i$—are grouped into the combinations

$$\begin{aligned} \boldsymbol{E}_l &:= \frac{1}{2} l(l-1)\, \boldsymbol{H}_l + (l-1)\, \boldsymbol{H}_l^1 - \frac{1}{2}\, \boldsymbol{H}_l^2 \quad (l \geq 2), \\ \boldsymbol{F}_l &:= \frac{1}{3} l(2l-1)\, \boldsymbol{D}_l - \frac{1}{6} l(l+1)\, \boldsymbol{H}_l - \frac{1}{2}\, (\boldsymbol{H}_l^1 + \boldsymbol{H}_l^2) \quad (l \geq 1)\,, \end{aligned} \tag{2.52}$$

because it simplifies notably the results[4]. Among the constant coefficients $\tilde{M}_l$, $\tilde{J}_l$, $\tilde{A}_l$ and $\tilde{B}_l$, the first two are mass and angular Thorne-Geroch-Hansen multipole moments (Thorne, 1980; Geroch, 1970; Hansen, 1974), respectively, and the last two parametrize the gauge, in the sense that they belong to a part of the solution that can be eliminated with a suitable change of coordinates. As long as one keeps working with asymptotically Cartesian and mass centred coordinates, of which the harmonic ones we use are a subset, changes of coordinates only modify the value of $\tilde{A}_l$ and $\tilde{B}_l$. Also, the index l runs only on even numbers because the equatorial symmetry only allows for even parity of tensors, except for $\boldsymbol{Z}_l$, which must be odd to give negative angular moment when the angular velocity ω is reversed.

In the interior, the solution has to be regular at the origin, what modifies the dependence on the radial coordinate r and the definitions of the spherical harmonic tensor combinations so that

$$\boldsymbol{h}^-_{\text{hom}} = \sum_{l=0,2}^{\infty} \tilde{m}_l\, r^l\, (\boldsymbol{T}_l + \boldsymbol{D}_l) + \sum_{l=1,3}^{\infty} \tilde{j}_l\, r^l\, \boldsymbol{Z}_l + \sum_{l=0,2}^{\infty} \left(\tilde{a}_l\, r^l \boldsymbol{E}^*_l + \tilde{b}_{l+2}\, \boldsymbol{F}^*_l \right), \tag{2.53}$$

with[5]

$$\begin{aligned} \boldsymbol{E}^*_l &:= \frac{1+l}{6}\, [(6+4l)\boldsymbol{D}_l - l\boldsymbol{H}_l] - \frac{1}{2}(\boldsymbol{H}_l^1 + \boldsymbol{H}_l^2), \\ \boldsymbol{F}^*_l &:= \frac{1}{2}(l+1)(l+2)\boldsymbol{H}_l - (l+2)\boldsymbol{H}_l^1 - \frac{1}{2}\boldsymbol{H}_l^2. \end{aligned} \tag{2.54}$$

Here, again, we have a purely gauge part of the solution, the one containing $\tilde{a}_l$ and $\tilde{b}_l$, but contrary to what happens in the exterior, the remaining part is not gauge invariant, so $\tilde{m}_l$ and $\tilde{j}_l$ are expected to vary under coordinate changes.

2.3. *The approximate solution of the homogeneous system*

The expressions (2.47) and (2.53) for $\boldsymbol{h}^{\pm}_{\text{hom}}$ are infinite expansions in tensors which are increasingly complex in terms of θ dependence. To work with them, we must

[4] Note that the definitions from Cabezas *et al.* (2007) have been modified. Now $\boldsymbol{E}_2$ has spherical symmetry.

[5] The definition of $\boldsymbol{E}^*_l$ is different from the one used in Cabezas *et al.* (2007). Also, $\boldsymbol{E}^*_0 := \boldsymbol{D}_0$ has now spherical symmetry and the first $\tilde{b}_l$ constant is $\tilde{b}_2$.

truncate these expansions. To do it, we introduce a new approximation parameter Ω related with the rotation that measures the degree of deformation of the fluid. It must be noted though, that the normalization condition for the 4-velocity of the fluid $u_\alpha u^\alpha = -1$ gives

$$\psi = \left[-\left(g_{tt} + 2\omega\, g_{t\varphi} + \omega^2 g_{\varphi\varphi} \right) \right]^{-\frac{1}{2}} \tag{2.55}$$

and hence since the base post-Minkowskian expansion of $\boldsymbol{h}$ to give a static spacetime when $\omega = 0$ is

$$h_{00} = \lambda h^{(1)}_{00} + \lambda^2 h^{(2)}_{00} + \cdots, \tag{2.56}$$

$$h_{ij} = \lambda h^{(1)}_{ij} + \lambda^2 h^{(2)}_{ij} + \cdots, \tag{2.57}$$

$$h_{0i} = \omega(\lambda h^{(1)}_{0i} + \lambda^2 h^{(2)}_{0i} + \cdots), \tag{2.58}$$

we have that for the equation $\psi =$ const. to define spheres instead of cylindrical surfaces, we need $\omega^2 \sim \lambda$ at least. This two conditions led to introduce Ω as

$$\Omega^2 := \frac{r_s^2 \omega^2}{\lambda} \tag{2.59}$$

with r_s the coordinate radius of the static spherical fluid mass. It causes that h_{0i} terms, naturally possessing odd powers of Ω to give the expected behaviour under reversal of rotation direction, have an expansion of the form

$$h_{0i} = \lambda^{3/2} h^{(1)}_{0i} + \lambda^{5/2} h^{(2)}_{0i} + \mathcal{O}(\lambda^{7/2}). \tag{2.60}$$

We can give Ω a more intuitive expression. Defining λ to characterise the strength of the gravitational field in terms of parameters of the source as

$$\lambda := \frac{m}{r_s} \tag{2.61}$$

with m the Newtonian mass of the source in the static case, then

$$\Omega^2 = \frac{r_s \omega^2}{m/r_s^2}, \tag{2.62}$$

gives the ratio between the classical centrifugal and gravitational energies (also used by e.g. Hartle, 1967), what one should expect as a measure of source deformation because of rotation.

Now, to truncate the expansions and to extract the i-th post-Minkowskian solution from eqs. (2.47) and (2.53) we must find the expression of their constant

coefficients in terms of (λ, Ω). Starting with the exterior, the dimensional analysis of the first multipole moments gives the base dependence

$$\tilde{M}_0 = mM_0 = \lambda r_s M_0 \,, \tag{2.63}$$

$$\tilde{J}_1 = m\omega r_s^2 J_1 = \lambda^{\frac{3}{2}} \Omega r_s^2 J_1 \,. \tag{2.64}$$

where the untilded M_0 and J_1 are series expansions of λ and Ω with constant dimensionless coefficients. Superior multipole moments have dynamic origin and hence they depend on the Ω power that correspond to their multipole order, i.e.

$$\tilde{M}_l = \lambda \Omega^l r_s^{l+1} M_l \,, \tag{2.65}$$

$$\tilde{J}_l = \lambda^{\frac{3}{2}} \Omega^l r_s^{l+1} J_l \,. \tag{2.66}$$

It is worth noting that this is the kind of dependence that the multipole moments of the MacLaurin ellipsoids have when they are expanded in Ω. The gauge part coefficients are left with the most general base dependence that gives A_l and B_l dimensionless expansions with the only caveat that while $\boldsymbol{E}_2$ has spherical symmetry, $\boldsymbol{F}_2$ does not and thus cannot be present in the static limit. Accordingly, we get

$$\tilde{A}_l = \lambda \Omega^l r_s^{l+1} A_l \tag{2.67}$$

$$\tilde{B}_l = \lambda \Omega^l r_s^{l+1} B_l \tag{2.68}$$

but the summation of the $\boldsymbol{F}_l$ terms must start at $l = 2$. Summing up, the expression of the metric deviation up to $\mathcal{O}(\Omega^3)$, which is as far as we will go regarding Ω in this work, is

$$\begin{aligned} \boldsymbol{h}^{+}_{\text{hom}} = 2 \sum_{l=0,2} \lambda \Omega^l r_s^{l+1} \frac{M_l}{r^{l+1}} \left(\boldsymbol{T}_l + \boldsymbol{D}_l\right) + 2 \sum_{l=1,3} \lambda^{\frac{3}{2}} \Omega^l r_s^{l+1} \frac{J_l}{r^{l+1}} \boldsymbol{Z}_l \\ + \sum_{l=0,2} \lambda \Omega^l r_s^{l+3} \frac{A_l}{r^{l+3}} \boldsymbol{E}_{l+2} + \lambda \Omega^2 r_s^3 \frac{B_2}{r^3} \boldsymbol{F}_2 + \mathcal{O}(\Omega^4) \,. \end{aligned} \tag{2.69}$$

For the interior solution, we lack the multipole moments reference of the exterior. We can but make an educated guess and follow the same procedure we have applied to the exterior. Since $\boldsymbol{E}^*_0$ and $\boldsymbol{F}^*_0$ behave in the same fashion as their exterior counterparts, we have

$$\begin{aligned} \boldsymbol{h}^{-}_{\text{hom}} = \sum_{l=0,2} \lambda \Omega^l \frac{m_l}{r_s^l} r^l \left(\boldsymbol{T}_l + \boldsymbol{D}_l\right) + \sum_{l=1,3} \lambda^{\frac{3}{2}} \Omega^l \frac{j_l}{r_s^l} r^l \boldsymbol{Z}_l \\ + \sum_{l=0,2} \lambda \Omega^l \frac{a_l}{r_s^l} r^l \boldsymbol{E}^*_l + \lambda \Omega^2 b_2 \boldsymbol{F}^*_0 + \mathcal{O}(\Omega^4) \,. \end{aligned} \tag{2.70}$$

Metric	Free parameters	Constant coefficients
Exterior	r_s, ω	M_0, M_2, J_1, J_2, A_0, A_2, B_2
Interior	r_s, ω	m_0, m_2, j_1, j_2, a_0, a_2, b_2

Table 2.1: Remaining constants in the solutions of the homogeneous system for a certain EOS. The constant coefficients are fixed when the metrics are fully matched. The free parameters remain so. Then, one can select different members of the family of metrics choosing values for them.

2.4. *The particular solution of the complete system*

With the solution of the homogeneous system at every λ-order, we only need to find a way to obtain particular solutions of the full harmonic post-Minkowskian equations (2.45). Regarding $N^{(i)}_{\alpha\beta}$ and $H^{(i)}_{\alpha}$, we already got formulas to compute them in Section 1.4. To find the approximate expression of $t_{\alpha\beta}$ for the interior problem, the only non-straightforward step is finding the $\epsilon(\psi)$ and $p(\psi)$ relations.

The assumptions of perfect fluid, circularity and rigid rotation allows us to obtain from the Euler equations $\nabla_\alpha T^\alpha_\beta = 0$ (Boyer, 1965) that

$$\frac{dp}{(\epsilon + p)} = d \ln \psi \tag{2.71}$$

which, making use of the $\epsilon(p)$ relation of the fluid, gives a separable ordinary differential equation for $p(\psi)$. If we are able to integrate it, using eq. (2.55) we get the expressions of ϵ and p we need. In the cases we study in this work, $(\epsilon^{(i)}, p^{(i)})$ depend only on $\boldsymbol{h}^{[i-1]}$, leading to a rhs of the Poisson equation fully known. It must be noted that it is not always the case, though. For example, for a polytropic fluid one ends up having to deal with a Lane-Endem equation at each iteration (Martín *et al.*, 2008).

In the cases when the rhs of the Poisson equation is completely known, the advantage of working with spherical harmonic tensor becomes clear because the rhs is a sum of terms of the form $f(r)Y_l(\theta, \phi)$ which verify

$$\Delta \left(f(r)\, Y_l(\theta, \phi) \right) = \frac{1}{r^2} \left[\partial_r (r^2 \partial_r f(r)) - l(l+1) f(r) \right] Y_l(\theta, \phi). \tag{2.72}$$

Then, we can start from the full rhs and correct the r dependence and numeric factors appropriately to get the particular solution.

The last step is ensuring that the solutions of the Poisson equation $\boldsymbol{h}^{\pm}_{\text{Poisson}}$ verify the harmonic condition as well. A solution $\boldsymbol{h}^{\pm}_{\text{full}}$ of the complete system is also

a solution of the Poisson equation. Now, since two solutions of a certain Poisson equation can only differ in a solution of the corresponding Laplace equations, we can find a solution of the complete system adding to the Poisson solutions a solution of the Laplace equation

$$h^{\pm}_{\text{full}} = h^{\pm}_{\text{Poisson}} + h^{\pm}_{\text{Laplace}} \tag{2.73}$$

with its coefficients adjusted so that the combination verifies the harmonic condition. In the exterior this step is unnecessary since h^{+}_{Poisson} is already written in harmonic coordinates. In the interior, we add a solution of the form

$$h^{\pm}_{\text{Laplace}} = a\boldsymbol{E}_2 + b\boldsymbol{E}_4 + c\boldsymbol{F}_2. \tag{2.74}$$

Note that inserting interior combinations $\boldsymbol{E}^*_l$, $\boldsymbol{F}^*_l$, would not work since they have been built to satisfy the interior harmonic condition in the same way as were the exterior ones in Appendix B and would therefore vanish.

2.5. *Surface of the source and matching*

Once we have the approximate solutions $\boldsymbol{g}^{\pm}$ in the two separate spacetimes $\mathcal{V}^{\pm}$, to build a stellar model we need to match them across the $p = 0$ surface of the fluid. In Cabezas *et al.* (2007) and Martín *et al.* (2008), the surface was introduced as an ansatz using an expansion in Legendre polynomials

$$r_{\Sigma}(\theta) = r_s \left\{1 + \Omega^2 \left[\varsigma_0 + \varsigma_2 P_2(\cos\theta)\right]\right\} + \mathcal{O}(\Omega^4) \tag{2.75}$$

with ς_n constants to be found. It was then used as the base for the matching. There, they imposed that the metrics $\boldsymbol{g}^{\pm}$ and its first derivatives were continuous through the surface—Lichnerowicz matching conditions—. This fixed the value of the constant coefficients of $h^{\pm}_{\text{hom}}$ and then they got the metric of the global spacetime of the stellar model, which depends only on the values of ω, r_s and the free parameters of the equation of state of the fluid.

Nevertheless, it has been argued that in some situations this kind of matching may not lead to the most general stellar model. Also, in general matching theory, the surface is actually one of the results of the matching procedure, so prescribing it at the beginning of the process can again lead to lack of generality. This problem will be treated in full care in the next chapter.

Note also that even after fixing the gauge, the rescaling freedom in the radial coordinate will affect the possible values of r_s. This does not affect the capability of CMMR to give explicit values for the metric and other quantities as we will discuss later.

Chapter Three

The linear EOS solution

In this chapter we apply CMMR to obtain the global solution for a non-convective fluid with a linear energy density-pressure relation, $\epsilon + (1-n)p = \epsilon_0$, what we will from now on call linear EOS unless otherwise stated[1]. Among the relevant EOS it includes are the ones corresponding to constant density ($n = 1$), the Wahlquist and Whittaker fluid ($n = -2$) and $n = 4$ which corresponds to the simple MIT bag model EOS that has been frequently used to study the properties of strange quark matter. The latter as constituent of at least a class of compact stars is currently an exciting possibility in astrophysics (Weber, 2005; Weissenborn *et al.*, 2011; Lattimer, 2011) as was discussed in Chapter 1. We also show that the full matching procedure used in CMMR can be made completely general using Darmois-Israel matching conditions (Darmois, 1927; Israel, 1966) instead of Lichnerowicz ones (Lichnerowicz, 1955), as well as ensuring the generality of the assumptions made on the embeddings of the matching surface. Later, we use the approximate metric to exclude as candidate sources of stellar models those Petrov type II interiors with this EOS that admit a CMMR expansion. This is unexpected. This fact coincides with a lack of exact stationary axisymmetric perfect fluid solutions of that Petrov type (Senovilla, 1993), what leads us to wonder if this can be the case irrespective of the EOS. The $\boldsymbol{Q}$ matrix of a metric with Papapetrou's structure like ours rules out Petrov type III, and the combination of its symmetries and EOS discards type N as well (Carminati, 1988) and hence we get that the possible Petrov types of matchable rotating interiors with this EOS are I or D. Our analysis, though approximate, shows as well that the stationary (non-static) constant density case can only have Petrov type I. Finally, we obtain the conditions for our interior to correspond to an approximate Wahlquist metric and recover the result that Wahlquist can not be matched with stationary axisymmetric asymptotically flat exteriors Bradley *et al.* (2000); Sarnobat and Hoenselaers (2006). We also show that our interior can not be a source of Kerr metric.

[1] The equation of state of a temperature independent substance is actually given by two relations, $\epsilon(n)$ and $p(n)$, with n the particle number. It contains more information than the $\epsilon(p)$ relation, but it is common to abuse the term and refer to it as equation of state as well.

1. Interior Solution

We begin finding the approximate interior. All CMMR needs as input are the $\epsilon(\psi)$, $p(\psi)$ relations, hence we first look for them.

1.1. Source characterization

We will study a fluid with EOS

$$\epsilon + (1-n)p = \epsilon_0, \tag{3.1}$$

where n is a real number and ϵ_0 is a constant with units of energy density. This linear barotropic EOS contains the ones of two significant exact solutions: $n = 1$ corresponds to constant density of the Schwarzschild interior and $n = -2$ gives the EOS of the Wahlquist family of metrics (Wahlquist, 1968) which has Whittaker's solution (Whittaker, 1968) as static limit.

As we saw in Chapter 2, the information about the EOS of the source fluid enters the Einstein equations through the $\epsilon(\psi)$ and $p(\psi)$ relations, which we need to integrate using Euler's equations. Since our perfect fluid is in rigid rotation and verifies the circularity condition, Euler's equations are reduced to eq. (2.71) and give for this EOS, when $n \neq 0$,

$$\epsilon = \frac{\epsilon_0}{n}\left[(n-1)\left(\frac{\psi}{\psi_\Sigma}\right)^n + 1\right], \tag{3.2}$$

$$p = \frac{\epsilon_0}{n}\left[\left(\frac{\psi}{\psi_\Sigma}\right)^n - 1\right], \tag{3.3}$$

and if $n = 0$,

$$\epsilon = \epsilon_0\left(1 - \log\frac{\psi}{\psi_\Sigma}\right), \tag{3.4}$$

$$p = \epsilon_0 \log\frac{\psi}{\psi_\Sigma}\,. \tag{3.5}$$

The value of ψ depends in turn on the metric components through eq. (2.55), which have a post-Minkowskian expansion. Since we choose ξ^- to be a unit time translation at Minkowskian level, the first terms of ψ are

$$\psi = 1 + \lambda\psi^{(1)} + \lambda^2\psi^{(2)} + \mathcal{O}\left(\lambda^3\right) \tag{3.6}$$

with an equivalent expansion for ψ_Σ. This makes that the expansions of ϵ, p for the $n \neq 0$ case

$$\begin{aligned}\frac{\epsilon}{\epsilon_0} &= 1 + \lambda\left(n\left(\psi^{(1)} - \psi_\Sigma^{(1)}\right) + \psi_\Sigma^{(1)} - \psi^{(1)}\right) \\ &+ \lambda^2\left\{n^2\left[-\psi^{(1)}\psi_\Sigma^{(1)} + \frac{1}{2}\left(\psi_\Sigma^{(1)}\right)^2 + \frac{1}{2}\left(\psi^{(1)}\right)^2\right] + n\left(\psi^{(1)}\psi_\Sigma^{(1)} - \psi_\Sigma^{(2)} - \left(\psi^{(1)}\right)^2 + \psi^{(2)}\right)\right. \\ &\left. - \frac{1}{2}\left(\psi_\Sigma^{(1)}\right)^2 + \psi_\Sigma^{(2)} + \frac{1}{2}\left(\psi^{(1)}\right)^2 - \psi^{(2)}\right\} + \mathcal{O}\left(\lambda^3\right), \qquad (3.7)\end{aligned}$$

$$\begin{aligned}\frac{p}{\epsilon_0} &= \lambda\left(\psi^{(1)} - \psi_\Sigma^{(1)}\right) + \lambda^2\left\{n\left[-\psi^{(1)}\psi_\Sigma^{(1)} + \frac{1}{2}\left(\psi_\Sigma^{(1)}\right)^2 + \frac{1}{2}\left(\psi^{(1)}\right)^2\right]\right. \\ &\left. + \frac{1}{2}\left(\psi_\Sigma^{(1)}\right)^2 - \psi_\Sigma^{(2)} - \frac{1}{2}\left(\psi^{(1)}\right)^2 + \psi^{(2)}\right\} + \mathcal{O}\left(\lambda^3\right), \qquad (3.8)\end{aligned}$$

coincide making $n = 0$ with the ones derived from eqs. (3.4) and (3.5)

$$\frac{\epsilon}{\epsilon_0} = 1 + \lambda\left(\psi_\Sigma^{(1)} - \psi^{(1)}\right) + \frac{1}{2}\lambda^2\left[-\left(\psi_\Sigma^{(1)}\right)^2 + 2\psi_\Sigma^{(2)} + \left(\psi^{(1)}\right)^2 - 2\psi^{(2)}\right] + \mathcal{O}\left(\lambda^3\right), \qquad (3.9)$$

$$\frac{p}{\epsilon_0} = \lambda\left(\psi^{(1)} - \psi_\Sigma^{(1)}\right) + \frac{1}{2}\lambda^2\left[\left(\psi_\Sigma^{(1)}\right)^2 - 2\psi_\Sigma^{(2)} - \left(\psi^{(1)}\right)^2 + 2\psi^{(2)}\right] + \mathcal{O}\left(\lambda^3\right). \qquad (3.10)$$

Therefore, eqs. (3.7) and (3.8) actually cover every possible value of n. It is also very important to note that the zeroth order of ϵ is just ϵ_0, which is one of the free parameters of the solution. Hence, $t_{\alpha\beta}^{(i)}$ is fully derivable from $g_{\alpha\beta}^{[i-1]}$, allowing for an easy obtention of the i-th order particular solution of the Poisson equation.

The definition of λ (2.61) taking ϵ_0 as average energy density becomes

$$\lambda = \frac{4}{3}\pi r_s^2 \epsilon_0. \qquad (3.11)$$

This causes that the lowest term of the energy density and pressure behave likely

$$\epsilon \sim \mathcal{O}(\lambda), \qquad (3.12)$$

$$p \sim \mathcal{O}\left(\lambda^2\right). \qquad (3.13)$$

A relation of this kind also holds for spherical configurations in Newtonian theory (Bradley and Fodor, 2009).

1.2. *Approximate solution*

Once we have fully determined $t_{\alpha\beta}^{(1)}$, following the steps summarised in Chapter 2 leads to the following solution for the interior metric

$$
\begin{aligned}
g^- = &-\boldsymbol{T}_0 + \boldsymbol{D}_0 + \lambda\Big\{\left(m_0 - \eta^2\right)\boldsymbol{T}_0 + \left(a_0 + m_0 - \eta^2\right)\boldsymbol{D}_0 + \\
&\quad + \Omega^2\left[m_2\eta^2\boldsymbol{T}_2 + (5a_2 + m_2)\,\eta^2\boldsymbol{D}_2 + b_2\boldsymbol{H}_0 + a_2\eta^2\boldsymbol{F}_2\right]\Big\} \\
&+ \lambda^2\eta^2\left\{\left(-a_0 - \frac{m_0}{2}(n+2) + (n+2)S + (2+3n)\,\frac{\eta^2}{20}\right)\boldsymbol{T}_0\right. \\
&\quad + \left(-2a_0 - \frac{m_0}{2}(n+2) + (n-2)S + \left(\frac{13}{3} + \frac{3n}{2}\right)\frac{\eta^2}{10}\right)\boldsymbol{D}_0 \\
&\quad + \left(-\frac{m_0}{5} + \frac{2S}{5} + \frac{2\eta^2}{21}\right)\boldsymbol{E}_2 \\
&\quad + \Omega^2\left[\left(-\frac{3}{5} - \frac{n}{10}\right)\eta^2\boldsymbol{T}_0 + \left(\frac{1}{15} - \frac{n}{10}\right)\eta^2\boldsymbol{D}_0\right. \\
&\quad + \left(\frac{6}{7} - 3a_2 + \frac{m_2}{7} + \frac{n}{7} - \frac{3}{14}m_2 n\right)\eta^2\boldsymbol{T}_2 \\
&\quad + \left(\frac{2}{7} - 8a_2 - m_2 + \frac{n}{7} - \frac{3}{14}m_2 n\right)\eta^2\boldsymbol{D}_2 \\
&\quad - \left(b_2 + (1+m_2)\frac{\eta^2}{15}\right)\boldsymbol{H}_0 - \frac{2\eta^2}{21}\boldsymbol{E}_2 + \left(\frac{1}{3} - \frac{m_2}{2}\right)\frac{\eta^2}{105}\boldsymbol{E}_4 \\
&\quad \left.\left. - \left(\frac{m_2}{5}(2m_0 + a_0) + \left(a_2 + \frac{2}{21}(2 - m_2)\right)\eta^2\right)\boldsymbol{F}_2\right]\right\} \\
&+ \lambda^{3/2}\Omega\eta\left[\left(j_1 - \frac{6\eta^2}{5}\right)\boldsymbol{Z}_1 + \Omega^2 j_3\eta^2\boldsymbol{Z}_3\right] \\
&+ \lambda^{5/2}\Omega\eta^3\frac{1}{5}\left\{\left(j_1 - 12(a_0 + m_0) - 3m_0 n + 6nS + \left(\frac{27}{7} + \frac{15n}{14}\right)\eta^2\right)\boldsymbol{Z}_1\right. \\
&\quad + \Omega^2\left[-\left(\frac{42b_2}{5} + j_1 m_2 + \left(4 - 3m_2 - \frac{nm_2}{2} + 2n - \frac{42a_2}{5}\right)\frac{3\eta^2}{7}\right)\boldsymbol{Z}_1\right. \\
&\quad \left.\left. + \left(\frac{4}{9} - \frac{48a_2}{5} + \frac{5j_3}{9} - \frac{4m_2}{3} + \frac{2n}{9} - \frac{m_2 n}{3}\right)\eta^2\boldsymbol{Z}_3\right]\right\} \\
&+ \mathcal{O}(\lambda^3, \Omega^4)
\end{aligned}
\tag{3.14}
$$

where $\eta := r/r_s$ and the constant S comes from the expansion of ψ on the surface,

$$\psi_\Sigma = 1 + S\lambda + \mathcal{O}(\lambda^2). \tag{3.15}$$

It takes the value

$$S = \frac{m_0 - 1}{2} + \frac{\Omega^2}{3} + \mathcal{O}(\Omega^4) \tag{3.16}$$

but leaving S undetermined in the expression of $g^-_{\alpha\beta}$ will be useful in Chapter 4

The first order part of eq. (3.14) corresponds to the constant energy density problem already solved in Cabezas *et al.* (2007). It is so due to the dependence on λ of ϵ and p—eqs. (3.12) and (3.13)—.

2. Global Solution

After getting the interior, we have to find a suitable exterior and match both spacetimes together. In this section we will do this using two sets of matching conditions and then analyse both results.

2.1. Exterior Solution

The EOS does not play any role in the obtention of the exterior and it can be obtained directly from the considerations in Chapter 2. Notice though that the coordinates in eq. (2.47) have been named as the ones used in $\mathcal{V}^-$ but they are not the same in principle. Even after the Darmois matching, the coordinates will only be C^0 on the surface. Properly speaking, $\{t, \phi, r, \theta\}$ should be replaced by $\{T, \Phi, R, \Theta\}$ by now.

The general vacuum solution is

$$
\begin{aligned}
g^+ = -\boldsymbol{T}_0 + \boldsymbol{D}_0 + \lambda\frac{1}{\eta}\Bigg[&2M_0(\boldsymbol{T}_0 + \boldsymbol{D}_0) + \frac{A_0}{\eta^2}\boldsymbol{E}_2 \\
&+ \Omega^2\frac{1}{\eta^2}\left(2M_2(\boldsymbol{T}_2 + \boldsymbol{D}_2) + B_2\boldsymbol{F}_2 + \frac{A_2}{\eta^2}\boldsymbol{E}_4\right)\Bigg] \\
+ \lambda^2\frac{1}{\eta^2}\Bigg\{&\left(-2M_0^2 - \frac{A_0M_0}{\eta^2}\right)\boldsymbol{T}_0 + \left(\frac{4M_0^2}{3} - \frac{A_0M_0}{\eta^2} + \frac{3{A_0}^2}{2\eta^4}\right)\boldsymbol{D}_0 \\
&+ \left(-\frac{{M_0}^2}{3} + \frac{2A_0M_0}{\eta^2} - \frac{9{A_0}^2}{4\eta^4}\right)\boldsymbol{E}_2 \\
&+ \Omega^2\frac{1}{\eta^2}\Bigg[A_0\left(\frac{6B_2}{5\eta^2} + \frac{2M_2}{5\eta^2} - \frac{3A_2}{2\eta^4}\right)\boldsymbol{H}_0 \\
&+ \left(2M_0(B_2 - 2M_2) - \frac{3A_2M_0}{\eta^2} - \frac{3A_0M_2}{\eta^2}\right)\boldsymbol{T}_2 \\
&+ \left(2M_0\left(B_2 + \frac{32M_2}{21}\right) - \frac{A_0}{7\eta^2}(12B_2 - 13M_2) - \frac{3A_2M_0}{\eta^2} + \frac{66A_0A_2}{7\eta^4}\right)\boldsymbol{D}_2 \\
&+ \left(2M_0\left(B_2 - \frac{2M_2}{21}\right) - \frac{A_0}{7\eta^2}(15B_2 - 4M_2) + \frac{30A_0A_2}{7\eta^4}\right)\boldsymbol{F}_2
\end{aligned}
$$

$$+\left(-\frac{M_0M_2}{7}+\frac{A_0}{35\eta^2}(33B_2+6M_2)+\frac{2A_2M_0}{\eta^2}-\frac{53A_0A_2}{14\eta^4}\right)\boldsymbol{E}_4\Bigg]\Bigg\}$$
$$+\lambda^{3/2}\Omega\frac{2}{\eta^2}\left(J_1\boldsymbol{Z}_1+\Omega^2\frac{J_3}{\eta^2}\boldsymbol{Z}_3\right)+\lambda^{5/2}\Omega\frac{1}{\eta^3}\Bigg\{\left(-2J_1M_0-\frac{A_0J_1}{\eta^2}\right)\boldsymbol{Z}_1$$
$$+\Omega^2\frac{1}{\eta^2}\Bigg[\left(\frac{4B_2J_1}{5}+\frac{9A_2J_1}{5\eta^2}\right)\boldsymbol{Z}_1$$
$$+\left(\frac{6B_2J_1}{5}-J_3M_0-J_1M_2+\frac{A_2J_1}{5\eta^2}-\frac{3A_0J_3}{\eta^2}\right)\boldsymbol{Z}_3\Bigg]\Bigg\}+\mathcal{O}(\lambda^3,\Omega^4). \tag{3.17}$$

2.2. *Matching*

The last step to build our global spacetime $\mathcal{M}$ is the matching of $(\mathcal{V}^-,\boldsymbol{g}^-)$ and $(\mathcal{V}^+,\boldsymbol{g}^+)$. The general problem involves finding a hypersurface Σ with its embeddings into $\mathcal{V}^-$ and $\mathcal{V}^+$

$$\Sigma^- = \chi_-(\Sigma) \qquad \text{and} \qquad \Sigma^+ = \chi_+(\Sigma) \tag{3.18}$$

along which the identification of the two spacetimes to form a manifold $\mathcal{M}$ that has Lorentzian geometry and on which the Einstein's equations are well defined (a wider summary can be found in Fayos *et al.*, 1996). Several sets of matching or junction conditions have been used in the literature. Bonnor and Vickers (1981) showed that among them, the more general ones are due to Darmois (1927)—see also Israel (1966)—. They read as follows. Denoting with $\chi_\pm^*$ the pull-backs of $\chi_\pm$ and with $\chi_{\pm *}$ their push-forwards, let

$$\boldsymbol{q}^\pm = \chi_\pm^*\boldsymbol{g}^\pm \tag{3.19}$$

be the first fundamental forms of $\Sigma^\pm$ and $\kappa^\pm_{ab}$ $(a,b=0,\dots,\dim\mathcal{V}^\pm-1)$

$$\kappa^\pm_{ab} = -n^\pm_\mu e^{\pm\nu}_a\nabla^\pm_\nu e^{\pm\mu}_b \tag{3.20}$$

its second fundamental forms, with $\boldsymbol{e}_a$ the basis of the tangent space of Σ, $e^{\pm\mu}_a$ the components of

$$\chi_{\pm *}(\boldsymbol{e}_a) = \frac{\partial\chi^\mu_\pm}{\partial\zeta^a}\frac{\partial}{\partial x^\mu_\pm} \equiv \boldsymbol{e}^\pm_a, \tag{3.21}$$

where ζ^a and $x^\alpha_\pm$ are coordinates on Σ and $\mathcal{V}^\pm$ respectively. The unit vectors $n^\pm_\alpha$ are normal to $\boldsymbol{e}^\pm_a$ and have a suitable orientation. Then two spacetimes are *matchable* when the Darmois-Israel conditions

$$\begin{aligned} q^+_{ab} &= q^-_{ab}, \\ \kappa^+_{ab} &= \kappa^-_{ab}, \end{aligned} \tag{3.22}$$

are satisfied for a certain Σ. In particular, these imply that for every point of Σ there is a local set of coordinates in which the metric and its first derivatives are continuous

$$\begin{aligned} g^{+}_{\alpha\beta}\Big|_{\Sigma^+} &= g^{-}_{\alpha\beta}\Big|_{\Sigma^-}, \\ \partial_\gamma g^{+}_{\alpha\beta}\Big|_{\Sigma^+} &= \partial_\gamma g^{-}_{\alpha\beta}\Big|_{\Sigma^-}. \end{aligned} \tag{3.23}$$

These are known as *Lichnerowicz matching conditions* (Lichnerowicz, 1955); they are verified on a local set of *admissible coordinates* when the spacetimes are matchable.

Darmois-Israel and Lichnerowicz matching conditions are equivalent in the sense that the latter are the practical realization of the former in a certain set of coordinates. Nevertheless, when two *families* of spacetimes are to be matched using Lichnerowicz matching, these equations give the conditions for the families to be matched in the particular set of coordinates used, i.e., the family members for which the coordinates used are admissible. Then, if some members of the exterior and interior families are matchable in a different set of coordinates, they would not be present in the final matched spacetime. In this sense, when dealing with spacetime families Lichnerowicz matching conditions are more restrictive than the Darmois-Israel ones.

Here, we are going to match the most general exterior and interior solutions for our problem. This generality is expressed in the practice through all the free constants in both metrics. We are then matching spacetime families and therefore, although our primary goal is to find the fully matched spacetime, we will first analyse the result of the Darmois-Israel conditions to ensure that we find all the possible global solutions.

Matching surface

Now, we are going to match the exterior and interior solutions given in the previous sections keeping all the free constants they have. First, let us start discussing how to choose the matching surface. In a general matching of spacetimes the surface, along with its embeddings, is actually part of the solution and can not be given beforehand without risk of losing generality (see Mars *et al.* (2007) and Mars and Senovilla (1998) for a discussion of this topic). In our case and in stellar model building, Σ^- is uniquely characterized in $\mathcal{V}^-$ as the locus of points where $p = 0$ and it is the only relevant matching surface. The zero pressure surface $r = r_\Sigma(\theta)$ of our interior metric is defined implicitly by the equation $\psi(r, \theta) = \psi_\Sigma$ (see [3.3]). Therefore, we may write

$$\Sigma^- = \{t = \tau,\, \phi = \varphi,\, r = r_\Sigma(\vartheta),\, \theta = \vartheta)\}. \tag{3.24}$$

where $\{\tau, \varphi, \vartheta\}$ are coordinates of Σ.

To simplify the resolution of the matching, we are interested in using a common expression for Σ^+ and Σ^- in terms of the interior an exterior coordinates, that is to say

$$\Sigma^+ = \{T = \tau, \Phi = \varphi, R_\Sigma = r_\Sigma(\vartheta), \Theta_\Sigma = \vartheta)\}, \tag{3.25}$$

$\{T, \Phi, R, \Theta\}$ being coordinates in $\mathcal{V}^+$. This assumption implies no loss of generality if we prove that the coordinates that verify the above equations for Σ^- and Σ^+ belong to the class of coordinates we use to write the metrics. Then we can go along with the matching using the expressions for the interior and exterior metrics we got in the previous sections.

Let us set up the problem. The following expression for Σ^+,

$$\Sigma^+ = \{T = \tau, \Phi = \varphi, R = R(\vartheta), \Theta = \Theta(\vartheta)\}. \tag{3.26}$$

is well suited to the symmetries of the exterior field and how they have been implemented in the metric (3.17). Coordinates T and Φ are adapted to the Killing fields, and they have been chosen to ensure that the metric tends to the flat metric in standard spherical coordinates at infinity. They are unique up to an additive constant we can set equal to zero. On the other hand, coordinates R and Θ are not completely set. Any pair of functions $F(R, \Theta)$ and $H(R, \Theta)$ leading to a set of Cartesian-like harmonic coordinates

$$X' = F(R, \Theta) \cos \Phi, \tag{3.27}$$

$$Y' = F(R, \Theta) \sin \Phi, \tag{3.28}$$

$$Z = H(R, \Theta), \tag{3.29}$$

defines implicitly a couple of new coordinates by means of these two equations

$$R' \cos \Theta' = F(R, \Theta), \tag{3.30}$$

$$R' \cos \Theta' = H(R, \Theta). \tag{3.31}$$

Nevertheless, we must impose some conditions on the two functions in order to preserve the good behaviour of the coordinates at infinity, namely

$$F(R, \Theta) \to R \sin \Theta\,, \quad H(R, \Theta) \to R \cos \Theta\,. \qquad (R \to \infty) \tag{3.32}$$

This freedom is actually included in our metric (3.17) by means of the constants A_0, A_2 and B_2.

The harmonic condition requires F (and H) to be a solution of a second order elliptic equation. If we add to the boundary condition at infinity mentioned above this other one on Σ^+,

$$F\left((R_\Sigma(\vartheta), \Theta_\Sigma(\vartheta)\right) = r_\Sigma(\vartheta) \sin \vartheta\,, \quad H\left(R_\Sigma(\vartheta), \Theta_\Sigma(\vartheta)\right) = r_\Sigma(\vartheta) \cos \vartheta\,, \tag{3.33}$$

we get a Dirichlet problem. We assume by now that it admits a solution. We will later show that this is indeed the case, at least up to the order considered, since we are able to find a solution of the Lichnerowicz matching in these coordinates. The equation of the surface Σ^+ in the new coordinates (we drop out the primes) can then take the form we want, eq. (3.25).

There is another problem which should be mentioned here, even though it has no consequences on the equation for the matching surface itself. It has been pointed out that coordinates T and Φ can not be naively identified with t and ϕ on the matching surface as we have done in the precedent paragraph (Mars and Senovilla, 1998). Anyhow it can be done by making a suitable linear change $t = at'$ and $\phi = \phi' + abt'$ preserving the regularity of the symmetry axis.

In order to make such a change compatible with the approximate interior metric (eq. [3.14]), we have to assume an expansion of these two constants in powers of λ as follows

$$a = 1 + \mathcal{O}(\lambda), \tag{3.34}$$

$$b = \mathcal{O}(\lambda^{1/2}). \tag{3.35}$$

The first one and the lack of a $\mathcal{O}(\lambda^0)$ term in b just take into account that the starting point of our approximation is the flat metric; the reason behind the semi-integer expansion of b is that under this change the angular velocity of the fluid reads $\omega - b$, and within the CMMR scheme this quantity must be of order $\mathcal{O}(\lambda^{1/2})$. These infinitesimal expansions actually do not keep the structure of the interior metric because $g^-_{t'\phi'}$ contains a $\mathcal{O}(\lambda^{1/2})$ term proportional to b which is absent in $g^-_{t\phi}$ (that starts at $\mathcal{O}(\lambda^{3/2})$). It does not matter. The matching sets it equal to zero because the component $g^+_{T\Phi}$ can not have a $\mathcal{O}(\lambda^{1/2})$ term unless it violates the asymptotic conditions on the coordinates. Moreover, the rest of the contribution of a and b to the metric in the new coordinates can be absorbed into the free constants m_0, a_0 and j_1.

We actually think that the choice of t and ϕ discussed above has already been considered in the CMMR scheme from the very beginning. Dropping out a $\mathcal{O}(\lambda^{1/2})$ in $g^-_{t\phi}$ at the linear level of the approximation is a way of choosing the inner coordinates t and ϕ, and also the angular velocity ω in a sense, since we assumed $g^+_{T\Phi}$ to be proportional to ω in eq. (2.58).

These kind of assumptions are meaningful in a perturbation scheme but they cannot be easily implemented in an exact matching problem. The continuity of the Killing fields on the surface matching used in Mars and Senovilla (1998) is a smart reasonable assumption to make an exhaustive use of the symmetries of the problem. The arguments sketched above show how this point of view has not

been forgotten in our scheme. Therefore, we can argue that our approach is in accordance with it.

Lastly, let us simplify a little more the matching process by introducing an ansatz for the explicit equation of the surface. Being this an axisymmetric problem, the zero pressure surface can be expanded as a power series in Legendre polynomials, and the reflection symmetry allows us to rule out every odd degree term in the expansion. Coherently with the assignment of dependence on Ω we made for the approximate solutions of the homogeneous linear Einstein equations, we have then

$$r_\Sigma(\theta) = r_s \left\{1 + \Omega^2 \left[\varsigma_0 + \varsigma_2 P_2(\cos\theta)\right]\right\} + \mathcal{O}(\Omega^4) \tag{3.36}$$

where $\varsigma_{0,2}$ are constants expandable in (λ, Ω) to be determined while matching. This, which is the original ansatz in CMMR, is also coherent with the kind of expression we need for r to solve the implicit equation $\psi(r, \theta) = \psi_\Sigma$ of the surface.

Darmois matching

First we impose Darmois-Israel conditions on the surface (3.36) to match $\{\mathcal{V}^-, g^-\}$ and $\{\mathcal{V}^+, g^+\}$ up to $\mathcal{O}(\lambda^{5/2}, \Omega^3)$ in the metrics. They are satisfied when the constants associated to the multipole moments are

$$M_0 = 1 + \lambda\left[\frac{3a_0}{2} + \frac{n}{5} + \frac{14}{5} + \frac{2}{15}\Omega^2(4-n)\right] + \mathcal{O}(\lambda^2, \Omega^4), \tag{3.37}$$

$$M_2 = -\frac{1}{2} + \lambda\left(-\frac{5a_0}{4} + \frac{n}{14} - \frac{37}{35}\right) + \mathcal{O}(\lambda^2, \Omega^2), \tag{3.38}$$

$$J_1 = \frac{2}{5} + \frac{\Omega^2}{3} + \lambda\left[a_0 + \frac{2n}{35} + \frac{16}{7} + \Omega^2\left(\frac{5a_0}{6} - \frac{3n}{35} + \frac{176}{105}\right)\right] + \mathcal{O}(\lambda^2, \Omega^4), \tag{3.39}$$

$$J_3 = -\frac{1}{7} + \lambda\left(-\frac{a_0}{2} + \frac{11n}{441} - \frac{496}{735}\right) + \mathcal{O}(\lambda^2, \Omega^2), \tag{3.40}$$

while their interior counterparts take the values

$$m_0 = 3 + \lambda\left[3a_0 + \frac{3n}{4} + \frac{9}{2} + \Omega^2\left(1 - \frac{n}{2}\right)\right] + \mathcal{O}(\lambda^2, \Omega^4), \tag{3.41}$$

$$m_2 = -1 + \lambda\left(-a_0 + 2b_2 - \frac{3n}{14} - \frac{29}{35}\right) + \mathcal{O}(\lambda^2, \Omega^2), \tag{3.42}$$

$$j_1 = 2 + \frac{2\Omega^2}{3} + \lambda\left[4a_0 + \frac{n}{2} + \frac{49}{5} + \Omega^2\left(\frac{4a_0}{3} + 2b_2 - \frac{5n}{14} + \frac{289}{105}\right)\right] + \mathcal{O}(\lambda^2, \Omega^4), \tag{3.43}$$

$$j_3 = -\frac{2}{7} + \lambda\left(-\frac{4a_0}{7} + 2a_2 + \frac{12b_2}{25} - \frac{3n}{49} - \frac{326}{245}\right) + \mathcal{O}(\lambda^2, \Omega^2) \tag{3.44}$$

and finally, the exterior gauge constants are

$$A_0 = a_0 + \lambda\left(\frac{3a_0^2}{4} - 3a_0 - \frac{237}{35} - \frac{22\Omega^2}{35}\right) + \mathcal{O}(\lambda^2, \Omega^4), \tag{3.45}$$

$$A_2 = -\frac{a_0}{2} + a_2 + \lambda\left(\frac{a_0 n}{7} - \frac{7a_0^2}{8} + a_2 a_0 + \frac{139a_0}{70} - 3a_2 + \frac{383}{90}\right) + \mathcal{O}(\lambda^2, \Omega^2), \tag{3.46}$$

$$B_2 = \frac{a_0}{2} + b_2 + \lambda\left(-\frac{a_0 n}{7} + \frac{3a_0^2}{8} - \frac{25a_0}{14} - 3b_2 - \frac{7}{2}\right) + \mathcal{O}(\lambda^2, \Omega^2)\,. \tag{3.47}$$

The matching surface on which the matching conditions hold is

$$\eta_\Sigma = 1 + P_2(\cos\theta)\Omega^2\left[-\frac{5}{6} + \lambda\left(-\frac{3a_2}{2} + b_2 + \frac{5n}{21} + \frac{10}{21}\right)\right] + \mathcal{O}(\lambda^2, \Omega^4). \tag{3.48}$$

These results require some comments. Here, the only free parameters are a_0, a_2 and b_2, (which, as already mentioned, parametrize changes of harmonic coordinates in $\mathcal{V}^-$), r_s (which depends on the size of the source *but also on the coordinates*), ϵ_0, ω (which are part of the definitions of λ and Ω) and the EOS parameter n. Then, for a fixed set of source parameters

$$s := \{n, \epsilon_0, \omega\} \tag{3.49}$$

and r_s,[2] the interior metric that can be matched is unique up to changes of coordinates. Since the asymptotically flat exterior of a certain source spacetime in rotation is unique (Mars and Senovilla, 1998) then, given a set of source parameters s and r_s, there is only one possible global spacetime, i.e., only a couple of metrics $\left(\hat{g}^-, \hat{g}^+\right)$ among the families g^- and g^+ give spacetimes that can be matched. Nevertheless, this could seem contradictory with the apparent fact that the value of mass and angular multipole moments depend on the value of a_0 as eqs. (3.37) to (3.40). This apparent dependence happens because these constants are not the only gauge dependent quantities in the expressions. There is coordinate dependence hidden in λ, which, unlike Ω, depends on r_s.

This problem can be solved finding their expression in terms of physical variables because they are gauge invariant. A convenient way of doing it is using the

[2] Note that r_s has been excluded from s because of its coordinate dependence. It contains information necessary to fully characterise the source, though.

mass monopole moment $\tilde{M}_0$ to redefine λ. In CMMR, λ is defined as $\lambda := \frac{4\pi}{3}\epsilon_0 r_s^2$ so that

$$\tilde{M}_0 = -\lim_{r\to\infty} \frac{1}{2} g^{+}_{tt,r} r^2 = \lambda r_s M_0 \tag{3.50}$$

and $M_0 = 1 + \mathcal{O}(\lambda)$ reflecting the fact that λ and r_s were chosen to reproduce the Newtonian mass of the source. Now, if we define $\{\lambda', r_s'\}$ to give the general relativistic mass monopole moment $\tilde{M}_0$ and keep the same relation between them, i.e. ,

$$\lambda' := \frac{4\pi}{3}\epsilon_0 r_s'^2, \tag{3.51}$$

$$\lambda' r_s' := \tilde{M}_0, \tag{3.52}$$

inserting eq. (3.51) into eq. (3.52) and using the expression of M_0 (3.37) to find $\tilde{M}_0 = \lambda r_s M_0$, we obtain that

$$\lambda' = \lambda\left(1 + \lambda\left\{a_0 + \frac{2}{3}\left[\frac{n}{5} + \frac{14}{5} + \frac{2}{15}\Omega^2(4-n)\right]\right\}\right) + \mathcal{O}(\lambda^3, \Omega^4), \tag{3.53}$$

$$r_s' = r_s\left(1 + \lambda\left\{\frac{a_0}{2} + \frac{1}{3}\left[\frac{n}{5} + \frac{14}{5} + \frac{2}{15}\Omega^2(4-n)\right]\right\}\right) + \mathcal{O}(\lambda^2, \Omega^4). \tag{3.54}$$

Using these changes,

$$M_0 = 1 + \mathcal{O}(\lambda'^2) \tag{3.55}$$

as required and the dependence on the gauge constant a_0 of the multipole moments $\tilde{M}_2$, $\tilde{J}_1$ and $\tilde{J}_3$ disappears. In this way, the set of parameters to completely specify the interior would become ϵ_0, n, ω and $\tilde{M}_0$.

This procedure can be followed as well using the central pressure p_c instead of $\tilde{M}_0$ to characterise the interior as is sometimes done in astrophysics.

From the $\mathcal{O}(\lambda^2)$ metric we can obtain the pressure up to the next order

$$\begin{aligned}
\frac{p}{8\pi} r_s^2 = {} & \lambda^2\left\{3 - 3\eta^2 + \Omega^2\left[-2 + 2\eta^2 + \eta^2\left(-2 + 3m_2\right)P_2\right]\right\} \\
& + \lambda^3\left(\frac{6}{5} + \frac{9n}{5} + 3a_0 + 3m_0 + \eta^2\left(-3 - 3n - 3a_0 - 3m_0\right) + \left(\frac{9}{5} + \frac{6n}{5}\right)\eta^4\right. \\
& + \Omega^2\left\{-1 - \frac{17n}{10} - 2a_0 + 4j_1 - 4m_0 + \eta^2\left(2 + 3n + 2a_0 - 4j_1 + 4m_0\right)\right. \\
& + \left(-1 - \frac{13n}{10}\right)\eta^4 + \left[\eta^2\left(-n - 2a_0 + 4j_1 - 4m_0 + \frac{3nm_2}{2} + 3m_0 m_2\right)\right. \\
& \left.\left.\left. + \eta^4\left(\frac{62}{35} + \frac{10n}{7} - 9a_2 - \frac{18m_2}{7} - \frac{15nm_2}{7}\right)\right]P_2\right\}\right) + \mathcal{O}(\lambda^4, \Omega^4)
\end{aligned} \tag{3.56}$$

and its value at $r = 0$, p_c

$$\frac{p_c}{8\pi} r_s^2 = \lambda^2 \left(3 - 2\Omega^2\right) + \lambda^3 \left[\frac{6}{5} + \frac{9n}{5} + 3a_0 + 3m_0 + \Omega^2 \left(-1 - \frac{17n}{10} - 2a_0 + 4j_1 - 4m_0\right)\right] + \mathcal{O}(\lambda^4, \Omega^4). \quad (3.57)$$

Using the Darmois-Israel matching results it is reduced to the form

$$\frac{p_c}{8\pi} r_s^2 = \lambda^2 \left(3 - 2\Omega^2\right) + \lambda^3 \left[\frac{51}{5} + \frac{9n}{5} + 3a_0 + \Omega^2 \left(-5 - \frac{17n}{10} - 2a_0\right)\right] + \mathcal{O}(\lambda^4, \Omega^4) \quad (3.58)$$

and now, using the definition of λ, can be rewritten as

$$p_c \left(\frac{4\Omega^2}{3\epsilon_0} + \frac{2}{\epsilon_0}\right) = \lambda + \lambda^2 \left[a_0 + \frac{3n}{5} + \frac{17}{5} + \Omega^2 \left(\frac{3}{5} - \frac{n}{6}\right)\right] + \mathcal{O}(\lambda^3, \Omega^4). \quad (3.59)$$

Next, defining the coordinate independent parameter

$$\Lambda := p_c \frac{2}{\epsilon_0} \left(1 + \frac{2}{3}\Omega^2\right) + \mathcal{O}(\Omega^4). \quad (3.60)$$

eq. (3.59) leads to

$$\Lambda = \lambda \left\{1 + \lambda \left[a_0 + \frac{3n}{5} + \frac{17}{5} + \Omega^2 \left(\frac{3}{5} - \frac{n}{6}\right)\right]\right\} + \mathcal{O}(\lambda^3, \Omega^4), \quad (3.61)$$

Keeping a relation of the form of eq. (3.51), the associated radial coordinate changes as

$$r_\Lambda = r_0 \left\{1 + \lambda \left[\frac{a_0}{2} + \frac{3n}{10} + \frac{17}{10} + \Omega^2 \left(\frac{3}{10} - \frac{n}{12}\right)\right]\right\} + \mathcal{O}(\lambda^2, \Omega^4). \quad (3.62)$$

Again, as one expects, with these changes the expressions for the multipole moments become manifestly coordinate independent.

Thus, with these last results, the exterior (3.17) and the interior (3.14) with their constants taking the values in eqs. (3.37) to (3.47) give the most general approximate family of global asymptotically flat solutions for the kind of source studied. Each of its members characterized only by the values of $\{n, \epsilon_0, \omega\}$ and r_0' or r_Λ that, with the first three fixed, depend only on $\tilde{M}_0$ and p_c, respectively. Additionally, they also point out the behaviour one intuitively expects as a generalization of the theorem by Rendall and Schmidt (1991), i.e., that for a stationary axisymmetric singularity free compact rotating perfect fluid, its asymptotically flat exterior is unique once the EOS, central pressure and rotation speed are fixed.

Lichnerowicz matching

Now we impose Lichnerowicz conditions. The $\mathcal{O}(\lambda^{5/2}, \Omega^3)$ metric is then matched in the global set of coordinates when its multipole moments and $\{m_l, j_l\}$ constants take the values

$$M_0 = 1 + \lambda\left[\frac{n}{5} + \frac{14}{5} + \Omega^2\left(\frac{8}{15} - \frac{2n}{15}\right)\right] + \mathcal{O}(\lambda^2, \Omega^4), \tag{3.63}$$

$$M_2 = -\frac{1}{2} + \lambda\left(\frac{n}{14} - \frac{37}{35}\right) + \mathcal{O}(\lambda^2, \Omega^2), \tag{3.64}$$

$$J_1 = \frac{2}{5} + \frac{\Omega^2}{3} + \lambda\left[\frac{2n}{35} + \frac{16}{7} + \Omega^2\left(\frac{176}{105} - \frac{3n}{35}\right)\right] + \mathcal{O}(\lambda^2, \Omega^4), \tag{3.65}$$

$$J_3 = -\frac{1}{7} + \lambda\left(\frac{11n}{441} - \frac{496}{735}\right) + \mathcal{O}(\lambda^2, \Omega^2), \tag{3.66}$$

$$m_0 = 3 + \lambda\left[\frac{3n}{4} + \frac{9}{2} + \Omega^2\left(1 - \frac{n}{2}\right)\right] + \mathcal{O}(\lambda^2, \Omega^4), \tag{3.67}$$

$$m_2 = -1 + \lambda\left(-\frac{3n}{14} - \frac{29}{35}\right) + \mathcal{O}(\lambda^2, \Omega^2), \tag{3.68}$$

$$j_1 = 2 + \frac{2\Omega^2}{3} + \lambda\left[\frac{n}{2} + \frac{49}{5} + \Omega^2\left(\frac{289}{105} - \frac{5n}{14}\right)\right] + \mathcal{O}(\lambda^2, \Omega^4), \tag{3.69}$$

$$j_3 = -\frac{2}{7} + \lambda\left(-\frac{3n}{49} - \frac{326}{245}\right) + \mathcal{O}(\lambda^2, \Omega^2), \tag{3.70}$$

and the coordinate-parametrizing constants are

$$\begin{aligned} A_0 &= \frac{4\lambda}{35}\left(2 + \frac{\Omega^2}{3}\right) + \mathcal{O}(\lambda^2, \Omega^4), & a_0 &= \lambda\left(7 + \frac{2\Omega^2}{3}\right) + \mathcal{O}(\lambda^2, \Omega^4), \\ A_2 &= -\frac{4\lambda}{63} + \mathcal{O}(\lambda^2, \Omega^2), & a_2 &= -\frac{86\lambda}{105} + \mathcal{O}(\lambda^2, \Omega^2), \\ B_2 &= \mathcal{O}(\lambda^2, \Omega^2), & b_2 &= \mathcal{O}(\lambda^2, \Omega^2). \end{aligned} \tag{3.71}$$

The value of these parameters is unique for each set of parameters $\{n, \epsilon_0, \omega, r_s\}$ and verify the relations obtained with Darmois-Israel conditions as is to be expected. Nevertheless, it proves the existence of a harmonic and asymptotically Cartesian global system of coordinates up to the approximation order considered.

In spite of the attention drew to Darmois-Israel matching before, it is important to remark that the real focus of the approximation scheme is the obtention of totally matched spacetimes in the sense that even the gauge constants are fully fixed and the Lichnerowicz admissible coordinates are found. In fact, only Lichnerowicz conditions were used in Cabezas *et al.* (2007) and Martín *et al.* (2008)

although the generality of the results in them can be verified with the same techniques used here. Besides, one needs the fully matched spacetime for many practical purposes, as for example to compare with numerical results for stellar models built using global coordinates, as we will see in Chapter 5

3. Petrov classification

We will now analyse the possible Petrov types of the unmatched interior metric. They are given by the possible Jordan canonical forms of the $Q^{\alpha}{}_{\beta}$ matrix—which is symmetric and tracefree in an orthonormal cobasis—defined from the Weyl tensor $C^{\alpha}_{\beta\gamma\delta}$ as

$$Q^{\alpha}{}_{\beta} := \left(C^{\alpha}{}_{\lambda\beta\mu} + \mathrm{i}{}^{\star}C^{\alpha}{}_{\lambda\beta\mu}\right) v^{\lambda}v^{\mu} := \overset{+}{C}{}_{\lambda\mu}v^{\lambda}v^{\mu}, \tag{3.72}$$

where $\star$ denotes the left Hodge dual and v^{α} is a unit timelike vector. We use $u^{i} = 0$ for simplicity. A full reminder of the Petrov classification in the form we use here appears in Appendix D.

This $Q_{\alpha\beta}$ matrix can be directly calculated from $\overset{+}{\boldsymbol{C}}$ using the timelike unit vector $v = (1/\sqrt{-g_{tt}})\partial_t$ since the contraction $\overset{+}{C}{}_{\alpha\beta\gamma\delta}v^{\beta}v^{\delta}$ picks out the fourth 3×3 element of $\overset{+}{C}{}_{AB}$ as can be seen from the definition of the 2-form cobasis (D.15) and then we have

$$\overset{+}{C}{}_{\alpha\beta\gamma\delta}u^{\beta}u^{\delta} = \frac{-1}{g_{tt}}\begin{pmatrix} 0 & \mathbf{0} \\ \mathbf{0} & -\boldsymbol{Q} \end{pmatrix} \equiv \frac{1}{g_{tt}}Q_{\alpha\gamma} \tag{3.73}$$

where $Q_{\alpha\gamma}$ contains the components of the $\boldsymbol{Q}$ matrix expressed in the coordinate cobasis. Thus, we have to solve the eigenvalue problem

$$Q_{\alpha\beta}V^{\beta} = \varepsilon V_{\alpha} = \varepsilon g_{\alpha\beta}V^{\beta} \tag{3.74}$$

or equivalently

$$\left(Q_{\alpha\beta} - \varepsilon g_{\alpha\beta}\right)V^{\beta} = \left(Q^{\alpha}{}_{\beta} - \varepsilon\delta^{\alpha}_{\beta}\right)V^{\beta} = 0. \tag{3.75}$$

When studying Petrov types one generally chooses an orthonormal cobasis at a point what makes the components and structure of $Q_{\alpha\beta}$ and $Q^{\alpha}{}_{\beta}$ be the same

$$Q^{\alpha}{}_{\beta} = \begin{pmatrix} 0 & \mathbf{0} \\ \mathbf{0} & Q^{i}{}_{j} \end{pmatrix}. \tag{3.76}$$

If one does not use an orthonormal cobasis this is not true in general. In the particular case of a metric with Papapetrou's structure, we can compute $\boldsymbol{Q}$ and see

$$Q_{\alpha\beta} = \begin{pmatrix} 0 & 0 & 0 & 0 \\ 0 & Q_{rr} & Q_{r\theta} & 0 \\ 0 & Q_{\theta r} & Q_{\theta\theta} & 0 \\ 0 & 0 & 0 & Q_{\phi\phi} \end{pmatrix} \longrightarrow Q^{\alpha}{}_{\beta} = \begin{pmatrix} 0 & 0 & 0 & Q^{t}{}_{\phi} \\ 0 & Q^{r}{}_{r} & Q^{r}{}_{\theta} & 0 \\ 0 & Q^{\theta}{}_{r} & Q^{\theta}{}_{\theta} & 0 \\ 0 & 0 & 0 & Q^{\phi}{}_{\phi} \end{pmatrix}. \tag{3.77}$$

The only possible Jordan canonical forms of $Q^{\alpha}{}_{\beta}$ at each point must still be those of a 3×3 matrix though, completely irrespective of the kind of coordinates we use. This can be made apparent in this case considering the following. First, we rearrange components of $Q^{\alpha}{}_{\beta}$ so that

$$Q^{\alpha}{}_{\beta} = \begin{pmatrix} 0 & Q^{t}{}_{\phi} & 0 & 0 \\ 0 & Q^{\phi}{}_{\phi} & 0 & 0 \\ 0 & 0 & Q^{r}{}_{r} & Q^{r}{}_{\theta} \\ 0 & 0 & Q^{\theta}{}_{r} & Q^{\theta}{}_{\theta} \end{pmatrix} \tag{3.78}$$

and it is clear that the eigenvectors of the $\{r, \theta\}$ subspace are orthogonal to those of the $\{t, \phi\}$ subspace so we can analyse these subspaces separately. Considering the $\{t, \phi\}$ box, it can only be similar to the Jordan canonical forms

$$\text{if } Q^{\phi}{}_{\phi} = 0 : \begin{cases} \begin{pmatrix} 0 & 1 \\ 0 & 0 \end{pmatrix} & \text{when } Q^{t}{}_{\phi} \neq 0 \\ \begin{pmatrix} 0 & 0 \\ 0 & 0 \end{pmatrix} & \text{when } Q^{t}{}_{\phi} = 0 \end{cases} \tag{3.79}$$

$$\text{if } Q^{\phi}{}_{\phi} \neq 0 : \quad \begin{pmatrix} 0 & 0 \\ 0 & Q^{\phi}{}_{\phi} \end{pmatrix}. \tag{3.80}$$

Since the inverse of a metric with Papapetrou's structure has also Papapetrou's structure, the components of $Q^{\alpha}{}_{\beta} = g^{\alpha\lambda} Q_{\alpha\beta}$ are

$$Q^{t}{}_{\phi} = g^{\alpha t} Q_{\alpha\phi} = g^{tt} Q_{t\phi} + g^{\phi t} Q_{\phi\phi} = g^{\phi t} Q_{\phi\phi}, \tag{3.81}$$

$$Q^{\phi}{}_{\phi} = g^{\alpha\phi} Q_{\alpha\phi} = g^{t\phi} Q_{t\phi} + g^{\phi\phi} Q_{\phi\phi} = g^{\phi\phi} Q_{\phi\phi}\,, \tag{3.82}$$

i.e., for an axi-stationary metric $Q^{t}{}_{\phi} = 0$ only when $Q^{\phi}{}_{\phi} = 0$. Hence the only possible Jordan form of the $\{t, \phi\}$ subspace is

$$\begin{pmatrix} 0 & 0 \\ 0 & Q^{\phi}{}_{\phi} \end{pmatrix} \quad \text{for any value of } Q^{\phi}{}_{\phi} \tag{3.83}$$

and then, the classification of eq. (3.78) is equivalent to the one of

$$Q^i{}_j = \begin{pmatrix} Q^r{}_r & Q^r{}_\theta & 0 \\ Q^\theta{}_r & Q^\theta{}_\theta & 0 \\ 0 & 0 & Q^\phi{}_\phi \end{pmatrix}, \tag{3.84}$$

that keeps the greatly simplifying property of possessing two orthogonal blocks, so that we can write all its possible Jordan canonical forms as

$$\boldsymbol{J}_Q = \begin{pmatrix} \varepsilon_1 & a & 0 \\ 0 & \varepsilon_2 & 0 \\ 0 & 0 & \varepsilon_3 \end{pmatrix}, \tag{3.85}$$

with $a = 0$ or 1, the latter being a possibility only if $\varepsilon_1 = \varepsilon_2$.

The eigenvalues ε_1 and ε_2 of the r-θ subspace are degenerate iff the discriminant of the roots of its characteristic equation is zero, ,

$$\left(Q^r{}_r - Q^\theta{}_\theta\right)^2 + 4Q^r{}_\theta Q^\theta{}_r = 0 \tag{3.86}$$

which using the traceless property gives

$$Q^r{}_r Q^\theta{}_\theta - Q^r{}_\theta Q^\theta{}_r - \frac{1}{4}\left(Q^\phi{}_\phi\right)^2 = 0. \tag{3.87}$$

The condition for either ε_1 or ε_2 to be degenerate with $\varepsilon_3 = Q^\phi{}_\phi$ is

$$Q^r{}_r Q^\theta{}_\theta - Q^r{}_\theta Q^\theta{}_r + 2(Q^\phi{}_\phi)^2 = 0\,, \tag{3.88}$$

that has the same expression as eq. (3.87) switching the numerical factor. The structure of $Q^i{}_j$, see (3.84), allows the following possibilities.

1. First, no degeneracy at all. This is the general case and corresponds to Petrov type I, whose Segrè symbol is {111}.[3]

2. The second, degeneracy in only two eigenvalues. It can come from eq. (3.87), in which case it can lead to types D –Segrè symbol {(11)1}– and II –{21}–, or from eq. (3.88) that can only give rise to type D because from the structure of (3.85) we see that the degenerate eigenvalues would then belong to orthogonal subspaces.

[3] In a Segrè symbol, each number gives the dimension of one of the invariant subspaces. Numbers associated to subspaces with degenerate eigenvalues are written inside parenthesis.

3. Last, three degenerate eigenvalues, what happens if both eq. (3.87) and (3.88) are fulfilled. This can lead only to types N –{(21)}– and O –{(111)}– since type III –{3}– is directly excluded again by the form of (3.85).

We get the following conditions on the metric parameters (in which the trivial case $\lambda = 0$ is not considered) extracting from (3.87) and (3.88) the relevant information up to this order of approximation.

We will first analyse the general rotating case separately from the static case for clarity. The relevant condition eq. (3.86) for $\varepsilon_1 = \varepsilon_2$, even considering only its terms up to $\mathcal{O}(\lambda^3, \Omega^3)$

$$-\mathrm{i}\lambda^{5/2}\Omega^3\frac{54r}{5r_s^5}m_2P_1(\cos\theta) + \lambda^3\Omega^2\frac{3r^2}{25r_s^6}\times \\ \times\{5m_2(n-1)\left[4P_2(\cos\theta)-1\right]-108\} + \mathcal{O}(\lambda^{7/2},\Omega^4) = 0 \quad (3.89)$$

can not be satisfied everywhere unless $\Omega = 0$ and therefore we can not have $\varepsilon_1 = \varepsilon_2$ degeneracy out of the static case. The conditions for the other possible degeneracies $\varepsilon_1 = \varepsilon_3$ or $\varepsilon_2 = \varepsilon_3$ are given by eq. (3.88), that yields

$$-\lambda^3\Omega^2\frac{3r^2}{25r_s^6}\left[P_2(\cos\theta)-1\right]\left[5m_2(n-1)+18\right] + \mathrm{i}\lambda^{7/2}\Omega^3\frac{18r^3}{175r_s^7}\times \\ \times\left[P_1(\cos\theta)-P_3(\cos\theta)\right]\left[2\left(35j_3+3\right)(n-1)+m_2(23-14n)\right] \\ +\mathcal{O}(\lambda^4,\Omega^4) = 0. \quad (3.90)$$

They are satisfied in the static case and, if $\Omega \neq 0$, when the constants of the metric verify

$$m_2 = \frac{18}{5(1-n)} \quad \text{and} \quad j_3 = \frac{3(n+8)(8-5n)}{175(n-1)^2}, \quad (3.91)$$

which can never be satisfied in the constant energy density case.

Concerning the static case, equation (3.86) gives conditions different from eq. (3.89). They are satisfied only when $n = 1$, while the other degeneracy possibility condition (3.88) is always verified. This can be seen straightaway from the form the $Q^i{}_j$ matrix takes

$$Q^i{}_j = \frac{1}{5}\frac{\eta^2}{r_s^2}\lambda^2\begin{pmatrix}2(n-1) & 0 & 0\\ 0 & 1-n & 0\\ 0 & 0 & 1-n\end{pmatrix} + \mathcal{O}(\lambda^3) \quad (3.92)$$

as well as the fact that the only possible Petrov types are D ($n \neq 1$) and O ($n = 1$) as must be the case for a spherically symmetric spacetime (Stephani *et al.*, 2003,

p. 228). The condition on n for type O is expectable since any conformally flat perfect fluid solution with our symmetries must be Schwarzschild's interior solution (Collinson, 1976). From the equations (3.86) and (3.88) alone one can not say whether this behaviour will endure further approximations because extra conditions could impose a more general Petrov type, but these theorems on spherical symmetry and constant energy density give a strong hint about its endurance.

Therefore, collecting the results together from the rotating and static cases, we conclude that

- An invariant subspace of dimension 3 for the eigenvalue problem, which would lead to Petrov type III, is ruled out by the structure of $\boldsymbol{Q}$ associated to the Papapetrou structure of the metric. From our perturbation theory results, we see that the only option for a bidimensional invariant subspace appears in the static limit, where its existence is forbidden by the fact that the spherical symmetry associated imposes types D or O. Accordingly, the $\boldsymbol{Q}$ matrix of our interior spacetime is always diagonalizable.

- In general, the Petrov type is I. Out of the static case, it will only be type D when eq. (3.91) are satisfied provided $n \neq 1$. In the static case, it will always be type D unless $n = 1$, in which case the Petrov type is O. Then, the constant energy density case can only be type I ($\Omega \neq 0$) or O ($\Omega = 0$).

It could be argued that our approximate results do not necessarily hold for exact solutions. Nevertheless, as long as an exact solution for the source we work with exists, a series development of it following the CMMR approach must lead to our results. Because of this, while any property compatible with a truncated series development is not necessarily a property of the exact solution, a behaviour ruled out already in the truncated solution can not be a property of the hypothetical exact solution.

4. Some implications

Besides any theoretical result we can extract from it, a key point is knowing when this linear EOS metric gives a good approximation for a specific problem. Its range of applicability is given by the set of values (r_s, μ_0, ω). The parameter λ will be small whenever r_s or μ_0 are small enough. For Ω, small values ω are in principle required, but the greater λ is, the higher ω can be. This comes from the fact that a strongly gravitationally bounded source deforms much less with rotation than a lightly bounded one. We will focus deeply on this topic on Chapter 5.

We make now some connections with known exact solutions and possible future ones. It has long been suspected that the Kerr metric can not represent the exterior of any stellar model. We can easily check that it is indeed the case here using the kind of analysis that appears in Cabezas *et al.* (2007).

The first three Kerr multipole moments are (Hansen, 1974)[4]

$$M_0^{\rm Kerr} = m, \qquad J_1^{\rm Kerr} = ma, \qquad M_2^{\rm Kerr} = -ma^2. \tag{3.93}$$

If our two first multipole moments were equal to the Kerr ones, $M_2^{\rm Kerr}$ should have the expression

$$\left.\begin{aligned} M_0^{\rm Kerr} &= m = \lambda r_s M_0 \\ J_1^{\rm Kerr} &= ma = \lambda^{3/2}\Omega r_s^2 J_1 \end{aligned}\right\} \longrightarrow -ma^2 = -\frac{(\lambda^{3/2}\Omega r_s^2 J_1)^2}{\lambda r_s M_0} = -\lambda^2\Omega^2 r_s^3 \frac{J_1^2}{M_0}$$

i.e. , the first λ-order component of $\tilde{M}_2$ should vanish. This in in contradiction with eq. (3.64) and hence neither our interior nor any exact metric of which it could be an approximation can be a source of Kerr.

Now we focus on the Wahlquist family of metrics (Wahlquist, 1968). That is to say to a stationary axisymmetric rigidly rotating perfect fluid with EOS $\epsilon + 3p =$ const. and Petrov type D (Kramer, 1986; Senovilla, 1987). In the non-static case, the conditions for Petrov type D for our interior family are given by eq. (3.91). Then, in the case when $n = -2$ and eq. (3.91) is satisfied, g^- is of type D and our interior is an approximation to the Wahlquist family.

It must be noted nevertheless that, despite the fact that Wahlquist's family is a subcase of our general interior solution (as must be expected), the values m_2 and j_3 imposed by the matching with the asymptotically flat exterior *do not* satisfy eq. (3.91). Then, we recover and give an independent derivation of the known result that, within perturbation theory, Wahlquist's family can not correspond to an isolated source (Bradley *et al.*, 2000; Sarnobat and Hoenselaers, 2006).

A last comment. If one looks for stationary axisymmetric perfect fluid solutions with a static limit as candidates to represent the interior of a stellar model, considering the Penrose chart of how a certain Petrov type can lead to another through degeneration, one should then only take into account those metrics whose Petrov type can lead to the types D and O corresponding to spherical symmetry (Senovilla, 1993). A type N, rigidly rotating perfect fluid with barotropic EOS and $\epsilon + p \neq 0$ can not be axisymmetric (Carminati, 1988), therefore we must discard types III and N, but all the rest should, to the best of our knowledge, be considered. It seems reasonable that a type II exact metric with the properties we demand can

[4]Here m stands for the Kerr mass parameter.

be approximated by our solutions. Nevertheless, the Petrov type II is not included among the possible types of our general interior metric and hence, we conjecture that *there is no stationary axisymmetric rigidly rotating perfect fluid metric with EOS* $\epsilon + (1 - n)p = const.$ *of type II possessing a static limit and a surface of zero pressure.* This is in accordance with the weird fact that, even dropping the demand of zero pressure surface, it has not been found any type II exact interior metric suitable to be part of a stellar model, while the harder field of type I solutions is not empty (Senovilla, 1993).

Chapter Four

An approximate Wahlquist solution from the CMMR linear EOS metric

The question we try to answer in this chapter is whether or not we can include an appropriate approximation of the Wahlquist solution in our family of approximate solutions for the linear EOS (which we will generally call CGMR[1] from now on) There are two ways to answer. One of them is asking our $n = -2$ solution to be of Petrov type D, since a metric with its characteristics and this Petrov type must belong to the Wahlquist family (Senovilla, 1987). The other way is finding a coordinate change to make them to coincide.

Regarding the first one, we have already verified that our solution can take Petrov type D in Chapter 3. Some of its free constants are then fixed and we have found their values do not coincide with the ones they are forced to take when we matched our interior solution with an asymptotically flat exterior solution, as one expects.

The coordinate change way involves writing our solution in a co-rotating frame, and then making a series expansion of Wahlquist's solution with μ_0—rest-mass density at the zero pressure surface—as post-Minkowskian parameter. When the parameter μ_0 tends to zero the Wahlquist solution becomes Minkowski's metric, what shows that μ_0 plays an equivalent role to the one of the parameter λ in our scheme. This way is more meaningful since, in spite of any result we can get from our approximate metric alone, there is always the question of whether our solution really corresponds to a parametric expansion of an exact metric. Working this way we verify explicitly this correspondence.

In Section 1 we write the CGMR interior metric for $n = -2$ and perform the rotation to write our metric in a co-rotating coordinate system. In Section 2 we give the Wahlquist metric, write it in spheroidal-like coordinates and then write the approximate post-Minkowskian Wahlquist metric. Finally, in Section 3 we compare

[1]It stands for the initials of the authors of Cuchí *et al.* (2013a), which covers the material en Chapter 4. The present chapter contains the work published in Cuchí *et al.* (2013b)

both solutions and determine the value of our constants and the relation between r_0 and the rotation parameter.

1. The approximate interior metric

The main goal of this chapter is attempting to get an approximation of Wahlquist's metric using the CMMR approach. Since Wahlquist's metric is only valid in a non-empty spacetime, we will only need here to work with the interior part of the CMMR solution for the linear EOS $\epsilon + (n-1)p = \epsilon_0$ (CGMR) from now on. To ease the work of comparison with Wahlquist's metric, we will keep the notation used for it in Stephani *et al.* (2003)—which in turn is mainly adopted from Senovilla (1993)— . The only modification is the use of $\hat{\eta}$ instead of η to denote one of Wahlquist's coordinates. Also, we will work with rest-mass density parameters μ, μ_0 instead of energy density ones ϵ, ϵ_0.

To match the kind of fluid in the Wahlquist metric, first we need the EOS

$$\mu + 3p = \mu_0. \tag{4.1}$$

which is the $n = -2$ interior subcase of CGMR, what, using eqs. (3.2) and (3.3), involves these expressions for the $\mu(\psi)$, $p(\psi)$ relations

$$\begin{aligned} p &= \frac{\mu_0}{2}\left(1 - \frac{\psi_\Sigma^2}{\psi^2}\right), \\ \mu &= \frac{\mu_0}{2}\left(3\frac{\psi_\Sigma^2}{\psi^2} - 1\right). \end{aligned} \tag{4.2}$$

For $n = -2$, the components $\gamma_{\alpha\beta}$ of the CGMR interior metric in the orthonormal cobasis (2.49) are, up to $\mathcal{O}(\lambda^2, \Omega^3)$

$$\begin{aligned} \gamma_{rr}^{\text{CGMR}} &= 1 + \lambda\left[m_0 - \frac{r^2}{r_s^2}\left(1 - m_2\Omega^2 P_2\right)\right] \\ &\quad + \frac{2\lambda^2}{5}\frac{r^2}{r_s^2}\left\{m_0 - 12S - 4m_0 m_2\Omega^2 P_2 - \frac{r^2}{r_s^2}\left[\Omega^2\left(\frac{5}{3}P_2 - \frac{8}{7}\right) + \frac{1}{7}\right]\right\} \\ &\quad + \mathcal{O}(\lambda^3, \Omega^4), \end{aligned} \tag{4.3}$$

$$\gamma_{r\theta}^{\text{CGMR}} = -\lambda^2\Omega^2\frac{r^2}{r_s^2}P_2^1\left[\frac{1}{5}m_0 m_2 + \frac{1}{63}\frac{r^2}{r_s^2}\left(1 - 6m_2\right)\right] + \mathcal{O}(\lambda^3, \Omega^4), \tag{4.4}$$

$$\gamma_{\theta\theta}^{\text{CGMR}} = 1 + \lambda\left[m_0 - \frac{r^2}{r_s^2}\left(1 - m_2\Omega^2 P_2\right)\right]$$

$$+\lambda^2\frac{r^2}{r_s^2}\left(-\frac{1}{5}\left[18S+m_0+2m_0m_2\Omega^2(2P_2-1)\right]\right.$$
$$\left.+\frac{1}{7}\frac{r^2}{r_s^2}\left\{\frac{8}{5}-\frac{\Omega^2}{3}\left[\frac{m_2}{2}-\frac{134}{15}+\left(\frac{31}{3}+\frac{23m_2}{2}\right)P_2\right]\right\}\right)$$
$$+\mathcal{O}(\lambda^3,\Omega^4), \tag{4.5}$$

$$\gamma^{\mathrm{CGMR}}_{\phi\phi}=1+\lambda\left[m_0-\frac{r^2}{r_s^2}\left(1-m_2\Omega^2P_2\right)\right]+\lambda^2\frac{r^2}{r_s^2}\left(-\frac{1}{5}\left(18S+m_0+2m_0m_2\Omega^2\right)\right.$$
$$\left.+\frac{1}{7}\frac{r^2}{r_s^2}\left\{\frac{8}{5}+\frac{\Omega^2}{3}\left[\frac{m_2}{2}-\frac{26}{15}+\left(\frac{1}{3}-\frac{25m_2}{2}\right)P_2\right]\right\}\right)+\mathcal{O}(\lambda^3,\Omega^4), \tag{4.6}$$

$$\gamma^{\mathrm{CGMR}}_{t\phi}=\lambda^{3/2}\Omega\frac{r}{r_s}\left[\left(j_1-\frac{6}{5}\frac{r^2}{r_s^2}\right)P_1^1+j_3\Omega^2\frac{r^2}{r_s^2}P_3^1\right]+\mathcal{O}(\lambda^{5/2},\Omega^5), \tag{4.7}$$

$$\gamma^{\mathrm{CGMR}}_{tt}=-1+\lambda\left[m_0-\frac{r^2}{r_s^2}\left(1-m_2\Omega^2P_2\right)\right]-\lambda^2\frac{r^4}{r_s^4}\left[\frac{1}{5}\left(1+2\Omega^2\right)-\frac{4}{7}\Omega^2(1+m_2)P_2\right]$$
$$+\mathcal{O}(\lambda^3,\Omega^4). \tag{4.8}$$

Note that the original CGMR includes $\mathcal{O}(\lambda^{5/2},\Omega^3)$ terms as well, but we will not work with them here. The reason will become apparent later in the chapter. Also, and again only in this chapter, to mirror the already published formulae, we work in $8\pi G=1$ units, so the value of λ we work here with is

$$\lambda=\frac{1}{6}\mu_0r_s^2. \tag{4.9}$$

With the EOS fixed, the interior in CGMR depends on nine free constants. Two of them, r_s and ω, are part of the approximation parameters λ and Ω. The other seven are $(m_0, m_2, j_1, j_3, a_0, a_2, b_2)$. These arise from the harmonic expansion we use to solve the homogeneous part of the Einstein equations at each order. The first four of them are the ones that a Darmois matching fixes and choosing values for them amounts to choosing a "particular metric" from the CGMR family—although in a strict sense, such particular metric would still be a family of metrics because of the free values of λ and Ω—. The last three parametrize changes between the harmonic coordinates used. Here, to simplify we have taken these purely gauge constants

$$a_0=0,\quad a_2=0,\quad b_2=0, \tag{4.10}$$

without losing generality because they are not needed hereafter. The static limit ($\Omega=0$) of CGMR for a certain EOS is characterised with only (r_s, m_0) (see Table 4.1).

Table 4.1: Free parameters in the CGMR interior. The last column is a subset of the previous ones.

Parameters	Harmonic expansion constants	Static limit
μ_0, n, r_s, ω	m_0, m_2, j_1, j_3	μ_0, n, r_s, m_0

The constant S is defined as

$$\psi_\Sigma = 1 + \lambda\left(-\frac{1}{2} + \frac{\Omega^2}{3} + \frac{m_0}{2}\right) + \mathcal{O}(\lambda^2, \Omega^4) := 1 + \lambda S + \mathcal{O}(\lambda^2, \Omega^4). \tag{4.11}$$

This value ψ_Σ comes from the value of ψ

$$\begin{aligned}\psi = 1 &+ \lambda\left\{-\frac{r^2}{2r_s^2} + \frac{m_0}{2} + \Omega^2\left[\frac{r^2}{3r_s^2} + \frac{r^2}{r_s^2}\left(-\frac{1}{3} + \frac{m_2}{2}\right)P_2\right]\right\} \\ &+ \lambda^2\left(\frac{11r^4}{40r_s^4} - \frac{3m_0r^2}{4r_s^2} + \frac{3m_0^2}{8} + \Omega^2\left\{-\frac{7r^4}{30r_s^4} + \frac{r^2}{r_s^2}\left(-\frac{2j_1}{3} + \frac{5m_0}{6}\right)\right.\right. \\ &\left.\left. + \left[\frac{r^4}{r_s^4}\left(\frac{67}{210} - \frac{13m_2}{28}\right) + \frac{r^2}{r_s^2}\left(\frac{2j_1}{3} - \frac{5m_0}{6} + \frac{3m_0m_2}{4}\right)\right]P_2\right\}\right) + \mathcal{O}(\lambda^2, \Omega^2)\end{aligned} \tag{4.12}$$

on the zero pressure surface

$$r_\Sigma = r_s\left(1 + \left\{\left(-\frac{1}{3} + \frac{m_2}{2}\right) + \lambda\left[\frac{1}{21}\left(-1 + 14j_1 - 7m_0\right) + \frac{3m_2}{35}\right]\right\}\Omega^2P_2\right) + \mathcal{O}(\lambda^2, \Omega^2). \tag{4.13}$$

We have not replaced S in the expressions for both brevity and to check the behaviour of ψ_Σ when we compare with the parameters in the Wahlquist solution. These expressions for ψ and ψ_Σ lead to the following one for the pressure

$$\frac{p}{\mu_0} = \lambda\left\{\frac{1}{2} - \frac{r^2}{2r_s^2} + \Omega^2\left[-\frac{1}{3} + \frac{r^2}{3r_s^2} + \frac{r^2}{r_s^2}\left(-\frac{1}{3} + \frac{m_2}{2}\right)P_2\right]\right\} + \mathcal{O}(\lambda^2, \Omega^4). \tag{4.14}$$

This solution is apparently less interesting than the Wahlquist exact solution for the same kind of source because it is an approximation. Nevertheless, it is more general in a sense because it is a Petrov type I solution unless

$$m_2 = \frac{6}{5} + \mathcal{O}(\lambda, \Omega^2), \quad j_3 = \frac{36}{175} + \mathcal{O}(\lambda, \Omega^2), \tag{4.15}$$

in which case it becomes a Petrov type D solution. It is worth noticing though that when finding the Petrov type of a metric, the more special the algebraic type is, the bigger is the number of conditions to verify. Then, while an approximate metric can satisfy these constraints up to a certain order, it is possible that its higher

orders do not. Accordingly, the Petrov type of an approximate metric must be regarded generally as an upper bound to the algebraic speciality of its Weyl tensor (see Chapter 3).

Another feature of the CGMR interior is that, as we saw in Chapter 3, imposing Darmois-Israel matching conditions shows that when

$$m_0 = 3 + \lambda\left(3 + 2\Omega^2\right) + \mathcal{O}(\lambda^2, \Omega^4), \tag{4.16}$$

$$m_2 = -1 - \frac{2}{5}\lambda + \mathcal{O}(\lambda^2, \Omega^2), \tag{4.17}$$

$$j_1 = 2 + \frac{2\Omega^2}{3} + \lambda\left(\frac{44}{5} + \frac{52}{15}\Omega^2\right) + \mathcal{O}(\lambda^2, \Omega^4), \tag{4.18}$$

$$j_3 = -\frac{2}{7} - \frac{296}{245}\lambda + \mathcal{O}(\lambda^2, \Omega^2), \tag{4.19}$$

the interior can be matched with an asymptotically flat vacuum exterior. There is no known asymptotically flat exterior for Wahlquist, though. Additionally, in our solution the parameter $\omega = u^\phi/u^t$ is the angular velocity of the fluid with respect to our harmonic coordinate frame and its vanishing leads to a static solution (i.e. , $\gamma_{t\phi} = 0$). There is no parameter in Wahlquist's metric with these two features.

If we want to compare this approximate solution with Wahlquist's metric we have to start finding their expressions in the same coordinates. The first problem is that the Wahlquist metric is written in a co-rotating coordinate system and CGMR is not, so first we must choose between the two kinds of coordinates. Changing the CGMR interior to a co-rotating system is straightforward doing

$$\phi \to \phi + \frac{\lambda^{1/2}\Omega}{r_s}t, \quad t \to t \tag{4.20}$$

and then in the co-rotating system the metric components are:

$$\begin{aligned}\gamma_{tt}^{\text{CGMR}} = &-1 + \lambda\left\{m_0 + \frac{r^2}{r_s^2}\left[-1 + \frac{1}{3}\Omega^2\left(2 + (3m_2 - 2)P_2\right)\right]\right\} \\ &+ \lambda^2\frac{r^2}{r_s^2}\left\{\frac{2}{3}\Omega^2(2j_1 - m_0)(P_2 - 1) - \frac{1}{5}\frac{r^2}{r_s^2}\left[1 - \frac{2}{3}\Omega^2\left(4 + \frac{1}{7}(30m_2 - 19)P_2\right)\right]\right\} \\ &+ \mathcal{O}(\lambda^3, \Omega^4),\end{aligned} \tag{4.21}$$

$$\begin{aligned}\gamma_{t\phi}^{\text{CGMR}} = &-\Omega\lambda^{1/2}\frac{r}{r_s}\left(P_1^1 + \lambda\left\{\left[m_0 - j_1 + \frac{1}{5}\frac{r^2}{r_s^2}\left(1 - \Omega^2 m_2\right)\right]P_1^1\right.\right. \\ &\left.\left. - \Omega^2\frac{r^2}{r_s^2}\left(j_3 - \frac{m_2}{5}\right)P_3^1\right\}\right) + \mathcal{O}(\lambda^{5/2}, \Omega^4)\end{aligned} \tag{4.22}$$

and the other components remain unchanged. Let us remark that the $\gamma_{t\phi}$ component is now of order $\lambda^{1/2}$ instead of the order $\lambda^{3/2}$ it was in the original coordinates.

2. The Wahlquist metric

The next steps in the comparison are, using the singularity free Wahlquist metric, first expand it in the appropriate approximation parameters and then make coordinate changes to reduce it to a particular case of the CGMR interior.

The singularity free Wahlquist metric reads (Wahlquist, 1968; Stephani *et al.*, 2003)[2]

$$ds^2 = -f(dt + A\,d\phi)^2 + r_0^2(\xi^2+\hat{\eta}^2)\left[\frac{c^2 h_1 h_2}{h_1 - h_2}\,d\phi^2 + \frac{d\xi^2}{(1-k^2\xi^2)h_1} + \frac{d\hat{\eta}^2}{(1+k^2\hat{\eta}^2)h_2}\right], \tag{4.23}$$

where

$$f(\xi,\hat{\eta}) := \frac{h_1 - h_2}{\xi^2+\hat{\eta}^2}, \quad A := c\,r_0\left(\frac{\xi^2 h_2 + \hat{\eta}^2 h_1}{h_1 - h_2} - \hat{\eta}_0^2\right), \tag{4.24}$$

$$h_1(\xi) := 1 + \xi^2 + \frac{\xi}{b^2}\left[\xi - \frac{1}{k}(1-k^2\xi^2)^{1/2}\arcsin(k\,\xi)\right], \tag{4.25}$$

$$h_2(\hat{\eta}) := 1 - \hat{\eta}^2 - \frac{\hat{\eta}}{b^2}\left[\hat{\eta} - \frac{1}{k}(1+k^2\hat{\eta}^2)^{1/2}\mathrm{arcsinh}(k\,\hat{\eta})\right] \tag{4.26}$$

and

$$k^2 := \frac{1}{2}\,\mu_0\, r_0^2 b^2\,. \tag{4.27}$$

Here μ_0, b, r_0 are free constants and $\hat{\eta}_0$ and c are related with the behaviour of the solution on the axis. The symmetry axis is located at $\hat{\eta} = \hat{\eta}_0$ where

$$h_2(\hat{\eta}_0) = 0\,, \tag{4.28}$$

and to satisfy the regularity condition of axisymmetry, c must be

$$\frac{1}{c} = \frac{1}{2}(1+k^2\hat{\eta}_0^2)^{1/2}\left.\frac{dh_2}{d\hat{\eta}}\right|_{\hat{\eta}=\hat{\eta}_0}. \tag{4.29}$$

Therefore $\hat{\eta}_0$ and c become functions of the constants μ_0, r_0 and b, which thus characterise completely the singularity free Wahlquist's solution. It is generated by a perfect fluid with 4-velocity

$$\boldsymbol{u} = f^{-1/2}\,\partial_t \qquad (g_{\alpha\beta}u^\alpha u^\beta = -1)\,, \tag{4.30}$$

[2] Here ξ is a coordinate not to be mistaken with any quantity related with the stationary Killing vector ξ of CGMR.

and with energy density and pressure are given by

$$\mu = \frac{1}{2}\mu_0(3b^2 f - 1), \tag{4.31}$$

$$p = \frac{1}{2}\mu_0(1 - b^2 f), \tag{4.32}$$

where we can see now more clearly that the constants b and μ_0 are the values of the normalization factor $f^{-1/2}$ and the energy density on the matching surface of zero pressure (see also [4.2]).

Regarding rotation in Wahlquist's solution, the full expression of the module of its twist vector $\varpi^{\mathrm{W}}(\hat{\eta}, \xi)$ can be found in Wahlquist (1968) and its value at ($\hat{\eta} = 0$, $\xi = 0$) is

$$\varpi^{\mathrm{W}}(0, 0) = \frac{1}{3}\mu_0 r_0. \tag{4.33}$$

We can also get a static limit for it—Whittaker's metric (Whittaker, 1968)—making the change

$$\{\xi, \hat{\eta}\} \to \{R, \chi\} : \ \{\xi = \frac{R}{r_0}, \hat{\eta} = \cos\chi\} \tag{4.34}$$

and letting r_0 go to zero (Wahlquist, 1968) although it must be noted that this coordinate change is singular when $r_0 = 0$.

Expression (4.33) and the limiting procedure suggest a relation between r_0 and the rotation of the fluid. It is actually the case since

$$\lim_{r_0 \to 0} \varpi^{\mathrm{W}} = 0 \tag{4.35}$$

everywhere so $r_0 \to 0$ implies vanishing rotation and should lead to a static spacetime. Nevertheless, it must be done through the limiting procedure (4.34). It is also worth noticing that the only other parameter choice capable of giving $\varpi^{\mathrm{W}} = 0$ everywhere is $\mu_0 = 0$ but it gives an empty interior.

The parameters $\{r_0, \mu_0\}$ will be the natural choice for us to make the formal expansions—they do not need to be small at all—of the Wahlquist metric if we want to compare with the post-Minkowskian and slow rotation expansions of CGMR, but first we must find the change to spherical-like coordinates.

2.1. The Wahlquist metric written in spherical–like coordinates

Our approximate metric (4.3) to (4.6), (4.21) and (4.22) is written in "standard" spherical coordinates—in the sense that when $\lambda = 0$ the metric becomes the Minkowski metric in standard spherical coordinates—so we need to find a consistent

way to write the Wahlquist metric in a set of coordinates as close to ours as possible to begin with.

In this regard we note first that if we put $\mu_0 = 0$ in the Wahlquist metric (4.23) we obtain the Minkowski metric in oblate spheroidal coordinates $\{\xi, \hat{\eta}\}$, whose coordinate lines are oblate confocal ellipses and confocal orthogonal hyperbolas. From these coordinates it is easy to go to Kepler coordinates $\{R, \chi\}$ changing $\xi = R/r_0, \hat{\eta} = \cos\chi$, where R represents the semi-minor axis of the ellipses, χ the Kepler eccentric polar angle and r_0 the focal length. Finally we get standard spherical coordinates $\{r, \theta\}$ by changing

$$\sqrt{R^2 + r_0^2}\sin\chi = r\sin\theta, \quad R\cos\chi = r\cos\theta. \tag{4.36}$$

Moreover, the limiting procedure (4.34) from Wahlquist's solution to its static limit (the Whittaker metric) has a similar form, in this case leading to Kepler-like coordinates.

These considerations suggest to look for a change of coordinates in the Wahlquist metric (prior to any limit) so that the new coordinates "directly represent" spheroidal-like coordinates. We use a heuristic approach here and start plotting the graphs of $h_1(\xi)$ and $h_2(\hat{\eta})$ (Fig. 4.1.) We can see that these curves have the appearance of a hyperbolic cosine and a squared sine for some values of b and k, respectively. Taking this into account we write as an educated guess

$$\{\xi, \hat{\eta}\} \to \{R, \chi\} : \quad \begin{cases} h_1(\xi) = 1 + \dfrac{R^2}{r_0^2} := 1 + \dfrac{R_1^2}{r_0^2} \\ 1 - h_2(\hat{\eta}) = \cos^2\chi := \dfrac{R_2^2}{r_0^2}\,. \end{cases} \tag{4.37}$$

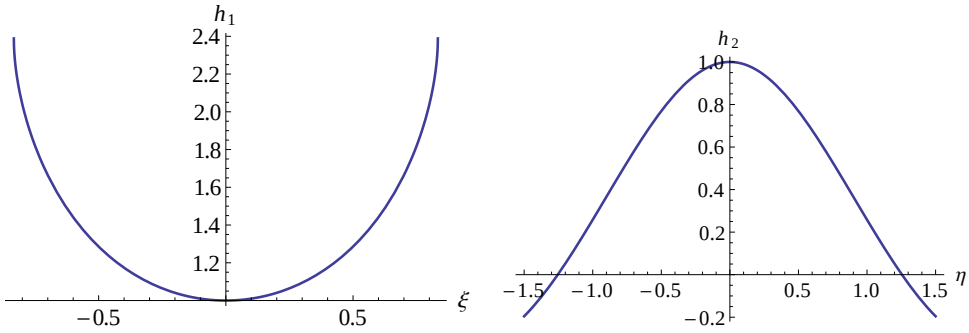

Figure 4.1: Behaviour of the $h_1(\xi)$ and $h_2(\hat{\eta})$ functions for $k = 1.2$, $b = 1$ and $k = 1.248$, $b = 1$, respectively.

where we introduce R_1, R_2 just to simplify calculations later. Let us write now the two dimensional metric spanned by $\{\xi, \hat{\eta}\}$

$$d\Sigma^2 = f_1 d\xi^2 + f_2 d\hat{\eta}^2 \tag{4.38}$$

in terms of $\{R_1, R_2\}$. Since

$$d\xi = \frac{dh_1}{dh_1/d\xi} \quad \text{and} \quad d\hat{\eta} = \frac{dh_2}{dh_2/d\hat{\eta}}, \tag{4.39}$$

taking h_1, h_2 as functions of R_1 and R_2

$$dh_1 = \frac{2R_1}{r_0^2} dR_1, \quad -dh_2 = \frac{2R_2}{r_0^2} dR_2, \tag{4.40}$$

we get

$$d\Sigma^2 = m_{11}\left(\frac{2R_1}{r_0^2} dR_1\right)^2 + m_{22}\left(\frac{2R_2}{r_0^2} dR_2\right)^2, \tag{4.41}$$

where

$$m_{11} = \frac{f_1}{(dh_1/d\xi)^2}, \quad m_{22} = \frac{f_2}{(dh_2/d\hat{\eta})^2}. \tag{4.42}$$

Now let us do another coordinate change to a kind of spherical coordinates $\{r, \theta\}$ using the previous relations eqs. (4.36) and (4.37). Then, R_1 and R_2 are the following functions of r and θ

$$\{R_1, R_2\} \to \{r, \theta\} : \begin{cases} R_1 = \sqrt{\frac{1}{2}\left(r^2 - r_0^2 + \sqrt{(r^2 - r_0^2)^2 + 4r^2 r_0^2 \cos^2\theta}\right)}, \\ R_2 = \sqrt{\frac{1}{2}\left(r_0^2 - r^2 + \sqrt{(r^2 - r_0^2)^2 + 4r^2 r_0^2 \cos^2\theta}\right)}, \end{cases} \tag{4.43}$$

and if we define the function

$$F = (r^2 - r_0^2)^2 + 4r^2 r_0^2 \cos^2\theta,$$

we have that the metric (4.38) in $\{r, \theta\}$ coordinates

$$d\Sigma^2 = g_{rr} dr^2 + 2g_{r\theta} dr d\theta + g_{\theta\theta} d\theta^2$$

has the coefficients

$$g_{rr} = \frac{2r^2}{r_0^4 F}\left[\sqrt{F}(r^2 - r_0^2 + 2r_0^2\cos^2\theta)(m_{11} - m_{22})\right.$$

$$+ (F - 2r_0^4 \sin^2\theta\cos^2\theta)(m_{11} + m_{22})\Big], \tag{4.44}$$

$$g_{r\theta} = -\sin\theta\cos\theta\frac{2r^3}{r_0^2 F}\Big[\sqrt{F}\,(m_{11} - m_{22}) + \left(r^2 - r_0^2 + 2r_0^2\cos^2\theta\right)(m_{11} + m_{22})\Big], \tag{4.45}$$

$$g_{\theta\theta} = \sin^2\theta\cos^2\theta\frac{4r^4}{F}(m_{11} + m_{22}). \tag{4.46}$$

Only the terms $m_{11} + m_{22}$ and $m_{11} - m_{22}$ depend on both $\{\mu_0, r_0\}$; the remaining terms depend on r_0 alone.

Now we are going to write the full metric in terms of $\{r, \theta\}$; notice that the inversion can only be approximately done (in a series of μ_0). First, we determine $\hat{\eta}_0$ up to order μ_0^2, and then c to the same order. This last series depends on b^2, so before that must determine how b depends on μ_0. We recall that in the $\mu_0 = 0$ limit the Wahlquist metric becomes Minkowski's metric written in oblate spheroidal coordinates so

$$\lim_{\mu_0\to 0} f = 1, \tag{4.47}$$

and hence, since $b = f^{-1/2}\big|_{p=0}$, its series expansion must begin as $b^2 = 1 + \mathcal{O}(\mu_0)$. Besides, since eq. (4.32) takes the form

$$p = \frac{1}{2}\mu_0\left\{1 - b^2[1 + \mathcal{O}(\mu_0)]\right\}, \tag{4.48}$$

the expansion of b makes the pressure start with $p \sim \mu_0^2$, behaving like in CGMR. Accordingly, we are going to use

$$b^2 = 1 + \frac{1}{3}\mu_0\sigma_1 + \mu_0^2\sigma_2 + \mathcal{O}(\mu_0^3) \tag{4.49}$$

where σ_1 and σ_2 are two new constants introduced merely for calculation convenience. Inserting it into eqs. (4.27) to (4.29), we obtain for the constants $\hat{\eta}_0$ and c up to $\mathcal{O}(\mu_0^3)$

$$\hat{\eta}_0 = 1 + \frac{1}{12}\mu_0 r_0^2\left\{1 + \frac{1}{120}\mu_0 r_0^2\left[11 + \mu_0\left(\frac{73}{28}r_0^2 - 8\sigma_1\right)\right]\right\} + \mathcal{O}(\mu_0^4), \tag{4.50}$$

$$c = -1 + \frac{1}{12}r_0^2\mu_0^2\left[\sigma_1 - \frac{r_0^2}{3} + \mu_0\left(3\sigma_2 - \frac{r_0^4}{30}\right)\right] + \mathcal{O}(\mu_0^4). \tag{4.51}$$

Next, we invert the change of coordinates eq. (4.37), which gives

$$\xi^2 = \frac{R_1^2}{r_0^2}\left(1 - \frac{1}{6}\mu_0 R_1^2\left\{1 - \frac{1}{15}\mu_0 R_1^2\left[2 - \mu_0\left(\sigma_1 + \frac{37}{84}R_1^2\right)\right]\right\}\right) + \mathcal{O}(\mu_0^4) \tag{4.52}$$

$$\hat{\eta}^2 = \frac{R_2^2}{r_0^2}\left(1+\frac{1}{6}\mu_0 R_2^2\left\{1+\frac{1}{15}\mu_0 R_2^2\left[2-\mu_0\left(\sigma_1-\frac{37}{84}R_2^2\right)\right]\right\}\right)+\mathcal{O}(\mu_0^4) \tag{4.53}$$

And finally, by doing the coordinate change $\{R_1, R_2\} \to \{r, \theta\}$ we obtain the metric coefficients up to $\mathcal{O}(\mu_0^3)$ in the spherical-like coordinates desired

$$\begin{aligned}\gamma^{\mathrm{W}}_{rr} = 1 &+ \frac{\mu_0}{6}(r_0^2-r^2)+\frac{\mu_0^2}{6}\left[\sigma_1(r^2-r_0^2\sin^2\theta)+r_0^2\left(\frac{4r^2}{5}-\frac{r_0^2}{3}\right)\cos^2\theta\right.\\ &\left.+\frac{7}{15}(r_0^2-r^2)^2\right]+\frac{\mu_0^3}{90}\left\{\frac{\sigma_1}{2}\left[r_0^2\left(5r_0^2-7r^2\right)\cos^2\theta-7(r_0^2-r^2)^2\right]\right.\\ &+45\sigma_2(r^2-r_0^2\sin^2\theta)+\frac{r_0^2}{21}(r_0^2-r^2)(85r^2-28r_0^2)\cos^2\theta\\ &\left.+\frac{149}{84}(r_0^2-r^2)^3-\frac{r_0^4}{2}r^2\cos^4\theta\right\},\end{aligned} \tag{4.54}$$

$$\begin{aligned}\gamma^{\mathrm{W}}_{\theta\theta} = 1 &+ \frac{\mu_0}{6}(r_0^2-r^2)+\frac{\mu_0^2}{9}\left[r_0^2\left(\frac{r^2}{5}+\frac{r_0^2}{2}-\frac{3}{2}\sigma_1\right)\cos^2\theta+\frac{1}{5}(r^2-r_0^2)^2\right]\\ &+\frac{\mu_0^3}{180}\left\{\sigma_1\left[r_0^2(3r^2-5r_0^2)\cos^2\theta-2(r_0^2-r^2)^2\right]-90\sigma_2 r_0^2\cos^2\theta\right.\\ &\left.+\frac{r_0^2}{21}(r_0^2-r^2)(37r^2+56r_0^2)\cos^2\theta+r_0^4r^2\cos^4\theta+\frac{37}{42}(r_0^2-r^2)^3\right\},\end{aligned} \tag{4.55}$$

$$\begin{aligned}\gamma^{\mathrm{W}}_{r\theta} = &\frac{\mu_0^2 r_0^2}{18}\sin\theta\cos\theta\left\{r_0^2-r^2-3\sigma_1\right.\\ &\left.-\frac{\mu_0}{10}\left[5\sigma_1(r_0^2-r^2)+90\sigma_2-r_0^2r^2\cos\theta^2-\frac{8}{3}(r_0^2-r^2)^2\right]\right\},\end{aligned} \tag{4.56}$$

$$\begin{aligned}\gamma^{\mathrm{W}}_{\phi\phi} = 1 &+ \frac{\mu_0}{6}(r_0^2-r^2)-\frac{\mu_0^2}{6}\left\{r_0^2\left[\sigma_1-\frac{1}{15}\left(7r_0^2-\frac{13}{2}r^2\right)\right]-\frac{3}{10}r_0^2r^2\cos^2\theta\right.\\ &\left.-\frac{2}{15}r^4\right\}+\frac{\mu_0^3}{90}\left\{\sigma_1\left[\frac{r_0^2}{2}(9r^2-7r_0^2)-r_0^2r^2\cos^2\theta-r^4\right]-45r_0^2\sigma_2\right.\\ &\left.+\frac{149}{84}r_0^6-\frac{43}{14}r_0^4r^2+\frac{11}{7}r_0^2r^4-\frac{37}{84}r^6-\frac{1}{84}r_0^2r^2(95r^2-151r_0^2)\cos^2\theta\right\},\end{aligned} \tag{4.57}$$

$$\begin{aligned}\gamma^{\mathrm{W}}_{t\phi} = -&\frac{\mu_0 r_0}{6}r\sin\theta\left\{1+\frac{\mu_0}{30}(r^2+3r_0^2)+\frac{\mu_0^2}{15}\left[\sigma_1\left(r^2-\frac{13}{4}r_0^2\right)\right.\right.\\ &\left.\left.+\frac{r_0^2}{84}(97r_0^2-41r^2)+\frac{4}{21}r^4+\frac{3}{28}r_0^2r^2\cos^2\theta\right]\right\},\end{aligned} \tag{4.58}$$

$$\gamma^{\mathrm{W}}_{tt} = -1 + \frac{\mu_0}{6}(r_0^2 - r^2) - \frac{\mu_0^2}{180}\left\{(r_0^2 - r^2)^2 - 4r^2 r_0^2 \cos^2\theta\right\} + \frac{\mu_0^3}{90}\left\{(r_0^2 - r^2)\times \right.$$
$$\left.\times\left[\frac{4}{21}(r_0^2 - r^2)^2 + \frac{3}{14}r^2 r_0^2\cos^2\theta\right] - \sigma_1\left[(r^2 - r_0^2)^2 + r^2 r_0^2\cos^2\theta\right]\right\}. \tag{4.59}$$

3. Comparing the approximate Wahlquist solution with the CGMR solution in co-rotating coordinates

Now we face the problem of identification of the parameters and to perform the final adjustments of coordinates needed to make every term in Wahlquist's metric and the CGMR interior equal.

To get an idea of the problems arising, we analyze first the static limit. Using eq. (4.9) and making $r_0 = 0$ in eq. (4.54) we obtain the expression for the γ_{rr} coefficient of the static metric

$$\gamma^{\mathrm{W}}_{rr}(r_0 = 0) = 1 - \frac{r^2\lambda}{{r_s}^2} + \frac{2r^2\lambda^2\left(7r^2 + 15\sigma_1\right)}{5{r_s}^4} + \mathcal{O}(\lambda^3) \tag{4.60}$$

and upon comparison with the corresponding static limit of CGMR

$$\gamma^{\mathrm{CGMR}}_{rr}(\Omega = 0) = 1 + m_0\lambda - \frac{r^2\lambda}{{r_s}^2} - \frac{2r^4\lambda^2}{35{r_s}^4} + \frac{2m_0 r^2\lambda^2}{5{r_s}^2} - \frac{24r^2 S\lambda^2}{5{r_s}^2} + \mathcal{O}(\lambda^3) \tag{4.61}$$

we can see that there are discrepancies among r^4 terms in the sense that they can not be made equal adjusting parameters. To some extent this was to be expected since CGMR was written in coordinates associated to harmonic ones and no such condition has been imposed on the Wahlquist metric. In this particular case, the two metrics can be rendered exactly equal with a change of radial coordinate in $\gamma^{\mathrm{W}}_{\alpha\beta}(r_0 = 0)$

$$r \to r'\left[1 + \left(-\frac{2r'^4}{7r_s^4} - \frac{9r'^2 S}{5r_s^2}\right)\lambda^2\right] + \mathcal{O}(\lambda^3) \tag{4.62}$$

and making $m_0 = 0$, $\sigma_1 = r_s^2 S$.

3.1. *Adjusting parameters*

We go back now to the non-static case. If we compare the lowest order term in $g_{t\phi}$ and g_{tt} of both solutions—eqs. (4.21), (4.22), (4.58) and (4.59)—we can see that the relation between λ and μ_0 is (4.9) as expected and the constant Ω of the CGMR solution must be related with the r_0 constant of the Wahlquist metric as

$$r_0 = -\frac{\kappa\, r_s \Omega}{\lambda^{1/2}} \tag{4.63}$$

with κ a factor to be determined later on. If we perform this identification we get to a new difficulty because Wahlquist's solution has λ-free terms with Ω dependence. These terms appear associated with powers of $\mu_0 r_0^2$ (or $\kappa^2\Omega^2$ using eq. [4.63]). This is not possible in our self-gravitating solution building scheme. This issue can be solved using the remaining freedom in time scale and $\{r, \theta\}$ coordinates. The changes we can do are[3]

$$t = T\left(1 + \mu_0 F_1 + \mu_0^2 F_2 + \cdots\right), \tag{4.64}$$

$$\begin{aligned} r &= R\left[1 + \mu_0 G_1(R,\Theta) + \mu_0^2 G_2(R,\Theta) + \cdots\right], \\ \theta &= \Theta + \mu_0 \sin\Theta\left[H_1(R,\Theta) + \mu_0 H_2(R,\Theta) + \cdots\right], \end{aligned} \tag{4.65}$$

with F_i constants depending on the parameters and G_i, H_i undetermined functions. Imposing vanishing of these unwanted terms, we get the time scale change

$$t = T\left\{1 + \frac{\mu_0 r_0^2}{12}\left[1 + \frac{11\mu_0 r_0^2}{120}\left(1 + \frac{73\mu_0 r_0^2}{308}\right)\right]\right\} + \mathcal{O}(\mu_0^4) \tag{4.66}$$

and the $\{r,\ \theta\}$ changes

$$r = R\left\{1 - \frac{\mu_0 r_0^2}{12}\left(1 + \frac{\mu_0 r_0^2}{3}\left[\frac{41}{40} - \cos^2\Theta + \frac{\mu_0 r_0^2}{60}\left(\frac{191}{56} - \cos^2\Theta\right)\right]\right)\right\} + \mathcal{O}(\mu_0^4), \tag{4.67}$$

$$\theta = \Theta - \frac{\mu_0^2 r_0^4}{36}\sin\Theta\cos\Theta\left(1 + \frac{\mu_0 r_0^2}{10}\right) + \mathcal{O}(\mu_0^4). \tag{4.68}$$

Note that the symmetry axis for the old coordinates is located at $\theta = 0,\ \pi$ and due to the presence of the $\sin\Theta$ it remains at $\Theta = 0, \pi$. We will maintain this condition for all the coordinate changes of the θ coordinate.

Now, we introduce these changes in our last expression of Wahlquist metric obtaining up to $\mathcal{O}(\mu_0^3)$

$$\begin{aligned} \gamma^{\mathrm{W}}_{RR} = 1 &- \frac{\mu_0}{6}R^2 + \mu_0^2\left\{\frac{7}{90}R^4 + \frac{\sigma_1}{6}R^2 + r_0^2\left[\frac{R^2}{10}\left(\frac{4}{3}\cos^2\Theta - 1\right) - \frac{\sigma_1}{6}\sin^2\Theta\right]\right\} \\ &+ \mu_0^3 r_0^2\left[\frac{17}{42}R^4\left(\frac{1}{20} - \frac{1}{9}\cos^2\Theta\right) - \frac{\sigma_2}{2}\sin^2\Theta + \frac{\sigma_1}{45}R^2\left(1 - \frac{7}{4}\cos^2\Theta\right)\right], \end{aligned} \tag{4.69}$$

$$\gamma^{\mathrm{W}}_{R\Theta} = -\sin\Theta\cos\Theta\frac{\mu_0^2 r_0^2}{6}\left[\sigma_1 + \frac{1}{3}R^2 + \mu_0\left(3\sigma_2 - \frac{\sigma_1}{6}R^2 - \frac{4}{45}R^4\right)\right], \tag{4.70}$$

[3] Here R is a totally new coordinate not to be mistaken with the one used in eq. (4.36)

$$\gamma^{\mathrm{W}}_{\Theta\Theta} = 1 - \frac{\mu_0}{6}R^2 + \frac{1}{45}\mu_0^2\left\{R^4 + r_0^2\left[R^2\left(\cos\Theta^2 + \frac{1}{2}\right) - \frac{15}{2}\sigma_1\cos^2\Theta\right]\right\} + \frac{\mu_0^3}{2}r_0^2\left[\frac{\sigma_1}{90}R^2\left(4 + 3\cos\Theta^2\right) + \frac{1}{140}R^4\left(1 - \frac{74}{27}\cos^2\Theta\right) - \sigma_2\cos^2\Theta\right], \quad (4.71)$$

$$\gamma^{\mathrm{W}}_{\phi\phi} = 1 - \frac{\mu_0}{6}R^2 + \frac{\mu_0^2}{3}\left\{\frac{1}{15}R^4 + \frac{1}{2}r_0^2\left[\frac{R^2}{10}(3\cos\Theta^2 - 1) - \sigma_1\right]\right\} + \mu_0^3 r_0^2\left[\frac{\sigma_1}{90}R^2\left(\frac{9}{2} - \cos^2\Theta\right) + \frac{R^4}{63}\left(\frac{2}{5} - \frac{19}{24}\cos^2\Theta\right) - \frac{\sigma_2}{2}\right], \quad (4.72)$$

$$\gamma^{\mathrm{W}}_{t\phi} = -\frac{\mu_0}{6}r_0 R\sin\Theta\left\{1 + \frac{\mu_0}{30}\left(R^2 + \frac{r_0^2}{2}\right) + \frac{\mu_0^2}{20}r_0^2\left[\frac{R^2}{7}\left(\cos^2\Theta - \frac{103}{18}\right) - \frac{13}{3}\sigma_1\right]\right\}, \quad (4.73)$$

$$\gamma^{\mathrm{W}}_{tt} = -1 - \frac{\mu_0}{6}R^2 - \frac{\mu_0^2}{180}\left[R^4 - 2r_0^2R^2\left(1 + 2\cos^2\Theta\right)\right] + \mu_0^3\frac{r_0^2}{90}\left[\sigma_1 R^2(2 - \cos^2\Theta) + \frac{R^4}{14}\left(\frac{55}{6} - 3\cos^2\Theta\right)\right]. \quad (4.74)$$

After dealing with μ_0 and r_0, we have to find expressions for b and κ. Recalling eq. (4.49), we wrote b^2 as a series in μ_0 with coefficients σ_1, σ_2. To help with its determination, we can give more details about σ_1 and σ_2. When b^2 is written in terms of λ and Ω, its $\mathcal{O}(\lambda^0)$ terms will in general contain order Ω^2 terms. These arise from $\mu_0 r_0^2$ factors and, using dimensional arguments, we can redefine

$$\sigma_1 \to \sigma_1 r_s^2 + r_0^2\nu_1 \quad (4.75)$$

$$\sigma_2 \to (\sigma_2 r_s^2 + r_0^2\nu_2)r_s^2 \quad (4.76)$$

to make this possibility more explicit during calculations.

Now we can write the approximate Wahlquist metric in terms of our parameters λ and Ω using (4.63). Comparing the lower terms in λ for $g_{t\phi}$ of the CGMR co-rotating interior solution and the approximate Wahlquist metric just built, we can determine the proportionality constant κ to be a series in our rotation parameter Ω

$$\kappa = 1 - \frac{\Omega^2}{10} + \mathcal{O}(\Omega^3) \quad (4.77)$$

3.2. Adjusting terms

Once the relations between the approximation parameters of both metrics are determined we can obtain the expression of the approximate Wahlquist metric writ-

ten in the same parameters we have used for the CGMR co-rotating interior. With the coordinate change in eqs. (4.66) to (4.68) we eliminated terms that can not be present in CGMR. Now, to make both solutions coincide we can use changes of coordinates in the Wahlquist metric as long as they do not reintroduce undesired terms. Also, we have freedom to adjust the (m_0, m_2, j_1, j_3) constants of CGMR. Regarding the first, the remaining freedom is a change in the $\{r, \theta\}$ coordinates of the type displayed in eq. (4.65). If we make this change in the Wahlquist metric

$$r \to r\left\{1 + \lambda\Omega^2\left(3\sigma_1 \sin^2\theta - \frac{1}{2}\frac{r^2}{r_s^2}\cos^2\theta\right) - \lambda^2\left[\frac{9}{5}\frac{r^2}{r_s^2}\sigma_1 + \frac{2}{7}\frac{r^4}{r_s^4} - \frac{1}{70}\Omega^2\frac{r^4}{r_s^4}\left(\frac{13}{3} + 33\cos^2\theta\right)\right]\right\} + \mathcal{O}(\lambda^3, \Omega^4), \tag{4.78}$$

$$\theta \to \theta + \lambda\Omega^2 \sin\theta\cos\theta\left(\frac{1}{2}\frac{r^2}{r_s^2} + 3\sigma_1 - \frac{29}{210}\lambda\frac{r^4}{r_s^4}\right) + \mathcal{O}(\lambda^3, \Omega^4), \tag{4.79}$$

we get that, for the two metrics to be exactly equal up to $\mathcal{O}(\lambda^2, \Omega^3)$ the free constants (apart from λ and Ω) of the CGMR co-rotating interior must be

$$m_0 = \mathcal{O}(\lambda^2, \Omega^4), \qquad m_2 = \frac{6}{5}(1 + 2\lambda S) + \mathcal{O}(\lambda^2, \Omega^2), \tag{4.80}$$

$$j_1 = \frac{9}{5}\Omega^2 S + \mathcal{O}(\lambda, \Omega^4), \qquad j_3 = \frac{36}{175} + \mathcal{O}(\lambda, \Omega^2) \tag{4.81}$$

and the free constants of the approximate Wahlquist metric must be

$$\sigma_1 = S, \quad \sigma_2 = 0, \quad \nu_1 = \frac{1}{2}, \quad \nu_2 = \frac{1}{18}. \tag{4.82}$$

This gives b^2 as

$$b^2 = (1 + \Omega^2)(1 + 2\lambda S) + \mathcal{O}(\lambda^2, \Omega^4), \tag{4.83}$$

thus coinciding with the expansion of ψ_Σ^2 from (4.11) if we take into account that the term $(1+\Omega^2)$ comes from the change of the normalization factor over the transformation of the temporal coordinate eq. (4.66) we have done. This gives a first check of the consistency of the comparison since b is the Wahlquist counterpart of ψ_Σ.

The final expressions for the metric components of either Wahlquist's solution or the CGMR interior in the orthonormal basis are, up to $\mathcal{O}(\lambda^2, \Omega^2)$—and $\mathcal{O}(\lambda^{1/2}, \Omega^3)$ in $\gamma_{t\phi}$—,

$$\gamma_{rr} = 1 - \lambda\frac{r^2}{r_s^2}\left\{1 - \frac{6}{5}\Omega^2 P_2\right\} + \frac{2}{5}\lambda^2\left\{-12S - \frac{1}{7}\frac{r^2}{r_s^2} + \Omega^2\left[\frac{8}{7}\frac{r^2}{r_s^2} + \left(6S - \frac{5}{3}\frac{r^2}{r_s^2}\right)P_2\right]\right\}\frac{r^2}{r_s^2}, \tag{4.84}$$

$$\gamma_{r\theta} = \frac{31}{315}\lambda^2\Omega^2\frac{r^4}{r_s^4}P_2^1, \tag{4.85}$$

$$\gamma_{\theta\theta} = 1 - \lambda\frac{r^2}{r_s^2}\left(1 - \frac{6}{5}\Omega^2 P_2\right) - \lambda^2\frac{2r^2}{21r_s^2}\left\{\frac{189}{5}S - \frac{12}{5}\frac{r^2}{r_s^2} - \Omega^2\left[\frac{25}{6}\frac{r^2}{r_s^2} - \frac{1}{5}\left(\frac{181}{3}\frac{r^2}{r_s^2} - 126S\right)P_2\right]\right\}, \tag{4.86}$$

$$\gamma_{\phi\phi} = 1 - \lambda\frac{r^2}{r_s^2}\left(1 - \frac{6}{5}\Omega^2 P_2\right) - \frac{2}{105}\lambda^2\frac{r^2}{r_s^2}\left\{189S - 12\frac{r^2}{r_s^2} + \Omega^2\left[\frac{17}{6}\frac{r^2}{r_s^2} + \left(\frac{110}{3}\frac{r^2}{r_s^2} - 126S\right)P_2\right]\right\}, \tag{4.87}$$

$$\gamma_{t\phi} = -\lambda^{1/2}\Omega\frac{r}{r_s}\left(P_1^1 + \frac{\lambda}{5}\left\{\frac{r^2}{r_s^2}P_1^1 - 3\Omega^2\left[\left(3S + \frac{2}{5}\frac{r^2}{r_s^2}\right)P_1^1 - \frac{2}{35}P_3^1\right]\right\}\right), \tag{4.88}$$

$$\gamma_{tt} = -1 - \lambda\frac{r^2}{r_s^2}\left[1 - \frac{2}{3}\Omega^2\left(1 + \frac{4}{5}P_2\right)\right] + \frac{\lambda^2}{5}\frac{r^2}{r_s^2}\left\{-\frac{r^2}{r_s^2} + \Omega^2\left[\frac{8}{3}\frac{r^2}{r_s^2} + \left(12S + \frac{34}{21}\frac{r^2}{r_s^2}\right)P_2\right]\right\}. \tag{4.89}$$

To give another check of the whole procedure we can compare now with the conditions necessary for our $n = -2$ approximate metric to be of Petrov type D, i.e., eq. (4.15). They are compatible with the values of the constants m_2 and j_3 we have just found in (4.80) and (4.81), as wished. Also, when matched with an asymptotically flat vacuum exterior, m_2, j_3 and the rest of the free constants of the metric can only have the expressions we found in Chapter 3. Since the $n = -2$ fluid for a type D interior does not satisfy the matched expressions, we concluded then that it can not be the source of such exterior in accordance with previous works (Wahlquist, 1968; Bradley *et al.*, 2000; Sarnobat and Hoenselaers, 2006). Nevertheless, it is worth noting here that CGMR contains a $n = -2$ subcase that lacks this problem and can indeed be matched that way. It has then all the characteristics of Wahlquist's fluid but Petrov type I instead of D.

Note, finally, that the Cartesian coordinates associated to the spherical-like coordinates used above are not harmonic. Nevertheless, since eqs. (4.84) to (4.89) correspond as well to the co-rotating $n = -2$ CGMR interior with particular values of the free constants, undoing the change (4.20) they become harmonic again.

4. Remarks

In this chapter we have taken the singularity-free Wahlquist metric and managed to transform it into the form the CGMR interior metric takes when written in a co-rotating coordinate system. We have started from a formal expansion of Wahlquist's solution in (μ_0, r_0) and found its expression in terms of the parameters of CGMR, so it possesses the range of applicability already discussed for CGMR.

We have identified Wahlquist's parameters corresponding to λ and Ω of Cabezas *et al.* (2007). Doing this, we have found an expansion of the parameter r_0 of Wahlquist's metric in terms of our Ω. Accordingly, now we have an approximate expression of r_0 in terms of the better characterised quantities ω and μ_0

$$r_0 = -\frac{r_s}{\sqrt{\lambda}}\Omega\left(1-\frac{\Omega^2}{10}\right)+\mathcal{O}(\Omega^4) = -\frac{6}{\mu_0}\omega\left(1-\frac{3\omega^2}{5\mu_0}\right)+\mathcal{O}\left(\frac{\omega^4}{\mu_0^2}\right). \tag{4.90}$$

To the best of our knowledge its qualitative relation with the angular velocity was previously only guessed through the singular limiting procedure that takes the Wahlquist solution and leads to Whittaker's metric but no parametrization of it in terms of well defined quantities had been given.

In the context of fixed EOS, this last equation, together with eq. (4.83), completes the map from the free parameters of Wahlquist's solution (b, r_0) to the free parameters of a particular CGMR metric (r_s, ω). Curiously, we have gained insight in both sets. The role of r_0 as key to a vanishing twist vector and its good behaviour in the comparison with Ω shows far more clearly than the limiting procedure eq. (4.34) its relation with the rotation in the Wahlquist metric. But also, the role of b as fundamental parameter in Wahlquist's solution hints towards the possibility of trying to build our post-Minkowskian approximation with a stronger emphasis on ψ_Σ instead of the coordinate dependent r_s.

Last, notice that the usual interpretation of $\omega = u_\phi/u_t$ as angular velocity of the fluid as seen from the infinite lacks sense if we deal with a metric that is not matched with an asymptotically flat exterior. In our interior though, it is still singled out by the harmonic coordinate condition. Besides, the definition of stationarity and axisymmetry allows a change of coordinates

$$\{t = t',\ \phi = \phi' + at'\} \tag{4.91}$$

that can modify the value of ω to

$$\omega' = u'_\phi/u'_t = \omega - a \tag{4.92}$$

or make it zero (the case of co-rotating frames). Nevertheless, when dealing with a family of metrics explicitly dependent on ω, its value can be important. In the case of, e.g. , CGMR, we see that written in co-rotating coordinates $u_{t'}/u_{\phi'} = 0$ but ω is part of the metric functions and actually, $\omega \to 0$ still leads to a static metric. It is actually the only way for the module of the CGMR twist vector

$$\varpi^{\mathrm{CGMR}} = \frac{2\lambda^{1/2}\Omega}{r_s} + \mathcal{O}(\lambda^2, \Omega^4) = 2\omega + \mathcal{O}(\lambda^2, \Omega^4) \tag{4.93}$$

to vanish (its $\mathcal{O}(\lambda^2, \Omega^4)$ terms are proportional to ω as well). In this sense, the characterization (4.90) of r_0 is meaningful.

Chapter Five

Comparison of results with a numerical code

The CMMR scheme works on several assumptions. Among them, the most prominent are:

1. the λ expansion of $g_{t\phi}$ components starts with $\mathcal{O}(\lambda^{\frac{3}{2}})$ terms,
2. the parametrization of the multipole moments of the exterior metric and their associated constants of the interior in terms of r_s, λ and Ω,
3. the harmonic gauge is completely non-restrictive in our Lichnerowicz matching, and
4. the post-Minkowskian approximation still holds inside the source.

Some of them have been shown to be non-restrictive at least up to second order in our post-Minkowskian approximation. This is the case for items 1 and 3. For item 2 we have given not even a partial proof. Also, one could certainly expect that the post-Minkowskian approximation starts to crash when the deformation of a spacetime begins to be of importance, but when should we start to mistrust its results? It would remain a matter of rather subjective evaluation if we did not give some error estimation or cross-checked our results. This will be the main purpose of this chapter.

We can give error estimations easily, but provided there is a reliable set of previous results from other methods, a comprehensive comparison of results would be far superior in terms of quantity of information that can be obtained about the behaviour of our scheme. The ideal situation would be having at one's disposal some exact global metrics. This would give us the best density of information and precision possible but, out of the static constant density case, it is not an option. The next best option in terms of information density would be having well tested results from other global analytic approximation for our EOS. Nevertheless, they are not so substantially different from CMMR so as to be sure that they do not suffer the same possible issues. This, united to the effort required to use other scheme for our EOS, makes this option not so interesting. Thus, if we want a reliable but fundamentally different approach, we are led to numerical results.

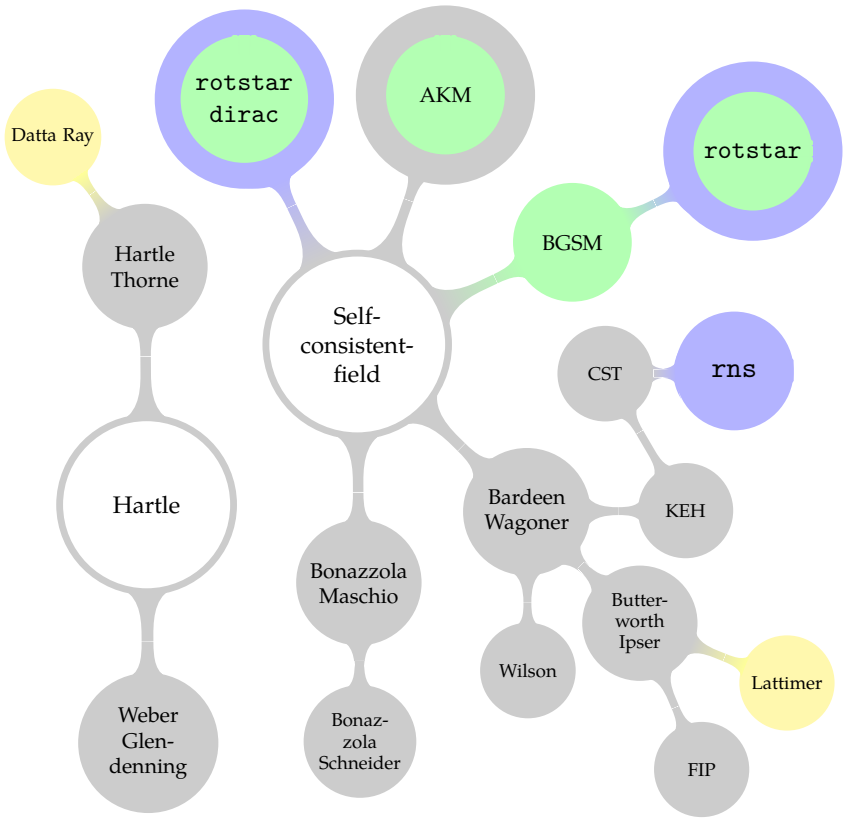

Figure 5.1: Evolution of approaches and numerical codes for relativistic stellar models and some characteristics. Green circles indicate the use of spectral methods instead of finite differences, concentric circles indicate multi-domain codes and light purple refers to open-source codes. Yellow circles correspond to relevant applications.

It would also be interesting to know how CMMR behaves when going to higher approximation orders, the rate of improvement of the results and actually whether they show convergence or not. To answer this, we have computed two additional post-Minkowskian iterations getting the $\mathcal{O}(\lambda^{9/2}, \Omega^3)$ CGMR metric that can be found in Appendix F. We will compare these three CGMR metrics of increasing precision with highly precise numerical stellar models. Thus, we start selecting one code among the several possibilities.

1. Choice of code

Axistationary rotating sources are fundamental in Astrophysics. In the case of compact stars models and observation can impose constraints on the largely unknown EOS of dense nuclear matter (see Haensel *et al.*, 2008, Trümper, 2011, Bagchi, 2010, Lattimer, 2012 and references therein). The great importance of this topics is in direct contrast with the lack of analytic results and has eventually led to the development of several different numerical approaches to compute stellar models in General Relativity.

The first numerical results—in the sense that they are not completely analytical—for rotating stars are due to Hartle and Thorne (1968) and based on the formalism introduced by Hartle (1967). It has been applied to several different EOS by Datta and Ray (1983) and other works reviewed by Datta (1988). Later, Weber and Glendenning (1991) and Weber *et al.* (1991) also used Hartle's method and eventually gave an improved version (Weber and Glendenning, 1992). Being based in Hartle's work, they use a slow-rotation approximation, and only resort to numerical methods to integrate some final expressions. It has been already reviewed in the Introduction.

But one can compute stellar models without making any approximation. Most the codes to follow are based on the *self-consistent-field* approach of Ostriker and Mark (1968). Although originally designed for Newtonian stars, Bonazzola and Maschio (1971) made its first relativistic version, which was later improved (Bonazzola and Schneider, 1974).

A different adaptation of the self-consistent-field to GR (Bardeen and Wagoner, 1971) gave rise to the codes of Wilson (1972), Butterworth and Ipser (1976) (with later applications by Friedman *et al.*, 1986, 1989 (FIP) and Lattimer *et al.*, 1990), and finally to the one by Komatsu *et al.* (1989a,b) (KEH). This last code has been subsequently improved by Cook *et al.* (1992) (CST) and Stergioulas and Friedman (1995) to give the public domain code `rns`.

Three other independent applications of the self-consistent-field method are quite remarkable. The first one (Bonazzola *et al.*, 1993) (BGSM) was the first of these codes to implement spectral methods. Later, it was improved to work on multiple domains, i.e., solve Einstein's equations on different spacetimes and then match the results at each iteration (Bonazzola *et al.*, 1998; Gourgoulhon *et al.*, 1999b). This code, called `rotstar` is also public domain and part of the LORENE library. A similar approach in a different gauge (Dirac instead of the usual quasi-isotropic) was performed by Lin and Novak (2006), resulting in the `rotstar-dirac` code. The third one (Ansorg *et al.*, 2002, 2003) (AKM) is spectral and multi-domain as well, and has been the first code to achieve machine accuracy, i.e. , 16 meaningful

	AKM	KEH	`rns`	BGSM	`rotstar`
p_c	1				
R_p/R_{eq}	0.7			1×10^{-3}	
ω	1.411	1×10^{-2}	3×10^{-4}	1×10^{-2}	9×10^{-6}
$\tilde{M}_0$	0.1357	2×10^{-2}	2×10^{-5}	9×10^{-3}	2×10^{-4}
M_b	0.1863	2×10^{-3}	2×10^{-4}	1×10^{-2}	2×10^{-4}
$\mathcal{R}_{circ}$	0.3454	1×10^{-3}	3×10^{-5}	3×10^{-3}	5×10^{-5}
$\tilde{J}_1$	0.01405	2×10^{-2}	4×10^{-4}	2×10^{-2}	2×10^{-5}
z_p	1.707	6×10^{-2}	4×10^{-5}	2×10^{-2}	1×10^{-5}
z_{eq}^+	−0.1625	2×10^{-2}	2×10^{-3}	4×10^{-2}	2×10^{-4}
z_{eq}^-	11.353	2×10^{-1}	7×10^{-5}	8×10^{-2}	7×10^{-6}
|GRV3|	4×10^{-13}	1×10^{-1}	3×10^{-5}	4×10^{-3}	3×10^{-6}

Table 5.1: Relative errors of some numerical codes with respect to the values given by AKM for a rotating constant density model. The quantities compared are defined in Section 4. Table obtained from Stergioulas (2003).

digits when working with double precision programs, what gives errors of order 10^{-15}. Stergioulas (2003) and Gourgoulhon (2010) have made more detailed reviews on these codes.

To choose between these codes for the task at hand, the determining factor is precision. The main tool here is the so-called *GRV3* identity. For stationary spacetimes, it is the general relativistic generalization of the Newtonian virial identity and was introduced by Gourgoulhon and Bonazzola (1994). Its value for an exact metric should be zero, so any deviation from it gives a measure of the error of a numerical code or approximation scheme. In every code its value depends on the configuration, giving worse results at higher rotations (and especially near the mass-shedding limit, as one could expect) but the result from AKM is consistently better than any other. Table 5.1 shows a comparison of codes and their performance for a particular configuration. Another interesting characteristic to consider is whether the code is adapted to work on several domains or not. Since some EOS lead to density discontinuities on the surface of the source, mono-domain codes suffer Gibbs phenomena in the metric potentials near the surface. Multi-domain codes were born to deal with this and other situations where space-time matching is the natural approach, so it is another desirable feature. AKM is multi-domain as well, and though not public domain, it is available as online complement of a book by Meinel *et al.* (2008) from `http://www.tpi.uni-jena.de/gravity/relastro/rfe/`, and is the code we chose to work with.

1.1. Building stellar models with AKM

The AKM code is able to compute the metric of a stellar model characterised by the value of two physical parameters and its EOS. These two parameters can be any of a list including the multipole moments $\tilde{M}_0$ and $\tilde{J}_1$, baryon mass M_b (it will be later defined in Section 4.1), rotation speed ω and some others. Regarding the EOS, the code has three modes: constant density, relativistic polytrope ($p = K\mu_b^\gamma$, with K and γ the polytropic constant and exponent respectively and μ_b the baryon mass density) and custom EOS. To use the custom EOS mode, one needs first to find the $p(h)$ relation, where

$$h := \frac{\epsilon + p}{\mu_b} \tag{5.1}$$

is the specific enthalpy. From the Gibbs–Duhem relation at zero temperature

$$dp = n_b d\hat{\mu}, \tag{5.2}$$

where n_b is the baryon number density in the fluid frame and $\hat{\mu}$ its chemical potential, since

$$h = \frac{\hat{\mu}}{m_b}, \tag{5.3}$$

(with m_b the mass per baryon) we have

$$dh = \frac{1}{\mu_b} dp \tag{5.4}$$

and thus

$$\frac{dh}{h} = \frac{dp}{\epsilon + p} \quad \longrightarrow \quad h(p) = h(0) \exp \int_0^p \frac{dp'}{\epsilon(p') + p'} \tag{5.5}$$

which is integrated knowing $\epsilon(p)$. Once inverted, replacing h for

$$H = \frac{h}{h(0)} - 1 \tag{5.6}$$

leads to $p(H)$. Finally, if we can express this relation as

$$p = C \sum_{i=1}^{N} p_i H^i \tag{5.7}$$

with C a constant and p_i some constant coefficients, these p_i is what the code requires to specify the custom EOS.

AKM works on Lewis–Papapetrou (LP) coordinates $\{\varrho, \zeta, \phi, t\}$, the cylindrical coordinates associated to quasi-isotropic coordinates $\{R, \Theta, \phi, t\}$, i.e.

$$\varrho = R \sin\Theta, \quad \zeta = R \cos\Theta. \tag{5.8}$$

In these coordinates, the line-element of the axistationary interior and exterior reads

$$ds^2 = \mathrm{e}^{2\alpha}\left(d\varrho^2 + d\zeta^2\right) + W^2\mathrm{e}^{-2\nu}\left(d\phi - \hat{\omega}dt\right)^2 - \mathrm{e}^{2\nu}dt^2 \tag{5.9}$$

and defining

$$\hat{B} := \frac{W}{\varrho}, \quad \mathrm{e}^{\hat{u}} := \frac{\mathrm{e}^{\nu}}{\hat{B}}, \tag{5.10}$$

it can be rewritten as

$$ds^2 = -\hat{B}^2\mathrm{e}^{2\hat{u}}dt^2 + \mathrm{e}^{2\alpha}\left(d\zeta^2 + d\varrho^2\right) + \varrho^2 e^{-2\hat{u}}\left(d\phi - \hat{\omega}dt\right)^2. \tag{5.11}$$

The code obtains the four functions $\hat{B}$, $\hat{u}$, α, and $\hat{\omega}$ which are necessary to fully determine both metrics. It finds their values on a $\{\varrho, \zeta\}$ grid of custom resolution and then writes them in a file. It also gives several physical parameters of the stellar model computed. All these results are given in an EOS dependent unit system. It works on units where $c = G = 1$ and the third constant is

1. $\epsilon_0 = 1$ in the case of constant density,
2. $K = 1$ for relativistic polytropes and
3. $C = 1$ for custom EOS

2. Choice of source

Having chosen the code for the comparison, the next step is the selection of the kind of matter to study. Its EOS must allow to get a finite expansion of eq. (5.7) and also be a subcase of the linear EOS of CMMR. It should nevertheless correspond to a physically interesting source. We will now look for a candidate source of compact stars with such an EOS, but since many of the available results focus on the more fundamental thermodynamic potential instead of the EOS, we start reminding the relation between the two of them. Then we will review some results for a very interesting class of sources and see to what extent they are contained in the linear EOS.

2.1. Thermodynamics and strange stars

The thermodynamic potentials are the fundamental tool for the thermodynamic characterization of a system, in the sense that when one knows their expression in terms of their natural variables, partial derivatives give all the thermodynamic properties. Working with matter where number of particles fluctuates, e.g. the kind of matter expected to constitute compact stars, the natural choice is the gran-canonical ensemble, what leads to work with the specific grand potential $\hat{\Omega}$. It comes from a Legendre transformation of the specific Helmholtz free energy $f = \epsilon - Ts$, where ϵ is the energy density, T temperature and s specific entropy, that substitutes as natural variables the particle number densities n_i for their chemical potentials $\hat{\mu}_i$, i.e.

$$\hat{\Omega} = f - \sum_i \hat{\mu}_i n_i. \tag{5.12}$$

It can be made more manageable using the relation

$$\epsilon = Ts - p + \sum_i \hat{\mu}_i n_i \tag{5.13}$$

to give

$$\hat{\Omega} = -p. \tag{5.14}$$

From eq. (5.14), working at $T = 0$ (it is a good approximation for almost degenerate matter, see Introduction for details) and knowing $\hat{\Omega}(\hat{\mu}_i)$ we can get the equations of state $p(n_i)$ and $\epsilon(n_i)$ just doing

$$\left.\begin{aligned} p &= -\hat{\Omega} \\ n_i &= -\partial_{\hat{\mu}_i}\hat{\Omega} \end{aligned}\right\} \longrightarrow \epsilon = -p + \sum_i \hat{\mu}_i n_i. \tag{5.15}$$

The grand potential is thus the main focus of the research field of the thermodynamics of nuclear and quark matter (see Kurkela *et al.* (2010) for a critical review of previous computations and an modern example).

In what follows we give two examples of obtention of equations of state from grand potentials, in the particular case of strange matter. They will be useful later when we relate them with our linear EOS. Witten (1984) modelled SQM with the simple MIT bag model, in which the grand potential is $\hat{\Omega} = \hat{\Omega}(\hat{\mu}_i, m_s, \alpha_s, B)$, with $\hat{\mu}_i$ the chemical potentials of the three flavors, m_s the mass of the s quark, α_s the strong interaction coupling constant and B the bag constant. Neglecting m_s and the effects of strong interactions ($m_s = \alpha_s = 0$), the grand potential for the ultra-

relativistic gas of *uds* quarks is

$$\hat{\Omega} = \sum_{i=1}^{3} \hat{\Omega}_i + B \tag{5.16}$$

with

$$\hat{\Omega}_i = \frac{-\hat{\mu}_i^4}{4\pi^2\hbar^3}. \tag{5.17}$$

When m_s is considered zero, the electron number density n_e vanishes and we get, from weak interactions equilibrium and charge neutrality (see Haensel *et al.* (2006), pg. 365), that the quark chemical potentials $\hat{\mu}_i$ and number densities n_i verify

$$\hat{\mu}_u = \hat{\mu}_d = \hat{\mu}_s := \hat{\mu} \qquad n_u = n_d = n_s = n_\mathrm{b} \tag{5.18}$$

so that eq. (5.16) becomes

$$\hat{\Omega} = \frac{-3}{4\pi^2\hbar^3}\hat{\mu}^4 + B. \tag{5.19}$$

and leads to the EOS (see also Haensel *et al.*, 1986)

$$p = \frac{1}{3}(\epsilon - 4B). \tag{5.20}$$

With increasing value of m_s, the abundance of strange quarks decreases so that the effect of neglecting m_s is less than 4% from the full calculations (Alcock *et al.*, 1986), making eq. (5.20) a useful simplification.

The MIT bag model is only one of the attempts to implement some of the main features of Quantum ChromoDynamics (QCD) into the behaviour of matter. QCD equations can not be solved as of now, and wherever the strong interaction coupling constant α_s is not expected to be very small (e.g., compact stars interiors), the only option available is to work with non-perturbative models of QCD. Here the main choices are phenomenological models (MIT bag model and others, see the paper by Li *et al.*, 2011) and dynamical models and Dyson-Schwinger equation models (Weber, 2005). Recently, Alford *et al.* (2005) showed that a phenomenological parametrization of the 3-flavor quark matter grand potential

$$\hat{\Omega}_\mathrm{QM} = -\frac{3}{4\pi^2}A_4\hat{\mu}^4 + \frac{3}{4\pi^2}A_2\hat{\mu}^2 + B_\mathrm{eff} \tag{5.21}$$

with A_4, A_2, B_eff independent of $\hat{\mu}$ can approximate several $\mathcal{O}(\alpha_s^2)$ perturbative QCD effects.

- With $A_4 := 1 - \hat{c}$, quark matter made of three non-interacting flavors has $\hat{c} = 0$. For interacting quarks, Fraga *et al.* (2001) showed that $\mathcal{O}(\alpha_s^2)$ results can be approximated with $\hat{c}$ with a value of order 0.3.

- The quadratic $\hat{\mu}$ term can arise from strange quark mass and color superconductivity (also known as *pairing*). Strange quark mass increases A_2 and pairing reduces it.

It is important to note that, setting $A_2 = 0$, the grand potential $\hat{\Omega}_{\rm QM}$ gives the $\epsilon(\hat{\mu})$, $p(\hat{\mu})$ equations

$$p = (1-\hat{c})\frac{3}{4\pi^2}\hat{\mu}^4 - B_{\rm eff}, \tag{5.22}$$

$$\epsilon = 3(1-\hat{c})\frac{3}{4\pi^2}\hat{\mu}^4 + B_{\rm eff} \tag{5.23}$$

and they lead to the EOS

$$\epsilon = 3p + 4B_{\rm eff} \tag{5.24}$$

what evidences that the term corresponding to quark interactions in the approach of Fraga *et al.* (2001) has no effect in the $\epsilon(p)$ EOS.

2.2. *The linear EOS and the simple MIT bag model*

We are finally led to the question of what kind of grand potentials can lead to our linear EOS metric, and what kind of source matter among the ones previously discussed we will finally study. A reasonable first guess for the grand potential is

$$\hat{\Omega} = a\hat{\mu}^n + b, \tag{5.25}$$

with a and b constants, leads to the $n_{\rm b}(\hat{\mu})$, $p(\hat{\mu})$ and $\epsilon(\hat{\mu})$ relations

$$n_{\rm b} = -an\hat{\mu}^{n-1}, \tag{5.26}$$

$$p = -a\hat{\mu}^n - b, \tag{5.27}$$

$$\epsilon = -a(n-1)\hat{\mu}^n + b. \tag{5.28}$$

and to our linear EOS

$$\epsilon = (n-1)p + nb. \tag{5.29}$$

with $nb =: \epsilon_0$. Accordingly, we work from now on with a source described by eq. (5.25). This EOS corresponds to several *different* situations. In particular, when $n = 4$, it corresponds to the simple MIT bag model of SQM (eq. [5.19]) and the case $A_2 = 0$ of eq. (5.21). In the remainder of the chapter we will perform the comparison between AKM and CMMR for the simple MIT bag model, but we will give formulae in terms of (a, b, n) whenever possible.

Nevertheless, it must be taken into account eqs. (5.26) to (5.28) have been derived under the assumption that eq. (5.25) gives the behaviour of some kind of

matter with only one component. Whenever we are interested in the numerical densities n_i of a system of N kinds of particles (as is the case of SQM in the simple MIT bag model, where $N = 3$) or in obtaining $p(n_i)$, $\epsilon(n_i)$, we must use eq. (5.15). In this way, when a grand potential that can be written as eq. (5.25) is actually

$$\hat{\Omega} = \sum_{i=1}^{N} \frac{a}{N} \hat{\mu}_i^n + b, \tag{5.30}$$

then

$$n_i = -\frac{an}{N} \hat{\mu}_i^{n-1}. \tag{5.31}$$

In the case all $\hat{\mu}_i$ and n_i are equal it gives, defining $\hat{\mu} := \hat{\mu}_i$, the $p(\hat{\mu})$, $\epsilon(\hat{\mu})$ relations already found in eqs. (5.27) and (5.28), but

$$p = -a\left(-\frac{Nn_i}{an}\right)^{\frac{n}{n-1}} - b, \tag{5.32}$$

$$\epsilon = \left[-\frac{1}{an} + a\left(-\frac{N}{an}\right)^n\right]^{\frac{1}{n-1}} (Nn_i)^{\frac{n}{n-1}} + b, \tag{5.33}$$

differ from the ones we would have obtained from eq. (5.26). The EOS is eq. (5.29) again, since it is insensitive to the value of a.

It is worth giving two more comments. First, as we already calculated in Chapter 2, the hydrostatic equilibrium of a perfect fluid leads to eq. (2.71)

$$\frac{d\psi}{\psi} = \frac{dp}{\epsilon(p) + p} \tag{5.34}$$

and, by integration,

$$\epsilon = b\left[(n-1)\left(\frac{\psi}{\psi_\Sigma}\right)^n + 1\right], \tag{5.35}$$

$$p = b\left[\left(\frac{\psi}{\psi_\Sigma}\right)^n - 1\right]. \tag{5.36}$$

Now, because of eq. (5.1) and eq. (5.3), h and $\hat{\mu}$ verify

$$\frac{dh}{h} = \frac{d\hat{\mu}}{\hat{\mu}} = \frac{dp}{\epsilon(p) + p} \tag{5.37}$$

as well so that

$$\frac{\psi}{\psi_\Sigma} = \frac{h}{h(0)} = \frac{\hat{\mu}}{\hat{\mu}(0)} \tag{5.38}$$

and accordingly, the dependence of ϵ and p on these three variables is the same, i.e.

$$\epsilon\left(\frac{\psi}{\psi_\Sigma}\right) = \epsilon\left(\frac{h}{h(0)}\right) = \epsilon\left(\frac{\hat{\mu}}{\hat{\mu}(0)}\right), \tag{5.39}$$

$$p\left(\frac{\psi}{\psi_\Sigma}\right) = p\left(\frac{h}{h(0)}\right) = p\left(\frac{\hat{\mu}}{\hat{\mu}(0)}\right). \tag{5.40}$$

These relations are useful to compare different calculation approaches, since numerical methods usually build stellar models with a heavy focus on h instead of our ψ. It also allows us to directly write eq. (5.36) in the form

$$p = b\left[(H+1)^n - 1\right] \tag{5.41}$$

that determines the p_i coefficients in eq. (5.7) that AKM uses as input.

Last, for the particular case we will study, $n = 4$ so that

$$p_1 = 4, \quad p_2 = 6, \quad p_3 = 4 \quad \text{and} \quad p_4 = 1. \tag{5.42}$$

The constant C of the AKM system of units when working with custom EOS corresponds to b in the linear EOS grand potential and to B in the simple MIT bag model. In the uniform density case, the third AKM dimensional constant is ϵ_0 instead, but since $n = 1$ it is again b in our linear EOS. Accordingly, we will work in $c = G = b = 1$ units unless otherwise stated, making explicit if $b = \epsilon_0$ or $b = B$ in some particular cases.

3. Comparing metric functions

Both CMMR and AKM compute all that is required to know the metric inside and outside a stellar model source with a certain EOS. Since it is an axisymmetric problem with equatorial symmetry, it is enough to find its value on a 90° sector. Then, the most straightforward way to compare their results in finding the absolute value of the relative difference between each metric component on every point of that sector. Nevertheless, two limitations arise from the use of a numerical the code.

1. First, the size of the sector computed by AKM is finite. Despite its internal use of conformal transformations to deal with asymptotic conditions, its results are restricted to a square region with the centre of the star in one vertex. Its size is customizable, as well as its resolution (see the next point), so getting information about big portions of the spacetime comes at the cost of either detail or computation time in both the AKM computation and the comparison procedure.

2. Next, AKM gives us the value of the functions necessary to find the 5 components of a metric written in LP coordinates but it only gives their values at the nodes of a coordinate grid. The number of nodes can be modified, nonetheless.

These features condition all the comparison procedure. We must choose the square sector of the spacetime to compare. We are interested in seeing both the interior and exterior behaviour of CMMR, but being a post-Minkowskian approximation it will give very good results in the far field zone, so we will focus on the spacetime inside and immediately around the source, where troubles may arise. AKM needs the size of the sector before attempting to build the model, but it can be adjusted through trial and error (or using data from similar models) to get the desired detail on the source. Additionally, we can only compare on the grid nodes of AKM. Hence we need in principle to find the coordinate change from our spherical-like coordinates to LP coordinates, take the AKM grid points and evaluate CMMR on them. Nevertheless, to build our matched spacetime on that grid we will need to decide if a certain point belongs to the interior or the exterior, so we have will have to resort to our surface and it is easier to deal with it in quasi-isotropic (QI) coordinates. Since they are simply related by eq. (5.8), we will use QI coordinates during the first part of the comparison. We will find the QI coordinates of each node of the AKM grid, and we could do the same with CMMR, getting the spherical-like label of each node of the grid, obtaining in this way the value of the metric functions in AKM and CMMR for each point. However, this would require as many coordinate changes as points in the grid so finding the expression of CMMR in QI coordinates straightaway is less resolution dependent and it is the procedure we choose. As a last step, from the set of grid points and relative errors on them we will build interpolate plots to show the behaviour of the error in every point of the sector, not just the nodes. This part requires the grids to be written in cylindrical-like coordinates, so we will change the QI labels of the points to the LP ones we already have from the original AKM input.

3.1. Finding quasi-isotropic coordinates

If we want to write in QI coordinates $\{t, R, \Theta, \phi\}$ a line-element with general Papapetrou structure, it is easier to find LP coordinates $\{t, \varrho, \zeta, \phi\}$, first. To do so, we require a conformal change from its expression on the bidimensional $\{t = \text{const.}, \phi = \text{const.}\}$ planes

$$dl^2 = g_{rr}dr^2 + 2g_{r\theta}drd\theta + g_{\theta\theta}d\theta^2 \tag{5.43}$$

to

$$dl^2 = f(\varrho,\zeta)\left(d\varrho^2 + d\zeta^2\right). \tag{5.44}$$

A simple way to do it is the following. If we decompose eq. (5.44) in two factors

$$dl^2 = f(\varrho,\zeta)\left(d\varrho^2 + d\zeta^2\right) = e(\varrho,\zeta)\bar{e}(\varrho,\zeta)\left(d\varrho + \mathrm{i}d\zeta\right)\left(d\varrho - \mathrm{i}d\zeta\right) \tag{5.45}$$

we see that if we do the same with eq. (5.43)

$$\begin{aligned} dl^2 &= g_{rr}dr^2 + 2g_{r\theta}drd\theta + g_{\theta\theta}d\theta^2 \\ &= \left(\sqrt{g_{rr}}dr + \frac{g_{r\theta} + \mathrm{i}\sqrt{\hat{g}}}{\sqrt{g_{rr}}}d\theta\right)\left(\sqrt{g_{rr}}dr + \frac{g_{r\theta} - \mathrm{i}\sqrt{\hat{g}}}{\sqrt{g_{rr}}}d\theta\right) \end{aligned} \tag{5.46}$$

where $\hat{g} := g_{rr}g_{\theta\theta} - g_{r\theta}^2$, all we need to do is to find the coordinate change $\varphi : (r,\theta) \to \left(\varrho : \varrho(r,\theta),\ \zeta = \zeta(r,\theta)\right)$ that verifies

$$\left(\sqrt{g_{rr}}dr + \frac{g_{r\theta} + \mathrm{i}\sqrt{\hat{g}}}{\sqrt{g_{rr}}}d\theta\right) = \varphi_*\left(e\left(d\varrho + \mathrm{i}d\zeta\right)\right) \tag{5.47}$$

$$= \varphi^{-1}(e)\left[\left(\frac{\partial\varrho}{\partial r} + \mathrm{i}\frac{\partial\zeta}{\partial r}\right)dr + \left(\frac{\partial\varrho}{\partial\theta} + \mathrm{i}\frac{\partial\zeta}{\partial\theta}\right)d\theta\right]. \tag{5.48}$$

This leads to

$$\left[\sqrt{g_{rr}} - \varphi^{-1}(e)\left(\frac{\partial\varrho}{\partial r} + \mathrm{i}\frac{\partial\zeta}{\partial r}\right)\right]dr = 0, \tag{5.49}$$

$$\left[\frac{g_{r\theta} + \mathrm{i}\sqrt{\hat{g}}}{\sqrt{g_{rr}}} - \varphi^{-1}(e)\left(\frac{\partial\varrho}{\partial\theta} + \mathrm{i}\frac{\partial\zeta}{\partial\theta}\right)\right]d\theta = 0, \tag{5.50}$$

and from here we can extract partial differential equations on φ eliminating $\varphi^{-1}(e)$ so that

$$\left(\frac{\partial\varrho}{\partial r} + \mathrm{i}\frac{\partial\zeta}{\partial r}\right) = \frac{g_{rr}}{g_{r\theta} + \mathrm{i}\sqrt{\hat{g}}}\left(\frac{\partial\varrho}{\partial\theta} + \mathrm{i}\frac{\partial\zeta}{\partial\theta}\right), \tag{5.51}$$

whose real and imaginary parts give the equations

$$g_{r\theta}\frac{\partial\varrho}{\partial r} - \sqrt{\hat{g}}\frac{\partial\zeta}{\partial r} = g_{rr}\frac{\partial\varrho}{\partial\theta}, \tag{5.52}$$

$$\sqrt{\hat{g}}\frac{\partial\varrho}{\partial r} + g_{r\theta}\frac{\partial\zeta}{\partial r} = g_{rr}\frac{\partial\zeta}{\partial\theta}, \tag{5.53}$$

that can be rearranged giving finally the conditions on φ

$$\begin{cases} \dfrac{\partial\varrho}{\partial r} = \dfrac{1}{\sqrt{\hat{g}}}\left(g_{rr}\dfrac{\partial\zeta}{\partial\theta} - g_{r\theta}\dfrac{\partial\zeta}{\partial r}\right), \\ \dfrac{\partial\varrho}{\partial\theta} = \dfrac{1}{\sqrt{\hat{g}}}\left(g_{r\theta}\dfrac{\partial\zeta}{\partial\theta} - g_{\theta\theta}\dfrac{\partial\zeta}{\partial r}\right). \end{cases} \tag{5.54a}$$

and

$$\begin{cases} \dfrac{\partial\zeta}{\partial r} = \dfrac{1}{\sqrt{\hat{g}}}\left(g_{r\theta}\dfrac{\partial\varrho}{\partial r} - g_{rr}\dfrac{\partial\varrho}{\partial\theta}\right), \\ \dfrac{\partial\zeta}{\partial\theta} = \dfrac{1}{\sqrt{\hat{g}}}\left(g_{\theta\theta}\dfrac{\partial\varrho}{\partial r} - g_{r\theta}\dfrac{\partial\varrho}{\partial\theta}\right). \end{cases} \tag{5.54b}$$

These equations (their derivation can be found in Dubrovin *et al.*, 1985) have two good properties. On one hand, imposing integrability conditions on them so that

$$\frac{\partial}{\partial\theta}\frac{\varrho}{\partial r} = \frac{\partial}{\partial r}\frac{\varrho}{\partial\theta} \quad \text{and} \quad \frac{\partial}{\partial\theta}\frac{\zeta}{\partial r} = \frac{\partial}{\partial r}\frac{\zeta}{\partial\theta}, \tag{5.55}$$

we get

$$\begin{aligned} \epsilon^{ab}\partial_a\left(\frac{1}{\sqrt{\hat{g}}}\epsilon^{cd}g_{bc}\partial_d\right)\zeta = 0, \\ \epsilon^{ab}\partial_a\left(\frac{1}{\sqrt{\hat{g}}}\epsilon^{cd}g_{bc}\partial_d\right)\varrho = 0, \end{aligned} \qquad (a,b,c,d = 1,2) \tag{5.56}$$

respectively, where ϵ^{ab} is the bidimensional Levi-Civita symbol. Because of their structure, they can be rewritten as Laplace equations

$$g^{ab}\nabla_a\nabla_b\zeta = 0, \tag{5.57}$$

$$g^{ab}\nabla_a\nabla_b\varrho = 0 \tag{5.58}$$

and hence when g_{ab} components are analytical these equations are solvable and accordingly the systems eqs. (5.54a) and (5.54b) are integrable. On the other hand, if we take eq. (5.54a) and use it to replace the terms $\partial\varrho/\partial r$ and $\partial\varrho/\partial\theta$ appearing in eq. (5.54b), we get an identity. Thus, we can find the change to quasi-isotropic coordinates if first we find a function $\zeta(r,\theta)$ satisfying the Laplacian equation eq. (5.57). Since its general solution is a power series of r^i with positive (in the interior) or negative (in the exterior) exponents and Legendre polynomials, it can be found adjusting coefficients in a general enough ansatz. Then, we use it to build the rhs of eq. (5.54a) and solve it to get ϱ. Because of the form of ζ, the integration of this differential equation is straightforward. Once we find ϱ we have finished since, as already discussed, this set of (ζ,ϱ) identically satisfies eq. (5.54b).

Using this procedure with the CGMR metric eqs. (3.14) and (3.17), once we solve these two differential equations, we get the $\mathcal{O}(\lambda^2,\Omega^2)$ change in the interior

$$\frac{\varrho_I}{r\sin\theta} = 1+\lambda^2\eta^2\left\{\frac{c_1}{\eta^2}+\frac{3}{20}-\frac{\eta^2}{28}+\Omega^2\left[-\frac{5\eta^2}{448}-\frac{1}{35}+c_2+\cos 2\theta\left(-\frac{5\eta^2}{96}+2c_2\right)\right]\right\}, \tag{5.59}$$

$$\frac{\zeta_I}{r\cos\theta} = 1+\lambda^2\eta^2\left\{\frac{c_1}{\eta^2}+\frac{3}{20}-\frac{\eta^2}{28}+\Omega^2\left[-\frac{43\eta^2}{1344}+\frac{4}{35}-c_2+\cos 2\theta\left(-\frac{5\eta^2}{96}+2c_2\right)\right]\right\} \tag{5.60}$$

and the exterior

$$\frac{\varrho_E}{r\sin\theta} = 1+\frac{\lambda^2}{\eta^2}\left\{\frac{4}{35\eta}+d_1+\Omega^2\left[-\frac{1}{14\eta^3}+\frac{2}{105\eta}+\frac{1}{32\eta^2}+\frac{d_2}{\eta^2}\right.\right.$$
$$\left.\left.+\cos 2\theta\left(-\frac{5}{42\eta^3}+\frac{2d_2}{\eta^2}\right)\right]\right\}, \tag{5.61}$$

$$\frac{\zeta_E}{r\cos\theta} = 1+\frac{\lambda^2}{\eta^2}\left\{\frac{4}{35\eta}-\frac{1}{2}-d_1+\Omega^2\left[\frac{1}{42\eta^3}+\frac{2}{105\eta}-\frac{5}{32\eta^2}+\frac{d_2}{\eta^2}\right.\right.$$
$$\left.\left.+\cos 2\theta\left(-\frac{5}{42\eta^3}+\frac{5}{16\eta^2}-\frac{2d_2}{\eta^2}\right)\right]\right\}. \tag{5.62}$$

In these expression we have used the same r, θ in $\mathcal{V}^-$ and $\mathcal{V}^+$ trying not to overload notation. Also, the constants c_1, c_2, d_1, d_2 are not necessary for the change to LP coordinates so we could drop them, but if we want to preserve the C^1 character of the metrics across the surface, we need to impose continuity of each pair $\{\varrho_I, \varrho_E\}$ and $\{\zeta_I, \zeta_E\}$ and their derivatives on the surface. From these conditions, we get the values of the constants:

$$\begin{cases} c_1 = -\dfrac{1}{4}-\dfrac{\Omega^2}{96}, \\ c_2 = \dfrac{5}{112}, \end{cases} \qquad \begin{cases} d_1 = -\left(\dfrac{1}{4}+\dfrac{\Omega^2}{16}\right), \\ d_2 = \dfrac{5}{64}. \end{cases} \tag{5.63}$$

With this we have determined φ. Together with eq. (5.8) it gives us $R(r,\theta)$, $\Theta(r,\theta)$, and inverting these relations we finally have the change to QI coordinates. Its expression inside the source is (dropping I and E subindices in coordinates where there is no need of extra clarification), for the radial coordinate

$$\frac{r}{R} = 1+\lambda^2\left\{\frac{1}{4}-\frac{3\hat{R}^2}{20}+\frac{\hat{R}^4}{28}+\Omega^2\left[\frac{1}{96}+\frac{41\hat{R}^2}{560}-\frac{55\hat{R}^4}{1344}+\cos^2\Theta\left(-\frac{13\hat{R}^2}{56}+\frac{\hat{R}^4}{8}\right)\right]\right\}$$
$$+\mathcal{O}(\lambda^3,\Omega^4) \tag{5.64}$$

and for the azimuthal

$$\cos\theta = \cos\Theta+\frac{1}{336}\lambda^2\Omega^2\hat{R}^2\left(-18+7\hat{R}^2\right)\sin^2\Theta\cos\Theta+\mathcal{O}(\lambda^3,\Omega^4). \tag{5.65}$$

With them, the line element of the $t = \phi = $ const. surfaces has the expression $f^I(R,\Theta)(dR^2 + R^2 d\Theta^2)$ with

$$f^I(R,\Theta) = 1 + \lambda\left(3 - \hat{R}^2 - \Omega^2\hat{R}^2 P_2\right) + \lambda^2\left(12 + \frac{3n}{4} + \left(-\frac{11}{2} - \frac{n}{2}\right)\hat{R}^2 + \left(\frac{3}{5} + \frac{3n}{20}\right)\hat{R}^4 + \Omega^2\left\{\frac{27}{16} - \frac{n}{2} + \left(-\frac{23}{24} + \frac{n}{3}\right)\hat{R}^2 + \left(\frac{127}{480} - \frac{n}{10}\right)\hat{R}^4 + \left[\left(-\frac{303}{70} - \frac{3n}{14}\right)\hat{R}^2 + \left(\frac{37}{42} + \frac{5n}{14}\right)\hat{R}^4\right]P_2\right\}\right) + \mathcal{O}(\lambda^3, \Omega^4) \tag{5.66}$$

where P_i^j stand now for the associated Legendre polynomials $P_i^j(\cos\Theta)$ and we have introduced $\hat{R} = \frac{R}{r_s}$, the equivalent in QI coordinates of η to simplify the expressions. The other metric components are

$$g^I_{tt} = -1 + \lambda\left(3 - \hat{R}^2 - \Omega^2\hat{R}^2 P_2\right) + \lambda^2\left(\frac{9}{2} + \frac{3n}{4} + \left(-1 - \frac{n}{2}\right)\hat{R}^2 + \left(\frac{1}{10} + \frac{3n}{20}\right)\hat{R}^4 + \Omega^2\left\{1 - \frac{n}{2} + \left(\frac{2}{3} + \frac{n}{3}\right)\hat{R}^2 + \left(-\frac{3}{5} - \frac{n}{10}\right)\hat{R}^4 + \left[\left(-\frac{29}{35} - \frac{3n}{14}\right)\hat{R}^2 + \left(\frac{5}{7} + \frac{5n}{14}\right)\hat{R}^4\right]P_2\right\}\right) + \mathcal{O}(\lambda^3, \Omega^4), \tag{5.67}$$

$$g^I_{t\phi} = \lambda^{3/2}\left(\Omega\left(2\hat{R} - \frac{6\hat{R}^3}{5}\right)P_1^1 + \Omega^3\left(\frac{2\hat{R}}{3}P_1^1 - \frac{2\hat{R}^3}{7}P_3^1\right)\right) + \lambda^{5/2}\left(\Omega\left[\left(\frac{49}{5} + \frac{n}{2}\right)\hat{R} + \left(-\frac{34}{5} - \frac{3n}{5}\right)\hat{R}^3 + \left(\frac{27}{35} + \frac{3n}{14}\right)\hat{R}^5\right]P_1^1 + \Omega^3\left\{\left[\left(\frac{289}{105} - \frac{5n}{14}\right)\hat{R} + \left(\frac{8}{15} + \frac{2n}{5}\right)\hat{R}^3 + \left(-\frac{3}{5} - \frac{3n}{14}\right)\hat{R}^5\right]P_1^1 + \left[\left(-\frac{326}{245} - \frac{3n}{49}\right)\hat{R}^3 + \left(\frac{34}{105} + \frac{n}{9}\right)\hat{R}^5\right]P_3^1\right\}\right) + \mathcal{O}(\lambda^{7/2}, \Omega^5), \tag{5.68}$$

$$g^I_{\phi\phi} = 1 + \lambda\left(3 - \hat{R}^2 - \Omega^2\hat{R}^2 P_2\right) + \lambda^2\left(\frac{23}{2} + \frac{3n}{4} + \left(-\frac{26}{5} - \frac{n}{2}\right)\hat{R}^2 + \left(\frac{37}{70} + \frac{3n}{20}\right)\hat{R}^4 + \Omega^2\left\{\frac{5}{3} - \frac{n}{2} + \left(-\frac{16}{105} + \frac{n}{3}\right)\hat{R}^2 + \left(-\frac{193}{630} - \frac{n}{10}\right)\hat{R}^4 + \left[\left(-\frac{517}{105} - \frac{3n}{14}\right)\hat{R}^2 + \left(\frac{167}{126} + \frac{5n}{14}\right)\hat{R}^4\right]P_2\right\}\right) + \mathcal{O}(\lambda^3, \Omega^4). \tag{5.69}$$

Now, in the exterior, the change to QI coordinates is

$$\frac{r}{R} = 1 + \lambda^2 \left\{ \frac{1}{4\hat{R}^2} - \frac{4}{35\hat{R}^3} + \Omega^2 \left[\frac{1}{16\hat{R}^2} - \frac{2}{105\hat{R}^3} + \frac{3}{64\hat{R}^4} - \frac{1}{21\hat{R}^5} + \left(-\frac{1}{8\hat{R}^2} - \frac{1}{8\hat{R}^4} + \frac{1}{7\hat{R}^5} \right) \cos^2\Theta \right] \right\} + \mathcal{O}(\lambda^3, \Omega^4)$$

and

$$\cos\theta = \cos\Theta - \lambda^2\Omega^2 \frac{\left(32 - 63\hat{R} + 42\hat{R}^3\right)}{336\hat{R}^5} \sin^2\Theta \cos\Theta + \mathcal{O}(\lambda^3, \Omega^4) \tag{5.70}$$

what gives the line element $f^E(R, \Theta)(dR^2 + R^2 d\Theta^2)$ with

$$f^E(R, \Theta) = 1 + \lambda \left(\frac{2}{\hat{R}} - \frac{1}{\hat{R}^3}\Omega^2 P_2 \right) + \lambda^2 \left(\left(\frac{28}{5} + \frac{2n}{5} \right) \frac{1}{\hat{R}} + \frac{3}{2\hat{R}^2} + \Omega^2 \left\{ \left(\frac{16}{15} - \frac{4n}{15} \right) \frac{1}{\hat{R}} - \frac{1}{24\hat{R}^2} - \frac{1}{32\hat{R}^4} + \left[\frac{1}{6\hat{R}^2} + \left(-\frac{74}{35} + \frac{n}{7} \right) \frac{1}{\hat{R}^3} - \frac{3}{2\hat{R}^4} \right] P_2 \right\} \right) + \mathcal{O}(\lambda^3, \Omega^4) \tag{5.71}$$

and the rest of the exterior metric is

$$g^E_{tt} = -1 + \lambda \left(\frac{2}{\hat{R}} - \frac{1}{\hat{R}^3}\Omega^2 P_2 \right) + \lambda^2 \left(\left(\frac{28}{5} + \frac{2n}{5} \right) \frac{1}{\hat{R}} - \frac{2}{\hat{R}^2} + \Omega^2 \left\{ \left(\frac{16}{15} - \frac{4n}{15} \right) \frac{1}{\hat{R}} + \left[\left(-\frac{74}{35} + \frac{n}{7} \right) \frac{1}{\hat{R}^3} + \frac{2}{\hat{R}^4} \right] P_2 \right\} \right) + \mathcal{O}(\lambda^3, \Omega^4), \tag{5.72}$$

$$g^E_{t\phi} = \lambda^{3/2} \left[\frac{4}{5} \frac{1}{\hat{R}^2} \Omega P_1^1 + \Omega^3 \left(\frac{2}{3\hat{R}^2} P_1^1 - \frac{2}{7\hat{R}^4} P_3^1 \right) \right] + \lambda^{5/2} \left(\Omega \left[\left(\frac{32}{7} + \frac{4n}{35} \right) \frac{1}{\hat{R}^2} - \frac{4}{5\hat{R}^3} \right] P_1^1 + \Omega^3 \left\{ \left[\left(\frac{352}{105} - \frac{6n}{35} \right) \frac{1}{\hat{R}^2} - \frac{2}{3\hat{R}^3} \right] P_1^1 + \left[\left(-\frac{992}{735} + \frac{22n}{441} \right) \frac{1}{\hat{R}^4} + \frac{12}{35\hat{R}^5} \right] P_3^1 \right\} \right) + \mathcal{O}(\lambda^{7/2}, \Omega^4), \tag{5.73}$$

$$g^E_{\phi\phi} = 1 + \lambda \left(\frac{2}{\hat{R}} - \frac{1}{\hat{R}^3}\Omega^2 P_2 \right) + \lambda^2 \left(\left(\frac{28}{5} + \frac{2n}{5} \right) \frac{1}{\hat{R}} + \frac{1}{\hat{R}^2} + \frac{8}{35\hat{R}^3} + \Omega^2 \left\{ \left(\frac{16}{15} - \frac{4n}{15} \right) \frac{1}{\hat{R}} + \frac{4}{105\hat{R}^3} + \frac{1}{6\hat{R}^4} - \frac{4}{63\hat{R}^5} + \left[\left(-\frac{74}{35} + \frac{n}{7} \right) \frac{1}{\hat{R}^3} - \frac{7}{6\hat{R}^4} - \frac{20}{63\hat{R}^5} \right] P_2 \right\} \right) + \mathcal{O}(\lambda^3, \Omega^4). \tag{5.74}$$

3.2. *Setting up the metrics for comparison*

After a successful run, AKM gives, besides some properties of the source, the line-element of the sector of spacetime in the form

$$ds^2 = -\hat{B}^2 \mathrm{e}^{2\hat{u}} dt^2 + \mathrm{e}^{2\alpha}\left(d\zeta^2 + d\varrho^2\right) + \varrho^2 e^{-2\hat{u}}\left(d\phi - \hat{\omega} dt\right)^2 . \tag{5.75}$$

It is contained in a multi-column file where each row gives all the data corresponding to each point. It is organised as follows.

- Columns #1 and #2 give ϱ^2 and ζ^2, respectively.
- Column #3 contains the value of $\hat{u}$ and #4 and #5 its partial derivatives with respect to ϱ^2 and ζ^2.
- Columns #6, #7 and #8 corresponds to the function $\hat{B}$ and its derivatives,
- columns #9, #10 and #11 to $\hat{\omega}$ and its derivatives and
- finally, columns #12 – #14 give α and its derivatives as well.

From the two first columns we can extract the LP coordinates of all the grid points. We can obtain the value of the metric components on each of them from the rest of the columns straightforwardly as

$$g_{tt} = -\hat{B}^2 \mathrm{e}^{2\hat{u}} + \mathrm{e}^{-2\hat{u}} \varrho^2 \hat{\omega}^2, \tag{5.76}$$
$$g_{t\phi} = -\mathrm{e}^{-2\hat{u}} \varrho^2 \hat{\omega} \tag{5.77}$$
$$g_{\phi\phi} = \mathrm{e}^{-2\hat{u}} \varrho^2 \tag{5.78}$$
$$g_{\varrho\varrho} = \mathrm{e}^{2\alpha} \tag{5.79}$$
$$g_{\zeta\zeta} = \mathrm{e}^{2\alpha} \tag{5.80}$$

Now we can focus on building the corresponding part of spacetime from CGMR. First we take the AKM grid and change its points to QI coordinates inverting eq. (5.8) to get the usual

$$R = \sqrt{\varrho^2 + \zeta^2}, \qquad \Theta = \arcsin \frac{\varrho}{\sqrt{\varrho^2 + \zeta^2}}. \tag{5.81}$$

Next, we evaluate the surface equation at the corresponding approximation order at each grid point p_g. If the R coordinate of the point is lower than $R_\Sigma(\Theta(p_g))$, we use the QI interior eq. (5.69) to find $g_{\alpha\beta}(p_g)$. Otherwise, we use the exterior formulae eq. (5.74). Afterwards, we revert the coordinates of the grid points to

LP coordinates and find the relative error between the AKM and CGMR value of each component $g_{\alpha\beta}(p_g)$

$$\varepsilon\left[g_{\alpha\beta}(p_g)\right] = \left|\frac{g^{\mathrm{AKM}}_{\alpha\beta}(p_g) - g^{\mathrm{CGMR}}_{\alpha\beta}(p_g)}{g^{\mathrm{AKM}}_{\alpha\beta}(p_g)}\right|. \tag{5.82}$$

Finally, we take each set of grid and relative error and make interpolated contour plots of the data using a modification of the `ContourPlot` command from *Mathematica*.

3.3. *The surfaces*

To get a better understanding of the behaviour of the plots of the relative errors $\varepsilon\left[g_{\alpha\beta}(p_g)\right]$, knowing the shape and position of the AKM and CGMR surfaces is a key step. In the case of CGMR, this points can be identified noticing where the switch from interior to exterior metric occurs. This must be done ranging first along ϱ = const. lines and afterwards following ζ = const. ones to ensure that no point is missing, but otherwise it is just an algorithmic exercise. The AKM case is a little different. AKM gives a file with the coordinates of the surface points (and the ergosurface, if any), and while it is straightforward to make them appear in the plots, they do not necessarily belong to the grid the program used to compute the metric. Since we want to compare the surfaces mainly to give information about the metric component plots, we need to get both of them in terms of the original grid points. We have found no other way to do so in the AKM case but finding the grid points lying closest to the ones in the surface file.

4. Physical properties compared

We can get more information about how well CMMR performs if, besides the direct comparison of metric functions, we extract as many physical parameters from our metric as possible and compare them with the ones AKM provides. We can see if and how the precision obtained in the metric functions correlates with the one in the physical properties, check which of them are more sensitive to higher values of mass and rotation and also get estimates about the behaviour of errors. With the calculation of these properties we will be obtaining from CMMR a kind of information that we have not cared about before, setting up the bridge from the more theoretical focus of previous chapters to different line of work, the analysis of our solutions to shed some light about source models and observation.

Here we give the definitions of the physical properties that will be later used in the comparison with AKM, along with some others that, while not being part of

the AKM output, are commonly found in other relevant works such as Friedman *et al.* (1986); Nozawa *et al.* (1998); Gourgoulhon *et al.* (1999a). We write the corresponding approximate expressions obtained from the $\mathcal{O}(\lambda^{9/2}, \Omega^3)$ CGMR metric as well.

4.1. Masses, energies and moments

We start with the definitions of quantities associated with masses, energies and momenta of the source.

- Baryon mass $M_{\rm b}$. Let us define $n_{\rm b}$ as the particle density as seen by an observer at rest with the fluid. Now, due to the kind of flow inside the source we deal with,

$$u^\alpha = \psi\left(\xi^\alpha + \omega\zeta^\alpha\right), \tag{5.83}$$

the baryon 4-current in the fluid $j^\alpha_{\rm b} := n_{\rm b}u^\alpha$ is a conserved quantity ($\nabla_\alpha j^\alpha_{\rm b} = 0$). Thanks to this, we can evaluate the integral that defines the total number of baryons in the source

$$N_{\rm b} := -\int_{\Sigma_t} j^\alpha_{\rm b} n_\alpha \sqrt{\gamma} dx^1 dx^2 dx^3 \tag{5.84}$$

independently of the time-like hypersurface Σ_t chosen. In this expression, n^α is the unit normal vector to Σ_t and γ is the determinant of the restriction of the metric to this hypersurface, $\gamma_{ij} = g_{ij} + n_i n_j$. The most convenient choice of Σ_t gives

$$\boldsymbol{n} = -\sqrt{-g_{tt}}dt \tag{5.85}$$

so that $\gamma_{ij} = g_{ij}$ and $(x^1, x^2, x^3) = (R, \Theta, \phi)$. Having fixed n_α in this way, we have $u^\alpha n_\alpha = -\psi\sqrt{-g_{tt}}$ and then

$$N_{\rm b} = \int_{\Sigma_t} \psi\sqrt{-g_{tt}} n_{\rm b} \sqrt{\gamma} dR d\Theta d\phi \tag{5.86}$$

It is worth noting that in $-j^\alpha_b n_\alpha = \psi\sqrt{-g_{tt}} n_{\rm b}$ gives the number density that would be measured by the observers following the congruence n^α, that in this case corresponds to locally non-rotating observers (Bardeen, 1970), and $\psi\sqrt{-g_{tt}}$ is the associated Lorentz correction. With $N_{\rm b}$, the total baryon mass is defined as $M_{\rm b} = m_{\rm b}N_{\rm b}$, where $m_{\rm b}$ is the mean rest mass per baryon that is usually taken as $m_{\rm b} = 1.66 \times 10^{-27}$ kg. This standard approach is followed, e.g., by Gourgoulhon *et al.* (1999a). Nevertheless, when one is interested in working in the units AKM uses for custom EOS, i.e. units where ($c = G =$

$b = 1$) with b a constant with energy density units, one must first find the value of the dimensionless $\bar{m}_\mathrm{b}$ in

$$m_\mathrm{b} = \bar{m}_\mathrm{b} \frac{c^4}{G^{3/2} b^{1/2}} \tag{5.87}$$

and this implies fixing a value for b. We are interested in giving scalable results, and the common solution for this is to pick a reference value, b_ref, calculate the new value of the dimensionless part $\bar{m}'_\mathrm{b}$ with it and rewrite m_b in terms of the dimensionless ratio $b_\# := b/b_\mathrm{ref}$ so that

$$m_\mathrm{b} = \bar{m}'_\mathrm{b} b_\#^{1/2} \frac{c^4}{G^{3/2} b^{1/2}} \tag{5.88}$$

remains constant independently of the b we choose. Accordingly, the baryon mass in AKM units $\bar{M}_\mathrm{b}$ is

$$\frac{\bar{M}_\mathrm{b}}{b_\#^{1/2}} = \bar{m}'_\mathrm{b} N_\mathrm{b}. \tag{5.89}$$

The presence of $b_\#$ is usual in models for, e.g., strange stars, but it can be avoided if we are able to introduce the constant m_b into the problem through a quantity expressively in terms of only c and G. Actually, this is what AKM does. One of its input data is the specific enthalpy at zero pressure, $h(0)$ (5.5), that from the definition of specific enthalpy (5.1) can be written as

$$h(0) = \frac{\epsilon(0)}{\mu_\mathrm{b}(0)} = \frac{\epsilon(0)}{m_\mathrm{b} n_\mathrm{b}(0)} = \bar{h}(0) c^2. \tag{5.90}$$

They use it to find an alternate expression for $\mu_\mathrm{b} = m_\mathrm{b} n_\mathrm{b}$ and integrate it to directly get M_b as

$$M_\mathrm{b} = \int_{\Sigma_t} \psi \sqrt{-g_{tt}} \mu_\mathrm{b} \sqrt{\gamma} dR d\Theta d\phi. \tag{5.91}$$

This alternate expression is essentially the Gibbs-Duhem relation (5.4) that, using eq. (5.6), they rewrite to work inside their code as

$$\mu_\mathrm{b} = \frac{1}{h(0)} \frac{dp}{dH}. \tag{5.92}$$

We can find the equivalent expression in terms of ψ using equations (5.36) and (5.38) so that

$$p = b \left[\left(\frac{\psi}{\psi_\Sigma} \right)^n - 1 \right] = b \left[\left(\frac{h}{h(0)} \right)^n - 1 \right] \tag{5.93}$$

and then

$$\mu_{\rm b} = \frac{dp}{dh} = \frac{nb}{h(0)}\left(\frac{h}{h(0)}\right)^{n-1} = \frac{nb}{h(0)}\left(\frac{\psi}{\psi_\Sigma}\right)^{n-1}, \tag{5.94}$$

that allows us to give $M_{\rm b}$ in $c = G = b = 1$ units totally free of any $b_\#$ to compare directly with the AKM result.

Working this way the CGMR baryon rest-mass is

$$\begin{aligned}\frac{h(0)}{r_s}M_{\rm b} = {}& \lambda + \lambda^2\left[\frac{17}{5} + \frac{n}{5} + \left(\frac{1}{3} - \frac{2n}{15}\right)\Omega^2\right] \\ & + \lambda^3\left[\frac{969}{70} + \frac{72n}{35} + \frac{3n^2}{35} + \left(\frac{403}{105} - \frac{25n}{21} - \frac{8n^2}{105}\right)\Omega^2\right] \\ & + \lambda^4\left[\frac{12997}{210} + \frac{1441n}{90} + \frac{767n^2}{525} + \frac{74n^3}{1575}\right. \\ & \left. + \left(\frac{98369}{3150} - \frac{1257n}{175} - \frac{2059n^2}{1575} - \frac{4n^3}{75}\right)\Omega^2\right] + \mathcal{O}(\lambda^5, \Omega^4).\end{aligned} \tag{5.95}$$

We obtain the value of $h(0)$ for the general linear EOS imposing $p = 0$ on eqs. (5.31) to (5.33) to get

$$n_{\rm b}(0) = \frac{nb}{N}\left(-\frac{a}{b}\right)^{1/n} \tag{5.96}$$

$$\epsilon_0 = nb \tag{5.97}$$

that gives

$$h(0) = \frac{\epsilon_0}{m_{\rm b} n_{\rm b}(0)} = \frac{N}{m_{\rm b}}\left(-\frac{b}{a}\right)^{1/n}. \tag{5.98}$$

For the simple MIT bag model for SQM considered, where $a = -\frac{3}{4\pi^2}\frac{1}{(c\hbar)^3}$, $b = B$, $n = 4$ and $N = 3$, it takes the value (in B, c units)

$$\begin{aligned}h(0) &= \frac{3^{3/4}\left(Bc^3\hbar^3\right)^{1/4}\sqrt{2\pi}}{m_{\rm b}} = \frac{3^{3/4}c^2\bar{\hbar}^{3/4}\sqrt{2\pi}}{\bar{m}_{\rm b}} \\ &= 0.899124c^2.\end{aligned} \tag{5.99}$$

- Gravitational mass $\tilde{M}_0$. It can be read directly from the exterior metric or integrated from the interior spacetime using (see Wald, 1984, e.g.)

$$\tilde{M}_0 = 2\int_{\Sigma_t}\left(T_{\lambda\mu} - \frac{1}{2}T^{\nu}{}_{\nu}g_{\lambda\mu}\right)n^{\lambda}\xi^{\mu}\sqrt{\gamma}d^3x. \tag{5.100}$$

We get it directly from the Lichnerowicz matching

$$\begin{aligned}\frac{\tilde{M}_0}{r_s} &= \lambda + \lambda^2\left[\frac{14}{5} + \frac{n}{5} + \left(\frac{8}{15} - \frac{2n}{15}\right)\Omega^2\right] \\ &+ \lambda^3\left[\frac{73}{7} + \frac{64n}{35} + \frac{3n^2}{35} + \left(\frac{488}{105} - \frac{36n}{35} - \frac{8n^2}{105}\right)\Omega^2\right] \\ &+ \lambda^4\left[\frac{13894}{315} + \frac{4169n}{315} + \frac{2116n^2}{1575} + \frac{74n^3}{1575} + \left(\frac{1468}{45} - \frac{918n}{175} - \frac{376n^2}{315}\right.\right. \\ &\left.\left. - \frac{4n^3}{75}\right)\Omega^2\right] + \mathcal{O}(\lambda^5, \Omega^4),\end{aligned} \tag{5.101}$$

though evaluating the integral as well could lead to an estimation of the error. We will compute GRV3 for this purpose, though.

- Proper mass $M_{\rm p}$. Represents the energy of the configuration excluding rotational and gravitational potential energies (Cook *et al.*, 1992). Has a definition similar to the baryon mass, but including the internal energy density $\epsilon_{\rm int}$ between the particles. Since the energy density is the result of adding it to the energy due to the rest-mass of the particles, $\epsilon = \epsilon_{\rm b} + \epsilon_{\rm int}$, its expression is

$$M_{\rm p} = \int_{\Sigma_t}\epsilon\psi\sqrt{-g_{tt}}\,\sqrt{\gamma}dRd\Theta d\phi. \tag{5.102}$$

what leads to

$$\begin{aligned}\frac{M_{\rm p}}{r_s} &= \lambda + \lambda^2\left[\frac{17}{5} + \frac{n}{5} + \left(\frac{1}{3} - \frac{2n}{15}\right)\Omega^2\right] \\ &+ \lambda^3\left[\frac{967}{70} + \frac{73n}{35} + \frac{3n^2}{35} + \left(\frac{407}{105} - \frac{43n}{35} - \frac{8n^2}{105}\right)\Omega^2\right] \\ &+ \lambda^4\left[\frac{194029}{3150} + \frac{51287n}{3150} + \frac{334n^2}{225} + \frac{74n^3}{1575} + \left(\frac{33161}{1050} - \frac{3938n}{525}\right.\right. \\ &\left.\left. - \frac{47n^2}{35} - \frac{4n^3}{75}\right)\Omega^2\right] + \mathcal{O}(\lambda^5, \Omega^4)\end{aligned} \tag{5.103}$$

- Binding energy $E_{\rm bind}$. Is the difference between the gravitational and baryon masses

$$E_{\rm bind} = \tilde{M}_0 - M_{\rm b}. \tag{5.104}$$

It is not different enough from the separate expressions of both quantities to be worth writing.

- Mass quadrupole M_2. Can be read directly from the exterior metric

$$\begin{aligned}\frac{M_2}{r_s^3} = &-\frac{\lambda\Omega^2}{2} + \left(-\frac{37}{35} + \frac{n}{14}\right)\lambda^2\Omega^2 + \left(-\frac{83927}{22050} + \frac{128n}{735} + \frac{10n^2}{441}\right)\lambda^3\Omega^2 \\ &+ \left(-\frac{4856219}{282975} - \frac{476479n}{1697850} + \frac{6443n^2}{33957} + \frac{67n^3}{6174}\right)\lambda^4\Omega^2 + \mathcal{O}(\lambda^5, \Omega^4).\end{aligned} \tag{5.105}$$

- Angular momentum $\tilde{J}_1$. Appears in the exterior metric as well

$$\begin{aligned}\frac{\tilde{J}_1}{r_s^2} = &\lambda^{3/2}\left(\frac{2\Omega}{5} + \frac{\Omega^3}{3}\right) + \lambda^{5/2}\left[\left(\frac{16}{7} + \frac{2n}{35}\right)\Omega + \left(\frac{176}{105} - \frac{3n}{35}\right)\Omega^3\right] \\ &+ \lambda^{7/2}\left[\left(\frac{18896}{1575} + \frac{76n}{75} + \frac{34n^2}{1575}\right)\Omega + \left(\frac{34889}{3675} - \frac{494n}{735} - \frac{124n^2}{3675}\right)\Omega^3\right] \\ &+ \lambda^{9/2}\left[\left(\frac{120744}{1925} + \frac{181352n}{17325} + \frac{10376n^2}{17325} + \frac{64n^3}{5775}\right)\Omega\right. \\ &\left. + \left(\frac{67472308}{1157625} - \frac{3080233n}{848925} - \frac{1664972n^2}{2546775} - \frac{49393n^3}{2546775}\right)\Omega^3\right] \\ &+ \mathcal{O}(\lambda^{11/2}, \Omega^5)\end{aligned} \tag{5.106}$$

although, as $\tilde{M}_0$, can be integrated from the source using

$$\tilde{J}_1 = -\int_{\Sigma_t} T_{\lambda\mu} n^\lambda \zeta^\nu \sqrt{\gamma} d^3x. \tag{5.107}$$

- J_3. Again from the Lichnerowicz matched exterior,

$$\begin{aligned}\frac{J_3}{r_s^4} = &-\frac{1}{7}\lambda^{3/2}\Omega^3 + \left(-\frac{496}{735} + \frac{11n}{441}\right)\lambda^{5/2}\Omega^3 + \left(-\frac{2703854}{848925} + \frac{358n}{5775} + \frac{1234n^2}{169785}\right)\lambda^{7/2}\Omega^3 \\ &+ \left(-\frac{1396705292}{89137125} - \frac{4293174n}{8583575} + \frac{608000n^2}{9270261} + \frac{10433n^3}{3090087}\right)\lambda^{9/2}\Omega^3 + \mathcal{O}(\lambda^{11/2}, \Omega^5).\end{aligned} \tag{5.108}$$

- Rotational energy T. It is defined as

$$T = \frac{1}{2}\int \Omega d\tilde{J}_1 = \frac{1}{2}\Omega \tilde{J}_1 \tag{5.109}$$

so can be obtained directly from eq. (5.106). Again, its definition using integrals over the source

$$T = \frac{1}{2}\Omega \int_{\Sigma_t} T_{\lambda\mu} n^\lambda \zeta^\nu \sqrt{\gamma} d^3x. \tag{5.110}$$

could be used for an error check.

- Moment of inertia about the rotation axis I. For a rigidly rotating star, it has the usual definition

$$I = \frac{\tilde{J}_1}{\omega}. \tag{5.111}$$

The result obtained directly dividing instead of using a Taylor expansion is

$$\begin{aligned}
\frac{I}{r_s^3} &= \lambda\left(\frac{2}{5}+\frac{\Omega^2}{3}\right) + \lambda^2\left[\frac{16}{7}+\frac{2n}{35}+\left(\frac{176}{105}-\frac{3n}{35}\right)\Omega^2\right] \\
&+ \lambda^3\left[\frac{18896}{1575}+\frac{76n}{75}+\frac{34n^2}{1575}+\left(\frac{34889}{3675}-\frac{494n}{735}-\frac{124n^2}{3675}\right)\Omega^2\right] \\
&+ \lambda^4\left[\frac{120744}{1925}+\frac{181352n}{17325}+\frac{10376n^2}{17325}+\frac{64n^3}{5775}\right. \\
&\left.+\left(\frac{67472308}{1157625}-\frac{3080233n}{848925}-\frac{1664972n^2}{2546775}-\frac{49393n^3}{2546775}\right)\Omega^2\right] \\
&+ \mathcal{O}(\lambda^5, \Omega^4),
\end{aligned} \tag{5.112}$$

and leads in the static case to the classical expression for a uniform density sphere at $\mathcal{O}(\lambda)$, as desirable. This is also the reason behind the kind of expansion of T and gives, by the way, a result that we have not been able to find in numerical codes, probably because of the difficulties of dividing by quantities close to zero.

- Gravitational energy W. It is the rotational energy plus the difference between gravitational and proper masses

$$W = T + M_\mathrm{p} - \tilde{M}_0, \tag{5.113}$$

with its $\mathcal{O}(\lambda^{9/2}, \Omega^3)$ CGMR expression

$$\frac{W}{r_s} = \lambda^2\left(\frac{3}{5}+\frac{\Omega^4}{6}\right) + \lambda^3\left[\frac{237}{70}+\frac{9n}{35}+\left(\frac{13}{35}-\frac{6n}{35}\right)\Omega^2+\left(\frac{88}{105}-\frac{3n}{70}\right)\Omega^4\right]$$

$$+\lambda^4\left[\frac{6121}{350}+\frac{457n}{150}+\frac{74n^2}{525}+\left(\frac{15619}{3150}-\frac{306n}{175}-\frac{218n^2}{1575}\right)\Omega^2+\left(\frac{34889}{7350}-\frac{247n}{735}-\frac{62n^2}{3675}\right)\Omega^4\right]+\lambda^5\left[\left(\frac{60372}{1925}+\frac{90676n}{17325}+\frac{5188n^2}{17325}+\frac{32n^3}{5775}\right)\Omega^2+\left(\frac{33736154}{1157625}-\frac{3080233n}{1697850}-\frac{832486n^2}{2546775}-\frac{49393n^3}{5093550}\right)\Omega^4\right]. \tag{5.114}$$

In this case we keep the $\mathcal{O}(\lambda^5)$ contribution because it is the only way to have an expansion leading to the result obtained adding the independently evaluated terms of (5.113). It must be noted that the $\mathcal{O}(\lambda^5)$ part will not be fully known until the $\mathcal{O}(\lambda^5)$ metric is known.

4.2. Radii

Using the information in the expression of the source surface

$$\begin{aligned}\frac{R_\Sigma}{r_s}=1&-\frac{5\Omega^2P_2}{6}+\left(\frac{10}{21}+\frac{5n}{21}\right)\lambda\Omega^2P_2\\&+\lambda^2\left\{-\frac{19}{140}+\Omega^2\left[-\frac{47}{6720}+\left(\frac{22877}{17640}+\frac{548n}{735}+\frac{41n^2}{882}\right)P_2\right]\right\}\\&+\lambda^3\left\{-\frac{1213}{1575}-\frac{179n}{3150}+\Omega^2\left[-\frac{1987}{8400}+\frac{403n}{11200}\right.\right.\\&\left.\left.+\left(\frac{24643463}{5093550}+\frac{134431687n}{40748400}+\frac{238556n^2}{509355}+\frac{188n^3}{9261}\right)P_2\right]\right\}\\&+\mathcal{O}(\lambda^4,\Omega^4),\end{aligned} \tag{5.115}$$

we get different characterizations of the size of the source. First

- the coordinate radii $R_{\rm eq}$ and $R_{\rm p}$, the values of coordinate R on the $p=0$ surface where $\Theta=\frac{\pi}{2}$ and $\Theta=0$, respectively:

$$\begin{aligned}\frac{R_{\rm eq}}{r_s}=1&+\frac{5\Omega^2}{12}+\left(-\frac{5}{21}-\frac{5n}{42}\right)\lambda\Omega^2-\lambda^2\left[\frac{19}{140}+\left(\frac{18499}{28224}+\frac{274n}{735}+\frac{41n^2}{1764}\right)\Omega^2\right]\\&-\lambda^3\left[\frac{1213}{1575}+\frac{179n}{3150}+\left(\frac{108212789}{40748400}+\frac{52599703n}{32598720}+\frac{119278n^2}{509355}+\frac{94n^3}{9261}\right)\Omega^2\right]\\&+\mathcal{O}(\lambda^4,\Omega^4),\end{aligned} \tag{5.116}$$

$$\frac{R_{\rm p}}{r_s}=1-\frac{5\Omega^2}{6}+\left(\frac{10}{21}+\frac{5n}{21}\right)\lambda\Omega^2+\lambda^2\left[-\frac{19}{140}+\left(\frac{182029}{141120}+\frac{548n}{735}+\frac{41n^2}{882}\right)\Omega^2\right]$$

$$+\lambda^3\left[-\frac{1213}{1575}-\frac{179n}{3150}+\left(\frac{187508767}{40748400}+\frac{543591607n}{162993600}+\frac{238556n^2}{509355}+\frac{188n^3}{9261}\right)\Omega^2\right]+\mathcal{O}(\lambda^4,\Omega^4). \tag{5.117}$$

- Circumpherential radius $\mathcal{R}_{\rm circ}$. It is a commonly used coordinate-independent way to measure the stellar radius. Its definition (Gourgoulhon, 2010) is $\mathcal{R}_{\rm circ}=\frac{\mathcal{C}_{\rm eq}}{2\pi}$ with $\mathcal{C}_{\rm eq}$ the length of the equator, i.e.,

$$\mathcal{R}_{\rm circ}=\frac{1}{2\pi}\oint_{\substack{R=R_{\rm eq}\\ \Theta=\pi/2}} ds = g_{\phi\phi}\left(R_{\rm eq},\frac{\pi}{2}\right). \tag{5.118}$$

what in CGMR gives

$$\begin{aligned}\frac{\mathcal{R}_{\rm circ}}{r_s} &= 1+\frac{5\Omega^2}{12}+\lambda\left[1+\left(\frac{1}{84}-\frac{5n}{42}\right)\Omega^2\right]\\ &+\lambda^2\left[\frac{102}{35}+\frac{n}{5}+\left(\frac{9467}{17640}-\frac{531n}{980}-\frac{41n^2}{1764}\right)\Omega^2\right]\\ &+\lambda^3\left[\frac{17417}{1575}+\frac{2948n}{1575}+\frac{3n^2}{35}+\left(\frac{98503871}{20374200}-\frac{1135571n}{407484}\right.\right.\\ &\left.\left.-\frac{163861n^2}{509355}-\frac{94n^3}{9261}\right)\Omega^2\right]+\mathcal{O}(\lambda^4,\Omega^4).\end{aligned} \tag{5.119}$$

An alternate way of giving the size of the source is the straightforward integration of the equatorial radius $\mathcal{R}_{\rm eq}$

$$\mathcal{R}_{\rm eq}:=\int_{R=0}^{R=R_{\rm eq}} g_{RR}\left(R',\frac{\pi}{2}\right)dR', \tag{5.120}$$

i.e. ,

$$\begin{aligned}\frac{\mathcal{R}_{\rm eq}}{r_s} &= 1+\frac{5\Omega^2}{12}+\lambda\left[\frac{4}{3}+\left(\frac{11}{42}-\frac{5n}{42}\right)\Omega^2\right]\\ &+\lambda^2\left[\frac{4313}{1050}+\frac{23n}{75}+\left(\frac{38351}{29400}-\frac{27031n}{44100}-\frac{41n^2}{1764}\right)\Omega^2\right]\\ &+\lambda^3\left[\frac{176003}{11025}+\frac{31811n}{11025}+\frac{169n^2}{1225}+\left(\frac{42650147}{5093550}-\frac{8195204n}{2546775}\right.\right.\\ &\left.\left.-\frac{3773639n^2}{10187100}-\frac{94n^3}{9261}\right)\Omega^2\right]+\mathcal{O}(\lambda^4,\Omega^4).\end{aligned} \tag{5.121}$$

We can get the polar radius $\mathcal{R}_{\rm p}$ in a similar fashion with

$$\mathcal{R}_{\rm p} := \int_{R=0}^{R=R_{\rm p}} g_{RR}(R',0)dR', \tag{5.122}$$

obtaining

$$\begin{aligned}\frac{\mathcal{R}_{\rm p}}{r_s} = 1 - \frac{5\Omega^2}{6} + \lambda\left[\frac{4}{3} + \left(-\frac{11}{21} + \frac{5n}{21}\right)\Omega^2\right] \\ + \lambda^2\left[\frac{4313}{1050} + \frac{23n}{75} + \left(-\frac{7327}{14700} + \frac{13507n}{22050} + \frac{41n^2}{882}\right)\Omega^2\right] \\ + \lambda^3\left[\frac{176003}{11025} + \frac{31811n}{11025} + \frac{169n^2}{1225} + \left(\frac{6620767}{2546775} + \frac{3887302n}{2546775}\right.\right. \\ \left.\left. + \frac{1880363n^2}{5093550} + \frac{188n^3}{9261}\right)\Omega^2\right] + \mathcal{O}(\lambda^4, \Omega^4).\end{aligned} \tag{5.123}$$

In our case, these *proper radii* would correspond to the ones measured integrating the spatial metric on the quotient space to observers that follow the normal vectors to the t = const. surfaces, i.e. , ZAMO observers.

4.3. *Eccentricity and proper radii*

The eccentricity of an ellipsoidal object is defined as

$$\varepsilon = \sqrt{1 - \left(\frac{r_{\rm p}}{r_{\rm eq}}\right)^2}, \tag{5.124}$$

with $r_{\rm p}$ and $r_{\rm eq}$ the lengths of the polar and equatorial radii. Accordingly, the natural generalization in General Relativity comes from taking a congruence of observers and using their associated quotient metric to integrate these lengths. This leads to the definition used, e.g. , in Cook *et al.* (1994)

$$\varepsilon_{\rm proper} = \sqrt{1 - \left(\frac{\mathcal{R}_{\rm p}}{\mathcal{R}_{\rm eq}}\right)^2}, \tag{5.125}$$

with $\mathcal{R}_{\rm p}$ and $\mathcal{R}_{\rm eq}$ the so-called proper radii.

Nevertheless, some have also used a different definition (Friedman *et al.*, 1986; Nozawa *et al.*, 1998). They take the restriction of the metric of the spacetime to the surface R_Σ and find its isometrical embedding into $\mathbb{R}^3$. Then, the surface is described by the coordinates

$$R_s(\Theta) = \sqrt{g_{\phi\phi}(R_\Sigma, \Theta)} \tag{5.126}$$

$$z_s(\Theta) = \int_{\Theta}^{\pi/2} d\Theta \sqrt{g_{RR}(R_\Sigma,\Theta)\left(\frac{dR_\Sigma}{d\Theta}\right)^2 + g_{\Theta\Theta}(R_\Sigma,\Theta) - \left(\frac{d\sqrt{g_{\phi\phi}}}{d\Theta}\right)^2} \tag{5.127}$$

and they take the *coordinates* of the equator and pole to define the eccentricity as

$$\varepsilon_{\text{FIP}} = \sqrt{1 - \left(\frac{z_s(\Theta=0)}{R_s(\Theta=\pi/2)}\right)^2}. \tag{5.128}$$

This procedure is questionable because it implicitly integrates in the flat space and this is extrinsic to the surface. Only intrinsic properties are kept in the isometrical embedding. We can check if it is somehow related with the circumpherential lengths $\mathcal{C}_{\text{p}}$ and $\mathcal{C}_{\text{eq}}$, quantities completely intrinsic to the surface. From eq. (5.126) we see that $\mathcal{C}_{\text{eq}} = 2\pi R_s(\Theta = \pi/2)$, i.e., the circumpherential equatorial radius is equal to $R_s(\Theta = \pi/2)$. Nevertheless, the polar circumpherence

$$\mathcal{C}_{\text{p}} = 2\int_0^{\pi} d\Theta \sqrt{g_{RR}(R_\Sigma,\Theta)\frac{dR_\Sigma}{d\Theta} + g_{\Theta\Theta}(R_\Sigma,\Theta)}, \tag{5.129}$$

coincides with $2\pi\, z_s(\Theta = 0)$ in the static case but in general differs from it. With the current CGMR metric, its expression is

$$\begin{aligned}\frac{\mathcal{C}_{\text{p}}}{2\pi r_s} &= 1 - \frac{5\Omega^2}{24} + \lambda\left[1 + \left(-\frac{1}{168} + \frac{5n}{84}\right)\Omega^2\right] \\ &\quad + \lambda^2\left[\frac{102}{35} + \frac{n}{5} + \left(\frac{3953}{7056} + \frac{139n}{1960} + \frac{41n^2}{3528}\right)\Omega^2\right] \\ &\quad + \lambda^3\left[\frac{17417}{1575} + \frac{2948n}{1575} + \frac{3n^2}{35} + \left(\frac{196281697}{40748400} - \frac{3860173n}{20374200}\right.\right. \\ &\qquad \left.\left. + \frac{47437n^2}{1018710} + \frac{47n^3}{9261}\right)\Omega^2\right] + \mathcal{O}(\lambda^4, \Omega^4)\end{aligned} \tag{5.130}$$

We will compute this different generalization of the eccentricity as well

$$\varepsilon_{\text{intrinsic}} = \sqrt{1 - \left(\frac{\mathcal{C}_p}{\mathcal{C}_e}\right)^2}, \tag{5.131}$$

as an alternative to eqs. (5.125) and (5.128) using only quantities intrinsic to the surface.

4.4. GRV3)

Gourgoulhon and Bonazzola (1994) introduced a generalization of the Newtonian virial identity to stationary spacetimes in General Relativity. Their codes, part of the LORENE library, use it to measure precision, and although the AKM code we use does not, some published AKM results incorporate it. Defining

$$M^2 := -g_{tt} + \frac{g_{t\phi^2}}{g_{\phi\phi}}, \qquad D^2 := \frac{g_{\phi\phi}}{R^2 \sin^2\Theta}, \tag{5.132}$$

$$A^2 := g_{RR}, \qquad \nu := \log M, \tag{5.133}$$

$$S := 3p + (\epsilon + p)\left[\frac{D}{M}\left(\omega + \frac{g_{t\phi}}{g_{\phi\phi}}\right) R \sin\Theta\right]^2, \tag{5.134}$$

and

$$GRV3_1 := \frac{1}{A^2}\left[\left(\frac{\partial \nu}{\partial R}\right)^2 + \frac{1}{R^2}\left(\frac{\partial \nu}{\partial \Theta}\right)^2 - \frac{1}{2AD}\left(\frac{\partial A}{\partial R}\frac{\partial D}{\partial R} + \frac{1}{R^2}\frac{\partial A}{\partial \Theta}\frac{\partial D}{\partial \Theta}\right)\right] \tag{5.135}$$

$$GRV3_2 := \frac{1}{2R}\left(\frac{1}{A^2} - \frac{1}{D^2}\right)\left[\frac{1}{A}\left(\frac{\partial A}{\partial R} + \frac{1}{R\tan\Theta}\frac{\partial A}{\partial \Theta}\right) - \frac{1}{2D}\left(\frac{\partial D}{\partial R} + \frac{1}{R\tan\Theta}\frac{\partial D}{\partial \Theta}\right)\right] \tag{5.136}$$

$$GRV3_3 := \frac{3R^2D^2\sin^2\Theta}{8A^2M^2}\left[\left(\frac{\partial(g_{t\phi}/g_{\phi\phi})}{\partial R}\right)^2 + \frac{1}{R^2}\left(\frac{\partial(g_{t\phi}/g_{\phi\phi})}{\partial \Theta}\right)^2\right] \tag{5.137}$$

the GRV3 is integrated with

$$GRV3 = \int_{\Sigma_t} (4\pi S - GRV3_1 + GRV3_2 + GRV3_3)\sqrt{\gamma} dR d\Theta d\phi. \tag{5.138}$$

We intended to use it to measure error in our approximation as well. Nevertheless, using CMMR metrics this virial identity holds exactly at each order. This happens because after the matching, the primitive of the integral is evaluated at $R = 0$ and $R = \infty$, and at these two points our spacetime is exactly Minkowski.

4.5. Thermodynamic properties at the centre of the source

AKM gives the value at $R = 0$ of the pressure, rest mass density and specific enthalpy $h_c = h(0)\frac{\psi}{\psi_\Sigma}\Big|_{R=0}$. For us, they have the expressions

$$p_c 4\pi r_s^2 = \lambda^2\left(\frac{3}{2} - \Omega^2\right) + \lambda^3\left[\frac{51}{10} + \frac{9n}{10} + \left(-\frac{5}{2} - \frac{17n}{20}\right)\Omega^2\right]$$

$$
\begin{aligned}
&+\lambda^4\left[\frac{3001}{140}+\frac{2013n}{280}+\frac{83n^2}{140}+\left(-\frac{169}{25}-\frac{44n}{7}-\frac{101n^2}{140}\right)\Omega^2\right]\\
&+\lambda^5\left[\frac{2472}{25}+\frac{204881n}{4200}+\frac{65621n^2}{8400}+\frac{139n^3}{336}\right.\\
&\left.+\left(-\frac{68423}{6300}-\frac{473747n}{12600}-\frac{235013n^2}{25200}-\frac{10331n^3}{16800}\right)\Omega^2\right]\\
&+\mathcal{O}(\lambda^6,\Omega^4),
\end{aligned}
\tag{5.139}
$$

$$
\begin{aligned}
\mu_c 4\pi r_s^2 &= 3\lambda+\lambda^2\left(-\frac{3}{2}+\frac{3n}{2}+(1-n)\Omega^2\right)\\
&+\lambda^3\left[-\frac{51}{10}+\frac{21n}{5}+\frac{9n^2}{10}+\left(\frac{5}{2}-\frac{33n}{20}-\frac{17n^2}{20}\right)\Omega^2\right]\\
&+\lambda^4\left[-\frac{3001}{140}+\frac{3989n}{280}+\frac{1847n^2}{280}+\frac{83n^3}{140}+\left(\frac{169}{25}-\frac{83n}{175}-\frac{779n^2}{140}-\frac{101n^3}{140}\right)\Omega^2\right]\\
&+\mathcal{O}(\lambda^5,\Omega^4),
\end{aligned}
\tag{5.140}
$$

$$
\begin{aligned}
\frac{h_c}{h(0)} &= 1+\lambda\left(\frac{1}{2}-\frac{\Omega^2}{3}\right)+\lambda^2\left[\frac{73}{40}+\frac{7n}{40}+\left(-1-\frac{7n}{60}\right)\Omega^2\right]\\
&+\lambda^3\left[\frac{4489}{560}+\frac{183n}{112}+\frac{5n^2}{56}+\left(-\frac{1967}{600}-\frac{43n}{35}-\frac{23n^2}{280}\right)\Omega^2\right]\\
&+\lambda^4\left[\frac{855517}{22400}+\frac{248681n}{20160}+\frac{278359n^2}{201600}+\frac{5389n^3}{100800}\right.\\
&\left.+\left(-\frac{84481}{9450}-\frac{1370969n}{151200}-\frac{42239n^2}{30240}-\frac{353n^3}{5600}\right)\Omega^2\right]+\mathcal{O}(\lambda^5,\Omega^4).
\end{aligned}
\tag{5.141}
$$

4.6. Properties related with geodesic motion of particles near the source

We will now re-derive the formulas describing redshifts of photons emitted by the source and circular orbits of massive and massless particles around it. They can be found spread in the literature (Shibata and Sasaki, 1998; Gourgoulhon, 2010) for particular expressions of the metric and using quasi-isotropic coordinates, but here we will collect these results together. We will use the following subsections to give here their expression for a general metric with Papapetrou structure as well as a reminder of their main features. All the quantities we will deal with can be obtained making use of normalization conditions and the fact that when an affinely parametrized geodesic vector $u^\alpha\nabla_\alpha u^\beta = 0$ is contracted with a Killing

vector ξ^α, it verifies

$$u^\lambda \nabla_\lambda (\xi^\mu u_\mu) = u^\lambda (u_\mu \nabla_\lambda \xi^\mu + \xi^\mu \nabla_\lambda u_\mu) = u^\lambda u_\mu \nabla_\lambda \xi^\mu = u^\lambda u^\mu \nabla_\lambda \xi_\mu = 0, \tag{5.142}$$

i.e., the vector product $\xi^\alpha u_\alpha$ is constant along the geodesic defined by u^α.

In what follows it is assumed that the coordinates are adapted to the Killings and the metric has Papapetrou's structure.

Redshifts

The redshift of a photon of 4-momentum p^α with emitted and received wavelengths $\lambda_{\rm em}$ and $\lambda_{\rm rec}$ is defined as

$$z = \frac{\lambda_{\rm rec} - \lambda_{\rm em}}{\lambda_{\rm em}} = \frac{E_{\rm em}}{E_{\rm rec}} - 1 \tag{5.143}$$

where $u^\alpha_{\rm obs} p_\alpha = -E_{\rm obs}$ is the energy measured by a geodesic observer $u^\alpha_{\rm obs}$. When the photon is emitted at the surface of the fluid $u^\alpha_{\rm em} = u^t_{\rm em}\left(\xi^\alpha + \omega \eta^\alpha\right)$ and measured by an stationary observer $u^\alpha_{\rm obs} = \xi^\alpha$ at $r = r_{\rm ob}$ we have

$$z = \frac{u^t_{\rm em}\left(\xi^\alpha + \omega\eta^\alpha\right) p_\alpha\Big|_{\rm em}}{u^t_{\rm rec}\xi^\alpha p_\alpha\Big|_{\rm rec}} - 1 = \frac{u^t_{\rm em}}{u^t_{\rm rec}}\left(1 + \omega \frac{\eta^\alpha p_\alpha|_{\rm em}}{\xi^\alpha p_\alpha|_{\rm rec}}\right) - 1 \tag{5.144}$$

where we have used $\xi^\alpha p_\alpha|_{\rm em} = \xi^\alpha p_\alpha|_{\rm rec}$.

There are two simple cases. The first one corresponds to photons emitted from the poles of the fluid, where $\omega = 0$. eq. (5.144) leads then to

$$z_{\rm p} = \frac{u^t_{\rm em}}{u^t_{\rm rec}} - 1 = \sqrt{\frac{g_{tt}|_{\rm rec}}{g_{tt}|_{\rm em}}} - 1. \tag{5.145}$$

and in CGMR,

$$\begin{aligned} z_{\rm p} = {} & \lambda\left(1 + \frac{\Omega^2}{3}\right) + \lambda^2\left[\frac{33}{10} + \frac{n}{5} + \left(\frac{5}{3} - \frac{2n}{15}\right)\Omega^2\right] \\ & + \lambda^3\left[\frac{953}{70} + \frac{71n}{35} + \frac{3n^2}{35} + \left(\frac{3387}{350} - \frac{19n}{21} - \frac{8n^2}{105}\right)\Omega^2\right] \\ & + \lambda^4\left[\frac{260263}{4200} + \frac{49951n}{3150} + \frac{913n^2}{630} + \frac{74n^3}{1575} + \left(\frac{555199}{9450} - \frac{3586n}{945}\right.\right. \\ & \left.\left. - \frac{5587n^2}{4725} - \frac{4n^3}{75}\right)\Omega^2\right] + \mathcal{O}(\lambda^5, \Omega^4). \end{aligned} \tag{5.146}$$

The second one, photons emitted from the equator and following a geodesic contained in the equatorial plane, so that $p^\alpha = p^t\xi^\alpha + p^\phi\eta^\alpha$. For them, using again that $\xi^\alpha p_\alpha$ and $\eta^\alpha p_\alpha$ are constant along the path of the photon,

$$\frac{\eta^\alpha p_\alpha|_{\text{em}}}{\xi^\alpha p_\alpha|_{\text{rec}}} = \frac{\eta^\alpha p_\alpha}{\xi^\alpha p_\alpha} = \frac{g_{t\phi} + \alpha g_{\phi\phi}}{g_{tt} + \alpha g_{t\phi}} \tag{5.147}$$

with $\alpha := p^\phi/p^t$. Now, the normalization

$$p^\alpha p_\alpha = g_{tt} + 2g_{t\phi}\alpha + g_{\phi\phi}\alpha^2 = 0 \tag{5.148}$$

renders eq. (5.147) into

$$\frac{g_{t\phi} + \alpha g_{\phi\phi}}{g_{tt} + \alpha g_{t\phi}} = -\frac{1}{\alpha} \tag{5.149}$$

which, solving eq. (5.148) for α allows us to finally write eq. (5.144) as

$$z_{\text{eq}} + 1 = \sqrt{\frac{(g_{tt} + 2g_{t\phi}\omega + g_{\phi\phi}\omega^2)|_{\text{em}}}{g_{tt}|_{\text{rec}}}}\left(1 + \omega\frac{g_{\phi\phi}}{g_{t\phi} \mp \sqrt{g_{t\phi}{}^2 - g_{\phi\phi}g_{tt}}}\right). \tag{5.150}$$

The particular sign to use depends on the direction of emission of the photon. If it is emitted forwards, $p^\phi > 0$. The product of the future oriented ξ^α and p_α is always $\xi^\alpha p_\alpha < 0$, and in this situation $\eta^\alpha p_\alpha \geq 0$. This makes

$$\frac{\eta^\alpha p_\alpha}{\xi^\alpha p_\alpha} \leq 0 \Leftrightarrow \frac{\eta^\alpha p_\alpha}{\xi^\alpha p_\alpha} = \frac{g_{\phi\phi}}{g_{t\phi} - \sqrt{g_{t\phi}{}^2 - g_{\phi\phi}g_{tt}}} \tag{5.151}$$

and the situation is reversed when $p^\phi < 0$. Hence, we have

$$z^{\pm}_{\text{eq}} = z_a \mp z_b \tag{5.152}$$

with

$$\begin{aligned} z_a = 1 &+ \lambda\left(-1 - \frac{\Omega^2}{3}\right) + \lambda^2\left[-\frac{23}{10} - \frac{n}{5} + \left(-\frac{1}{5} + \frac{2n}{15}\right)\Omega^2\right] \\ &+ \lambda^3\left[-\frac{561}{70} - \frac{57n}{35} - \frac{3n^2}{35} + \left(-\frac{601}{1050} + \frac{31n}{35} + \frac{8n^2}{105}\right)\Omega^2\right] \\ &+ \lambda^4\left[-\frac{27509}{840} - \frac{34903n}{3150} - \frac{557n^2}{450} - \frac{74n^3}{1575} + \left(-\frac{49933}{9450}\right.\right. \\ &\qquad \left.\left. + \frac{24338n}{4725} + \frac{727n^2}{675} + \frac{4n^3}{75}\right)\Omega^2\right] + \mathcal{O}(\lambda^5, \Omega^4) \end{aligned} \tag{5.153}$$

and

$$z_b = \sqrt{\lambda}\left(\Omega + \frac{5\Omega^3}{12}\right) + \lambda^{3/2}\left[\Omega + \left(-\frac{41}{84} - \frac{5n}{42}\right)\Omega^3\right] + \lambda^{5/2}\left[\left(\frac{102}{35} + \frac{n}{5}\right)\Omega + \left(-\frac{20521}{17640} - \frac{531n}{980} - \frac{41n^2}{1764}\right)\Omega^3\right] + \lambda^{7/2}\left[\left(\frac{17417}{1575} + \frac{2948n}{1575} + \frac{3n^2}{35}\right)\Omega + \left(-\frac{5481737}{4074840} - \frac{6463717n}{2037420} - \frac{163861n^2}{509355} - \frac{94n^3}{9261}\right)\Omega^3\right] + \mathcal{O}(\lambda^{9/2}, \Omega^5). \tag{5.154}$$

Innermost stable circular orbit

The normalization condition of the 4-momentum p^α of a particle of mass m when the metric of an axisymmetric spacetime has Papapetrou's structure is

$$\begin{aligned} -m^2 &= p^\lambda p_\lambda \\ &= g^{tt}p_t^2 + 2g^{t\phi}p_t p_\phi + g^{\phi\phi}p_\phi^2 + g^{rr}p_r^2 + 2g^{r\theta}p_r p_\theta + g^{\theta\theta}p_\theta^2. \end{aligned} \tag{5.155}$$

Since the coordinates are adapted to the Killing vectors

$$\boldsymbol{\xi} = \partial_t, \qquad \boldsymbol{\eta} = \partial_\phi, \tag{5.156}$$

the p_t and p_ϕ components are

$$\xi^\lambda p_\lambda = p_t \equiv -E, \tag{5.157}$$

$$\eta^\lambda p_\lambda = p_\phi \equiv L, \tag{5.158}$$

which are constant along the geodesics defined by p^α. With this, eq. (5.155) is then

$$-m^2 = g^{tt}E^2 - 2g^{t\phi}EL + g^{\phi\phi}L^2 + g^{rr}p_r^2 + 2g^{r\theta}p_r p_\theta + g^{\theta\theta}p_\theta^2. \tag{5.159}$$

We will only work with geodesics in the equatorial plane of the source (it can be shown that equatorial orbits are plane), so we fix $\theta = \pi/2$ and $p^\theta = 0$. Hence,

$$p_\theta = g_{\theta\lambda}p^\lambda = g_{\theta r}p^r \tag{5.160}$$

and eq. (5.159) together with

$$-E = p_t = g_{tt}p^t + g_{t\phi}p^\phi, \tag{5.161}$$

$$L = p_\phi = g_{t\phi}p^t + g_{\phi\phi}p^\phi, \tag{5.162}$$

allow us to obtain (p^t, p^r, p^ϕ), or for a massive particle $(m\frac{dt}{d\tau}, m\frac{dr}{d\tau}, m\frac{d\phi}{d\tau})$, in terms of the constants E, L and the metric components.

Expressing the inverse metric functions $g^{\alpha\beta}$ in terms of the metric,

$$\begin{aligned} g^{tt} &= \frac{g_{\phi\phi}}{-g_2}, \quad g^{\phi\phi} = \frac{g_{tt}}{-g_2}, \quad g^{t\phi} = \frac{g_{t\phi}}{g_2}, \quad \left(g_2 := g_{t\phi}^2 - g_{tt}g_{\phi\phi}\right), \\ g^{rr} &= \frac{g_{\theta\theta}}{-g_1}, \quad g^{\theta\theta} = \frac{g_{rr}}{-g_1}, \quad g^{r\theta} = \frac{g_{r\theta}}{g_1}, \quad \left(g_1 := g_{r\theta}^2 - g_{rr}g_{\theta\theta}\right), \end{aligned} \tag{5.163}$$

the p^α components can be solved from eqs. (5.159), (5.161) and (5.162) and reduced to

$$p^t = \frac{g_{\phi\phi}E + g_{t\phi}L}{g_2}, \tag{5.164}$$

$$p^\phi = -\frac{g_{t\phi}E + g_{tt}L}{g_2}, \tag{5.165}$$

$$(p^r)^2 = \frac{1}{g_{rr}}\left(-m^2 + \frac{g_{\phi\phi}}{g_2}E^2 + 2\frac{g_{t\phi}}{g_2}EL + \frac{g_{tt}}{g_2}L^2\right), \tag{5.166}$$

which give all the information needed to integrate trajectories and orbits of particles moving in the equatorial plane. From them we get the expressions of $dx^\alpha/d\lambda$

$$\frac{dt}{d\lambda} = \frac{g_{\phi\phi}\bar{E} + g_{t\phi}\bar{L}}{g_2}, \tag{5.167}$$

$$\frac{d\phi}{d\lambda} = -\frac{g_{t\phi}\bar{E} + g_{tt}\bar{L}}{g_2}, \tag{5.168}$$

$$\left(\frac{dr}{d\lambda}\right)^2 = \frac{1}{g_{rr}}\left(-a + \frac{g_{\phi\phi}}{g_2}\bar{E}^2 + 2\frac{g_{t\phi}}{g_2}\bar{E}\bar{L} + \frac{g_{tt}}{g_2}\bar{L}^2\right) := V, \tag{5.169}$$

where, for time-like particles we take the proper time τ as affine parameter $\lambda = \tau$, $a = 1$, $\bar{L} = L/m$ and $\bar{E} = E/m$. For massless ones $a = 0$, $\bar{L} = L$ and $\bar{E} = E$. Out of the static case, neither for time-like or massless particles can eq. (5.169) get the form

$$\left(\frac{dr}{d\lambda}\right)^2 = \text{const} - V_{\text{eff}}(r) \tag{5.170}$$

with an energy independent V_{eff} which would allow the intuitive analysis one can make of orbits in Schwarzschild metric, but we can nonetheless study circular orbits quite easily. Circular orbits satisfy

$$\frac{dr}{d\lambda} = \frac{d^2r}{d\lambda^2} = 0, \tag{5.171}$$

which in turn imply that, first,

$$V = 0. \tag{5.172}$$

Hence

$$\frac{d^2r}{d\lambda^2} = \frac{d\sqrt{V}}{dr}\frac{dr}{d\lambda} = \frac{1}{2}\frac{dV}{dr} \tag{5.173}$$

so

$$\frac{dV}{dr} = 0. \tag{5.174}$$

They are then located in a $r = r_{\text{circ}}$ such that $V(r) = 0$ and have an extremal value. They will be stable(unstable) circular orbits when d^2V/dr^2 is greater(lower) than zero, and marginally stable when

$$\frac{d^2V}{dr^2} = 0. \tag{5.175}$$

This marginally stable circular orbit corresponds to the lower limit of r_{circ} for stable orbits and thus defines the radius of the innermost stable circular orbit (ISCO). This is calculated in the exterior spacetime, and only when r_{ISCO} is bigger than r_Σ will there be a real limit to the radii of circular stable orbits.

We can attempt to give eqs. (5.172), (5.174) and (5.175) a simpler form. If we write eq. (5.172) as

$$V \equiv \frac{1}{g_{rr}}V^* = 0 \Leftrightarrow V^* = 0, \tag{5.176}$$

then eq. (5.174) is equivalent to

$$\frac{d}{dr}\left(\frac{1}{g_{rr}}V^*\right) = \frac{-1}{g_{rr^2}}V^* + \frac{1}{g_{rr}}\frac{dV^*}{dr} = 0 \quad \text{and then} \quad \frac{dV}{dr} = 0 \Leftrightarrow \frac{dV^*}{dr} = 0 \tag{5.177}$$

which in turn makes eq. (5.175) give

$$\frac{d}{dr}\frac{dV}{dr} = \frac{d}{dr}\left(\frac{-V^*}{g_{rr^2}}\right)\frac{dg_{rr}}{dr} - \frac{V^*}{g_{rr^2}}\frac{d^2g_{rr}}{dr^2} + \frac{d}{dr}\frac{1}{g_{rr}}\frac{dV^*}{dr} + \frac{1}{g_{rr}}\frac{d^2V^*}{dr^2} = 0 \tag{5.178}$$

so that

$$\frac{d^2V}{dr^2} = 0 \Leftrightarrow \frac{d^2V^*}{dr^2} = 0. \tag{5.179}$$

Now, using the expression of V^* from eq. (5.169), these three conditions for the location and existence of ISCO, denoting $\frac{d^k f}{dr^k} \equiv f^{k)}$, can be written together as

$$g^{k)}_{\phi\phi}\bar{E}^2 + 2g^{k)}_{t\phi}\bar{E}\bar{L} + g^{k)}_{tt}\bar{L}^2 - ag^{k)}_2 = 0 \qquad (k = 0, 1, 2). \tag{5.180}$$

Next, we can analyse the solution to these equations for the time-like and massless cases separately. In the case of particles with mass, where $a = 1$, the equations for $k = 0, 1$ can be solved in a quite compact form for $\bar{E}$ and $\bar{L}$ in terms of $\omega_{\rm orb}$ defined as

$$p^\alpha = p^t \left(\xi^\alpha + \omega_{\rm orb}\eta^\alpha\right) \tag{5.181}$$

so that $\omega_{\rm orb} = \frac{d\phi}{dt}$. If we write it in terms of $\bar{E}$ and $\bar{L}$ as

$$\omega_{\rm orb} = \frac{d\phi}{d\lambda}\frac{d\lambda}{dt} = -\frac{g_{t\phi}\bar{E} + g_{tt}\bar{L}}{g_{\phi\phi}\bar{E} + g_{t\phi}\bar{L}} \tag{5.182}$$

we can get $\bar{E} = \bar{E}(\omega_{\rm orb}, \bar{L})$ and use this to solve eq. (5.180) for $k = 0$ obtaining

$$\bar{L} = \frac{\pm(g_{t\phi} + g_{\phi\phi}\omega_{\rm orb})}{\sqrt{-g_{tt} - 2\omega_{\rm orb}g_{t\phi} - \omega_{\rm orb}^2 g_{\phi\phi}}}, \tag{5.183}$$

$$\bar{E} = \frac{\mp(g_{tt} + g_{t\phi}\omega_{\rm orb})}{\sqrt{-g_{tt} - 2\omega_{\rm orb}g_{t\phi} - \omega_{\rm orb}^2 g_{\phi\phi}}}. \tag{5.184}$$

Substituting in eq. (5.180) for $k = 1$ we finally get that these equations give $(\bar{E}, \bar{L})$ for a particle in a circular orbit when

$$\omega_{\rm orb} = \frac{-g_{t\phi,r} \pm \sqrt{(g_{t\phi,r})^2 - g_{tt,r}g_{\phi\phi,r}}}{g_{\phi\phi,r}} \tag{5.185}$$

where the upper sign in eqs. (5.183) to (5.185) corresponds to prograde orbits and the lower one to the retrograde ones.

Expressions are actually equivalent in QI coordinates because we are only dealing with orbits in the equatorial plane, so no $g_{r\theta}$ component appears. Switching now to these coordinates, inserting eqs. (5.183) to (5.185) into the $k = 2$ case of eq. (5.180), we get, working in the equatorial plane, an equation for $R^{\pm}_{\rm ISCO}$. The equations for the pro- and retrograde cases are

$$\frac{1}{\hat{R}}(a_1 \mp \hat{R}^{3/2}a_2) = 0 \tag{5.186}$$

with

$$a_1 = \lambda\left(-2 + \frac{3}{2}\frac{1}{\hat{R}^2}\Omega^2\right) + \lambda^2\left\{-\frac{28}{5} - \frac{2n}{5} + 8\frac{1}{\hat{R}} + \left[-\frac{16}{15} + \frac{4n}{15} + \left(\frac{111}{35} - \frac{3n}{14}\right)\frac{1}{\hat{R}^2}\right.\right.$$
$$\left.\left. + 18\frac{1}{\hat{R}^3}\right]\Omega^2\right\} + \lambda^3\left\{-\frac{146}{7} - \frac{128n}{35} - \frac{6n^2}{35} + \left(\frac{224}{5} + \frac{16n}{5}\right)\frac{1}{\hat{R}} + \frac{11}{2}\frac{1}{\hat{R}^2}\right.$$

$$+\left[-\frac{976}{105}+\frac{72n}{35}+\frac{16n^2}{105}+\left(\frac{128}{15}-\frac{32n}{15}\right)\frac{1}{\hat{R}}+\left(\frac{346733}{29400}-\frac{128n}{245}-\frac{10n^2}{147}\right)\frac{1}{\hat{R}^2}\right.$$
$$\left.+\left(\frac{15592}{175}+\frac{36n}{35}\right)\frac{1}{\hat{R}^3}+\frac{5455}{224}\frac{1}{\hat{R}^4}\right]\Omega^2\Bigg\}+\lambda^4\left\{-\frac{27788}{315}-\frac{8338n}{315}-\frac{4232n^2}{1575}-\frac{148n^3}{1575}\right.$$
$$+\left(\frac{40176}{175}+\frac{6688n}{175}+\frac{296n^2}{175}\right)\frac{1}{\hat{R}}+\left(\frac{231}{5}+\frac{33n}{10}\right)\frac{1}{\hat{R}^2}+12\frac{1}{\hat{R}^3}$$
$$+\left[-\frac{2936}{45}+\frac{1836n}{175}+\frac{752n^2}{315}+\frac{8n^3}{75}+\left(\frac{51584}{525}-\frac{2176n}{105}-\frac{288n^2}{175}\right)\frac{1}{\hat{R}}\right.$$
$$+\left(\frac{6098614}{94325}-\frac{11012261n}{9055200}-\frac{6443n^2}{11319}-\frac{67n^3}{2058}\right)\frac{1}{\hat{R}^2}+\left(\frac{21394}{49}+\frac{33368n}{1225}+\frac{52n^2}{245}\right)\frac{1}{\hat{R}^3}$$
$$\left.\left.+\left(\frac{3828481}{19600}+\frac{9819n}{1568}\right)\frac{1}{\hat{R}^4}+\frac{404}{7}\frac{1}{\hat{R}^5}\right]\Omega^2\right\}+\mathcal{O}(\lambda^5,\Omega^4), \tag{5.187}$$

$$a_2=\lambda^2\left[\frac{24\Omega}{5}+\left(4+\frac{513}{35}\frac{1}{\hat{R}^2}\right)\Omega^3\right]+\lambda^3\left\{\left(\frac{5976}{175}+\frac{204n}{175}+\frac{36}{5}\frac{1}{\hat{R}}\right)\Omega\right.$$
$$\left.+\left[\frac{4724}{175}-\frac{166n}{175}+6\frac{1}{\hat{R}}+\left(\frac{4425}{49}-\frac{2791n}{2450}\right)\frac{1}{\hat{R}^2}+\frac{2253}{70}\frac{1}{\hat{R}^3}\right]\Omega^3\right\}$$
$$+\lambda^4\left\{\left(\frac{532072}{2625}+\frac{17132n}{875}+\frac{191n^2}{375}+\left(\frac{12492}{175}+\frac{558n}{175}\right)\frac{1}{\hat{R}}+\frac{102}{5}\frac{1}{\hat{R}^2}\right)\Omega\right.$$
$$+\left[\frac{1076144}{6125}-\frac{10034n}{1225}-\frac{6773n^2}{12250}+\left(\frac{10698}{175}-\frac{207n}{175}\right)\frac{1}{\hat{R}}+\left(\frac{957188417}{1886500}\right.\right.$$
$$\left.\left.\left.+\frac{1080019n}{134750}-\frac{1747819n^2}{3773000}\right)\frac{1}{\hat{R}^2}+\left(\frac{3571299}{12250}+\frac{18171n}{4900}\right)\frac{1}{\hat{R}^3}+\frac{56501}{560}\frac{1}{\hat{R}^4}\right]\Omega^3\right\}$$
$$+\mathcal{O}(\lambda^5,\Omega^4) \tag{5.188}$$

We have not been able to find an approximate expression for it, so we have resorted to make a numerical solution of the equation to get $R^{\pm}_{\rm ISCO}$. The orbital frequency depends on the ISCO positions through

$$\omega^{\pm}_{\rm orb}=\frac{1}{R}\frac{1}{\sqrt{\hat{R}}}(\hat{R}^{3/2}b_1\pm b_2) \tag{5.189}$$

with b_1, b_2 given by

$$b_1=\lambda^{3/2}\left[-\frac{2\Omega}{5}+\left(-\frac{1}{3}-\frac{9}{14}\frac{1}{\hat{R}^2}\right)\Omega^3\right]+\lambda^{5/2}\left\{\left(-\frac{16}{7}-\frac{2n}{35}+\frac{6}{5}\frac{1}{\hat{R}}\right)\Omega\right.$$
$$\left.+\left[-\frac{176}{105}+\frac{3n}{35}+\frac{1}{\hat{R}}+\left(-\frac{744}{245}+\frac{11n}{98}\right)\frac{1}{\hat{R}^2}+\frac{11}{7}\frac{1}{\hat{R}^3}\right]\Omega^3\right\}$$

$$+\lambda^{7/2}\left\{\left[-\frac{18896}{1575}-\frac{76n}{75}-\frac{34n^2}{1575}+\left(\frac{1788}{175}+\frac{72n}{175}\right)\frac{1}{\hat{R}}-\frac{21}{10}\frac{1}{\hat{R}^2}\right]\Omega\right.$$
$$+\left[-\frac{34889}{3675}+\frac{494n}{735}+\frac{124n^2}{3675}+\left(\frac{1482}{175}-\frac{38n}{175}\right)\frac{1}{\hat{R}}+\left(-\frac{12079371}{754600}+\frac{537n}{1925}\right.\right.$$
$$\left.\left.+\frac{617n^2}{18865}\right)\frac{1}{\hat{R}^2}+\left(\frac{2934}{245}+\frac{4n}{147}\right)\frac{1}{\hat{R}^3}-\frac{3277}{1120}\frac{1}{\hat{R}^4}\right]\Omega^3\Bigg\}+\mathcal{O}(\lambda^{9/2},\Omega^5), \tag{5.190}$$

$$b_2=\sqrt{\lambda}\left(1+\frac{3}{8}\frac{1}{\hat{R}^2}\Omega^2\right)+\lambda^{3/2}\left\{\frac{7}{5}+\frac{n}{10}-\frac{3}{2}\frac{1}{\hat{R}}+\left[\frac{4}{15}-\frac{n}{15}+\left(\frac{15}{56}-\frac{51n}{560}\right)\frac{1}{\hat{R}^2}\right.\right.$$
$$\left.-\frac{11}{16}\frac{1}{\hat{R}^3}\right]\Omega^2\Bigg\}+\lambda^{5/2}\left\{\frac{741}{175}+\frac{271n}{350}+\frac{53n^2}{1400}+\left(-\frac{63}{10}-\frac{9n}{20}\right)\frac{1}{\hat{R}}+\frac{3}{2}\frac{1}{\hat{R}^2}\right.$$
$$+\left[\frac{1024}{525}-\frac{47n}{105}-\frac{11n^2}{350}+\left(-\frac{6}{5}+\frac{3n}{10}\right)\frac{1}{\hat{R}}+\left(\frac{93851}{117600}-\frac{6277n}{19600}-\frac{5197n^2}{235200}\right)\frac{1}{\hat{R}^2}\right.$$
$$\left.\left.+\left(-\frac{6541}{2800}+\frac{33n}{1120}\right)\frac{1}{\hat{R}^3}+\frac{969}{896}\frac{1}{\hat{R}^4}\right]\Omega^2\right\}+\lambda^{7/2}\left\{\frac{126992}{7875}+\frac{80483n}{15750}+\frac{34103n^2}{63000}\right.$$
$$+\frac{2483n^3}{126000}+\left(-\frac{4878}{175}-\frac{3321n}{700}-\frac{603n^2}{2800}\right)\frac{1}{\hat{R}}+\left(\frac{21}{2}+\frac{3n}{4}\right)\frac{1}{\hat{R}^2}-\frac{5}{4}\frac{1}{\hat{R}^3}$$
$$+\left[\frac{98054}{7875}-\frac{1851n}{875}-\frac{3674n^2}{7875}-\frac{21n^3}{1000}+\left(-\frac{2124}{175}+\frac{183n}{70}+\frac{141n^2}{700}\right)\frac{1}{\hat{R}}\right.$$
$$+\left(\frac{248086339}{45276000}-\frac{61376113n}{36220800}-\frac{6699761n^2}{30184000}-\frac{2167n^3}{219520}\right)\frac{1}{\hat{R}^2}+\left(-\frac{32256341}{3528000}\right.$$
$$\left.\left.-\frac{168089n}{588000}+\frac{21131n^2}{1411200}\right)\frac{1}{\hat{R}^3}+\left(\frac{971793}{156800}+\frac{10659n}{62720}\right)\frac{1}{\hat{R}^4}-\frac{1965}{1792}\frac{1}{\hat{R}^5}\right]\Omega^2\Bigg\}$$
$$+\mathcal{O}(\lambda^{9/2},\Omega^4). \tag{5.191}$$

In the case of massless particles $a=0$ and eq. (5.180) becomes

$$g_{\phi\phi}{}^{k)}\bar{E}^2+2g_{t\phi}{}^{k)}\bar{E}\bar{L}+g_{tt}{}^{k)}\bar{L}^2=0, \qquad (k=0,1,2) \tag{5.192}$$

which we can simplify focusing on $\bar{L}\neq 0$ particles. Introducing $\bar{b}=\bar{L}/\bar{E}$ in the $k=0$ equation we get

$$\frac{1}{\bar{b}}=\frac{-g^{k)}_{t\phi}\pm\sqrt{\left(g^{k)}_{t\phi}\right)^2-g^{k)}_{tt}g^{k)}_{\phi\phi}}}{g^{k)}_{\phi\phi}}. \tag{5.193}$$

This reduces the $k = 1$ case of eq. (5.192) to a $f(R) = 0$ equation giving the position of circular orbits. To get their frequency we start from eq. (5.182) and get

$$\frac{1}{\bar{b}} = -\frac{\omega_{\rm orb} g_{t\phi} + g_{tt}}{g_{t\phi} + \omega_{\rm orb} g_{\phi\phi}} \tag{5.194}$$

what allows us to solve for $\omega_{\rm orb}$ as

$$\omega_{\rm null} = \frac{-g_{t\phi} \pm \sqrt{\left(g_{t\phi}\right)^2 - g_{tt} g_{\phi\phi}}}{g_{\phi\phi}} \tag{5.195}$$

and hence, again, the upper signs corresponds to prograde orbits. The $k = 2$ equation gives the stability of the orbit. Since circular orbits of massless particles are unstable (Bardeen *et al.*, 1972), we can use it to discard unphysical solutions to the previous equations. As we will see later in Section 6, time-like ISCOs appear only at quite high masses. We omit massless results here because, according to them, there is no massless ISCOs for baryon rest masses below $2\,M_\odot$ and the higher rotation frequency observed. Besides, they are rather problematic to compute probably due to their closeness to $R = 0$.

5. Comparison with AKM results

With the EOS fixed through the p_i parameters, using the procedure described in Section 4.1 to obtain the value $h(0)$ of the specific enthalpy on the $p = 0$ surface and fixing two of its default output quantities (but the polar redshift $z_{\rm p}$), the AKM code gives us the values of the rest of them. It also produces a file with the values of the metric potentials in a grid of points near the source. Here we will compare these two kinds of results with the corresponding CGMR values of the quantities and metric functions.

The default AKM output parameters are listed in Table 5.2 (page 114) and deserve two comments. First, there is a quantity not yet defined. It is the mass-shed parameter β that measures how close the source is to start losing matter at the equator due to the fast rotation. Since it is only relevant in regimes of really strong source deformation (at the onset of the mass-shedding a cusp appears at the equator, a conjecture of Bardeen, 1971, confirmed first by Eriguchi and Sugimoto, 1981), we have not included it in our calculations. Second, although the default AKM gives only these quantities, it actually computes four more and fortunately we can make them appear on screen editing the source code.

Several of the physical properties of the source discussed in Section 4 are not computed by AKM but are commonly found in other computations (see Cook

et al., 1992, 1994; Nozawa *et al.*, 1998). We will give their analytic expressions (as well as the AKM comparison ones) and also their particular values for some of the models discussed to ease possible future comparisons by others.

To obtain particular results from the analytical expressions of CGMR with a fixed EOS it is enough to specify the value of ω and r_s. While the first one is a very mainstream quantity as well as part of the AKM results and poses no problem, r_s is, as we saw in Chapter 3 coordinate dependent and has a not very observational definition, though. This could seem problematic, but to obtain a model for, let us say, a certain $(\tilde{M}_0, \omega)$ combination, all we have to do is find the r_s that gives the desired value of $\tilde{M}_0$. In fact, this characteristic makes CMMR quite versatile since every quantity depends on r_s and hence a very wide range of parameters can be used to adjust its value.

We start studying the behaviour of relative errors when we include further approximation orders in CGMR. After that, we will compare a given AKM model with results of CMMR using $\tilde{M}_0$, R_{eq}, p_{c} and $\tilde{J}_1$ to adjust the value of r_s and see what kind of adjustment gives better results. Then, we will analyze some relevant constant density and simple MIT bag model configurations to check the range of applicability of CMMR.

5.1. Relations between error and order of approximation

It is known that some other analytical approximation schemes (e.g., the post-Newtonian) may display a weird oscillating behaviour of their error. This means that going to higher orders in the approximation, in some intermediate steps it may grow instead of decrease as one would expect (Arun *et al.*, 2005). It is important to check if this happens for the kind of stellar models we will study later. Besides this oddity, one may also wish to know the evolution of error while going to higher approximation levels since it can tell us

- whether it is worthy undertaking the increasingly long calculations,
- the rate of change of the increment of precision and
- what are the applicability limits of CMMR.

Regarding the first point, the troubles generated by the calculations are twofold. There is the base difficulty of having to deal with increasingly long expressions in each iteration of the solution of the Einstein relaxed equations, what gives us the next λ-order. This translates in not only longer calculation times but also—since manual calculation is truly unpractical in expressions with hundreds

Quantity	Definition
$\tilde{M}_0$	gravitational mass
ω	angular velocity
M_b	baryon rest mass
$\tilde{J}_1$	Angular moment
β	mass-shed parameter
$-\ln\psi_\Sigma$	ln of the surface potential
z_p	polar redshift
R_{eq}	equatorial QI radial coordinate
R_p	polar QI radial coordinate
R_p/R_{eq}	ratio of main QI radial coordinates
ϵ_c	central energy density
p_c	central pressure
μ_{bc}	central baryon rest mass density
h_c	central specific enthalpy
$\hat{B}_c$	central value of $\hat{B}$ (see eq. [5.11])
E_{bind}	binding energy
$\mathcal{R}_{circ}$	circumpherential radius
M_p	proper mass
T	gravitational energy
W	rotational energy
T/W	gravitational vs rotational energies ratio

Table 5.2: Output parameters of the AKM numerical code. The first of them are given by the default AKM code. The last four are also computed by default but not printed on screen.

of thousands of terms—really serious RAM memory consumption of the *Mathematica* programs we use. The results of this Section make use of the $\mathcal{O}(\lambda^{9/2}, \Omega^3)$ CGMR and a lot of depuration of the codes has been necessary. Even after that and using remote *Mathematica* kernels on bigger linux machines for the worst parts of the calculations, at least 3.5 Gb of RAM are necessary for these comparisons. But all-in-all, this is essentially a "merely" resources issue and currently the obtention of the next λ-order is totally automatic. The other degree of difficulty comes when trying to go to higher Ω-orders. For this, the expansion of the homogeneous solution—eqs. (2.47) and (2.53)—must include new harmonic spherical tensors, and the surface ansatz eq. (2.75) additional Legendre polynomials. This implies important modifications on the programs at many levels and is therefore a more serious issue.

We consider first a static stellar model. It corresponds to a constant density source of $M_b = 8\times10^{-4}$ (we will use the AKM values of quantities to label the models). This value—as any other unless otherwise stated—is given in $c = G =$

		$\mathcal{O}(\lambda^2)$		$\mathcal{O}(\lambda^3)$		$\mathcal{O}(\lambda^4)$	
Quantity	AKM	CMMR	ε	CMMR	ε	CMMR	ε
M_0	7.93325_{-4}	7.933_{-4}	0.0	7.9333_{-4}	5.5_{-16}	7.93325_{-4}	2.7_{-16}
M_b	8.00000_{-4}	7.995_{-4}	6.5_{-4}	7.9996_{-4}	5.0_{-5}	7.99997_{-4}	3.8_{-6}
M_p	8.00000_{-4}	7.995_{-4}	6.5_{-4}	7.9996_{-4}	5.0_{-5}	7.99997_{-4}	3.8_{-6}
E_{bind}	6.67467_{-6}	6.156_{-6}	7.8_{-2}	6.6350_{-6}	5.9_{-3}	6.67159_{-6}	4.6_{-4}
W	6.67467_{-6}	6.156_{-6}	7.8_{-2}	6.6350_{-6}	5.9_{-3}	6.67159_{-6}	4.6_{-4}
$\mathcal{R}_{circ}$	5.74276_{-2}	5.744_{-2}	1.7_{-4}	5.7429_{-2}	1.6_{-5}	5.74277_{-2}	1.3_{-6}
z_p	1.41074_{-2}	1.409_{-2}	1.4_{-3}	1.4106_{-2}	9.8_{-5}	1.41073_{-2}	7.4_{-6}
$-\ln\psi_\Sigma$	-1.40088_{-2}	-1.400_{-2}	7.9_{-4}	-1.4008_{-2}	5.3_{-5}	-1.40087_{-2}	3.8_{-6}
R_p	5.66315_{-2}	5.668_{-2}	7.7_{-4}	5.6634_{-2}	5.0_{-5}	5.66317_{-2}	3.5_{-6}
R_{eq}	5.66315_{-2}	5.668_{-2}	7.7_{-4}	5.6634_{-2}	5.0_{-5}	5.66317_{-2}	3.5_{-6}
R_p/R_{eq}	1.00000	1.000	7.0_{-13}	1.0000	7.0_{-13}	1.00000	7.0_{-13}
ϵ_c	1.00000	1.000	0.0	1.0000	0.0	1.00000	0.0
p_c	7.10379_{-3}	7.089_{-3}	2.0_{-3}	7.1027_{-3}	1.6_{-4}	7.10370_{-3}	1.3_{-5}
μ_{bc}	1.00000	1.000	0.0	1.0000	0.0	1.00000	0.0
h_c	1.00710	1.007	1.4_{-5}	1.0071	1.1_{-6}	1.00710	8.8_{-8}

Table 5.3: Behaviour of relative error ε in CMMR with respect to AKM with increasing λ-order of the computation. Both AKM and CMMR values are given in $c = G = \epsilon_0 = 1$ units. This model corresponds to the static configuration of a constant density sequence with $M_b = 8\times10^{-4}$, the $\omega = 0$ version of the model in Table 5.5 (page 118). We use the shorthand notation $a_b = a\times10^b$. The value of the approximation parameter is $\lambda \simeq 0.013$.

$\epsilon_0 = 1$ units. It is important to note that written in $c = G = 1$ units, it is $M_b = 8\times10^{-4}\,\epsilon_0^{-1/2} = 8\times10^{-4}\,\mu_0^{-1/2}$ and accordingly corresponds to widely different models, depending on the value of μ_0. In particular, if using the standard neutron star density $\mu_0 = 4\times10^{17}\,\mathrm{kg\,m^{-3}}$, it is $M_b = 3.14\times10^{-2}\,M_\odot$, too low to be interesting for that kind of sources; however, if $\mu_0 = 1408\,\mathrm{kg\,m^{-3}}$, the mean solar density, it corresponds to $M_b \simeq 5.29\times10^5\,M_\odot$, a more than fair amount of matter. In what follows, tables will in general give $c = G = \epsilon_0 = 1$ values but in several situations they will use more common units to ease the check of applicability of CMMR. In that cases, the value of B or μ_0 used will be given.

The reason for using the baryon rest mass M_b as main parameter here instead of the gravitational mass is that when one wish to compare configurations of the same object for different values of ω the amount of rotation increases the gravitational mass while the number of baryons and accordingly M_b is not modified. This is the standard way to build *evolutionary sequences* (Miller, 1977).

Table 5.3 shows the AKM and CMMR quantities comparison for this model. It gives the AKM value and the CGMR results with increasing λ-order, from $\mathcal{O}(\lambda^2)$ to $\mathcal{O}(\lambda^4)$ and the relative error with respect to AKM. It shows a consistent im-

provement of more than one order of magnitude in the relative error ε in every quantity except in R_p/R_{eq}, though it is rather artificial since the values of $R_{eq,p}$ follow the trend. The error is quite homogeneous, but bigger in W and E_{bind}. These two quantities are very sensitive to error because they are linear combinations of other quantities (see eqs. [5.104] and [5.113]) and in this case give rise to error two orders of magnitude bigger than the ones of the quantities they are obtained from. This will consistently happen in all the following models. The extremely low error in $\tilde{M}_0$ is artificial of course, since the CMMR model has been adjusted to give the AKM value through r_s fixing.

The $\mathcal{O}(\lambda^4, \Omega^3)$ results are comparable to the best ones in the numeric results comparison of Table 5.1 (page 76) and the improvement rate is fairly constant up to this point, so going further in λ-order will probably give even better results.

Concerning the metric potentials, their relative errors in a sector around the source are depicted in Fig. 5.2 (following page) with the lower left corner of each graph corresponding to the source centre. They are plotted in LP coordinates and correspond to g_{tt} and g_{RR} in the three different approximation levels. They show the expectable spherical symmetry of a static configuration and their relative error ranges from $\varepsilon_c \sim 10^{-5}$ in the centre of the source and $\varepsilon_{2\varrho_{eq}} \sim 10^{-6}$ at two times ϱ_{eq} when using $\mathcal{O}(\lambda^2)$ results down to $(\varepsilon_c, \varepsilon_{2\varrho_{eq}}) \sim (10^{-7}, 10^{-8})$ with $\mathcal{O}(\lambda^4)$ data. These results are summarized in Table 5.4. Thus, the decrement in error follows the same pattern as the one previously seen in the model properties of Table 5.3 (facing page).

Now we put these same amount of matter in rotation to see how different its error behaviour is. We take a $M_b = 8 \times 10^{-4}$ and $\omega = 0.2$ source. This angular velocity in $c = G = 1$ units is $\omega = 0.2\mu_0^{1/2}$ and gives 2.14 times the solar rotation rate for solar mean density or $\omega = 164.5\,\text{Hz}$ for standard neutron star density.

In Table 5.5 (page 118) we see that this model shows the same tendency of the static one, with error dropping an order of magnitude per λ-order in several of them but in the step from $\mathcal{O}(\lambda^{7/2}, \Omega^3)$ to $\mathcal{O}(\lambda^{9/2}, \Omega^3)$ this is not the case for all

	g_{tt}		g_{RR}	
Approx. order	$\varepsilon(\varrho = 0)$	$\varepsilon(\varrho = 2\varrho_{eq})$	$\varepsilon(\varrho = 0)$	$\varepsilon(\varrho = 2\varrho_{eq})$
$\mathcal{O}(\lambda^2)$	$\sim 1.8 \times 10^{-5}$	$\sim 6.0 \times 10^{-6}$	$\sim 9.5 \times 10^{-5}$	$\sim 6.0 \times 10^{-6}$
$\mathcal{O}(\lambda^3)$	$\sim 1.4 \times 10^{-6}$	$\sim 4.8 \times 10^{-7}$	$\sim 7.0 \times 10^{-6}$	$\sim 4.6 \times 10^{-7}$
$\mathcal{O}(\lambda^4)$	$\sim 1.1 \times 10^{-7}$	$\sim 3.8 \times 10^{-8}$	$\sim 5.3 \times 10^{-7}$	$\sim 3.3 \times 10^{-8}$

Table 5.4: Evolution of relative error in metric functions g_{tt} and g_{RR} from Fig. 5.2 (following page) at the source centre and at the $\varrho = 2\varrho_{eq}$ sphere.

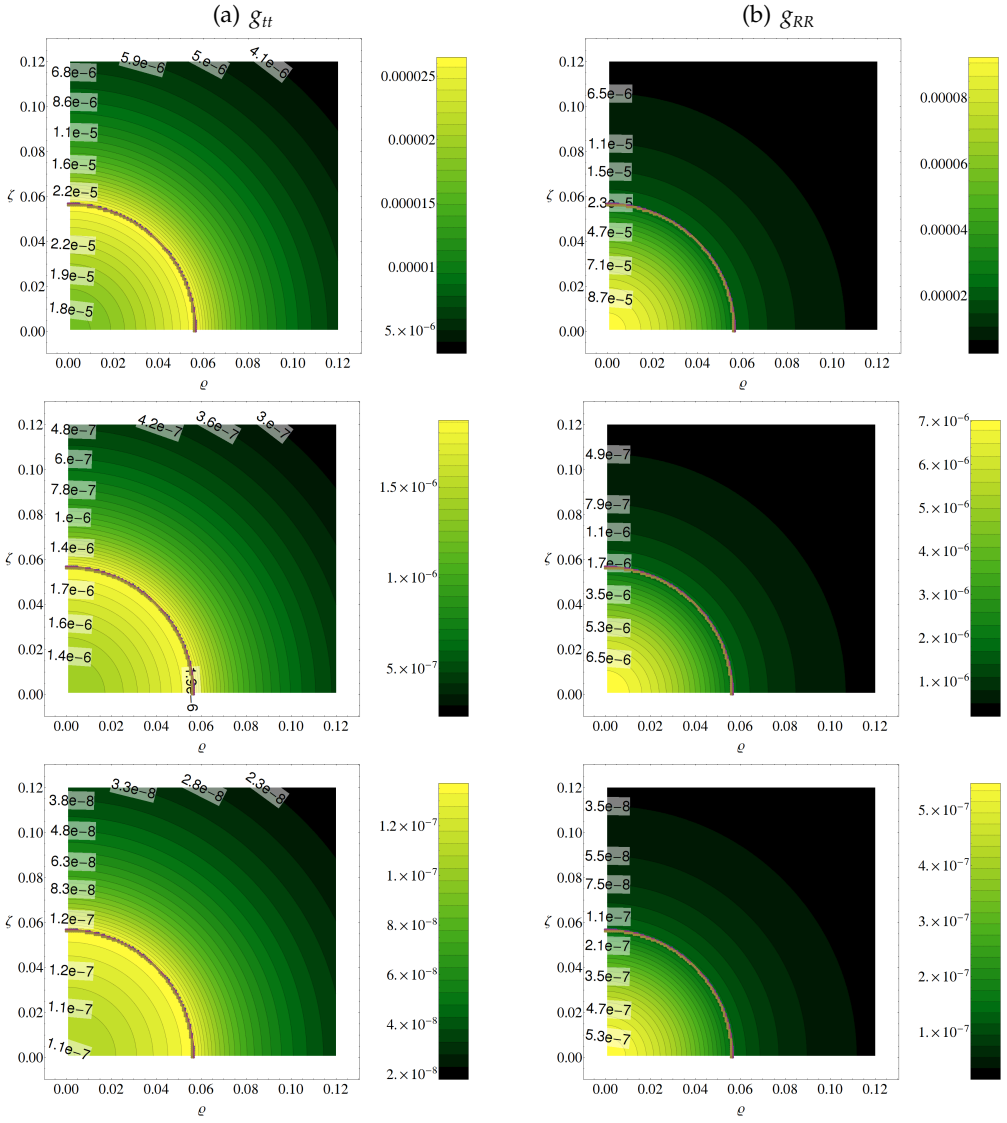

Figure 5.2: Relative error in g_{tt} and g_{RR}, between AKM and CMMR for a constant density source with $M_b = 8 \times 10^{-4}$, $\omega = 0$ for different approximation orders, using $\tilde{M}_0$ to adjust r_s. The first row refers to $\mathcal{O}(\lambda^2)$, second row to $\mathcal{O}(\lambda^3)$ and third row to $\mathcal{O}(\lambda^4)$. The thin dotted lines represent the AKM and CMMR surfaces (indistinguishable in this model).

Quantity	AKM	$\mathcal{O}(\lambda^{5/2}, \Omega^3)$ CMMR	ε	$\mathcal{O}(\lambda^{7/2}, \Omega^3)$ CMMR	ε	$\mathcal{O}(\lambda^{9/2}, \Omega^3)$ CMMR	ε
$\tilde{M}_0$	7.93347_{-4}	7.933_{-4}	4.1_{-16}	7.9335_{-4}	6.8_{-16}	7.93347_{-4}	4.1_{-16}
ω	2.00000_{-1}	2.000_{-1}		2.0000_{-1}		2.00000_{-1}	
$\tilde{J}_1$	2.13498_{-7}	2.130_{-7}	2.1_{-3}	2.1343_{-7}	3.0_{-4}	2.13473_{-7}	1.1_{-4}
M_b	8.00000_{-4}	7.995_{-4}	6.5_{-4}	7.9996_{-4}	4.9_{-5}	7.99997_{-4}	3.5_{-6}
M_p	8.00000_{-4}	7.995_{-4}	6.5_{-4}	7.9996_{-4}	4.9_{-5}	7.99997_{-4}	3.5_{-6}
E_bind	6.65323_{-6}	6.136_{-6}	7.8_{-2}	6.6138_{-6}	5.9_{-3}	6.65041_{-6}	4.2_{-4}
T	2.13498_{-8}	2.130_{-8}	2.1_{-3}	2.1343_{-8}	3.0_{-4}	2.13473_{-8}	1.1_{-4}
W	6.67458_{-6}	6.157_{-6}	7.7_{-2}	6.6352_{-6}	5.9_{-3}	6.67176_{-6}	4.2_{-4}
T/W	3.19867_{-3}	3.460_{-3}	8.2_{-2}	3.2167_{-3}	5.6_{-3}	3.19965_{-3}	3.1_{-4}
$\mathcal{R}_\mathrm{circ}$	5.76540_{-2}	5.766_{-2}	1.4_{-4}	5.7653_{-2}	2.5_{-5}	5.76517_{-2}	3.9_{-5}
z_p	1.41529_{-2}	1.413_{-2}	1.4_{-3}	1.4151_{-2}	1.1_{-4}	1.41526_{-2}	2.0_{-5}
$-\ln\psi_\Sigma$	-1.40537_{-2}	-1.404_{-2}	8.0_{-4}	-1.4053_{-2}	6.5_{-5}	-1.40534_{-2}	1.6_{-5}
R_p	5.61837_{-2}	5.623_{-2}	8.0_{-4}	5.6189_{-2}	8.5_{-5}	5.61859_{-2}	3.9_{-5}
R_eq	5.68560_{-2}	5.690_{-2}	7.3_{-4}	5.6856_{-2}	8.8_{-6}	5.68538_{-2}	3.8_{-5}
$R_\mathrm{p}/R_\mathrm{eq}$	9.88177_{-1}	9.882_{-1}	7.2_{-5}	9.8825_{-1}	7.7_{-5}	9.88252_{-1}	7.7_{-5}
ϵ_c	1.00000	1.000	0.0	1.0000	0.0	1.00000	0.0
p_c	7.05840_{-3}	7.045_{-3}	2.0_{-3}	7.0577_{-3}	9.4_{-5}	7.05876_{-3}	5.1_{-5}
μ_bc	1.00000	1.000	0.0	1.0000	0.0	1.00000	0.0
h_c	1.00706	1.007	1.4_{-5}	1.0071	6.6_{-7}	1.00706	3.6_{-7}

Table 5.5: Behaviour of relative error ε in CMMR with respect to AKM with increasing λ-order of the computation. Both AKM and CMMR values are given in $c = G = \epsilon_0 = 1$ units. This model corresponds to a constant density configuration of $M_\mathrm{b} = 3.14 \times 10^{-2} M_\odot$, $\omega = 164.5\,\mathrm{Hz}$ if $\mu_0 = 4 \times 10^{17}\,\mathrm{kg\,m^{-3}}$ (standard neutron star density), or $M_\mathrm{b} \approx 5.29 \times 10^5 M_\odot$, $\omega = 9.7 \times 10^{-6}\,\mathrm{Hz}$ if $\mu_0 = 1408\,\mathrm{kg\,m^{-3}}$ (mean solar density). The value of the approximation parameters is $(\lambda, \Omega) \simeq (0.013, 0.097)$.

the quantities. In particular $\tilde{J}_1$, T, p_c, h_c and the surface quantities show a lower decrement. It even grows in the case of $\mathcal{R}_\mathrm{circ}$ and R_eq.

Fig. 5.3 (following page) shows also a quite different pattern from the corresponding static case. Here the plots belong to g_{tt} and $g_{t\phi}$, the g_{ii} ones being quite similar to g_{tt}, and again each row is the result of a increasingly higher λ-order. Looking at the first row we see that the error distribution is almost spherical again, with only a little deviation from it in $g_{t\phi}$. Now, if we had access to only this first row, we could think that the rotation has little impact in both the shape of the source and the error. The first is actually true if we check the value of $R_\mathrm{p}/R_\mathrm{eq}$ from Table 5.5. The second is not. In the second row, where $\mathcal{O}(\lambda^{7/2}, \Omega^3)$ are displayed, the spherical symmetry in the error is clearly lost in $g_{t\phi}$, and this effect grows in the the next row with $\mathcal{O}(\lambda^{9/2}, \Omega^3)$ results, making itself evident even in g_{tt}. This behaviour is totally different from the static case and thus a consequence of ro-

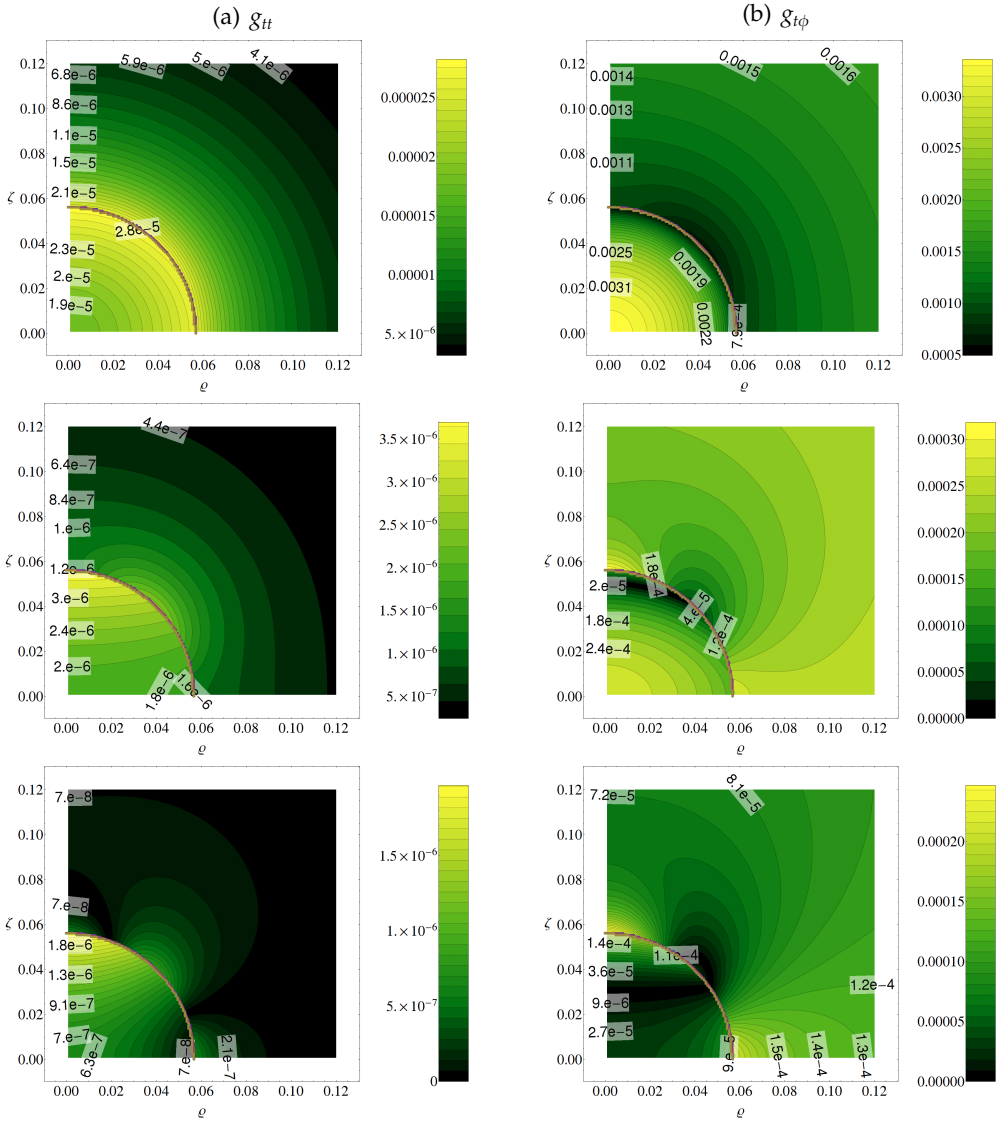

Figure 5.3: Relative error for constant density for the model $M_b = 8 \times 10^{-4}$, $\omega = 0.2$ in (a): g_{tt}, (b) $g_{t\phi}$ using $\tilde{M}_0$ to adjust r_s. The first row refers to $\mathcal{O}(\lambda^{5/2}, \Omega^3)$, second row to $\mathcal{O}(\lambda^{7/2}, \Omega^3)$ and third row to $\mathcal{O}(\lambda^{9/2}, \Omega^3)$. The thin dotted lines represent the AKM and CMMR surfaces (indistinguishable in this picture size).

tation. The error has now a lobular appearance that, together with the rotational origin, points towards the truncation of the tensor spherical harmonics expansion of the solution of the homogeneous post-Minkowskian system —eqs. (2.47) and (2.53)—and the surface as a cause. Hence, this lobular appearance is a direct consequence of the Ω-order of the approximation, and can be present even with small source deformation. Nevertheless, in this case it is an effect that makes itself apparent only at higher λ-orders. From this series of results we see that the solution truncation in Ω is the main source of error when the lobular pattern appears. This is key to ascertain when going to higher Ω-orders may be more productive than going forward in the post-Minkowskian approximation. Alternatively, when the results can be substantially improved with ease going to the next λ-order and when it would involve cumbersome modifications in the *Mathematica* codes to get a higher Ω-order.

Concerning the values of the error, we see that similarly to what happens with the quantities in Table 5.5 (page 118), it drops an order of magnitude from $\lambda^{5/2}$ to $\lambda^{7/2}$ but the drop is not homogeneous in the next iteration and it is smaller in the equatorial and polar areas, what is likely the cause of the heterogeneous results in the table.

		$M_0^{\text{AKM}} = M_0^{\text{CMMR}}$		$R_{\text{eq}}^{\text{AKM}} = R_{\text{eq}}^{\text{CMMR}}$		$p_{\text{c}}^{\text{AKM}} = p_{\text{c}}^{\text{CMMR}}$	
Quantity	AKM	CMMR	ε	CMMR	ε	CMMR	ε
$\tilde{M}_0$	7.93325_{-4}	7.93325_{-4}	2.7_{-16}	7.93317_{-4}	1.1_{-5}	7.93340_{-4}	1.8_{-5}
M_{b}	8.00000_{-4}	7.99997_{-4}	3.8_{-6}	7.99988_{-4}	1.5_{-5}	8.00012_{-4}	1.5_{-5}
M_{p}	8.00000_{-4}	7.99997_{-4}	3.8_{-6}	7.99988_{-4}	1.5_{-5}	8.00012_{-4}	1.5_{-5}
E_{bind}	6.67467_{-6}	6.67159_{-6}	4.6_{-4}	6.67147_{-6}	4.8_{-4}	6.67179_{-6}	4.3_{-4}
W	6.67467_{-6}	6.67159_{-6}	4.6_{-4}	6.67147_{-6}	4.8_{-4}	6.67179_{-6}	4.3_{-4}
$\mathcal{R}_{\text{circ}}$	5.74276_{-2}	5.74277_{-2}	1.3_{-6}	5.74275_{-2}	2.3_{-6}	5.74281_{-2}	7.4_{-6}
z_{p}	1.41074_{-2}	1.41073_{-2}	7.4_{-6}	1.41071_{-2}	1.5_{-5}	1.41074_{-2}	5.1_{-6}
$-\ln\psi_{\Sigma}$	-1.40088_{-2}	-1.40087_{-2}	3.8_{-6}	-1.40086_{-2}	1.1_{-5}	-1.40089_{-2}	8.5_{-6}
R_{p}	5.66315_{-2}	5.66317_{-2}	3.5_{-6}	5.66315_{-2}	7_{-13}	5.66321_{-2}	9.4_{-6}
R_{eq}	5.66315_{-2}	5.66317_{-2}	3.5_{-6}	5.66315_{-2}	1.2_{-16}	5.66321_{-2}	9.4_{-6}
$R_{\text{p}}/R_{\text{eq}}$	1.00000	1.00000	7.0_{-13}	1.00000	7_{-13}	1.00000	7_{-13}
ϵ_{c}	1.00000	1.00000	0.0	1.00000	0	1.00000	0
p_{c}	7.10379_{-3}	7.10370_{-3}	1.3_{-5}	7.10365_{-3}	2_{-5}	7.10379_{-3}	0
μ_{bc}	1.00000	1.00000	0.0	1.00000	0	1.00000	0
h_{c}	1.00710	1.00710	8.8_{-8}	1.00710	1.4_{-7}	1.00710	2.2_{-16}

Table 5.6: Comparison results for the model in Table 5.3 (page 115) of error between AKM and $\mathcal{O}(\lambda^4, \Omega^2)$ CMMR using different adjustments. The last three pairs of columns correspond to CMMR results using $\tilde{M}_0$, R_{eq} and p_{c} to fix the value of r_s, respectively.

Quantity	$\tilde{M}_0^{\mathrm{AKM}} = \tilde{M}_0^{\mathrm{CMMR}}$ CMMR	ε	$R_{\mathrm{eq}}^{\mathrm{AKM}} = R_{\mathrm{eq}}^{\mathrm{CMMR}}$ CMMR	ε	$p_{\mathrm{c}}^{\mathrm{AKM}} = p_{\mathrm{c}}^{\mathrm{CMMR}}$ CMMR	ε	$\tilde{J}_1^{\mathrm{AKM}} = \tilde{J}_1^{\mathrm{CMMR}}$ CMMR	ε
$\tilde{M}_0$	7.9335_{-4}	4.1_{-16}	7.9344_{-4}	1.2_{-4}	7.9329_{-4}	7.4_{-5}	7.9340_{-4}	6.8_{-5}
ω	2.0000_{-1}		2.0000_{-1}		2.0000_{-1}		2.0000_{-1}	
$\tilde{J}_1$	2.1347_{-7}	1.1_{-4}	2.1351_{-7}	8.1_{-5}	2.1345_{-7}	2.4_{-4}	2.1350_{-7}	1.2_{-16}
M_{b}	8.0000_{-4}	3.5_{-6}	8.0009_{-4}	1.1_{-4}	7.9994_{-4}	7.8_{-5}	8.0005_{-4}	6.5_{-5}
M_{p}	8.0000_{-4}	3.5_{-6}	8.0009_{-4}	1.1_{-4}	7.9994_{-4}	7.8_{-5}	8.0005_{-4}	6.5_{-5}
E_{bind}	6.6504_{-6}	4.2_{-4}	6.6517_{-6}	2.3_{-4}	6.6496_{-6}	5.5_{-4}	6.6512_{-6}	3.1_{-4}
T	2.1347_{-8}	1.1_{-4}	2.1351_{-8}	8.1_{-5}	2.1345_{-8}	2.4_{-4}	2.1350_{-8}	8.4_{-12}
W	6.6718_{-6}	4.2_{-4}	6.6731_{-6}	2.3_{-4}	6.6709_{-6}	5.5_{-4}	6.6725_{-6}	3.1_{-4}
T/W	3.1997_{-3}	3.1_{-4}	3.1997_{-3}	3.1_{-4}	3.1997_{-3}	3.1_{-4}	3.1997_{-3}	3.1_{-4}
$\mathcal{R}_{\mathrm{circ}}$	5.7652_{-2}	3.9_{-5}	5.7654_{-2}	7.1_{-7}	5.7650_{-2}	6.4_{-5}	5.7653_{-2}	1.7_{-5}
z_{p}	1.4153_{-2}	2_{-5}	1.4154_{-2}	5.9_{-5}	1.4152_{-2}	7.1_{-5}	1.4153_{-2}	2.6_{-5}
$-\ln \psi_{\Sigma}$	-1.4053_{-2}	1.6_{-5}	-1.4055_{-2}	6.3_{-5}	-1.4053_{-2}	6.6_{-5}	-1.4054_{-2}	3_{-5}
R_{p}	5.6186_{-2}	3.9_{-5}	5.6188_{-2}	7.7_{-5}	5.6185_{-2}	1.5_{-5}	5.6187_{-2}	6.1_{-5}
R_{eq}	5.6854_{-2}	3.8_{-5}	5.6856_{-2}	2.4_{-16}	5.6852_{-2}	6.2_{-5}	5.6855_{-2}	1.6_{-5}
$R_{\mathrm{p}}/R_{\mathrm{eq}}$	9.8825_{-1}	7.7_{-5}	9.8825_{-1}	7.7_{-5}	9.8825_{-1}	7.7_{-5}	9.8825_{-1}	7.7_{-5}
ϵ_{c}	1.0000	0	1.0000	0	1.0000	0	1.0000	0
p_{c}	7.0588_{-3}	5.1_{-5}	7.0593_{-3}	1.3_{-4}	7.0584_{-3}	0	7.0591_{-3}	9.8_{-5}
μ_{bc}	1.0000	0	1.0000	0	1.0000	0	1.0000	0
h_{c}	1.0071	3.6_{-7}	1.0071	9.2_{-7}	1.0071	2.2_{-16}	1.0071	6.8_{-7}

Table 5.7: Comparison results for the model in Table 5.5 (page 118) of error between AKM and $\mathcal{O}(\lambda^{9/2}, \Omega^3)$ CMMR using different adjustments. These are the CMMR values obtained using $\tilde{M}_0$, R_{eq}, p_{c} and $\tilde{J}_1$ to fix the value of r_s.

5.2. *Adjusting with different quantities*

In the previous results we saw that relative error is generally bigger inside the source. Also, the quantities more closely related with the source are the ones that show a discordant behaviour when rotation starts to be a noticeable contribution to error. Besides, the error plots for $g_{t\phi}$ in Fig. 5.3 (page 119) seem to indicate that it does not improve far from the source, contrarily to what happens with other metric functions. We obtained all these results adjusting with $\tilde{M}_0$, i.e. , choosing r_s so that the CMMR value of $\tilde{M}_0$ equalled the one provided by AKM. Doing this we granted a good behaviour of g_{tt} at least far away from the source. Now the question is, can we adjust with other parameters to lower the error inside the source? Could we fix the strange behaviour of $g_{t\phi}$ using $\tilde{J}_1$ to adjust r_s instead? Is there an all-round better adjustment procedure? We check now these other adjustments for the two models already discussed.

Table 5.6 (facing page) collects the comparisons using $\tilde{M}_0$, R_{eq} and p_{c} to extract the value of r_s for the static $M_{\mathrm{b}} = 8.0 \times 10^{-4}$ model. There we see that at least in this case adjusting with R_{eq} gives also the best error in R_{p} and using p_{c} leads to the best value of h_{c} but the $\tilde{M}_0$ adjustment gives better results in general.

Table 5.7, which gives the data of the $\omega = 0.2$ model, is consistent with this

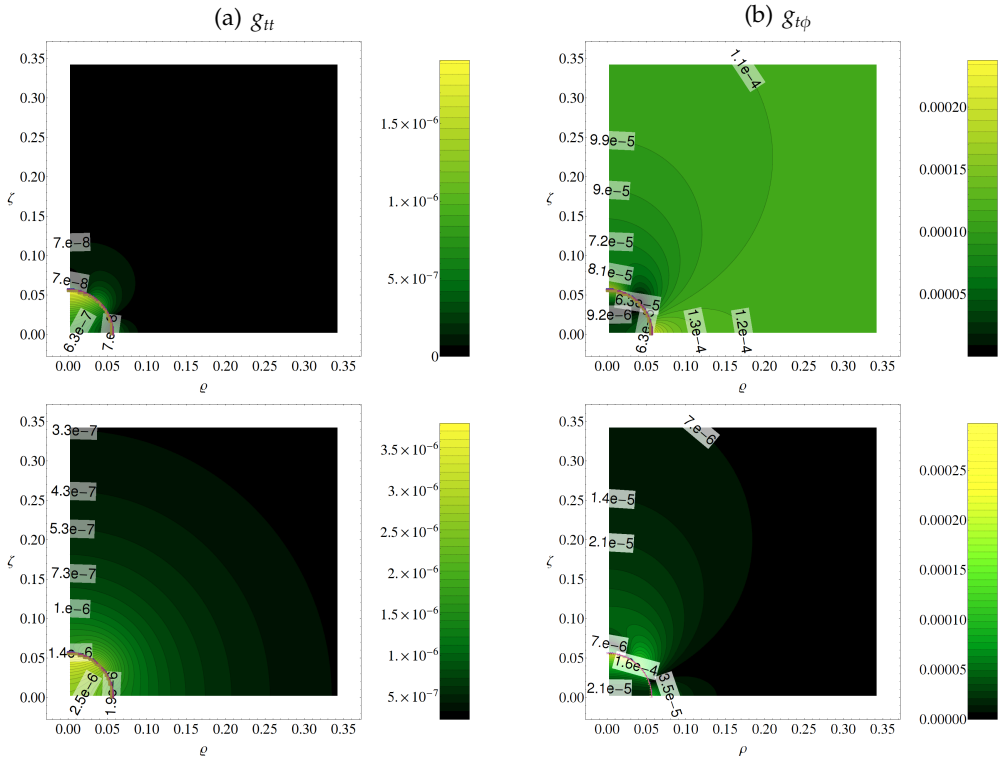

Figure 5.4: Relative error between $\mathcal{O}(\lambda^{9/2}, \Omega^3)$ CMMR and AKM for $M_b = 8.0 \times 10^{-4}$, $\omega = 0.2$ using $\tilde{M}_0$ adjustment (first row) and $\tilde{J}_1$ adjustment (second row). Column (a) groups g_{tt} components and (b) $g_{t\phi}$ ones.

tendency, although in E_{bind} we get a weird behaviour for R_{eq} adjustment, since it has the worst error in $\tilde{M}_0$ and M_b but the best value of E_{bind}. Nevertheless, we see here that the $\tilde{J}_1$ adjustment is comparable to the $\tilde{M}_0$ one. In this model and using $\tilde{M}_0$ adjustment $g_{t\phi}$ does not seem to tend to lower values far from the source, contrarily to the rest of the metric components and what one would expect of post-Minkowskian results for an asymptotically flat spacetime. The first row of graphs in Fig. 5.4 shows that this is indeed the situation at least at up to a coordinate distance of $6R_{\text{eq}}$. From the results in the second row, that collects g_{tt} and $g_{t\phi}$ for $\tilde{J}_1$ adjustment, we get that this is fixed using $\tilde{J}_1$ instead of $\tilde{M}_0$ to get r_s. Additionally, contrarily to what one could fear, it introduces no odd behaviour in g_{tt}. It seems to reduce its angular dependence, though it could be a consequence of the higher in average error. Unless otherwise stated, we will use $\tilde{J}_1$ adjustment in what follows. In static models, $\tilde{M}_0$ adjustment will be the choice since $\tilde{J}_1 = 0$.

5.3. Constant density models

We will study now some relevant configurations of gravitational mass and angular velocity to get information on the range of applicability of CMMR.

We start using models containing a source of constant density. These are not realistic (e.g., sound speed is infinite) but serve our purpose nonetheless. In the first one we focus on stellar-like objects, so we take for it the same parameters as the Sun, i.e., a gravitational mass of $\tilde{M}_0 = 1\,M_\odot$ and an angular velocity of $\omega \simeq 4.56\times10^{-6}\,\mathrm{Hz}$. Using the mean solar density $\mu_0 = 1408\,\mathrm{kg\,m^{-3}}$, this leads to models where the $c = G = \epsilon_0 = 1$ values of $\tilde{M}_0$ and ω must verify

$$1\,M_\odot \simeq \tilde{M}_0\,\frac{c^3}{\sqrt{G^3\mu_0}}, \tag{5.196}$$

$$4.56\times10^{-6}\,\mathrm{Hz} \simeq \omega\,\frac{\sqrt{G\mu_0}}{2\pi c}, \tag{5.197}$$

i.e.,

$$\tilde{M}_0 \simeq 1.51\times10^{-9}, \tag{5.198}$$

$$\omega \simeq 9.35\times10^{-2}. \tag{5.199}$$

Its compared data appear in Table 5.9 (following page). We see there that relative error is $\varepsilon \sim 10^{-6}$ or better except in E_{bind}. These are very good results, as could be expected from the very low values the approximation parameters take here: $(\lambda,\,\Omega) \simeq (2.12\times10^{-6},\,4.57\times10^{-2})$.

Relative error in the metric functions—Fig. 5.5 (following page)—is accordingly small as well, though far lower in $g_{\alpha\alpha}$ than in $g_{t\phi}$. This, and the very clear angular dependence in $g_{t\phi}$ is related with the strong difference existing between the approximation parameters.

	μ_0	Quantity	Value	$c = G = 1$ units	
Table 5.9	$1408\,\mathrm{kg\,m^{-3}}$	$\tilde{M}_0$	$1M_\odot$	$1.51\times10^{-9}\,\mu_0^{-1/2}$	p. 124
		ω	$4.56\times10^{-6}\,\mathrm{Hz}$	$9.35\times10^{-2}\,\mu_0^{1/2}$	
Table 5.11	$4\times10^{17}\,\mathrm{kg\,m^{-3}}$	$\tilde{M}_0$	$1M_\odot$	$2.54\times10^{-2}\,\mu_0^{-1/2}$	p. 127
		ω	$1.3\,\mathrm{Hz}$	$1.58\times10^{-3}\,\mu_0^{1/2}$	
Table 5.12	$4\times10^{17}\,\mathrm{kg\,m^{-3}}$	$\tilde{M}_0$	$1M_\odot$	$2.54\times10^{-2}\,\mu_0^{-1/2}$	p. 128
		ω	$350\,\mathrm{Hz}$	$4.26\times10^{-1}\,\mu_0^{1/2}$	

Table 5.8: Constant density models studied.

Quantity	AKM	CMMR	ε	$\text{CMMR}_{\text{conv}}$	Units
$\tilde{M}_0$	1.509790_{-9}	1.509794_{-9}	2.9_{-6}	1.000003	$M_\odot$
ω	9.350770_{-2}	9.350770_{-2}		4.561591_{-6}	Hz
$\tilde{J}_1$	2.865059_{-17}	2.865059_{-17}	4.3_{-16}	1.256899_1	$GM_\odot^2/c$
M_b	1.509792_{-9}	1.509796_{-9}	2.9_{-6}	1.000004	$M_\odot$
M_p	1.509792_{-9}	1.509796_{-9}	2.9_{-6}	1.000004	$M_\odot$
E_bind	1.924035_{-15}	1.920477_{-15}	1.8_{-3}	1.272016_{-6}	$M_\odot c^2$
T	1.339525_{-18}	1.339525_{-18}	6.7_{-14}	8.872260_{-10}	$M_\odot c^2$
W	1.921804_{-15}	1.921817_{-15}	6.6_{-6}	1.272903_{-6}	$M_\odot c^2$
T/W	6.970145_{-4}	6.970099_{-4}	6.6_{-6}		
$\mathcal{R}_\text{circ}$	7.122860_{-4}	7.122853_{-4}	1.1_{-6}	6.966679_5	km
z_p	2.122972_{-6}	2.122975_{-6}	1.3_{-6}		
$-\ln\psi_\Sigma$	-2.122970_{-6}	-2.122973_{-6}	1.3_{-6}		
R_p	7.104249_{-4}	7.104268_{-4}	2.7_{-6}	6.948502_5	km
R_eq	7.122845_{-4}	7.122837_{-4}	1.1_{-6}	6.966664_5	km
R_p/R_eq	9.973893_{-1}	9.973930_{-1}	3.7_{-6}		
ϵ_c	1.000000	1.000000	0	7.898302_{-13}	MeV fm^{-3}
p_c	1.059269_{-6}	1.059274_{-6}	4.9_{-6}	1.322927_9	atm
μ_bc	1.000000	1.000000	0	9.778020_{-47}	MeV c^2 fm^{-3}
h_c	1.000001	1.000001	5.2_{-12}	1.000001	c^2

Table 5.9: Relative error in the comparison for a constant density model of $\tilde{M}_0 = 1\,M_\odot$ and solar period using mean solar density and $\mathcal{O}(\lambda^{9/2}, \Omega^3)$ results. The second and third columns give $c = G = \epsilon_0 = 1$ values and the fifth one CMMR values corresponding to the convenient units of column six. Here $\lambda \simeq 2.12 \times 10^{-6}$ and $\Omega \simeq 4.57 \times 10^{-2}$.

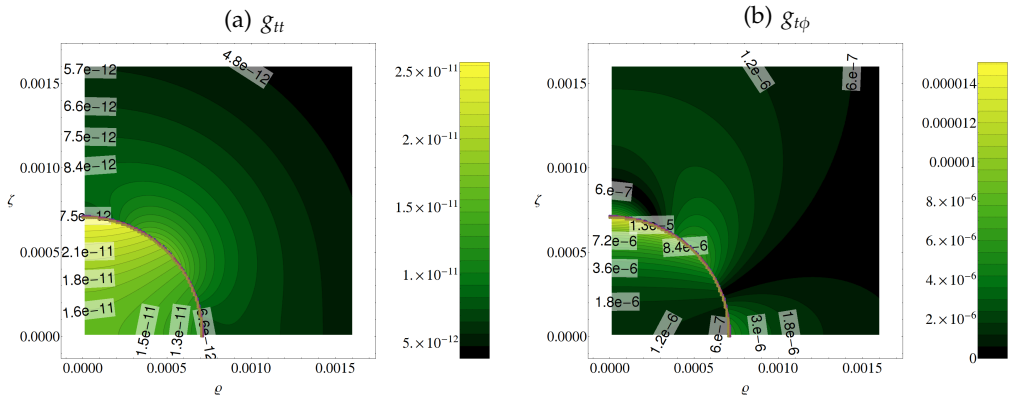

Figure 5.5: Relative error between AKM and $\mathcal{O}(\lambda^{9/2}, \Omega^3)$ CMMR in metric functions for $\tilde{M}_0 = 1\,M_\odot$ with solar mean density $\mu_0 = 1408\,\text{kg}\,\text{m}^{-3}$ and solar rotation rate $\omega \simeq 4.56 \times 10^{-6}$ Hz, the model of Table 5.9.

The error in the different quantities is comparable to the one obtained in the previous tables, which correspond to $M_b \simeq 5.29 \times 10^5 M_\odot$ and approximately two times the solar period for this density. Hence, CMMR provides very accurate results for objects in this order of compactness and angular velocity. The next models cover the kind of compactness found in compact stars. In particular, we take μ_0 to be the standard neutron star density, i.e., $\mu_0 = 4 \times 10^{17}\,\mathrm{kg\,m^{-3}}$. The typical mass of compact stars is $\tilde{M}_0 = 1.4\,M_\odot$, although several observations are compatible with lower masses (Lattimer, 2011). Their most common frequency is close $\omega = 1.3\,\mathrm{Hz}$—see Fig. 5.6 (following page)—although it can reach much higher values as in the case of millisecond pulsars, the fastest of them is J1748-2446ad with a frequency $\omega = 716\,\mathrm{Hz}$ (Hessels *et al.*, 2006). Kaaret *et al.* (2007) claimed to have found a 1122 Hz pulsar, but it has not been confirmed yet.

Table 5.11 (page 127) contains the data comparison for a source corresponding to $\tilde{M}_0 = 1\,M_\odot$ and $\omega = 1.3\,\mathrm{Hz}$, which arises from the model family of

$$\tilde{M}_0 \simeq 2.54 \times 10^{-2}, \tag{5.200}$$

$$\omega \simeq 1.58 \times 10^{-3} \tag{5.201}$$

in $c = G = \epsilon_0 = 1$ units. There we see that relative error is in general $\sim 1.5 \times 10^{-2}$ except in the quantities that are obtained from linear combinations of others and thus are more sensitive to errors. Regarding the metric functions—Fig. 5.7 (page 127), also part of the summary in Table 5.10 (following page)—we have that g_{tt} and $g_{t\phi}$ show an almost completely spherical symmetry as well. This is in contrast with what happens in Fig. 5.4 (page 122) because of two connected reasons. Here the approximation parameters are $(\lambda, \Omega) = (0.107, 7.72 \times 10^{-4})$, so contribution from the post-Minkowskian part of the approximation is dominant here, and hides the angular dependence of error that comes from the Ω truncation. But additionally, in Fig. 5.4 we got a higher value of $\Omega = 4.57 \times 10^{-2}$ despite having a far lower angular velocity. This comes from the relation of λ and Ω with r_s (eqs. [2.61, 2.62]). For compacter sources m/r_s gets higher thus increasing λ but decreasing Ω. Hence, *the compacter the source the faster it can spin before the contribution of the slow-rotation approximation becomes dominant*. In the last constant density case we keep this $\tilde{M}_0 = 1\,M_\odot$ but increase the angular velocity up to $\omega = 350\,\mathrm{Hz}$. To study it, we build the

$$\tilde{M}_0 \simeq 2.54 \times 10^{-2} \tag{5.202}$$

$$\omega \simeq 4.26 \times 10^{-1} \tag{5.203}$$

family of models. It is a faster rotating version of the previous one with slightly smaller M_b. Table 5.12 (page 128) shows its comparison results. We see that although the angular velocity is much bigger it affects very little the quality of the

CMMR data. In Fig. 5.8 (page 128) we have the same situation, a slight angular dependence in $g_{t\phi}$ but relative errors very close to those of $\omega = 1.3\,\mathrm{Hz}$.

This happens even though now $\lambda \simeq 0.107$, which is roughly the same as before, but $\Omega \simeq 0.208$, two orders of magnitude bigger than in Fig. 5.4 (page 122), and actually twice the value of the current λ. Hence, for models of this compactness

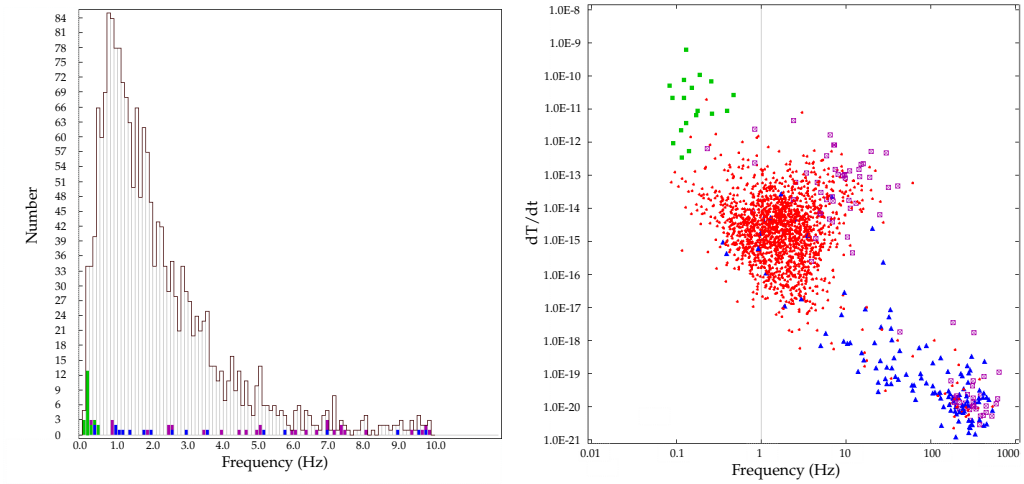

(a) Number vs. rotation frequency.

(b) Time derivative of period vs. rotation frequency.

Figure 5.6: (a): Number of pulsars in the ATNF Pulsar Catalogue for frequencies up to 10 Hz. (b): Time derivative of the rotation period vs. rotation frequency for all the pulsars in the Catalogue. The scales are logarithmic. Data for both figures obtained from `http://www.atnf.csiro.au`. (Manchester *et al.*, 2005). Colors code the kind of source; green for anomalous X-ray pulsars or soft gamma-ray repeaters, blue for binary pulsars, purple for high energy sources and red for other kinds.

$(\tilde{M}_0,\, \omega)$:	$1\,M_\odot$, 1.3 Hz		$1\,M_\odot$, 350 Hz	
	$\varepsilon\left(0,\, \frac{\pi}{2}\right)$	$\varepsilon\left(2\varrho_{\mathrm{eq}},\, \frac{\pi}{2}\right)$	$\varepsilon\left(0,\, \frac{\pi}{2}\right)$	$\varepsilon\left(2\varrho_{\mathrm{eq}},\, \frac{\pi}{2}\right)$
g_{tt}:	~ 0.02	~ 0.007	~ 0.019	~ 0.0072
$g_{t\phi}$:	~ 0.044	~ 0.014	~ 0.044	~ 0.015

Table 5.10: Relative error between AKM and $\mathcal{O}(\lambda^{9/2}, \Omega^3)$ CMMR in the g_{tt} and $g_{t\phi}$ metric functions for two configurations using the standard neutron star density $\mu_0 = 4 \times 10^{17}\,\mathrm{kg\,m^{-3}}$.

Quantity	AKM	CMMR	ε	Value	Units
$\tilde{M}_0$	2.545_{-2}	2.619_{-2}	2.9_{-2}	1.029	$M_\odot$
ω	1.581_{-3}	1.581_{-3}		1.300	Hz
$\tilde{J}_1$	6.129_{-7}	6.129_{-7}	6.9_{-16}	9.465_{-4}	$GM_\odot^2/c$
M_b	2.797_{-2}	2.842_{-2}	1.6_{-2}	1.117	$M_\odot$
M_p	2.797_{-2}	2.842_{-2}	1.6_{-2}	1.117	$M_\odot$
E_bind	2.520_{-3}	2.237_{-3}	1.1_{-1}	8.793_{-2}	$M_\odot c^2$
T	4.845_{-10}	4.845_{-10}	1.3_{-9}	1.904_{-8}	$M_\odot c^2$
W	2.520_{-3}	2.237_{-3}	1.1_{-1}	8.793_{-2}	$M_\odot c^2$
T/W	1.923_{-7}	2.165_{-7}	1.3_{-1}		
$\mathcal{R}_\mathrm{circ}$	1.825_{-1}	1.851_{-1}	1.4_{-2}	1.074_{1}	km
z_p	1.776_{-1}	1.765_{-1}	6.6_{-3}		
$-\ln\psi_\Sigma$	-1.635_{-1}	-1.645_{-1}	5.8_{-3}		
R_p	1.560_{-1}	1.593_{-1}	2.2_{-2}	9.246	km
R_eq	1.560_{-1}	1.593_{-1}	2.2_{-2}	9.246	km
$R_\mathrm{p}/R_\mathrm{eq}$	1.000_{0}	1.000_{0}	3.3_{-9}		
ϵ_c	1.000	1.000	0	2.244_{2}	MeV fm^{-3}
p_c	9.747_{-2}	9.499_{-2}	2.6_{-2}	3.370_{28}	atm
μ_bc	1.000	1.000	0	2.778_{-32}	MeV c^2 fm^{-3}
h_c	1.097	1.095	2.3_{-3}	1.095	c^2

Table 5.11: Relative error in the comparison for a constant density model of $\tilde{M}_0 = 1\,M_\odot$ and $\omega = 1.3\,\mathrm{Hz}$ using $\mu_0 = 4\times10^{17}\,\mathrm{kg\,m^{-3}}$ and $\mathcal{O}(\lambda^{9/2}, \Omega^3)$ results. The second and third columns give $c = G = \epsilon_0 = 1$ values and the fifth one has CMMR values corresponding to the units of column six. Here $\lambda \simeq 0.107$ and $\Omega \simeq 7.72\times10^{-4}$.

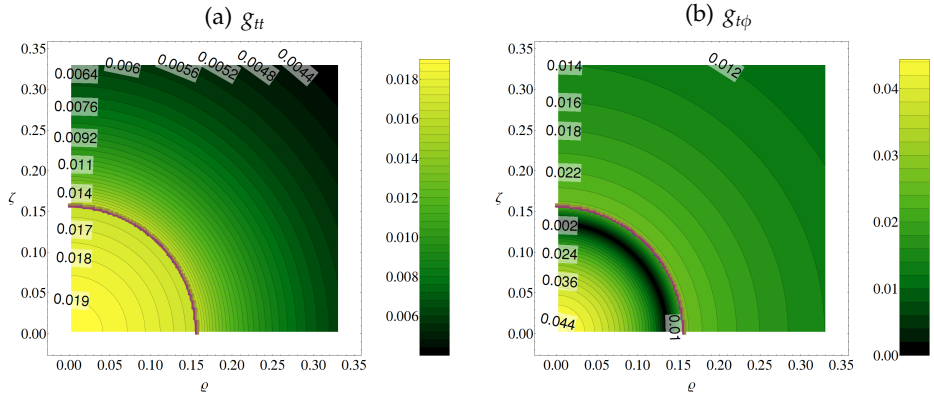

Figure 5.7: Relative error between AKM and $\mathcal{O}(\lambda^{9/2}, \Omega^3)$ CMMR in metric functions for $\tilde{M}_0 = 1\,M_\odot$ and a period of 1.3 s using constant standard neutron star density, the model of Table 5.11.

Quantity	AKM	CMMR	ε	$\text{CMMR}_{\text{conv}}$	Units
$\tilde{M}_0$	2.545_{-2}	2.619_{-2}	2.9_{-2}	1.029	$M_\odot$
ω	4.257_{-1}	4.257_{-1}		3.500_2	Hz
$\tilde{J}_1$	1.695_{-4}	1.695_{-4}	1.6_{-16}	2.617_{-1}	$GM_\odot^2/c$
M_{b}	2.792_{-2}	2.839_{-2}	1.7_{-2}	1.115	$M_\odot$
M_{p}	2.792_{-2}	2.839_{-2}	1.7_{-2}	1.115	$M_\odot$
E_{bind}	2.477_{-3}	2.199_{-3}	1.1_{-1}	8.641_{-2}	$M_\odot c^2$
T	3.607_{-5}	3.607_{-5}	1.3_{-14}	1.417_{-3}	$M_\odot c^2$
W	2.513_{-3}	2.235_{-3}	1.1_{-1}	8.783_{-2}	$M_\odot c^2$
T/W	1.435_{-2}	1.614_{-2}	1.2_{-1}		
$\mathcal{R}_{\text{circ}}$	1.851_{-1}	1.877_{-1}	1.4_{-2}	1.089_1	km
z_{p}	1.803_{-1}	1.791_{-1}	7_{-3}		
$-\ln\psi_\Sigma$	-1.658_{-1}	-1.667_{-1}	5.6_{-3}		
R_{p}	1.509_{-1}	1.542_{-1}	2.2_{-2}	8.949	km
R_{eq}	1.583_{-1}	1.617_{-1}	2.1_{-2}	9.384	km
$R_{\text{p}}/R_{\text{eq}}$	9.528_{-1}	9.537_{-1}	9.3_{-4}		
ϵ_{c}	1.000	1.000	0	2.244_2	MeV fm^{-3}
p_{c}	9.461_{-2}	9.229_{-2}	2.5_{-2}	3.274_{28}	atm
μ_{bc}	1.000	1.000	0	2.778_{-32}	MeV c^2 fm^{-3}
h_{c}	1.095	1.092	2.1_{-3}	1.092	c^2

Table 5.12: Relative error in the comparison for a constant density model of $\tilde{M}_0 = 1\,M_\odot$ and $\omega = 350\,\text{Hz}$ using $\mu_0 = 4\times10^{17}\,\text{kg m}^{-3}$ and $\mathcal{O}(\lambda^{9/2}, \Omega^3)$ results. The second and third columns give $c = G = \epsilon_0 = 1$ values and the fifth one has CMMR values corresponding to the units of column six. Here $\lambda \simeq 0.107$ and $\Omega \simeq 0.208$.

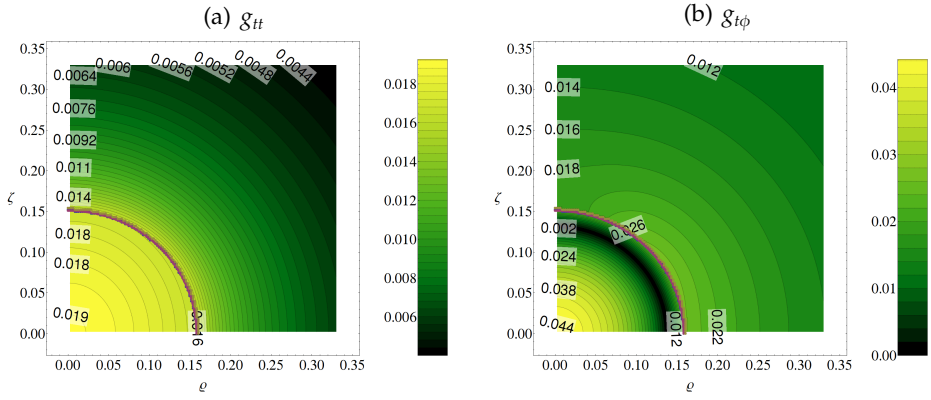

Figure 5.8: Relative error between AKM and $\mathcal{O}(\lambda^{9/2}, \Omega^3)$ CMMR in metric functions for $\tilde{M}_0 = 1\,M_\odot$ and $\omega = 350\,\text{Hz}$ using constant standard neutron star density, the model of Table 5.12.

and mass high rotation has little impact in the error when compared with the post-Minkowskian truncation order and accordingly, these could be improved going to higher λ-orders, the easier way.

5.4. Linear EOS-strange matter models

We turn our attention now to models that make better use of the freedom of the linear EOS (5.29). In particular, we choose $n = 4$, $b = B$ models corresponding to the simple MIT bag model energy-pressure EOS

$$\epsilon - 3p = \epsilon_0 = 4B \tag{5.204}$$

that gives the approximate behaviour of strange matter. Will use $c = G = B = 1$ units in general, as AKM does. This implies a little caveat.

Quantity	AKM	CMMR	ε	$\text{CMMR}_{\text{conv}}$	Units
$\tilde{M}_0$	$1.81 \cdot 10^{-2}$	$1.85 \cdot 10^{-2}$	$2.3 \cdot 10^{-2}$	1.41	$M_\odot$
ω	$3.06 \cdot 10^{-3}$	$3.06 \cdot 10^{-3}$		1.30	Hz
$\tilde{J}_1$	$2.34 \cdot 10^{-7}$	$2.34 \cdot 10^{-7}$	$2.3 \cdot 10^{-16}$	$1.36 \cdot 10^{-3}$	$GM_\odot^2/c$
M_{b}	$2.30 \cdot 10^{-2}$	$2.26 \cdot 10^{-2}$	$1.7 \cdot 10^{-2}$	1.72	$M_\odot$
M_{p}	$2.09 \cdot 10^{-2}$	$2.04 \cdot 10^{-2}$	$2.5 \cdot 10^{-2}$	1.55	$M_\odot$
E_{bind}	$4.86 \cdot 10^{-3}$	$4.05 \cdot 10^{-3}$	$1.7 \cdot 10^{-1}$	$3.08 \cdot 10^{-1}$	$M_\odot c^2$
T	$3.58 \cdot 10^{-10}$	$3.58 \cdot 10^{-10}$	$6.9 \cdot 10^{-9}$	$2.73 \cdot 10^{-8}$	$M_\odot c^2$
W	$2.73 \cdot 10^{-3}$	$1.80 \cdot 10^{-3}$	$3.4 \cdot 10^{-1}$	$1.37 \cdot 10^{-1}$	$M_\odot c^2$
T/W	$1.31 \cdot 10^{-7}$	$1.99 \cdot 10^{-7}$	$5.1 \cdot 10^{-1}$		
$\mathcal{R}_{\text{circ}}$	$9.56 \cdot 10^{-2}$	$1.01 \cdot 10^{-1}$	$5.2 \cdot 10^{-2}$	$1.13 \cdot 10^{1}$	km
z_{p}	$2.69 \cdot 10^{-1}$	$2.41 \cdot 10^{-1}$	$1.1 \cdot 10^{-1}$		
$-\ln \psi_\Sigma$	$-2.39 \cdot 10^{-1}$	$-2.22 \cdot 10^{-1}$	$6.8 \cdot 10^{-2}$		
R_{p}	$7.64 \cdot 10^{-2}$	$8.35 \cdot 10^{-2}$	$9.3 \cdot 10^{-2}$	9.38	km
R_{eq}	$7.64 \cdot 10^{-2}$	$8.35 \cdot 10^{-2}$	$9.3 \cdot 10^{-2}$	9.38	km
$R_{\text{p}}/R_{\text{eq}}$	$1.00 \cdot 10^{0}$	$1.00 \cdot 10^{0}$	$4.5 \cdot 10^{-8}$		
ϵ_{c}	6.94	5.57	$2{\cdot}10^{-1}$	$3.34 \cdot 10^{2}$	MeV fm^{-3}
p_{c}	$9.80 \cdot 10^{-1}$	$6.38 \cdot 10^{-1}$	$3.5 \cdot 10^{-1}$	$6.04 \cdot 10^{28}$	atm
μ_{bc}	7.43	6.15	$1.7 \cdot 10^{-1}$	$4.55 \cdot 10^{-32}$	MeV c^2 fm^{-3}
h_{c}	1.07	1.03	$3.8 \cdot 10^{-2}$	1.03	c^2

Table 5.13: Relative error in the comparison for a simple MIT bag model of $\tilde{M}_0 = 1.38\, M_\odot$ and $\omega = 1.3$ Hz using $\epsilon_0 = 4B = 4 \times 60$ MeV fm^{-3} and $\mathcal{O}(\lambda^{9/2}, \Omega^3)$ results. The second and third columns give $c = G = B = 1$ values and the fifth one has CMMR values corresponding to the units of column six. Here $\lambda \simeq 0.117$ and $\Omega \simeq 7.48 \times 10^{-4}$.

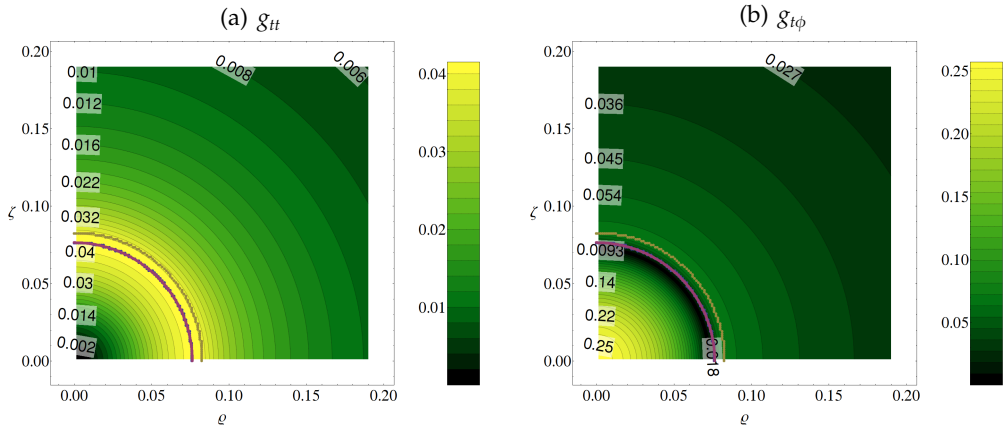

Figure 5.9: Relative error between AKM and $\mathcal{O}(\lambda^{9/2}, \Omega^3)$ CMMR in metric functions for $\tilde{M}_0 = 1.38\,M_\odot$ and $\omega = 1.3$ Hz using constant standard neutron star density, the model of Table 5.13 (facing page). The CMMR surface is the outer (lighter) pixeled line, slightly bigger than the AKM (darker) one.

When ϵ_0 is one of the three dimensional constants, with the others (c, G) fixed to one so that $r_s = \bar{r}_s \epsilon_0^{-1/2}$ and $\omega = \bar{\omega}\epsilon_0^{1/2}$, the approximation parameters keep the form they would take simply making $\epsilon_0 = 1$

$$\lambda = \frac{4}{3}\pi r_s^2 \epsilon_0 = \frac{4}{3}\pi \bar{r}_0^2, \tag{5.205}$$

$$\Omega = \frac{r_s \omega}{\lambda^{1/2}} = \sqrt{\frac{3}{4\pi}}\bar{\omega}, \tag{5.206}$$

because they are dimensionless. In the present case, ϵ_0 is not one of the three dimensional constants and thus the expression of λ and Ω changes, so that, whenever we are working with a third dimensional constant b definable as $\epsilon_0 = nb$ with n a dimensionless constant,

$$\lambda = \frac{4}{3}\pi r_s^2 \epsilon_0 = \frac{4}{3}\pi n \bar{r}_0^2, \tag{5.207}$$

$$\Omega = \frac{r_s \omega}{\lambda^{1/2}} = \sqrt{\frac{3}{4n\pi}}\bar{\omega}. \tag{5.208}$$

Taking this into account we can proceed as in previous cases. We will analyse first the model of a strange star with typical pulsar parameters $M = 1.38\,M_\odot$ and $\omega = 1.3$ Hz. If we take the common value for the bag constant $B = 60$ MeV fm^{-3} or equivalently

$$\mu_0 = 4B = 4 \times 1.067 \times 10^{17}\ \text{kg m}^{-3} \tag{5.209}$$

we have that this is a particular case of the family of models with

$$\tilde{M}_0 \simeq 1.81 \times 10^{-2} B^{-1/2}, \tag{5.210}$$

$$\omega \simeq 3.06 \times 10^{-3} B^{1/2}. \tag{5.211}$$

The comparison of quantities appears in Table 5.13 (page 129), where we see that ε is in general located between orders 10^{-1}-10^{-2}. Something similar happens in the metric functions on Fig. 5.9 (facing page), though falling quite fast to 10^{-3} in g_{tt} and 10^{-2} in $g_{t\phi}$ with bigger distances to the source. We can also see in this case a noticeable difference between AKM and CMMR masses—recall that we are using $\tilde{J}_1$ adjustment in non-static cases—and this is partly responsible for the bigger radius of the CMMR surface, but not exclusively since it happens with $\tilde{M}_0$ adjustment as well.

In this case error starts to be of importance, but again its distribution indicate that is λ dominated. Thus, it may be worthy to go to further λ-orders for a reasonable easy improvement of the results.

The previous $1.4\,M_\odot$ is a very common measured value for pulsars, and also a value easily reachable with most neutron star EOS. Nevertheless, neutron and strange stars have very different mass-radius (MR) relations. While neutron stars increase their mass for lower radii, what imposes a minimum size for them, strange star behave in the opposite way, with mass increasing with the radius. This gives them totally different zones in a MR diagram—see Fig. 1.1 (page 7)—, with strange stars favouring lower masses. There are at least two observed objects with estimated masses substantially below the canonical $1.38\,M_\odot$ that in fact defy explanation with most neutron star models, hinting towards SQM composition:

- 4U 1728-34. Li *et al.* (1999b) were the first to give an estimation for its mass and radius, establishing an upper bound of $\tilde{M}_0 \lesssim 1.1\,M_\odot$ for the first and $R \lesssim 10\,\text{km}$ for the second. Later, Shaposhnikov *et al.* (2003) gave estimates depending on the distance to the source, ranging from $\tilde{M}_0 = 0.91\,M_\odot$, $R = 8.66\,\text{km}$ at $4\,\text{kpc}$ to $\tilde{M}_0 = 1.61\,M_\odot$, $R = 9.60\,\text{km}$ at $5\,\text{kpc}$, the latter being probably the upper limit. Last, Majczyna and Madej (2005) gave $\tilde{M}_0 = 0.4^{0.7}_{0.1}\,M_\odot$, $R = 4.58^{7.7}_{1.4}\,\text{km}$ and $\tilde{M}_0 = 0.63^{1.2}_{0.1}\,M_\odot$, $R = 5.27^{9.1}_{1.4}\,\text{km}$ as best fits and $1-\sigma$ confidence ranges depending on the kind of atmosphere of the source.

- SAX J1808.4-3658. Li *et al.* (1999a) determined the allowed region of MR configurations for this $\omega = 401\,\text{Hz}$ source, showing it to be incompatible with the neutron star EOS considered and favouring strange quark matter ones. The latest MR estimation for this object is due to Leahy *et al.* (2008) to our knowledge. It gives two different results. A first one, using bolometric

light curves, gives a very wide 3-σ region ranging from the lightest configuration $\tilde{M}_0 = 0.4\,M_\odot$, $R = 6.5\,\mathrm{km}$ to the heaviest $\tilde{M}_0 = 1.4\,M_\odot$, $R = 10.6\,\mathrm{km}$ with a best fit in $\tilde{M}_0 = 0.99\,M_\odot$, $R = 4.87\,\mathrm{km}$. A second one, using only two band light curves, gives a heaviest configuration with $\tilde{M}_0 = 1.1\,M_\odot$, $R = 5.4\,\mathrm{km}$ and a lightest one with $\tilde{M}_0 = 0.8\,M_\odot$, $R = 4\,\mathrm{km}$, with best fit in $\tilde{M}_0 = 0.96\,M_\odot$, $R = 4.72\,\mathrm{km}$. This last one has much narrower confidence levels, points towards SQM EOS and is in better agreement with the previous results of Poutanen and Gierliński (2003), where the quality of the fits decreases rapidly for $\tilde{M}_0 \gtrsim 1\,M_\odot$

Hence, this two objects probably have masses close to $1\,M_\odot$ or even lower. Their frequencies are quite close (and high), too close to give rise to big differences between them. Taking this into account we are going to study now a model corresponding to $\tilde{M}_0 = 1\,M_\odot$ and one of their frequencies, $\omega = 364\,\mathrm{Hz}$, i.e. , models of the

$$\tilde{M}_0 \simeq 1.31 \times 10^{-2} B^{-1/2}, \tag{5.212}$$
$$\omega \simeq 0.857 B^{1/2}. \tag{5.213}$$

family. We will also calculate the

$$\tilde{M}_0 \simeq 1.31 \times 10^{-2} B^{-1/2}, \tag{5.214}$$
$$\omega \simeq 3.06 \times 10^{-3} B^{1/2}. \tag{5.215}$$

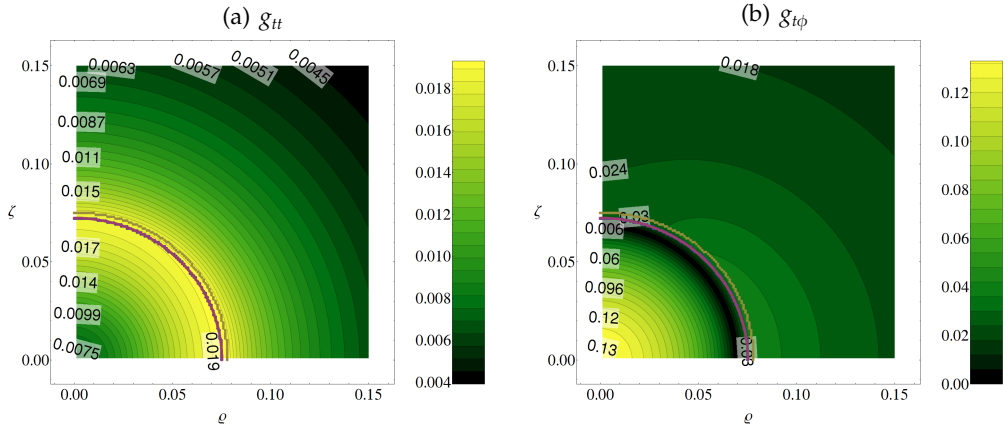

Figure 5.10: Relative error between AKM and $\mathcal{O}(\lambda^{9/2}, \Omega^3)$ CMMR in metric functions for $\tilde{M}_0 = 1\,M_\odot$ and $\omega = 364\,\mathrm{Hz}$ using the simple MIT bag model and $\epsilon_0 = 4B = 4 \times 60\,\mathrm{MeV\,fm^{-3}}$, the model of Table 5.14(a) (following page).

(a) $\omega = 364\,\mathrm{Hz}$

Quantity	AKM	CMMR	ε	$\mathrm{CMMR}_{\mathrm{conv}}$	Units
$\tilde{M}_0$	$1.314 \cdot 10^{-2}$	$1.339 \cdot 10^{-2}$	$1.8 \cdot 10^{-2}$	1.018	$M_\odot$
ω	$8.571 \cdot 10^{-1}$	$8.571 \cdot 10^{-1}$		$3.640 \cdot 10^{2}$	Hz
$\tilde{J}_1$	$3.997 \cdot 10^{-5}$	$3.997 \cdot 10^{-5}$	$1.7 \cdot 10^{-16}$	$2.313 \cdot 10^{-1}$	$GM_\odot^2/c$
M_{b}	$1.614 \cdot 10^{-2}$	$1.608 \cdot 10^{-2}$	$3.2 \cdot 10^{-3}$	1.224	$M_\odot$
M_{p}	$1.457 \cdot 10^{-2}$	$1.448 \cdot 10^{-2}$	$6.1 \cdot 10^{-3}$	1.101	$M_\odot$
E_{bind}	$2.993 \cdot 10^{-3}$	$2.699 \cdot 10^{-3}$	$9.8 \cdot 10^{-2}$	$2.054 \cdot 10^{-1}$	$M_\odot c^2$
T	$1.713 \cdot 10^{-5}$	$1.713 \cdot 10^{-5}$	$1.6 \cdot 10^{-12}$	$1.303 \cdot 10^{-3}$	$M_\odot c^2$
W	$1.440 \cdot 10^{-3}$	$1.110 \cdot 10^{-3}$	$2.3 \cdot 10^{-1}$	$8.443 \cdot 10^{-2}$	$M_\odot c^2$
T/W	$1.189 \cdot 10^{-2}$	$1.543 \cdot 10^{-2}$	$3 \cdot 10^{-1}$		
$\mathcal{R}_{\mathrm{circ}}$	$8.913 \cdot 10^{-2}$	$9.158 \cdot 10^{-2}$	$2.7 \cdot 10^{-2}$	$1.029 \cdot 10^{1}$	km
z_{p}	$1.965 \cdot 10^{-1}$	$1.868 \cdot 10^{-1}$	$4.9 \cdot 10^{-2}$		
$-\ln \psi_\Sigma$	$-1.794 \cdot 10^{-1}$	$-1.744 \cdot 10^{-1}$	$2.8 \cdot 10^{-2}$		
R_{p}	$7.236 \cdot 10^{-2}$	$7.562 \cdot 10^{-2}$	$4.5 \cdot 10^{-2}$	8.496	km
R_{eq}	$7.530 \cdot 10^{-2}$	$7.874 \cdot 10^{-2}$	$4.6 \cdot 10^{-2}$	8.846	km
$R_{\mathrm{p}}/R_{\mathrm{eq}}$	$9.610 \cdot 10^{-1}$	$9.604 \cdot 10^{-1}$	$5.9 \cdot 10^{-4}$		
ϵ_{c}	5.669	5.184	$8.6 \cdot 10^{-2}$	$3.103 \cdot 10^{2}$	$\mathrm{MeV\,fm^{-3}}$
p_{c}	$5.563 \cdot 10^{-1}$	$4.559 \cdot 10^{-1}$	$1.8 \cdot 10^{-1}$	$4.315 \cdot 10^{28}$	atm
μ_{bc}	6.199	5.731	$7.5 \cdot 10^{-2}$	$4.247 \cdot 10^{-32}$	$\mathrm{MeV}\,c^2\,\mathrm{fm^{-3}}$
h_{c}	1.004	$9.916 \cdot 10^{-1}$	$1.3 \cdot 10^{-2}$	$9.916 \cdot 10^{-1}$	c^2

(b) $\omega = 0$

Quantity	AKM	CMMR	ε	$\mathrm{CMMR}_{\mathrm{conv}}$	Units
$\tilde{M}_0$	$1.314 \cdot 10^{-2}$	$1.314 \cdot 10^{-2}$	$1.3 \cdot 10^{-16}$	1.000	$M_\odot$
M_{b}	$1.616 \cdot 10^{-2}$	$1.580 \cdot 10^{-2}$	$2.2 \cdot 10^{-2}$	1.202	$M_\odot$
M_{p}	$1.459 \cdot 10^{-2}$	$1.422 \cdot 10^{-2}$	$2.5 \cdot 10^{-2}$	1.082	$M_\odot$
E_{bind}	$3.016 \cdot 10^{-3}$	$2.657 \cdot 10^{-3}$	$1.2 \cdot 10^{-1}$	$2.021 \cdot 10^{-1}$	$M_\odot c^2$
W	$1.447 \cdot 10^{-3}$	$1.079 \cdot 10^{-3}$	$2.5 \cdot 10^{-1}$	$8.208 \cdot 10^{-2}$	$M_\odot c^2$
$\mathcal{R}_{\mathrm{circ}}$	$8.799 \cdot 10^{-2}$	$8.988 \cdot 10^{-2}$	$2.2 \cdot 10^{-2}$	$1.010 \cdot 10^{1}$	km
z_{p}	$1.942 \cdot 10^{-1}$	$1.817 \cdot 10^{-1}$	$6.4 \cdot 10^{-2}$		
$-\ln \psi_\Sigma$	$-1.775 \cdot 10^{-1}$	$-1.699 \cdot 10^{-1}$	$4.2 \cdot 10^{-2}$		
R_{p}	$7.426 \cdot 10^{-2}$	$7.737 \cdot 10^{-2}$	$4.2 \cdot 10^{-2}$	8.693	km
R_{eq}	$7.426 \cdot 10^{-2}$	$7.737 \cdot 10^{-2}$	$4.2 \cdot 10^{-2}$	8.693	km
$R_{\mathrm{p}}/R_{\mathrm{eq}}$	$1.000 \cdot 10^{0}$	1.000	$1.2 \cdot 10^{-14}$		
ϵ_{c}	5.727	5.203	$9.2 \cdot 10^{-2}$	$3.114 \cdot 10^{2}$	$\mathrm{MeV\,fm^{-3}}$
p_{c}	$5.757 \cdot 10^{-1}$	$4.622 \cdot 10^{-1}$	$2 \cdot 10^{-1}$	$4.375 \cdot 10^{28}$	atm
μ_{bc}	6.257	5.751	$8.1 \cdot 10^{-2}$	$4.262 \cdot 10^{-32}$	$\mathrm{MeV}\,c^2\,\mathrm{fm^{-3}}$
h_{c}	1.007	$9.927 \cdot 10^{-1}$	$1.5 \cdot 10^{-2}$	$9.927 \cdot 10^{-1}$	c^2

Table 5.14: Relative error in the comparison for a simple MIT bag EOS model of $\tilde{M}_0 = 1\,M_\odot$ in the static and $\omega = 364\,\mathrm{Hz}$ cases ($\mu_0 \simeq 1.067 \times 10^{17}\,\mathrm{kg\,m^{-3}}$, or equivalently $\epsilon_0 = 4B = 4 \times 60\,\mathrm{MeV\,fm^{-3}}$) using $\mathcal{O}(\lambda^{9/2}, \Omega^3)$ results. The second and third columns give $c = G = B = 1$ values and the fifth one CMMR values corresponding to the units of column six. Here $\lambda \simeq 0.102$ and $\Omega \simeq 0.209$; $\lambda \simeq 0.101$ in the static case.

model leading to $\omega = 1.3\,\mathrm{Hz}$ and the static case to see the influence of rotation:

- Table 5.14(a) (facing page) gives the quantities comparison for the $\tilde{M}_0 = 1\,M_\odot$, $\omega = 364\,\mathrm{Hz}$ case, improving by roughly a $\frac{1}{2}$ factor with respect to the ones $\tilde{M}_0 = 1.38\,M_\odot$ ones of Table 5.13 (page 129). Fig. 5.10 (page 132) shows the familiar almost spherical error distribution, as well as closely fitted surfaces.

- In Table 5.14(b) (facing page) we list the results for the static case, with $\tilde{M}_0$ adjustment. It shows no big departure from the 364 Hz case, and something similar happens with the metric functions of Fig. 5.11.

- Last, Table 5.16 (page 136) lists the ε for $\omega = 1.3\,\mathrm{Hz}$, with the metric functions compared in Fig. 5.12 (page 136). The results are very similar to the static ones.

Therefore for this frequency range the results show very little rotation dependence and again can be significatively improved going to next post-Minkowskian iteration, which should lead to $\varepsilon \sim 10^{-3}$ as general value. Table 5.15 (following page) summarizes the error in the metric functions for these three angular velocities.

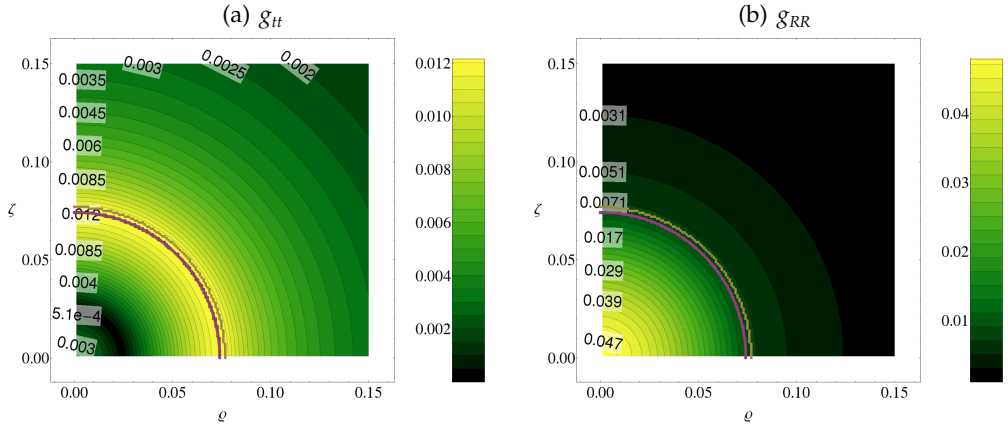

Figure 5.11: Relative error between AKM and $\mathcal{O}(\lambda^4)$ CGMR in metric functions for $\tilde{M}_0 = 1\,M_\odot$ using a static simple MIT bag model and $\epsilon_0 = 4B = 4 \times 60\,\mathrm{MeV\,fm^{-3}}$, the model of Table 5.14(b) (facing page).

$(\tilde{M}_0,\, \omega)$:	$1\,M_\odot$, 0 Hz		$1\,M_\odot$, 1.3 Hz		$1\,M_\odot$, 350 Hz	
	$\varepsilon\left(0,\, \frac{\pi}{2}\right)$	$\varepsilon\left(2\varrho_{\text{eq}},\, \frac{\pi}{2}\right)$	$\varepsilon\left(0,\, \frac{\pi}{2}\right)$	$\varepsilon\left(2\varrho_{\text{eq}},\, \frac{\pi}{2}\right)$	$\varepsilon\left(0,\, \frac{\pi}{2}\right)$	$\varepsilon\left(2\varrho_{\text{eq}},\, \frac{\pi}{2}\right)$
g_{tt}:	~ 0.003	~ 0.0035	~ 0.0077	~ 0.0069	~ 0.0075	~ 0.0069
$g_{t\phi}$:			~ 0.13	~ 0.024	~ 0.13	~ 0.025
g_{RR}:	~ 0.12	~ 0.0057	~ 0.12	~ 0.004	~ 0.10	~ 0.004

Table 5.15: Relative error between AKM and $\mathcal{O}(\lambda^{9/2}, \Omega^3)$ CGMR in the g_{tt}, $g_{t\phi}$ and g_{RR} metric functions for three configurations using the simple MIT bag model with $\epsilon_0 = 4B = 4 \times 60\,\text{MeV fm}^{-3}$.

6. Other results

In Section 4 we introduced some quantities that, while the standard AKM code does not compute, appear in different works. We list them for both their physical relevance and to allow for a fast further comparison of our results.

In what follows, we use our analytical expressions to give values for these quantities for the stellar models studied in the previous section.

- Table 5.17 (page 137) contains the data corresponding to constant density sources with $M_{\text{b}} = 8 \times 10^{-4}$, static and rotating at $\omega = 350\,\text{Hz}$.
- Table 5.18(a) (page 138) concerns $\tilde{M}_0 = 1\,M_\odot$ constant density models for two different densities and solar, average and 350 Hz angular velocities.
- Table 5.18(b) (page 138) corresponds to the $\tilde{M}_0 = 1\,M_\odot$ strange star models rotating at $\omega = 0$, $\omega = 1.3\,\text{Hz}$ and $\omega = 363\,\text{Hz}$.

Among them, the data regarding the ISCO (or the circular orbit for massless particles) deserves a more careful look. We did not find a way to expand its radial coordinate coherently with the rest of the approximation; hence, the radii come from the numerical solution of the $k = 2$ case of eq. (5.186) and the $k = 1$ one from eq. (5.192). Fig. 5.13 (page 140) shows the behaviour of prograde and retrograde ISCO of time-like particles for strange star sources of $M_{\text{b}} \simeq 0.11$, 0.95 and $1.71\,M_\odot$ corresponding to gravitational masses of approximately $\tilde{M}_0 \simeq 0.1$, 0.8 and $1.4\,M_\odot$, and ranging from $\omega = 0$ to $\omega = 2$—slightly faster than the fastest spinning source known, $\omega = 1.7 \overset{\text{SI}}{\simeq} 716\,\text{Hz}$. In that Figure, the left column contains $\mathcal{O}(\lambda^{9/2}, \Omega^3)$ results and the right one those of the $\mathcal{O}(\lambda^{5/2}, \Omega^3)$ approximation. To check accuracy, the plots also display a dot at the position of the Schwarzschild ISCO, which is $r_{\text{stnd}} = 6M$ in Schwarzschild standard coordinates. Changing coordinates from

Quantity	AKM	CMMR	ε	$\text{CMMR}_{\text{conv}}$	Units
$\tilde{M}_0$	$1.314 \cdot 10^{-2}$	$1.340 \cdot 10^{-2}$	$2{\cdot}10^{-2}$	1.020	$M_\odot$
ω	$3.061 \cdot 10^{-3}$	$3.061 \cdot 10^{-3}$		1.300	Hz
$\tilde{J}_1$	$1.393 \cdot 10^{-7}$	$1.393 \cdot 10^{-7}$	0	$8.060 \cdot 10^{-4}$	$GM_\odot^2/c$
M_{b}	$1.616 \cdot 10^{-2}$	$1.612 \cdot 10^{-2}$	$2.3 \cdot 10^{-3}$	1.227	$M_\odot$
M_{p}	$1.459 \cdot 10^{-2}$	$1.451 \cdot 10^{-2}$	$5.4 \cdot 10^{-3}$	1.104	$M_\odot$
E_{bind}	$3.016 \cdot 10^{-3}$	$2.721 \cdot 10^{-3}$	$9.8 \cdot 10^{-2}$	$2.070 \cdot 10^{-1}$	$M_\odot c^2$
T	$2.131 \cdot 10^{-10}$	$2.131 \cdot 10^{-10}$	$7.3 \cdot 10^{-12}$	$1.621 \cdot 10^{-8}$	$M_\odot c^2$
W	$1.447 \cdot 10^{-3}$	$1.111 \cdot 10^{-3}$	$2.3 \cdot 10^{-1}$	$8.453 \cdot 10^{-2}$	$M_\odot c^2$
T/W	$1.473 \cdot 10^{-7}$	$1.918 \cdot 10^{-7}$	$3{\cdot}10^{-1}$		
$\mathcal{R}_{\text{circ}}$	$8.799 \cdot 10^{-2}$	$9.045 \cdot 10^{-2}$	$2.8 \cdot 10^{-2}$	$1.016 \cdot 10^{1}$	km
z_{p}	$1.942 \cdot 10^{-1}$	$1.846 \cdot 10^{-1}$	$4.9 \cdot 10^{-2}$		
$-\ln \psi_\Sigma$	$-1.775 \cdot 10^{-1}$	$-1.725 \cdot 10^{-1}$	$2.8 \cdot 10^{-2}$		
R_{p}	$7.426 \cdot 10^{-2}$	$7.772 \cdot 10^{-2}$	$4.6 \cdot 10^{-2}$	8.731	km
R_{eq}	$7.426 \cdot 10^{-2}$	$7.772 \cdot 10^{-2}$	$4.6 \cdot 10^{-2}$	8.731	km
$R_{\text{p}}/R_{\text{eq}}$	$1.000 \cdot 10^{0}$	$1.000 \cdot 10^{0}$	$2{\cdot}10^{-8}$		
ϵ_{c}	5.727	5.221	$8.8 \cdot 10^{-2}$	$3.125 \cdot 10^{2}$	MeV fm^{-3}
p_{c}	$5.757 \cdot 10^{-1}$	$4.706 \cdot 10^{-1}$	$1.8 \cdot 10^{-1}$	$4.454 \cdot 10^{28}$	atm
μ_{bc}	6.257	5.771	$7.8 \cdot 10^{-2}$	$4.277 \cdot 10^{-32}$	MeV c^2 fm^{-3}
h_{c}	1.007	$9.943 \cdot 10^{-1}$	$1.3 \cdot 10^{-2}$	$9.943 \cdot 10^{-1}$	c^2

Table 5.16: Relative error in the comparison for a simple MIT bag model EOS of $\tilde{M}_0 = 1\,M_\odot$ and $\omega = 1.3$ Hz using $\epsilon_0 = 4B = 4 \times 60$ MeV fm^{-3} and $\mathcal{O}(\lambda^{9/2}, \Omega^3)$ results. The second and third columns give $c = G = B = 1$ values and the fifth one has CMMR values corresponding to the units of column six. Here $\lambda \simeq 0.102$ and $\Omega \simeq 7.48 \times 10^{-4}$.

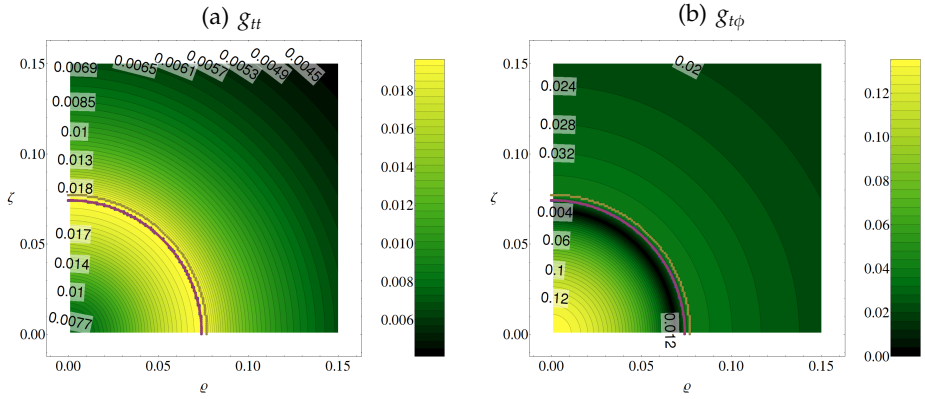

Figure 5.12: Relative error between AKM and $\mathcal{O}(\lambda^{9/2}, \Omega^3)$ CMMR in metric functions for $\tilde{M}_0 = 1\,M_\odot$ and $\omega = 1.3$ Hz using the simple MIT bag model with $\epsilon_0 = 4B = 4 \times 60$ MeV fm^{-3}, the model of Table 5.16.

standard to isotropic ones with

$$R = \frac{r_{\text{stnd}}}{2} - \frac{2\tilde{M}_0}{4} + \sqrt{\frac{r_{\text{stnd}}}{4}(r_{\text{stnd}} - 2\tilde{M}_0)}, \tag{5.216}$$

we get the position of the Schwarzschild ISCO in isotropic coordinates—which are equal to the quasi-isotropic ones in the spherical limit—, i.e.

$$R_{\text{ISCO}}^{\text{Schw}} = \left(\frac{5}{2} + \sqrt{6}\right)\tilde{M}_0. \tag{5.217}$$

The behaviour is far better for low masses as expectable and shows a significant improvement with the higher approximation. It is also apparent that with the current results, the mass and/or angular velocity needed for the presence of an ISCO ($R_{\text{ISCO}}^{\pm} > R_{\text{eq}}$) is still visibly higher than what the Schwarzschild result suggest, though. The circular orbits of massless particles have always smaller radii than ISCOs and do not lie above R_{eq} for any of the cases studied and we do not

	$\omega = 0\,\text{Hz}$		$\omega = 350\,\text{Hz}$		
Quantity	CMMR	$\text{CMMR}_{\text{conv}}$	CMMR	$\text{CMMR}_{\text{conv}}$	Unit
r_0	5.663323_{-2}	5.53915_{7}	5.663395_{-2}	5.539221_{7}	km
$\tilde{M}_2$	0	0	-1.197716_{-8}	-2.386673_{3}	$M_\odot \mathcal{R}_{\text{circ}}^2$
$\tilde{J}_3$	0	0	-2.27517_{-12}	-3.002869_{8}	$GM_\odot^2 \mathcal{R}_{\text{circ}}^2/c$
I	1.059112_{-6}	2.127073_{5}	1.067488_{-6}	2.127171_{5}	$M_\odot \mathcal{R}_{\text{circ}}^2$
$c\tilde{J}_1/G\tilde{M}_0^2$	0		3.391625_{-1}		
$\tilde{M}_2/\tilde{M}_0\mathcal{R}_{\text{circ}}^2$	0		-4.541685_{-3}		
$c^4\tilde{M}_2/G^2\tilde{M}_0^3$	0		-2.398147_{1}		
z_{eq}^+	9.860889_{-1}		9.745158_{-1}		
z_{eq}^-	9.860889_{-1}		9.975755_{-1}		
R_{ISCO}^+	3.798184_{-3}	3.714906_{6}	8.318422_{-3}	8.136035_{6}	km
R_{ISCO}^-	3.798184_{-3}	3.714906_{6}	9.537823_{-3}	9.3287_{6}	km
R_{null}^+	0	0	3.794365_{-3}	3.71117_{6}	km
R_{null}^-	0	0	4.236964_{-3}	4.144065_{6}	km
$\mathcal{R}_{\text{p}}$	5.769543_{-2}	5.643042_{7}	5.724346_{-2}	5.598836_{7}	km
$\mathcal{C}_{\text{p}}$	3.608289_{-1}	3.529175_{8}	3.601286_{-1}	3.522325_{8}	km
$\varepsilon_{\text{proper}}$	0		1.526887_{-1}		
$\varepsilon_{\text{int.}}$	0		1.079286_{-1}		

Table 5.17: Some other quantities corresponding to the constant density models with $M_{\text{b}} = 8 \times 10^{-4}$ of Table 5.3 (page 115) and Table 5.5 (page 118) using $\mathcal{O}(\lambda^{9/2}, \Omega^3)$ results. Each pair of data columns lists the $c = G = \epsilon_0 = 1$ value and its value in some convenient units when $\mu_0 = 4 \times 10^{17}\,\text{kg}\,\text{m}^{-3}$.

(a) Constant density models of Table 5.9 (page 124), Table 5.11 (page 127) and Table 5.12 (page 128) with $\tilde{M}_0 = 1\,M_\odot$ with mean solar density (first pair) and $\mu_0 = 4 \times 10^{17}\,\mathrm{kg\,m^{-3}}$ (last two pairs).

	$\omega = 4.56 \times 10^{-6}$ Hz		$\omega = 1.3$ Hz		$\omega = 350$ Hz		
Quantity	CMMR	CMMR$_{\mathrm{conv}}$	CMMR	CMMR$_{\mathrm{conv}}$	CMMR	CMMR$_{\mathrm{conv}}$	Unit
r_0	7.117_{-4}	6.961_5	1.597_{-1}	9.27	1.596_{-1}	9.263	km
$\tilde{M}_2$	-7.981_{-19}	-1.042_{-3}	-1.736_{-10}	-1.993_{-7}	-1.253_{-5}	-1.398_{-2}	$M_\odot \mathcal{R}^2_{\mathrm{circ}}$
$\tilde{J}_3$	-1.08_{-26}	-9.338_{-3}	-2.808_{-15}	-1.266_{-10}	-5.443_{-8}	-2.387_{-3}	$GM_\odot^2 \mathcal{R}^2_{\mathrm{circ}}/c$
I	3.064_{-16}	4_{-1}	3.877_{-4}	4.449_{-1}	3.981_{-4}	4.442_{-1}	$M_\odot \mathcal{R}^2_{\mathrm{circ}}$
$c\tilde{J}_1/G\tilde{M}_0^2$	1.257_1		8.937_{-4}		2.471_{-1}		
$\tilde{M}_2/\tilde{M}_0\mathcal{R}^2_{\mathrm{circ}}$	-1.042_{-3}		-1.936_{-7}		-1.359_{-2}		
$c^4\tilde{M}_2/G^2\tilde{M}_0^3$	-2.319_8		-9.669_{-6}		-6.977_{-1}		
z^+_{eq}	9.999_{-1}		8.465_{-1}		7.659_{-1}		
z^-_{eq}	1		8.471_{-1}		9.252_{-1}		
R^+_{ISCO}	2.817_{-5}	2.755_4	1.021_{-1}	5.925	1.049_{-1}	6.086	km
R^-_{ISCO}	2.817_{-5}	2.755_4	1.022_{-1}	5.933	1.368_{-1}	7.938	km
R^+_{null}	3.047_{-6}	2.98_3	5.07_{-2}	2.942	5.221_{-2}	3.03	km
R^-_{null}	3.049_{-6}	2.983_3	5.076_{-2}	2.946	6.716_{-2}	3.897	km
$\mathcal{R}_{\mathrm{p}}$	7.104_{-4}	6.949_5	1.943_{-1}	1.127_1	1.881_{-1}	1.092_1	km
$\mathcal{C}_{\mathrm{p}}$	4.47_{-3}	4.372_6	1.163	6.747_1	1.153	6.692_1	km
$\varepsilon_{\mathrm{proper}}$	7.216_{-2}		1.13_{-3}		2.985_{-1}		
$\varepsilon_{\mathrm{int.}}$	5.104_{-2}		7.84_{-4}		2.084_{-1}		

(b) Simple MIT bag models of models of Table 5.14 (page 133) and Table 5.16 (page 136) with $\tilde{M}_0 = 1\,M_\odot$ using $\epsilon_0 = 4B = 4 \times 60\,\mathrm{MeV\,fm^{-3}}$.

	$\omega = 363$ Hz		$\omega = 0$ Hz		$\omega = 1.3$ Hz		
Quantity	CMMR	CMMR$_{\mathrm{conv}}$	CMMR	CMMR$_{\mathrm{conv}}$	CMMR	CMMR$_{\mathrm{conv}}$	Unit
r_0	7.789_{-2}	8.751	7.756_{-2}	8.714	7.791_{-2}	8.753	km
$\tilde{M}_2$	-1.31_{-6}	-1.189_{-2}	0	0	-1.673_{-11}	-1.556_{-7}	$M_\odot \mathcal{R}^2_{\mathrm{circ}}$
$\tilde{J}_3$	-2.713_{-9}	-1.873_{-3}	0	0	-1.238_{-16}	-8.757_{-11}	$GM_\odot^2 \mathcal{R}^2_{\mathrm{circ}}/c$
I	4.663_{-5}	4.23_{-1}	4.409_{-5}	4.152_{-1}	4.549_{-5}	4.23_{-1}	$M_\odot \mathcal{R}^2_{\mathrm{circ}}$
$c\tilde{J}_1/G\tilde{M}_0^2$	2.231_{-1}		0		7.753_{-4}		
$\tilde{M}_2/\tilde{M}_0\mathcal{R}^2_{\mathrm{circ}}$	-1.167_{-2}		0		-1.526_{-7}		
$c^4\tilde{M}_2/G^2\tilde{M}_0^3$	-5.464_{-1}		0		-6.95_{-6}		
z^+_{eq}	7.597_{-1}		8.411_{-1}		8.386_{-1}		
z^-_{eq}	9.162_{-1}		8.411_{-1}		8.391_{-1}		
R^+_{ISCO}	4.91_{-2}	5.516	4.698_{-2}	5.278	4.761_{-2}	5.349	km
R^-_{ISCO}	6.374_{-2}	7.161	4.698_{-2}	5.278	4.767_{-2}	5.356	km
R^+_{null}	2.786_{-2}	3.13	2.838_{-2}	3.189	2.837_{-2}	3.187	km
R^-_{null}	3.51_{-2}	3.943	2.838_{-2}	3.189	2.84_{-2}	3.19	km
$\mathcal{R}_{\mathrm{p}}$	9.263_{-2}	1.041_1	9.454_{-2}	1.062_1	9.52_{-2}	1.07_1	km
$\mathcal{C}_{\mathrm{p}}$	5.646_{-1}	6.343_1	5.648_{-1}	6.345_1	5.683_{-1}	6.385_1	km
$\varepsilon_{\mathrm{proper}}$	2.78_{-1}		0		1.009_{-3}		
$\varepsilon_{\mathrm{int.}}$	1.931_{-1}		0		6.973_{-4}		

Table 5.18: Extra quantities of $\mathcal{O}(\lambda^{9/2}, \Omega^3)$ CMMR results. Each pair of data columns lists the $c = G = b = 1$ value and its value in some convenient units.

present them. Additionally, some difficulties arise computing them, leading to an increment the precision needed for the numerical treatment. We think that it is a consequence of working relatively closer to $R = 0$ with a metric that is a multipole expansion around infinity.

Last, a comment on ratios of quantities. In Tables 5.17 and 5.18 and Section 4 we have introduced several dimensionless ratios of physical properties of the source without giving their analytical approximate expression. This is due to the fact that, for each particular stellar model, obtaining first the value of the quantities involved and then obtaining the ratio leads to a different value than the one provided making a series expansion of the quotient of the approximate expressions. Actually, this last procedure can lead to expressions that depend on negative powers of λ and Ω or on which expansion is done first. Hence, we take the consistent way of proceeding, computing ratios of values, despite loosing the goodness of an analytical expression.

7. Summary

In this Chapter we have chosen the AKM code to build exact numerical stellar models to compare with our analytic approximate results. Studying first a constant density source with $M_b = 8 \times 10^{-4}$—which would correspond to $M_b = 3.14 \times 10^{-2} M_\odot$ if $\mu_0 = 4 \times 10^{17}\,\mathrm{kg\,m^{-3}}$ and $M_b \simeq 5.29 \times 10^5 M_\odot$ if $\mu_0 = 1408\,\mathrm{kg\,m^{-3}}$—we saw that going from $\mathcal{O}(\lambda^2)$ to $\mathcal{O}(\lambda^4)$ results,

- there is a consistent improvement in the relative error with respect to AKM of the physical properties of our model of slightly more than one order of magnitude after each new post-Minkowskian iteration. There is higher error en W and E_{bind}—and also in subsequent models—because these quantities are linear combinations of others;

- relative error in the metric functions shows the expectable spherical symmetry of a static configuration and changes from $\varepsilon_c \sim 10^{-5}$ in the centre of the source and $\varepsilon_{2_{\varrho_{eq}}} \sim 10^{-6}$ at two times the radial coordinate of its equator to $(\varepsilon_c, \varepsilon_{2_{\varrho_{eq}}}) \sim (10^{-7}, 10^{-8})$ two iterations later.

For the same M_b but including rotation with $\omega = 0.2$—2.14 times the solar spin rate for its density and 164 Hz for neutron star density—we get the same trend except in quantities more strictly related with the source, like $\tilde{J}_1$, T, p_c and h_c, which have slightly higher errors. The error in metric functions shows a lobular appearance that increases with each post-Minkowskian iteration. It is related with the error introduced by the truncation in tensor spherical harmonics that comes

(a) $M_b \simeq 0.11\, M_\odot$

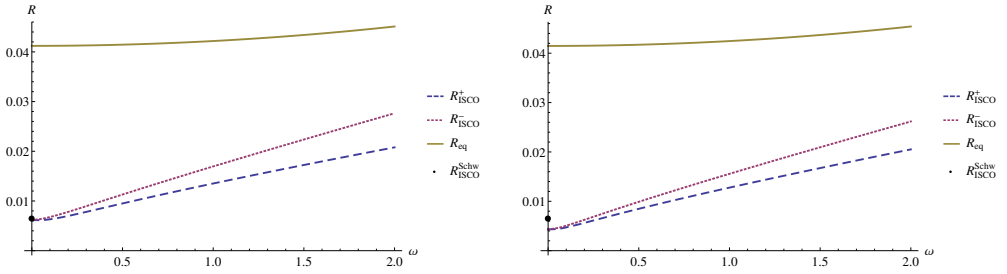

(b) $M_b \simeq 0.95\, M_\odot$

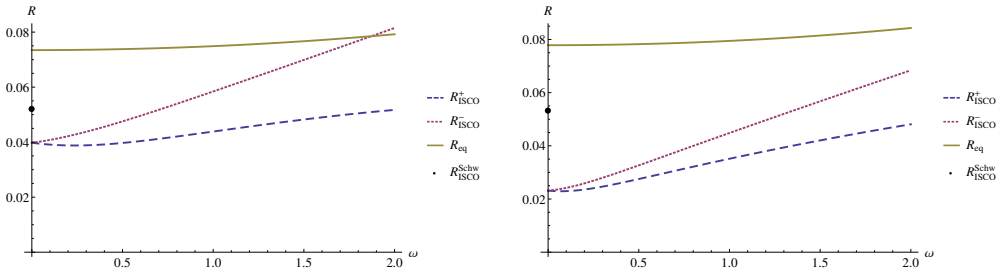

(c) $M_b \simeq 1.71\, M_\odot$

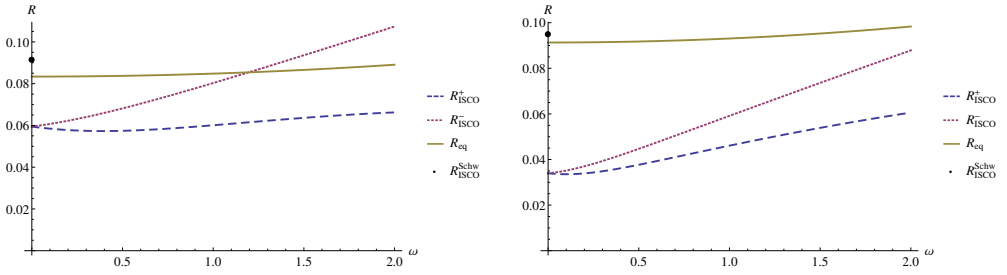

Figure 5.13: CGMR results for the radial coordinate of prograde and retrograde ISCO for massive particles and the surface as a function of the angular velocity of the source. All the cases correspond to $n = 4$ and $h(0) = 0.899124$. Plots on the left are obtained from $\mathcal{O}(\lambda^{9/2}, \Omega^3)$ CGMR and the ones on the right from $\mathcal{O}(\lambda^{5/2}, \Omega^3)$ CGMR.

from the slow-rotation approximation. This lobular distribution indicates when rotation is an important source of error.

The final check of the behaviour of error in CMMR was changing the pair of parameters used to adjust the values of r_s and ω. We saw that the best quantity, among $\tilde{M}_0$, p_c, R_{eq} and $\tilde{J}_1$ is the last one, and next $\tilde{M}_0$, which is the one to use in static configurations.

After understanding the general behaviour of CMMR, we turned to see its performance for interesting sources.

We started again with constant density models.

- Using typical solar parameters, we got $\varepsilon \sim 10^{-6}$ in physical properties and $g_{t\phi}$ inside and near the source, but much lower in g_{tt}, $\varepsilon \sim 10^{-11}$. This behaviour is similar to the one of the $M_b \simeq 5.29 \times 10^5\, M_\odot$ model, hinting that error depends more on compactness than in absolute mass.

- For average neutron star density and rotation—1.3 Hz—error is around 1.5×10^{-2}, and its distribution in metric functions is nearly spherical. We found that the compacter the source the faster it can spin before the slow rotation approximation becomes dominant and results for spin rates of 350 Hz are very similar.

Then, we studied a subcase of the linear EOS, $n = 4$, which corresponds to the simple MIT bag model EOS of SQM.

- First, using $B = 60\,\text{MeV fm}^{-3}$ for the common value of gravitational mass $\tilde{M}_0 = 1.38\, M_\odot$ and the most common rotation rate, 1.3 Hz, errors in physical properties are in the 10^{-1}-10^{-2} range, and similarly in the metric functions but falling fast to 10^{-3} in g_{tt} and 10^{-2} in $g_{t\phi}$. Again, the distribution is very spherical so dominated by error coming from the post-Minkowskian part of the approximation.

- There are astrophysical objects with lower masses, and in particular such lighter sources can be very relevant in the study of the SQM hypothesis. There are strong indications that 4U 1728-34 and SAX J1808.4-3658 have masses of $\tilde{M}_0 = 1\, M_\odot$ or less, and accordingly we have studied models with this gravitational mass. Their rotation rates are very close, so we picked one of the, 364 Hz. Here, error is a factor 0.5 better that with $\tilde{M}_0 = 1.38\, M_\odot$. We studied also the static and 1 Hz cases without finding big differences. For these models, the next post-Minkowskian iteration should give relative errors of 10^{-3}.

For the main cases of interest where error should be improved, the post-Minkowskian approximation is the main responsible. With the software developed in this work, it is essentially automatic to obtain the next post-Minkowskian iterations and hence, we expect to be able to improve our results with ease.

Beside the physical properties we compared with the ones AKM provides, we have computed the value of several other for all these models to allow a fast comparison with other codes. Particularly relevant was the study of the ISCO radii, for which we have not been able to find an analytical expression, but we intend to do it in the future. We compared our results for it with the one of Schwarzschild's exterior for $M_b = 0.11\,M_\odot$, with very good agreement; for $M_b = 0.95\,M_\odot$ we got an error of $\sim 20\%$ and one of 23% in $M_b = 1.71\,M_\odot$. We have no checks for the effect of rotation on it, though.

Chapter Six

Model with a bilayer interior

We have already seen in Chapters 3 and 4 that the CGMR interior cannot be a source of a Kerr exterior nor be an approximate Wahlquist if matched with the asymptotically flat exterior. It seems that the perfect fluid restriction is important in forbidding the Kerr exterior since anisotropic interiors for it have been found (Wiltshire, 2012). We can check if a more complex structure, with two different layers of perfect fluid can, keeping the isotropy of the stress-energy tensor, give rise to Kerr, though. Similarly, an additional layer of fluid adds flexibility in the matching so one could expect that this bilayer source could contain a inner one corresponding to Wahlquist and yet be matchable with the asymptotically flat exterior. These are the two main checks for this chapter, apart from the possible application to more realistic compact stars.

We know of three kinds of compact stars: black holes, neutron stars and white dwarfs. If the SQM hypothesis is right, a fourth, strange stars, should be added. The intensity of gravity inside a compact star can lead to pressures of more than ten times the one inside ordinary atomic nuclei and thus create an environment with energy available to generate particles or structures very different from those present in nuclear matter. In Chapter 5 we have already discussed one of such compositions, i.e. , strange quark matter. The pressure is not everywhere the same, though, giving rise to stratified layers with different environments and particles, like

- hyperon and baryon resonances,
- deconfined quark matter,
- boson condensates and
- the hypothesised strange quark matter

are to be expected in high pressure layers in the most general scenario.

The particular composition of a certain compact star depends mainly on its mass-radius parameters, but also on the behaviour of its components. It is dom-

inated by the strong interaction and thus currently subject of important undeterminacies regarding their EOS. Eventually, they all need to be consistent with the observations, which in turn are not trivial at all. It leads to the present picture: several different compact star models which researchers try to improve to lead to discrepancies with the slowly increasing number of observational constraints in order to gain insight on both astrophysical objects and behaviour of fundamental particles. Hence, multi-layer stellar models have a very interesting number of practical applications.

In this chapter we build a global solution for a bilayer source. In both layers the EOS is the familiar linear one, using different n, ϵ_0 parameters. It may be used to make a better approximation of bare SQM cores due to the extra freedom of parameters, but the main purpose is to illustrate the procedure of layering within the CMMR scheme.

1. The spacetimes and matter content

We want to study a rigidly rotating stationary perfect fluid source with two non-convective layers of different composition immersed in asymptotically flat vacuum. We build this configuration up from three different spacetimes. The first one, $(\mathcal{V}^i, g^i)$ will form the inner layer of the source. A second one, $(\mathcal{V}^s, g^s)$ will describe the outer layer and $(\mathcal{V}^+, g^+)$ the asymptotically flat exterior. Each spacetime is stationary and axisymmetric and we can apply the CMMR approximation scheme straightforwardly.

In $\mathcal{V}^i$, the EOS is

$$\epsilon + (1 - n_1)p = \epsilon_1 \tag{6.1}$$

and the ansatz for its surface is

$$r_{\Sigma_i} = r_i \left[1 + \varsigma_i \, \Omega^2 P_2(\cos\theta)\right]. \tag{6.2}$$

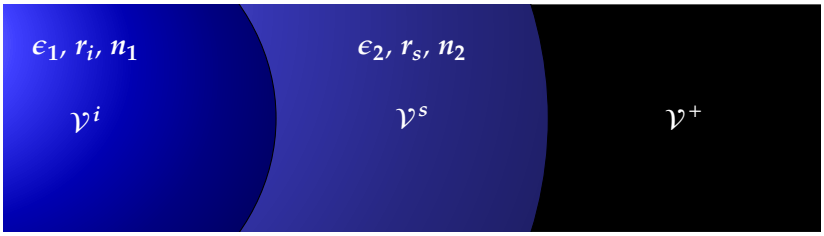

Figure 6.1: Configuration of spacetimes to study and their associated free parameters. From left to right, the inner layer, exterior layer and exterior spacetime.

Note that we have dropped the σ_0 factor that was present in eq. (3.36) because it is not necessary.

Similarly, in $\mathcal{V}^s$ we have

$$\epsilon + (1 - n_2)p = \epsilon_2, \tag{6.3}$$

$$r_{\Sigma_s} = r_s \left[1 + \varsigma_s \, \Omega^2 P_2(\cos\theta)\right]. \tag{6.4}$$

With the EOS, we can integrate the simplified form of Euler's equations eq. (2.71) and obtain the $p(\psi)$ relation in both spacetimes

$$p = \frac{\epsilon_a}{n_a}\left[\left(C_a\psi\right)^{n_a} - 1\right], \qquad (a = 1, 2) \tag{6.5}$$

where C_a is the integration constant. In the outer surface, it must be adjusted so that $\psi(p = 0) = \psi_s$. This gives $C_2 = \psi_s^{-n_2}$ and hence, in the outer layer

$$p = \frac{\epsilon_2}{n_2}\left[\left(\frac{\psi}{\psi_s}\right)^{n_2} - 1\right]. \tag{6.6}$$

On the inner surface, we define $\psi(r_{\Sigma_i}) := \psi_i$. The continuity of pressure on through the surface gives then

$$\frac{\epsilon_1}{n_1}\left[\left(C_1\psi_i\right)^{n_1} - 1\right] = \frac{\epsilon_2}{n_2}\left[\left(\frac{\psi_i}{\psi_s}\right)^{n_2} - 1\right]. \tag{6.7}$$

Thus,

$$C_1^{n_1} = \psi_i^{-n_1}\left\{\frac{\epsilon_2 n_1}{\epsilon_1 n_2}\left[\left(\frac{\psi_i}{\psi_s}\right)^{n_2} - 1\right] + 1\right\} \tag{6.8}$$

and the pressure on $\mathcal{V}^i$ is

$$p = \frac{\left(\frac{\psi}{\psi_i}\right)^{n_1}\left\{\epsilon_2 n_1\left[\left(\frac{\psi_i}{\psi_s}\right)^{n_2} - 1\right] + \epsilon_1 n_2\right\} - \epsilon_1 n_2}{n_1 n_2}, \tag{6.9}$$

with the energy densities of both layers obtainable from p through the EOS.

Regarding the post-Minkowskian approximation parameter, in the monolayer case of Chapter 3, its definition was $\lambda = \frac{4}{3}\pi r_s^2 \epsilon_0$, essentially the Newtonian static mass divided the characteristic length. Here we are interested in keeping a simple enough similar relation that allows us to recover the original parameter when either $\epsilon_1 = \epsilon_2$ or $r_i = r_s$. One possible choice is then

$$\lambda = \frac{4}{3}\pi\left[r_s^2\epsilon_2 + r_i^2\left(\epsilon_1 - \epsilon_2\right)\right]. \tag{6.10}$$

In particular, if $\epsilon_2 = q\epsilon_1$, we have

$$\lambda = \frac{4}{3}\pi\left[qr_s^2 - (q-1)r_i^2\right]\epsilon_1 \tag{6.11}$$

that recovers the familiar expression $\lambda = \frac{4}{3}\pi r_o^2\epsilon_1$ defining

$$r_o := \sqrt{qr_s^2 - (q-1)r_i^2} \tag{6.12}$$

as characteristic length.

2. Approximate metrics of the fluid layers

Next, we need the solution of the homogeneous part of the system (2.45) in the three spacetimes, $\boldsymbol{h}^+_{\rm hom}$, $\boldsymbol{h}^s_{\rm hom}$ and $\boldsymbol{h}^i_{\rm hom}$. Recall that eqs. (2.69) and (2.70) are, considering the symmetries, the most general of such solutions which are regular at infinity and at $r = 0$, respectively. Hence, the expressions of $\boldsymbol{h}^+_{\rm hom}$ and $\boldsymbol{h}^i_{\rm hom}$ are identical to eq. (2.69) and eq. (2.70), replacing r_s with r_o. In the outer layer of the source the general solution of the Laplace equation does not need to fulfil these regularity conditions, since we work with a piece of spacetime that does not get near infinity nor $r = 0$. Hence, the solution contains both positive and negative powers of r with the same form the previous ones had, i.e.

$$\begin{aligned}\boldsymbol{h}^s_{\rm hom} = {} & 2\sum_{l=0,2}\lambda\Omega^l\left(r_o^{l+1}\frac{\bar{M}_l}{r^{l+1}} + \frac{\bar{m}_l}{2r_o^l}\,r^l\right)(\boldsymbol{T}_l + \boldsymbol{D}_l) + 2\sum_{l=1,3}\lambda^{\frac{3}{2}}\Omega^l\left(r_o^{l+1}\frac{\bar{J}_l}{r^{l+1}} + \frac{\bar{j}_l}{2r_o^l}\,r^l\right)\boldsymbol{Z}_l \\ & + \sum_{l=0,2}\lambda\Omega^l\left(r_o^{l+3}\frac{\bar{A}_l}{r^{l+3}}\boldsymbol{E}_{l+2} + \frac{\bar{a}_l}{r_o^l}\,r^l\boldsymbol{E}^*_l\right) + \lambda\Omega^2\left(r_o^3\frac{\bar{B}_2}{r^3}\,\boldsymbol{F}_2 + \bar{b}_2\,\boldsymbol{F}^*_0\right) + \mathcal{O}(\Omega^4)\,.\end{aligned} \tag{6.13}$$

In this chapter we keep the notation of upper case letters $\{M_l, J_l, A_l, B_2\}$ for the exterior free coefficients of $\boldsymbol{h}^+_{\rm hom}$, lower case letters $\{m_l, j_l, a_l, b_2\}$ for those in $\boldsymbol{h}^+_{\rm hom}$ and a barred combination of both depending on whether they multiply a positive or negative power of r for the outer layer solution.

The remaining steps are not different from the ones in Chapter 3. The resulting general solutions of the full harmonic post-Minkowskian system appear in Appendix G

3. Lichnerowicz matching of the three spacetimes

We match the three separate spacetimes into the final one imposing Lichnerowicz conditions. The procedure is again similar to the matchings in Chapter 3, taking

care of one surface at a time. We get first the conditions on the free coefficients in the outer layer, obtaining all the outer layer constants $\{\bar{X}_l, \bar{x}_l\}$ as functions of the exterior ones

$$\begin{aligned} \bar{X}_l &= \bar{X}_l(M_l, J_l, A_l, B_2), \\ \bar{x}_l &= \bar{x}_l(M_l, J_l, A_l, B_2). \end{aligned} \tag{6.14}$$

Then we proceed in the same fashion on the inner surface, getting the relations

$$\begin{aligned} \bar{X}_l &= \bar{X}_l(m_l, j_l, a_l, b_2), \\ \bar{x}_l &= \bar{x}_l(m_l, j_l, a_l, b_2). \end{aligned} \tag{6.15}$$

In this way, we get the final system of equations that only involve the inner layer constants and the exterior ones and is formally equivalent to, again, the one we met in Chapter 3. This fixes the exterior and inner layer constants and through eqs. (6.14) and (6.15) those of the outer layer as well. The final values of X_l and x_l appear in Appendix G. We also write the outer layer constants as functions of the inner layer ones there.

3.1. Some subcases of the matching

As a check, we can take these matched coefficients and see how they behave when $r_i = r_s$. The exterior and inner layer constants of the $\mathcal{O}(\lambda^{5/2}, \Omega^3)$ solutions are reduced to

$$\begin{aligned} M_0 &= 1 + \frac{1}{15}\lambda\left[\Omega^2(8-2n_1) + (42+3n_1)\right], & A_0 &= \lambda\left(\frac{8}{35} + \frac{4\Omega^2}{105}\right), \\ M_2 &= -\frac{1}{2} + \frac{1}{70}\lambda(-74+5n_1), & A_2 &= -\frac{4\lambda}{63}, \\ J_1 &= \frac{2}{5} + \frac{\Omega^2}{3} + \frac{1}{105}\lambda\left[\Omega^2(176-9n_1) + (240+6n_1)\right], & B_2 &= 0, \\ J_3 &= -\frac{1}{7} + \frac{1}{2205}\lambda(-1488+55n_1) \end{aligned} \tag{6.16}$$

and the inner layer ones to

$$\begin{aligned} m_0 &= 3 + \frac{1}{4}\lambda\left[\Omega^2(4-2n_1) + (18+3n_1)\right], & a_0 &= \lambda\left(7 + \frac{2\Omega^2}{3}\right), \\ m_2 &= -1 + \lambda\left(-\frac{29}{35} - \frac{3n_1}{14}\right), & a_2 &= -\frac{86\lambda}{105}, \\ j_1 &= 2 + \frac{2\Omega^2}{3} + \frac{1}{210}\lambda\left[\Omega^2(578-75n_1) + (2058+105n_1)\right], & b_2 &= 0, \\ j_3 &= -\frac{2}{7} + \frac{1}{245}\lambda(-326-15n_1), \end{aligned} \tag{6.17}$$

i.e., the same values we found in Chapter 3. The situation is very different in the outer layer. There, when $r_i = r_s$ we obtain

$$\bar{M}_0 = 1 - q + \lambda\left[\frac{14}{5} - 7q + \frac{21q^2}{5} + \frac{n_1}{5} - \frac{qn_2}{2} + \frac{3q^2n_2}{10} + \Omega^2\left(\frac{8}{15} - \frac{8q}{15} - \frac{2n_1}{15} + \frac{2qn_2}{15}\right)\right], \tag{6.18}$$

$$\bar{M}_2 = -\frac{1}{10}(q-1)(-2+3m_2) + \frac{1}{700}\lambda\left[-2\left(283 - 958q + 675q^2\right) + (95 - 145q)n_1 - 25q(-5+3q)n_2\right], \tag{6.19}$$

$$\bar{J}_1 = -\frac{2}{5}(q-1) + \frac{\Omega^2}{15}(q-1)(-2+3m_2) + \lambda\left\{-\frac{16}{7}(q-1) + \frac{39}{35}(q-1)q + \frac{2n_1}{35} - \frac{qn_2}{10} + \frac{3q^2n_2}{70} + \Omega^2\left[-\frac{793}{525}(q-1) + \frac{29}{35}(q-1)q + \frac{1}{210}(-27+29q)n_1 - \frac{17qn_2}{210} + \frac{q^2n_2}{14}\right]\right\}, \tag{6.20}$$

$$\bar{J}_3 = -\frac{1}{35}(q-1)(-2+3m_2) + \frac{\lambda}{44100}\left\{(1910 - 2610q)n_1 - 7\left[3804 - 5954q + 2150q^2 + 25q(-7+3q)n_2\right]\right\}, \tag{6.21}$$

$$\bar{A}_0 = \lambda\left[\frac{2}{105}\left(12 - 21q + 9q^2\right) + \frac{2}{105}(2-2q)\Omega^2\right], \tag{6.22}$$

$$\bar{A}_2 = \frac{1}{63}\left(-4 + 7q - 3q^2\right)\lambda, \tag{6.23}$$

$$\bar{B}_2 = -\frac{47}{35}(q-1)q\lambda, \tag{6.24}$$

$$\bar{m}_0 = -3 + 3q + m_0 + \lambda\left\{-\frac{9}{2} + 18q - \frac{27q^2}{2} - \frac{3n_1}{4} + 3qn_2 - \frac{9q^2n_2}{4} + \Omega^2\left(q - 1 + \frac{n_1}{2} - \frac{qn_2}{2}\right)\right\}, \tag{6.25}$$

$$\bar{m}_2 = \frac{1}{5}\left(2 - 2q + (2+3q)m_2\right) + \frac{1}{350}\lambda\left[116 - 466q + 350q^2 + 5(6+29q)n_1 - 175q^2n_2\right], \tag{6.26}$$

$$\bar{j}_1 = 2(q-1) + j_1 - \frac{2\Omega^2}{15}(q-1)(-2+3m_2) + \lambda\left\{-\frac{49}{5} + \frac{64q}{5} - 3q^2 - \frac{n_1}{2} - \frac{1}{2}q(-4+3q)n_2 + \Omega^2\left[-\frac{1271}{525} + \frac{746q}{525} + q^2 + \frac{1}{210}(93 - 58q)n_1 + \frac{1}{6}q(-4+3q)n_2\right]\right\}, \tag{6.27}$$

$$\bar{j}_3 = j_3 + \frac{1}{35}\left[2(q-1)\left(3m_2-2\right)\right] + \frac{\lambda}{1225}\left[5(6+29q)n_1 - 7\left(-208+98q+110q^2+25q^2n_2\right)\right], \tag{6.28}$$

$$\bar{a}_0 = a_0 + \lambda\left[-7-8q+15q^2+\left(-\frac{2}{3}+\frac{2q}{3}\right)\Omega^2\right], \tag{6.29}$$

$$\bar{a}_2 = a_2 - \frac{86}{105}\left(q-1^2\right)\lambda, \tag{6.30}$$

$$\bar{b}_2 = b_2 + (q-1)q\lambda \tag{6.31}$$

what gives a solution completely different from the inner layer one. Even if different, one would expect the solution to vanish. We only recover a source with the behaviour of the inner layer

$$\begin{aligned} &\bar{M}_0 = 0, \quad \bar{M}_2 = 0, \quad \bar{J}_1 = 0, \quad \bar{J}_3 = 0, \\ &\bar{A}_0 = 0, \quad \bar{A}_2 = 0, \quad \bar{B}_2 = 0, \end{aligned} \tag{6.32}$$

$$\begin{aligned} &\bar{m}_0 = m_0, \quad \bar{m}_2 = m_2, \quad \bar{j}_1 = j_1, \quad \bar{j}_3 = j_3, \\ &\bar{a}_0 = a_0, \quad \bar{a}_2 = a_2, \quad \bar{b}_2 = b_2 \end{aligned} \tag{6.33}$$

when both $q = 1$ and $n_1 = n_2$.

It is also interesting the behaviour of the three solutions when $r_i = 0$. In the outer layer we obtain

$$\begin{aligned} &\bar{M}_0 = 0, \quad \bar{M}_2 = 0, \quad \bar{J}_1 = 0, \quad \bar{J}_3 = 0, \\ &\bar{A}_0 = 0, \quad \bar{A}_2 = 0, \quad \bar{B}_2 = 0, \end{aligned} \tag{6.34}$$

for the coefficients of negative powers of r. This is the expected behaviour when the source has only one layer. The rest of coefficients are

$$\bar{m}_0 = m_0\,, \tag{6.35}$$

$$\bar{m}_2 = \frac{1}{5}\left(2-2q+(2+3q)m_2\right) + \frac{\lambda\left(-8-54q+62q^2+25q^2n_1-25qn_2\right)}{20+30q}, \tag{6.36}$$

$$\bar{j}_1 = j_1\,, \tag{6.37}$$

$$\bar{j}_3 = \frac{1}{35}\left[35j_3+2(-1+q)\left(-2+3m_2\right)\right] + \frac{\lambda\left(262-324q+62q^2+25q^2n_1-25qn_2\right)}{70+105q}, \tag{6.38}$$

$$\bar{a}_0 = a_0\,, \tag{6.39}$$

$$\bar{a}_2 = \frac{6(1-q)\lambda}{2+3q} + a_2\,, \tag{6.40}$$

$$\bar{b}_2 = b_2\,, \tag{6.41}$$

which depend on the inner layer constants. These inner constants become

$$m_0 = 3 + \lambda\left[-\frac{\Omega^2\,(-2+n_2)}{2q} + \frac{3}{4}\,(6+n_2)\right], \tag{6.42}$$

$$m_2 = \frac{-7+2q}{2+3q} + \frac{\lambda\left[-60+204q-434q^2-175q^2n_1+10(-3+13q)n_2\right]}{14(2+3q)^2}, \tag{6.43}$$

$$j_1 = 2 + \frac{2\Omega^2}{3q} + \lambda\left[\frac{49}{5} + \frac{n_2}{2} + \Omega^2\left(\frac{289}{105q} - \frac{5n_2}{14q}\right)\right], \tag{6.44}$$

$$j_3 = \frac{2(-7+2q)}{7(2+3q)} + \lambda\frac{-875q^2n_1+2\left[-2576-2043q+544q^2+25(-3+13q)n_2\right]}{245(2+3q)^2}, \tag{6.45}$$

$$a_0 = \lambda\left(7 + \frac{2\Omega^2}{3q}\right), \tag{6.46}$$

$$a_2 = \lambda\frac{2(-401+186q)}{105(2+3q)}, \tag{6.47}$$

$$b_2 = 0, \tag{6.48}$$

and the exterior ones are reduced to

$$M_0 = \frac{1}{\sqrt{q}} + \lambda\left[\frac{14}{5\sqrt{q}} + \frac{n_2}{5\sqrt{q}} + \Omega^2\left(\frac{8}{15q^{3/2}} - \frac{2n_2}{15q^{3/2}}\right)\right], \tag{6.49}$$

$$M_2 = -\frac{1}{2q^{5/2}} + \frac{\lambda\,(-74+5n_2)}{70q^{5/2}}, \tag{6.50}$$

$$J_1 = \frac{2}{5q^{3/2}} + \frac{\Omega^2}{3q^{5/2}} + \lambda\left[\frac{16}{7q^{3/2}} + \frac{2n_2}{35q^{3/2}} + \Omega^2\left(\frac{176}{105q^{5/2}} - \frac{3n_2}{35q^{5/2}}\right)\right], \tag{6.51}$$

$$J_3 = -\frac{1}{7q^{7/2}} + \frac{\lambda\,(-1488+55n_2)}{2205q^{7/2}}, \tag{6.52}$$

$$A_0 = \lambda\left(\frac{8}{35q^{3/2}} + \frac{4\Omega^2}{105q^{5/2}}\right), \tag{6.53}$$

$$A_2 = -\frac{4\lambda}{63q^{7/2}}, \tag{6.54}$$

$$B_2 = 0. \tag{6.55}$$

Both of these two last sets become the expected CGMR results only when $q = 1$.

Last, the case $q = 0$, that can arise from having $\epsilon_2 = 0$, requires to work with the full expression of the metric because q appears not only in the $(X_l, x_l, \bar{X}_l, \bar{x}_l)$ constants. It gives the usual CGMR metric in the inner layer, transforms the outer layer into the CGMR vacuum and the exterior is the CGMR one as well, as could be expected. All these particular cases are summarized in Table 6.1 (following page).

Regarding the surfaces, both η_i and η_s behave as one should expect: they become the CGMR result imposing just $r_i = r_s$. Particularly, $\eta_i = 0$ when $r_i = 0$.

4. Remarks and some implications

Repeating the kind of analysis that lead us to conclude that the CGMR interior can not be matched with a Kerr exterior (see Chapter 3, Section 4), here we have, since $M_l^{\text{Kerr}} = m(\mathrm{i}a)^l$

$$M_0^{\text{Kerr}} = m = \lambda r_s M_0 \,, \tag{6.56}$$

$$M_1^{\text{Kerr}} := J_1^{\text{Kerr}} = ma = \lambda^{3/2}\Omega r_s^2 J_1 \,, \tag{6.57}$$

the value of the next two multipole moments must be

$$M_2^{\text{Kerr}} = -ma^2 = -\frac{(\lambda^{3/2}\Omega r_s^2 J_1)^2}{\lambda r_s M_0} = -\lambda^2\Omega^2 r_s^3 \frac{J_1^2}{M_0} \,, \tag{6.58}$$

$$J_3^{\text{Kerr}} = -ma^3 = -\lambda^{5/2}\Omega^3 r_s^4 \frac{J_1^3}{M_0^2} \,. \tag{6.59}$$

Thus, our M_2 and J_3 should not have any $\mathcal{O}(\lambda^0)$ term, to begin with. None of the subcases considered in the previous section allow this, not even the $r_i = 0$ one, where q seems to give some freedom but it is actually not the case because in this situation q can be factored out of λ and r_o and exactly cancel the $q^{a/2}$ denominators. In can be checked in general using the formulae of Appendix G.

One can try to get a Kerr exterior introducing singularities in the source. We actually managed to to this in (Cuchí *et al.*, 2011) inserting a singular term in the inner layer, but it would be interesting to be able to turn the inner layer directly into a singularity. Here we have worked with the EOS energy density parameters $\epsilon_{1,2}$ through q, but with this goal in mind it would probably be more convenient to have the three solutions written explicitly in terms of the $\epsilon_{1,2}$.

Table 6.1: Subcases of the matching results of the three spacetimes considered in Section 3.1.

	Inner layer	Outer layer	Exterior
$r_i = r_s$	CGMR results, $x_l(n_1)$	$\bar{X}_l(n_1, n_2, q)$ $\bar{x}_l(n_1, n_2, q)$	CGMR results, $X_l(n_1)$
$r_i = 0$	$x_l(n_1, n_2, q)$	$\bar{X}_l = 0$ $\bar{x}_l(n_1, n_2, q)$	$X_l(n_2, q)$
$q = 1$, $n_1 = n_2$	CGMR results	$\bar{X}_l = 0$ $\bar{x}_l = x_l$	CGMR results
$q = 0$	CGMR results	CGMR exterior	CGMR results

Something similar happens when one tries to get the solution corresponding to $\epsilon_1 = 0$, a kind of solution that includes the one that would represent an inner layer of a photon gas ($n_1 = 4$) inside the outer layer of matter[1]. This value of ϵ_1 makes $\lambda = 0$. This can be amended with a different choice of post-Minkowskian parameter, though. Instead of building it as in eq. (6.11), one can start with the Newtonian mass of the uniform fluid sphere

$$m = \frac{4}{3}\pi\left(\epsilon_1 r_i^3 + \epsilon_2(r_s^3 - r_i^3)\right) \tag{6.60}$$

and introduce the relations

$$r_i := \tau r_s \qquad \epsilon_1 = \kappa_1 \mu_o \qquad \epsilon_2 := \kappa_2 \mu_o \tag{6.61}$$

with μ_0 the average density so that

$$\lambda = \frac{m}{r_s} = \frac{4}{3}\pi r_s^2 \mu_o. \tag{6.62}$$

In this situation, not all the parameters are independent, but they keep the relation

$$\kappa_1 \tau^3 + \kappa_2\left(1 - \tau^3\right) = 1. \tag{6.63}$$

Building the metrics with these parameters gives a more direct control over the densities, but one gets a similar problem if attempts to study subcases of different radii values, which are now encoded in the τ ratio. Having full control of the energy density parameters of the EOS and the radii at the same time is possible, but would increase the number of parameters and length of the solutions.

We can also analyze the inner layer in relation with the Wahlquist metric. Recall that this metric can not be matched with an asymptotically flat exterior but it is possible that adding a perfect fluid layer around it gives us enough freedom to allow a matching. In that case, Wahlquist's solution could describe the inner layer of some asymptotically flat sources. When $n_1 = -2$, the first terms of m_2 and j_3 are

$$m_2 = \frac{6(q-1)q r_i^5 - 10(q-1)^2 r_i^3 r_s^2 + 2q(2q-7)r_s^5}{5\left(-3q^2+q+2\right) r_i^3 r_s^2 + 9(q-1)q r_i^5 + 2q(3q+2)r_s^5} + \mathcal{O}(\lambda), \tag{6.64}$$

$$j_3 = \frac{4\left[3(q-1)q r_i^5 - 5(q-1)^2 r_i^3 r_s^2 + q(2q-7)r_s^5\right]}{7\left[5\left(-3q^2+q+2\right) r_i^3 r_s^2 + 9(q-1)q r_i^5 + 2q(3q+2)r_s^5\right]} + \mathcal{O}(\lambda), \tag{6.65}$$

[1] This case is curious because it would not be possible without the outer matter envelope.

As we saw in Chapter 3, these two coefficients must verify eq. (3.91) for the metric to be of Petrov type D and correspond to an approximation of Wahlquist's solution. Here we have 3 parameters for two equations, a promising flexibility. Nevertheless, imposing the first of the Petrov type D conditions

$$m_2 = \frac{6}{5} + \mathcal{O}(\lambda) \tag{6.66}$$

and solving it for q leads to

$$q = \frac{\pm 1}{8\left(3r_i^5 - 5r_i^3 r_s^2 + 2r_s^5\right)}\left(-12r_i^5 - 35r_i^3 r_s^2 + 47r_s^5 \right.$$
$$\left. + \sqrt{144r_i^{10} - 1800r_i^8 r_s^2 + 5625r_i^6 r_s^4 - 1128r_i^5 r_s^5 - 5050r_i^3 r_s^7 + 2209r_s^{10}}\right) \tag{6.67}$$

what, introduced in eq. (6.65), gives

$$j_3 = \frac{12}{35} + \mathcal{O}(\lambda), \tag{6.68}$$

directly incompatible with the second type D condition $j_3 = \frac{36}{175} + \mathcal{O}(\lambda)$, eliminating all our parameter freedom. Hence Wahlquist cannot be the central part of a bilayer configuration like ours when matched with and asymptotically flat exterior. The type D condition is surprisingly restrictive.

Summing up, the process of matching an exterior to a source made up from two different layers is quite straightforward within CMMR. The particular choice of post-Minkowskian parameter is able to give results that are more suited to study some specific configurations than others. In any case, with the different choices we have worked with, a common characteristic is that the length of the expressions is far bigger than with one layer, placing more stringent limitations to the computation of the next orders of approximation than those present in the monolayer source. Renouncing completely to write them anywhere, it should be feasible to go up to the fourth λ-order, though. In any case, if one is to undertake the work needed, it would be more interesting to use a polytropic outer layer. Additionally, a numerical check of these and eventual new solutions would also be worth the effort, specially taking into account that there is an unpublished version of AKM designed for multi-layer interiors.

Chapter Seven

Conclusions

We have highlighted the main original results of this work in the final sections of Chapters 3 to 6 and set up the context for the problem of analytical approximations for stellar models in GR in the Introduction. Now, we will summarise the most relevant contributions made and fit them into the current knowledge on the matter. The first two sections cover results of the monolayer interior model, leaving the bilayer source for the last section to simplify the exposition.

1. On the properties of the analytical stellar model

In this work we have expanded the use of the CMMR scheme in four ways. First, we have provided a new approximate global model for a linear EOS, where previous uses of CMMR have focused on uniform density—which is a subcase of the linear EOS—and a Newtonian polytrope. The two free parameters of this EOS gives it a lot of flexibility. It contains the EOS of well-known exact solutions, e.g. Schwarzschild interior (static) or the Wahlquist solution, but not exclusively. Most if not all the rigidly rotating known exact solutions have a linear EOS, probably because it makes the integration of the field equations simpler (Senovilla, 1993). From them, the only one to correspond to our kind of interior is Wahlquist's solution, but if a new candidate is discovered it is likely to have this kind of EOS. It is interesting because new testing grounds for the scheme can be found there and it can be used again to ascertain some aspects of these exact solutions if they are discovered. The versatility of the EOS concerns not only the field of exact solutions. It also represents several physically realistic compositions, such as the photon gas or the behaviour of strange quark matter in the simplest form of the MIT bag model (Witten, 1984) and even modern realistic SQM EOS like the one of Dey *et al.* (1998) finding appropriate fittings for the parameters (Zdunik, 2000; Gondek-Rosinska *et al.*, 2000). Recently, Bradley and Fodor (2009) have used in a Hartle interior an even more flexible EOS with four parameters that includes the linear one but also Newtonian and relativistic polytropes. Although in their work the final solutions have to be numerically integrated as usual in the Hartle scheme,

and considering that the polytropic case in CMMR (Martín *et al.*, 2008) depends on the zeros of the Lane-Emden function, this four-parameter EOS could be an interesting possibility for future work taking into consideration that wide kinds of degenerate matter are modelled with polytropes (more on this below). Second, we have increased the complexity of the studied interior to include bilayer configurations (see more about this below).

We have also improved the matching procedure originally used in previous CMMR works. First, besides doing a Lichnerowicz matching and getting the fully matched global metric in admissible coordinates, we have used Darmois-Israel matching conditions to ensure the generality of the results. This has led us also to study changes of post-Minkowskian parameter to get a coordinate independent one to get rid of the apparent coordinate dependence in the multipole moments. Second, we have analysed and solved the possible issues of loss of generality derived from the use of coordinates in the ansatz of the zero pressure surface (Mars and Senovilla, 1998).

Last, we have completed two post-Minkowskian iterations more than any previous CMMR calculation. Thankfully, the approximate expressions of the different physical quantities obtained are rather compact, and while the final expressions for the metric are lengthy, they are smaller than several intermediate expressions. Handling this kind of calculations is unpractical without symbolic computation software. We chose to work with *Mathematica*, and we have managed to create a package of functions that makes the calculation of each new order of the metric automatically. One handicap of going to higher approximation orders is the extensive RAM consumption, but this has been solved parallelizing parts of the computation to distribute this memory use through different machines. We have made some improvements to the simplification function of *Mathematica* and avoided procedures that take longer times, but it would be naive to think that the computing times can not be improved.[1]

This analytical approximation of a global model with a linear EOS source contributes to fill an important gap in the range of stellar models available. In this work we have not paid attention to spherically symmetric solutions because stellar models need rotating sources, but the spherically symmetric exact solutions that can describe interiors are numerous. Nevertheless, for this EOS such solution is only known in some cases of anisotropic fluid (Sharma and Maharaj, 2007; de Avellar and Horvath, 2010), and even there, where the integration of Einstein's equations is by far simpler than in the rotating case, the energy density profile $\epsilon(r)$ of the source is enforced, overdetermining the problem.

[1] Publishing the code in written version in a traditional way is utterly unpractical these days. Copies and support of the packages can be asked for at `jecuchi@gmail.com`

Out of the fully analytical domain, for this EOS there is the already discussed Hartle interior by Bradley and Fodor (2009) but mainly the options are non-approximate fully numerical models (Stergioulas *et al.*, 1999; Gourgoulhon *et al.*, 1999a; Gondek-Rosinska *et al.*, 2000; Ansorg *et al.*, 2003; Lin and Novak, 2006) made to study compact stars. Results from these modern codes can reach machine accuracy and are very consistent among them. Hence, they are more accurate than those from our linear model, but they have disadvantages beyond those related with the possibility to work with analytical expressions. To find a particular model they must fix at least one of its EOS parameters when computing. The other, ϵ_0, can be used to build dimensionless variables and later, using the scaling laws (Haensel *et al.*, 1986; Cook *et al.*, 1994), one can extract information for models with any ϵ_0. Contrarily, in our final expressions the linear EOS is left complete general, what gives our results an important advantage studying the consequences of the linear EOS in a stellar model. Besides, when the numerical code needs an initial configuration to find the GR model, as in the case of AKM, it is not trivial to obtain it for any EOS. In particular, this code allows to obtain initial data for a certain EOS starting from initial data of another, but to make it so it must compute intermediate sequences of stellar models. If any of these intermediate states does not correspond to a physical possibility, the code fails to converge and one must find appropriate physical parameters for the intermediate configurations, what can not be trivial, at least in our experience[2].

This advantage of analytical models has led to interesting mixtures as of late, consisting of exact or approximate analytical exteriors that are matched to numerical interiors. Berti and Stergioulas (2004) used a three-parameter version of the exact metric by Manko *et al.* (2000) successfully, although it cannot be matched in slow-rotating cases, where one can use the approximate Hartle and Thorne (1968) exterior (Berti *et al.*, 2005). Teichmüller *et al.* (2011) built approximate exteriors with an increasing number of parameters and unknowns related with the source surface, and last of all, Pappas and Apostolatos (2013) used the exact two-soliton solution of Manko *et al.* (1995), in the four parameter version, which contains the three-parameter one of Manko *et al.* but works for any rotation rate. All these approaches are useful and give important analytical expressions, but they rely on the information extracted from numerical interiors, and the matching is usually made through the multipole moments, an approach not so well established as Darmois-Israel conditions. Our approximate exterior could also be used in this way, although the global character of our calculations allows us to give the full spacetime inside and outside the source prescribing—once the EOS is fixed—only *two*

[2]The possibility of discovering this issue one week before a conference presentation is dangerous

parameters, what one expects intuitively and as a generalization of the theorem of Rendall and Schmidt (1991). It is also worth noting that it would still depend only on two parameters even if we included an arbitrary number of multipole moments going further in the slow-rotation approximation.

1.1. *Petrov classification of the CGMR interior metric*

We have studied all the possible Petrov types of the monolayer interior. We found that in the static case, the only possibilities are types D ($n \neq 0$) and O ($n = 0$), in accordance with known results (Stephani *et al.*, 2003, p. 228; Collinson, 1976). Also, the constant density case can only be of types I (if rotating) or O (if static), and more generally, that for the linear EOS the only possible types are I, D or O. This made us conjecture that exact solutions for the interior of stellar models may not exist in the type II class, what is in accordance with current knowledge. We have found recently that this result had already been reached by Fodor and Perjés (2000), who established using a slightly modified Hartle interior that "circularly and rigidly rotating perfect fluids of Petrov type II must reduce to the de Sitter space-time in the slow-rotation limit" and hence no stellar models with EOS satisfying the weak energy condition can be found to have Petrov type II. They also found that a "slowly and circularly rotating incompressible perfect fluid space-time with an asymptotically flat vacuum exterior cannot be Petrov type D". Our result on incompressible fluids possessing only types I and O is irrespective of the matchability with the exterior, though. The overlap of results regarding type II stellar models is somewhat dissapointing but interesting taking into account that both results have been obtained through different schemes of analytical approximation.

2. Comparisons, precision and range of applicability

2.1. *Concerning Wahlquist's metric*

Petrov type D constrains the value of some of the interior constants. These constraints are incompatible with the value the constants take when matched with the asymptotically flat exterior, ruling out the $n = -2$ subcase, which must correspond to Wahlquist (Senovilla, 1987), as the interior of a stellar model. This was, again, already known from different approximate calculations, e.g. , Bradley *et al.* (2000).

The Wahlquist metric served us to check if our interior can be cast into the form a perturbative expansion of Wahlquist's solution takes, though. Moreover,

the type D constraints on the interior constants are automatically satisfied by this form. This way we have given the CMMR interior a valuable test. In the process, we had to identify a rotation parameter in Wahlquist. We found that r_0 is the only variable that can make Wahlquist's twist vector to vanish everywhere and hence it was the only possible candidate to be the rotation parameter of Wahlquist's solution and we gave the relation between this parameter and well characterised quantities in our scheme. Bradley *et al.* (2000) and Sarnobat and Hoenselaers (2006) also used r_0 as slow rotation parameter, and already in the original paper (Wahlquist, 1968) it was used to get the Whittaker metric—a static metric—through a singular change of coordinates letting $r_0 \to 0$, so it is not surprising and yet this limiting procedure was the only hint of the relation of r_0 with the rotation before our work. In fact, it seems that Wahlquist only considered it as the radial coordinate of a particular point in the spacetime. We have related it with our ω which, although lacking interpretability as angular velocity seen by an observer at rest with respect to infinity when the interior can not be matched with an asymptotically flat exterior, is also the only parameter that can make the twist vector of our interior zero.

2.2. Facing numerical results

After checking the interior with the approximate Wahlquist metric, we went on to test the global character of the approximation confronting our results with exact models—in the sense that they do not include any approximation and results have machine accuracy—which we computed using the AKM numerical code. It turned out that the exterior behaviour is better than the interior one, although the obtained relative errors are quite close inside the source and the exterior near zone.

Many of the original motivations behind this work were purely theoretical but we have found the approximation gives very low error in several situations.

- For a model with uniform density and solar parameters of mass, average density and angular velocity, we got relative errors of $\varepsilon \sim 10^{-6}$ in the physical quantities compared, and in the $\varepsilon \sim 10^{-5}$-10^{-8} range for the metric components inside and near the source.

- Constant density models with $M_0 = 1\,M_\odot$, $\omega = 1.3\,\mathrm{Hz}$ and the typical neutron star density $4 \times 10^{17}\,\mathrm{kg\,m^{-3}}$ gave relative errors mainly close to 1.5×10^{-2} in compared physical quantities and $\sim 2 \times 10^{-2}$-10^{-3} in metric functions, with spherical distribution of error meaning that error coming from the post-Minkowskian part of the approximation is dominant. Results for a 350 Hz source are very similar, and we saw that the compacter the source

the faster it can spin before the contribution of the slow-rotation approximation becomes dominant.

- With linear EOS models we analysed the typical configuration of $M = 1.38\,M_\odot$ and $\omega = 1.3\,\mathrm{Hz}$, getting a ε located in general between orders 10^{-1}-10^{-2}, although falling quite fast in metric functions to 10^{-3} in g_{tt} and 10^{-2} in $g_{t\phi}$.

  For $M_0 = 1\,M_\odot$ and frequency $\omega = 364\,\mathrm{Hz}$, results improved roughly by a $\frac{1}{2}$ factor with respect to the $M_0 = 1.38\,M_\odot$ ones. Results are similar with lower frequencies and we concluded that, due to the small rotation dependence, results for this frequency range can be significatively improved going to next post-Minkowskian iteration, which should lead to $\varepsilon \sim 10^{-3}$. It is is worth stressing that at least two of the strange star candidates—4U 1728-34. (Li *et al.*, 1999b); SAX J1808.4-3658. (Li *et al.*, 1999a)—have this masses or lower, as we discussed in detail in Chapter 5

We have also obtained analytical approximate formulae for most of the standard quantities of AKM output and also many other parameters of astrophysical interest obtained in other works (Cook *et al.*, 1994; Nozawa *et al.*, 1998; Gourgoulhon *et al.*, 1999a). Our formulae have the advantage of not having any of the EOS parameters fixed, as discussed above, contrarily to what happens using scaling laws from numerical results. Modern numerical results are more accurate that our predictions, though. The only important quantity where we have not been able to obtain an analytical final result is the ISCO radii, where we have resorted to numerical solution of the final equation. There is a number of analytical approximate expressions for it (Shibata and Sasaki, 1998; Abramowicz *et al.*, 2003; Bejger *et al.*, 2010; Sanabria-Gómez *et al.*, 2010), and as we saw in the Chapter 1 it is a very important observable in compact stars. It would be very interesting to obtain an approximate expression, and we are already planning on using the approach in Abramowicz *et al.* (2003) or Galindo and Mars (2013) to get it.

Currently, to obtain the final value from our analytical formulae we need to specify the value of the angular velocity ω and the r_s parameter, which is not as well defined. Its value must be obtained fixing one of the physical parameters, like $\tilde{M}_0$ or $\tilde{J}_1$, what gives us flexibility. At the same time we have seen that the comparison results vary slightly depending on which physical parameter one uses. This can be a drawback in the cases when there is very little information on the source, what can happen with astrophysical observations, and one is forced to use a not optimal parameter. Fortunately, in Chapter 3 we saw how to modify the post-Minkowskian parameter to release it from the r_s dependence, changing it for some physical property, in particular, the central pressure of the source.

Last, in what regards to the different numerical codes available, it is worth recalling that before the arrival of multi-domain codes like `rotstar`–the improved version of BGSM (Bonazzola *et al.*, 1993)—or AKM, density discontinuities in the source, as happens naturally in the surface of uniform density models, gave rise to Gibbs phenomena that affected precision near the surface (Nozawa *et al.*, 1998). It affects codes as widely used as `rns`. Our global models are totally free of this kind of issues.

3. The bilayer interior and its possible uses

Finally, we have built a stellar model with two layers with linear EOS $\epsilon + (1 - n_i)p = \epsilon_i$, $i = 1, 2$. Behind this lies the quest for reasonable interiors that can be source of a Kerr exterior. We have found that both the monolayer and this bilayer configurations of perfect fluid are impossible to match with Kerr, continuing the work of the previous CMMR applications and a trend that probably started with the numerical results of Bardeen and Wagoner (1971) which showed that for disks of dust the quadrupole of the exterior is always bigger than the Kerr one unless the disk is relativistic. Eventually, it was proved for the the exact disk of dust solution (Neugebauer and Meinel, 1995; Klein, 2001), which stands as the only axysimmetric perfect fluid source of Kerr known to date. Recently, Bradley and Fodor (2009) showed that this difference between quadrupoles is a quite general feature of rotating perfect fluids[3] and Filter and Kleinwächter (2009) have conjectured that this can happen with every other multipole moment.

In other work (Cuchí *et al.*, 2011), we explicitly included a singular term in the inner layer solution, what allowed the matching with a Kerr exterior. Because of the singularity it is not a viable stellar model though, as neither is the also Kerr-matchable source of Wiltshire (2012), whose anisotropic stress-energy tensor is composed by three different perfect fluid components and has ellipsoidal shape. Our work deepens the belief that no spheroidal perfect fluid stellar model can have a Kerr exterior, and also what kind of modifications to the simple perfect fluid interior are key to allow it.

Also, we have found that despite the great freedom in the fully matched inner layer, imposing a Wahlquist fluid and the type D conditions that if verified would imply that the layer is an approximation of the Wahlquist metric, all the freedom in the relevant metric constants m_2 and j_3 is removed. The value they take is incompatible with the possibility of representing Wahlquist's solution. Then, despite

[3] One of the EOS they prove it for is the linear one. It is worth noting that our results on the linear EOS where presented in Cuchí *et al.* (2008b,a).

the matching flexibility that the extra layer provides, this important metric cannot be the central layer of bilayer asymptotically flat sources of the kind discussed in this work.

Finally, we saw in Chapter 5 that the linear EOS contains the one of the simple MIT bag model that has been frequently used to study strange quark matter. These results are lengthier than those of monolayer interior and here we have only reached the second order in the post-Minkowskian expansion. Whether it is worth going to higher orders or not depends mainly on its applicability, and it depends in turn on the main field of potential applicability of these metrics, i.e. , compact stars. We end up with a brief summary of future possible uses of the bilayer interior in the CMMR scheme in this field and what we have learnt building it.

- The EOS of white dwarfs is now well understood Baym *et al.* (1971) and can be well approximated using two layers with polytropic equations. In the outer one, where the electrons in the Fermi gas are not relativistic, the adiabatic coefficient is $\Gamma = \frac{5}{3}$. In the inner layer, if the mass of the white dwarf is big enough to give rise to relativistic electrons in the gas, $\Gamma = \frac{4}{3}$.

- In neutron stars, the structure is richer. Around the core, there is a crust, which is divided in two layers. The outer crust is a solid lattice of neutron rich nuclei neutralized by electrons (Alcock *et al.*, 1986), and is well described by the EOS by Baym *et al.* (1971) and Haensel and Pichon (1994). For both of them, it behaves like a $\Gamma = \frac{4}{3}$ polytrope (see Haensel *et al.* (2006), pg. 156). The inner crust starts when the crust reaches a density of $\sim 10^{11}$ g cm^{-3} that releases the neutrons from the nuclei—neutron drip—. According to Read *et al.* (2009), there is consensus in that this layer is well described by the EOS of Douchin and Haensel (2001) and use three layers of polytrope to approximate it with good results. Regarding the core, they have shown that many predictions of physical EOS for the wide variety of possible compositions can be reproduced using another three layers of polytrope. In some cases, two layers is enough.

- Strange stars are simpler in composition because when matter falls into it, it is converted in SQM. This seems to imply that these stars are always *bare*. It is not necessarily the case, though. Models with a quark s mass $m_s \gtrsim 200$ MeV have a non-zero density of electrons (Alford, 2001) that can escape some hundreds of fm out of the surface, that together with the distribution of s quarks creates an electric dipole in the surface with an outward directed field of at least 10^{17} V cm^{-1} (Alcock *et al.*, 1986). For m_s under that value there are no electrons (Rajagopal and Wilczek, 2001), but the color-flavor locked phase

in which the quarks are expected to be gives a positive charge on the surface of a similar strength (Madsen, 2000, 2001; Usov, 2004). This Coulomb barrier can sustain a levitating neutron star crust, but only the outer part since the inner crust of free neutrons would be absorbed by the SQM. Hence, the general strange star can be modelled with an EOS for quark matter and a $\Gamma = \frac{4}{3}$ polytrope. The crust in this situation has a mass of $\sim 10^{-5}\,\mathrm{M}$ and a thickness of not more than 300 m for stars of $M = 1\text{-}1.4\,M_{\odot}$ (Haensel *et al.*, 2006).

- Finally, the SQM hypothesis allows for the existence of two new kinds of white dwarfs, strange white dwarfs, which have a core of SQM. There is an stability gap that makes that ordinary white dwarfs with densities bigger than 10^9 g cm^{-3} transitions to neutron or strange stars of 10^{14} g cm^{-3}. In this case, there is a wide layer of white dwarf over the SQM core. But the presence of a SQM core can also give stability to intermediate configurations, with white dwarf matter containing nuclear matter up to the neutron drip density on top of the SQM core (Glendenning *et al.*, 1995). There is no new phase in these stars, so they can be modelled again with a combination of polytrope and quark matter EOSs.

Summing up, the whole spectrum of degenerate compact stars can be modelled with layers of polytrope and MIT bag model EOS, which are within the kind of metrics obtained by now with CMMR. In the particular case of strange stars with crust, only two layers would be required. It could be argued that for small mass stars it is too thin to really be worth the effort, but it deforms easier than the SQM core at high angular velocities and can be of importance in the measurements of ISCO (Zdunik *et al.*, 2001).

Appendix A

Perturbations and gauge

In order to calculate perturbations, we need to be able to make Taylor expansions. We are going to deal with situations in which the metric of the spacetime depends on a parameter and are such that when that parameter takes a particular value (zero in general), the spacetime—the *background*—is known. We work then with families of metrics and hence, families of different spacetimes. Nevertheless, Taylor expansions need to be carried on a single spacetime and then, require an identification map between the family of manifolds.

The idea of considering perturbations of a given background spacetime as a uniparametric family of spacetimes and embedding all of them within a new 5-dimensional manifold $\mathcal{M}$ (an approach started by Sachs 1964; Geroch 1969) allowed a mathematically precise treatment of the problem. The key point in this construction is to allow the separation of "standard" coordinate changes, in which the points of all the different members of the spacetimes family are transformed in the same way, from the changes of the identification map between the different manifolds of the family. This second kind can be translated into infinitesimal changes of coordinates on each manifold and corresponds to what one refers to as *gauge transformations*.

Within linear theory, the framework was settled by Stewart and Walker (1974), emphasising the importance (and difficulty) of finding gauge invariant quantities in order to get rid of the spurious solutions introduced by gauge freedom. In the context of perturbations of FRW cosmology, this was achieved by Bardeen (1980) and later reworked in a covariant manner by Stewart (1990). Recently, with the generalised increment in computational power and interest in high-sensitivity measurements, higher order perturbation theory has won importance along with the treatment of the gauge problem. Continuing the work of Stewart and Walker (1974), the general mathematical formalism has been expanded to arbitrary order in Bruni *et al.* (1997); Sonego and Bruni (1998); Bruni and Sonego (1999) and even to two-parameter perturbation theory (Bruni *et al.*, 2003)[1].

[1] Also, several gauge-invariant schemes have followed the first attempts (Nakamura, 2003, 2005, 2007; Ellis and Bruni, 1989; Bruni *et al.*, 1992; Giesel *et al.*, 2010). See the last one for a comparison

In what follows we will summarise the known formalism to see how this identification or gauge choice is supplied by a one-parameter group of diffeomorphisms, how the change of gauge requires the use of one-parameter *families* of diffeomorphisms and its translation into the common language of (extended) infinitesimal transformations.

1. Gauge choices and Taylor expansions

Consider a smooth nowhere vanishing vector field X on $\mathcal{M}$, with $\mathcal{M}$ the five dimensional manifold foliated by M_λ, and transversal to every M_λ. A point $p_\lambda \in M_\lambda$ will be identified and considered the same as a point $p_{\lambda'} \in M_{\lambda'}$ if it belongs to the integral curve of X. Thus, the one-parameter group of diffeomorphisms $\phi_\lambda : \mathcal{M} \to \mathcal{M}$ defined locally by X is such that its restriction to M_0 verifies

$$\phi_\lambda|_{M_0} \colon M_0 \to M_\lambda \,, \tag{A.1}$$

where $M_0 := M_{\lambda=0}$. This ϕ_λ is the identification map associated with X and a choice of either of them is a choice of identification gauge.

Once we have a gauge choice, for a certain quantity Q defined on each manifold M_λ we can make a Taylor expansion of its value on the background as (Bruni *et al.*, 1997)

$$\phi_\lambda^* Q = \sum_{l=0}^{+\infty} \frac{\lambda^l}{l!} \pounds_X^l Q\big|_{M_0} \tag{A.2}$$

where the Lie derivative appears as a consequence of applying the Taylor expansion around $\lambda = 0$ to a pullbacked quantity. It is worth noting that this expression makes explicit use of the properties of the one-parameter group. Then we get the usual definition of the perturbation as the rhs of

$$\phi_\lambda^* Q_\lambda - Q_0 = \lambda Q^{(1)} + \lambda^2 Q^{(2)} + \mathcal{O}(\lambda^3) \tag{A.3}$$

where $Q_0 := Q|_{M_0}$ and the first l-th order terms $Q^{(l)}$ of the field Q with respect to the gauge choice ϕ_λ are, according to eq. (A.2)

$$Q^{(1)} := \pounds_X Q|_{M_0} \,, \qquad Q^{(2)} := \frac{1}{2} \pounds_X^2 Q\big|_{M_0} \,. \tag{A.4}$$

between them.

2. Changing the gauge

Once we have laid a precise framework for perturbations, we can handle the issue of how their value changes when the gauge choice is modified. In the linear approximation the question is a simple one (Stewart and Walker, 1974). Indeed, if X and Y are two different vector fields associated to identification maps on $\mathcal{M}$, then the respective linearized perturbations $Q^{(1)}$ and $\bar{Q}^{(1)}$ are such that verify

$$\begin{aligned} \lambda Q^{1)} - \lambda \bar{Q}^{1)} &= \lambda(\pounds_X Q|_{M_0} - \pounds_Y Q|_{M_0}) \\ &= \lambda \pounds_{X-Y} Q|_{M_0} \\ &= \pounds_{\lambda X'} Q|_{M_0}\,, \end{aligned} \tag{A.5}$$

with X' defined as the difference between the vector fields $X - Y$ on M_0, which actually belongs to TM_0. What is happening from the geometric point of view is that, if ψ_λ and ϕ_λ are the one-parameter groups associated with Y and X respectively, a point q on M_λ is pullbacked to $p = \phi_{-\lambda}(q)$ and $\bar{p} = \psi_{-\lambda}(q)$. Now, to get the difference between the values of the perturbation on p, first we need to pullback the value of $\psi_{-\lambda}(q)$ to p and Taylor expand. This step would have an equivalent expression to eq. (A.2) if the map

$$\begin{aligned} \Phi_\lambda : M_0 &\longrightarrow M_0 \\ p &\longmapsto \bar{p} \equiv (\psi_{-\lambda} \circ \phi_\lambda)(p) \end{aligned} \tag{A.6}$$

were a one-parameter group of diffeomorphisms. It is not the case unless X and Y commute (Bruni *et al.*, 1997) so we need a generalization of eq. (A.2) for one-parameter families of diffeomorphisms to deal with gauge changes.

It can be shown (Bruni *et al.*, 1997) that any Φ_λ can be approximated as a composition of different one-parameter groups $\phi^{(l)}_\lambda$

$$\Phi_\lambda = \ldots \circ \phi^{(l)}_{\lambda^l/l!} \circ \ldots \circ \phi^{(2)}_{\lambda^2/2} \circ \phi^{(1)}_\lambda \tag{A.7}$$

for a suitably high l. Such a composition of n one-parameter groups $\phi^{(l)}_\lambda$ is called a *knight diffeormorphism* of rank n. With such a decomposition, the pullback of a tensor field T can now be expanded around $\lambda = 0$ as

$$\Phi^*_\lambda T = \sum_{k_1=0}^{+\infty} \sum_{k_2=0}^{+\infty} \ldots \sum_{k_l=0}^{+\infty} \ldots \frac{\lambda^{k_1+2k_2+\cdots+lk_l+\cdots}}{2^{k_2} \cdots (l!)^{k_l} \cdots k_1! \, k_2! \cdots k_l! \cdots} \times \\ \times \pounds^{k_1}_{V(1)} \pounds^{k_2}_{V(2)} \cdots \pounds^{k_l}_{V(l)} \cdots T. \tag{A.8}$$

Applying it to the case $T := \phi^*_\lambda Q\big|_{M_0}$, we get that the value of $\psi^*_\lambda Q\big|_{M_0}$ can be expanded in terms of the other gauge choice as

$$\psi^*_\lambda Q\big|_{M_0} = \phi^*_\lambda Q\big|_{M_0} + \lambda \pounds_{V(1)}(\phi^*_\lambda Q\big|_{M_0}) + \lambda^2 \frac{1}{2}\left(\pounds_{V(1)^2} + \pounds_{V(2)}\right)\phi^*_\lambda Q\big|_{M_0} + \mathcal{O}(\lambda^3) \quad \text{(A.9)}$$

and now, introducing the Taylor expansions for $\psi^*_\lambda Q\big|_{M_0}$ and $\phi^*_\lambda Q\big|_{M_0}$ in eq. (A.9), the differences between the value of the perturbation at each order $Q^{(1)}, Q^{(2)}, \ldots$ due to the gauge change are

$$\bar{Q}^{(1)} - Q^{(1)} = \pounds_{V(1)} Q_0, \quad \text{(A.10)}$$

$$\bar{Q}^{(2)} - Q^{(2)} = \left(\pounds^2_{V(1)} + \pounds_{V(2)}\right) Q_0 + 2\pounds_{V(1)} Q^{(1)}, \quad \text{(A.11)}$$

$$\bar{Q}^{(3)} - Q^{(3)} = \left(\pounds^3_{V(1)} + 3\pounds_{V(1)}\pounds_{V(2)} + \pounds_{V(3)}\right) Q_0 + \\ + 3\left(\pounds^2_{V(1)} + \pounds_{V(2)}\right) Q^{(1)} + 3\pounds_{V(1)} Q^{(2)} \quad \text{(A.12)}$$

$$\cdots$$

with the first $V(i)$ vectors

$$V_{(1)} = Y - X, \quad \text{(A.13)}$$

$$V_{(2)} = [X, Y], \quad \text{(A.14)}$$

$$V_{(3)} = [2X - Y, [X, Y]], \quad \text{(A.15)}$$

$$\cdots$$

Now, in practical computations what one usually does is to choose a coordinate system (x^α, λ) on $\mathcal{M}$ and write eq. (A.3) in components, obscuring all the structure behind it. In this situation, the effects of the gauge change can be directly translated into an infinitesimal change of coordinates. Considering them as a tensor on $\mathcal{M}$, its expression can be obtained from eqs. (A.9) to (A.12), getting that the new coordinates y^α of a point p on each M_λ are

$$y^\alpha = x^\alpha - \lambda V^\alpha_{(1)} + \frac{1}{2}\lambda^2\left(V^\alpha_{(1),\beta} V^\alpha_{(1)} - V^\alpha_{(2)}\right) + \cdots \quad \text{(A.16)}$$

with $V_{(i)}$ given by eqs. (A.13) to (A.15) and expressed in the the coordinate system x^α. It is worth noting that because of how we have parametrized the identification maps, the parameter of the infinitesimal transformation corresponding to a gauge change is the same as the approximation parameter. This last fact can be unclear without the full picture in mind.

Equation (A.16) can be generalised straightforwardly to a case of two parameter perturbation theory (Bruni *et al.*, 2003) like the one we use. Expressions are messier, but only because gauge choices and changes involve then two-parameter groups and families of diffeomorphisms, respectively.

Appendix B

Solution of the homogeneous system

Here we find the general solution of the equations

$$\begin{cases} \triangle h_{\alpha\beta} = 0, \\ \partial^k \left(h_{k\alpha} - \dfrac{1}{2} h \eta_{k\alpha} \right) = 0, \end{cases} \tag{B.1}$$

that arise in the harmonic post-Minkowskian approximation for both exterior and interior stationary spacetimes. We start finding the general solution and then simplify it using the axisymmetry of the spacetimes, Papapetrou's structure of the metric and finally the harmonic conditions.

1. Expansions in spherical harmonic tensors

In this section we define a cobasis of spherical harmonic tensors suited to describe metrics with Papapetrou's structure and in harmonic gauge, taking the usual decomposition of the general solution of Laplace's equation into tracefree symmetric tensors.

We start with some previous notation. We define r as the usual spherical-like radial coordinate, $\boldsymbol{x} = x^i \boldsymbol{e}_i$ as a Cartesian-like 3-vector such that $r^2 = x^i x_i$ and $\boldsymbol{n} = \boldsymbol{x}/r$, so that $n_i = x_i/r$. Round brackets around a pair of indices mean taking the symmetric part, as usual.

Now, if we take successively ∂_i derivatives with respect to the Cartesian-like coordinates of the $\frac{1}{r}$ function, using the shorthand $\partial_{ij} = \partial_i \partial_j$, we have

$$\partial_j \frac{1}{r} = -\frac{1}{r^2} n_j \,, \tag{B.2}$$

$$\partial_{jk} \frac{1}{r} = \frac{3}{r^3} \left(n_j n_k - \frac{1}{3} \delta_{jk} \right) , \tag{B.3}$$

$$\partial_{jkp} \frac{1}{r} = -\frac{3 \cdot 5}{r^4} \left(n_j n_k n_p - \frac{1}{5} \delta_{jk} n_p - \frac{1}{5} \delta_{kp} n_j - \frac{1}{5} \delta_{pj} n_k \right) , \tag{B.4}$$

$$\cdots \tag{B.5}$$

$$\partial_{i_1 i_2 \ldots i_l} \frac{1}{r} = (-1)^l \frac{(2l-1)!!}{r^{l+1}} (n_{i_1} n_{i_2} \ldots n_{i_l})^{\text{STF}} , \tag{B.6}$$

where the STF superindex means taking the symmetric and tracefree part of the tensor.

The flat Laplacian of these derivatives is, since out of origin of coordinates we have $\Delta \frac{1}{r} = 0$,

$$\Delta \left(\partial_{i_1 i_2 \ldots i_l} \frac{1}{r} \right) = \partial_{i_1 i_2 \ldots i_l} \Delta \frac{1}{r} = 0 , \tag{B.7}$$

so these symmetric and tracefree tensors are solution of the Laplace equation around infinity. Splitting the Laplacian in

$$\Delta = \frac{\partial^2}{\partial r^2} + \frac{2}{r} \frac{\partial}{\partial r} - \frac{L^2}{r^2} \tag{B.8}$$

where L^2 contains the angular derivatives, we get that

$$\Delta \left[\frac{1}{r^{l+1}} (n_{i_1} n_{i_2} \ldots n_{i_l})^{\text{STF}} \right] = \frac{1}{r^{l+3}} \left[l(l+1) - L^2 \right] (n_{i_1} n_{i_2} \ldots n_{i_l})^{\text{STF}} = 0, \tag{B.9}$$

leading us to the way L^2 operates on STF tensors

$$L^2 (n_{i_1} n_{i_2} \ldots n_{i_l})^{\text{STF}} = l(l+1) (n_{i_1} n_{i_2} \ldots n_{i_l})^{\text{STF}}, \tag{B.10}$$

what shows that STF tensors are actually spherical harmonic tensors as well.

We have now the basic tools to deal with the exterior problem. We need to find solutions of the Laplace equation that work at $r = 0$ to deal with the interior, too. Simplifying the notation

$$n_{i_1 \ldots i_l} := (n_{i_1} \ldots n_{i_l})^{\text{STF}} \tag{B.11}$$

and using

$$\Delta \, x_{i_1 \ldots i_l} = 0 = \Delta (r^l n_{i_1 \ldots i_l}) , \tag{B.12}$$

we have

$$\Delta \left(r^l n_{i_1 \ldots i_l} \right) = r^{l-2} \left[l(l+1) - L^2 \right] n_{i_1 \ldots i_l} = 0 . \tag{B.13}$$

Again, $n_{i_1 \ldots i_l}$ is solution of the angular part of the Laplace equation. In this way the exterior (regular at infinity) and the interior (regular at the origin) solutions differ only on the radial part. We will focus now in solving the exterior problem, since the interior allows for a very similar treatment.

It is well known that Einstein equations can be decomposed into three separate and independent sets. When we deal with their homogeneous post-Minkowskian expression the equations are

$$\Delta h_{00} = 0, \tag{B.14}$$

$$\Delta h_{0j} = 0, \tag{B.15}$$

$$\Delta h_{ij} = 0, \tag{B.16}$$

scalar, vector and tensor equations respectively. Summing up, we can state now that the most general solution of the Laplace equation around infinity is

$$h_{00} = \sum_{l=0} \frac{1}{r^{l+1}} M^{i_1 \dots i_l} n_{i_1 \dots i_l}, \tag{B.17}$$

$$h_{0j} = \sum_{l=0} \frac{1}{r^{l+1}} M_{j,i_1 \dots i_l} n^{i_1 \dots i_l}, \tag{B.18}$$

$$h_{ij} = \sum_{l=0} \frac{1}{r^{l+1}} M_{ij,i_1 \dots i_l} n^{i_1 \dots i_l}, \tag{B.19}$$

with r^l replacing $r^{-(l+1)}$ for the solution around the origin. $M_{\alpha\beta i_1 \dots i_l}$ is a tensor with constant components, which we will call scalar, vector and tensor depending on the equation they are involved in. It is already symmetric and tracefree in the indices which are contracted with the spherical harmonic tensor ones, but there are free indices in the vector and tensor equations. We find a STF tensor decomposition for these parts in what follows.

1.1. Decomposition of $\boldsymbol{M}$ into STF tensors

We find now the STF decomposition of an arbitrary $\boldsymbol{M}$ tensor with constant components of rank $n + 2$. We will later use it to find its contraction with rank n spherical harmonic tensors.

From now on, for the sake of clarity, we will denote STF tensors with calligraphic types and add a bracketed subindex stating the number of components added or subtracted from with respect to n.

The scalar components already have the desired form

$$M^{k_1 \cdots k_n} = M^{(k_1 \cdots k_n)^{TF}} := \mathcal{M}^{k_1 \cdots k_n}_{[0]}. \tag{B.20}$$

Focusing now in the vectorial components, we start from

$$M^{j,k_1 \cdots k_n} = M^{j,(k_1 \cdots k_n)^{TF}}. \tag{B.21}$$

We can decompose it, as any other vector, in its symmetric and antisymmetric parts. The main goal now is rewriting its antisymmetric part in terms of objects *check* which are antisymmetric in their two (first) indices

$$M^{j,k_1\cdots k_n} = M^{(j,k_1\cdots k_n)} + \frac{2}{n+1}\Big[\epsilon^{jk_1}{}_{q}N^{q,k_2\cdots k_n} + \epsilon^{jk_2}{}_{q}N^{q,k_1k_3\cdots k_n} + \cdots + \epsilon^{jk_n}{}_{q}N^{q,k_1\cdots k_{n-1}}\Big], \tag{B.22}$$

$$N^{q,k_2\cdots k_n} := \frac{1}{2}\epsilon^{q}{}_{sk_1}M^{s,k_1k_2\cdots k_n}, \tag{B.23}$$

which, from its definition and the properties of the last $n-1$ indices,

$$\begin{cases} N^{q,k_2\cdots k_n} = N^{q,(k_2\cdots k_n)^{TF}}, \\ \delta_{qk_2}N^{q,k_2k_3\cdots k_n} = 0. \end{cases} \tag{B.24}$$

are tracefree and then

$$N^{(q,k_2\cdots k_n)} = N^{(q,k_2\cdots k_n)^{TF}} := \mathcal{J}^{qk_2\cdots k_n}_{[0]}. \tag{B.25}$$

We still need totally symmetric objects. We could keep on decomposing iteratively in this way $N^{q,k_2\cdots k_n}$

$$N^{q,k_2\cdots k_n} = N^{(q,k_2\cdots k_n)} + \frac{2}{n}\Big[\epsilon^{qk_2}{}_{h}P^{h,k_3\cdots k_n} + \epsilon^{qk_3}{}_{h}P^{h,k_2k_4\cdots k_n} + \cdots + \epsilon^{qk_n}{}_{h}P^{h,k_2\cdots k_{n-1}}\Big], \tag{B.26}$$

in a process with n iterations. Nevertheless, taking into account that from its definition

$$\begin{aligned} P^{h,k_3\cdots k_n} &:= \frac{1}{2}\epsilon^{h}{}_{sk_2}N^{s,k_2k_3\cdots k_n} \\ &= \frac{1}{4}\epsilon^{h}{}_{sk_2}\epsilon^{s}{}_{rk_1}M^{r,k_1k_2\cdots k_n} \\ &= \frac{1}{4}M_{s}{}^{,shk_3\cdots k_n}, \end{aligned} \tag{B.27}$$

the h index actually belongs to the original totally symmetric part. Hence, the process truncates itself leading to

$$P^{h,k_3\cdots k_n} = P^{(h,k_3\cdots k_n)^{TF}} := \mathcal{U}^{hk_3\cdots k_n}_{[-1]} \tag{B.28}$$

and then

$$N^{q,k_2\cdots k_n} = \mathcal{J}^{qk_2\cdots k_n}_{[0]} + \frac{2}{n}\Big[\epsilon^{qk_2}{}_{h}\mathcal{U}^{hk_3\cdots k_n}_{[-1]}$$

$$+ \epsilon^{qk_3}{}_h \mathcal{U}^{hk_2k_4\cdots k_n}_{[-1]} + \cdots + \epsilon^{qk_n}{}_h \mathcal{U}^{hk_3\cdots k_{n-1}}_{[-1]} \Big], \tag{B.29}$$

leaving the antisymmetric part of $M^{j,k_1\cdots k_n}$ completely expressed in STF tensors. Focusing now in its symmetric part, it can be decomposed as

$$M^{(j,k_1\cdots k_n)} = M^{(j,k_1\cdots k_n)^{TF}} + \tfrac{4n}{2n+1}\delta^{j(k_1}\mathcal{U}^{k_2\cdots k_n)}_{[-1]}, \tag{B.30}$$

since the only non-zero traces are those involving the j index and the rest are symmetric. Note as well that the tracefree part is already in the desired form. Then, substituting in the initial decomposition eq. (B.22), and taking into account that, from its definition

$$\epsilon^{jk_1}{}_q \epsilon^{qk_2}{}_h P^{h,k_3\cdots k_n} = \delta^{jk_2}\mathcal{U}^{k_1,k_3\cdots k_n}_{[-1]} - \delta^{k_1k_2}\mathcal{U}^{j,k_3\cdots k_n}_{[-1]}, \tag{B.31}$$

we get that

$$\begin{aligned} M^{j,k_1\cdots k_n} = {} & \tfrac{2(n-1)}{n+1}\Big[\delta^{j(k_1}\mathcal{U}^{k_2\cdots k_n)}_{[-1]} - \mathcal{U}^{j(k_1\cdots k_{n-2}}_{[-1]}\delta^{k_{n-1}k_n)}\Big] \\ & + \tfrac{2n}{n+1}\epsilon^{j(k_1}{}_q \mathcal{J}^{k_2\cdots k_n)q}_{[0]} \\ & + \mathcal{V}^{jk_1\cdots k_n}_{[1]} + \tfrac{4n}{2n+1}\delta^{j(k_1}\mathcal{U}^{k_2\cdots k_n)}_{[-1]}, \end{aligned} \tag{B.32}$$

with the calligraphic components standing for

$$\mathcal{U}^{k_2\cdots k_n}_{[-1]} := \tfrac{1}{4}M_s{}^{sk_2\cdots k_n} \tag{B.33}$$

$$\mathcal{J}^{k_2\cdots k_nq}_{[0]} := \tfrac{1}{2}M^{s,k_1(k_2\cdots k_n}\epsilon^{q)}{}_{sk_1} \tag{B.34}$$

$$\mathcal{V}^{jk_1\cdots k_n}_{[1]} := M^{(j,k_1\cdots k_n)^{TF}}. \tag{B.35}$$

The decomposition is then complete. Inserting it in the solution of the vector Laplace equation, its contracted with the spherical harmonics, leading to, for a solution around infinity

$$\begin{aligned} M^{j,k_1\cdots k_n}\partial_{k_1\cdots k_n}\frac{1}{r} = {} & 2\,\tfrac{4n^2+n-1}{(2n+1)(n+1)}\mathcal{U}^{k_2\cdots k_n}_{[-1]}\partial^j{}_{k_2\cdots k_n}\frac{1}{r} \\ & + \tfrac{2n}{n+1}\epsilon^{jk_1}{}_q\mathcal{J}^{k_2\cdots k_nq}_{[0]}\partial_{k_1\cdots k_n}\frac{1}{r} \\ & + \mathcal{V}^{jk_1\cdots k_n}_{[1]}\partial_{k_1\cdots k_n}\frac{1}{r}. \end{aligned} \tag{B.36}$$

We can apply this kind of process to symmetrize any number of indices. In particular, we must use it twice for the tensorial components $M^{ij,k_1\cdots k_n}$. The first decomposition leads to an expression similar to (B.36)

$$M^{ij,k_1\cdots k_n}\partial_{k_1\cdots k_n}\frac{1}{r} = \tfrac{4n^2+n-1}{(2n+1)(n+1)}U^{i,k_2\cdots k_n}\partial^j{}_{k_2\cdots k_n}\frac{1}{r} + (i \leftrightarrow j)$$

$$+ \tfrac{n}{n+1}\epsilon^{jk_1}{}_q J^{i,k_2\cdots k_n q}\partial_{k_1\cdots k_n}\frac{1}{r} + (i\leftrightarrow j)$$
$$+ \tfrac{1}{2}V^{i,jk_1\cdots k_n}\partial_{k_1\cdots k_n}\frac{1}{r} + (i\leftrightarrow j)\,, \tag{B.37}$$

where

$$U^{i,k_2\cdots k_n} := \tfrac{1}{4}M^{i}{}_{s}{}^{,sk_2k_3\cdots k_n}, \tag{B.38}$$
$$J^{i,k_2\cdots k_n q} := \tfrac{1}{2}M^{is,k_1(k_2\cdots k_n}\epsilon^{q)}{}_{sk_1}\,, \tag{B.39}$$
$$V^{i,jk_1\cdots k_n} := M^{i(j,k_1\cdots k_n)^{TF}}, \tag{B.40}$$

with no STF component yet. Now, noticing that index j already belongs to the STF part, we can decompose again getting, for $V^{i,jk_1\cdots k_n}$,

$$\begin{aligned} V^{i,jk_1\cdots k_n} &= \mathcal{Q}^{ijk_1\cdots k_n}_{[2]} + \tfrac{4(n+1)}{2n+3}\delta^{i(j}\mathcal{Q}^{k_1\cdots k_n)}_{[0]} \\ &+ 2\,\tfrac{(n+1)}{n+2}\epsilon^{i(j}{}_q\mathcal{Q}^{k_1\cdots k_n)q}_{[1]} \\ &+ 2\,\tfrac{n}{n+2}\left[\delta^{i(j}\mathcal{Q}^{k_1\cdots k_n)}_{[0]} - \mathcal{Q}^{i(jk_1\cdots k_{n-2}}_{[0]}\delta^{k_{n-1}k_n)}\right] \end{aligned} \tag{B.41}$$

with the STF base

$$\mathcal{Q}^{ijk_1\cdots k_n}_{[2]} := V^{(i,jk_1\cdots k_n)^{TF}}, \tag{B.42}$$
$$\mathcal{Q}^{k_1\cdots k_n q}_{[1]} := \tfrac{1}{2}V^{r,s(k_1k_2\cdots k_n}\epsilon^{q)}{}_{rs}, \tag{B.43}$$
$$\mathcal{Q}^{k_1\cdots k_n}_{[0]} := \tfrac{1}{4}V_{s}{}^{,sk_1\cdots k_n}\,, \tag{B.44}$$

so that, grouping terms,

$$\begin{aligned} \frac{1}{2}V^{i,jk_1\cdots k_n}\partial_{k_1\cdots k_n} + (i\leftrightarrow j) &= \mathcal{Q}^{ijk_1\cdots k_n}_{[2]}\partial_{k_1\cdots k_n}\frac{1}{r} \\ &+ \frac{n}{n+2}\epsilon^{ik_1}{}_q\mathcal{Q}^{k_2\cdots k_n jq}_{[1]}\partial_{k_1\cdots k_n}\frac{1}{r} + (i\leftrightarrow j) \\ &+ \frac{2(4n^2+9n+4)}{(n+1)(n+2)(2n+3)}\delta^{ij}\mathcal{Q}^{k_1\cdots k_n}_{[0]}\partial_{k_1\cdots k_n}\frac{1}{r} \\ &+ \frac{n(4n^2+5n-2)}{(n+1)(n+2)(2n+3)}\mathcal{Q}^{ik_2\cdots k_n}_{[0]}\partial^{j}{}_{k_2\cdots k_n}\frac{1}{r} + (i\leftrightarrow j)\,. \end{aligned} \tag{B.45}$$

In the same fashion, we can write the $J^{i,k_2\cdots k_n q}$ components as

$$J^{i,k_2\cdots k_n q} = \mathcal{R}^{ik_2\cdots k_n q}_{[1]} + \frac{4n}{2n+1}\delta^{i(k_2}\mathcal{R}^{k_3\cdots k_n q)}_{[-1]} + \frac{2n}{n+1}\epsilon^{i(k_2}{}_p\mathcal{R}^{k_3\cdots k_n q)p}_{[0]}$$

$$+ 2\,\frac{n-1}{n+1}\Big[\delta^{i(k_2}\mathcal{R}^{k_3\cdots k_n q)}_{[-1]} - \mathcal{R}^{i(k_2\cdots k_{n-1}}_{[-1]}\delta^{k_n q)}\Big] \tag{B.46}$$

with the definitions

$$\mathcal{R}^{ik_2\cdots k_n q}_{[1]} := J^{(i,k_2\cdots k_n q)^{TF}}, \tag{B.47}$$

$$\mathcal{R}^{k_3\cdots k_n qp}_{[0]} := \frac{1}{2}J^{s,k_2(k_3\cdots k_n q}\epsilon^{p)}{}_{sk_2}, \tag{B.48}$$

$$\mathcal{R}^{k_3\cdots k_n q}_{[-1]} := \frac{1}{4}J_s{}^{,sk_3\cdots k_n q}, \tag{B.49}$$

and hence,

$$\begin{aligned}\frac{n}{n+1}\epsilon^{jk_1}{}_q J^{i,k_2\cdots k_n q}\partial_{k_1\cdots k_n}\frac{1}{r} + (i\leftrightarrow j) &= \tfrac{n}{n+1}\epsilon^{jk_1}{}_q\mathcal{R}^{ik_2\cdots k_n q}_{[1]}\partial_{k_1\cdots k_n}\frac{1}{r} + (i\leftrightarrow j)\\ &+ \frac{2(n-1)(4n^2+n-1)}{(n+1)^2(2n+1)}\epsilon^{ik_2}{}_q\mathcal{R}^{k_3\cdots k_n q}_{[-1]}\partial^j{}_{k_2\cdots k_n}\frac{1}{r} + (i\leftrightarrow j)\\ &- \frac{4n^2}{(n+1)^2}\delta^{ij}\mathcal{R}^{k_1\cdots k_n}_{[0]}\partial_{k_1\cdots k_n}\frac{1}{r}\\ &+ \frac{2n(2n-1)}{(n+1)^2}\mathcal{R}^{ik_2\cdots k_n}_{[0]}\partial^j{}_{k_2\cdots k_n}\frac{1}{r} + (i\leftrightarrow j)\,.\end{aligned} \tag{B.50}$$

Last, the decomposition of the remaining components $U^{i,k_2\cdots k_n}$ is

$$\begin{aligned}U^{i,k_2\cdots k_n} &= S^{ik_2\cdots k_n}_{[0]} + \frac{4(n-1)}{2n-1}\delta^{i(k_2}S^{k_3\cdots k_n)}_{[-2]} + \frac{2(n-1)}{n}\epsilon^{i(k_2}{}_p S^{k_3\cdots k_n)p}_{[-1]}\\ &+ 2\,\frac{n-2}{n}\Big[\delta^{i(k_2}S^{k_3\cdots k_n)}_{[-2]} - S^{j(k_2\cdots k_{n-2}}_{[-2]}\delta^{k_{n-1}k_n)}\Big],\end{aligned} \tag{B.51}$$

with the same notation as before for the basis

$$S^{ik_2\cdots k_n}_{[0]} := U^{(i,k_2\cdots k_n)^{TF}} \tag{B.52}$$

$$S^{k_3\cdots k_n p}_{[-1]} := \frac{1}{2}U^{s,k_2(k_3\cdots k_n}\epsilon^{p)}{}_{sk_2} \tag{B.53}$$

$$S^{k_3\cdots k_n}_{[-2]} := \frac{1}{4}U_s{}^{,sk_3\cdots k_n}, \tag{B.54}$$

so, finally,

$$\begin{aligned}\frac{4n^2+n-1}{(n+1)(2n+1)}U^{i,k_2\cdots k_n}\partial^j{}_{k_1\cdots k_n}\frac{1}{r} + (i\leftrightarrow j) &= \frac{4n^2+n-1}{(n+1)(2n+1)}S^{ik_2\cdots k_n}_{[0]}\partial^j{}_{k_2\cdots k_n}\frac{1}{r} + (i\leftrightarrow j)\\ &+ \frac{2(n-1)(4n^2+n-1)}{n(n+1)(2n+1)}\epsilon^{ik_2}{}_p S^{k_3\cdots k_n q}_{[-1]}\partial^j{}_{k_2\cdots k_n}\frac{1}{r} + (i\leftrightarrow j)\end{aligned}$$

$$+\frac{4(4n^2-7n+2)(4n^2+n-1)}{n(n+1)(2n-1)(2n+1)}S^{k_3\cdots k_n}_{[-2]}\partial^{ij}{}_{k_3\cdots k_n}\frac{1}{r}\,. \tag{B.55}$$

Accordingly, the decomposition in STF tensors of any rank two tensor is

$$\begin{aligned}M^{ij,k_1\cdots k_n}\partial_{k_1\cdots k_n}\frac{1}{r} &= \mathcal{D}^{k_3\cdots k_n}_{[-2]}\partial^{ij}{}_{k_3\cdots k_n}\frac{1}{r}+\epsilon^{ik_2}{}_p\mathcal{E}^{k_3\cdots k_nq}_{[-1]}\partial^{j}{}_{k_2\cdots k_n}\frac{1}{r}\ +(i\leftrightarrow j)\\ &\quad+\delta^{ij}\mathcal{G}^{k_1\cdots k_n}_{[0]}\partial_{k_1\cdots k_n}\frac{1}{r}+\mathcal{H}^{ik_2\cdots k_n}_{[0]}\partial^{j}{}_{k_2\cdots k_n}\frac{1}{r}\ +(i\leftrightarrow j)\\ &\quad+\epsilon^{ik_1}{}_q\mathcal{I}^{k_2\cdots k_njq}_{[1]}\partial_{k_1\cdots k_n}\frac{1}{r}\ +(i\leftrightarrow j)+\mathcal{K}^{ijk_1\cdots k_n}_{[2]}\partial_{k_1\cdots k_n}\frac{1}{r}\,,\end{aligned} \tag{B.56}$$

where we have introduced the redefinitions

$$\mathcal{D}^{k_3\cdots k_n}_{[-2]} := \frac{4(4n^2-7n+2)(4n^2+n-1)}{n(n+1)(2n-1)(2n+1)}\mathcal{S}^{k_3\cdots k_n}_{[-2]}\,, \tag{B.57}$$

$$\mathcal{E}^{k_3\cdots k_nq}_{[-1]} := \frac{2(n-1)(4n^2+n-1)}{(n+1)^2(2n+1)}\mathcal{R}^{k_3\cdots k_nq}_{[-1]}+\frac{2(n-1)(4n^2+n-1)}{n(n+1)(2n+1)}\mathcal{S}^{k_3\cdots k_nq}_{[-1]}\,, \tag{B.58}$$

$$\begin{aligned}\mathcal{G}^{k_1\cdots k_n}_{[0]} &:= \frac{2(4n^2+9n+4)}{(n+1)(n+2)(2n+3)}\mathcal{Q}^{k_1\cdots k_n}_{[0]}-\frac{4n^2}{(n+1)^2}\mathcal{R}^{k_1\cdots k_n}_{[0]}\,,\\ \mathcal{H}^{ik_2\cdots k_n}_{[0]} &:= \frac{n(4n^2+5n-2)}{(n+1)(n+2)(2n+3)}\mathcal{Q}^{ik_2\cdots k_n}_{[0]}+\frac{2n(2n-1)}{(n+1)^2}\mathcal{R}^{ik_2\cdots k_n}_{[0]}\\ &\quad+\frac{4n^2+n-1}{(n+1)(2n+1)}\mathcal{S}^{ik_2\cdots k_n}_{[0]}\,,\end{aligned} \tag{B.59}$$

$$\mathcal{I}^{k_2\cdots k_njq}_{[1]} := \frac{n}{n+2}\mathcal{Q}^{k_2\cdots k_njq}_{[1]}+\frac{n}{n+1}\mathcal{R}^{ik_2\cdots k_nq}_{[1]}\,, \tag{B.60}$$

$$\mathcal{K}^{ijk_1\cdots k_n}_{[2]} := \mathcal{Q}^{ijk_1\cdots k_n}_{[2]}\,. \tag{B.61}$$

1.2. STF decomposition and harmonic constraints

To solve the homogeneous system of equations of the harmonic Post-Minkowskian approximation, we are looking for a general solution of Laplace's equations which also satisfies the linear part of the harmonic condition

$$\partial^k\left(h_{k\alpha}-\frac{1}{2}h\eta_{k\alpha}\right)=0. \tag{B.62}$$

We start with the scalar component eq. (B.20). The axisymmetry of the space-time makes it time independent, so the first term of eq. (B.62) is already zero.

Now, since it consists of only a STF tensor, the trace $h^{\text{scalar}} = 0$ as well. Thus, the scalar component already complies with the linear harmonic condition.

The vector solution

$$h^{0j}(r,\boldsymbol{n}) = 2\sum_{l=1}^{\infty}\epsilon^{jk_1}{}_p\mathcal{J}^{pk_2\ldots k_l}\partial_{k_1k_2\ldots k_l}\frac{1}{r} + \partial^j\sum_{l=0}^{\infty}\mathcal{U}^{k_1\ldots k_l}\partial_{k_1\ldots k_l}\frac{1}{r} + \sum_{l=1}^{\infty}\mathcal{V}^{jk_2\ldots k_l}\partial_{k_2\ldots k_l}\frac{1}{r}\,, \tag{B.63}$$

has null trace again. Its divergence is

$$\partial_j h^{0j} = \sum_{l=1}^{\infty}\mathcal{V}^{k_1k_2\ldots k_l}\partial_{k_1k_2\ldots k_l}\frac{1}{r}\,, \tag{B.64}$$

and thus, since the linear harmonic condition for these components imposes $\partial_j h^{0j} = 0$, we have

$$\mathcal{V}^{k_1k_2\ldots k_l} = 0\,. \tag{B.65}$$

Regarding the tensor solution

$$\begin{aligned} h^{ij}(r,\boldsymbol{n}) = {}& \delta^{ij}\sum_{l=0}^{\infty}\mathcal{G}^{k_1\ldots k_l}\partial_{k_1\ldots k_l}\frac{1}{r} + \partial^{(i}\sum_{l=1}^{\infty}\mathcal{H}^{j)k_2\ldots k_l}\partial_{k_2\ldots k_l}\frac{1}{r} \\ & + \partial^{ij}\sum_{l=0}^{\infty}\mathcal{D}^{k_1\ldots k_l}\partial_{k_1\ldots k_l}\frac{1}{r} + \partial^{(i}\sum_{l=1}^{\infty}\epsilon^{j)k_1}{}_q\mathcal{E}^{qk_2\ldots k_l}\partial_{k_1k_2\ldots k_l}\frac{1}{r} \\ & + \sum_{l=2}^{\infty}\left[\mathcal{K}^{ijk_3\ldots k_l}\partial_{k_3\ldots k_l}\frac{1}{r} + \epsilon^{k_2}{}_q{}^{(i}\mathcal{I}^{j)qk_3\ldots k_l}\partial_{k_2k_3\ldots k_l}\frac{1}{r}\right], \end{aligned} \tag{B.66}$$

whose divergence and trace are

$$\begin{aligned} \partial_i h^{ij} = {}& \partial^j\sum_{l=0}^{\infty}\mathcal{G}^{k_1\ldots k_l}\partial_{k_1\ldots k_l}\frac{1}{r} + \frac{1}{2}\partial^j\sum_{l=1}^{\infty}\mathcal{H}^{k_1k_2\ldots k_l}\partial_{k_1k_2\ldots k_l}\frac{1}{r} \\ & + \sum_{l=2}^{\infty}\mathcal{K}^{jk_2k_3\ldots k_l}\partial_{k_2k_3\ldots k_l}\frac{1}{r} + \frac{1}{2}\sum_{l=2}^{\infty}\epsilon^{k_2}{}_q{}^j\mathcal{I}^{k_1qk_3\ldots k_l}\partial_{k_1k_2k_3\ldots k_l}\frac{1}{r} \end{aligned} \tag{B.67}$$

and

$$h = \sum_{l=0}^{\infty}(-\mathcal{M}^{k_1\ldots k_l} + 3\mathcal{G}^{k_1\ldots k_l})\partial_{k_1\ldots k_l}\frac{1}{r} + \sum_{l=1}^{\infty}\mathcal{H}^{k_1\ldots k_l}\partial_{k_1\ldots k_l}\frac{1}{r}\,, \tag{B.68}$$

respectively. This leads, imposing eq. (B.62), to

$$\begin{cases} \mathcal{G}^{k_1\dots k_l} = \mathcal{M}^{k_1\dots k_l}, \\ \mathcal{K}^{k_1 k_2\dots k_l} = 0, \\ \mathcal{I}^{k_1 k_2\dots k_l} = 0. \end{cases} \tag{B.69}$$

1.3. Axial symmetry and Papapetrou's structure

The last simplifications on the structure of the STF decomposition comes from the symmetries. Calling e^i to the components of a vector ∂_z such that

$$\partial_z = e^i \partial_{x_i} \quad \text{and} \quad e^i = (0,0,1) \tag{B.70}$$

and taking it to be parallel to the symmetry axis of the spacetime, the components of a STF tensor can only be related with the basis through e^{k_n} terms, i.e.

$$\mathcal{T}^{k_1\dots k_l} \propto (e^{k_1}\cdots e^{k_l})^{\mathrm{TF}} := e^{k_1\dots k_l}\,. \tag{B.71}$$

These components appear contracted with the ones belonging to the spherical harmonic tensors in two ways.

- The first one, $\mathcal{T}^{k_1\dots k_l} n_{k_1\cdots k_l}$. Starting from

$$\mathcal{T}^{k_1\dots k_l}\partial_{k_1\dots k_l}\frac{1}{r} \;\propto\; e^{k_1\dots k_l}\partial_{k_1\dots k_l}\frac{1}{r} \;=\; \left(e^k\partial_k\right)^l\frac{1}{r} \tag{B.72}$$

  and using the definition of the Legendre polynomials and $n_3 = \cos\theta$,

$$e^k\partial_k\frac{P_l(\cos\theta)}{r^{l+1}} = -(l+1)\frac{P_{l+1}(\cos\theta)}{r^{l+2}}\,. \tag{B.73}$$

  In particular,

$$e^k\partial_k\frac{1}{r} = e^k\partial_k\frac{P_0(\cos\theta)}{r} = -\frac{P_1(\cos\theta)}{r^2}, \tag{B.74}$$

  ...

$$\left(e^k\partial_k\right)^l\frac{1}{r} = (-1)^l l!\;\frac{P_l(\cos\theta)}{r^{n+1}}, \tag{B.75}$$

  so that these terms can be written as

$$\mathcal{T}^{k_1\dots k_l} n_{k_1\cdots k_l} = r^{l+1}\mathcal{T}^{k_1\dots k_l}\partial_{k_1\dots k_l}\frac{1}{r} \propto T_l P_l(\cos\theta) \tag{B.76}$$

  with T_l a constant.

- The other kind of contraction is $\epsilon^{jk_1}{}_p \mathcal{X}^{pk_2\ldots k_l} n_{k_1\cdots k_l}$. Working in similar fashion, we have for them that

$$\epsilon^{jk_1}{}_p \mathcal{X}^{pk_2\ldots k_l} \partial_{k_1\ldots k_l} \frac{1}{r} \;\propto\; \epsilon^{jk_1}{}_p e^{pk_2\ldots k_l} \partial_{k_1\ldots k_l} \frac{1}{r} \;=\; \epsilon^{jk_1}{}_p e^p \partial_{k_1} \left(e^m \partial_m\right)^{l-1} \frac{1}{r}. \tag{B.77}$$

  Now, using a more convenient basis, an orthonormal cylindrical-like one,

$$\begin{cases} \partial_\rho = k^i \partial_i = \cos\phi\ \partial_x - \sin\phi\ \partial_y \\ \dfrac{1}{\rho}\partial_\phi = m^i \partial_i = \sin\phi\ \partial_x + \cos\phi\ \partial_y \\ \partial_z = e^i \partial_i \end{cases} \tag{B.78}$$

  we can write

$$\epsilon^{jk_1}{}_p e^p = -2m^{[k_1} k^{j]}. \tag{B.79}$$

  Hence,

$$\begin{aligned} \epsilon^{jk_1}{}_p e^p \partial_{k_1} \left(e^m \partial_m\right)^{l-1} \frac{1}{r} &= -\left(m^{k_1} k^j - m^j k^{k_1}\right) \partial_{k_1} \left(e^m \partial_m\right)^{l-1} \frac{1}{r} \\ &= (-)^l (l-1)!\, k^j m^{k_1} \partial_{k_1} \frac{P_{l-1}(\cos\theta)}{r^l} \qquad \text{(B.80)} \\ &\qquad + (-1)^{l-1} (l-1)!\, m^j k^{k_1} \partial_{k_1} \frac{P_{l-1}(\cos\theta)}{r^l} \\ &= (-1)^{l-1} (l-1)!\, \frac{P_l^1(\cos\theta)}{r^{l+1}} m^j, \qquad \text{(B.81)} \end{aligned}$$

so, summing up,

$$\mathcal{T}^{k_1\ldots k_l} n_{k_1\cdots k_l} \propto T_l P_l(\cos\theta), \tag{B.82}$$

$$\epsilon^{jk_1}{}_p \mathcal{X}^{pk_2\ldots k_l} n_{k_1\cdots k_l} \propto X_l P_l^1(\cos\theta)\, m^j. \tag{B.83}$$

with X_l constants.

Finally, inserting these results in the three solutions we get that

1. the scalar solution is

$$h^{00} = 2\sum_{l=0}^{\infty} \frac{\tilde{M}_l}{r^{l+1}} P_l(\cos\theta)\ . \tag{B.84}$$

   where we have redefined $\tilde{M}_l$ to correspond with the usual expression of the multipole moments.

2. The vector solution is most easily written in the orthonormal spherical-like basis. Being $\omega^{\phi} = \rho d\phi$, we can use the previous results straightaway. Calling

$$\begin{cases} \partial_r = n^i \partial_i \,, \\ \dfrac{1}{r}\partial_\theta = s^i \partial_i \,, \end{cases} \tag{B.85}$$

to the components of the orthonormal spherical-like basis, we have

$$h^{0j} = \sum_{l=0}^{\infty} \underbrace{\frac{U_l}{r^{l+2}}\Big[-(l+1)P_l(\cos\theta)\, n^j + P_l^1(\cos\theta)\, s^j \Big]}_{\partial^j\left[U_l P_l(\cos\theta)/r^{l+1}\right]} + \sum_{l=1}^{\infty} \frac{\tilde{J}_l}{r^{l+1}} P_l^1(\cos\theta)\, m^j + \sum_{l=1}^{\infty} \frac{V_{l-1}^j}{r^l} P_{l-1}(\cos\theta) \,,$$

and hence

$$h^{0j} = \sum_{l=0}^{\infty} \frac{1}{r^{l+1}} \left[-(l+1)\frac{U_l}{r} n^j + V_l^j \right] P_l(\cos\theta) + \sum_{l=0}^{\infty} \frac{1}{r^{l+1}} \left(\frac{U_l}{r} s^j + \tilde{J}_l m^j \right) P_l^1(\cos\theta) \,. \tag{B.86}$$

Recalling Papapetrou's structure, we must preserve only those components which are proportional to m^j. This, together with the linear harmonic conditions, simplifies the vector solution and leads to

$$h^{0j} = 2 \sum_{l=0}^{\infty} \frac{1}{r^{l+1}} \tilde{J}_l P_l^1(\cos\theta) m^j \,, \tag{B.87}$$

where again we have extracted a 2 factor so that $\tilde{J}_l$ correspond to angular multipole moments.

3. For the tensor solution

$$h^{ij} = \sum_{l=0}^{\infty} \partial^{ij}\left[\frac{D_l}{r^{l+1}} P_l(\cos\theta) \right] + \sum_{l=1}^{\infty} \left\{ \partial^i \left[\frac{E_l}{r^{l+1}} P_l^1(\cos\theta)\, m^j \right] \right\}^S + \delta^{ij} \sum_{l=0}^{\infty} \frac{G_l}{r^{l+1}} P_l(\cos\theta) + \sum_{l=1}^{\infty} \left\{ \partial^i \left[\frac{H_{l-1}^j}{r^l} P_{l-1}(\cos\theta) \right] \right\}^S$$

$$+\sum_{l=2}^{\infty}\left\{\frac{I^i_{l-1}}{r^l}P^1_{l-1}(\cos\theta)\,m^j\right\}^S+\sum_{l=2}^{\infty}\frac{K^{ij}_{l-2}}{r^{l-1}}P_{l-2}(\cos\theta)\,, \tag{B.88}$$

we have

$$\begin{aligned}h^{ij}=&\sum_{l=0}^{\infty}\frac{1}{r^{l+1}}\left\{(l+1)\frac{D_l}{r^2}\left[-\delta^{ij}+(l+3)n^in^j\right]\right.\\&\left.-(l+1)\frac{H^{(i}_l n^{j)}}{r}+G_l\delta^{ij}+K^{ij}_l\right\}P_l(\cos\theta)\\&+\sum_{l=0}^{\infty}\frac{1}{r^{l+1}}\left\{\frac{D_l}{r^2}\left[\cot\theta(\delta^{ij}-n^in^j)-2(l+2)n^{(i}s^{j)}\right]\right.\\&\left.+\frac{1}{r}\left[-(l+2)E_ln^{(i}m^{j)}+H^{(i}_l s^{j)}\right]+I^{(i}_l m^{j)}\right\}P^1_l(\cos\theta)\\&+\sum_{l=0}^{\infty}\frac{1}{r^{l+2}}\left\{\frac{D_l}{r}s^is^j+E_ls^{(i}m^{j)}\right\}P^2_l(\cos\theta)\,.\end{aligned} \tag{B.89}$$

Again, since Papapetrou's structure admits only terms proportional to n^in^j, n^is^j, s^is^j and m^im^j and the linear harmonic conditions eq. (B.69), we get

$$\begin{aligned}h^{ij}=&\sum_{l=0}^{\infty}\frac{1}{r^{l+1}}\left\{(l+1)\frac{D_l}{r^2}\left[-\delta^{ij}+(l+3)n^in^j\right]-(l+1)\frac{H^{(i}_l n^{j)}}{r}+G_l\delta^{ij}\right\}P_l(\cos\theta)\\&+\sum_{l=0}^{\infty}\frac{1}{r^{l+1}}\left\{\frac{D_l}{r^2}\left[\cot\theta(\delta^{ij}-n^in^j)-2(l+2)n^{(i}s^{j)}\right]+\frac{1}{r}H^{(i}_l s^{j)}\right\}P^1_l(\cos\theta)\\&+\sum_{l=0}^{\infty}\frac{1}{r^{l+2}}\frac{D_l}{r}s^is^jP^2_l(\cos\theta).\end{aligned} \tag{B.90}$$

It is worth noticing that B.88 has some terms with a structure that corresponds to a gauge change

$$h^{ij}(r,\theta)=\delta^{ij}\sum_{l=0}^{\infty}\frac{G_l}{r^{l+1}}P_l(\cos\theta)\underbrace{-\partial^iw^j-\partial^jw^i}_{h^{ij}_{\text{gauge}}} \tag{B.91}$$

with

$$w^j:=\sum_{l=0}\frac{1}{r^{l+1}}\left[H_lP_l\,e^j+\frac{1}{l+1}H_{l+1}P^1_l\,n^j\right]+\partial^j\sum_{l=0}\frac{D_{l+1}}{r^{l+1}}P_l. \tag{B.92}$$

Redefining the constants of this part

$$\begin{aligned} \hat{A}_l &:= H_{l-1}\,, \\ \hat{B}_l &:= D_{l-1}\,, \end{aligned} \tag{B.93}$$

introducing the definitions

$$D_l^{ij} := \delta^{ij} P_l(\cos\theta), \tag{B.94}$$

$$H_l^{(0)ij} := (\delta^{ij} - 3e^i e^j) P_l(\cos\theta), \tag{B.95}$$

$$H_l^{(1)ij} := (k^i e^j + k^j e^i) P_l^1(\cos\theta), \tag{B.96}$$

$$H_l^{(2)ij} := (m^i m^j - k^i k^j) P_l^2(\cos\theta) \tag{B.97}$$

and grouping for convenience the tensor basis as

$$\begin{aligned} E_l^{ij} &:= \frac{1}{2} l(l-1)\, H_l^{(0)ij} + (l-1)\, H_l^{(1)ij} - \frac{1}{2}\, H_l^{(2)ij}\,, \quad (l \geq 2) \\ F_l^{ij} &:= \frac{1}{3} l(2l-1)\, D_l^{ij} - \frac{1}{6} l(l+1)\, H_l^{(0)ij} - \frac{1}{2}\, H_l^{(1)ij} + H_l^{(2)ij})\,, \quad (l \geq 1) \end{aligned} \tag{B.98}$$

we have then that the gauge part of the homogeneous solution is

$$h^{ij}_{\text{gauge}} = \sum_{l=1} \frac{(2l-1)\hat{A}_l}{l\, r^{l+1}} E_l^{ij} + \sum_{l=2} \frac{\hat{A}_l + l\hat{B}_l}{l\, r^{l+1}} F_l^{ij}\,. \tag{B.99}$$

Last, summing up the different components and regrouping the gauge part constants into $\tilde{A}_l$ and $\tilde{B}_l$, we get the expression we will use

$$\boldsymbol{h}^{+}_{\text{hom}} = 2\sum_{l=0}^{\infty} \frac{\tilde{M}_l}{r^{l+1}} (\boldsymbol{T}_l + \boldsymbol{D}_l) + 2\sum_{l=1,3}^{\infty} \frac{\tilde{J}_l}{r^{l+1}} \boldsymbol{Z}_l + \sum_{l=0,2}^{\infty} \frac{1}{r^{l+3}} \left(\tilde{A}_l \boldsymbol{E}_{l+2} + \tilde{B}_{l+2}\, \boldsymbol{F}_{l+2}\right). \tag{B.100}$$

Appendix C

$\mathcal{O}(\lambda^{5/2}, \Omega^3)$ *metric components after Lichnerowicz matching*

Here we give both metrics written in the orthonormal cobasis associated to $\{t, r, \theta, \phi\}$. These result from the substitution of eqs. (3.63) to (3.71) in eqs. (3.14) and (3.17). The exterior components are

$$\begin{aligned}
\gamma^+_{tt} &= -1 + \lambda\frac{1}{\eta}\left(2 - \frac{1}{\eta^2}\Omega^2 P_2\right) + \lambda^2\frac{1}{\eta}\left\{\frac{28}{5} + \frac{2n}{5} - \frac{2}{\eta}\right. \\
&\quad \left. + \Omega^2\left[\frac{16}{15} - \frac{4n}{15} + \frac{1}{\eta^2}\left(-\frac{74}{35} + \frac{n}{7} + \frac{2}{\eta}\right)P_2\right]\right\} + \mathcal{O}(\lambda^3, \Omega^4), \qquad \text{(C.1)} \\
\gamma^+_{t\phi} &= \lambda^{3/2}\frac{1}{\eta^2}\left[\frac{4}{5}\Omega P^1_1 + \Omega^3\left(\frac{2}{3}P^1_1 - \frac{2}{7\eta^2}P^1_3\right)\right] \\
&\quad + \lambda^{5/2}\frac{1}{\eta^2}\left\{\left(\frac{32}{7} + \frac{4n}{35} - \frac{4}{5\eta}\right)\Omega P^1_1 + \Omega^3\left[\left(\frac{352}{105} - \frac{6n}{35} - \frac{2}{3\eta}\right)P^1_1\right.\right. \\
&\quad \left.\left. + \frac{1}{\eta^2}\left(-\frac{992}{735} + \frac{22n}{441} + \frac{12}{35\eta}\right)P^1_3\right]\right\} + \mathcal{O}(\lambda^{7/2}, \Omega^5), \qquad \text{(C.2)} \\
\gamma^+_{rr} &= 1 + \lambda\frac{1}{\eta}\left(2 - \frac{1}{\eta^2}\Omega^2 P_2\right) + \lambda^2\frac{1}{\eta}\left\{\left(\frac{28}{5} + \frac{2n}{5}\right) + 2\frac{1}{\eta} - \frac{16}{35\eta^2}\right. \\
&\quad \left. + \Omega^2\left[\frac{16}{15} - \frac{4n}{15} - \frac{8}{105\eta^2} + \frac{1}{\eta^2}\left(-\frac{74}{35} + \frac{n}{7} - 2\frac{1}{\eta} + \frac{16}{21\eta^2}\right)P_2\right]\right\} + \mathcal{O}(\lambda^3, \Omega^4), \qquad \text{(C.3)} \\
\gamma^+_{\theta\theta} &= 1 + \lambda\frac{1}{\eta}\left(2 - \frac{1}{\eta^2}\Omega^2 P_2\right) \\
&\quad + \lambda^2\frac{1}{\eta}\left\{\frac{28}{5} + \frac{2n}{5} + \frac{1}{\eta} + \frac{8}{35\eta^2} + \Omega^2\left[\frac{16}{15} - \frac{4n}{15} + \frac{4}{105\eta^2}\right.\right. \\
&\quad \left.\left. - \frac{1}{6\eta^3} + \frac{4}{63\eta^4} + \frac{1}{\eta^2}\left(-\frac{74}{35} + \frac{n}{7} - \frac{5}{6\eta} - \frac{4}{9\eta^2}\right)P_2\right]\right\} + \mathcal{O}(\lambda^3, \Omega^4), \qquad \text{(C.4)}
\end{aligned}$$

$$\gamma^+_{r\theta} = \lambda^2\Omega^2\frac{1}{\eta^4}\left(\frac{1}{3} - \frac{16}{63\eta}\right)P_2^1 + \mathcal{O}(\lambda^3, \Omega^4), \tag{C.5}$$

$$\begin{aligned}\gamma^+_{\phi\phi} = 1 &+ \lambda\frac{1}{\eta}\left(2 - \frac{1}{\eta^2}\Omega^2 P_2\right)\\ &+ \lambda^2\frac{1}{\eta}\left\{\left(\frac{28}{5} + \frac{2n}{5}\right) + \frac{1}{\eta} + \frac{8}{35\eta^2} + \Omega^2\left[\frac{16}{15} - \frac{4n}{15} + \frac{4}{105\eta^2}\right.\right.\\ &\left.\left. + \frac{1}{6\eta^3} - \frac{4}{63\eta^4} + \frac{1}{\eta^2}\left(-\frac{74}{35} + \frac{n}{7} - \frac{7}{6\eta} - \frac{20}{63\eta^2}\right)P_2\right]\right\} + \mathcal{O}(\lambda^3, \Omega^4).\end{aligned} \tag{C.6}$$

The results for the interior metric are

$$\begin{aligned}\gamma^-_{tt} = -1 &+ \lambda\left(3 - \eta^2 - \eta^2\Omega^2 P_2\right)\\ &+ \lambda^2\left\{\frac{9}{2} + \frac{3n}{4} - \left(1 + \frac{n}{2}\right)\eta^2 + \left(\frac{1}{10} + \frac{3n}{20}\right)\eta^4 + \Omega^2\left[1 - \frac{n}{2} + (2+n)\frac{\eta^2}{3}\right.\right.\\ &\left.\left. + \left(-\frac{3}{5} - \frac{n}{10}\right)\eta^4 + \eta^2\left(-\frac{29}{35} - \frac{3n}{14} + \left(\frac{5}{7} + \frac{5n}{14}\right)\eta^2\right)P_2\right]\right\} + \mathcal{O}(\lambda^3, \Omega^4),\end{aligned} \tag{C.7}$$

$$\begin{aligned}\gamma^-_{t\phi} = &\lambda^{3/2}\eta\left[\Omega\left(2 - \frac{6\eta^2}{5}\right)P_1^1 + \Omega^3\left(\frac{2}{3}P_1^1 - \frac{2}{7}\eta^2 P_3^1\right)\right]\\ &+ \lambda^{5/2}\eta\left\{\left[\frac{49}{5} + \frac{n}{2} - \left(\frac{34}{5} + \frac{3n}{5}\right)\eta^2 + \left(\frac{27}{35} + \frac{3n}{14}\right)\eta^4\right]\Omega P_1^1\right.\\ &+ \Omega^3\left[\left(\frac{289}{105} - \frac{5n}{14} + \left(\frac{8}{15} + \frac{2n}{5}\right)\eta^2 - \left(\frac{3}{5} + \frac{3n}{14}\right)\eta^4\right)P_1^1\right.\\ &\left.\left. + \eta^2\left(-\frac{326}{245} - \frac{3n}{49} + \left(\frac{34}{105} + \frac{n}{9}\right)\eta^2\right)P_3^1\right]\right\} + \mathcal{O}(\lambda^{7/2}, \Omega^5),\end{aligned} \tag{C.8}$$

$$\begin{aligned}\gamma^-_{rr} = 1 &+ \lambda\left(3 - \eta^2 - \eta^2\Omega^2 P_2\right)\\ &+ \lambda^2\left\{\frac{23}{2} + \frac{3n}{4} + \left(-\frac{23}{5} - \frac{n}{2}\right)\eta^2 + \left(\frac{17}{70} + \frac{3n}{20}\right)\eta^4\right.\\ &+ \Omega^2\left[\frac{5}{3} - \frac{n}{2} + \left(-\frac{14}{15} + \frac{n}{3}\right)\eta^2 + \left(\frac{9}{35} - \frac{n}{10}\right)\eta^4\right.\\ &\left.\left. + \eta^2\left(-\frac{17}{5} - \frac{3n}{14} + \left(\frac{1}{21} + \frac{5n}{14}\right)\eta^2\right)P_2\right]\right\} + \mathcal{O}(\lambda^3, \Omega^4),\end{aligned} \tag{C.9}$$

$$\begin{aligned}\gamma^-_{\theta\theta} = 1 &+ \lambda\left(3 - \eta^2 - \eta^2\Omega^2 P_2\right)\\ &+ \lambda^2\left\{\frac{23}{2} + \frac{3n}{4} + \left(-\frac{26}{5} - \frac{n}{2}\right)\eta^2 + \left(\frac{37}{70} + \frac{3n}{20}\right)\eta^4\right.\\ &+ \Omega^2\left[\frac{5}{3} - \frac{n}{2} + \left(-\frac{32}{35} + \frac{n}{3}\right)\eta^2 + \left(\frac{157}{630} - \frac{n}{10}\right)\eta^4\right.\end{aligned}$$

$$+\eta^2\left(-\frac{437}{105}-\frac{3n}{14}+\left(\frac{97}{126}+\frac{5n}{14}\right)\eta^2\right)P_2\Bigg]\Bigg\}+\mathcal{O}(\lambda^3,\Omega^4), \tag{C.10}$$

$$\gamma^-_{r\theta}=\lambda^2\Omega^2\eta^2\left(\frac{4}{21}-\frac{\eta^2}{9}\right)P_2^1+\mathcal{O}(\lambda^3,\Omega^4), \tag{C.11}$$

$$\begin{aligned}\gamma^-_{\phi\phi}&=1+\lambda\left(3-\eta^2-\eta^2\Omega^2P_2\right)\\&\quad+\lambda^2\left\{\frac{23}{2}+\frac{3n}{4}-\left(\frac{26}{5}+\frac{n}{2}\right)\eta^2+\left(\frac{37}{70}+\frac{3n}{20}\right)\eta^4\right.\\&\quad+\Omega^2\left[\frac{5}{3}-\frac{n}{2}+\left(-\frac{16}{105}+\frac{n}{3}\right)\eta^2-\left(\frac{193}{630}+\frac{n}{10}\right)\eta^4\right.\\&\quad\left.\left.+\eta^2\left(-\frac{517}{105}-\frac{3n}{14}+\left(\frac{167}{126}+\frac{5n}{14}\right)\eta^2\right)P_2\right]\right\}+\mathcal{O}(\lambda^3,\Omega^4).\end{aligned} \tag{C.12}$$

Appendix D

Reminder on the Petrov classification

The Petrov classification allows us to classify the spacetimes in an algebraic way, working with the Weyl tensor in a point p of the manifold. The amount of symmetries and properties of the Weyl tensor is such that the apparently gruesome task of classifying a four dimensional matrix of 4 indices can be reduced to study the Jordan canonical form of a 3×3 matrix generally called the Q matrix. There are several ways of determining the Petrov type; in Chapter 3 we use the most algebraic one, though it is not easy to find a comprehensive review in the literature so here we make a summary of it following closely the text of Hall (2004).

We start considering a general class of tensors $\boldsymbol{W}$ possessing the following symmetries

$$\begin{aligned} W_{\alpha\beta\gamma\delta} &= -W_{\beta\alpha\gamma\delta} = -W_{\alpha\beta\delta\gamma}\,, \\ W_{\alpha\beta\gamma\delta} &= W_{\gamma\delta\alpha\beta} \end{aligned} \tag{D.1}$$

and

$$W_{\alpha\beta\gamma\delta} + W_{\alpha\gamma\delta\beta} + W_{\alpha\delta\beta\gamma} = 0\,. \tag{D.2}$$

They also imply $W_{\alpha[\beta\gamma\delta]} = 0$. If we define the left and right Hodge duals as

$${}^{\star}W_{\alpha\beta\gamma\delta} = \frac{1}{2}\epsilon_{\alpha\beta\epsilon\zeta}W^{\epsilon\zeta}{}_{\gamma\delta}\,, \qquad\qquad W^{\star}_{\alpha\beta\gamma\delta} = \frac{1}{2}W_{\alpha\beta}{}^{\epsilon\zeta}\epsilon_{\gamma\delta\epsilon\zeta} \tag{D.3}$$

we can see that this tensors satisfy the Ruse-Lanczos identity

$${}^{\star}W^{\star}_{\alpha\beta\gamma\delta} + W_{\alpha\beta\gamma\delta} = 2g_{\alpha[\gamma}\tilde{W}_{\delta]\beta} + 2g_{\beta[\delta}\tilde{W}_{\gamma]\alpha} \tag{D.4}$$

where $W_{\alpha\beta} \equiv W^{\gamma}{}_{\alpha\gamma\beta}$, $\tilde{W}_{\alpha\beta} \equiv W_{\alpha\beta} - \frac{1}{4}Wg_{\alpha\beta}$, and $W \equiv W^{\alpha}{}_{\alpha}$. This identity implies ${}^{\star}W^{\star}_{\alpha[\beta\gamma\delta]} = 0$ and also, noting that (D.3) implies

$${}^{\star\star}W_{\alpha\beta\gamma\delta} = -W_{\alpha\beta\gamma\delta}\,, \quad \text{and} \quad W^{\star\star}_{\alpha\beta\gamma\delta} = -W_{\alpha\beta\gamma\delta}\,, \tag{D.5}$$

a contraction of (D.4) with the inverse metric gives the equivalent relations

$${}^{\star}W^{\star}_{\alpha\beta\gamma\delta} = -W_{\alpha\beta\gamma\delta}\,, \tag{D.6}$$

$$ {}^\star W_{\alpha\beta\gamma\delta} = W^\star_{\alpha\beta\gamma\delta}\,, \tag{D.7} $$

$$ \tilde{W}_{\alpha\beta} = 0\,. \tag{D.8} $$

Ending this collection of properties of $\boldsymbol{W}$, it is also worth noticing that the two in (D.1) are enough to give the equivalent relations

$$ W_{\alpha[\beta\gamma\delta]} = 0\,, \quad W^{\star\alpha}{}_{\beta\alpha\delta} = 0\,. \tag{D.9} $$

The Riemann tensor is naturally among the tensors with the symmetries described in (D.1). They are shared by the Weyl tensor, too, as it can be checked from its definition

$$ C^\alpha{}_{\beta\gamma\delta} = R^\alpha{}_{\beta\gamma\delta} - \frac{1}{n-2}\left(R^\alpha{}_\gamma g_{\beta\delta} + R_{\beta\delta}\delta^\alpha_\delta - R_{\beta\gamma}\delta^\alpha_\delta - R^\alpha{}_\delta g_{\beta\gamma}\right) - \frac{R}{(n-1)(n-2)}\left(g_{\beta\gamma}\delta^\alpha_\delta - g_{\beta\delta}\delta^\alpha_\gamma\right) \tag{D.10} $$

that is, the tracefree part of the $R^\alpha{}_{\beta\gamma\delta}$. This means $C^\alpha{}_{\beta\alpha\delta} \equiv C_{\beta\delta} = 0$, and then (D.4) reduces to

$$ {}^\star C^\star_{\alpha\beta\gamma\delta} = -C_{\alpha\beta\gamma\delta} \quad \text{and} \quad {}^\star C_{\alpha\beta\gamma\delta} = C^\star_{\alpha\beta\gamma\delta} \tag{D.11} $$

Using the second relation in (D.1) and the definition of Hodge duals, we can see that ${}^\star C_{\alpha\beta\gamma\delta} = {}^\star C_{\gamma\delta\alpha\beta}$, so $\boldsymbol{C}^\star$ satisfies (D.1) and then also, from (D.9),

$$ C^\star_{\alpha[\beta\gamma\delta]} = 0\,, \quad \text{and} \quad C^{\star\alpha}{}_{\beta\alpha\delta} = 0\,. \tag{D.12} $$

This means that that ${}^\star C$ and $C^\star$ share the $\boldsymbol{W}$ symmetries. From this, we can build another tensor

$$ \overset{+}{C}_{\alpha\beta\gamma\delta} = C_{\alpha\beta\gamma\delta} + \mathrm{i}\,{}^\star C_{\alpha\beta\gamma\delta} \tag{D.13} $$

that also belongs to the $\boldsymbol{W}$ class besides $\overset{+}{C}{}^\alpha{}_{\beta\alpha\delta} = 0$. Its Hodge left dual is ${}^\star\overset{+}{\boldsymbol{C}} = -\mathrm{i}\,\overset{+}{\boldsymbol{C}}$, which is the definition of the self-duality property (defining the complex conjugated of this relation the *anti*-self duality), and thus $\overset{+}{\boldsymbol{C}}$ is called the complex self-dual Weyl tensor. It will be key in the final steps of the classification.

Before that, we can make an important simplification if we use the antisymmetry of $\boldsymbol{W}$ under interchange of indices inside the first and second pair (first property in [D.1]). We can work in an antisymmetrized base for each pair of indices, grouping

$$ \begin{aligned} dx^\alpha dx^\beta dx^\gamma dx^\delta - dx^\beta dx^\alpha dx^\gamma dx^\delta &\longrightarrow dx^\alpha \wedge dx^\beta dx^\gamma dx^\delta \\ dx^\alpha dx^\beta dx^\gamma dx^\delta - dx^\alpha dx^\beta dx^\delta dx^\gamma &\longrightarrow dx^\alpha dx^\beta dx^\delta \wedge dx^\gamma \end{aligned} \tag{D.14} $$

and defining the 2-form cobasis

$$\begin{aligned} \boldsymbol{\omega}^1 &\equiv dx^2 \wedge dx^3\,, \quad \boldsymbol{\omega}^4 \equiv dx^1 \wedge dx^0\,, \\ \boldsymbol{\omega}^2 &\equiv dx^3 \wedge dx^1\,, \quad \boldsymbol{\omega}^5 \equiv dx^2 \wedge dx^0\,, \\ \boldsymbol{\omega}^3 &\equiv dx^1 \wedge dx^2\,, \quad \boldsymbol{\omega}^6 \equiv dx^3 \wedge dx^0\,, \end{aligned} \tag{D.15}$$

we can write $\boldsymbol{W}$ as W_{AB}, where A and B are called p-form indices. For obvious reasons, this is called 6×6 *notation*. One can also get a sense of where all this is going noticing that $W_{AB} = W_{BA}$, but first we need to introduce some notions.

A complex 2-form is a complex second order antisymmetric covariant tensor whose real and imaginary parts are real 2-forms. We will call the set of complex 2-forms at a point p of the manifold $C\Omega(p)$. It is a six dimensional vector space and can be split in two subspaces defined by, for a complex 2-form $\boldsymbol{H}$

$$\begin{aligned} \boldsymbol{H} \in S^+(p) &\Leftrightarrow {}^\star\boldsymbol{H} = -\mathrm{i}\,\boldsymbol{H} \\ \boldsymbol{H} \in S^-(p) &\Leftrightarrow {}^\star\boldsymbol{H} = \mathrm{i}\,\boldsymbol{H}\,. \end{aligned} \tag{D.16}$$

Those 2-forms in $S^+(p)$ are called *self-dual* and those in $S^-(p)$ *anti self-dual*. We can see simply writing out

$$\boldsymbol{H} = \frac{1}{2}\left(\boldsymbol{H} + \mathrm{i}\,{}^\star\boldsymbol{H}\right) + \frac{1}{2}\left(\boldsymbol{H} - \mathrm{i}\,{}^\star\boldsymbol{H}\right) \tag{D.17}$$

that $S^+(p)$ and $S^-(p)$ span the whole $C\Omega(p)$ and

$$C\Omega(p) = S^+(p) \oplus S^-(p)\,. \tag{D.18}$$

Also, if we write $\boldsymbol{H}$ as $\boldsymbol{H} = \boldsymbol{A} + \mathrm{i}\,\boldsymbol{B}$, with $\boldsymbol{A}$ and $\boldsymbol{B}$ real 2-forms, conditions (D.16) lead to $\boldsymbol{B} = {}^\star\boldsymbol{A}$ if $\boldsymbol{H} \in S^+(p)$ and $\boldsymbol{B} = -{}^\star\boldsymbol{A}$ in the case $\boldsymbol{H} \in S^-(p)$. This means also that any complex 2-form has a uniquely associated real 2-form.

We can go on with the classification now. We have seen that we can write a tensor belonging to the $\boldsymbol{W}$ class as the symmetric W_{AB} using 2-form indices. The next step is to state that $F_{\alpha\beta}$ is an eigen-2-form of $\boldsymbol{W}$ if

$$W_{\alpha\beta\gamma\delta}F^{\gamma\delta} = \lambda F_{\alpha\beta}\,, \qquad \lambda \in \mathbb{C}\,,\ F_{\alpha\beta} \in C\Omega(p) \tag{D.19}$$

and λ is the associated eigenvalue. Working in the 2-form cobasis we have $C_{AB}F^B = \lambda F_A$ and we can face the algebraic classification of $\boldsymbol{C}$ on the point p. We have allowed F_A to belong to the set of complex 2-forms $C\Omega(p)$ because although $\boldsymbol{C}$ and its eigen-2-forms are all real, if one regards it as a $\mathbb{C}^6 \longrightarrow \mathbb{C}^6$ map and notices that

$${}^\star(\boldsymbol{C}\boldsymbol{H}) = {}^\star\boldsymbol{C}\boldsymbol{H} = (\boldsymbol{C}{}^\star\boldsymbol{H}) = \boldsymbol{C}({}^\star\boldsymbol{H}) \tag{D.20}$$

(what comes from the $\star$ definition and the property [D.12]) then $\boldsymbol{C}$ maps $S^+(p) \longrightarrow S^+(p)$ and $S^-(p) \longrightarrow S^-(p)$. Then, considering (D.18), $\boldsymbol{C}$ is fully described by its restrictions

$$\begin{aligned} &\boldsymbol{C}_1 : S^+(p) \longrightarrow S^+(p) \qquad \text{and} \\ &\boldsymbol{C}_2 : S^-(p) \longrightarrow S^-(p)\,. \end{aligned} \tag{D.21}$$

Furthermore, $S^+(p)$ and $S^-(p)$ are isomorphic under conjugation operation k, so $\boldsymbol{C}_2 = k \circ \boldsymbol{C}_1 \circ k^{-1}$ and their Jordan form is the same modulo conjugation. If we work now a little with the self-dual Weyl tensor $\overset{+}{\boldsymbol{C}}$, we see

$$\begin{aligned} &\boldsymbol{H} \in S^+(p) \Rightarrow \overset{+}{\boldsymbol{C}}\boldsymbol{H} = (\boldsymbol{C} + \mathrm{i}\,\boldsymbol{C}^\star)\,\boldsymbol{H} = \boldsymbol{C}\boldsymbol{H} + \mathrm{i}\,\boldsymbol{C}\,(^\star\boldsymbol{H}) = 2\boldsymbol{C}\boldsymbol{H} \in S^+(p)\,, \\ &\boldsymbol{H} \in S^-(p) \Rightarrow \overset{+}{\boldsymbol{C}}\boldsymbol{H} = (\boldsymbol{C} + \mathrm{i}\,\boldsymbol{C}^\star)\,\boldsymbol{H} = \boldsymbol{C}\boldsymbol{H} + \mathrm{i}\,\boldsymbol{C}\,(^\star\boldsymbol{H}) = 0\,. \end{aligned} \tag{D.22}$$

Then the restriction of $\overset{+}{\boldsymbol{C}}$ to $S^-(p)$ is represented by the zero 3×3 matrix and it is enough to know the Jordan form of $\overset{+}{\boldsymbol{C}}$ on its restriction to $S^+(p)$, $\overset{+}{\boldsymbol{C}}_1$, to classify it. Additionally, $\overset{+}{\boldsymbol{C}}_1$ is just $2\boldsymbol{C}_1$ and hence *the problem of the classification of the Weyl tensor is reduced to computing the Jordan canonical form of the* 3×3 *matrix* $\overset{+}{\boldsymbol{C}}_1(p)$.

Again, the symmetries of the problem will allow extra simplification. Now we will show that it will not be necessary to compute the restriction $\overset{+}{\boldsymbol{C}}_1(p)$. Writing C_{AB} as the 6×6 matrix

$$C_{AB} = \begin{pmatrix} \boldsymbol{M} & \boldsymbol{N}^T \\ \boldsymbol{N} & \boldsymbol{P} \end{pmatrix} \tag{D.23}$$

where $\boldsymbol{M}$, $\boldsymbol{N}$ and $\boldsymbol{P}$ are 3×3 matrices, $\boldsymbol{M}$ and $\boldsymbol{P}$ symmetric. The first Bianchi identity (D.2) tells us that N is tracefree and, *introducing an orthonormal frame* to compute $C^{\alpha}{}_{\beta\alpha\delta} = g^{\alpha\gamma}C_{\gamma\beta\alpha\delta} = 0$, we can also get that $\boldsymbol{N} = \boldsymbol{N}^T$, $\boldsymbol{P} = -\boldsymbol{M}$ and $\mathrm{tr}\boldsymbol{M} = 0$. Transforming $\epsilon_{\alpha\beta\gamma\delta}$ and $G_{\alpha\beta\gamma\delta} = g_{\alpha[\beta}g_{\gamma]\delta}$—that rises and lowers indices of 2-forms—to 6×6 notation, we get

$$\epsilon_{AB} = \begin{pmatrix} 0 & \boldsymbol{I}_3 \\ \boldsymbol{I}_3 & 0 \end{pmatrix} \qquad \text{and} \qquad G_{AB} = \frac{1}{2}\begin{pmatrix} \boldsymbol{I}_3 & 0 \\ 0 & -\boldsymbol{I}_3 \end{pmatrix}. \tag{D.24}$$

With this, for a 2-form $F_A = (F_1, F_2, F_3, F_4, F_5, F_6)$ its dual is

$$^\star F_A = 2\epsilon_{AB}G^{BC}F_C \tag{D.25}$$

what means $^\star F_A = (-F_4, -F_5, -F_6, F_1, F_2, F_3)$. Grouping each triple into $\boldsymbol{R}, \boldsymbol{S} \in \mathbb{C}^3$ so that $F_A = (\boldsymbol{R}, \boldsymbol{S})$, then $^\star F_A = (-\boldsymbol{S}, \boldsymbol{R})$ and we see that $\boldsymbol{F} \in S^+(p) \Leftrightarrow F_A = (\boldsymbol{R}, i\boldsymbol{R})$ and $\boldsymbol{F} \in S^-(p) \Leftrightarrow F_A = (\boldsymbol{R}, -i\boldsymbol{R})$. With the results for $\boldsymbol{C}$ in mind, the dual Weyl tensor is

$$\overset{+}{C}_{AB} = C_{AB} + \mathrm{i}\,{}^\star C_{AB} = C_{AB} + 2i\epsilon_{AC}G^{CD}C_{BD} \tag{D.26}$$

$$= \begin{pmatrix} \boldsymbol{M} - i\boldsymbol{N} & \boldsymbol{N} + i\boldsymbol{M} \\ \boldsymbol{N} + i\boldsymbol{M} & -\boldsymbol{M} + i\boldsymbol{N} \end{pmatrix} \equiv \begin{pmatrix} \boldsymbol{Q} & i\boldsymbol{Q} \\ i\boldsymbol{Q} & -\boldsymbol{Q} \end{pmatrix} \tag{D.27}$$

and then

$$\begin{aligned} \overset{+}{C}_{AB} F^A = \overset{+}{C}_{AB} G^{AC} F_C &= \begin{pmatrix} \boldsymbol{Q} & i\boldsymbol{Q} \\ i\boldsymbol{Q} & -\boldsymbol{Q} \end{pmatrix} \begin{pmatrix} \boldsymbol{I}_3 & 0 \\ 0 & -\boldsymbol{I}_3 \end{pmatrix} \begin{pmatrix} \boldsymbol{R} \\ \boldsymbol{S} \end{pmatrix} \\ &= \begin{pmatrix} \boldsymbol{Q}(\boldsymbol{R} - i\boldsymbol{S}) \\ \boldsymbol{Q}(i\boldsymbol{R} + \boldsymbol{S}) \end{pmatrix} \equiv \begin{pmatrix} \boldsymbol{D} \\ i\boldsymbol{D} \end{pmatrix}. \end{aligned} \tag{D.28}$$

As we can see, $(\boldsymbol{D}, i\boldsymbol{D}) \in S^+(p)$ reinforcing what we already knew and the fact that any eigen-2-form of $\overset{+}{\boldsymbol{C}}$ with non-zero eigenvalue is self-dual. Furthermore, for any of its self-dual eigen-2-forms $F_A = (\boldsymbol{R}, i\boldsymbol{R})$,

$$\overset{+}{C}_{AB} F^B = \varepsilon F_A \Leftrightarrow Q^A_{\ B} R^B = \frac{\varepsilon}{2} R^B \tag{D.29}$$

and the problem is then reduced to determine the canonical form of the complex symmetric tracefree matrix $\boldsymbol{Q}$.

Now, the possible Segre types of the matrix $\boldsymbol{Q}$ at a point p are

1. {111} with three different eigenvalues ε_i satisfying $\varepsilon_1 + \varepsilon_2 + \varepsilon_3 = 0$. This is the so-called Petrov type I.

2. {(11)1}, two degenerate eigenvalues ε_1 with unidimensional invariant subspaces –the associated elementary divisor is simple– and ε_2 satisfying $2\varepsilon_1 + \varepsilon_2 = 0 \longrightarrow \varepsilon_2 = -2\varepsilon_1$. This is Petrov type D (for "degenerate I").

3. {(111)} implies the three eigenvalues are degenerate so $\varepsilon = 0$, and the elementary divisor is simple. This means $\boldsymbol{Q} = 0$ and the Petrov type is O.

4. {(2)1}, two different eigenvalues with the degenerate one ε_1 associated with a two dimensional invariant subspace and again, $\varepsilon_2 = -2\varepsilon_1$. This is Petrov type II.

5. {(21)} means only one eigenvalue, so $\varepsilon = 0$, but keeping a unidimensional invariant subspace. This is Petrov type N (for "null II")

6. {3} with a only a three-dimensional invariant subspace and $\varepsilon = 0$. This is Petrov type III.

Appendix E

Q matrix components

The result for the contraction $\overset{+}{C}_{\alpha\beta\gamma\mu}v^\beta v^\mu = -Q_{\alpha\gamma}$ is

$$Q_{\alpha\gamma} = (v^0)^2 \begin{pmatrix} 0 & 0 & 0 & 0 \\ 0 & C_{0101} + i\sqrt{-g}C_{01}{}^{23} & C_{0102} + i\sqrt{-g}C_{02}{}^{23} & C_{0103} + i\sqrt{-g}C_{03}{}^{23} \\ 0 & C_{0201} - i\sqrt{-g}C_{01}{}^{13} & C_{0202} - i\sqrt{-g}C_{02}{}^{13} & C_{0203} - i\sqrt{-g}C_{03}{}^{13} \\ 0 & C_{0301} + i\sqrt{-g}C_{01}{}^{12} & C_{0302} + i\sqrt{-g}C_{02}{}^{12} & C_{0303} + i\sqrt{-g}C_{03}{}^{12} \end{pmatrix} \tag{E.1}$$

that leads, using a timelike unit vector v to the components of the Q^i_j matrix up to $\mathcal{O}\left(\lambda^{5/2}, \Omega^3\right)$

$$\begin{aligned} Q^r{}_r r_s^2 = {} & \lambda\Omega^2 m_2 P_2 + \lambda^2 \left\{ \left(-\frac{2}{5} + \frac{2n}{5} \right) \eta^2 \right. \\ & \left. + \Omega^2 \left[\left(-\frac{14}{15} - \frac{4n}{15} \right) \eta^2 + \left(-2b_2 - a_0 m_2 + \eta^2 \left(\frac{52}{21} + \frac{11n}{21} + \frac{13m_2}{7} - \frac{11nm_2}{14} \right) \right) P_2 \right] \right\} \\ & + \mathrm{i}\,\lambda^{3/2} \left(-\frac{12}{5}\eta\Omega P_1 + 12\eta\Omega^3 j_3 P_3 \right) \\ & + \mathrm{i}\,\lambda^{5/2} \left(\Omega \left[\left(-\frac{12}{7} + \frac{6n}{7} \right) \eta^3 + \eta \left(\frac{12nS}{5} - \frac{6a_0}{5} + \frac{12j_1}{5} - \frac{12m_0}{5} - \frac{6nm_0}{5} \right) \right] P_1 \right. \\ & + \Omega^3 \left\{ \left[\eta^3 \left(-\frac{48}{35} - \frac{24n}{35} + \frac{27a_2}{5} + \frac{516m_2}{175} + \frac{6nm_2}{35} \right) + \eta \left(\frac{6b_2}{25} - \frac{6j_1 m_2}{5} \right) \right] P_1 \right. \\ & + \left[\eta^3 \left(\frac{32}{15} + \frac{16n}{15} - 9a_2 + \frac{80j_3}{3} - \frac{88m_2}{25} - \frac{8nm_2}{5} \right) \right. \\ & \left. \left. \left. + \eta \left(-\frac{18b_2}{5} - 12a_2 j_1 - 18a_0 j_3 - 12j_3 m_0 - \frac{6j_1 m_2}{5} \right) \right] P_3 \right\} \right), \end{aligned} \tag{E.2}$$

$$\begin{aligned} Q^r{}_\theta r_s = {} & \frac{1}{2}\eta\lambda\Omega^2 m_2 P_2^1 + \lambda^2\Omega^2 \left\{ \eta^3 \left[\frac{9}{7} + \frac{3n}{14} + \left(\frac{5}{7} - \frac{9n}{28} \right) m_2 \right] + \eta \left[-b_2 - \frac{a_0 m_2}{2} \right] \right\} P_2^1 \\ & + \mathrm{i}\,\lambda^{3/2} \left(-\frac{9}{5}\eta^2\Omega P_1^1 + 4\eta^2\Omega^3 j_3 P_3^1 \right) \end{aligned}$$

$$
\begin{aligned}
&+\mathrm{i}\,\lambda^{5/2}\left(\Omega\left\{\left(-\frac{33}{35}+\frac{15n}{14}\right)\eta^4+\eta^2\left[\frac{9nS}{5}-\frac{9a_0}{10}+\frac{9j_1}{5}+\left(-\frac{9}{5}-\frac{9n}{10}\right)m_0\right]\right\}P_1^1\right.\\
&+\Omega^3\left\{\left[\eta^4\left(-\frac{12}{7}-\frac{6n}{7}-\frac{27a_2}{10}+\left(\frac{246}{175}+\frac{3n}{14}\right)m_2\right)+\eta^2\left(\frac{72b_2}{25}-\frac{9j_1m_2}{10}\right)\right]P_1^1\right.\\
&+\left[\eta^4\left(\frac{2}{3}+\frac{n}{3}-\frac{27a_2}{10}+\frac{22j_3}{3}+\left(-\frac{23}{25}-\frac{n}{2}\right)m_2\right)\right.\\
&\left.\left.\left.+\eta^2\left(-\frac{6b_2}{5}-4a_2j_1-6a_0j_3-4j_3m_0-\frac{2j_1m_2}{5}\right)\right]P_3^1\right\}\right),
\end{aligned}
\tag{E.3}
$$

$$
\begin{aligned}
Q^{\theta}_{r}r_s^3 &= \frac{\lambda\Omega^2m_2P_2^1}{2\eta}+\lambda^2\Omega^2\left\{\eta\left[\frac{9}{7}+\frac{3n}{14}+\left(\frac{5}{7}-\frac{9n}{28}\right)m_2\right]+\frac{-b_2-\frac{a_0m_2}{2}}{\eta}\right\}P_2^1\\
&+\mathrm{i}\,\lambda^{3/2}\left(-\frac{9}{5}\Omega P_1^1+4\Omega^3j_3P_3^1\right)\\
&+\mathrm{i}\,\lambda^{5/2}\left(\Omega\left\{\left(-\frac{33}{35}+\frac{15n}{14}\right)\eta^2+\left[\frac{9nS}{5}-\frac{9a_0}{10}+\frac{9j_1}{5}+\left(-\frac{9}{5}-\frac{9n}{10}\right)m_0\right]\right\}P_1^1\right.\\
&+\Omega^3\left\{\left[\eta^2\left(-\frac{12}{7}-\frac{6n}{7}-\frac{27a_2}{10}+\left(\frac{246}{175}+\frac{3n}{14}\right)m_2\right)+\left(-\frac{63b_2}{25}-\frac{9j_1m_2}{10}\right)\right]P_1^1\right.\\
&+\left[\eta^2\left(\frac{2}{3}+\frac{n}{3}-\frac{27a_2}{10}+\frac{22j_3}{3}+\left(-\frac{23}{25}-\frac{n}{2}\right)m_2\right)\right.\\
&\left.\left.\left.+\left(-\frac{6b_2}{5}-4a_2j_1-6a_0j_3-4j_3m_0-\frac{2j_1m_2}{5}\right)\right]P_3^1\right\}\right),
\end{aligned}
\tag{E.4}
$$

$$
\begin{aligned}
Q^{\theta}_{\theta}r_s^2 &= \lambda\Omega^2\left(\frac{m_2}{2}-m_2P_2\right)\\
&+\lambda^2\left(\left(\frac{1}{5}-\frac{n}{5}\right)\eta^2+\Omega^2\left\{-b_2-\frac{a_0m_2}{2}+\eta^2\left(\frac{199}{105}+\frac{43n}{210}+\left(\frac{1}{14}-\frac{3n}{28}\right)m_2\right)\right.\right.\\
&\left.\left.+\left[2b_2+a_0m_2+\eta^2\left(-\frac{8}{3}-\frac{n}{3}+\left(-1+\frac{n}{2}\right)m_2\right)\right]P_2\right\}\right)\\
&+\mathrm{i}\,\lambda^{3/2}\left[\frac{6}{5}\eta\Omega P_1+\Omega^3\left(6\eta j_3P_1-12\eta j_3P_3\right)\right]\\
&+\mathrm{i}\,\lambda^{5/2}\left(\Omega\left\{\left(\frac{6}{7}-\frac{3n}{7}\right)\eta^3+\eta\left[-\frac{6nS}{5}+\frac{3a_0}{5}-\frac{6j_1}{5}+\left(\frac{6}{5}+\frac{3n}{5}\right)m_0\right]\right\}P_1\right.\\
&+\Omega^3\left\{\left[\eta\left(-\frac{48b_2}{25}-6a_2j_1-9a_0j_3-6j_3m_0\right)\right.\right.\\
&\left.\left.\left.+\eta^3\left(\frac{52}{35}+\frac{26n}{35}-\frac{27a_2}{5}+4j_3+\left(-\frac{12}{7}-\frac{24n}{35}\right)m_2\right)\right]P_1\right.
\end{aligned}
$$

$$+\left[\eta^3\left(-\frac{28}{15}-\frac{14n}{15}+\frac{36a_2}{5}-\frac{52j_3}{3}+\left(2+\frac{7n}{5}\right)m_2\right)\right.$$
$$\left.\left.+\eta\left(\frac{18b_2}{5}+12a_2j_1+18a_0j_3+12j_3m_0+\frac{6j_1m_2}{5}\right)\right]P_3\right\}\Bigg), \tag{E.5}$$

$$\begin{aligned}
Q^{\phi}_{\phi}r_s^2 = &-\frac{1}{2}\lambda\Omega^2m_2+\mathrm{i}\,\lambda^{3/2}\left(\frac{6}{5}\eta\Omega P_1-6\eta\Omega^3j_3P_1\right)\\
&+\lambda^2\left\{\left(\frac{1}{5}-\frac{n}{5}\right)\eta^2+\Omega^2\left[b_2+\frac{a_0m_2}{2}+\eta^2\left(-\frac{101}{105}+\frac{13n}{210}+\left(-\frac{1}{14}+\frac{3n}{28}\right)m_2\right)\right.\right.\\
&\left.\left.+\eta^2\left(\frac{4}{21}-\frac{4n}{21}+\left(-\frac{6}{7}+\frac{2n}{7}\right)m_2\right)P_2\right]\right\}\\
&+\mathrm{i}\,\lambda^{5/2}\left(\Omega\left\{\left(\frac{6}{7}-\frac{3n}{7}\right)\eta^3+\eta\left[-\frac{6nS}{5}+\frac{3a_0}{5}-\frac{6j_1}{5}+\left(\frac{6}{5}+\frac{3n}{5}\right)m_0\right]\right\}P_1\right.\\
&+\Omega^3\left\{\left[\eta^3\left(-\frac{4}{35}-\frac{2n}{35}-4j_3+\left(-\frac{216}{175}+\frac{18n}{35}\right)m_2\right)\right.\right.\\
&\left.+\eta\left(\frac{42b_2}{25}+6a_2j_1+9a_0j_3+6j_3m_0+\frac{6j_1m_2}{5}\right)\right]P_1\\
&\left.\left.+\eta^3\left[-\frac{4}{15}-\frac{2n}{15}+\frac{9a_2}{5}-\frac{28j_3}{3}+\left(\frac{38}{25}+\frac{n}{5}\right)m_2\right]P_3\right\}\right).
\end{aligned} \tag{E.6}$$

Appendix F

The $\mathcal{O}(\lambda^{9/2}, \Omega^3)$ CGMR metric

1. Metric components

1.1. Exterior

The unmatched metric components of the CGMR exterior metric, in the orthonormal spherical-like cobasis, are

$$
\begin{aligned}
\gamma^{+}_{\hat{t}\hat{t}} = &-1 + \lambda\left(2\frac{1}{\eta}M_0 + 2\frac{1}{\eta^3}\Omega^2 M_2 P_2\right)\\
&+ \lambda^2\left\{-\frac{1}{\eta^4}A_0 M_0 - 2\frac{1}{\eta^2}M_0^2 + \Omega^2\left[\frac{1}{\eta^4}M_0\left(2B_2 - 4M_2\right) + \frac{1}{\eta^6}\left(-3A_2 M_0 - 3A_0 M_2\right)\right]P_2\right\}\\
&+ \lambda^3\left\{\frac{3}{2}\frac{1}{\eta^7}A_0^2 M_0 + 2\frac{1}{\eta^5}A_0 M_0^2 + 2\frac{1}{\eta^3}M_0^3 + \Omega^2\left[\frac{2}{3}\frac{1}{\eta^4}J_1^2 + \left(\frac{4}{3}\frac{1}{\eta^4}J_1^2 + \frac{1}{\eta^5}M_0^2\left(-4B_2 + \frac{44M_2}{7}\right)\right.\right.\right.\\
&\left.\left.\left. + \frac{1}{\eta^9}\left(12A_0 A_2 M_0 + 6A_0^2 M_2\right) + \frac{1}{\eta^7}\left(6A_2 M_0^2 + M_0\left(-6A_0 B_2 + 8A_0 M_2\right)\right)\right)P_2\right]\right\}\\
&+ \lambda^4\left\{-3\frac{1}{\eta^{10}}A_0^3 M_0 - \frac{7}{2}\frac{1}{\eta^8}A_0^2 M_0^2 - \frac{18}{5}\frac{1}{\eta^6}A_0 M_0^3 - \frac{8}{3}\frac{1}{\eta^4}M_0^4 + \Omega^2\left[-\frac{4}{3}\frac{1}{\eta^7}A_0 J_1^2 - 2\frac{1}{\eta^5}J_1^2 M_0\right.\right.\\
&+ \left(-\frac{8}{3}\frac{1}{\eta^7}A_0 J_1^2 - \frac{26}{7}\frac{1}{\eta^5}J_1^2 M_0 + \frac{1}{\eta^6}M_0^3\left(\frac{222B_2}{35} - \frac{58M_2}{5}\right) + \frac{1}{\eta^{12}}\left(-\frac{165}{4}A_0^2 A_2 M_0 - \frac{55}{4}A_0^3 M_2\right)\right.\\
&+ \frac{1}{\eta^8}\left(-\frac{37}{3}A_2 M_0^3 + M_0^2\left(14A_0 B_2 - \frac{1889A_0 M_2}{105}\right)\right) + \frac{1}{\eta^{10}}\left(-27A_0 A_2 M_0^2\right.\\
&\left.\left.\left.\left. + M_0\left(18A_0^2 B_2 - 18A_0^2 M_2\right)\right)\right)P_2\right]\right\} + \mathcal{O}(\lambda^5\Omega^4)
\end{aligned}
\tag{F.1}
$$

$$
\begin{aligned}
\gamma^{+}_{\hat{t}\hat{\phi}} = &\lambda^{3/2}\left(2\frac{1}{\eta^2}\Omega J_1 P_{11} + 2\frac{1}{\eta^4}\Omega^3 J_3 P_{31}\right) + \lambda^{5/2}\left\{\Omega\left(-\frac{1}{\eta^5}A_0 J_1 - 2\frac{1}{\eta^3}J_1 M_0\right)P_{11}\right.\\
&\left.+ \Omega^3\left[\left(\frac{9}{5}\frac{1}{\eta^7}A_2 J_1 + \frac{4}{5}\frac{1}{\eta^5}B_2 J_1\right)P_{11} + \left(\frac{1}{\eta^7}\left(\frac{A_2 J_1}{5} - 3A_0 J_3\right) + \frac{1}{\eta^5}\left(\frac{6B_2 J_1}{5} - J_3 M_0 - J_1 M_2\right)\right)P_{31}\right]\right\}\\
&+ \lambda^{7/2}\left\{\Omega\left(\frac{3}{2}\frac{1}{\eta^8}A_0^2 J_1 + 2\frac{1}{\eta^6}A_0 J_1 M_0 + 2\frac{1}{\eta^4}J_1 M_0^2\right)P_{11}\right.\\
&\left.+ \Omega^3\left[\left(-\frac{27}{5}\frac{1}{\eta^{10}}A_0 A_2 J_1 + \frac{1}{\eta^8}\left(-\frac{3}{5}A_0 B_2 J_1 - \frac{12}{5}A_2 J_1 M_0\right) + \frac{1}{\eta^6}M_0\left(-\frac{2}{5}B_2 J_1 - \frac{24J_1 M_2}{35}\right)\right)P_{11}\right.\right.
\end{aligned}
$$

$$
\begin{aligned}
&+\left(\frac{1}{\eta^{10}}\left(\frac{2}{5}A_0A_2J_1+6A_0^2J_3\right)+\frac{1}{\eta^8}\left(-\frac{12}{5}A_0B_2J_1+\left(\frac{2A_2J_1}{5}+2A_0J_3\right)M_0+2A_0J_1M_2\right)\right.\\
&\left.+\frac{1}{\eta^6}\left(2J_3M_0^2+M_0\left(-\frac{8}{5}B_2J_1+\frac{16J_1M_2}{15}\right)\right)\right)P_{31}\Bigg]\Bigg\}\\
&+\lambda^{9/2}\left\{\Omega\left(-3\frac{1}{\eta^{11}}A_0^3J_1-\frac{7}{2}\frac{1}{\eta^9}A_0^2J_1M_0-\frac{18}{5}\frac{1}{\eta^7}A_0J_1M_0^2-\frac{8}{3}\frac{1}{\eta^5}J_1M_0^3\right)P_{11}\right.\\
&+\Omega^3\left[\left(\frac{63}{4}\frac{1}{\eta^{13}}A_0^2A_2J_1-\frac{38}{35}\frac{1}{\eta^6}J_1^3+9\frac{1}{\eta^{11}}A_0A_2J_1M_0+\frac{1}{\eta^7}M_0^2\left(\frac{174B_2J_1}{175}+\frac{248J_1M_2}{175}\right)\right.\right.\\
&\left.+\frac{1}{\eta^9}\left(5A_2J_1M_0^2+M_0\left(-\frac{2}{5}A_0B_2J_1+\frac{58}{35}A_0J_1M_2\right)\right)\right)P_{11}\\
&+\left(-\frac{8}{15}\frac{1}{\eta^6}J_1^3+\frac{1}{\eta^{13}}\left(-\frac{13}{4}A_0^2A_2J_1-\frac{55}{4}A_0^3J_3\right)+\frac{1}{\eta^{11}}\left(6A_0^2B_2J_1+\left(-3A_0A_2J_1-\frac{9}{2}A_0^2J_3\right)M_0\right.\right.\\
&\left.-\frac{9}{2}A_0^2J_1M_2\right)+\frac{1}{\eta^7}\left(-\frac{10}{3}J_3M_0^3+M_0^2\left(\frac{486B_2J_1}{175}-\frac{2902J_1M_2}{1575}\right)\right)\\
&\left.\left.+\frac{1}{\eta^9}\left(\left(-\frac{7}{9}A_2J_1-\frac{34A_0J_3}{5}\right)M_0^2+M_0\left(\frac{22}{5}A_0B_2J_1-\frac{902}{315}A_0J_1M_2\right)\right)\right)P_{31}\Bigg]\Bigg\}+\mathcal{O}(\lambda^{11/2},\Omega^5),
\end{aligned}
\tag{F.2}
$$

$$
\begin{aligned}
\gamma^+_{rr}=1&+\lambda\left(2\frac{1}{\eta}M_0+2\frac{1}{\eta^3}\Omega^2M_2P_2\right)+\lambda^2\left\{\frac{3}{2}\frac{1}{\eta^6}A_0^2-\frac{1}{\eta^4}A_0M_0+\frac{4}{3}\frac{1}{\eta^2}M_0^2\right.\\
&\left.+\Omega^2\left[\frac{87}{7}\frac{1}{\eta^8}A_0A_2+\frac{1}{\eta^4}M_0\left(2B_2+\frac{64M_2}{21}\right)+\frac{1}{\eta^6}\left(-\frac{144}{35}A_0B_2-3A_2M_0-\frac{93A_0M_2}{35}\right)\right]P_2\right\}\\
&+\lambda^3\left\{-\frac{11}{2}\frac{1}{\eta^9}A_0^3+\frac{9}{2}\frac{1}{\eta^7}A_0^2M_0-\frac{12}{5}\frac{1}{\eta^5}A_0M_0^2+\frac{2}{3}\frac{1}{\eta^3}M_0^3\right.\\
&+\Omega^2\left[-\frac{4}{9}\frac{1}{\eta^4}J_1^2+\left(-\frac{534}{7}\frac{1}{\eta^{11}}A_0^2A_2+\frac{1346}{315}\frac{1}{\eta^4}J_1^2+\frac{1}{\eta^5}M_0^2\left(\frac{148B_2}{35}+\frac{44M_2}{15}\right)\right.\right.\\
&+\frac{1}{\eta^9}\left(\frac{864}{35}A_0^2B_2+\frac{1272}{35}A_0A_2M_0+\frac{54}{7}A_0^2M_2\right)+\frac{1}{\eta^7}\left(-\frac{2642}{315}A_2M_0^2\right.\\
&\left.\left.\left.+M_0\left(-\frac{486}{35}A_0B_2-\frac{2096A_0M_2}{315}\right)\right)\right)P_2\right]\Bigg\}\\
&+\lambda^4\left\{\frac{75}{4}\frac{1}{\eta^{12}}A_0^4-\frac{31}{2}\frac{1}{\eta^{10}}A_0^3M_0+\frac{21}{2}\frac{1}{\eta^8}A_0^2M_0^2-\frac{26}{15}\frac{1}{\eta^6}A_0M_0^3+\Omega^2\left[\frac{40}{63}\frac{1}{\eta^7}A_0J_1^2\right.\right.\\
&+\frac{2}{9}\frac{1}{\eta^5}J_1^2M_0+\left(\frac{729}{2}\frac{1}{\eta^{14}}A_0^3A_2-\frac{1958}{315}\frac{1}{\eta^7}A_0J_1^2+\frac{122}{315}\frac{1}{\eta^5}J_1^2M_0+\frac{1}{\eta^6}M_0^3\left(\frac{274B_2}{105}+\frac{22M_2}{35}\right)\right.\\
&+\frac{1}{\eta^{12}}\left(-\frac{810}{7}A_0^3B_2-\frac{5811}{28}A_0^2A_2M_0-\frac{99}{4}A_0^3M_2\right)+\frac{1}{\eta^8}\left(-\frac{419}{63}A_2M_0^3+M_0^2\left(-\frac{1436}{49}A_0B_2\right.\right.\\
&\left.\left.\left.-\frac{3821A_0M_2}{441}\right)\right)+\frac{1}{\eta^{10}}\left(\frac{29269}{315}A_0A_2M_0^2+M_0\left(\frac{2544}{35}A_0^2B_2+\frac{50839A_0^2M_2}{2205}\right)\right)\right)P_2\Bigg]\Bigg\}+\mathcal{O}(\lambda^5,\Omega^4),
\end{aligned}
\tag{F.3}
$$

$$
\gamma^+_{\theta\theta}=1+\lambda\left(2\frac{1}{\eta}M_0+2\frac{1}{\eta^3}\Omega^2M_2P_2\right)+\lambda^2\left\{\frac{3}{2}\frac{1}{\eta^6}A_0^2-\frac{1}{\eta^4}A_0M_0+\frac{4}{3}\frac{1}{\eta^2}M_0^2\right.
$$

$$
\begin{aligned}
&+\Omega^2\left[\frac{3}{2}\frac{1}{\eta^8}A_0A_2+\frac{1}{\eta^6}\left(-\frac{6}{5}A_0B_2-\frac{2A_0M_2}{5}\right)\right.\\
&\left.+\left(\frac{45}{7}\frac{1}{\eta^8}A_0A_2+\frac{1}{\eta^4}M_0\left(2B_2+\frac{64M_2}{21}\right)+\frac{1}{\eta^6}\left(\frac{24A_0B_2}{35}-3A_2M_0-\frac{37A_0M_2}{35}\right)\right)P_2\right]\Bigg\}\\
&+\lambda^3\left\{-\frac{11}{2}\frac{1}{\eta^9}A_0^3+\frac{9}{2}\frac{1}{\eta^7}A_0^2M_0-\frac{12}{5}\frac{1}{\eta^5}A_0M_0^2+\frac{2}{3}\frac{1}{\eta^3}M_0^3\right.\\
&+\Omega^2\left[-12\frac{1}{\eta^{11}}A_0^2A_2-\frac{1}{45}\frac{1}{\eta^4}J_1^2+\frac{1}{\eta^5}M_0^2\left(\frac{2B_2}{5}+\frac{2M_2}{15}\right)\right.\\
&+\frac{1}{\eta^9}\left(\frac{57}{10}A_0^2B_2+\frac{18}{5}A_0A_2M_0+\frac{3}{2}A_0^2M_2\right)+\frac{1}{\eta^7}\left(-\frac{2}{5}A_2M_0^2+M_0\left(-\frac{14}{5}A_0B_2-\frac{22A_0M_2}{35}\right)\right)\\
&+\left(-\frac{198}{7}\frac{1}{\eta^{11}}A_0^2A_2+\frac{814}{315}\frac{1}{\eta^4}J_1^2+\frac{1}{\eta^5}M_0^2\left(\frac{92B_2}{35}+\frac{12M_2}{5}\right)+\frac{1}{\eta^9}\left(\frac{66}{35}A_0^2B_2+\frac{768}{35}A_0A_2M_0\right.\right.\\
&\left.\left.\left.+\frac{12}{7}A_0^2M_2\right)+\frac{1}{\eta^7}\left(-\frac{2138}{315}A_2M_0^2+M_0\left(-\frac{94}{35}A_0B_2-\frac{1304A_0M_2}{315}\right)\right)\right)P_2\right]\Bigg\}\\
&+\lambda^4\left\{\frac{75}{4}\frac{1}{\eta^{12}}A_0^4-\frac{31}{2}\frac{1}{\eta^{10}}A_0^3M_0+\frac{21}{2}\frac{1}{\eta^8}A_0^2M_0^2-\frac{26}{15}\frac{1}{\eta^6}A_0M_0^3\right.\\
&+\Omega^2\left[\frac{513}{8}\frac{1}{\eta^{14}}A_0^3A_2-\frac{44}{315}\frac{1}{\eta^7}A_0J_1^2+\frac{8}{45}\frac{1}{\eta^5}J_1^2M_0+\frac{1}{\eta^6}M_0^3\left(\frac{2B_2}{15}-\frac{8M_2}{105}\right)\right.\\
&+\frac{1}{\eta^8}M_0^2\left(-\frac{209}{35}A_0B_2-A_0M_2\right)+\frac{1}{\eta^{12}}\left(-\frac{51}{2}A_0^3B_2-\frac{117}{4}A_0^2A_2M_0-\frac{21}{4}A_0^3M_2\right)\\
&+\frac{1}{\eta^{10}}\left(\frac{113}{10}A_0A_2M_0^2+M_0\left(\frac{147}{10}A_0^2B_2+\frac{17}{5}A_0^2M_2\right)\right)+\left(108\frac{1}{\eta^{14}}A_0^3A_2-\frac{982}{315}\frac{1}{\eta^7}A_0J_1^2\right.\\
&+\frac{178}{315}\frac{1}{\eta^5}J_1^2M_0+\frac{1}{\eta^6}M_0^3\left(\frac{218B_2}{105}+\frac{14M_2}{15}\right)+\frac{1}{\eta^{12}}\left(-\frac{96}{7}A_0^3B_2-\frac{2535}{28}A_0^2A_2M_0-\frac{15}{4}A_0^3M_2\right)\\
&+\frac{1}{\eta^8}\left(-\frac{419}{63}A_2M_0^3+M_0^2\left(-\frac{1328}{245}A_0B_2-\frac{2057A_0M_2}{441}\right)\right)\\
&\left.\left.+\frac{1}{\eta^{10}}\left(\frac{15031}{315}A_0A_2M_0^2+M_0\left(\frac{486}{35}A_0^2B_2+\frac{20851A_0^2M_2}{2205}\right)\right)\right)P_2\right]\Bigg\}+\mathcal{O}(\lambda^5,\Omega^4),
\end{aligned}
\tag{F.4}
$$

$$
\begin{aligned}
\gamma^+_{\phi\phi}=1&+\lambda\left(2\frac{1}{\eta}M_0+2\frac{1}{\eta^3}\Omega^2M_2P_2\right)+\lambda^2\left\{\frac{3}{2}\frac{1}{\eta^6}A_0^2-\frac{1}{\eta^4}A_0M_0+\frac{4}{3}\frac{1}{\eta^2}M_0^2\right.\\
&+\Omega^2\left[-\frac{3}{2}\frac{1}{\eta^8}A_0A_2+\frac{1}{\eta^6}\left(\frac{6A_0B_2}{5}+\frac{2A_0M_2}{5}\right)\right.\\
&\left.+\left(\frac{66}{7}\frac{1}{\eta^8}A_0A_2+\frac{1}{\eta^4}M_0\left(2B_2+\frac{64M_2}{21}\right)+\frac{1}{\eta^6}\left(-\frac{12}{7}A_0B_2-3A_2M_0-\frac{13A_0M_2}{7}\right)\right)P_2\right]\Bigg\}\\
&+\lambda^3\left\{-\frac{11}{2}\frac{1}{\eta^9}A_0^3+\frac{9}{2}\frac{1}{\eta^7}A_0^2M_0-\frac{12}{5}\frac{1}{\eta^5}A_0M_0^2+\frac{2}{3}\frac{1}{\eta^3}M_0^3\right.\\
&+\Omega^2\left[12\frac{1}{\eta^{11}}A_0^2A_2-\frac{13}{15}\frac{1}{\eta^4}J_1^2+\frac{1}{\eta^5}M_0^2\left(-\frac{2B_2}{5}-\frac{2M_2}{15}\right)\right.\\
&\left.+\frac{1}{\eta^9}\left(-\frac{57}{10}A_0^2B_2-\frac{18}{5}A_0A_2M_0-\frac{3}{2}A_0^2M_2\right)+\frac{1}{\eta^7}\left(\frac{2}{5}A_2M_0^2+M_0\left(\frac{14A_0B_2}{5}+\frac{22A_0M_2}{35}\right)\right)\right.
\end{aligned}
$$

$$
\begin{aligned}
&+\left(-\frac{366}{7}\frac{1}{\eta^{11}}A_0^2A_2+\frac{24}{7}\frac{1}{\eta^4}J_1^2+\frac{1}{\eta^5}M_0^2\left(\frac{24B_2}{7}+\frac{8M_2}{3}\right)+\frac{1}{\eta^9}\left(\frac{93}{7}A_0^2B_2\right.\right.\\
&\left.\left.+\frac{204}{7}A_0A_2M_0+\frac{33}{7}A_0^2M_2\right)+\frac{1}{\eta^7}\left(-\frac{478}{63}A_2M_0^2+M_0\left(-\frac{58}{7}A_0B_2-\frac{340A_0M_2}{63}\right)\right)\right)P_2\Bigg]\Bigg\}\\
&+\lambda^4\left\{\frac{75}{4}\frac{1}{\eta^{12}}A_0^4-\frac{31}{2}\frac{1}{\eta^{10}}A_0^3M_0+\frac{21}{2}\frac{1}{\eta^8}A_0^2M_0^2-\frac{26}{15}\frac{1}{\eta^6}A_0M_0^3\right.\\
&+\Omega^2\left[-\frac{513}{8}\frac{1}{\eta^{14}}A_0^3A_2+\frac{148}{105}\frac{1}{\eta^7}A_0J_1^2+\frac{4}{15}\frac{1}{\eta^5}J_1^2M_0+\frac{1}{\eta^6}M_0^3\left(-\frac{2B_2}{15}+\frac{8M_2}{105}\right)\right.\\
&+\frac{1}{\eta^8}M_0^2\left(\frac{209A_0B_2}{35}+A_0M_2\right)+\frac{1}{\eta^{12}}\left(\frac{51}{2}A_0^3B_2+\frac{117}{4}A_0^2A_2M_0+\frac{21}{4}A_0^3M_2\right)\\
&+\frac{1}{\eta^{10}}\left(-\frac{113}{10}A_0A_2M_0^2+M_0\left(-\frac{147}{10}A_0^2B_2-\frac{17}{5}A_0^2M_2\right)\right)\\
&+\left(\frac{945}{4}\frac{1}{\eta^{14}}A_0^3A_2-\frac{14}{3}\frac{1}{\eta^7}A_0J_1^2+\frac{10}{21}\frac{1}{\eta^5}J_1^2M_0+\frac{1}{\eta^6}M_0^3\left(\frac{82B_2}{35}+\frac{82M_2}{105}\right)+\frac{1}{\eta^{12}}\left(-\frac{453}{7}A_0^3B_2\right.\right.\\
&\left.\left.-\frac{4173}{28}A_0^2A_2M_0-\frac{57}{4}A_0^3M_2\right)+\frac{1}{\eta^8}\left(-\frac{419}{63}A_2M_0^3+M_0^2\left(-\frac{4254}{245}A_0B_2-\frac{2939A_0M_2}{441}\right)\right)\right.\\
&\left.\left.+\frac{1}{\eta^{10}}\left(\frac{4430}{63}A_0A_2M_0^2+M_0\left(\frac{303}{7}A_0^2B_2+\frac{7169}{441}A_0^2M_2\right)\right)\right)P_2\Bigg]\Bigg\}+\mathcal{O}(\lambda^5,\Omega^4),
\end{aligned}
\tag{F.5}
$$

$$
\begin{aligned}
\gamma^+_{r\theta}=&\lambda^2\Omega^2\left[\frac{3}{2}\frac{1}{\eta^8}A_0A_2+\frac{1}{\eta^6}\left(-\frac{6}{5}A_0B_2-\frac{2A_0M_2}{5}\right)\right]P_{21}\\
&+\lambda^3\Omega^2\left\{-12\frac{1}{\eta^{11}}A_0^2A_2+\frac{19}{45}\frac{1}{\eta^4}J_1^2+\frac{1}{\eta^5}M_0^2\left(\frac{2B_2}{5}+\frac{2M_2}{15}\right)\right.\\
&\left.+\frac{1}{\eta^9}\left(\frac{57}{10}A_0^2B_2+\frac{18}{5}A_0A_2M_0+\frac{3}{2}A_0^2M_2\right)+\frac{1}{\eta^7}\left[-\frac{2}{5}A_2M_0^2+M_0\left(-\frac{14}{5}A_0B_2-\frac{22A_0M_2}{35}\right)\right]\right\}P_{21}\\
&+\lambda^4\Omega^2\left\{\frac{513}{8}\frac{1}{\eta^{14}}A_0^3A_2-\frac{244}{315}\frac{1}{\eta^7}A_0J_1^2-\frac{2}{45}\frac{1}{\eta^5}J_1^2M_0+\frac{1}{\eta^6}M_0^3\left(\frac{2B_2}{15}-\frac{8M_2}{105}\right)\right.\\
&+\frac{1}{\eta^8}M_0^2\left(-\frac{209}{35}A_0B_2-A_0M_2\right)+\frac{1}{\eta^{12}}\left(-\frac{51}{2}A_0^3B_2-\frac{117}{4}A_0^2A_2M_0-\frac{21}{4}A_0^3M_2\right)\\
&\left.+\frac{1}{\eta^{10}}\left[\frac{113}{10}A_0A_2M_0^2+M_0\left(\frac{147}{10}A_0^2B_2+\frac{17}{5}A_0^2M_2\right)\right]\right\}P_{21}+\mathcal{O}(\lambda^5,\Omega^4).
\end{aligned}
\tag{F.6}
$$

1.2. Interior components

The interior ones are

$$
\begin{aligned}
\gamma^-_{\mathrm{tt}}=&-1+\lambda\left(-\eta^2+m_0+\eta^2\Omega^2m_2P_2\right)+\lambda^2\left\{\left(\frac{1}{10}+\frac{3n}{20}\right)\eta^4+\eta^2\left(-1-\frac{n}{2}-a_0\right)\right.\\
&\left.+\Omega^2\left[\left(\frac{2}{3}+\frac{n}{3}\right)\eta^2+\left(-\frac{3}{5}-\frac{n}{10}\right)\eta^4+\eta^4\left(\frac{6}{7}+\frac{n}{7}-3a_2+\left(\frac{1}{7}-\frac{3n}{14}\right)m_2\right)P_2\right]\right\}\\
&+\lambda^3\left\{\left(\frac{1}{7}-\frac{3n}{70}-\frac{n^2}{35}\right)\eta^6+\eta^4\left(-\frac{7}{10}+\frac{n}{4}+\frac{3n^2}{20}+\frac{a_0}{5}+\frac{3na_0}{10}+\left(\frac{1}{10}+\frac{3n}{20}\right)m_0\right)\right.
\end{aligned}
$$

$$
\begin{aligned}
&+\eta^2\left(-\frac{2}{5}-\frac{4n}{5}-\frac{3n^2}{10}-2a_0-na_0+\left(-1-\frac{n}{2}+a_0\right)m_0+m_0^2\right)\\
&+\Omega^2\left[\left(\frac{271}{525}+\frac{n}{7}+\frac{13n^2}{420}\right)\eta^6+\eta^4\left(\frac{7}{15}-\frac{7n}{15}-\frac{3n^2}{20}-\frac{6a_0}{5}-\frac{na_0}{5}-\frac{2j_1}{5}+\frac{nj_1}{5}+\left(-\frac{6}{5}-\frac{n}{5}\right)m_0\right)\right.\\
&+\eta^2\left(\frac{1}{3}+\frac{11n}{15}+\frac{17n^2}{60}+\frac{4a_0}{3}+\frac{2na_0}{3}-\frac{4j_1}{3}-\frac{2nj_1}{3}+\frac{2j_1^2}{3}+\left(\frac{4}{3}+\frac{2n}{3}\right)m_0\right)\\
&+\left(\eta^6\left(-\frac{509}{1575}-\frac{37n}{210}-\frac{5n^2}{126}+\frac{3a_2}{5}+\frac{9na_2}{10}+\left(-\frac{38}{105}+\frac{n}{35}+\frac{5n^2}{84}\right)m_2\right)\right.\\
&+\eta^4\left(\frac{3n}{7}+\frac{n^2}{14}+\frac{12a_0}{7}+\frac{2na_0}{7}-3a_2-\frac{3na_2}{2}-\frac{24b_2}{35}-\frac{6nb_2}{35}-\frac{4j_1}{35}-\frac{2nj_1}{7}\right.\\
&\left.\left.\left.+\left(\frac{23}{35}+\frac{n}{14}-\frac{3n^2}{28}+\frac{26a_0}{35}-\frac{3na_0}{14}\right)m_2+m_0\left(\frac{12}{7}+\frac{2n}{7}+3a_2+\left(\frac{47}{35}-\frac{3n}{14}\right)m_2\right)\right)\right)P_2\right]\Bigg\}\\
&+\lambda^4\left\{\left(-\frac{177}{1400}-\frac{649n}{12600}+\frac{913n^2}{50400}+\frac{61n^3}{10080}\right)\eta^8+\eta^6\left(\frac{221}{350}+\frac{129n}{350}-\frac{31n^2}{280}-\frac{3n^3}{70}+\frac{3a_0}{7}\right.\right.\\
&\left.-\frac{9na_0}{70}-\frac{3n^2a_0}{35}+\left(\frac{2}{7}-\frac{3n}{35}-\frac{2n^2}{35}\right)m_0\right)\\
&+\eta^4\left(-\frac{27}{25}-\frac{67n}{100}+\frac{31n^2}{100}+\frac{51n^3}{400}-\frac{21a_0}{10}+\frac{3na_0}{4}+\frac{9n^2a_0}{20}+\frac{a_0^2}{10}+\frac{3na_0^2}{20}\right.\\
&\left.+\left(-\frac{7}{5}+\frac{n}{2}+\frac{3n^2}{10}\right)m_0+\left(-\frac{1}{10}-\frac{3n}{20}\right)m_0^2\right)+\eta^2\left(-\frac{41}{105}-\frac{67n}{105}-\frac{37n^2}{60}-\frac{83n^3}{420}-\frac{6a_0}{5}\right.\\
&\left.-\frac{12na_0}{5}-\frac{9n^2a_0}{10}-a_0^2-\frac{na_0^2}{2}+\left(-\frac{4}{5}-\frac{8n}{5}-\frac{3n^2}{5}\right)m_0+\left(1+\frac{n}{2}\right)m_0^2\right)\\
&+\Omega^2\left[\left(-\frac{158}{1575}-\frac{117n}{700}-\frac{283n^2}{6300}-\frac{n^3}{112}\right)\eta^8+\eta^6\left(-\frac{137}{105}+\frac{148n}{525}+\frac{101n^2}{420}+\frac{5n^3}{84}\right.\right.\\
&\left.+\frac{271a_0}{175}+\frac{3na_0}{7}+\frac{13n^2a_0}{140}+\frac{58j_1}{525}-\frac{13n^2j_1}{210}+\left(\frac{271}{175}+\frac{3n}{7}+\frac{13n^2}{140}\right)m_0\right)\\
&+\eta^4\left(\frac{13}{10}+\frac{33n}{50}-\frac{21n^2}{40}-\frac{33n^3}{200}+\frac{7a_0}{5}-\frac{7na_0}{5}-\frac{9n^2a_0}{20}-\frac{3a_0^2}{5}-\frac{na_0^2}{10}\right.\\
&-\frac{14j_1}{15}+\frac{2nj_1}{15}+\frac{3n^2j_1}{10}-\frac{2a_0j_1}{5}+\frac{1}{5}na_0j_1+\frac{j_1^2}{5}-\frac{nj_1^2}{10}\\
&\left.+\left(\frac{7}{5}-\frac{7n}{5}-\frac{9n^2}{20}-\frac{6a_0}{5}-\frac{na_0}{5}-\frac{2j_1}{5}+\frac{nj_1}{5}\right)m_0+\left(-\frac{3}{5}-\frac{n}{10}\right)m_0^2\right)\\
&+\eta^2\left(\frac{6}{25}+\frac{338n}{525}+\frac{26n^2}{35}+\frac{101n^3}{420}+a_0+\frac{11na_0}{5}+\frac{17n^2a_0}{20}+\frac{2a_0^2}{3}+\frac{na_0^2}{3}\right.\\
&-\frac{2j_1}{3}-\frac{22nj_1}{15}-\frac{17n^2j_1}{30}-\frac{4a_0j_1}{3}-\frac{2}{3}na_0j_1+\frac{2j_1^2}{3}+\frac{nj_1^2}{3}-\frac{2}{3}a_0j_1^2\\
&+\left(1+\frac{11n}{5}+\frac{17n^2}{20}+\frac{4a_0}{3}+\frac{2na_0}{3}-\frac{4j_1}{3}-\frac{2nj_1}{3}-\frac{2j_1^2}{3}\right)m_0+\left(\frac{2}{3}+\frac{n}{3}\right)m_0^2\Big)+\left(\eta^8\left(\frac{167}{40425}\right.\right.\\
&\left.+\frac{4243n}{40425}+\frac{23n^2}{420}+\frac{n^3}{90}+\frac{108a_2}{77}-\frac{27na_2}{70}-\frac{9n^2a_2}{35}+\left(\frac{1787}{5390}+\frac{1399n}{8085}-\frac{113n^2}{3080}-\frac{n^3}{60}\right)m_2\right)\\
&+\eta^4\left(\frac{6n}{35}+\frac{2n^2}{7}+\frac{3n^3}{70}+\frac{9na_0}{7}+\frac{3n^2a_0}{14}+\frac{6a_0^2}{7}+\frac{na_0^2}{7}-\frac{6a_2}{5}-\frac{12na_2}{5}-\frac{9n^2a_2}{10}-3a_0a_2\right.
\end{aligned}
$$

$$
\begin{aligned}
&- \frac{3}{2} n a_0 a_2 - \frac{24 b_2}{25} - \frac{6 n b_2}{7} - \frac{6 n^2 b_2}{35} - \frac{24 a_0 b_2}{35} - \frac{6}{35} n a_0 b_2 - \frac{2 n j_1}{35} - \frac{n^2 j_1}{7} - \frac{4 a_0 j_1}{35} \\
&- \frac{2}{7} n a_0 j_1 + \frac{58 j_1^2}{105} + \left(\frac{6}{7} + \frac{n}{7} \right) m_0^2 + \left(\frac{46}{175} + \frac{74 n}{175} - \frac{9 n^3}{140} + \frac{67 a_0}{35} + \frac{31 n a_0}{70} - \frac{3 n^2 a_0}{14} \right) m_2 \\
&+ m_0 \left(\frac{9 n}{7} + \frac{3 n^2}{14} + \frac{12 a_0}{7} + \frac{2 n a_0}{7} - \frac{4 j_1}{35} - \frac{2 n j_1}{7} + \left(\frac{88}{35} + \frac{26 n}{35} - \frac{3 n^2}{14} \right) m_2 \right) \Bigg) \\
&+ \eta^6 \Bigg(\frac{56}{45} - \frac{139 n}{450} - \frac{257 n^2}{1260} - \frac{5 n^3}{126} - \frac{509 a_0}{525} - \frac{37 n a_0}{70} - \frac{5 n^2 a_0}{42} - \frac{24 a_2}{5} + \frac{3 n a_2}{2} \\
&+ \frac{9 n^2 a_2}{10} + \frac{3 a_0 a_2}{5} + \frac{9}{10} n a_0 a_2 - \frac{2 b_2}{15} + \frac{n b_2}{5} + \frac{11 n^2 b_2}{210} - \frac{782 j_1}{1575} + \frac{n j_1}{15} \\
&+ \frac{5 n^2 j_1}{63} + \left(-\frac{51}{70} - \frac{127 n}{210} + \frac{59 n^2}{840} + \frac{5 n^3}{84} - \frac{443 a_0}{525} - \frac{43 n a_0}{350} + \frac{5 n^2 a_0}{42} \right) m_2 \\
&+ m_0 \left(-\frac{509}{525} - \frac{37 n}{70} - \frac{5 n^2}{42} + \left(-\frac{506}{525} - \frac{53 n}{175} + \frac{5 n^2}{42} \right) m_2 \right) \Bigg) P_2 \Bigg] \Bigg\} + \mathcal{O}(\lambda^5, \Omega^4),
\end{aligned}
\tag{F.7}
$$

$$
\begin{aligned}
\gamma^-_{t\phi} = {} & \lambda^{3/2} \left[\Omega \left(-\frac{6 \eta^3}{5} + \eta j_1 \right) P_{11} + \eta^3 \Omega^3 j_3 P_{31} \right] \\
&+ \lambda^{5/2} \Bigg\{ \Omega \left(\left(\frac{27}{35} + \frac{3 n}{14} \right) \eta^5 + \eta^3 \left(-\frac{3 n}{5} - \frac{12 a_0}{5} + \frac{j_1}{5} - \frac{12 m_0}{5} \right) \right) P_{11} \\
&+ \Omega^3 \Bigg[\left(\eta^5 \left(-\frac{12}{35} - \frac{6 n}{35} + \frac{18 a_2}{25} + \left(\frac{9}{35} + \frac{3 n}{70} \right) m_2 \right) + \eta^3 \left(\frac{2 n}{5} - \frac{42 b_2}{25} - \frac{j_1 m_2}{5} \right) \right) P_{11} \\
&+ \eta^5 \left(\frac{4}{45} + \frac{2 n}{45} - \frac{48 a_2}{25} + \frac{j_3}{9} + \left(-\frac{4}{15} - \frac{n}{15} \right) m_2 \right) P_{31} \Bigg] \Bigg\} \\
&+ \lambda^{7/2} \Bigg\{ \Omega \Bigg[\left(-\frac{29}{225} - \frac{323 n}{1050} - \frac{2 n^2}{45} \right) \eta^7 + \eta^5 \left(-\frac{261}{175} + \frac{69 n}{70} + \frac{3 n^2}{14} + \frac{81 a_0}{35} + \frac{9 n a_0}{14} \right. \\
&\left. - \frac{17 j_1}{70} - \frac{9 n j_1}{140} + \left(\frac{81}{35} + \frac{9 n}{14} \right) m_0 \right) \\
&+ \eta^3 \left(-\frac{6 n}{25} - \frac{9 n^2}{25} - \frac{9 n a_0}{5} - \frac{6 a_0^2}{5} + \frac{4 j_1}{5} + \frac{n j_1}{10} + \frac{a_0 j_1}{5} + \left(-\frac{9 n}{5} - \frac{12 a_0}{5} + \frac{j_1}{5} \right) m_0 - \frac{6 m_0^2}{5} \right) \Bigg] P_{11} \\
&+ \Omega^3 \Bigg[\left(\eta^7 \left(\frac{362}{1575} + \frac{179 n}{525} + \frac{37 n^2}{630} - \frac{162 a_2}{175} - \frac{9 n a_2}{35} + \left(-\frac{248}{1575} - \frac{2 n}{15} - \frac{n^2}{63} \right) m_2 \right) \right. \\
&+ \eta^5 \left(\frac{174}{175} - \frac{29 n}{35} - \frac{8 n^2}{35} - \frac{36 a_0}{35} - \frac{18 n a_0}{35} + \frac{9 n a_2}{25} + \frac{18 a_0 a_2}{25} + \frac{153 b_2}{175} + \frac{3 n b_2}{10} \right. \\
&+ \frac{24 j_1}{35} + \frac{27 n j_1}{70} - \frac{3 a_2 j_1}{25} + \left(\frac{9 n}{70} + \frac{3 n^2}{140} + \frac{324 a_0}{875} + \frac{3 n a_0}{35} - \frac{j_1}{35} \right) m_2 \\
&\left. + m_0 \left(-\frac{48}{35} - \frac{24 n}{35} + \frac{18 a_2}{25} + \left(\frac{423}{875} + \frac{9 n}{70} \right) m_2 \right) \right) + \eta^3 \left(\frac{n}{5} + \frac{17 n^2}{50} + \frac{6 n a_0}{5} - \frac{21 n b_2}{25} \right. \\
&\left. \left. - \frac{42 a_0 b_2}{25} - \frac{8 j_1}{15} - \frac{13 n j_1}{15} + \frac{12 b_2 j_1}{25} + m_0 \left(\frac{8 n}{5} - \frac{42 b_2}{25} - \frac{j_1 m_2}{5} \right) \right) \right) P_{11} \\
&+ \left(\eta^7 \left(-\frac{34}{1575} - \frac{1324 n}{17325} - \frac{n^2}{77} + \frac{297 a_2}{175} + \frac{33 n a_2}{70} - \frac{2089 j_3}{6930} - \frac{9 n j_3}{220} + \left(\frac{113}{825} + \frac{163 n}{1155} + \frac{3 n^2}{154} \right) m_2 \right) \right.
\end{aligned}
$$

$$
\begin{aligned}
&+\eta^5\left(\frac{2n}{45}+\frac{n^2}{45}+\frac{4a_0}{15}+\frac{2na_0}{15}-\frac{24na_2}{25}-\frac{48a_0a_2}{25}-\frac{24b_2}{175}-\frac{4nb_2}{105}-\frac{13j_1}{63}-\frac{11nj_1}{105}\right.\\
&+\frac{47a_2j_1}{225}+\frac{47j_3}{45}+\frac{nj_3}{18}+\frac{a_0j_3}{9}+\left(-\frac{2n}{15}-\frac{n^2}{30}-\frac{56a_0}{375}-\frac{2na_0}{15}+\frac{5j_1}{126}+\frac{nj_1}{42}\right)m_2\\
&\left.+m_0\left(\frac{16}{45}+\frac{8n}{45}-\frac{48a_2}{25}+\frac{j_3}{9}+\left(-\frac{4}{125}-\frac{n}{5}\right)m_2\right)\right)\Big]\Big\}\\
&+\lambda^{9/2}\left\{\Omega\left[\left(-\frac{59023}{242550}+\frac{29647n}{161700}+\frac{2753n^2}{27720}+\frac{61n^3}{6160}\right)\eta^9+\eta^7\left(\frac{3173}{1575}-\frac{23n}{150}-\frac{1681n^2}{3150}-\frac{n^3}{15}\right.\right.\right.\\
&-\frac{116a_0}{225}-\frac{646na_0}{525}-\frac{8n^2a_0}{45}+\frac{46j_1}{525}+\frac{239nj_1}{3150}+\frac{n^2j_1}{63}+\left(-\frac{116}{225}-\frac{646n}{525}-\frac{8n^2}{45}\right)m_0\Big)\\
&+\eta^5\left(-\frac{522}{875}-\frac{2181n}{1750}+\frac{171n^2}{175}+\frac{51n^3}{280}-\frac{1044a_0}{175}+\frac{138na_0}{35}+\frac{6n^2a_0}{7}+\frac{81a_0^2}{35}\right.\\
&+\frac{9na_0^2}{14}-\frac{53j_1}{350}-\frac{43nj_1}{140}-\frac{9n^2j_1}{140}-\frac{17a_0j_1}{35}-\frac{9}{70}na_0j_1\\
&\left.+\left(-\frac{1044}{175}+\frac{138n}{35}+\frac{6n^2}{7}+\frac{162a_0}{35}+\frac{9na_0}{7}-\frac{17j_1}{35}-\frac{9nj_1}{70}\right)m_0+\left(\frac{81}{35}+\frac{9n}{14}\right)m_0^2\right)\\
&+\eta^3\left(-\frac{41n}{175}-\frac{93n^2}{350}-\frac{83n^3}{350}-\frac{24na_0}{25}-\frac{36n^2a_0}{25}-\frac{9na_0^2}{5}+\frac{8j_1}{25}+\frac{13nj_1}{25}+\frac{3n^2j_1}{50}\right.\\
&\left.\left.+\frac{8a_0j_1}{5}+\frac{1}{5}na_0j_1+\left(-\frac{24n}{25}-\frac{36n^2}{25}-\frac{18na_0}{5}+\frac{8j_1}{5}+\frac{nj_1}{5}\right)m_0-\frac{9nm_0^2}{5}\right)\right]P_{11}\\
&+\Omega^3\left[\left(\eta^9\left(\frac{49373}{3031875}-\frac{11551n}{40425}-\frac{2801n^2}{17325}-\frac{829n^3}{46200}+\frac{1963a_2}{9625}+\frac{969na_2}{1750}+\frac{2n^2a_2}{25}\right.\right.\right.\\
&\left.+\left(-\frac{29497}{404250}+\frac{15397n}{115500}+\frac{39n^2}{700}+\frac{n^3}{200}\right)m_2\right)+\eta^7\left(-\frac{1222}{675}+\frac{59n}{315}+\frac{3502n^2}{4725}\right.\\
&+\frac{13n^3}{126}+\frac{1448a_0}{1575}+\frac{716na_0}{525}+\frac{74n^2a_0}{315}+\frac{1692a_2}{875}-\frac{207na_2}{175}-\frac{9n^2a_2}{35}-\frac{324a_0a_2}{175}\\
&-\frac{18}{35}na_0a_2+\frac{247b_2}{7875}-\frac{2153nb_2}{5250}-\frac{104n^2b_2}{1575}-\frac{122j_1}{1575}-\frac{1153nj_1}{1575}-\frac{173n^2j_1}{1260}+\frac{51a_2j_1}{175}\\
&+\frac{27}{350}na_2j_1+\left(\frac{149}{315}-\frac{487n}{3150}-\frac{13n^2}{90}-\frac{n^3}{63}-\frac{754a_0}{2625}-\frac{61na_0}{175}-\frac{n^2a_0}{21}+\frac{43j_1}{525}+\frac{83nj_1}{3150}+\frac{n^2j_1}{252}\right)m_2\\
&\left.+m_0\left(\frac{362}{315}+\frac{179n}{105}+\frac{37n^2}{126}-\frac{324a_2}{175}-\frac{18na_2}{35}+\left(-\frac{292}{1125}-\frac{226n}{525}-\frac{4n^2}{63}\right)m_2\right)\right)\\
&+\eta^5\left(\frac{87}{175}+\frac{1262n}{875}-\frac{817n^2}{700}-\frac{171n^3}{700}+\frac{696a_0}{175}-\frac{116na_0}{35}-\frac{32n^2a_0}{35}-\frac{36a_0^2}{35}\right.\\
&-\frac{18na_0^2}{35}+\frac{18na_2}{125}+\frac{27n^2a_2}{125}+\frac{18}{25}na_0a_2-\frac{11727b_2}{4375}+\frac{411nb_2}{350}+\frac{3n^2b_2}{10}\\
&+\frac{306a_0b_2}{175}+\frac{3}{5}na_0b_2-\frac{991j_1}{525}+\frac{391nj_1}{210}+\frac{73n^2j_1}{140}+\frac{48a_0j_1}{35}+\frac{27}{35}na_0j_1\\
&-\frac{12a_2j_1}{25}-\frac{3}{50}na_2j_1-\frac{24b_2j_1}{175}-\frac{9}{175}nb_2j_1-\frac{762j_1^2}{875}-\frac{8nj_1^2}{35}\\
&\left.+\left(\frac{9n}{175}+\frac{3n^2}{35}+\frac{9n^3}{700}+\frac{549na_0}{1750}+\frac{9n^2a_0}{140}+\frac{99a_0^2}{875}+\frac{3na_0^2}{70}-\frac{41j_1}{175}-\frac{nj_1}{70}-\frac{4a_0j_1}{875}\right)m_2\right.
\end{aligned}
$$

$$
\begin{aligned}
&+ m_0^2\left(-\frac{12}{5} - \frac{6n}{5} + \left(\frac{396}{875} + \frac{6n}{35}\right)m_2\right) + m_0\left(\frac{174}{35} - \frac{29n}{7} - \frac{8n^2}{7} - \frac{108a_0}{35} - \frac{54na_0}{35} + \frac{18na_2}{25}\right.\\
&\left.+ \frac{306b_2}{175} + \frac{3nb_2}{5} + \frac{72j_1}{35} + \frac{81nj_1}{70} + \left(\frac{324n}{875} + \frac{3n^2}{35} + \frac{396a_0}{875} + \frac{6na_0}{35} - \frac{8j_1}{875}\right)m_2\right)\Bigg)\\
&+ \eta^3\left(\frac{18n}{125} + \frac{11n^2}{35} + \frac{101n^3}{350} + \frac{4na_0}{5} + \frac{34n^2a_0}{25} + \frac{6na_0^2}{5} - \frac{42nb_2}{125} - \frac{63n^2b_2}{125} - \frac{42}{25}na_0b_2\right.\\
&- \frac{4j_1}{15} - \frac{133nj_1}{150} - \frac{221n^2j_1}{300} - \frac{16a_0j_1}{15} - \frac{26}{15}na_0j_1 + \frac{18b_2j_1}{25} + \frac{6}{25}nb_2j_1 + \frac{16j_1^2}{15}\\
&\left.+ \frac{8nj_1^2}{15} + \frac{j_1^3}{15} + \left(n + \frac{17n^2}{10} + \frac{18na_0}{5} - \frac{42nb_2}{25} - \frac{8j_1}{5} - \frac{13nj_1}{5}\right)m_0 + m_0^2\left(\frac{14n}{5} - \frac{j_1m_2}{5}\right)\right)\Bigg)P_{11}\\
&+ \left(\eta^9\left(-\frac{2553}{56875} + \frac{54017n}{1051050} + \frac{54101n^2}{1576575} + \frac{11n^3}{2925} - \frac{24782a_2}{86625} - \frac{323na_2}{375} - \frac{28n^2a_2}{225}\right.\right.\\
&\left.+ \frac{973j_3}{6435} + \frac{6973nj_3}{90090} + \frac{n^2j_3}{91} + \left(\frac{536831}{5255250} - \frac{1283617n}{10510500} - \frac{61031n^2}{1051050} - \frac{11n^3}{1950}\right)m_2\right)\\
&+ \eta^7\left(\frac{298}{2475} + \frac{118n}{5775} - \frac{2963n^2}{34650} - \frac{n^3}{77} - \frac{136a_0}{1575} - \frac{5296na_0}{17325} - \frac{4n^2a_0}{77} - \frac{3207a_2}{875}\right.\\
&+ \frac{759na_2}{350} + \frac{33n^2a_2}{70} + \frac{594a_0a_2}{175} + \frac{33}{35}na_0a_2 + \frac{734b_2}{28875} + \frac{3076nb_2}{28875} + \frac{83n^2b_2}{5775}\\
&+ \frac{8j_1}{525} + \frac{647nj_1}{3850} + \frac{43n^2j_1}{1386} - \frac{4709a_2j_1}{17325} - \frac{387na_2j_1}{3850} - \frac{2561j_3}{6930} - \frac{949nj_3}{2772}\\
&- \frac{9n^2j_3}{220} - \frac{2089a_0j_3}{3465} - \frac{9}{110}na_0j_3 + \left(-\frac{2962}{5775} + \frac{607n}{5775} + \frac{13n^2}{84} + \frac{3n^3}{154} + \frac{688a_0}{9625}\right.\\
&\left.+ \frac{181na_0}{550} + \frac{9n^2a_0}{154} - \frac{592j_1}{17325} - \frac{653nj_1}{23100} - \frac{n^2j_1}{132}\right)m_2 + m_0\left(-\frac{34}{315} - \frac{1324n}{3465}\right.\\
&\left.\left.- \frac{5n^2}{77} + \frac{594a_2}{175} + \frac{33na_2}{35} - \frac{2089j_3}{3465} - \frac{9nj_3}{110} + \left(-\frac{3782}{28875} + \frac{2171n}{5775} + \frac{6n^2}{77}\right)m_2\right)\right)\\
&+ \eta^5\left(\frac{4n}{225} + \frac{8n^2}{225} + \frac{n^3}{75} + \frac{8na_0}{45} + \frac{4n^2a_0}{45} + \frac{4a_0^2}{15} + \frac{2na_0^2}{15} - \frac{48na_2}{125} - \frac{72n^2a_2}{125} - \frac{48}{25}na_0a_2 -\right.\\
&\frac{688b_2}{4375} - \frac{92nb_2}{525} - \frac{4n^2b_2}{105} - \frac{48a_0b_2}{175} - \frac{8}{105}na_0b_2 - \frac{13nj_1}{126} - \frac{11n^2j_1}{210} - \frac{26a_0j_1}{63}\\
&- \frac{22}{105}na_0j_1 + \frac{98a_2j_1}{225} + \frac{47}{450}na_2j_1 + \frac{13b_2j_1}{105} + \frac{2}{525}nb_2j_1 + \frac{2018j_1^2}{7875} + \frac{2nj_1^2}{63} + \frac{94j_3}{225}\\
&+ \frac{146nj_3}{225} + \frac{n^2j_3}{30} + \frac{94a_0j_3}{45} + \frac{1}{9}na_0j_3 + \left(-\frac{4n}{75} - \frac{7n^2}{75} - \frac{n^3}{50} - \frac{26na_0}{125} - \frac{n^2a_0}{10}\right.\\
&\left.+ \frac{44a_0^2}{375} - \frac{na_0^2}{15} + \frac{31j_1}{630} + \frac{5nj_1}{252} + \frac{n^2j_1}{84} - \frac{11a_0j_1}{5250} + \frac{1}{42}na_0j_1\right)m_2 + m_0^2\left(\frac{28}{45} + \frac{14n}{45}\right.\\
&\left.+ \left(\frac{176}{375} - \frac{4n}{15}\right)m_2\right) + m_0\left(\frac{2n}{9} + \frac{n^2}{9} + \frac{4a_0}{5} + \frac{2na_0}{5} - \frac{48na_2}{25} - \frac{48b_2}{175} - \frac{8nb_2}{105} - \frac{13j_1}{21}\right.\\
&\left.\left.\left.- \frac{11nj_1}{35} + \frac{94j_3}{45} + \frac{nj_3}{9} + \left(-\frac{56n}{375} - \frac{2n^2}{15} + \frac{176a_0}{375} - \frac{4na_0}{15} - \frac{11j_1}{2625} + \frac{nj_1}{21}\right)m_2\right)\right)P_{31}\right]\Bigg\}\\
&+ \mathcal{O}(\lambda^{11/2}, \Omega^5),
\end{aligned}
\tag{F.8}
$$

$$
\begin{aligned}
\gamma^{-}_{rr} = 1 &+ \lambda\left\{-\eta^2 + a_0 + m_0 + \Omega^2\left[-2b_2 + \eta^2\left(9a_2 + m_2\right)\right]P_2\right\} \\
&+ \lambda^2\left\{\left(\frac{17}{70} + \frac{3n}{20}\right)\eta^4 + \eta^2\left(\frac{7}{5} - \frac{n}{2} - 2a_0 - 2m_0\right) + \Omega^2\left[\left(-\frac{14}{15} + \frac{n}{3}\right)\eta^2 + \left(\frac{9}{35} - \frac{n}{10}\right)\eta^4\right.\right. \\
&\left.\left. + \left(\eta^4\left(-\frac{8}{21} + \frac{n}{7} - 12a_2 + \left(-\frac{3}{7} - \frac{3n}{14}\right)m_2\right) + \eta^2\left(2b_2 - \frac{4a_0m_2}{5} - \frac{8m_0m_2}{5}\right)\right)P_2\right]\right\} \\
&+ \lambda^3\left\{\left(\frac{23}{45} - \frac{52n}{315} - \frac{n^2}{35}\right)\eta^6 + \eta^4\left(-\frac{197}{70} + \frac{11n}{28} + \frac{3n^2}{20} + \frac{51a_0}{70} + \frac{9na_0}{20} + \left(\frac{51}{70} + \frac{9n}{20}\right)m_0\right)\right. \\
&+ \eta^2\left(\frac{14}{25} + \frac{16n}{25} - \frac{3n^2}{10} + \frac{21a_0}{5} - \frac{3na_0}{2} - a_0^2 + \left(\frac{21}{5} - \frac{3n}{2} - 2a_0\right)m_0 - m_0^2\right) \\
&+ \Omega^2\left[\left(-\frac{11}{35} + \frac{8n}{105} + \frac{13n^2}{420}\right)\eta^6 + \eta^4\left(\frac{197}{105} - \frac{2n}{15} - \frac{3n^2}{20} + \frac{27a_0}{35} - \frac{3na_0}{10} - \frac{38j_1}{35} + \frac{nj_1}{5} + \left(\frac{36}{35}\right.\right.\right. \\
&\left.\left. - \frac{2n}{5}\right)m_0\right) + \eta^2\left(-\frac{7}{15} - \frac{47n}{75} + \frac{17n^2}{60} - \frac{14a_0}{5} + na_0 + \frac{28j_1}{15} - \frac{2nj_1}{3} + \frac{2j_1^2}{5} + \left(-\frac{56}{15} + \frac{4n}{3}\right)m_0\right) \\
&+ \left(\eta^6\left(\frac{1009}{1575} - \frac{821n}{6930} - \frac{5n^2}{126} + \frac{435a_2}{154} + \frac{9na_2}{4} + \left(-\frac{668}{495} + \frac{2447n}{6930} + \frac{5n^2}{84}\right)m_2\right)\right. \\
&+ \eta^4\left(-\frac{4n}{21} + \frac{n^2}{14} - \frac{8a_0}{7} + \frac{3na_0}{7} + \frac{99a_2}{5} - 6na_2 - 12a_0a_2 - \frac{3b_2}{5} - \frac{33nb_2}{70} + \frac{4j_1}{3}\right. \\
&\left.\left. - \frac{2nj_1}{7} + \left(\frac{87}{35} - \frac{3n}{14} - \frac{3n^2}{28} + \frac{54a_0}{35} - \frac{3na_0}{7}\right)m_2 + m_0\left(-\frac{32}{21} + \frac{4n}{7} - 12a_2 + \left(\frac{123}{35} - \frac{9n}{14}\right)m_2\right)\right)\right. \\
&\left.\left. + \eta^2\left(-\frac{28b_2}{25} + nb_2 + 2a_0b_2 - \frac{14j_1^2}{15} - \frac{8}{5}m_0^2m_2 + m_0\left(2b_2 - \frac{4a_0m_2}{5}\right)\right)\right)P_2\right]\right\} \\
&+ \lambda^4\left\{\left(-\frac{720259}{970200} - \frac{1179n}{15400} + \frac{32237n^2}{554400} + \frac{61n^3}{10080}\right)\eta^8 + \eta^6\left(\frac{1451}{630} + \frac{653n}{630} - \frac{247n^2}{840} - \frac{3n^3}{70}\right.\right. \\
&\left. + \frac{92a_0}{45} - \frac{208na_0}{315} - \frac{4n^2a_0}{35} + \left(\frac{92}{45} - \frac{208n}{315} - \frac{4n^2}{35}\right)m_0\right) \\
&+ \eta^2\left(\frac{41}{75} + \frac{223n}{525} + \frac{697n^2}{2100} - \frac{83n^3}{420} + \frac{56a_0}{25} + \frac{64na_0}{25} - \frac{6n^2a_0}{5} + \frac{21a_0^2}{5} - \frac{3na_0^2}{2}\right. \\
&\left. + \left(\frac{56}{25} + \frac{64n}{25} - \frac{6n^2}{5} + \frac{42a_0}{5} - 3na_0\right)m_0 + \left(\frac{21}{5} - \frac{3n}{2}\right)m_0^2\right) \\
&+ \eta^4\left(\frac{12}{35} - \frac{2057n}{700} + \frac{151n^2}{350} + \frac{51n^3}{400} - \frac{394a_0}{35} + \frac{11na_0}{7} + \frac{3n^2a_0}{5} + \frac{51a_0^2}{70} + \frac{9na_0^2}{20}\right. \\
&\left. + \left(-\frac{394}{35} + \frac{11n}{7} + \frac{3n^2}{5} + \frac{51a_0}{35} + \frac{9na_0}{10}\right)m_0 + \left(\frac{51}{70} + \frac{9n}{20}\right)m_0^2\right) \\
&+ \Omega^2\left[\left(\frac{73}{4410} + \frac{1637n}{11550} - \frac{149n^2}{2475} - \frac{n^3}{112}\right)\eta^8 + \eta^6\left(-\frac{1007}{945} - \frac{1229n}{945} + \frac{373n^2}{1260} + \frac{5n^3}{84} - \frac{44a_0}{35}\right.\right. \\
&\left. + \frac{32na_0}{105} + \frac{13n^2a_0}{105} + \frac{1886j_1}{945} - \frac{74nj_1}{945} - \frac{13n^2j_1}{210} + \left(-\frac{11}{7} + \frac{8n}{21} + \frac{13n^2}{84}\right)m_0\right) \\
&+ \eta^4\left(-\frac{51}{50} + \frac{1187n}{350} - \frac{111n^2}{280} - \frac{33n^3}{200} + \frac{788a_0}{105} - \frac{8na_0}{15} - \frac{3n^2a_0}{5} + \frac{27a_0^2}{35} - \frac{3na_0^2}{10}\right. \\
&\left.\left. - \frac{394j_1}{105} - \frac{2nj_1}{105} + \frac{3n^2j_1}{10} - \frac{76a_0j_1}{35} + \frac{2}{5}na_0j_1 - \frac{19j_1^2}{105} - \frac{nj_1^2}{10}\right.\right.
\end{aligned}
$$

$$
\begin{aligned}
&+\left(\frac{197}{21}-\frac{2n}{3}-\frac{3n^2}{4}+\frac{81a_0}{35}-\frac{9na_0}{10}-\frac{114j_1}{35}+\frac{3nj_1}{5}\right)m_0+\left(\frac{9}{5}-\frac{7n}{10}\right)m_0^2\Bigg)\\
&+\eta^2\Bigg(-\frac{42}{125}-\frac{46n}{75}-\frac{72n^2}{175}+\frac{101n^3}{420}-\frac{28a_0}{15}-\frac{188na_0}{75}+\frac{17n^2a_0}{15}-\frac{14a_0^2}{5}+na_0^2\\
&+\frac{14j_1}{15}+\frac{94nj_1}{75}-\frac{17n^2j_1}{30}+\frac{56a_0j_1}{15}-\frac{4}{3}na_0j_1-\frac{14j_1^2}{15}+\frac{nj_1^2}{3}\\
&+\left(-\frac{7}{3}-\frac{47n}{15}+\frac{17n^2}{12}-\frac{42a_0}{5}+3na_0+\frac{28j_1}{5}-2nj_1+\frac{2j_1^2}{5}\right)m_0+\left(-\frac{98}{15}+\frac{7n}{3}\right)m_0^2\Bigg)\\
&+\Bigg(\eta^8\Bigg(-\frac{1122431}{3153150}-\frac{210421n}{900900}+\frac{14753n^2}{180180}+\frac{n^3}{90}+\frac{53498a_2}{5005}-\frac{1289na_2}{455}-\frac{18n^2a_2}{35}\\
&+\left(\frac{514981}{210210}+\frac{659n}{2310}-\frac{19433n^2}{120120}-\frac{n^3}{60}\right)m_2\Bigg)+\eta^2\Bigg(-\frac{56b_2}{125}-\frac{34nb_2}{125}+\frac{3n^2b_2}{5}-\frac{56a_0b_2}{25}\\
&+2na_0b_2+\left(-\frac{56b_2}{25}+2nb_2-\frac{14j_1^2}{15}\right)m_0-\frac{4}{5}a_0m_0^2m_2-\frac{8}{5}m_0^3m_2\Bigg)+\eta^6\Bigg(-\frac{2386}{3465}+\frac{12191n}{11550}\\
&-\frac{2027n^2}{13860}-\frac{5n^3}{126}+\frac{4036a_0}{1575}-\frac{1642na_0}{3465}-\frac{10n^2a_0}{63}-\frac{36537a_2}{770}+\frac{1563na_2}{308}+\frac{9n^2a_2}{4}\\
&+\frac{435a_0a_2}{77}+\frac{9}{2}na_0a_2-\frac{688b_2}{495}+\frac{2129nb_2}{3465}+\frac{23n^2b_2}{210}-\frac{12514j_1}{4725}+\frac{1693nj_1}{10395}\\
&+\frac{5n^2j_1}{63}+\left(-\frac{5399}{1386}-\frac{1235n}{693}+\frac{10943n^2}{27720}+\frac{5n^3}{84}-\frac{10657a_0}{2310}+\frac{563na_0}{924}+\frac{5n^2a_0}{28}\right)m_2\\
&+m_0\left(\frac{1009}{315}-\frac{821n}{1386}-\frac{25n^2}{126}+\frac{435a_2}{77}+\frac{9na_2}{2}+\left(-\frac{22619}{3465}+\frac{3551n}{6930}+\frac{5n^2}{21}\right)m_2\right)\Bigg)\\
&+\eta^4\Bigg(-\frac{8n}{105}-\frac{3n^2}{35}+\frac{3n^3}{70}-\frac{16na_0}{21}+\frac{2n^2a_0}{7}-\frac{8a_0^2}{7}+\frac{3na_0^2}{7}+\frac{198a_2}{25}+\frac{237na_2}{25}\\
&-\frac{18n^2a_2}{5}+\frac{198a_0a_2}{5}-12na_0a_2+\frac{723b_2}{175}-\frac{15nb_2}{14}-\frac{33n^2b_2}{70}\\
&-\frac{6a_0b_2}{5}-\frac{33}{35}na_0b_2+\frac{2nj_1}{3}-\frac{n^2j_1}{7}+\frac{8a_0j_1}{3}-\frac{4}{7}na_0j_1+\frac{48j_1^2}{35}\\
&+\left(\frac{174}{175}+\frac{246n}{175}-\frac{6n^2}{35}-\frac{9n^3}{140}+\frac{612a_0}{175}+\frac{39na_0}{70}-\frac{9n^2a_0}{28}+\frac{69a_0^2}{35}-\frac{3na_0^2}{14}\right)m_2\\
&+m_0^2\left(-\frac{8}{3}+n+\left(\frac{276}{35}-\frac{6n}{7}\right)m_2\right)+m_0\left(-\frac{20n}{21}+\frac{5n^2}{14}-\frac{24a_0}{7}+\frac{9na_0}{7}+\frac{198a_2}{5}-12na_2\right.\\
&\left.\left.\left.-\frac{6b_2}{5}-\frac{33nb_2}{35}+4j_1-\frac{6nj_1}{7}+\left(\frac{354}{175}+\frac{54n}{35}-\frac{3n^2}{7}+\frac{276a_0}{35}-\frac{6na_0}{7}\right)m_2\right)\right)\right)P_2\Bigg]\Bigg\}+\mathcal{O}(\lambda^5,\Omega^4),
\end{aligned}
\tag{F.9}
$$

$$
\begin{aligned}
\gamma^-_{\theta\theta}&=1+\lambda\left\{-\eta^2+a_0+m_0+\Omega^2\left[-\eta^2a_2-b_2+\left(2b_2+\eta^2\left(7a_2+m_2\right)\right)P_2\right]\right\}\\
&+\lambda^2\Bigg\{\left(\frac{37}{70}+\frac{3n}{20}\right)\eta^4+\eta^2\left(\frac{4}{5}-\frac{n}{2}-2a_0-2m_0\right)+\Omega^2\Bigg[\eta^4\left(\frac{71}{315}-\frac{n}{10}+a_2-\frac{m_2}{42}\right)\\
&+\eta^2\left(-\frac{8}{15}+\frac{n}{3}+b_2+\frac{a_0m_2}{5}+\frac{2m_0m_2}{5}\right)+\left(\eta^4\left(-\frac{13}{63}+\frac{n}{7}-10a_2+\left(-\frac{41}{42}-\frac{3n}{14}\right)m_2\right)\right.
\end{aligned}
$$

$$
\begin{aligned}
&+\eta^2\left(-2b_2-\frac{2a_0m_2}{5}-\frac{4m_0m_2}{5}\right)P_2\Bigg]\Bigg\}\\
&+\lambda^3\left\{\left(-\frac{13}{315}-\frac{73n}{315}-\frac{n^2}{35}\right)\eta^6+\eta^4\left(-\frac{23}{14}+\frac{19n}{28}+\frac{3n^2}{20}+\frac{111a_0}{70}+\frac{9na_0}{20}+\left(\frac{111}{70}+\frac{9n}{20}\right)m_0\right)\right.\\
&+\eta^2\left(\frac{8}{25}+\frac{7n}{25}-\frac{3n^2}{10}+\frac{12a_0}{5}-\frac{3na_0}{2}-a_0^2+\left(\frac{12}{5}-\frac{3n}{2}-2a_0\right)m_0-m_0^2\right)\\
&+\Omega^2\left[\eta^6\left(-\frac{562}{1575}+\frac{851n}{6930}+\frac{13n^2}{420}-\frac{377a_2}{770}-\frac{3na_2}{20}+\left(\frac{229}{6930}+\frac{8n}{3465}\right)m_2\right)\right.\\
&+\eta^4\left(\frac{23}{21}-\frac{107n}{315}-\frac{3n^2}{20}+\frac{71a_0}{105}-\frac{3na_0}{10}-a_2+\frac{na_2}{2}+a_0a_2-\frac{101b_2}{210}-\frac{3nb_2}{20}\right.\\
&-\frac{32j_1}{63}+\frac{nj_1}{5}+m_0\left(\frac{284}{315}-\frac{2n}{5}+a_2-\frac{33m_2}{70}\right)+\left(-\frac{1}{42}-\frac{n}{84}-\frac{26a_0}{105}\right)m_2\Bigg)\\
&+\eta^2\left(-\frac{4}{15}-\frac{43n}{150}+\frac{17n^2}{60}-\frac{8a_0}{5}+na_0-\frac{38b_2}{25}+\frac{nb_2}{2}+a_0b_2+\frac{16j_1}{15}\right.\\
&-\frac{2nj_1}{3}+\frac{j_1^2}{5}+\frac{2}{5}m_0^2m_2+m_0\left(-\frac{32}{15}+\frac{4n}{3}+b_2+\frac{a_0m_2}{5}\right)\Bigg)\\
&+\left(\eta^6\left(\frac{734}{1575}-\frac{1381n}{6930}-\frac{5n^2}{126}+\frac{5081a_2}{770}+\frac{39na_2}{20}+\left(\frac{29}{198}+\frac{719n}{1386}+\frac{5n^2}{84}\right)m_2\right)\right.\\
&+\eta^4\left(-\frac{13n}{126}+\frac{n^2}{14}-\frac{13a_0}{21}+\frac{3na_0}{7}+\frac{47a_2}{5}-5na_2-10a_0a_2+\frac{94b_2}{105}+\frac{9nb_2}{70}+\frac{94j_1}{315}-\frac{2nj_1}{7}\right.\\
&+\left(\frac{281}{210}-\frac{41n}{84}-\frac{3n^2}{28}+\frac{a_0}{21}-\frac{3na_0}{7}\right)m_2+m_0\left(-\frac{52}{63}+\frac{4n}{7}-10a_2+\left(\frac{15}{14}-\frac{9n}{14}\right)m_2\right)\Bigg)\\
&+\eta^2\left(\frac{76b_2}{25}-nb_2-2a_0b_2-\frac{2j_1^2}{15}-\frac{4}{5}m_0^2m_2+m_0\left(-2b_2-\frac{2a_0m_2}{5}\right)\right)\Bigg)P_2\Bigg]\Bigg\}\\
&+\lambda^4\left\{\left(-\frac{209467}{970200}+\frac{6779n}{46200}+\frac{41021n^2}{554400}+\frac{61n^3}{10080}\right)\eta^8\right.\\
&+\eta^6\left(\frac{2603}{1575}-\frac{97n}{6300}-\frac{331n^2}{840}-\frac{3n^3}{70}-\frac{52a_0}{315}-\frac{292na_0}{315}-\frac{4n^2a_0}{35}+\left(-\frac{52}{315}-\frac{292n}{315}-\frac{4n^2}{35}\right)m_0\right)\\
&+\eta^2\left(\frac{164}{525}+\frac{167n}{1050}+\frac{199n^2}{2100}-\frac{83n^3}{420}+\frac{32a_0}{25}+\frac{28na_0}{25}-\frac{6n^2a_0}{5}+\frac{12a_0^2}{5}-\frac{3na_0^2}{2}\right.\\
&+\left(\frac{32}{25}+\frac{28n}{25}-\frac{6n^2}{5}+\frac{24a_0}{5}-3na_0\right)m_0+\left(\frac{12}{5}-\frac{3n}{2}\right)m_0^2\Bigg)\\
&+\eta^4\left(-\frac{9}{175}-\frac{43n}{28}+\frac{118n^2}{175}+\frac{51n^3}{400}-\frac{46a_0}{7}+\frac{19na_0}{7}+\frac{3n^2a_0}{5}+\frac{111a_0^2}{70}+\frac{9na_0^2}{20}\right.\\
&+\left(-\frac{46}{7}+\frac{19n}{7}+\frac{3n^2}{5}+\frac{111a_0}{35}+\frac{9na_0}{10}\right)m_0+\left(\frac{111}{70}+\frac{9n}{20}\right)m_0^2\Bigg)\\
&+\Omega^2\left[\eta^8\left(\frac{5298541}{18918900}+\frac{16477n}{1801800}-\frac{53351n^2}{675675}-\frac{n^3}{112}-\frac{164a_2}{9009}+\frac{928na_2}{4095}+\frac{n^2a_2}{35}\right.\right.\\
&+\left(-\frac{4343}{180180}-\frac{223n}{27720}-\frac{n^2}{3276}\right)m_2\Bigg)+\eta^6\left(-\frac{8368}{10395}-\frac{55633n}{103950}+\frac{1891n^2}{4620}+\frac{5n^3}{84}-\frac{2248a_0}{1575}\right.\\
&+\frac{1702na_0}{3465}+\frac{13n^2a_0}{105}+\frac{1479a_2}{770}-\frac{197na_2}{308}-\frac{3n^2a_2}{20}-\frac{377a_0a_2}{385}-\frac{3}{10}na_0a_2-\frac{86b_2}{3465}+\frac{787nb_2}{3465}
\end{aligned}
$$

$$+\frac{n^2b_2}{35}+\frac{4412j_1}{4725}-\frac{2498nj_1}{10395}-\frac{13n^2j_1}{210}+\left(\frac{43}{6930}+\frac{7n}{198}+\frac{8n^2}{3465}+\frac{1138a_0}{5775}+\frac{853na_0}{23100}\right)m_2$$
$$+m_0\left(-\frac{562}{315}+\frac{851n}{1386}+\frac{13n^2}{84}-\frac{377a_2}{385}-\frac{3na_2}{10}+\left(\frac{5683}{17325}+\frac{2399n}{34650}\right)m_2\right)\Bigg)$$
$$+\eta^4\left(-\frac{13}{50}+\frac{2906n}{1575}-\frac{557n^2}{840}-\frac{33n^3}{200}+\frac{92a_0}{21}-\frac{428na_0}{315}-\frac{3n^2a_0}{5}+\frac{71a_0^2}{105}-\frac{3na_0^2}{10}-\frac{2a_2}{5}\right.$$
$$-\frac{2na_2}{5}+\frac{3n^2a_2}{10}-2a_0a_2+na_0a_2+\frac{2581b_2}{1050}-\frac{53nb_2}{84}-\frac{3n^2b_2}{20}-\frac{101a_0b_2}{105}-\frac{3}{10}na_0b_2$$
$$-\frac{46j_1}{21}+\frac{41nj_1}{63}+\frac{3n^2j_1}{10}-\frac{64a_0j_1}{63}+\frac{2}{5}na_0j_1-\frac{4j_1^2}{35}-\frac{nj_1^2}{10}+m_0^2\left(\frac{71}{45}-\frac{7n}{10}-\frac{94m_2}{105}\right)$$
$$+\left(-\frac{1}{105}-\frac{2n}{105}-\frac{n^2}{140}+\frac{9a_0}{70}-\frac{19na_0}{140}-\frac{47a_0^2}{210}\right)m_2+m_0\left(\frac{115}{21}-\frac{107n}{63}-\frac{3n^2}{4}+\frac{71a_0}{35}-\frac{9na_0}{10}\right.$$
$$\left.\left.-2a_2+na_2-\frac{101b_2}{105}-\frac{3nb_2}{10}-\frac{32j_1}{21}+\frac{3nj_1}{5}+\left(\frac{32}{105}-\frac{26n}{105}-\frac{94a_0}{105}\right)m_2\right)\right)$$
$$+\eta^2\left(-\frac{24}{125}-\frac{157n}{525}-\frac{43n^2}{350}+\frac{101n^3}{420}-\frac{16a_0}{15}-\frac{86na_0}{75}+\frac{17n^2a_0}{15}-\frac{8a_0^2}{5}+na_0^2-\frac{76b_2}{125}\right.$$
$$-\frac{89nb_2}{125}+\frac{3n^2b_2}{10}-\frac{76a_0b_2}{25}+na_0b_2+\frac{8j_1}{15}+\frac{43nj_1}{75}-\frac{17n^2j_1}{30}+\frac{32a_0j_1}{15}-\frac{4}{3}na_0j_1$$
$$-\frac{8j_1^2}{15}+\frac{nj_1^2}{3}+\left(-\frac{4}{3}-\frac{43n}{30}+\frac{17n^2}{12}-\frac{24a_0}{5}+3na_0-\frac{76b_2}{25}+nb_2+\frac{16j_1}{5}-2nj_1+\frac{j_1^2}{5}\right)m_0$$
$$\left.+\frac{2}{5}m_0^3m_2+m_0^2\left(-\frac{56}{15}+\frac{7n}{3}+\frac{a_0m_2}{5}\right)\right)$$
$$+\left(\eta^8\left(-\frac{210968}{429975}+\frac{3923n}{175175}+\frac{11819n^2}{108108}+\frac{n^3}{90}-\frac{818a_2}{6435}-\frac{15037na_2}{4095}-\frac{16n^2a_2}{35}\right.\right.$$
$$\left.+\left(\frac{119789}{180180}-\frac{84911n}{194040}-\frac{10849n^2}{51480}-\frac{n^3}{60}\right)m_2\right)+\eta^2\left(\frac{152b_2}{125}+\frac{178nb_2}{125}-\frac{3n^2b_2}{5}\right.$$
$$\left.+\frac{152a_0b_2}{25}-2na_0b_2+\left(\frac{152b_2}{25}-2nb_2-\frac{2j_1^2}{15}\right)m_0-\frac{2}{5}a_0m_0^2m_2-\frac{4}{5}m_0^3m_2\right)$$
$$+\eta^6\left(-\frac{986}{3465}+\frac{8251n}{11550}-\frac{1049n^2}{4620}-\frac{5n^3}{126}+\frac{2936a_0}{1575}-\frac{2762na_0}{3465}-\frac{10n^2a_0}{63}-\frac{3681a_2}{154}+\frac{2633na_2}{308}\right.$$
$$+\frac{39n^2a_2}{20}+\frac{5081a_0a_2}{385}+\frac{39}{10}na_0a_2-\frac{443b_2}{3465}-\frac{383nb_2}{3465}-\frac{n^2b_2}{210}-\frac{3944j_1}{4725}+\frac{4253nj_1}{10395}$$
$$+\frac{5n^2j_1}{63}+\left(-\frac{1844}{693}+\frac{4n}{495}+\frac{3107n^2}{5544}+\frac{5n^3}{84}-\frac{5084a_0}{5775}+\frac{26941na_0}{23100}+\frac{5n^2a_0}{28}\right)m_2$$
$$\left.+m_0\left(\frac{734}{315}-\frac{1381n}{1386}-\frac{25n^2}{126}+\frac{5081a_2}{385}+\frac{39na_2}{10}+\left(-\frac{35579}{17325}+\frac{44873n}{34650}+\frac{5n^2}{21}\right)m_2\right)\right)$$
$$+\eta^4\left(-\frac{13n}{315}-\frac{n^2}{30}+\frac{3n^3}{70}-\frac{26na_0}{63}+\frac{2n^2a_0}{7}-\frac{13a_0^2}{21}+\frac{3na_0^2}{7}+\frac{94a_2}{25}+\frac{91na_2}{25}-3n^2a_2+\frac{94a_0a_2}{5}\right.$$
$$-10na_0a_2-\frac{487b_2}{105}+\frac{43nb_2}{42}+\frac{9n^2b_2}{70}+\frac{188a_0b_2}{105}+\frac{9}{35}na_0b_2+\frac{47nj_1}{315}-\frac{n^2j_1}{7}+\frac{188a_0j_1}{315}$$
$$\left.-\frac{4}{7}na_0j_1+\frac{52j_1^2}{105}+\left(\frac{281}{525}+\frac{319n}{525}-\frac{47n^2}{140}-\frac{9n^3}{140}+\frac{747a_0}{350}-\frac{13na_0}{28}-\frac{9n^2a_0}{28}+\frac{43a_0^2}{42}-\frac{3na_0^2}{14}\right)m_2\right.$$

$$+ m_0^2\left(-\frac{13}{9}+n+\left(\frac{86}{21}-\frac{6n}{7}\right)m_2\right)+m_0\left(-\frac{65n}{126}+\frac{5n^2}{14}-\frac{13a_0}{7}+\frac{9na_0}{7}+\frac{94a_2}{5}\right.$$
$$\left.\left.\left.-10na_2+\frac{188b_2}{105}+\frac{9nb_2}{35}+\frac{94j_1}{105}-\frac{6nj_1}{7}+\left(\frac{836}{525}+\frac{n}{21}-\frac{3n^2}{7}+\frac{86a_0}{21}-\frac{6na_0}{7}\right)m_2\right)\right)P_2\right]\right\}$$
$$+\mathcal{O}(\lambda^5,\Omega^4), \tag{F.10}$$

$$\gamma^-_{\phi\phi}=1+\lambda\left\{-\eta^2+a_0+m_0+\Omega^2\left[\eta^2a_2+b_2+\eta^2\left(5a_2+m_2\right)P_2\right]\right\}$$
$$+\lambda^2\left\{\left(\frac{37}{70}+\frac{3n}{20}\right)\eta^4+\eta^2\left(\frac{4}{5}-\frac{n}{2}-2a_0-2m_0\right)+\Omega^2\left[\eta^4\left(-\frac{89}{315}-\frac{n}{10}-a_2+\frac{m_2}{42}\right)\right.\right.$$
$$\left.\left.+\eta^2\left(-\frac{8}{15}+\frac{n}{3}-b_2-\frac{a_0m_2}{5}-\frac{2m_0m_2}{5}\right)+\eta^4\left(\frac{19}{63}+\frac{n}{7}-8a_2+\left(-\frac{43}{42}-\frac{3n}{14}\right)m_2\right)P_2\right]\right\}$$
$$+\lambda^3\left\{\left(-\frac{13}{315}-\frac{73n}{315}-\frac{n^2}{35}\right)\eta^6+\eta^4\left(-\frac{23}{14}+\frac{19n}{28}+\frac{3n^2}{20}+\frac{111a_0}{70}+\frac{9na_0}{20}+\left(\frac{111}{70}+\frac{9n}{20}\right)m_0\right)\right.$$
$$+\eta^2\left(\frac{8}{25}+\frac{7n}{25}-\frac{3n^2}{10}+\frac{12a_0}{5}-\frac{3na_0}{2}-a_0^2+\left(\frac{12}{5}-\frac{3n}{2}-2a_0\right)m_0-m_0^2\right)$$
$$+\Omega^2\left[\eta^6\left(\frac{346}{1575}+\frac{1591n}{6930}+\frac{13n^2}{420}+\frac{377a_2}{770}+\frac{3na_2}{20}+\left(-\frac{229}{6930}-\frac{8n}{3465}\right)m_2\right)\right.$$
$$+\eta^4\left(\frac{23}{21}-\frac{187n}{315}-\frac{3n^2}{20}-\frac{89a_0}{105}-\frac{3na_0}{10}+a_2-\frac{na_2}{2}-a_0a_2+\frac{101b_2}{210}+\frac{3nb_2}{20}\right.$$
$$+\frac{124j_1}{315}+\frac{nj_1}{5}+m_0\left(-\frac{356}{315}-\frac{2n}{5}-a_2+\frac{33m_2}{70}\right)+\left(\frac{1}{42}+\frac{n}{84}+\frac{26a_0}{105}\right)m_2\Big)$$
$$+\eta^2\left(-\frac{4}{15}-\frac{43n}{150}+\frac{17n^2}{60}-\frac{8a_0}{5}+na_0+\frac{38b_2}{25}-\frac{nb_2}{2}-a_0b_2+\frac{16j_1}{15}-\frac{2nj_1}{3}\right.$$
$$\left.\left.+\frac{j_1^2}{15}-\frac{2}{5}m_0^2m_2+m_0\left(-\frac{32}{15}+\frac{4n}{3}-b_2-\frac{a_0m_2}{5}\right)\right)\right.$$
$$+\left(\eta^6\left(-\frac{58}{525}-\frac{101n}{330}-\frac{5n^2}{126}+\frac{4327a_2}{770}+\frac{33na_2}{20}+\left(\frac{491}{2310}+\frac{403n}{770}+\frac{5n^2}{84}\right)m_2\right)\right.$$
$$+\eta^4\left(\frac{19n}{126}+\frac{n^2}{14}+\frac{19a_0}{21}+\frac{3na_0}{7}+\frac{37a_2}{5}-4na_2-8a_0a_2-\frac{b_2}{15}-\frac{6nb_2}{35}-\frac{38j_1}{63}-\frac{2nj_1}{7}\right.$$
$$\left.\left.\left.+\left(\frac{271}{210}-\frac{43n}{84}-\frac{3n^2}{28}-\frac{47a_0}{105}-\frac{3na_0}{7}\right)m_2+m_0\left(\frac{76}{63}+\frac{4n}{7}-8a_2+\left(\frac{9}{70}-\frac{9n}{14}\right)m_2\right)\right)\right)P_2\right]\right\}$$
$$+\lambda^4\left\{\left(-\frac{209467}{970200}+\frac{6779n}{46200}+\frac{41021n^2}{554400}+\frac{61n^3}{10080}\right)\eta^8+\eta^6\left(\frac{2603}{1575}-\frac{97n}{6300}-\frac{331n^2}{840}-\frac{3n^3}{70}\right.\right.$$
$$\left.-\frac{52a_0}{315}-\frac{292na_0}{315}-\frac{4n^2a_0}{35}+\left(-\frac{52}{315}-\frac{292n}{315}-\frac{4n^2}{35}\right)m_0\right)$$
$$+\eta^2\left(\frac{164}{525}+\frac{167n}{1050}+\frac{199n^2}{2100}-\frac{83n^3}{420}+\frac{32a_0}{25}+\frac{28na_0}{25}-\frac{6n^2a_0}{5}+\frac{12a_0^2}{5}-\frac{3na_0^2}{2}\right.$$
$$\left.+\left(\frac{32}{25}+\frac{28n}{25}-\frac{6n^2}{5}+\frac{24a_0}{5}-3na_0\right)m_0+\left(\frac{12}{5}-\frac{3n}{2}\right)m_0^2\right)$$
$$+\eta^4\left(-\frac{9}{175}-\frac{43n}{28}+\frac{118n^2}{175}+\frac{51n^3}{400}-\frac{46a_0}{7}+\frac{19na_0}{7}+\frac{3n^2a_0}{5}+\frac{111a_0^2}{70}+\frac{9na_0^2}{20}\right.$$

$$+\left(-\frac{46}{7}+\frac{19n}{7}+\frac{3n^2}{5}+\frac{111a_0}{35}+\frac{9na_0}{10}\right)m_0+\left(\frac{111}{70}+\frac{9n}{20}\right)m_0^2\Bigg)$$
$$+\Omega^2\Bigg[\eta^8\left(-\frac{1120081}{18918900}-\frac{390253n}{1801800}-\frac{6311n^2}{61425}-\frac{n^3}{112}+\frac{164a_2}{9009}-\frac{928na_2}{4095}-\frac{n^2a_2}{35}\right.$$
$$\left.+\left(\frac{4343}{180180}+\frac{223n}{27720}+\frac{n^2}{3276}\right)m_2\right)+\eta^6\left(-\frac{14908}{10395}+\frac{3079n}{20790}+\frac{7153n^2}{13860}+\frac{5n^3}{84}+\frac{1384a_0}{1575}+\frac{3182na_0}{3465}\right.$$
$$+\frac{13n^2a_0}{105}-\frac{1479a_2}{770}+\frac{197na_2}{308}+\frac{3n^2a_2}{20}+\frac{377a_0a_2}{385}+\frac{3}{10}na_0a_2+\frac{86b_2}{3465}-\frac{787nb_2}{3465}$$
$$-\frac{n^2b_2}{35}-\frac{4j_1}{525}-\frac{512nj_1}{1155}-\frac{13n^2j_1}{210}+\left(-\frac{43}{6930}-\frac{7n}{198}-\frac{8n^2}{3465}-\frac{1138a_0}{5775}-\frac{853na_0}{23100}\right)m_2$$
$$\left.+m_0\left(\frac{346}{315}+\frac{1591n}{1386}+\frac{13n^2}{84}+\frac{377a_2}{385}+\frac{3na_2}{10}+\left(-\frac{5683}{17325}-\frac{2399n}{34650}\right)m_2\right)\right)$$
$$+\eta^4\left(-\frac{13}{50}+\frac{2746n}{1575}-\frac{137n^2}{168}-\frac{33n^3}{200}+\frac{92a_0}{21}-\frac{748na_0}{315}-\frac{3n^2a_0}{5}-\frac{89a_0^2}{105}-\frac{3na_0^2}{10}\right.$$
$$+\frac{2a_2}{5}+\frac{2na_2}{5}-\frac{3n^2a_2}{10}+2a_0a_2-na_0a_2-\frac{2581b_2}{1050}+\frac{53nb_2}{84}+\frac{3n^2b_2}{20}+\frac{101a_0b_2}{105}+\frac{3}{10}na_0b_2$$
$$-\frac{46j_1}{21}+\frac{347nj_1}{315}+\frac{3n^2j_1}{10}+\frac{248a_0j_1}{315}+\frac{2}{5}na_0j_1-\frac{46j_1^2}{105}-\frac{nj_1^2}{10}+m_0^2\left(-\frac{89}{45}-\frac{7n}{10}+\frac{94m_2}{105}\right)$$
$$+\left(\frac{1}{105}+\frac{2n}{105}+\frac{n^2}{140}-\frac{9a_0}{70}+\frac{19na_0}{140}+\frac{47a_0^2}{210}\right)m_2+m_0\left(\frac{115}{21}-\frac{187n}{63}-\frac{3n^2}{4}-\frac{89a_0}{35}-\frac{9na_0}{10}\right.$$
$$\left.\left.+2a_2-na_2+\frac{101b_2}{105}+\frac{3nb_2}{10}+\frac{124j_1}{105}+\frac{3nj_1}{5}+\left(-\frac{32}{105}+\frac{26n}{105}+\frac{94a_0}{105}\right)m_2\right)\right)$$
$$+\eta^2\left(-\frac{24}{125}-\frac{157n}{525}-\frac{43n^2}{350}+\frac{101n^3}{420}-\frac{16a_0}{15}-\frac{86na_0}{75}+\frac{17n^2a_0}{15}-\frac{8a_0^2}{5}+na_0^2+\frac{76b_2}{125}\right.$$
$$+\frac{89nb_2}{125}-\frac{3n^2b_2}{10}+\frac{76a_0b_2}{25}-na_0b_2+\frac{8j_1}{15}+\frac{43nj_1}{75}-\frac{17n^2j_1}{30}+\frac{32a_0j_1}{15}-\frac{4}{3}na_0j_1$$
$$-\frac{8j_1^2}{15}+\frac{nj_1^2}{3}+\left(-\frac{4}{3}-\frac{43n}{30}+\frac{17n^2}{12}-\frac{24a_0}{5}+3na_0+\frac{76b_2}{25}-nb_2+\frac{16j_1}{5}-2nj_1+\frac{j_1^2}{15}\right)m_0$$
$$\left.-\frac{2}{5}m_0^3m_2+m_0^2\left(-\frac{56}{15}+\frac{7n}{3}-\frac{a_0m_2}{5}\right)\right)+\left(\eta^8\left(-\frac{286397}{1891890}+\frac{142253n}{573300}+\frac{6541n^2}{49140}+\frac{n^3}{90}\right.\right.$$
$$\left.-\frac{7366a_2}{45045}-\frac{1883na_2}{585}-\frac{2n^2a_2}{5}+\left(\frac{111103}{180180}-\frac{8003n}{17640}-\frac{76163n^2}{360360}-\frac{n^3}{60}\right)m_2\right)$$
$$+\eta^6\left(\frac{398}{1155}+\frac{359n}{11550}-\frac{661n^2}{1980}-\frac{5n^3}{126}-\frac{232a_0}{525}-\frac{202na_0}{165}-\frac{10n^2a_0}{63}-\frac{15447a_2}{770}\right.$$
$$+\frac{2239na_2}{308}+\frac{33n^2a_2}{20}+\frac{4327a_0a_2}{385}+\frac{33}{10}na_0a_2-\frac{41b_2}{231}+\frac{397nb_2}{1155}+\frac{11n^2b_2}{210}+\frac{8j_1}{75}$$
$$+\frac{101nj_1}{165}+\frac{5n^2j_1}{63}+\left(-\frac{437}{165}+\frac{13n}{165}+\frac{5221n^2}{9240}+\frac{5n^3}{84}-\frac{936a_0}{1925}+\frac{9549na_0}{7700}+\frac{5n^2a_0}{28}\right)m_2$$
$$\left.\left.+m_0\left(-\frac{58}{105}-\frac{101n}{66}-\frac{25n^2}{126}+\frac{4327a_2}{385}+\frac{33na_2}{10}+\left(-\frac{1153}{825}+\frac{5519n}{3850}+\frac{5n^2}{21}\right)m_2\right)\right)+\eta^4\left(\frac{19n}{315}\right.\right.$$
$$\left.+\frac{5n^2}{42}+\frac{3n^3}{70}+\frac{38na_0}{63}+\frac{2n^2a_0}{7}+\frac{19a_0^2}{21}+\frac{3na_0^2}{7}+\frac{74a_2}{25}+\frac{71na_2}{25}-\frac{12n^2a_2}{5}+\frac{74a_0a_2}{5}$$

$$
\begin{aligned}
&- 8na_0a_2 + \frac{146b_2}{525} - \frac{5nb_2}{21} - \frac{6n^2b_2}{35} - \frac{2a_0b_2}{15} - \frac{12}{35}na_0b_2 - \frac{19nj_1}{63} - \frac{n^2j_1}{7} - \frac{76a_0j_1}{63} - \frac{4}{7}na_0j_1 \\
&+ \frac{86j_1^2}{105} + \left(\frac{271}{525} + \frac{299n}{525} - \frac{7n^2}{20} - \frac{9n^3}{140} + \frac{837a_0}{350} - \frac{103na_0}{140} - \frac{9n^2a_0}{28} + \frac{121a_0^2}{210} - \frac{3na_0^2}{14}\right)m_2 \\
&+ m_0^2\left(\frac{19}{9} + n + \left(\frac{242}{105} - \frac{6n}{7}\right)m_2\right) + m_0\left(\frac{95n}{126} + \frac{5n^2}{14} + \frac{19a_0}{7} + \frac{9na_0}{7} + \frac{74a_2}{5} - 8na_2\right. \\
&\left.\left.\left. - \frac{2b_2}{15} - \frac{12nb_2}{35} - \frac{38j_1}{21} - \frac{6nj_1}{7} + \left(\frac{1156}{525} - \frac{47n}{105} - \frac{3n^2}{7} + \frac{242a_0}{105} - \frac{6na_0}{7}\right)m_2\right)\right)P_2\right]\Bigg\} + \mathcal{O}(\lambda^5, \Omega^4),
\end{aligned}
\tag{F.11}
$$

$$
\begin{aligned}
\gamma^-_{r\theta} = {}& \lambda\Omega^2\left(\frac{\eta^2a_2}{2} - b_2\right)P_{21} + \lambda^2\Omega^2\left[\eta^4\left(-\frac{1}{63} - \frac{a_2}{2} + \frac{2m_2}{21}\right) + \eta^2\left(b_2 - \frac{a_0m_2}{10} - \frac{m_0m_2}{5}\right)\right]P_{21} \\
&+ \lambda^3\Omega^2\left\{\eta^6\left[-\frac{29}{1575} + \frac{5n}{693} - \frac{163a_2}{1540} + \frac{3na_2}{40} + \left(-\frac{634}{3465} - \frac{76n}{3465}\right)m_2\right]\right. \\
&+ \eta^4\left[-\frac{n}{126} - \frac{a_0}{21} + \frac{6a_2}{5} - \frac{na_2}{4} - \frac{a_0a_2}{2} - \frac{13b_2}{30} - \frac{3nb_2}{20} + \frac{64j_1}{315} + m_0\left(-\frac{4}{63} - \frac{a_2}{2} + \frac{17m_2}{35}\right)\right. \\
&\left.\left. + \left(\frac{2}{21} + \frac{n}{21} + \frac{61a_0}{210}\right)m_2\right] + \eta^2\left[-\frac{26b_2}{25} + \frac{nb_2}{2} + a_0b_2 - \frac{j_1^2}{5} - \frac{1}{5}m_0^2m_2 + m_0\left(b_2 - \frac{a_0m_2}{10}\right)\right]\right\}P_{21} \\
&+ \lambda^4\Omega^2\left\{\eta^8\left[\frac{1560061}{18918900} - \frac{3169n}{360360} - \frac{292n^2}{135135} + \frac{4493a_2}{6435} - \frac{47na_2}{1638} - \frac{n^2a_2}{70} + \left(\frac{53632}{315315} + \frac{23n}{315}\right.\right.\right. \\
&\left.\left. + \frac{17n^2}{3276}\right)m_2\right] + \eta^2\left[-\frac{52b_2}{125} - \frac{53nb_2}{125} + \frac{3n^2b_2}{10} - \frac{52a_0b_2}{25} + na_0b_2 + \left(-\frac{52b_2}{25} + nb_2 - \frac{j_1^2}{5}\right)m_0\right. \\
&\left. - \frac{1}{10}a_0m_0^2m_2 - \frac{1}{5}m_0^3m_2\right] + \eta^6\left[-\frac{9}{385} - \frac{194n}{17325} + \frac{5n^2}{693} - \frac{116a_0}{1575} + \frac{20na_0}{693} - \frac{3637a_2}{1540} - \frac{19na_2}{616}\right. \\
&+ \frac{3n^2a_2}{40} - \frac{163a_0a_2}{770} + \frac{3}{20}na_0a_2 - \frac{503b_2}{3465} + \frac{724nb_2}{3465} + \frac{n^2b_2}{35} - \frac{1556j_1}{4725} - \frac{74nj_1}{2079} \\
&+ \left(-\frac{64}{3465} - \frac{142n}{693} - \frac{76n^2}{3465} - \frac{12191a_0}{23100} - \frac{3733na_0}{46200}\right)m_2 + m_0\left(-\frac{29}{315} + \frac{25n}{693} - \frac{163a_2}{770}\right. \\
&\left.\left. + \frac{3na_2}{20} + \left(-\frac{23893}{34650} - \frac{8159n}{69300}\right)m_2\right)\right] + \eta^4\left[-\frac{n}{315} - \frac{n^2}{210} - \frac{2na_0}{63} - \frac{a_0^2}{21} + \frac{12a_2}{25} + \frac{31na_2}{50}\right. \\
&- \frac{3n^2a_2}{20} + \frac{12a_0a_2}{5} - \frac{1}{2}na_0a_2 + \frac{311b_2}{150} - \frac{7nb_2}{12} - \frac{3n^2b_2}{20} - \frac{13a_0b_2}{15} - \frac{3}{10}na_0b_2 + \frac{32nj_1}{315} \\
&+ \frac{128a_0j_1}{315} + \frac{23j_1^2}{105} + m_0^2\left(-\frac{1}{9} + \frac{82m_2}{105}\right) + \left(\frac{4}{105} + \frac{8n}{105} + \frac{n^2}{35} + \frac{8a_0}{175} + \frac{27na_0}{140} + \frac{41a_0^2}{210}\right)m_2 \\
&\left.\left. + m_0\left(-\frac{5n}{126} - \frac{a_0}{7} + \frac{12a_2}{5} - \frac{na_2}{2} - \frac{13b_2}{15} - \frac{3nb_2}{10} + \frac{64j_1}{105} + \left(-\frac{52}{525} + \frac{61n}{210} + \frac{82a_0}{105}\right)m_2\right)\right]\right\}P_{21} \\
&+ \mathcal{O}(\lambda^5, \Omega^4).
\end{aligned}
\tag{F.12}
$$

2. Constants of the solution of the homogeneous system after Lichnerowicz matching

First, we give the value of the constant factors of the exterior metric. The ones associated with multipole moments are

$$M_0 = 1 + \lambda\left[\frac{14}{5} + \frac{n}{5} + \left(\frac{8}{15} - \frac{2n}{15}\right)\Omega^2\right] + \lambda^2\left[\frac{73}{7} + \frac{64n}{35} + \frac{3n^2}{35} + \left(\frac{488}{105} - \frac{36n}{35} - \frac{8n^2}{105}\right)\Omega^2\right] + \lambda^3\left[\frac{13894}{315} + \frac{4169n}{315} + \frac{2116n^2}{1575} + \frac{74n^3}{1575} + \left(\frac{1468}{45} - \frac{918n}{175} - \frac{376n^2}{315} - \frac{4n^3}{75}\right)\Omega^2\right] + \mathcal{O}(\lambda^4, \Omega^4), \tag{F.13}$$

$$M_2 = -\frac{1}{2} + \lambda\left(-\frac{37}{35} + \frac{n}{14}\right) + \lambda^2\left(-\frac{83927}{22050} + \frac{128n}{735} + \frac{10n^2}{441}\right) + \lambda^3\left(-\frac{4856219}{282975} - \frac{476479n}{1697850} + \frac{6443n^2}{33957} + \frac{67n^3}{6174}\right) + \mathcal{O}(\lambda^4, \Omega^2), \tag{F.14}$$

$$J_1 = \frac{2}{5} + \frac{\Omega^2}{3} + \lambda\left[\frac{16}{7} + \frac{2n}{35} + \left(\frac{176}{105} - \frac{3n}{35}\right)\Omega^2\right] + \lambda^2\left[\frac{18896}{1575} + \frac{76n}{75} + \frac{34n^2}{1575} + \left(\frac{34889}{3675} - \frac{494n}{735} - \frac{124n^2}{3675}\right)\Omega^2\right] + \lambda^3\left[\frac{120744}{1925} + \frac{181352n}{17325} + \frac{10376n^2}{17325} + \frac{64n^3}{5775} + \left(\frac{67472308}{1157625} - \frac{3080233n}{848925} - \frac{1664972n^2}{2546775} - \frac{49393n^3}{2546775}\right)\Omega^2\right] + \mathcal{O}(\lambda^4, \Omega^4), \tag{F.15}$$

$$J_3 = -\frac{1}{7} + \lambda\left(-\frac{496}{735} + \frac{11n}{441}\right) + \lambda^2\left(-\frac{2703854}{848925} + \frac{358n}{5775} + \frac{1234n^2}{169785}\right) + \lambda^3\left(-\frac{1396705292}{89137125} - \frac{4293174n}{8583575} + \frac{608000n^2}{9270261} + \frac{10433n^3}{3090087}\right) + \mathcal{O}(\lambda^4, \Omega^2), \tag{F.16}$$

and the gauge constants

$$A_0 = \lambda\left(\frac{8}{35} + \frac{4\Omega^2}{105}\right) + \lambda^2\left[\frac{934}{1575} + \frac{136n}{1575} + \left(\frac{16}{35} - \frac{4n}{75}\right)\Omega^2\right] + \lambda^3\left[\frac{11908}{17325} + \frac{10942n}{17325} + \frac{256n^2}{5775} + \left(\frac{64004}{23625} - \frac{172n}{825} - \frac{716n^2}{17325}\right)\Omega^2\right] \tag{F.17}$$

$$A_2 = -\frac{4\lambda}{63} + \left(-\frac{15226}{121275} - \frac{68n}{24255}\right)\lambda^2 + \left(-\frac{720532}{18393375} - \frac{40358n}{1003275} - \frac{916n^2}{2207205}\right)\lambda^3 + \mathcal{O}(\lambda^4, \Omega^2), \tag{F.18}$$

$$B_2 = \left(\frac{1424}{11025} + \frac{8n}{2205}\right)\lambda^2 + \left(\frac{13238572}{12733875} + \frac{181792n}{2546775} + \frac{64n^2}{33957}\right)\lambda^3 + \mathcal{O}(\lambda^4, \Omega^2), \tag{F.19}$$

In the interior, the constants take the values

$$m_0 = 3 + \lambda\left[\frac{9}{2} + \frac{3n}{4} + \left(1 - \frac{n}{2}\right)\Omega^2\right] + \lambda^2\left[\frac{458}{35} + \frac{9n}{2} + \frac{7n^2}{20} + \left(\frac{733}{105} - \frac{12n}{5} - \frac{19n^2}{60}\right)\Omega^2\right] + \lambda^3\left[\frac{200357}{4200} + \frac{15359n}{600} + \frac{4477n^2}{1120} + \frac{45n^3}{224} + \left(\frac{22814}{525} - \frac{18763n}{2100} - \frac{1471n^2}{420} - \frac{391n^3}{1680}\right)\Omega^2\right] + \mathcal{O}(\lambda^4, \Omega^4), \tag{F.20}$$

$$m_2 = -1 + \lambda\left(-\frac{29}{35} - \frac{3n}{14}\right) + \lambda^2\left(-\frac{3413}{1225} - \frac{75n}{98} - \frac{47n^2}{588}\right) + \left(-\frac{23189521}{1697850} - \frac{126362n}{33957} - \frac{186041n^2}{271656} - \frac{1021n^3}{24696}\right)\lambda^3 + \mathcal{O}(\lambda^4, \Omega^2), \tag{F.21}$$

$$j_1 = 2 + \frac{2\Omega^2}{3} + \lambda\left[\frac{49}{5} + \frac{n}{2} + \left(\frac{289}{105} - \frac{5n}{14}\right)\Omega^2\right] + \lambda^2\left[\frac{4903}{105} + \frac{449n}{70} + \frac{7n^2}{30} + \left(\frac{196451}{11025} - \frac{26161n}{7350} - \frac{983n^2}{4410}\right)\Omega^2\right] + \lambda^3\left[\frac{34097}{150} + \frac{14117n}{252} + \frac{59071n^2}{12600} + \frac{15n^3}{112} + \left(\frac{3215569211}{25467750} - \frac{26642599n}{1131900} - \frac{43675099n^2}{10187100} - \frac{29951n^3}{185220}\right)\Omega^2\right] + \mathcal{O}(\lambda^4, \Omega^4), \tag{F.22}$$

$$j_3 = -\frac{2}{7} + \lambda\left(-\frac{326}{245} - \frac{3n}{49}\right) + \lambda^2\left(-\frac{51329}{8575} - \frac{397n}{490} - \frac{47n^2}{2058}\right) + \lambda^3\left(-\frac{458385352}{16506875} - \frac{50549n}{7203} - \frac{687657n^2}{1320550} - \frac{1021n^3}{86436}\right) + \mathcal{O}(\lambda^4, \Omega^2), \tag{F.23}$$

$$a_0 = \lambda\left(7 + \frac{2\Omega^2}{3}\right) + \lambda^2\left[\frac{544}{15} + \frac{107n}{30} + \left(\frac{158}{15} - \frac{34n}{15}\right)\Omega^2\right] + \lambda^3\left[\frac{53449}{300} + \frac{4043n}{105} + \frac{1191n^2}{560} + \left(\frac{295867}{3150} - \frac{2649n}{140} - \frac{871n^2}{420}\right)\Omega^2\right] + \mathcal{O}(\lambda^4, \Omega^4), \tag{F.24}$$

$$a_2 = -\frac{86\lambda}{105} + \lambda^2\left(-\frac{14836}{3675} - \frac{667n}{1470}\right) + \lambda^3\left(-\frac{13307503}{694575} - \frac{361421n}{77175} - \frac{231659n^2}{926100}\right) + \mathcal{O}(\lambda^4, \Omega^2), \tag{F.25}$$

$$b_2 = \lambda^2\left(-\frac{67}{175} - \frac{n}{210}\right) + \lambda^3\left(-\frac{1025011}{220500} - \frac{18097n}{88200} - \frac{5n^2}{1764}\right) + \mathcal{O}(\lambda^4, \Omega^2). \tag{F.26}$$

3. Changing to QI coordinates

3.1. Exterior

The original spherical-like coordinates $\{r, \theta\}$ change to the QI $\{R, \Theta\}$as

$$\frac{r}{R} = 1 + \lambda^2\left\{\frac{1}{4\hat{R}^2} - \frac{4}{35\hat{R}^3} + \Omega^2\left[\frac{1}{48\hat{R}^2} - \frac{2}{105\hat{R}^3} + \frac{1}{192\hat{R}^4} + \left(-\frac{1}{12\hat{R}^2} - \frac{1}{12\hat{R}^4} + \frac{2}{21\hat{R}^5}\right)P_2\right]\right\}$$

$$
\begin{aligned}
&+\lambda^3\left\{\left(\frac{7}{5}+\frac{n}{10}\right)\frac{1}{\hat{R}^2}+\left(-\frac{992}{1575}-\frac{68n}{1575}\right)\frac{1}{\hat{R}^3}\right.\\
&+\Omega^2\left[\left(\frac{379}{840}-\frac{141n}{2240}\right)\frac{1}{\hat{R}^2}+\left(-\frac{8}{35}+\frac{2n}{75}\right)\frac{1}{\hat{R}^3}+\left(\frac{39}{2800}+\frac{n}{3360}\right)\frac{1}{\hat{R}^4}\right.\\
&\left.\left.+\left(\left(-\frac{31}{42}-\frac{5n}{336}\right)\frac{1}{\hat{R}^2}+\left(\frac{1424}{11025}+\frac{8n}{2205}\right)\frac{1}{\hat{R}^3}+\left(-\frac{67}{175}-\frac{n}{210}\right)\frac{1}{\hat{R}^4}+\left(\frac{18008}{40425}+\frac{34n}{8085}\right)\frac{1}{\hat{R}^5}\right)P_2\right]\right\}\\
&+\lambda^4\left\{\left(\frac{2511}{350}+\frac{209n}{175}+\frac{37n^2}{700}\right)\frac{1}{\hat{R}^2}+\left(-\frac{54464}{17325}-\frac{8936n}{17325}-\frac{128n^2}{5775}\right)\frac{1}{\hat{R}^3}-\frac{2}{175\hat{R}^5}\right.\\
&+\Omega^2\left[\left(\frac{60273719}{14112000}-\frac{44477n}{78400}-\frac{70403n^2}{1411200}\right)\frac{1}{\hat{R}^2}+\left(-\frac{44602}{23625}+\frac{196n}{825}+\frac{358n^2}{17325}\right)\frac{1}{\hat{R}^3}\right.\\
&+\left(-\frac{5819}{423360}+\frac{793n}{176400}+\frac{13n^2}{211680}\right)\frac{1}{\hat{R}^4}+\frac{1}{350\hat{R}^5}-\frac{1}{1344\hat{R}^6}+\frac{1}{840\hat{R}^7}\\
&+\left(\left(-\frac{16943159}{3528000}-\frac{18889n}{58800}-\frac{2173n^2}{352800}\right)\frac{1}{\hat{R}^2}+\left(\frac{13238572}{12733875}+\frac{181792n}{2546775}+\frac{64n^2}{33957}\right)\frac{1}{\hat{R}^3}\right.\\
&+\left(-\frac{35375}{21168}-\frac{1297n}{11025}-\frac{13n^2}{13230}\right)\frac{1}{\hat{R}^4}+\left(\frac{36460142}{18393375}+\frac{42292n}{334425}+\frac{458n^2}{735735}\right)\frac{1}{\hat{R}^5}+\frac{1}{1344\hat{R}^6}\\
&\left.\left.\left.+\frac{124}{6615\hat{R}^7}\right)P_2\right]\right\}+\mathcal{O}(\lambda^5,\Omega^4),
\end{aligned}
\tag{F.27}
$$

$$
\begin{aligned}
\cos\theta = P_1 &+\lambda^2\Omega^2\left[\left(-\frac{1}{20\hat{R}^2}+\frac{3}{40\hat{R}^4}-\frac{4}{105\hat{R}^5}\right)P_1+\left(\frac{1}{20\hat{R}^2}-\frac{3}{40\hat{R}^4}+\frac{4\frac{1}{\hat{R}^5}}{105}\right)P_3\right]\\
&+\lambda^3\Omega^2\left\{\left[\left(-\frac{31}{70}-\frac{n}{112}\right)\frac{1}{\hat{R}^2}+\left(\frac{1424}{18375}+\frac{8n}{3675}\right)\frac{1}{\hat{R}^3}\right.\right.\\
&\left.+\left(\frac{631}{1750}+\frac{3n}{700}\right)\frac{1}{\hat{R}^4}+\left(-\frac{36016}{202125}-\frac{68n}{40425}\right)\frac{1}{\hat{R}^5}\right]P_1\\
&\left.+\left[\left(\frac{31}{70}+\frac{n}{112}\right)\frac{1}{\hat{R}^2}+\left(-\frac{1424}{18375}-\frac{8n}{3675}\right)\frac{1}{\hat{R}^3}-\left(\frac{631}{1750}+\frac{3n}{700}\right)\frac{1}{\hat{R}^4}+\left(\frac{36016}{202125}+\frac{68n}{40425}\right)\frac{1}{\hat{R}^5}\right]P_3\right\}\\
&+\lambda^4\Omega^2\left\{\left[\left(-\frac{16943159}{5880000}-\frac{18889n}{98000}-\frac{2173n^2}{588000}\right)\frac{1}{\hat{R}^2}+\left(\frac{13238572}{21223125}+\frac{181792n}{4244625}+\frac{64n^2}{56595}\right)\frac{1}{\hat{R}^3}\right.\right.\\
&+\left(\frac{25073}{14700}+\frac{1353n}{12250}+\frac{13n^2}{14700}\right)\frac{1}{\hat{R}^4}+\left(-\frac{24540328}{30655625}-\frac{84584n}{1672125}-\frac{916n^2}{3678675}\right)\frac{1}{\hat{R}^5}\\
&\left.-\frac{41}{2240\hat{R}^6}+\frac{463}{33075\hat{R}^7}-\frac{16}{3675\hat{R}^8}\right]P_1+\left[\left(\frac{16943159}{5880000}+\frac{18889n}{98000}+\frac{2173n^2}{588000}\right)\frac{1}{\hat{R}^2}\right.\\
&+\left(-\frac{13238572}{21223125}-\frac{181792n}{4244625}-\frac{64n^2}{56595}\right)\frac{1}{\hat{R}^3}+\left(-\frac{25073}{14700}-\frac{1353n}{12250}-\frac{13n^2}{14700}\right)\frac{1}{\hat{R}^4}\\
&\left.\left.+\left(\frac{24540328}{30655625}+\frac{84584n}{1672125}+\frac{916n^2}{3678675}\right)\frac{1}{\hat{R}^5}+\frac{41}{2240\hat{R}^6}-\frac{463}{33075\hat{R}^7}+\frac{16}{3675\hat{R}^8}\right]P_3\right\}+\mathcal{O}(\lambda^5,\Omega^4),
\end{aligned}
\tag{F.28}
$$

where $P_l := P_l(\cos\Theta)$ and $\hat{R} = R/r_s$. This makes the γ^+_{rr}, $\gamma^+_{\theta\theta}$ change to

$$
\gamma^+_{RR} = 1+\lambda\left(2\frac{1}{\hat{R}}-\frac{1}{\hat{R}^3}\Omega^2 P_2\right)+\lambda^2\left\{\left(\frac{28}{5}+\frac{2n}{5}\right)\frac{1}{\hat{R}}+\frac{3}{2\hat{R}^2}\right.
$$

$$
\begin{aligned}
&+\Omega^2\left[\left(\frac{16}{15}-\frac{4n}{15}\right)\frac{1}{\hat{R}}-\frac{1}{24\hat{R}^2}-\frac{1}{32\hat{R}^4}+\left(\frac{1}{6\hat{R}^2}+\left(-\frac{74}{35}+\frac{n}{7}\right)\frac{1}{\hat{R}^3}-\frac{3}{2\hat{R}^4}\right)P_2\right]\Bigg\}\\
&+\lambda^3\Bigg\{\left(\frac{146}{7}+\frac{128n}{35}+\frac{6n^2}{35}\right)\frac{1}{\hat{R}}+\left(\frac{42}{5}+\frac{3n}{5}\right)\frac{1}{\hat{R}^2}+\frac{1}{2\hat{R}^3}+\Omega^2\left[\left(\frac{976}{105}-\frac{72n}{35}-\frac{16n^2}{105}\right)\frac{1}{\hat{R}}\right.\\
&+\left(\frac{517}{420}-\frac{1369n}{3360}\right)\frac{1}{\hat{R}^2}-\frac{1}{8\hat{R}^3}+\left(-\frac{117}{1400}-\frac{n}{560}\right)\frac{1}{\hat{R}^4}-\frac{7}{96\hat{R}^5}+\left(\left(\frac{31}{21}+\frac{5n}{168}\right)\frac{1}{\hat{R}^2}\right.\\
&\left.\left.+\left(-\frac{156829}{22050}+\frac{256n}{735}+\frac{20n^2}{441}\right)\frac{1}{\hat{R}^3}+\left(-\frac{1262}{175}-\frac{3n}{35}\right)\frac{1}{\hat{R}^4}-\frac{61}{84\hat{R}^5}\right)P_2\right]\Bigg\}\\
&+\lambda^4\Bigg\{\left(\frac{27788}{315}+\frac{8338n}{315}+\frac{4232n^2}{1575}+\frac{148n^3}{1575}\right)\frac{1}{\hat{R}}+\left(\frac{7533}{175}+\frac{1254n}{175}+\frac{111n^2}{350}\right)\frac{1}{\hat{R}^2}\\
&+\left(\frac{21}{5}+\frac{3n}{10}\right)\frac{1}{\hat{R}^3}+\frac{1}{16\hat{R}^4}\\
&+\Omega^2\left[\left(\frac{2936}{45}-\frac{1836n}{175}-\frac{752n^2}{315}-\frac{8n^3}{75}\right)\frac{1}{\hat{R}}+\left(\frac{113048521}{7056000}-\frac{475849n}{117600}-\frac{219901n^2}{705600}\right)\frac{1}{\hat{R}^2}\right.\\
&+\left(-\frac{23}{35}-\frac{277n}{1120}\right)\frac{1}{\hat{R}^3}+\left(-\frac{2603}{35280}-\frac{793n}{29400}-\frac{13n^2}{35280}\right)\frac{1}{\hat{R}^4}\\
&+\left(-\frac{607}{1200}-\frac{3n}{160}\right)\frac{1}{\hat{R}^5}-\frac{61}{896\hat{R}^6}+\left(\left(\frac{16943159}{1764000}+\frac{18889n}{29400}+\frac{2173n^2}{176400}\right)\frac{1}{\hat{R}^2}\right.\\
&+\left(-\frac{8063098}{282975}-\frac{2526317n}{6791400}+\frac{12886n^2}{33957}+\frac{67n^3}{3087}\right)\frac{1}{\hat{R}^3}\\
&\left.\left.+\left(-\frac{49411}{1470}-\frac{2706n}{1225}-\frac{13n^2}{735}\right)\frac{1}{\hat{R}^4}+\left(-\frac{40447}{7350}-\frac{183n}{980}\right)\frac{1}{\hat{R}^5}-\frac{19}{224\hat{R}^6}\right)P_2\right]\Bigg\}+\mathcal{O}(\lambda^5,\Omega^4),
\end{aligned}
\tag{F.29}
$$

$$
\gamma^{+}_{\Theta\Theta}=R^2\gamma^{+}_{RR},
\tag{F.30}
$$

$$
\gamma^{+}_{R\Theta}=0.
\tag{F.31}
$$

with the rest of the components changing straighforwardly through eqs. (F.27) and (F.28).

3.2. *Interior*

In the interior, the coordinates change as

$$
\begin{aligned}
r/R=1+\lambda^2&\left\{\frac{1}{4}-\frac{3\hat{R}^2}{20}+\frac{\hat{R}^4}{28}+\Omega^2\left[\frac{1}{96}-\frac{\hat{R}^2}{240}+\frac{\hat{R}^4}{1344}+\left(-\frac{13\hat{R}^2}{84}+\frac{\hat{R}^4}{12}\right)P_2\right]\right\}\\
&+\lambda^3\left\{\frac{22}{15}+\frac{7n}{60}+\left(-\frac{24}{25}-\frac{9n}{100}\right)\hat{R}^2+\left(\frac{2}{7}+\frac{n}{28}\right)\hat{R}^4+\left(-\frac{1}{45}-\frac{n}{180}\right)\hat{R}^6+\right.\\
&\Omega^2\left[\frac{373}{840}-\frac{31n}{420}+\left(-\frac{2}{7}+\frac{953n}{16800}\right)\hat{R}^2+\left(\frac{143}{1680}-\frac{5n}{224}\right)\hat{R}^4+\left(-\frac{29}{4200}+\frac{23n}{6720}\right)\hat{R}^6\right.\\
&\left.\left.+\left(-\frac{67}{175}-\frac{n}{210}+\left(-\frac{709}{1225}-\frac{247n}{5880}\right)\hat{R}^2+\left(\frac{346}{735}+\frac{8n}{147}\right)\hat{R}^4+\left(-\frac{1921}{34650}-\frac{1079n}{55440}\right)\hat{R}^6\right)P_2\right]\right\}\\
&+\lambda^4\left\{\frac{132413}{16800}+\frac{2351n}{1680}+\frac{15n^2}{224}+\left(-\frac{15431}{2800}-\frac{771n}{700}-\frac{83n^2}{1400}\right)\hat{R}^2\right.
\end{aligned}
$$

$$
\begin{aligned}
&+\left(\frac{263}{140}+\frac{131n}{280}+\frac{17n^2}{560}\right)\hat{R}^4+\left(-\frac{1229}{5040}-\frac{17n}{180}-\frac{n^2}{120}\right)\hat{R}^6\\
&+\left(\frac{851}{61600}+\frac{219n}{30800}+\frac{61n^2}{61600}\right)\hat{R}^8+\Omega^2\left[\frac{1630711}{352800}-\frac{31433n}{47040}-\frac{2021n^2}{31360}\right.\\
&+\left(-\frac{135791689}{42336000}+\frac{183349n}{352800}+\frac{123737n^2}{2116800}\right)\hat{R}^2+\left(\frac{618419}{564480}-\frac{1689n}{7840}-\frac{4367n^2}{141120}\right)\hat{R}^4\\
&+\left(-\frac{24673}{169344}+\frac{3273n}{78400}+\frac{2507n^2}{282240}\right)\hat{R}^6+\left(\frac{49361}{6048000}-\frac{3359n}{1108800}-\frac{7387n^2}{6652800}\right)\hat{R}^8\\
&+\left(-\frac{771751}{220500}-\frac{16837n}{88200}-\frac{5n^2}{1764}+\left(-\frac{136037887}{74088000}-\frac{266743n}{617400}-\frac{15067n^2}{740880}\right)\hat{R}^2\right.\\
&+\left(\frac{727493}{308700}+\frac{4173n}{6860}+\frac{2231n^2}{61740}\right)\hat{R}^4+\left(-\frac{11542879}{23284800}-\frac{134611n}{529200}-\frac{17233n^2}{776160}\right)\hat{R}^6\\
&\left.\left.+\left(\frac{2323883}{54054000}+\frac{50371n}{1801800}+\frac{12443n^2}{2702700}\right)\hat{R}^8\right)P_2\right]\Bigg\}+\mathcal{O}(\lambda^5,\Omega^4),
\end{aligned}
\tag{F.32}
$$

$$
\begin{aligned}
\cos\theta = {}& P_1+\lambda^2\Omega^2\left[\left(-\frac{3\hat{R}^2}{140}+\frac{\hat{R}^4}{120}\right)P_1+\left(\frac{3\hat{R}^2}{140}-\frac{\hat{R}^4}{120}\right)P_3\right]\\
&+\lambda^3\Omega^2\left\{\left(-\frac{201}{875}-\frac{n}{350}+\left(\frac{263}{6125}-\frac{57n}{9800}\right)\hat{R}^2+\left(\frac{1}{294}+\frac{19n}{2940}\right)\hat{R}^4+\left(\frac{23}{57750}-\frac{179n}{92400}\right)\hat{R}^6\right)P_1\right.\\
&\left.+\left[\frac{201}{875}+\frac{n}{350}+\left(-\frac{263}{6125}+\frac{57n}{9800}\right)\hat{R}^2+\left(-\frac{1}{294}-\frac{19n}{2940}\right)\hat{R}^4+\left(-\frac{23}{57750}+\frac{179n}{92400}\right)\hat{R}^6\right]P_3\right\}\\
&+\lambda^4\Omega^2\left\{\left(-\frac{771751}{367500}-\frac{16837n}{147000}-\frac{n^2}{588}+\left(\frac{355916209}{370440000}+\frac{589n}{343000}-\frac{1159n^2}{411600}\right)\hat{R}^2\right.\right.\\
&+\left(-\frac{91779}{343000}+\frac{956n}{25725}+\frac{309n^2}{68600}\right)\hat{R}^4+\left(\frac{53983}{1108800}-\frac{13759n}{882000}-\frac{3013n^2}{1293600}\right)\hat{R}^6\\
&\left.+\left(-\frac{141311}{45045000}+\frac{1207n}{1001000}+\frac{1237n^2}{3003000}\right)\hat{R}^8\right)P_1+\left[\frac{771751}{367500}+\frac{16837n}{147000}+\frac{n^2}{588}\right.\\
&+\left(-\frac{355916209}{370440000}-\frac{589n}{343000}+\frac{1159n^2}{411600}\right)\hat{R}^2+\left(\frac{91779}{343000}-\frac{956n}{25725}-\frac{309n^2}{68600}\right)\hat{R}^4\\
&\left.\left.+\left(-\frac{53983}{1108800}+\frac{13759n}{882000}+\frac{3013n^2}{1293600}\right)\hat{R}^6+\left(\frac{141311}{45045000}-\frac{1207n}{1001000}-\frac{1237n^2}{3003000}\right)\hat{R}^8\right]P_3\right\}\\
&+\mathcal{O}(\lambda^5,\Omega^4),
\end{aligned}
\tag{F.33}
$$

with, again, $P_l := P_l(\cos\Theta)$ and $\hat{R} = R/r_s$. The r, θ components of the interior change to

$$
\begin{aligned}
\gamma^{-}_{\bar{R}R} = {}& 1+\lambda\left(3-\hat{R}^2-\hat{R}^2\Omega^2P_2\right)\\
&+\lambda^2\left\{12+\frac{3n}{4}+\left(-\frac{11}{2}-\frac{n}{2}\right)\hat{R}^2+\left(\frac{3}{5}+\frac{3n}{20}\right)\hat{R}^4+\Omega^2\left[\frac{27}{16}-\frac{n}{2}+\left(-\frac{23}{24}+\frac{n}{3}\right)\hat{R}^2\right.\right.\\
&\left.\left.+\left(\frac{127}{480}-\frac{n}{10}\right)\hat{R}^4+\left(\left(-\frac{303}{70}-\frac{3n}{14}\right)\hat{R}^2+\left(\frac{37}{42}+\frac{5n}{14}\right)\hat{R}^4\right)P_2\right]\right\}\\
&+\lambda^3\left\{\frac{753}{14}+\frac{83n}{10}+\frac{7n^2}{20}+\left(-\frac{283}{10}-\frac{59n}{10}-\frac{3n^2}{10}\right)\hat{R}^2+\left(\frac{9}{2}+\frac{21n}{10}+\frac{3n^2}{20}\right)\hat{R}^4\right.
\end{aligned}
$$

$$
\begin{aligned}
&+\left(-\frac{8}{35}-\frac{17n}{70}-\frac{n^2}{35}\right)\hat{R}^6\\
&+\Omega^2\left[\frac{31021}{1680}-\frac{337n}{70}-\frac{19n^2}{60}+\left(-\frac{4829}{420}+\frac{1893n}{560}+\frac{17n^2}{60}\right)\hat{R}^2+\left(\frac{4141}{1120}-\frac{1943n}{1680}-\frac{3n^2}{20}\right)\hat{R}^4\right.\\
&+\left(-\frac{3527}{8400}+\frac{139n}{1120}+\frac{13n^2}{420}\right)\hat{R}^6+\left(\left(-\frac{139163}{7350}-\frac{563n}{196}-\frac{47n^2}{588}\right)\hat{R}^2\right.\\
&\left.\left.+\left(\frac{2399}{490}+\frac{2873n}{735}+\frac{11n^2}{49}\right)\hat{R}^4+\left(-\frac{338}{1575}-\frac{125n}{168}-\frac{25n^2}{252}\right)\hat{R}^6\right)P_2\right]\Bigg\}\\
&+\lambda^4\left\{\frac{76873}{300}+\frac{285503n}{4200}+\frac{7009n^2}{1120}+\frac{45n^3}{224}+\left(-\frac{12241}{84}-\frac{41999n}{840}-\frac{4577n^2}{840}-\frac{83n^3}{420}\right)\hat{R}^2\right.\\
&+\left(\frac{10731}{400}+\frac{1911n}{100}+\frac{1149n^2}{400}+\frac{51n^3}{400}\right)\hat{R}^4+\left(-\frac{257}{140}-\frac{943n}{280}-\frac{211n^2}{280}-\frac{3n^3}{70}\right)\hat{R}^6\\
&+\left(\frac{191}{12600}+\frac{2713n}{12600}+\frac{547n^2}{7200}+\frac{61n^3}{10080}\right)\hat{R}^8+\Omega^2\left[\frac{11788857}{78400}-\frac{2341797n}{78400}\right.\\
&-\frac{268367n^2}{47040}-\frac{391n^3}{1680}+\left(-\frac{139920383}{1411200}+\frac{828619n}{39200}+\frac{360277n^2}{70560}+\frac{101n^3}{420}\right)\hat{R}^2\\
&+\left(\frac{12108443}{352800}-\frac{662993n}{94080}-\frac{196219n^2}{70560}-\frac{33n^3}{200}\right)\hat{R}^4\\
&+\left(-\frac{57449}{9600}+\frac{2699n}{2800}+\frac{5113n^2}{6720}+\frac{5n^3}{84}\right)\hat{R}^6+\left(\frac{204809}{504000}-\frac{43n}{2688}-\frac{8083n^2}{100800}-\frac{n^3}{112}\right)\hat{R}^8\\
&+\left(\left(-\frac{775698071}{9055200}-\frac{33553181n}{1358280}-\frac{210233n^2}{113190}-\frac{1021n^3}{24696}\right)\hat{R}^2\right.\\
&+\left(\frac{3274297}{154350}+\frac{6290503n}{205800}+\frac{497941n^2}{123480}+\frac{101n^3}{686}\right)\hat{R}^4\\
&+\left(\frac{20231}{39200}-\frac{777667n}{88200}-\frac{25021n^2}{11760}-\frac{395n^3}{3528}\right)\hat{R}^6\\
&\left.\left.\left.+\left(-\frac{57763}{173250}+\frac{102317n}{138600}+\frac{45257n^2}{138600}+\frac{n^3}{36}\right)\hat{R}^8\right)P_2\right]\right\}+\mathcal{O}(\lambda^5,\Omega^4),
\end{aligned}
\tag{F.34}
$$

$$
\gamma^{-}_{\Theta\Theta}=R^2\gamma^{-}_{RR}, \tag{F.35}
$$

$$
\gamma^{-}_{R\Theta}=0. \tag{F.36}
$$

Appendix G

The bilayer interior model

1. Metric components

Here we give the unmatched metric components in orthonormal cobasis for the source of the bilayer model. The unmatched exterior is the same as in CGMR and appears in Chapter 3 and, to a higher post-Minkowskian order, in Appendix F.

1.1. Inner layer

$$\begin{aligned}\gamma^i_{tt} = -1 + \lambda\left(-\eta^2 + m_0 + \eta^2\Omega^2 m_2 P_2\right) + \lambda^2\left\{\eta^4\left(\frac{1}{10} + \frac{3n_1}{20}\right) + \eta^2\left[-a_0 + m_0\left(-q - \frac{qn_1}{2}\right)\right.\right.\\ + \frac{r_i^2}{r_o^2}\left(-1 + q - \frac{n_1}{2} + \frac{qn_1}{2}\right) + \frac{r_o}{r_s}\left(2qM_0 + qM_0 n_1\right)\Big] + \Omega^2\left[\eta^4\left(-\frac{3}{5} - \frac{n_1}{10}\right) + \eta^4\left(\frac{6}{7} - 3a_2\right.\right.\\ \left.\left.\left. + m_2\left(\frac{1}{7} - \frac{3n_1}{14}\right) + \frac{n_1}{7}\right)P_2 - \frac{\eta^2}{3r_o^2}(2 + n_1)\left((-1+q)r_i^2 - qr_s^2\right)\right]\right\} + \mathcal{O}(\lambda^3, \Omega^4),\end{aligned} \tag{G.1}$$

$$\begin{aligned}\gamma^i_{t\phi} = \lambda^{3/2}\left[\Omega\left(-\frac{6\eta^3}{5} + \eta j_1\right)P_{11} + \eta^3\Omega^3 j_3 P_{31}\right]\\ + \lambda^{5/2}\left\{\Omega P_{11}\left[\eta^5\left(\frac{27}{35} + \frac{3n_1}{14}\right) + \eta^3\left(-\frac{12a_0}{5} + \frac{j_1}{5} - m_0\left(\frac{12}{5} + \frac{3qn_1}{5}\right) + \frac{3(-1+q)n_1 r_i^2}{5r_o^2} + \frac{6qM_0 n_1 r_o}{5r_s}\right)\right]\right.\\ + \Omega^3\left[\eta^5\left(\frac{4}{45} - \frac{48a_2}{25} + \frac{j_3}{9} + m_2\left(-\frac{4}{15} - \frac{n_1}{15}\right) + \frac{2n_1}{45}\right)P_{31} + P_{11}\left(\eta^5\left(-\frac{12}{35} + \frac{18a_2}{25}\right.\right.\right.\\ \left.\left.\left.\left. + m_2\left(\frac{9}{35} + \frac{3n_1}{70}\right) - \frac{6n_1}{35}\right) + \eta^3\left(-\frac{42b_2}{25} - \frac{j_1 m_2}{5} + \frac{2n_1}{5r_o^2}\left((1-q)r_i^2 + qr_s^2\right)\right)\right)\right]\Big\} + \mathcal{O}(\lambda^{7/2}, \Omega^5),\end{aligned} \tag{G.2}$$

$$\begin{aligned}\gamma^i_{rr} = 1 + \lambda\left\{-\eta^2 + a_0 + m_0 + \Omega^2\left[-2b_2 + \eta^2(9a_2 + m_2)\right]P_2\right\} + \lambda^2\left\{\eta^4\left(\frac{17}{70} + \frac{3n_1}{20}\right)\right.\\ + \eta^2\left[-2a_0 + m_0\left(-2 + \frac{7q}{5} - \frac{qn_1}{2}\right) + \frac{(-1+q)(-14+5n_1)r_i^2}{10r_o^2} + \frac{qM_0(-14+5n_1)r_o}{5r_s}\right]\\ + \Omega^2\left[\eta^4\left(\frac{9}{35} - \frac{n_1}{10}\right) + \left(\eta^2\left(2b_2 - \frac{4a_0 m_2}{5} - \frac{8m_0 m_2}{5}\right) + \eta^4\left(-\frac{8}{21} - 12a_2 - m_2\left(\frac{3}{7} + \frac{3n_1}{14}\right) + \frac{n_1}{7}\right)\right)P_2\right.\\ \left.\left. - \frac{\eta^2}{15r_o^2}(-14+5n_1)\left((-1+q)r_i^2 - qr_s^2\right)\right]\right\} + \mathcal{O}(\lambda^3, \Omega^4),\end{aligned} \tag{G.3}$$

$$\begin{aligned}\gamma^i_{\theta\theta} = 1 + \lambda\left\{-\eta^2 + a_0 + m_0 + \Omega^2\left[-\eta^2 a_2 - b_2 + \left(2b_2 + \eta^2\left(7a_2 + m_2\right)\right)P_2\right]\right\}\\ + \lambda^2\left\{\eta^4\left(\frac{37}{70} + \frac{3n_1}{20}\right) + \eta^2\left[-2a_0 + m_0\left(-2 + \frac{4q}{5} - \frac{qn_1}{2}\right) + \frac{(-1+q)(-8+5n_1)r_i^2}{10r_o^2}\right.\right.\\ \left. + \frac{qM_0(-8+5n_1)r_o}{5r_s}\right] + \Omega^2\left[\eta^4\left(\frac{71}{315} + a_2 - \frac{m_2}{42} - \frac{n_1}{10}\right) + \left(\eta^2\left(-2b_2 - \frac{2a_0m_2}{5} - \frac{4m_0m_2}{5}\right)\right.\right.\\ + \eta^4\left(-\frac{13}{63} - 10a_2 + m_2\left(-\frac{41}{42} - \frac{3n_1}{14}\right) + \frac{n_1}{7}\right)\Big)P_2\\ \left.\left. + \eta^2\left(b_2 + \frac{a_0m_2}{5} + \frac{2m_0m_2}{5} - \frac{1}{15r_o^2}(-8+5n_1)\left((-1+q)r_i^2 - qr_s^2\right)\right)\right]\right\} + \mathcal{O}(\lambda^3, \Omega^4),\end{aligned} \tag{G.4}$$

$$\begin{aligned}\gamma^i_{\phi\phi} = 1 + \lambda\left\{-\eta^2 + a_0 + m_0 + \Omega^2\left[\eta^2 a_2 + b_2 + \eta^2\left(5a_2 + m_2\right)P_2\right]\right\} + \lambda^2\left\{\eta^4\left(\frac{37}{70} + \frac{3n_1}{20}\right)\right.\\ + \eta^2\left[-2a_0 + m_0\left(-2 + \frac{4q}{5} - \frac{qn_1}{2}\right) + \frac{(-1+q)(-8+5n_1)r_i^2}{10r_o^2} + \frac{qM_0(-8+5n_1)r_o}{5r_s}\right]\\ + \Omega^2\left[\eta^4\left(-\frac{89}{315} - a_2 + \frac{m_2}{42} - \frac{n_1}{10}\right) + \eta^4\left(\frac{19}{63} - 8a_2 + m_2\left(-\frac{43}{42} - \frac{3n_1}{14}\right) + \frac{n_1}{7}\right)P_2\right.\\ \left.\left. + \eta^2\left(-b_2 - \frac{a_0m_2}{5} - \frac{2m_0m_2}{5} - \frac{1}{15r_o^2}(-8+5n_1)\left((-1+q)r_i^2 - qr_s^2\right)\right)\right]\right\} + \mathcal{O}(\lambda^3, \Omega^4),\end{aligned} \tag{G.5}$$

$$\gamma^i_{r\theta} = \lambda\Omega^2\left(\frac{\eta^2 a_2}{2} - b_2\right)P_{21} + \lambda^2\Omega^2\left[\eta^4\left(-\frac{1}{63} - \frac{a_2}{2} + \frac{2m_2}{21}\right) + \eta^2\left(b_2 - \frac{a_0m_2}{10} - \frac{m_0m_2}{5}\right)\right]P_{21} + \mathcal{O}(\lambda^3, \Omega^4), \tag{G.6}$$

1.2. Outer layer

$$\begin{aligned}\gamma^s_{tt} = -1 + \lambda\left[-q\eta^2 + \bar{m}_0 + \frac{2\bar{M}_0}{\eta} + \Omega^2 P_2\left(\eta^2\bar{m}_2 + \frac{2\bar{M}_2}{\eta^3}\right)\right]\\ + \lambda^2\left\{q^2\eta^4\left(\frac{1}{10} + \frac{3n_2}{20}\right) + \eta^2\left[\frac{1}{r_o^2 r_s}q(2+n_2)\left((1-q)r_i^3 + qr_s^3\right) - q\bar{a}_0 + q\left(-1 - \frac{n_2}{2}\right)\bar{m}_0\right]\right.\\ + q\eta(-10 - 3n_2)\bar{M}_0 - \frac{\bar{A}_0\bar{M}_0}{\eta^4} - \frac{2\bar{M}_0^2}{\eta^2} + \Omega^2\left[q\eta^4\left(-\frac{3}{5} - \frac{n_2}{10}\right) + \frac{q\eta^2(2+n_2)r_s^2}{3r_o^2}\right.\\ + P_2\left(\eta^4\left(q\left(\frac{6}{7} + \frac{n_2}{7}\right) - 3q\bar{a}_2 + q\left(\frac{1}{7} - \frac{3n_2}{14}\right)\bar{m}_2\right) + \eta\left(-3\bar{a}_2\bar{M}_0 - 2\bar{m}_2\bar{M}_0\right) + \frac{\bar{M}_0}{\eta^4}\left(2\bar{B}_2 - 4\bar{M}_2\right)\right.\\ \left.\left.\left. + \frac{2q\bar{B}_2 + \bar{A}_0\bar{m}_2 + 2\bar{b}_2\bar{M}_0 + q(6+n_2)\bar{M}_2}{\eta} + \frac{-3\bar{A}_2\bar{M}_0 - 3\bar{A}_0\bar{M}_2}{\eta^6}\right)\right]\right\} + \mathcal{O}(\lambda^3, \Omega^4),\end{aligned} \tag{G.7}$$

$$\begin{aligned}\gamma^s_{t\phi} = \lambda^{3/2}\left[\Omega P_{11}\left(-\frac{6q\eta^3}{5} + \eta\bar{j}_1 + \frac{2\bar{J}_1}{\eta^2}\right) + \Omega^3 P_{31}\left(\eta^3\bar{j}_3 + \frac{2\bar{J}_3}{\eta^4}\right)\right]\\ + \lambda^{5/2}\left\{\Omega P_{11}\left[q^2\eta^5\left(\frac{27}{35} + \frac{3n_2}{14}\right) - \frac{12q\bar{A}_0}{5} - 2q\bar{J}_1 - \frac{\bar{A}_0\bar{J}_1}{\eta^5}\right.\right.\\ \left.\left. + \eta^3\left(\frac{6qn_2}{5r_o^2r_s}\left((1-q)r_i^3 + qr_s^3\right) - \frac{12q\bar{a}_0}{5} + \frac{q\bar{j}_1}{5} + q\left(-\frac{12}{5} - \frac{3n_2}{5}\right)\bar{m}_0\right) + q\eta^2\left(-\frac{54}{5} - 3n_2\right)\bar{M}_0\right.\right.\end{aligned}$$

$$+2\bar{j}_1\bar{M}_0-\frac{2\bar{J}_1\bar{M}_0}{\eta^3}\Bigg]+\Omega^3\Bigg[P_{11}\Bigg(-\frac{42}{25}q\bar{B}_2+\frac{9}{5}\bar{a}_2\bar{J}_1+\frac{9\bar{A}_2\bar{J}_1}{5\eta^7}+\frac{4\bar{B}_2\bar{J}_1}{5\eta^5}+2\bar{J}_1\bar{m}_2$$
$$+\eta^5\left(q\left(-\frac{12}{35}-\frac{6n_2}{35}\right)+\frac{18q\bar{a}_2}{25}+q\left(\frac{9}{35}+\frac{3n_2}{70}\right)\bar{m}_2\right)+\eta^3\left(\frac{2qn_2r_s^2}{5r_o^2}-\frac{42q\bar{b}_2}{25}-\frac{1}{5}\bar{j}_1\bar{m}_2\right)$$
$$+q\left(-\frac{24}{5}-\frac{6n_2}{5}\right)\bar{M}_2\Bigg)+P_{31}\Bigg(\frac{12q\bar{B}_2}{25}+2\bar{A}_0\bar{j}_3+\frac{1}{5}\bar{a}_2\bar{J}_1+\frac{\frac{1}{5}\bar{A}_2\bar{J}_1-3\bar{A}_0\bar{J}_3}{\eta^7}$$
$$+\eta^5\left(-\frac{48}{25}q\bar{a}_2+q\left(\frac{4}{45}+\frac{2n_2}{45}+\frac{\bar{j}_3}{9}\right)+q\left(-\frac{4}{15}-\frac{n_2}{15}\right)\bar{m}_2\right)+\frac{2}{3}\eta^2\bar{j}_3\bar{M}_0+q\left(\frac{2}{5}+\frac{n_2}{5}\right)\bar{M}_2$$
$$-\frac{2}{25\eta^2}\left(24q\bar{A}_2-15\bar{b}_2\bar{J}_1+5q\bar{J}_3-5\bar{j}_1\bar{M}_2\right)+\frac{\frac{6}{5}\bar{B}_2\bar{J}_1-\bar{J}_3\bar{M}_0-\bar{J}_1\bar{M}_2}{\eta^5}\Bigg)\Bigg]\Bigg\}+\mathcal{O}(\lambda^{7/2},\Omega^5), \tag{G.8}$$

$$\gamma^s_{rr}=1+\lambda\left[-q\eta^2+\bar{a}_0+\bar{m}_0+\frac{2\bar{M}_0}{\eta}+\Omega^2P_2\left(-2\bar{b}_2+\eta^2\left(5\bar{a}_2+\bar{m}_2\right)+\frac{2\bar{M}_2}{\eta^3}\right)\right]$$
$$+\lambda^2\Bigg\{q^2\eta^4\left(\frac{13}{30}+\frac{3n_2}{20}\right)+\frac{3\bar{A}_0^2}{2\eta^6}+\eta^2\left(\frac{1}{r_o^2r_s}q\left(-2+n_2\right)\left(\left(1-q\right)r_i^3+qr_s^3\right)-2q\bar{a}_0+q\left(-1-\frac{n_2}{2}\right)\bar{m}_0\right)$$
$$+q\eta\left(-\frac{10}{3}-3n_2\right)\bar{M}_0-\frac{\bar{A}_0\bar{M}_0}{\eta^4}+\frac{4\bar{M}_0^2}{3\eta^2}+\frac{2\bar{a}_0\bar{M}_0+4\bar{m}_0\bar{M}_0}{\eta}+\Omega^2\Bigg[q\eta^4\left(\frac{1}{15}-\frac{n_2}{10}\right)+\frac{q\eta^2\left(-2+n_2\right)r_s^2}{3r_o^2}$$
$$+P_2\Bigg(\frac{87\bar{A}_0\bar{A}_2}{7\eta^8}+2q\eta^2\bar{b}_2+\eta^4\left(q\left(\frac{44}{105}+\frac{n_2}{7}\right)-8q\bar{a}_2-q\left(\frac{13}{15}+\frac{3n_2}{14}\right)\bar{m}_2\right)+\eta\left(7\bar{a}_2\bar{M}_0+\frac{10}{3}\bar{m}_2\bar{M}_0\right)$$
$$+\frac{\bar{M}_0\left(2\bar{B}_2+\frac{64\bar{M}_2}{21}\right)}{\eta^4}+\frac{1}{\eta}\left(\frac{1}{35}\bar{a}_2\bar{A}_0+2q\bar{B}_2+\frac{41}{35}\bar{A}_0\bar{m}_2-2\bar{b}_2\bar{M}_0+q\left(\frac{58}{105}+n_2\right)\bar{M}_2\right)$$
$$+\frac{6\bar{A}_0\bar{b}_2+14\left(\bar{a}_0+2\bar{m}_0\right)\bar{M}_2}{7\eta^3}-\frac{3}{35\eta^6}\left(35\bar{A}_2\bar{M}_0+\bar{A}_0\left(48\bar{B}_2+31\bar{M}_2\right)\right)\Bigg)\Bigg]\Bigg\}+\mathcal{O}(\lambda^3,\Omega^4), \tag{G.9}$$

$$\gamma^s_{r\theta}=-\lambda\Omega^2P_{21}\bar{b}_2+\lambda^2\Omega^2P_{21}\Bigg[\frac{3\bar{A}_0\bar{A}_2}{2\eta^8}+q\eta^2\bar{b}_2+\eta^4\left(\frac{q}{15}+\frac{q\bar{m}_2}{15}\right)+\frac{2}{3}\eta\bar{m}_2\bar{M}_0$$
$$+\frac{1}{\eta}\left(-\frac{27}{10}\bar{a}_2\bar{A}_0-\frac{1}{5}\bar{A}_0\bar{m}_2-2\bar{b}_2\bar{M}_0+\frac{4q\bar{M}_2}{5}\right)+\frac{-\frac{6}{5}\bar{A}_0\bar{B}_2-\frac{2}{5}\bar{A}_0\bar{M}_2}{\eta^6}\Bigg]+\mathcal{O}(\lambda^3,\Omega^4). \tag{G.10}$$

and the $\gamma_{\theta\theta}$ and $\gamma_{t\phi}$ are quite similar to the γ_{rr} ones, their differences being

$$\gamma^s_{rr}-\gamma^s_{\theta\theta}=\lambda\Omega^2(a-4aP_2)+\lambda^2\Omega^2(b-4bP_2)+\mathcal{O}(\lambda^3,\Omega^4), \tag{G.11}$$
$$\gamma^s_{rr}-\gamma^s_{\phi\phi}=\lambda\Omega^2(-a-2aP_2)+\lambda^2\Omega^2(-b-2bP_2)+\mathcal{O}(\lambda^3,\Omega^4), \tag{G.12}$$

with

$$a=\bar{b}_2, \tag{G.13}$$
$$b=-\frac{3\bar{A}_0\bar{A}_2}{2\eta^8}-q\eta^2\bar{b}_2-\frac{1}{15}q\eta^4\left(1+\bar{m}_2\right)-\frac{2}{3}\eta\bar{m}_2\bar{M}_0+\frac{2\bar{A}_0\left(3\bar{B}_2+\bar{M}_2\right)}{5\eta^6}$$
$$+\frac{27\bar{a}_2\bar{A}_0+2\bar{A}_0\bar{m}_2+20\bar{b}_2\bar{M}_0-8q\bar{M}_2}{10\eta}. \tag{G.14}$$

2. Matching results

2.1. Exterior

$$
\begin{aligned}
M_0 = \frac{r_i^3 - q r_i^3 + q r_s^3}{r_o^3} + \lambda \Bigg\{ & \frac{1}{15 r_o^5} \Omega^2 \left[\left(8 - 2n_1 + q\left(-8 + 5n_1 - 3n_2\right)\right) r_i^5 + q\left(-5n_1 + 5n_2\right) r_i^3 r_s^2 + q\left(8 - 2n_2\right) r_s^5 \right] \\
& + \frac{1}{10 r_o^5} \left(28 + 2n_1 + q\left(-70 + 10n_1 - 15n_2\right) + q^2\left(42 - 15n_1 + 18n_2\right)\right) r_i^5 \\
& + \frac{\left(q^2\left(10n_1 - 10n_2\right) + q\left(-10n_1 + 10n_2\right)\right) r_i^6}{r_s} + \left(q^2\left(-70 + 5n_1 - 10n_2\right) + q\left(70 + 5n_2\right)\right) r_i^3 r_s^2 \\
& + q^2\left(28 + 2n_2\right) r_s^5 \Bigg\} + \mathcal{O}(\lambda^2, \Omega^4),
\end{aligned}
\tag{G.15}
$$

$$
\begin{aligned}
M_2 = \frac{-5(-1+q)^2 r_i^8 r_s^2 + 8(-1+q) q r_i^5 r_s^5 - q(2+3q) r_s^{10}}{r_o^5 r_1} + \frac{1}{70 r_o^7 r_1^2} \lambda \Big\{ & \Big[q^3\left(-12600 + 9450n_1 - 3150n_2\right) \\
& + q^5\left(-2100 + 3150n_1 - 2100n_2\right) + q^2\left(8400 - 3150n_1 - 1050n_2\right) + q\left(-2100 + 1050n_2\right) \\
& + q^4\left(8400 - 9450n_1 + 5250n_2\right) \Big] r_i^{16} r_s + \Big[q\left(17280 + 630n_1\right) + q^4\left(-88992 + 12600n_1 - 16065n_2\right) \\
& + q^2\left(-75744 + 1890n_1 - 4725n_2\right) + q^5\left(23904 - 4725n_1 + 5670n_2\right) \\
& + q^3\left(123552 - 10395n_1 + 15120n_2\right) \Big] r_i^{15} r_s^2 + \Big[q^5\left(-17500 - 8750n_1\right) \\
& + q^3\left(-105000 - 26250n_1 - 26250n_2\right) + q\left(-17500 - 8750n_2\right) + q^4\left(70000 + 26250n_1 + 8750n_2\right) \\
& + q^2\left(70000 + 8750n_1 + 26250n_2\right) \Big] r_i^{14} r_s^3 + \Big[-7400 + 500n_1 + q^2\left(-27840 - 4750n_1 - 25700n_2\right) \\
& + q^5\left(-40140 + 14700n_1 - 9000n_2\right) + q\left(37460 - 2750n_1 + 10000n_2\right) \\
& + q^4\left(105160 - 38150n_1 + 12300n_2\right) + q^3\left(-67240 + 30450n_1 + 12400n_2\right) \Big] r_i^{13} r_s^4 \\
& + \left(8460q^2 - 24570q^3 + 23760q^4 - 7650q^5\right) r_i^{12} r_s^5 + \Big[q^4\left(-198800 - 17850n_1 - 28875n_2\right) \\
& + q^2\left(25200 - 4200n_1 - 5775n_2\right) + q\left(-34300 - 2100n_2\right) + q^5\left(77700 + 6825n_1 + 9450n_2\right) \\
& + q^3\left(130200 + 15225n_1 + 27300n_2\right) \Big] r_i^{11} r_s^6 + \Big[q\left(2600 + 1840n_1\right) \\
& + q^3\left(-63048 - 19460n_1 - 32660n_2\right) + q^5\left(-12672 - 16800n_1 - 2160n_2\right) \\
& + q^2\left(21288 + 120n_1 + 13700n_2\right) + q^4\left(51832 + 34300n_1 + 21120n_2\right) \Big] r_i^{10} r_s^7 \\
& + \Big[2240q + q^5\left(-24870 - 3150n_1\right) + q^2\left(-17700 - 2100n_2\right) + q^3\left(3810 + 2100n_1 - 1050n_2\right) \\
& + q^4\left(36520 + 1050n_1 + 3150n_2\right) \Big] r_i^8 r_s^9 + \Big[q^2\left(-1760 + 500n_1\right) + q^4\left(-21410 - 8750n_1 - 9375n_2\right) \\
& + q^5\left(6150 + 13125n_1 - 3750n_2\right) + q^3\left(17020 - 1750n_1 + 10000n_2\right) \Big] r_i^7 r_s^{10} \\
& + \Big[q^5\left(-21600 + 3150n_1 - 3600n_2\right) + q^4\left(14400 + 1050n_1 - 750n_2\right) + q\left(-9600 - 200n_2\right) \\
& + q^2\left(-9600 - 1400n_1 + 1200n_2\right) + q^3\left(26400 - 2800n_1 + 3350n_2\right) \Big] r_i^6 r_s^{11} + \Big[q\left(3920 + 280n_1\right) \\
& + q^3\left(-20220 + 2730n_1 - 5040n_2\right) + q^2\left(2856 + 2240n_1 - 2100n_2\right) + q^4\left(12 - 3150n_1 + 6580n_2\right) \\
& + q^5\left(13432 - 9100n_1 + 7560n_2\right) \Big] r_i^5 r_s^{12} + \Big[q^4\left(2670 + 2100n_1 - 2325n_2\right) \\
& + q^5\left(8010 + 1575n_1 - 2250n_2\right) + q^3\left(-7120 + 700n_1 - 100n_2\right) + q^2\left(-3560 + 300n_2\right) \Big] r_i^3 r_s^{14} \\
& + \Big[q^3\left(-1184 + 80n_2\right) + q^5\left(-2664 + 180n_2\right) + q^4\left(-3552 + 240n_2\right) \Big] r_s^{17} \Big\} + \mathcal{O}(\lambda^2, \Omega^2),
\end{aligned}
\tag{G.16}
$$

$$
\begin{aligned}
J_1 = {} & \frac{2\left[-(-1+q)r_i^5 + q r_s^5\right]}{5r_o^5} + \frac{2\Omega^2\left[5(-1+q)^2 r_i^8 r_s^2 - 8(-1+q)q r_i^5 r_s^5 + q(2+3q) r_s^{10}\right]}{3r_o^5 r_1} \\
& + \lambda\left\{\frac{1}{70r_o^7}\left(160 + 4n_1 + q\left(-350 + 28n_1 - 35n_2\right) + q^2\left(190 - 42n_1 + 45n_2\right)\right) r_i^7\right. \\
& + \frac{\left(q^2\left(28n_1 - 28n_2\right) + q\left(-28n_1 + 28n_2\right)\right) r_i^8}{r_s} + \left(140q + q^2\left(-140 + 14n_1 - 14n_2\right)\right) r_i^5 r_s^2 \\
& + \left(q^2\left(-210 - 7n_2\right) + q\left(210 + 7n_2\right)\right) r_i^3 r_s^4 + q^2\left(160 + 4n_2\right) r_s^7 \\
& + \frac{1}{105 r_o^7 r_1^2}\Omega^2\left[\left(q^2\left(648 - 324n_1\right) + q^5\left(-648 + 1134n_1 - 810n_2\right) + q^3\left(-1944 + 1782n_1 - 810n_2\right)\right.\right. \\
& + q^4\left(1944 - 2592n_1 + 1620n_2\right)\Big) r_i^{17} + \left(q^4\left(-8400 + 9450n_1 - 5250n_2\right) + q\left(2100 - 1050n_2\right)\right. \\
& + q^2\left(-8400 + 3150n_1 + 1050n_2\right) + q^5\left(2100 - 3150n_1 + 2100n_2\right) \\
& + q^3\left(12600 - 9450n_1 + 3150n_2\right)\Big) r_i^{16} r_s + \left(q\left(-27180 + 90n_1\right) + q^3\left(-178794 + 9081n_1 - 14886n_2\right)\right. \\
& + q^5\left(-32418 - 189n_1 - 1836n_2\right) + q^2\left(113958 - 4770n_1 + 6525n_2\right) \\
& + q^4\left(124434 - 4212n_1 + 10197n_2\right)\Big) r_i^{15} r_s^2 + \left(q^5\left(17500 + 8750n_1\right)\right. \\
& + q^2\left(-70000 - 8750n_1 - 26250n_2\right) + q^4\left(-70000 - 26250n_1 - 8750n_2\right) + q\left(17500 + 8750n_2\right) \\
& + q^3\left(105000 + 26250n_1 + 26250n_2\right)\Big) r_i^{14} r_s^3 + \left(17600 - 900n_1 + q\left(-63420 + 3750n_1 - 11000n_2\right)\right. \\
& + q^3\left(166180 - 34960n_1 - 8390n_2\right) + q^4\left(-205020 + 30110n_1 - 5760n_2\right) \\
& + q^5\left(71880 - 7770n_1 + 2970n_2\right) + q^2\left(12780 + 9770n_1 + 22180n_2\right)\Big) r_i^{13} r_s^4 + \left(q^2\left(-17496 + 288n_1\right)\right. \\
& + q^5\left(14436 + 1512n_1 - 1080n_2\right) + q^4\left(-46368 - 936n_1 + 360n_2\right) \\
& + q^3\left(49428 - 864n_1 + 720n_2\right)\Big) r_i^{12} r_s^5 + \left(q^3\left(-156450 - 11375n_1 - 31150n_2\right)\right. \\
& + q^5\left(-103950 - 9975n_1 - 6300n_2\right) + q\left(51800 - 1400n_1 + 3500n_2\right) \\
& + q^2\left(-51450 + 2800n_1 + 7175n_2\right) + q^4\left(260050 + 19950n_1 + 26775n_2\right)\Big) r_i^{11} r_s^6 \\
& + \left(q\left(11200 - 2160n_1\right) + q^4\left(13560 - 33916n_1 - 20376n_2\right) + q^2\left(-38456 + 360n_1 - 14500n_2\right)\right. \\
& + q^5\left(-14808 + 12768n_1 + 5148n_2\right) + q^3\left(28504 + 22948n_1 + 29728n_2\right)\Big) r_i^{10} r_s^7 \\
& + \left(-4480q + q^4\left(-61760 - 210n_1 - 5430n_2\right) + q^5\left(41280 + 5670n_1 - 1440n_2\right)\right. \\
& + q^3\left(-4800 - 4340n_1 + 2930n_2\right) + q^2\left(29760 - 1120n_1 + 3940n_2\right)\Big) r_i^8 r_s^9 + \left(q^2\left(5648 - 564n_1\right)\right. \\
& + q^3\left(-18284 + 1782n_1 - 10160n_2\right) + q^5\left(-1338 - 12621n_1 + 3390n_2\right) \\
& + q^4\left(13974 + 9278n_1 + 8895n_2\right)\Big) r_i^7 r_s^{10} + \left(q^3\left(-45100 + 2800n_1 - 2250n_2\right)\right. \\
& + q^2\left(16400 + 1400n_1 - 1600n_2\right) + q\left(16400 - 200n_2\right) + q^4\left(-24600 - 1050n_1 + 1350n_2\right) \\
& + q^5\left(36900 - 3150n_1 + 2700n_2\right)\Big) r_i^6 r_s^{11} + \left(q\left(-3920 - 280n_1\right) + q^5\left(-13960 + 8596n_1 - 7488n_2\right)\right. \\
& + q^4\left(1508 + 2478n_1 - 5764n_2\right) + q^2\left(-3752 - 2240n_1 + 2100n_2\right) \\
& + q^3\left(20124 - 2954n_1 + 5552n_2\right)\Big) r_i^5 r_s^{12} + \left(q^2\left(10360 - 620n_2\right) + q^3\left(20720 - 700n_1 - 540n_2\right)\right. \\
& + q^4\left(-7770 - 2100n_1 + 2565n_2\right) + q^5\left(-23310 - 1575n_1 + 2970n_2\right)\Big) r_i^3 r_s^{14} \\
& \left.\left. + \left(q^4\left(8448 - 432n_2\right) + q^5\left(6336 - 324n_2\right) + q^3\left(2816 - 144n_2\right)\right) r_s^{17}\right]\right\} + \mathcal{O}(\lambda^2, \Omega^4), \qquad \text{(G.17)}
\end{aligned}
$$

$$
\begin{aligned}
J_3 = {} & \frac{-10(-1+q)^2 r_i^{10} r_s^2 + 10(-1+q) q r_i^7 r_s^5 + 6(-1+q) q r_i^5 r_s^7 - 2q(2+3q) r_s^{12}}{7 r_o^7 r_1} \\
& - \frac{1}{4410 r_o^9 r_1^2} \lambda \Big\{ \left(-6048q^2 + 18144q^3 - 18144q^4 + 6048q^5\right) r_i^{19} + \Big[q^4 (-151200 + 170100 n_1 - 94500 n_2) \\
& + q (37800 - 18900 n_2) + q^2 (-151200 + 56700 n_1 + 18900 n_2) + q^5 (37800 - 56700 n_1 + 37800 n_2) \\
& + q^3 (226800 - 170100 n_1 + 56700 n_2) \Big] r_i^{18} r_s + \Big[q (-452280 - 9540 n_1) \\
& + q^3 (-3138786 + 188910 n_1 - 246285 n_2) + q^5 (-593982 + 85050 n_1 - 94635 n_2) \\
& + q^2 (1950822 - 37620 n_1 + 75825 n_2) + q^4 (2234226 - 226800 n_1 + 265095 n_2) \Big] r_i^{17} r_s^2 \\
& + \Big[q^5 (315000 + 157500 n_1) + q^2 (-1260000 - 157500 n_1 - 472500 n_2) \\
& + q^4 (-1260000 - 472500 n_1 - 157500 n_2) + q (315000 + 157500 n_2) \\
& + q^3 (1890000 + 472500 n_1 + 472500 n_2) \Big] r_i^{16} r_s^3 + [297600 - 11000 n_1 \\
& + q^3 (1985394 - 551100 n_1 - 324625 n_2) + q (-1091580 + 50500 n_1 - 169750 n_2) \\
& + q^4 (-2680554 + 686700 n_1 - 104475 n_2) + q^5 (959778 - 264600 n_1 + 121275 n_2) \\
& + q^2 (529362 + 89500 n_1 + 477575 n_2) \Big] r_i^{15} r_s^4 + \Big[q^2 (-210216 + 1800 n_1) \\
& + q^3 (627126 - 1800 n_1 - 9225 n_2) + q^5 (206694 - 7425 n_2) + q^4 (-623604 + 16650 n_2) \Big] r_i^{14} r_s^5 \\
& + \Big[q^3 (-942030 - 160650 n_1 - 233415 n_2) + q^5 (-885330 - 85050 n_1 - 65205 n_2) \\
& + q (571320 + 18900 n_2) + q^2 (-828630 + 37800 n_1 + 55755 n_2) \\
& + q^4 (2084670 + 207900 n_1 + 223965 n_2) \Big] r_i^{13} r_s^6 + \Big[q (213760 - 22960 n_1) \\
& + q^4 (41832 - 466200 n_1 - 284340 n_2) + q^2 (-783740 + 13720 n_1 - 180950 n_2) \\
& + q^5 (-199026 + 245700 n_1 + 22995 n_2) + q^3 (727174 + 229740 n_1 + 442295 n_2) \Big] r_i^{12} r_s^7 \\
& + \Big[q^3 (-1030050 - 113400 n_1 - 184275 n_2) + q^5 (-652050 - 37800 n_1 - 70875 n_2) \\
& + q (308700 + 9450 n_2) + q^2 (-274050 + 37800 n_1 + 42525 n_2) \\
& + q^4 (1647450 + 113400 n_1 + 203175 n_2) \Big] r_i^{11} r_s^8 + \Big[q (-25920 - 12960 n_1) \\
& + q^4 (-575316 - 113400 n_1 - 105030 n_2) + q^2 (376704 - 17280 n_1 - 40500 n_2) \\
& + q^5 (450090 + 37800 n_1 + 29565 n_2) + q^3 (-225558 + 105840 n_1 + 115965 n_2) \Big] r_i^{10} r_s^9 \\
& + \Big[q^2 (80224 - 4400 n_1) + q^3 (-154360 + 11400 n_1 - 67900 n_2) + q^5 (54108 - 94500 n_1 + 22050 n_2) \\
& + q^4 (20028 + 63000 n_1 + 70350 n_2) \Big] r_i^9 r_s^{10} + \Big[-30240 q + q^4 (-665760 - 56700 n_1 - 66780 n_2) \\
& + q^5 (418050 + 75600 n_1 - 6615 n_2) + q^2 (230820 + 14490 n_2) \\
& + q^3 (47130 - 18900 n_1 + 58905 n_2) \Big] r_i^8 r_s^{11} + \Big[q^2 (19008 - 5400 n_1) \\
& + q^3 (-69768 + 18900 n_1 - 104760 n_2) + q^5 (-174492 - 110250 n_1 + 35640 n_2) \\
& + q^4 (225252 + 94500 n_1 + 71370 n_2) \Big] r_i^7 r_s^{12} + \Big[q^3 (-616000 + 50400 n_1 - 58100 n_2) \\
& + q^2 (224000 + 25200 n_1 - 22400 n_2) + q (224000 + 2800 n_2) + q^4 (-336000 - 18900 n_1 + 14700 n_2) \\
& + q^5 (504000 - 56700 n_1 + 63000 n_2) \Big] r_i^6 r_s^{13} + \Big[q (-70560 - 5040 n_1) \\
& + q^5 (-215604 + 132300 n_1 - 126630 n_2) + q^4 (27012 + 56700 n_1 - 90090 n_2) \\
& + q^2 (-47376 - 40320 n_1 + 37800 n_2) + q^3 (306528 - 49140 n_1 + 84420 n_2) \Big] r_i^5 r_s^{14}
\end{aligned}
$$

$$+\left[q^2\left(150320-6520n_2\right)+q^3\left(300640-12600n_1-440n_2\right)+q^4\left(-112740-37800n_1+42690n_2\right)\right.$$
$$\left.+q^5\left(-338220-28350n_1+43020n_2\right)\right]r_i^3r_s^{16}+\left[q^4\left(142848-5280n_2\right)\right.$$
$$\left.+q^5\left(107136-3960n_2\right)+q^3\left(47616-1760n_2\right)\right]r_s^{19}\Big\}+\mathcal{O}(\lambda^2,\Omega^2), \tag{G.18}$$

$$A_0=-\frac{2}{105}\lambda\left\{\frac{\left(-12+21q-9q^2\right)r_i^7+\left(-21q+21q^2\right)r_i^3r_s^4-12q^2r_s^7}{r_o^7}+\frac{1}{r_o^7r_1}\Omega^2\left[\left(18q-36q^2+18q^3\right)r_i^{12}\right.\right.$$
$$+\left(-20+10q+40q^2-30q^3\right)r_i^{10}r_s^2+\left(-8q-4q^2+12q^3\right)r_i^7r_s^5+\left(18q^2-18q^3\right)r_i^5r_s^7$$
$$\left.\left.+\left(-20q-10q^2+30q^3\right)r_i^3r_s^9+\left(-8q^2-12q^3\right)r_s^{12}\right]\right\}+\mathcal{O}(\lambda^2,\Omega^4), \tag{G.19}$$

$$A_2=\frac{1}{63r_o^9r_1}2\lambda\left[\left(-20+55q-50q^2+15q^3\right)r_i^{12}r_s^2+\left(-20q+35q^2-15q^3\right)r_i^9r_s^5+\left(-27q+54q^2-27q^3\right)r_i^8r_s^6\right.$$
$$\left.+\left(-27q^2+27q^3\right)r_i^5r_s^9+\left(-8q-4q^2+12q^3\right)r_i^3r_s^{11}+\left(-8q^2-12q^3\right)r_s^{14}\right]+\mathcal{O}(\lambda^2,\Omega^2), \tag{G.20}$$

$$B_2=-\frac{2}{7r_o^7r_1}\lambda\left[\left(3q-6q^2+3q^3\right)r_i^{12}+\left(-10q+20q^2-10q^3\right)r_i^{10}r_s^2+\left(7q-14q^2+7q^3\right)r_i^8r_s^4\right.$$
$$\left.+\left(2q-9q^2+7q^3\right)r_i^7r_s^5+\left(10q^2-10q^3\right)r_i^5r_s^7+\left(-2q-q^2+3q^3\right)r_i^3r_s^9\right]+\mathcal{O}(\lambda^2,\Omega^2), \tag{G.21}$$

2.2. Inner layer

$$m_0=3+\lambda\left\{\frac{1}{2r_o^4}\Omega^2\left[\left(2-n_1+q\left(-2+2n_1-n_2\right)\right)r_i^4+q\left(-2n_1+2n_2\right)r_i^2r_s^2+q\left(2-n_2\right)r_s^4\right]\right.$$
$$+\frac{3}{4r_o^4}\left[\left(6+n_1+q\left(-24+4n_1-8n_2\right)+q^2\left(18-6n_1+9n_2\right)\right)r_i^4+\frac{4r_i^5}{r_s}\left(q^2\left(n_1-n_2\right)+q\left(-n_1+n_2\right)\right)\right.$$
$$\left.\left.+\left(q^2\left(-24-4n_2\right)+q\left(24+4n_2\right)\right)r_i^3r_s+q^2\left(2n_1-2n_2\right)r_i^2r_s^2+q^2\left(6+n_2\right)r_s^4\right]\right\}+\mathcal{O}(\lambda^2,\Omega^4), \tag{G.22}$$

$$m_2=\frac{6(-1+q)qr_i^5-10(-1+q)^2r_i^3r_s^2+2q(-7+2q)r_s^5}{r_1}$$
$$+\frac{1}{35r_o^2r_1^2}\lambda\left\{\left(-1404q^2+4698q^3-5184q^4+1890q^5\right)r_i^{12}+\left[q^5\left(10500+5250n_1\right)\right.\right.$$
$$+q^2\left(-5250n_1-5250n_2\right)+q^4\left(-28000-15750n_1-1750n_2\right)+q\left(-3500+1750n_2\right)$$
$$\left.+q^3\left(21000+15750n_1+5250n_2\right)\right]r_i^{11}r_s+\left[q^5\left(-23940-7875n_1\right)+q\left(21870+2475n_1\right)\right.$$
$$+q^2\left(-52350+600n_1-750n_2\right)+q^4\left(39270+21000n_1-450n_2\right)$$
$$\left.+q^3\left(15150-16200n_1+1200n_2\right)\right]r_i^{10}r_s^2+\left[q^5\left(-17500-8750n_1\right)\right.$$
$$+q^3\left(-105000-26250n_1-26250n_2\right)+q\left(-17500-8750n_2\right)+q^4\left(70000+26250n_1+8750n_2\right)$$
$$\left.+q^2\left(70000+8750n_1+26250n_2\right)\right]r_i^9r_s^3+\left[-2900+q^4\left(-50900-35000n_1\right)-750n_1\right.$$
$$\left.+q^5\left(32550+10500n_1\right)+q^2\left(1000-2250n_1-22750n_2\right)+q\left(10950-2125n_1+8750n_2\right)\right.$$

$$
\begin{aligned}
&+ q^3\,(9300 + 29625n_1 + 14000n_2)\Big] r_i^8 r_s^4 + \Big[q^2\,(-3162 + 1425n_1) + q^5\,(18270 + 7875n_1)\\
&+ q^4\,(-44112 - 5250n_1 - 9000n_2) + q^3\,(29004 - 2175n_1 + 7125n_2)\Big] r_i^7 r_s^5 + \Big[q^5\,(10500 + 7875n_1)\\
&+ q^4\,(-82250 - 10500n_1 - 15750n_2) + q^2\,(-5250 - 3500n_1 - 3500n_2) + q\,(-28000 - 1750n_2)\\
&+ q^3\,(105000 + 6125n_1 + 21000n_2)\Big] r_i^6 r_s^6 + \Big[q^5\,(-48720 - 21000n_1) + q\,(16180 - 350n_1)\\
&+ q^3\,(-81450 - 7175n_1 - 25900n_2) + q^2\,(-7250 + 525n_1 + 7000n_2)\\
&+ q^4\,(121240 + 22750n_1 + 24150n_2)\Big] r_i^5 r_s^7 + \Big[q^5\,(9450 + 2625n_1) + q^4\,(-5000 - 3750n_2)\\
&+ q^2\,(-4600 - 1000n_2) + q^3\,(150 + 1750n_1 + 375n_2)\Big] r_i^3 r_s^9 + \Big[q^2\,(3016 - 300n_1)\\
&+ q^5\,(11340 + 5250n_1) + q^4\,(-17104 - 3500n_1 - 3500n_2) + q^3\,(2748 - 1450n_1 + 3500n_2)\Big] r_i^2 r_s^{10}\\
&+ \Big[q^5\,(-4340 - 1750n_1) + q^3\,(-600 - 300n_2) + q^4\,(2040 + 1300n_2)\Big] r_s^{12}\Big\} + \mathcal{O}(\lambda^2, \Omega^2)
\end{aligned}
\tag{G.23}
$$

$$
\begin{aligned}
j_1 = 2 &+ \frac{4\Omega^2\left((-1+q)(-5+2q) r_i^5 r_s^2 - 5(-1+q) q r_i^2 r_s^5 + q(2+3q) r_s^7\right)}{3 r_o^2 r_1}\\
&+ \lambda\Bigg\{\frac{1}{10 r_o^4}\left(98 + 5n_1 + q\,(-268 + 20n_1 - 40n_2) + q^2\,(170 - 30n_1 + 45n_2)\right) r_i^4\\
&+ \frac{\left(q^2\,(-8 + 20n_1 - 20n_2) + q\,(8 - 20n_1 + 20n_2)\right) r_i^5}{r_s} + \left(q^2\,(-120 - 20n_2) + q\,(120 + 20n_2)\right) r_i^3 r_s\\
&+ \left(140q + q^2\,(-140 + 10n_1 - 10n_2)\right) r_i^2 r_s^2 + q^2\,(98 + 5n_2)\, r_s^4\\
&+ \frac{1}{105 r_o^4 r_1^2}\Omega^2\Bigg[\left(q^2\,(9558 - 2835n_1) + q^5\,(-9558 + 5670n_1 - 2835n_2)\right.\\
&+ q^3\,(-28674 + 11340n_1 - 2835n_2) + q^4\,(28674 - 14175n_1 + 5670n_2)\Big) r_i^{14}\\
&+ \frac{\left(-1512q^2 + 4536q^3 - 4536q^4 + 1512q^5\right) r_i^{15}}{r_s} + \Big(q^4\,(-10920 + 18900n_1 - 2940n_2)\\
&+ q\,(5880 - 2100n_2) + q^3\,(22680 - 18900n_1 - 1260n_2) + q^5\,(1680 - 6300n_1 + 1680n_2)\\
&+ q^2\,(-19320 + 6300n_1 + 4620n_2)\Big) r_i^{13} r_s + \Big(q\,(-57870 + 4365n_1)\\
&+ q^3\,(-173880 + 8145n_1 - 10845n_2) + q^4\,(59112 + 20790n_1 - 9360n_2)\\
&+ q^5\,(-738 - 15120n_1 + 9855n_2) + q^2\,(173376 - 18180n_1 + 10350n_2)\Big) r_i^{12} r_s^2\\
&+ \Big(q^5\,(9800 + 13300n_1) + q^2\,(-123200 - 13300n_1 - 39900n_2) + q^4\,(-67200 - 39900n_1 - 13300n_2)\\
&+ q\,(37800 + 13300n_2) + q^3\,(142800 + 39900n_1 + 39900n_2)\Big) r_i^{11} r_s^3 + (28900 - 3750n_1\\
&+ q\,(-74550 + 7185n_1 - 17500n_2) + q^5\,(62670 + 11550n_1 - 15525n_2)\\
&+ q^3\,(171908 - 66215n_1 - 8425n_2) + q^4\,(-188334 + 15925n_1 + 18450n_2)\\
&+ q^2\,(-594 + 35305n_1 + 23000n_2)\Big) r_i^{10} r_s^4 + \Big(q^2\,(-17334 + 1845n_1) + q^5\,(-8874 + 7560n_1 - 9855n_2)\\
&+ q^3\,(25794 - 3105n_1 - 2880n_2) + q^4\,(414 - 6300n_1 + 12735n_2)\Big) r_i^9 r_s^5\\
&+ \Big(q^3\,(-150430 - 700n_1 - 44555n_2) + q^5\,(-154350 - 16800n_1 + 3465n_2)\\
&+ q\,(55440 - 7000n_1 + 9100n_2) + q^2\,(-85120 - 2800n_1 + 15610n_2)\\
&+ q^4\,(334460 + 27300n_1 + 16380n_2)\Big) r_i^8 r_s^6 + \Big(q\,(10340 - 3990n_1)
\end{aligned}
$$

$$
\begin{aligned}
&+ q^4 (-51918 - 36680 n_1 - 35055 n_2) + q^2 (-25486 + 1605 n_1 - 16100 n_2) \\
&+ q^3 (39098 + 43925 n_1 + 21740 n_2) + q^5 (27966 - 8610 n_1 + 33165 n_2)\Big) r_i^7 r_s^7 + \Big(q^5 (63000 - 6300 n_1) \\
&+ q^2 (28000 + 2800 n_1 - 5600 n_2) + q (28000 - 2800 n_2) + q^3 (-77000 + 5600 n_1 + 2100 n_2) \\
&+ q^4 (-42000 - 2100 n_1 + 6300 n_2)\Big) r_i^6 r_s^8 + \Big(q (-5040 - 560 n_1) + q^5 (56514 + 25200 n_1 - 28125 n_2) \\
&+ q^4 (-72142 + 14700 n_1 - 10275 n_2) + q^2 (40016 - 10080 n_1 + 11000 n_2) \\
&+ q^3 (-19348 - 18760 n_1 + 16900 n_2)\Big) r_i^5 r_s^9 + \Big(q^2 (4216 - 660 n_1) + q^3 (-8380 + 1290 n_1 - 6160 n_2) \\
&+ q^5 (-10668 - 7980 n_1 - 2310 n_2) + q^4 (14832 + 9100 n_1 + 6720 n_2)\Big) r_i^4 r_s^{10} \\
&+ \Big(q^3 (32560 - 1400 n_1 - 4560 n_2) + q^2 (16280 - 2980 n_2) + q^4 (-12210 - 4200 n_1 + 6435 n_2) \\
&+ q^5 (-36630 - 3150 n_1 + 9855 n_2)\Big) r_i^3 r_s^{11} + \Big(1120 q^2 + q^4 (-2104 - 3360 n_1 + 40 n_2) \\
&+ q^3 (13712 - 1120 n_1 + 1480 n_2) + q^5 (-12728 + 980 n_1 + 1980 n_2)\Big) r_i^2 r_s^{12} \\
&+ \Big(q^4 (13872 - 1800 n_2) + q^5 (10404 - 1350 n_2) + q^3 (4624 - 600 n_2)\Big) r_s^{14}\Bigg\} + \mathcal{O}(\lambda^2, \Omega^4), \qquad \text{(G.24)}
\end{aligned}
$$

$$
\begin{aligned}
j_3 = &\frac{4\left[3(-1+q)q r_i^5 - 5(-1+q)^2 r_i^3 r_s^2 + q(-7+2q) r_s^5\right]}{7 r_1} \\
&+ \frac{2}{245 r_o^2 r_1^2}\lambda\Bigg\{\left(7344 q^2 - 21141 q^3 + 20250 q^4 - 6453 q^5\right) r_i^{12} + \frac{r_i^{15}}{r_s^3}\left(-162 q^2 + 486 q^3 - 486 q^4 + 162 q^5\right) \\
&+ \frac{\left(180 q + 2880 q^2 - 9720 q^3 + 10080 q^4 - 3420 q^5\right) r_i^{13}}{r_s} + \Big[q^5 (15750 + 5250 n_1) \\
&+ q^2 (5250 - 5250 n_1 - 5250 n_2) + q^4 (-40250 - 15750 n_1 - 1750 n_2) + q (-7000 + 1750 n_2) \\
&+ q^3 (26250 + 15750 n_1 + 5250 n_2)\Big] r_i^{11} r_s + \Big[q^5 (22347 - 7875 n_1) + q (24210 + 2475 n_1) \\
&+ q^2 (-96216 + 600 n_1 - 750 n_2) + q^4 (-92490 + 21000 n_1 - 450 n_2) \\
&+ q^3 (142149 - 16200 n_1 + 1200 n_2)\Big] r_i^{10} r_s^2 + \Big[q^5 (-17500 - 8750 n_1) \\
&+ q^3 (-105000 - 26250 n_1 - 26250 n_2) + q (-17500 - 8750 n_2) + q^4 (70000 + 26250 n_1 + 8750 n_2) \\
&+ q^2 (70000 + 8750 n_1 + 26250 n_2)\Big] r_i^9 r_s^3 + \Big[-16300 + q^4 (132490 - 35000 n_1) - 750 n_1 \\
&+ q^5 (-41295 + 10500 n_1) + q^2 (-11940 - 2250 n_1 - 22750 n_2) + q (55370 - 2125 n_1 + 8750 n_2) \\
&+ q^3 (-118325 + 29625 n_1 + 14000 n_2)\Big] r_i^8 r_s^4 + \Big[q^2 (10842 + 1425 n_1) + q^5 (-54 + 7875 n_1) \\
&+ q^4 (6990 - 5250 n_1 - 9000 n_2) + q^3 (-17778 - 2175 n_1 + 7125 n_2)\Big] r_i^7 r_s^5 + \Big[q^5 (40425 + 7875 n_1) \\
&+ q^4 (-149450 - 10500 n_1 - 15750 n_2) + q^2 (23800 - 3500 n_1 - 3500 n_2) + q (-46200 - 1750 n_2) \\
&+ q^3 (131425 + 6125 n_1 + 21000 n_2)\Big] r_i^6 r_s^6 + \Big[q^5 (3840 - 21000 n_1) + q (-9060 - 350 n_1) \\
&+ q^3 (-25706 - 7175 n_1 - 25900 n_2) + q^2 (29278 + 525 n_1 + 7000 n_2) \\
&+ q^4 (1648 + 22750 n_1 + 24150 n_2)\Big] r_i^5 r_s^7 + \Big[q^5 (-18810 + 2625 n_1) + q^4 (51730 - 3750 n_2) \\
&+ q^2 (-36140 - 1000 n_2) + q^3 (3220 + 1750 n_1 + 375 n_2)\Big] r_i^3 r_s^9 + \Big[q^2 (-4936 - 300 n_1) \\
&+ q^5 (2832 + 5250 n_1) + q^4 (-2340 - 3500 n_1 - 3500 n_2) + q^3 (4444 - 1450 n_1 + 3500 n_2)\Big] r_i^2 r_s^{10} \\
&+ \Big[q^5 (2176 - 1750 n_1) + q^3 (-10304 - 300 n_2) + q^4 (-8172 + 1300 n_2)\Big] r_s^{12}\Bigg\} + \mathcal{O}(\lambda^2, \Omega^2), \qquad \text{(G.25)}
\end{aligned}
$$

$$a_0 = \frac{\lambda}{r_o^4}\left\{-\frac{2}{3}\Omega^2\left[(-1+q)r_i^4 - qr_s^4\right] + \left(7-10q+3q^2\right)r_i^4 + \left(-8q+8q^2\right)r_i^3 r_s + \left(18q-18q^2\right)r_i^2 r_s^2 + 7q^2 r_s^4\right\} + \mathcal{O}(\lambda^2, \Omega^4), \tag{G.26}$$

$$a_2 = -\frac{4\lambda}{105 r_o^2 r_1}\left[\left(189q-378q^2+189q^3\right)r_i^7 + \frac{r_i^8}{r_s}\left(40q-80q^2+40q^3\right) + \left(215-845q+1274q^2-644q^3\right)r_i^5 r_s^2 + \left(275q-650q^2+375q^3\right)r_i^3 r_s^4 + \left(341q-567q^2+226q^3\right)r_i^2 r_s^5 + \left(401q^2-186q^3\right)r_s^7\right] + \mathcal{O}(\lambda^2, \Omega^2), \tag{G.27}$$

$$b_2 = \frac{\lambda}{r_o^4 r_1}\left[\left(3q-6q^2+3q^3\right)r_i^9 + \left(-8q+16q^2-8q^3\right)r_i^8 r_s + \left(5q-10q^2+5q^3\right)r_i^7 r_s^2 + \left(-5q^2+5q^3\right)r_i^5 r_s^4 + \left(2q+6q^2-8q^3\right)r_i^4 r_s^5 + \left(-2q-q^2+3q^3\right)r_i^3 r_s^6\right] + \mathcal{O}(\lambda^2, \Omega^2). \tag{G.28}$$

2.3. Outer layer

$$\bar{M}_0 = \frac{(1-q)r_i^3}{r_o^3} + \lambda\frac{1}{r_o^5}\left\{\left[\frac{14}{5} + \frac{n_1}{5} + q\left(-7+n_1-\frac{3n_2}{2}\right) + q^2\left(\frac{21}{5} - \frac{3n_1}{2} + \frac{9n_2}{5}\right)\right]r_i^5 + \left[q^2(n_1-n_2) + q(-n_1+n_2)\right]\frac{r_i^6}{r_s} + q^2\left(\frac{n_1}{2} - \frac{n_2}{2}\right)r_i^3 r_s^2 + \Omega^2\left[\left(\frac{8}{15} - \frac{2n_1}{15} + q\left(-\frac{8}{15} + \frac{n_1}{3} - \frac{n_2}{5}\right)\right)r_i^5 + q\left(-\frac{n_1}{3} + \frac{n_2}{3}\right)r_i^3 r_s^2\right]\right\} + \mathcal{O}(\lambda^2, \Omega^4), \tag{G.29}$$

$$\bar{M}_2 = \frac{1}{r_o^5}\left[\left(-\frac{1}{5} + \frac{q}{5}\right)r_i^5 + \left(\frac{3}{10} - \frac{3q}{10}\right)m_2 r_i^5\right] + \frac{1}{r_o^7 r_1}\lambda\left\{\left(-\frac{234q}{175} + \frac{783q^2}{175} - \frac{864q^3}{175} + \frac{9q^4}{5}\right)r_i^{12} + \left[q^4(10+5n_1) + q(-10-5n_2) + q^3(-30-10n_1-5n_2) + q^2(30+5n_1+10n_2)\right]r_i^{11} r_s + \left[-\frac{283}{35} + q^4\left(-\frac{99}{5} - \frac{15n_1}{2}\right) + \frac{19n_1}{14} + q^2\left(-\frac{3042}{35} - \frac{41n_1}{14} - \frac{215n_2}{14}\right) + q\left(\frac{1599}{35} - \frac{24n_1}{7} + \frac{95n_2}{14}\right) + q^3\left(\frac{2419}{35} + \frac{25n_1}{2} + \frac{60n_2}{7}\right)\right]r_i^{10} r_s^2 + \left[2q + q^4\left(-2 - \frac{5n_1}{2}\right) + q^2\left(-6 - \frac{5n_2}{2}\right) + q^3\left(6 + \frac{5n_1}{2} + \frac{5n_2}{2}\right)\right]r_i^8 r_s^4 + \left[q\left(-\frac{1571}{175} + \frac{19n_1}{14}\right) + q^4\left(\frac{81}{5} + \frac{15n_1}{2}\right) + q^3\left(-\frac{7976}{175} - 5n_1 - \frac{60n_2}{7}\right) + q^2\left(\frac{6712}{175} - \frac{29n_1}{14} + \frac{95n_2}{14}\right)\right]r_i^7 r_s^5 + \left[\frac{4q^2}{5} + q^4\left(-\frac{31}{5} - \frac{5n_1}{2}\right) + q^3\left(\frac{27}{5} + \frac{5n_2}{2}\right)\right]r_i^5 r_s^7\right\} + \mathcal{O}(\lambda^2, \Omega^2), \tag{G.30}$$

$$\bar{J}_1 = \left(\frac{2}{5} - \frac{2q}{5}\right)\frac{r_i^5}{r_o^5} + \frac{1}{r_o^5}\Omega^2\left[\left(\frac{2}{15} - \frac{2q}{15}\right)r_i^5 + \left(-\frac{1}{5} + \frac{q}{5}\right)m_2 r_i^5\right] + \frac{1}{r_o^7 r_1}\lambda\left\{\left[q\left(-\frac{144}{7} - \frac{18n_1}{35}\right) + q^3\left(-\frac{486}{7} + 9n_1 - \frac{72n_2}{7}\right) + q^2\left(\frac{459}{7} - \frac{108n_1}{35} + \frac{9n_2}{2}\right) + q^4\left(\frac{171}{7} - \frac{27n_1}{5} + \frac{81n_2}{14}\right)\right]r_i^{12}$$

$$
\begin{aligned}
&+\left[q^2\left(\frac{18n_1}{5}-\frac{18n_2}{5}\right)+q^4\left(\frac{18n_1}{5}-\frac{18n_2}{5}\right)+q^3\left(-\frac{36n_1}{5}+\frac{36n_2}{5}\right)\right]\frac{r_i^{13}}{r_s}+\Big[q^3\left(8n_1-8n_2\right)\\
&+q^2\left(2n_1-2n_2\right)+q\left(-4n_1+4n_2\right)+q^4\left(-6n_1+6n_2\right)\Big]r_i^{11}r_s+\left[\frac{160}{7}+\frac{4n_1}{7}\right.\\
&+q^4\left(-\frac{1929}{35}+\frac{54n_1}{5}-\frac{801n_2}{70}\right)+q\left(-\frac{270}{7}+\frac{30n_1}{7}-5n_2\right)+q^2\left(-\frac{1629}{35}-\frac{34n_1}{7}+\frac{55n_2}{14}\right)\\
&\left.+q^3\left(\frac{4108}{35}-\frac{54n_1}{5}+\frac{438n_2}{35}\right)\right]r_i^{10}r_s^2+\left[16q+q^2\left(-8+\frac{2n_1}{5}-\frac{2n_2}{5}\right)+q^3\left(-32+\frac{n_1}{5}-\frac{n_2}{5}\right)\right.\\
&\left.+q^4\left(24-\frac{3n_1}{5}+\frac{3n_2}{5}\right)\right]r_i^8r_s^4+\left[q\left(\frac{64}{7}+\frac{8n_1}{35}\right)+q^2\left(-\frac{44}{7}+\frac{68n_1}{35}-2n_2\right)+q^3\left(-\frac{134}{7}-\frac{3n_2}{7}\right)\right.\\
&\left.+q^4\left(\frac{114}{7}-\frac{18n_1}{5}+\frac{27n_2}{7}\right)\right]r_i^7r_s^5+\left[\frac{32q^2}{5}+q^4\left(-\frac{48}{5}+\frac{6n_1}{5}-\frac{6n_2}{5}\right)+q^3\left(\frac{16}{5}+\frac{4n_1}{5}-\frac{4n_2}{5}\right)\right]r_i^5r_s^7\\
&+\Omega^2\left[\left(-\frac{6q^4}{5}+q\left(\frac{36}{175}+\frac{12n_1}{35}\right)+q^3\left(\frac{456}{175}+\frac{6n_1}{5}-\frac{6n_2}{7}\right)+q^2\left(-\frac{282}{175}-\frac{54n_1}{35}+\frac{6n_2}{7}\right)\right)r_i^{12}\right.\\
&+\left(q^4\left(-\frac{20}{3}-\frac{10n_1}{3}\right)+q^2\left(-20-\frac{10n_1}{3}-\frac{20n_2}{3}\right)+q\left(\frac{20}{3}+\frac{10n_2}{3}\right)+q^3\left(20+\frac{20n_1}{3}+\frac{10n_2}{3}\right)\right)r_i^{11}r_s\\
&+\left(\frac{1586}{105}-\frac{9n_1}{7}+q^4\left(\frac{66}{5}+5n_1\right)+q\left(-\frac{6136}{105}+\frac{24n_1}{7}-\frac{115n_2}{21}\right)+q^3\left(-\frac{1912}{35}-\frac{173n_1}{15}-\frac{108n_2}{35}\right)\right.\\
&\left.+q^2\left(\frac{1780}{21}+\frac{461n_1}{105}+\frac{899n_2}{105}\right)\right)r_i^{10}r_s^2+\left(q^4\left(\frac{4}{3}+\frac{5n_1}{3}\right)+q^3\left(\frac{34}{3}+\frac{n_1}{3}-\frac{11n_2}{3}\right)\right.\\
&\left.+q\left(14-\frac{4n_1}{3}+\frac{4n_2}{3}\right)+q^2\left(-\frac{80}{3}-\frac{2n_1}{3}+\frac{7n_2}{3}\right)\right)r_i^8r_s^4+\left(q^4\left(-\frac{54}{5}-5n_1\right)+q\left(\frac{8002}{525}-\frac{37n_1}{35}\right)\right.\\
&\left.+q^2\left(-\frac{22294}{525}+\frac{59n_1}{35}-\frac{103n_2}{21}\right)+q^3\left(\frac{6654}{175}+\frac{62n_1}{15}+\frac{36n_2}{7}\right)\right)r_i^7r_s^5+\left(-\frac{16q}{15}+q^4\left(\frac{62}{15}+\frac{5n_1}{3}\right)\right.\\
&\left.\left.+q^3\left(-\frac{52}{3}-\frac{4n_1}{5}-\frac{13n_2}{15}\right)+q^2\left(\frac{214}{15}-\frac{8n_1}{15}+\frac{8n_2}{15}\right)\right)r_i^5r_s^7\right]\Big\}+\mathcal{O}(\lambda^2,\Omega^4),
\end{aligned}
\tag{G.31}
$$

$$
\begin{aligned}
\bar{J}_3=&\frac{1}{r_o^7}\left[\left(-\frac{2}{35}+\frac{2q}{35}\right)r_i^7+\left(\frac{3}{35}-\frac{3q}{35}\right)m_2r_i^7\right]+\frac{\lambda}{r_o^9r_1}\left\{\left(-\frac{1964q}{3675}+\frac{5818q^2}{3675}-\frac{5744q^3}{3675}+\frac{18q^4}{35}\right)r_i^{14}\right.\\
&+\left[q^4\left(\frac{20}{7}+\frac{10n_1}{7}\right)+q\left(-\frac{20}{7}-\frac{10n_2}{7}\right)-q^3\left(\frac{60}{7}+\frac{20n_1}{7}+\frac{10n_2}{7}\right)+q^2\left(\frac{60}{7}+\frac{10n_1}{7}+\frac{20n_2}{7}\right)\right]r_i^{13}r_s\\
&+\left[-\frac{634}{105}+q^4\left(-\frac{198}{35}-\frac{15n_1}{7}\right)+\frac{191n_1}{441}+q^2\left(-\frac{8894}{245}-\frac{41n_1}{49}-\frac{250n_2}{63}\right)\right.\\
&\left.+q\left(\frac{5973}{245}-\frac{452n_1}{441}+\frac{215n_2}{126}\right)+q^3\left(\frac{17359}{735}+\frac{25n_1}{7}+\frac{95n_2}{42}\right)\right]r_i^{12}r_s^2+\left[-\frac{36q}{7}+q^4\left(-\frac{4}{7}-\frac{5n_1}{7}\right)\right.\\
&\left.+q^2\left(\frac{68}{7}-\frac{5n_2}{7}\right)+q^3\left(-4+\frac{5n_1}{7}+\frac{5n_2}{7}\right)\right]r_i^{10}r_s^4+\left[q\left(-\frac{70498}{11025}+\frac{191n_1}{441}\right)+q^4\left(\frac{162}{35}+\frac{15n_1}{7}\right)\right.\\
&\left.+q^3\left(-\frac{20507}{1225}-\frac{10n_1}{7}-\frac{95n_2}{42}\right)+q^2\left(\frac{204031}{11025}-\frac{29n_1}{49}+\frac{215n_2}{126}\right)\right]r_i^9r_s^5\\
&+\left[-\frac{192q^2}{35}+q^4\left(-\frac{62}{35}-\frac{5n_1}{7}\right)+q^3\left(\frac{254}{35}+\frac{5n_2}{7}\right)\right]r_i^7r_s^7\Big\}+\mathcal{O}(\lambda^2,\Omega^2),
\end{aligned}
\tag{G.32}
$$

$$\bar{A}_0 = \frac{\lambda}{r_o^7 r_1}\left\{\Omega^2\left[\left(-\frac{12q}{35}+\frac{24q^2}{35}-\frac{12q^3}{35}\right)r_i^{12}+\left(\frac{8}{21}-\frac{4q}{21}-\frac{16q^2}{21}+\frac{4q^3}{7}\right)r_i^{10}r_s^2+\left(\frac{16q}{105}+\frac{8q^2}{105}-\frac{8q^3}{35}\right)r_i^7 r_s^5\right]\right.$$
$$+\left(-\frac{72q}{35}+\frac{198q^2}{35}-\frac{36q^3}{7}+\frac{54q^4}{35}\right)r_i^{12}+\left(\frac{16}{7}-\frac{20q}{7}-\frac{26q^2}{7}+\frac{48q^3}{7}-\frac{18q^4}{7}\right)r_i^{10}r_s^2$$
$$\left.+\left(\frac{32q}{35}-\frac{8q^2}{35}-\frac{12q^3}{7}+\frac{36q^4}{35}\right)r_i^7 r_s^5\right\}+\mathcal{O}(\lambda^2,\Omega^4), \tag{G.33}$$

$$\bar{A}_2 = \frac{\lambda}{r_o^9 r_1}\left[\left(-\frac{40}{63}+\frac{110q}{63}-\frac{100q^2}{63}+\frac{10q^3}{21}\right)r_i^{12}r_s^2+\left(-\frac{40q}{63}+\frac{10q^2}{9}-\frac{10q^3}{21}\right)r_i^9 r_s^5\right]+\mathcal{O}(\lambda^2,\Omega^2), \tag{G.34}$$

$$\bar{B}_2 = -\frac{2\lambda}{3r_o^7 r_1}\left[\left(\frac{9q}{7}-\frac{18q^2}{7}+\frac{9q^3}{7}\right)r_i^{12}+\left(-\frac{30q}{7}+\frac{60q^2}{7}-\frac{30q^3}{7}\right)r_i^{10}r_s^2+\left(-18q+36q^2-18q^3\right)r_i^8 r_s^4\right.$$
$$\left.+\left(\frac{6q}{7}-\frac{27q^2}{7}+3q^3\right)r_i^7 r_s^5+\left(-18q^2+18q^3\right)r_i^5 r_s^7\right]+\mathcal{O}(\lambda^2,\Omega^2), \tag{G.35}$$

$$\bar{m}_0 = m_0+\frac{(-3+3q)r_i^2}{r_o^2}+\frac{\lambda}{r_o^4}\left\{\Omega^2\left[\left(-1+\frac{n_1}{2}+q\left(1-n_1+\frac{n_2}{2}\right)\right)r_i^4+q\left(n_1-n_2\right)r_i^2 r_s^2\right]\right.$$
$$+\left[-\frac{9}{2}-\frac{3n_1}{4}+q^2\left(-\frac{27}{2}+\frac{9n_1}{2}-\frac{27n_2}{4}\right)+q\left(18-3n_1+6n_2\right)\right]r_i^4$$
$$\left.+\left[q\left(3n_1-3n_2\right)+q^2\left(-3n_1+3n_2\right)\right]\frac{r_i^5}{r_s}+q^2\left(-\frac{3n_1}{2}+\frac{3n_2}{2}\right)r_i^2 r_s^2\right\}+\mathcal{O}(\lambda^2,\Omega^4), \tag{G.36}$$

$$\bar{m}_2 = \frac{2}{5}-\frac{2q}{5}+\left(\frac{2}{5}+\frac{3q}{5}\right)m_2+\frac{\lambda}{r_o^2 r_1}\left\{\left(-\frac{3132q}{175}+\frac{5634q^2}{175}-\frac{1872q^3}{175}-\frac{18q^4}{5}\right)r_i^7+\left[q^4\left(-20-10n_1\right)\right.\right.$$
$$+q^2\left(-60-10n_1-20n_2\right)+q\left(20+10n_2\right)+q^3\left(60+20n_1+10n_2\right)\Big]r_i^6 r_s$$
$$+\left[\frac{116}{35}+\frac{6n_1}{7}+q^4\left(\frac{198}{5}+15n_1\right)+q^3\left(-\frac{2638}{35}-25n_1-10n_2\right)+q\left(-\frac{14}{5}+\frac{23n_1}{7}-10n_2\right)\right.$$
$$\left.+q^2\left(\frac{1234}{35}+\frac{41n_1}{7}+20n_2\right)\right]r_i^5 r_s^2+\left[-4q+q^4\left(4+5n_1\right)-q^3\left(12+5n_1+5n_2\right)+q^2\left(12+5n_2\right)\right]r_i^3 r_s^4$$
$$+\left[q^4\left(-\frac{162}{5}-15n_1\right)+q\left(-\frac{1508}{175}+\frac{6n_1}{7}\right)+q^2\left(-\frac{1374}{175}+\frac{29n_1}{7}-10n_2\right)\right.$$
$$\left.\left.+q^3\left(\frac{8552}{175}+10n_1+10n_2\right)\right]r_i^2 r_s^5+\left[-\frac{8q^2}{5}+q^4\left(\frac{62}{5}+5n_1\right)+q^3\left(-\frac{54}{5}-5n_2\right)\right]r_s^7\right\}+\mathcal{O}(\lambda^2,\Omega^2), \tag{G.37}$$

$$\bar{j}_1 = j_1+\frac{2(-1+q)r_i^2}{r_o^2}+\frac{\Omega^2}{r_o^2}\left[\left(-\frac{4}{15}+\frac{4q}{15}\right)r_i^2+\left(\frac{2}{5}-\frac{2q}{5}\right)m_2 r_i^2\right]+\frac{\lambda}{r_o^4 r_1}\left\{\Omega^2\left[\left(\frac{12q^4}{5}+q\left(\frac{1458}{175}-3n_1\right)\right.\right.\right.$$
$$\left.+q^2\left(-\frac{2496}{175}+9n_1-3n_2\right)+q^3\left(\frac{618}{175}-6n_1+3n_2\right)\right)r_i^9+\left(q^4\left(\frac{40}{3}+\frac{20n_1}{3}\right)+q\left(-\frac{40}{3}-\frac{20n_2}{3}\right)\right.$$
$$\left.+q^3\left(-40-\frac{40n_1}{3}-\frac{20n_2}{3}\right)+q^2\left(40+\frac{20n_1}{3}+\frac{40n_2}{3}\right)\right)r_i^8 r_s+\left(-\frac{2542}{105}+q^4\left(-\frac{132}{5}-10n_1\right)+\frac{31n_1}{7}\right.$$
$$\left.\left.+q^3\left(\frac{2412}{35}+\frac{98n_1}{3}-6n_2\right)+q^2\left(-\frac{8698}{105}-\frac{383n_1}{21}-\frac{2n_2}{3}\right)+q\left(\frac{968}{15}-\frac{62n_1}{7}+\frac{20n_2}{3}\right)\right)r_i^7 r_s^2\right.$$

$$
\begin{aligned}
&+\left(q^4\left(-\frac{8}{3}-\frac{10n_1}{3}\right)+q^2\left(\frac{136}{3}+\frac{10n_1}{3}-\frac{20n_2}{3}\right)+q\left(-24+\frac{20n_1}{3}-\frac{20n_2}{3}\right)\right.\\
&\left.+q^3\left(-\frac{56}{3}-\frac{20n_1}{3}+\frac{40n_2}{3}\right)\right)r_i^5r_s^4+\left(q\left(-\frac{9794}{525}+\frac{17n_1}{7}\right)+q^4\left(\frac{108}{5}+10n_1\right)\right.\\
&\left.+q^3\left(-\frac{9038}{175}-\frac{32n_1}{3}-3n_2\right)+q^2\left(\frac{25568}{525}-\frac{24n_1}{7}+\frac{14n_2}{3}\right)\right)r_i^4r_s^5+\left(-\frac{8q}{3}+q^4\left(-\frac{124}{15}-\frac{10n_1}{3}\right)\right.\\
&\left.+q^2\left(-\frac{404}{15}+\frac{8n_1}{3}-\frac{8n_2}{3}\right)+q^3\left(\frac{568}{15}+4n_1-\frac{2n_2}{3}\right)\right)r_i^2r_s^7\Big]+\Big[q\left(\frac{441}{5}+\frac{9n_1}{2}\right)\\
&+q^4\left(-153+27n_1-\frac{81n_2}{2}\right)+q^2\left(-\frac{1647}{5}+\frac{27n_1}{2}-36n_2\right)+q^3\left(\frac{1971}{5}-45n_1+\frac{153n_2}{2}\right)\Big]r_i^9\\
&+\left[q^3\left(36n_1-36n_2\right)+q^2\left(-18n_1+18n_2\right)+q^4\left(-18n_1+18n_2\right)\right]\frac{r_i^{10}}{r_s}+\Big[q^4\left(30n_1-30n_2\right)\\
&+q\left(20n_1-20n_2\right)+q^2\left(-10n_1+10n_2\right)+q^3\left(-40n_1+40n_2\right)\Big]r_i^8r_s+\Big[-98-5n_1\\
&+q^3\left(-739+54n_1-\frac{183n_2}{2}\right)+q^2\left(237+\frac{55n_1}{2}-25n_2\right)+q\left(219-\frac{45n_1}{2}+40n_2\right)\\
&+q^4\left(381-54n_1+\frac{153n_2}{2}\right)\Big]r_i^7r_s^2+\Big[-140q+q^4\left(-210+3n_1-3n_2\right)+q^3\left(280-n_1+n_2\right)\\
&+q^2\left(70-2n_1+2n_2\right)\Big]r_i^5r_s^4+\Big[q\left(-\frac{196}{5}-2n_1\right)+q^4\left(-102+18n_1-27n_2\right)+q^3\left(\frac{464}{5}+6n_2\right)\\
&+q^2\left(\frac{242}{5}-11n_1+16n_2\right)\Big]r_i^4r_s^5+\Big[-56q^2+q^3\left(-28-4n_1+4n_2\right)+q^4\left(84-6n_1+6n_2\right)\Big]r_i^2r_s^7\Big\}\\
&+\mathcal{O}(\lambda^2,\Omega^4),
\end{aligned}
\tag{G.38}
$$

$$
\begin{aligned}
\bar{j}_3=&\frac{4}{35}-\frac{4q}{35}+j_3+\left(-\frac{6}{35}+\frac{6q}{35}\right)m_2+\frac{\lambda}{r_o^2r_1}\left\{\left(\frac{3456q}{1225}-\frac{8172q^2}{1225}+\frac{5976q^3}{1225}-\frac{36q^4}{35}\right)r_i^7\right.\\
&+\left[q^4\left(-\frac{40}{7}-\frac{20n_1}{7}\right)+q^2\left(-\frac{120}{7}-\frac{20n_1}{7}-\frac{40n_2}{7}\right)+q\left(\frac{40}{7}+\frac{20n_2}{7}\right)\right.\\
&\left.+q^3\left(\frac{120}{7}+\frac{40n_1}{7}+\frac{20n_2}{7}\right)\right]r_i^6r_s+\left[\frac{416}{35}+\frac{12n_1}{49}+q^4\left(\frac{396}{35}+\frac{30n_1}{7}\right)\right.\\
&\left.-q^3\left(\frac{10056}{245}+\frac{50n_1}{7}+\frac{20n_2}{7}\right)+q\left(-\frac{10336}{245}+\frac{46n_1}{49}-\frac{20n_2}{7}\right)+q^2\left(\frac{14708}{245}+\frac{82n_1}{49}+\frac{40n_2}{7}\right)\right]r_i^5r_s^2\\
&+\left[\frac{100q}{7}+q^4\left(\frac{8}{7}+\frac{10n_1}{7}\right)+q^3\left(12-\frac{10n_1}{7}-\frac{10n_2}{7}\right)+q^2\left(-\frac{192}{7}+\frac{10n_2}{7}\right)\right]r_i^3r_s^4\\
&+\left[q^4\left(-\frac{324}{35}-\frac{30n_1}{7}\right)+q\left(\frac{16864}{1225}+\frac{12n_1}{49}\right)+q^2\left(-\frac{36808}{1225}+\frac{58n_1}{49}-\frac{20n_2}{7}\right)\right.\\
&\left.\left.+q^3\left(\frac{31284}{1225}+\frac{20n_1}{7}+\frac{20n_2}{7}\right)\right]r_i^2r_s^5+\left[\frac{524q^2}{35}+q^4\left(\frac{124}{35}+\frac{10n_1}{7}\right)+q^3\left(-\frac{648}{35}-\frac{10n_2}{7}\right)\right]r_s^7\right\}\\
&+\mathcal{O}(\lambda^2,\Omega^2),
\end{aligned}
\tag{G.39}
$$

$$
\bar{a}_0=a_0+\frac{\lambda}{r_o^4}\left[\left(-\frac{2}{3}+\frac{2q}{3}\right)\Omega^2r_i^4+\left(-7+10q-3q^2\right)r_i^4+\left(-18q+18q^2\right)r_i^2r_s^2\right]+\mathcal{O}(\lambda^2,\Omega^4),
\tag{G.40}
$$

$$\bar{a}_2 = a_2 + \frac{\lambda}{r_o^2 r_1}\left[\left(\frac{36q}{5} - \frac{72q^2}{5} + \frac{36q^3}{5}\right) r_i^7 + \left(\frac{172}{21} - \frac{676q}{21} + \frac{836q^2}{21} - \frac{332q^3}{21}\right) r_i^5 r_s^2 + \left(12q - 24q^2 + 12q^3\right) r_i^3 r_s^4 + \left(\frac{1364q}{105} - \frac{108q^2}{5} + \frac{904q^3}{105}\right) r_i^2 r_s^5 + \left(12q^2 - 12q^3\right) r_s^7\right] + \mathcal{O}(\lambda^2, \Omega^2), \tag{G.41}$$

$$\bar{b}_2 = b_2 + \frac{\lambda}{r_o^4 r_1}\left[\left(-3q + 6q^2 - 3q^3\right) r_i^9 + \left(-5q + 10q^2 - 5q^3\right) r_i^7 r_s^2 + \left(-2q - 6q^2 + 8q^3\right) r_i^4 r_s^5\right] + \mathcal{O}(\lambda^2, \Omega^2). \tag{G.42}$$

In the $r_i = r_s$ limit we have

$$\bar{M}_0 = 1 - q + \lambda\left[\frac{14}{5} - 7q + \frac{21q^2}{5} + \frac{n_1}{5} - \frac{qn_2}{2} + \frac{3q^2 n_2}{10} + \Omega^2\left(\frac{8}{15} - \frac{8q}{15} - \frac{2n_1}{15} + \frac{2qn_2}{15}\right)\right] + \mathcal{O}(\lambda^2, \Omega^4), \tag{G.43}$$

$$\bar{M}_2 = -\frac{1}{10}(-1+q)(-2+3m_2) + \frac{1}{700}\lambda\left[-2\left(283 - 958q + 675q^2\right) + (95 - 145q)n_1 - 25q(-5+3q)n_2\right] + \mathcal{O}(\lambda^2, \Omega^2), \tag{G.44}$$

$$\bar{J}_1 = -\frac{2}{5}(-1+q) + \frac{1}{15}(-1+q)\Omega^2(-2+3m_2) + \lambda\left\{-\frac{16}{7}(-1+q) + \frac{39}{35}(-1+q)q + \frac{2n_1}{35} - \frac{qn_2}{10} + \frac{3q^2 n_2}{70} + \Omega^2\left[-\frac{793}{525}(-1+q) + \frac{29}{35}(-1+q)q + \frac{1}{210}(-27+29q)n_1 - \frac{17qn_2}{210} + \frac{q^2 n_2}{14}\right]\right\} + \mathcal{O}(\lambda^2, \Omega^4), \tag{G.45}$$

$$\bar{J}_3 = -\frac{1}{35}(-1+q)(-2+3m_2) + \frac{\lambda}{44100}\left[(1910 - 2610q)n_1 - 7\left(3804 - 5954q + 2150q^2 + 25q(-7+3q)n_2\right)\right] + \mathcal{O}(\lambda^2, \Omega^2), \tag{G.46}$$

$$\bar{A}_0 = \lambda\left[\frac{2}{105}\left(12 - 21q + 9q^2\right) + \frac{2}{105}(2-2q)\Omega^2\right] + \mathcal{O}(\lambda^2, \Omega^4), \tag{G.47}$$

$$\bar{A}_2 = \frac{1}{63}\left(-4 + 7q - 3q^2\right)\lambda + \mathcal{O}(\lambda^2, \Omega^2), \tag{G.48}$$

$$\bar{B}_2 = -\frac{47}{35}(-1+q)q\lambda + \mathcal{O}(\lambda^2, \Omega^2), \tag{G.49}$$

$$\bar{m}_0 = -3 + 3q + m_0 + \lambda\left[-\frac{9}{2} + 18q - \frac{27q^2}{2} - \frac{3n_1}{4} + 3qn_2 - \frac{9q^2 n_2}{4} + \Omega^2\left(-1 + q + \frac{n_1}{2} - \frac{qn_2}{2}\right)\right] + \mathcal{O}(\lambda^2, \Omega^4), \tag{G.50}$$

$$\bar{m}_2 = \frac{1}{5}\left(2 - 2q + (2+3q)m_2\right) + \frac{1}{350}\lambda\left(116 - 466q + 350q^2 + 5(6+29q)n_1 - 175q^2 n_2\right) + \mathcal{O}(\lambda^2, \Omega^2), \tag{G.51}$$

$$\bar{j}_1 = 2(-1+q) + j_1 - \frac{2}{15}(-1+q)\Omega^2(-2+3m_2) + \lambda\left\{-\frac{49}{5} + \frac{64q}{5} - 3q^2 - \frac{n_1}{2} - \frac{1}{2}q(-4+3q)n_2\right.$$

$$+\Omega^2\left[-\frac{1271}{525}+\frac{746q}{525}+q^2+\frac{1}{210}(93-58q)n_1+\frac{1}{6}q(-4+3q)n_2\right]\Bigg\}+\mathcal{O}(\lambda^2,\Omega^4), \tag{G.52}$$

$$\bar{j}_3=\frac{1}{35}\left[35j_3+2(-1+q)\left(-2+3m_2\right)\right]+\frac{\lambda}{1225}\left[5(6+29q)n_1-7\left(-208+98q+110q^2+25q^2n_2\right)\right]+\mathcal{O}(\lambda^2,\Omega^2), \tag{G.53}$$

$$\bar{a}_0=\lambda\left[-7-8q+15q^2+\left(-\frac{2}{3}+\frac{2q}{3}\right)\Omega^2\right]+a_0 \tag{G.54}$$

$$\bar{a}_2=-\frac{86}{105}\left(-1+q^2\right)\lambda+a_2 \tag{G.55}$$

$$\bar{b}_2=(-1+q)q\lambda+b_2 \tag{G.56}$$

2.4. Surfaces

The interior surface is

$$\begin{aligned}\eta_i=&\frac{1}{r_o r_1}\Bigg\{\left(-9q+9q^2\right)r_i^6+\left(10+5q-15q^2\right)r_i^4r_s^2+\left(4q+6q^2\right)r_ir_s^5+\Omega^2P_2\left[\left(-\frac{25}{3}+\frac{25q}{3}\right)r_i^4r_s^2-\frac{25}{3}qr_ir_s^5\right]\Bigg\}\\&+\frac{1}{r_o^3r_1^2}\lambda\Omega^2P_2\Bigg\{\left(\frac{54q^2}{7}-\frac{108q^3}{7}+\frac{54q^4}{7}\right)r_i^{13}+\left[q^2\left(150-75n_2\right)+q^4\left(50-25n_2\right)+q\left(-50+25n_2\right)\right.\\&\left.+q^3\left(-150+75n_2\right)\right]r_i^{12}r_s+\left[q\left(\frac{1410}{7}+\frac{30n_1}{7}\right)+q^2\left(-\frac{4959}{7}-\frac{30n_1}{7}-\frac{75n_2}{7}\right)+q^4\left(-\frac{2139}{7}-\frac{45n_2}{7}\right)\right.\\&\left.+q^3\left(\frac{5688}{7}+\frac{120n_2}{7}\right)\right]r_i^{11}r_s^2+\left[q^3\left(-1250-250n_1-375n_2\right)+q\left(-\frac{1250}{3}-\frac{250n_1}{3}-125n_2\right)\right.\\&\left.+q^4\left(\frac{1250}{3}+\frac{250n_1}{3}+125n_2\right)+q^2\left(1250+250n_1+375n_2\right)\right]r_i^{10}r_s^3+\left[\frac{1000}{21}+q^4\left(120-200n_1\right)\right.\\&\left.+\frac{500n_1}{21}+q^2\left(-\frac{12940}{21}-\frac{1875n_1}{7}-325n_2\right)+q\left(\frac{890}{3}+\frac{250n_1}{7}+125n_2\right)\right.\\&\left.+q^3\left(\frac{3190}{21}+\frac{1225n_1}{3}+200n_2\right)\right]r_i^9r_s^4+\left[q^2\left(-\frac{834}{7}-\frac{75n_1}{7}\right)+q^4\left(-\frac{1443}{7}+\frac{225n_1}{2}-\frac{900n_2}{7}\right)\right.\\&\left.+q^3\left(\frac{2277}{7}-75n_1+\frac{1425n_2}{14}\right)\right]r_i^8r_s^5+\left[q^4\left(-925-225n_2\right)+q^2\left(-\frac{575}{3}-125n_1-50n_2\right)\right.\\&\left.+q\left(-\frac{1100}{3}-25n_2\right)+q^3\left(\frac{4450}{3}+125n_1+300n_2\right)\right]r_i^7r_s^6+\left[q\left(\frac{7040}{21}+\frac{130n_1}{3}\right)\right.\\&\left.+q^3\left(-\frac{33806}{21}-\frac{875n_1}{3}-370n_2\right)+q^2\left(\frac{1374}{7}+\frac{445n_1}{3}+100n_2\right)+q^4\left(\frac{7548}{7}+25n_1+345n_2\right)\right]r_i^6r_s^7\\&+\left[q^4\left(-\frac{465}{7}+\frac{25n_1}{2}-\frac{375n_2}{7}\right)+q^2\left(-\frac{820}{21}-\frac{100n_2}{7}\right)+q^3\left(\frac{2215}{21}+50n_1+\frac{75n_2}{14}\right)\right]r_i^4r_s^9\\&+\left[q^2\left(\frac{1480}{21}+\frac{200n_1}{21}\right)+q^4\left(-248-50n_1-50n_2\right)+q^3\left(\frac{3148}{21}+\frac{100n_1}{3}+50n_2\right)\right]r_i^3r_s^{10}\\&+\left[q^3\left(-\frac{68}{21}-\frac{30n_2}{7}\right)+q^4\left(\frac{1648}{21}+\frac{50n_1}{3}+\frac{130n_2}{7}\right)\right]r_ir_s^{12}\Bigg\}+\mathcal{O}(\lambda^2,\Omega^4).\end{aligned} \tag{G.57}$$

The exterior surface is

$$\begin{aligned}\eta_s = \frac{1}{r_o r_1}\Bigg\{&\left(q^2-q\right)9r_i^5 r_s + \left(10+5q-15q^2\right)r_i^3 r_s^3 + \left(4q+6q^2\right)r_s^6 + \Omega^2 P_2\left[(q-1)5r_i^5 r_s + \left(-\frac{10}{3}-5q\right)r_s^6\right]\Bigg\}\\
&+\frac{1}{r_o^3 r_1^2}\lambda\Omega^2 P_2\Big\{\Big[q^2(90-45n_2)+q^4(30-15n_2)+q(-30+15n_2)+q^3(-90+45n_2)\Big]r_i^{13}\\
&+\left[\frac{846q}{7}-351q^2+\frac{2376q^3}{7}-\frac{765q^4}{7}\right]r_i^{12}r_s+\Big[q^3(-750-150n_1-225n_2)+q(-250-50n_1-75n_2)\\
&+q^4(250+50n_1+75n_2)+q^2(750+150n_1+225n_2)\Big]r_i^{11}r_s^2+\Bigg[\frac{240}{7}+\frac{120n_1}{7}\\
&+q^2\left(-\frac{3418}{7}-165n_1-\frac{1465n_2}{7}\right)+q^4\left(-\frac{1950}{7}-75n_1-\frac{465n_2}{7}\right)+q\left(\frac{374}{7}+\frac{160n_1}{7}+\frac{475n_2}{7}\right)\\
&+q^3\left(\frac{4754}{7}+200n_1+\frac{1455n_2}{7}\right)\Bigg]r_i^{10}r_s^3+\Bigg[\frac{160}{3}+q^2\left(-\frac{965}{3}+25n_1-85n_2\right)+q\left(\frac{460}{3}-5n_2\right)\\
&+q^4(145-100n_1+30n_2)+q^3(-30+75n_1+60n_2)\Big]r_i^8r_s^5+\Bigg[q\left(-\frac{176}{7}+\frac{50n_1}{7}\right)\\
&+q^3\left(-\frac{2141}{7}-125n_1-\frac{1875n_2}{14}\right)+q^4\left(\frac{615}{7}+\frac{375n_1}{2}-\frac{375n_2}{7}\right)+q^2\left(\frac{1702}{7}-25n_1+\frac{1000n_2}{7}\right)\Bigg]r_i^7r_s^6\\
&+\Bigg[-\frac{400}{3}+q^4(-300+75n_1-75n_2)+q^3(200+25n_1-25n_2)+q\left(-\frac{400}{3}-\frac{100n_1}{3}+\frac{100n_2}{3}\right)\\
&+q^2\left(\frac{1100}{3}-\frac{200n_1}{3}+\frac{200n_2}{3}\right)\Bigg]r_i^6r_s^7+\Bigg[\frac{280}{3}+\frac{20n_1}{3}+q^2\left(-\frac{8026}{21}+65n_1-110n_2\right)\\
&+q\left(68+\frac{160n_1}{3}-50n_2\right)+q^3\left(-\frac{234}{7}-75n_1+120n_2\right)+q^4\left(\frac{1780}{7}-175n_1+165n_2\right)\Bigg]r_i^5r_s^8\\
&+\Bigg[q^4\left(-\frac{675}{7}+\frac{75n_1}{2}-\frac{480n_2}{7}\right)+q^3\left(-\frac{225}{7}+50n_1-\frac{845n_2}{14}\right)+q^2\left(\frac{600}{7}+\frac{50n_1}{3}+\frac{230n_2}{21}\right)\\
&+q\left(\frac{300}{7}+\frac{290n_2}{21}\right)\Bigg]r_i^3r_s^{10}+\Bigg[q^2\left(\frac{160}{21}+\frac{80n_2}{21}\right)+q^4\left(\frac{120}{7}+\frac{60n_2}{7}\right)+q^3\left(\frac{160}{7}+\frac{80n_2}{7}\right)\Bigg]r_s^{13}\Big\}\\
&+\mathcal{O}(\lambda^2,\Omega^4).\end{aligned}\tag{G.58}$$

They both lead to the usual equation for the surface when either $r_i = r_s$ or $q = 1$ and $n_1 = n_2$

Bibliography

Abramowicz, M. A., G. J. E. Almergren, W. Kluzniak, and A. V. Thampan (2003), "The Hartle–Thorne circular geodesics," arXiv preprint gr-qc/0312070 .

Abramowicz, M. A., and R. V. Wagoner (1976), "Variational analysis of rotating neutron stars," Astrophys. J. **204**, 896.

Abramowicz, M. A., and R. V. Wagoner (1977), "Analytic properties of relativistic, rotating bodies," Astrophys. J. **216**, 86.

Masood-ul Alam, A. K. M. (1987), "On the spherical symmetry of static perfect fluid spacetimes and the positive-mass theorem," Class. Quant. Grav. **4**, 625.

Masood-ul Alam, A. K. M. (1988), "A proof of the uniqueness of static stellar models with small $d\rho/dp$," Class. Quant. Grav. **5**, 409.

Masood-ul Alam, A. K. M. (2007), "Proof that static stellar models are spherical," Gen. Relativ. Gravit. **39** (1), 55.

Alcock, C., E. Farhi, and A. Olinto (1986), "Strange stars," Astrophys. J. **310**, 261.

Alford, M. (2001), "Color-superconducting quark matter," Ann. Rev. Nucl. Part. Sci. **51**, 131.

Alford, M., M. Braby, M. Paris, and S. Reddy (2005), "Hybrid stars that masquerade as neutron stars," Astrophys. J. **629**, 969.

Ansorg, M., T. Fischer, A. Kleinwächter, R. Meinel, D. Petroff, and K. Schöbel (2004), "Equilibrium configurations of homogeneous fluids in general relativity," Mon. Not. R. Astron. Soc. **355** (3), 682.

Ansorg, M., D. Gondek-Rosińska, and L. Villain (2009), "On the solution space of differentially rotating neutron stars in general relativity," Mon. Not. R. Astron. Soc. **396** (4), 2359.

Ansorg, M., A. Kleinwächter, and R. Meinel (2002), "Highly accurate calculation of rotating neutron stars," Astron. & Astrophys. **381** (3), L49.

Ansorg, M., A. Kleinwächter, and R. Meinel (2003), "Highly accurate calculation of rotating neutron stars. Detailed description of the numerical methods," Astron. & Astrophys. **405**, 711.

Arun, K. G., B. R. Iyer, B. S. Sathyaprakash, and P. A. Sundararajan (2005), "Parameter estimation of inspiralling compact binaries using 3.5 post-Newtonian gravitational wave phasing: The nonspinning case," Phys. Rev. D **71** (8), 084008, arXiv:gr-qc/0411146 .

de Avellar, M. G. B., and J. E. Horvath (2010), "Exact and quasi-exact models of strange stars," Int. J. Mod. Phys. D **19** (12), 1937.

Avez, A. (1964), "Le ds^2 de Schwarzschild parmi les ds^2 stationnaires," Ann. Inst. Henri Poincaré **1**, 291.

Bagchi, M. (2010), "Rotational parameters of strange stars in comparison with neutron stars," New Astron. **15** (1), 126.

Bagenal, F., T. E. Dowling, and W. B. McKinnon (2007), *Jupiter: the planet, satellites and magnetosphere*, Vol. 1 (Cambridge University Press).

Bardeen, J., and R. Wagoner (1971), "Relativistic disks. I. Uniform rotation," Astrophys. J. **167**, 359.

Bardeen, J. M. (1970), "A variational principle for rotating stars in general relativity," Astrophys. J. **162**, 71.

Bardeen, J. M. (1971), "A reexamination of the post-Newtonian Maclaurin spheroids," Astrophys. J. **167**, 425.

Bardeen, J. M. (1980), "Gauge-invariant cosmological perturbations," Phys. Rev. D **22** (8), 1882.

Bardeen, J. M., W. H. Press, and S. A. Teukolsky (1972), "Rotating black holes: locally nonrotating frames, energy extraction, and scalar synchrotron radiation," Astrophys. J. **178**, 347.

Barret, D., J.-F. Olive, and M. C. Miller (2006), "The coherence of kilohertz quasi-periodic oscillations in the X-rays from accreting neutron stars," Mon. Not. R. Astron. Soc. **370** (3), 1140.

Baym, G., C. Pethick, and P. Sutherland (1971), "The ground state of matter at high densities: equation of state and stellar models," Astrophys. J. **170**, 299.

Beig, R., and W. Simon (1991), "On the spherical symmetry of static perfect fluids in general relativity," Lett. Math. Phys. **21** (3), 245.

Beig, R., and W. Simon (1992), "On the uniqueness of static perfect-fluid solutions in general relativity," Comm. Math. Phys. **144** (2), 373.

Bejger, M., J. L. Zdunik, and P. Haensel (2010), "Approximate analytic expressions for circular orbits around rapidly rotating compact stars," Astron. & Astrophys. **520**, 16.

Bekenstein, J. D. (2004), "Relativistic gravitation theory for the modified Newtonian dynamics paradigm," Phys. Rev. D **70** (8), 083509.

Berti, E., and N. Stergioulas (2004), "Approximate matching of analytic and numerical solutions for rapidly rotating neutron stars," Mon. Not. R. Astron. Soc. **350** (4), 1416.

Berti, E., F. White, A. Maniopoulou, and M. Bruni (2005), "Rotating neutron stars: an invariant comparison of approximate and numerical space–time models," Mon. Not. R. Astron. Soc. **358** (3), 923.

Blanchet, L. (2006), "Gravitational radiation from post-Newtonian sources and inspiralling compact binaries," Living Reviews in Relativity **9** (4), Version: lrr-2006-4.

Bocquet, M., S. Bonazzola, E. Gourgoulhon, and J. Novak (1995), "Rotating neutron star models with a magnetic field." Astron. & Astrophys. **301**, 757.

Bodmer, A. R. (1971), "Collapsed nuclei," Phys. Rev. D **4** (6), 1601.

Bombaci, I., I. Parenti, and I. Vidaña (2004), "Quark deconfinement and implications for the radius and the limiting mass of compact stars," Astrophys. J. **614**, 314.

Bonazzola, S., E. Gourgoulhon, and J. A. Marck (1998), "Numerical approach for high precision 3D relativistic star models," Phys. Rev. D **58** (10), 104020.

Bonazzola, S., E. Gourgoulhon, M. Salgado, and J. A. Marck (1993), "Axisymmetric rotating relativistic bodies: A new numerical approach for 'exact' solutions," Astron. & Astrophys. **278**, 421.

Bonazzola, S., and G. Maschio (1971), "Models of rotating neutron stars in general relativity," in *The Crab Nebula*, IAU Symposium, Vol. 46, edited by R. D. Davies and F. Graham-Smith, p. 346.

Bonazzola, S., and J. Schneider (1974), "An exact study of rigidly and rapidly rotating stars in general relativity with application to the crab pulsar," Astrophys. J. **191**, 273.

Bonnor, W. B., and P. A. Vickers (1981), "Junction conditions in general relativity," Gen. Relativ. Gravit. **13** (1), 29.

Boyer, R. H. (1965), "Rotating fluid masses in General Relativity," in *Proc. Cambridge Philos. Soc.*, Vol. 61.

Bradley, M., D. Eriksson, G. Fodor, and I. Rácz (2007), "Slowly rotating fluid balls of Petrov type D," Phys. Rev. D **75** (2), 24013.

Bradley, M., and G. Fodor (2009), "Quadrupole moment of slowly rotating fluid balls," Phys. Rev. D **79**, 044018.

Bradley, M., G. Fodor, M. Marklund, and Z. Perjés (2000), "The Wahlquist metric cannot describe an isolated rotating body," Class. Quant. Grav. **17** (2), 351.

Bruni, M., P. K. S. Dunsby, and G. F. R. Ellis (1992), "Cosmological perturbations and the physical meaning of gauge-invariant variables," Astrophys. J. **395**, 34.

Bruni, M., L. Gualtieri, and C. F. Sopuerta (2003), "Two-parameter nonlinear spacetime perturbations: gauge transformations and gauge invariance," Class. Quant. Grav. **20** (3), 535.

Bruni, M., S. Matarrese, S. Mollerach, and S. Sonego (1997), "Perturbations of spacetime: gauge transformations and gauge invariance at second order and beyond," Class. Quant. Grav. **14**, 2585.

Bruni, M., and S. Sonego (1999), "Observables and gauge invariance in the theory of nonlinear spacetime perturbations," Class. Quant. Grav. **16**, L29.

Butterworth, E. M., and J. R. Ipser (1976), "On the structure and stability of rapidly rotating fluid bodies in general relativity. I-The numerical method for computing structure and its application to uniformly rotating homogeneous bodies," Astrophys. J. **204**, 200.

Cabezas, J. A., J. Martín, A. Molina, and E. Ruiz (2007), "An approximate global solution of Einstein's equations for a rotating finite body," Gen. Relativ. Gravit. **39** (6), 707.

Cabezas, J. A., and E. Ruiz (2006), "An approximate global solution to the gravitational field of a perfect fluid in slow rotation," gr-qc/0611099 .

Carleman, T. (1919), "Über eine isoperimetrische Aufgabe und ihre physikalischen Anwendungen," Math. Z. **3** (1), 1.

Carminati, J. (1988), "Type-N, shear-free, perfect-fluid spacetimes with a barotropic equation of state," Gen. Relativ. Gravit. **20** (12), 1239.

Carter, B. (1969), "Killing horizons and orthogonally transitive groups in space-time," J. Math. Phys. **10** (1), 70.

Carter, B. (1970), "The commutation property of a stationary, axisymmetric system," Comm. Math. Phys. **17** (3), 233.

Carter, B. (1973), "Black hole equilibrium states," in *Black holes - Les astres occlus*, Vol. 57, edited by C. DeWitt and B. DeWitt (Gordon and Breach, New York) pp. 61–124, Golden Oldie republication in http://dx.doi.org/10.1007/s10714-009-0888-5.

Chandrasekhar, S. (1969), *Ellipsoidal figures of equilibrium*, Vol. 9 (Yale University Press New Haven).

Chandrasekhar, S., and J. C. Miller (1974), "On slowly rotating homogeneous masses in general relativity," Mon. Not. R. Astron. Soc. **167**, 63.

Chinea, F. J., and L. M. González-Romero (1990), "Interior gravitational field of stationary, axially symmetric perfect fluid in irrotational motion," Class. Quant. Grav. **7** (5), L99.

Chodos, A., R. L. Jaffe, K. Johnson, C. B. Thorn, and V. F. Weisskopf (1974), "New extended model of hadrons," Phys. Rev. D **9** (12), 3471.

Choquet-Bruhat, Y. (1962), "The Cauchy problem," in *Gravitation: An introduction to current research*, edited by L. Witten (Wiley, New York).

Collinson, C. D. (1976), "The uniqueness of the Schwarzschild interior metric," Gen. Relativ. Gravit. **7** (5), 419.

Cook, G. B., S. L. Shapiro, and S. A. Teukolsky (1992), "Spin-up of a rapidly rotating star by angular momentum loss: Effects of general relativity," Astrophys. J. **398**, 203.

Cook, G. B., S. L. Shapiro, and S. A. Teukolsky (1994), "Rapidly rotating neutron stars in general relativity: Realistic equations of state," Astrophys. J. **424**, 823.

Copeland, E. J., M. Sami, and S. Tsujikawa (2006), "Dynamics of dark energy," Int. J. Mod. Phys. D **15** (11), 1753.

Crosta, M. T., and F. Mignard (2006), "Microarcsecond light bending by Jupiter," Class. Quant. Grav. **23** (15), 4853.

Cuchí, J., A. Gil-Rivero, A. Molina, and E. Ruiz (2008a), "An approximate global stationary metric with axial symmetry for a perfect fluid with equation of state $\mu + (1 - n)p = \mu_0$: Exterior Metric," in Oscoz *et al.* (2008), pp. 315–318.

Cuchí, J., A. Gil-Rivero, A. Molina, and E. Ruiz (2008b), "An approximate global stationary metric with axial symmetry for a perfect fluid with equation of state $\mu + (1 - n)p = \mu_0$: Interior Metric," in Oscoz *et al.* (2008), pp. 311–314.

Cuchí, J. E., A. Gil-Rivero, A. Molina, and E. Ruiz (2013a), "An approximate global solution of Einstein's equations for a rotating compact source with linear equation of state," Gen. Relativ. Gravit. **45** (7), 1433, published Online First: 4 April 2013.

Cuchí, J. E., J. Martín, A. Molina, and E. Ruiz (2013b), "Wahlquist's metric versus an approximate solution with the same equation of state," Gen. Relativ. Gravit. **45** (8), 1493.

Cuchí, J. E., A. Molina, and E. Ruiz (2011), "Double shell stars as source of the Kerr metric in the CMMR approximation," in *"Spanish Relativity Meeting (ERE 2010): Gravity as a Crossroad in Physics"*, Vol. 314, IOP Publishing (Journal of Physics: Conference Series) p. 012070.

Cutler, C., and L. Lindblom (1987), "The effect of viscosity on neutron star oscillations," Astrophys. J. **314**, 234.

Darmois, G. (1927), *Mémorial des Sciences Mathématiques*, Vol. XXV (Gauthier-Villars, Paris) Chapter V.

Datta, B. (1988), "Recent developments in neutron star physics," Fundam. Cosm. Phys. **12**, 151.

Datta, B., and A. Ray (1983), "Lower bounds on neutron star mass and moment of inertia implied by the millisecond pulsar," Mon. Not. R. Astron. Soc. **204**, 75P.

Davidson, W. (2008), "Stationary axisymmetric solutions of Einstein's equations for a perfect fluid in rigid or differential rotation," Advanced Studies in Theoretical Physics **2** (13), 597.

Davidson, W. (2009), "A GR axisymmetric solution that could represent a finite object in steady rigid body rotation," Advanced Studies in Theoretical Physics **3** (1), 1.

Demorest, P. B., T. Pennucci, S. M. Ransom, M. S. E. Roberts, and J. W. T. Hessels (2010), "A two-solar-mass neutron star measured using Shapiro delay," Nature **467** (7319), 1081.

Dey, M., I. Bombaci, J. Dey, S. Ray, and B. C. Samanta (1998), "Strange stars with realistic quark vector interaction and phenomenological density-dependent scalar potential," Phys. Lett. B **438** (1), 123.

Dodelson, S., and M. Liguori (2006), "Can cosmic structure form without dark matter?" Phys. Rev. Lett. **97** (23), 231301.

Douchin, F., and P. Haensel (2001), "A unified equation of state of dense matter and neutron star structure," Astron. & Astrophys. **380**, 151.

Dubrovin, B. A., A. T. Fomenko, and S. P. Novikov (1985), *Modern Geometry–methods and Applications: The Geometry Of Surfaces, Transformation Groups, And Fields*, Vol. 1 (Springer).

Ellis, G. F. R., and M. Bruni (1989), "Covariant and gauge-invariant approach to cosmological density fluctuations," Phys. Rev. D **40** (6), 1804.

Eriguchi, Y., and D. Sugimoto (1981), "Another equilibrium sequence of self-gravitating and rotating incompressible fluid," Prog. Theor. Phys **65**, 1870.

Farhi, E., and R. L. Jaffe (1984), "Strange matter," Phys. Rev. D **30** (11), 2379.

Fayos, F., J. M. M. Senovilla, and R. Torres (1996), "General matching of two spherically symmetric spacetimes," Phys. Rev. D **54** (8), 4862.

Filter, R., and A. Kleinwächter (2009), "On the multipole moments of a rigidly rotating fluid body," Ann. Phys. (Leipzig) **18** (2-3), 102.

Flowers, E., and N. Itoh (1976), "Transport properties of dense matter," Astrophys. J. **206**, 218.

Fodor, G., and Z. Perjés (2000), "Petrov types of slowly rotating fluid balls," Gen. Relativ. Gravit. **32** (12), 2319.

Foures-Bruhat, Y. (1952), "Théorème d'existence pour certains systèmes d'équations aux dérivées partielles non linéaires," Acta Math. **88** (1), 141.

Fraga, E. S., R. D. Pisarski, and J. Schaffner-Bielich (2001), "Small, dense quark stars from perturbative QCD," Phys. Rev. D **63** (12), 121702.

Friedman, J. L., and J. R. Ipser (1992), "Rapidly rotating relativistic stars," Philos. Trans. R. Soc. London, Ser. A **340** (1658), 391.

Friedman, J. L., J. R. Ipser, and L. Parker (1989), "Implications of a half-millisecond pulsar," Phys. Rev. Lett. **62** (26), 3015.

Friedman, J. L., L. Parker, and J. R. Ipser (1986), "Rapidly rotating neutron star models," Astrophys. J. **304**, 115.

Futamase, T., and Y. Itoh (2007), "The post-Newtonian approximation for relativistic compact binaries," Living Reviews in Relativity **10** (2), Version: lrr-2007-2.

Galindo, P., and M. Mars (2013), In preparation.

Geroch, R. (1969), "Limits of spacetimes," Comm. Math. Phys. **13** (3), 180.

Geroch, R. (1970), "Multipole moments. II. Curved space," J. Math. Phys. **11**, 2580.

Giesel, K., S. Hofmann, T. Thiemann, and O. Winkler (2010), "Manifestly gauge-invariant general relativistic perturbation theory: I. Foundations," Class. Quant. Grav. **27**, 055005.

Glendenning, N. K. (1992), "First-order phase transitions with more than one conserved charge: Consequences for neutron stars," Phys. Rev. D **46**, 1274.

Glendenning, N. K., C. Kettner, and F. Weber (1995), "Possible new class of dense white dwarfs," Phys. Rev. Lett. **74** (18), 3519.

Gondek-Rosinska, D., T. Bulik, L. Zdunik, E. Gourgoulhon, S. Ray, J. Dey, and M. Dey (2000), "Rapidly rotating compact strange stars," Astron. & Astrophys. **363**, 1005.

Gourgoulhon, É. (2010), "An introduction to the theory of rotating relativistic stars," Arxiv preprint arXiv:1003.5015 .

Gourgoulhon, E., and S. Bonazzola (1994), "A formulation of the virial theorem in general relativity," Class. Quant. Grav. **11** (2), 443.

Gourgoulhon, E., P. Haensel, R. Livine, E. Paluch, S. Bonazzola, and J. Marck (1999a), "Fast rotation of strange stars," Astron. & Astrophys. **349**, 851.

Gourgoulhon, E., P. Haensel, R. Livine, E. Paluch, S. Bonazzola, and J. A. Marck (1999b), "Fast rotation of strange stars," Astron. & Astrophys. **349**, 851.

Haensel, P., and B. Pichon (1994), "Experimental nuclear masses and the ground state of cold dense matter," Astron. & Astrophys. **283**, 313.

Haensel, P., A. Y. Potekhin, and D. G. Yakovlev (2006), *Neutron stars 1: Equation of state and structure*, Vol. 326 (Springer).

Haensel, P., J. L. Zdunik, and M. Bejger (2008), "Fast rotation of neutron stars and equation of state of dense matter," New Astron. Rev. **51** (10), 785.

Haensel, P., J. L. Zdunik, and R. Schaefer (1986), "Strange quark stars," Astron. & Astrophys. **160**, 121.

Hall, G. S. (2004), "Symmetries and curvature structure in general relativity," .

Hansen, R. O. (1974), "Multipole moments of stationary space-times," J. Math. Phys. **15**, 46.

Hartle, J. B. (1967), "Slowly rotating relativistic stars. I. Equations of structure," Astrophys. J. **150**, 1005.

Hartle, J. B., and K. S. Thorne (1968), "Slowly rotating relativistic stars. II. Models for neutron stars and supermassive stars," Astrophys. J. **153**, 807.

Hessels, J. W. T., S. M. Ransom, I. H. Stairs, P. C. C. Freire, V. M. Kaspi, and F. Camilo (2006), "A radio pulsar spinning at 716 Hz," Science **311**, 1901, arXiv:astro-ph/0601337 .

Hulse, R. A., and J. H. Taylor (1975), "Discovery of a pulsar in a binary system," Astrophys. J. **195**, L51.

Iorio, L. (2013), "A possible new test of general relativity with Juno," Class. Quant. Grav. **30** (19), 195011.

Israel, W. (1966), "Singular hypersurfaces and thin shells in general relativity," Nuovo Cimento B **44** (1), 1.

Kaaret, P., E. C. Ford, and K. Chen (1997), "Strong-field general relativity and quasi-periodic oscillations in X-ray binaries," Astrophys. J. Lett. **480**, L27.

Kaaret, P., Z. Prieskorn, S. Brandt, N. Lund, S. Mereghetti, D. Götz, E. Kuulkers, J. Tomsick, *et al.* (2007), "Evidence of 1122 Hz X-ray burst oscillations from the neutron star X-ray transient XTE J1739–285," Astrophys. J. Lett. **657** (2), L97.

Klein, C. (2001), "Exact relativistic treatment of stationary counterrotating dust disks: Boundary value problems and solutions," Phys. Rev. D **63**, 064033.

Klioner, S. A. (2003), "A practical relativistic model for microarcsecond astrometry in space," Astron. J. **125** (3), 1580.

Kluźniak, W. (1998), "General relativistic constraints on the equation of state of dense matter implied by kilohertz quasi-periodic oscillations in neutron-star X-ray binaries," Astrophys. J. Lett. **509**, L37.

Komatsu, H., Y. Eriguchi, and I. Hachisu (1989a), "Rapidly rotating general relativistic stars. I-Numerical method and its application to uniformly rotating polytropes," Mon. Not. R. Astron. Soc. **237**, 355.

Komatsu, H., Y. Eriguchi, and I. Hachisu (1989b), "Rapidly rotating general relativistic stars. II-Differentially rotating polytropes," Mon. Not. R. Astron. Soc. **239**, 153.

Kramer, D. (1986), "Rigidly rotating perfect fluids," Astron. Nachr. **307** (5), 309.

Kundt, W., and M. Trümper (1966), "Orthogonal decomposition of axi-symmetric stationary spacetimes," Z. Phys. A **192** (4), 419.

Künzle, H. (1971), "On the spherical symmetry of a static perfect fluid," Comm. Math. Phys. **20** (2), 85.

Künzle, H. P., and J. R. Savage (1980), "A global analysis approach to the general relativistic fluid ball problem," Gen. Relativ. Gravit. **12** (2), 155.

Kurkela, A., P. Romatschke, and A. Vuorinen (2010), "Cold quark matter," Phys. Rev. D **81** (10), 105021.

Lattimer, J. M. (2011), "Neutron stars and the dense matter equation of state," Astrophys. Space Sci. **336** (1), 67.

Lattimer, J. M. (2012), "The nuclear equation of state and neutron star masses," Ann. Rev. Nucl. Part. Sci. **62** (1), 485.

Lattimer, J. M., and M. Prakash (2007), "Neutron star observations: Prognosis for equation of state constraints," Phys. Rep. **442** (1), 109.

Lattimer, J. M., and M. Prakash (2010), "What a two solar mass neutron star really means," Arxiv preprint arXiv:1012.3208 .

Lattimer, J. M., M. Prakash, D. Masak, and A. Yahil (1990), "Rapidly rotating pulsars and the equation of state," Astrophys. J. **355**, 241.

Leahy, D. A., S. M. Morsink, and C. Cadeau (2008), "Limits on mass and radius for the millisecond-period X-ray pulsar SAX J1808.4-3658," Astrophys. J. **672**, 1119, arXiv:astro-ph/0703287 .

Li, A., G. X. Peng, and J. F. Lu (2011), "Strange star candidates revised within a quark model with chiral mass scaling," Res. Astron. Astrophys. **11** (4), 482.

Li, X. D., I. Bombaci, M. Dey, J. Dey, and E. P. J. van den Heuvel (1999a), "Is SAX J1808.4-3658 a strange star?" Phys. Rev. Lett. **83** (19), 3776.

Li, X. D., S. Ray, J. Dey, M. Dey, and I. Bombaci (1999b), "On the nature of the compact star in 4U 1728–34," Astrophys. J. Lett. **527** (1), L51.

Lichnerowicz, A. (1955), *Théories relativistes de la gravitation et de l'électromagnétisme: relativité générale et théories unitaires* (Masson).

Lin, L. M., and J. Novak (2006), "Rotating star initial data for a constrained scheme in numerical relativity," Class. Quant. Grav. **23** (14), 4545.

Lindblom, L. (1976), "Stationary stars are axisymmetric," Astrophys. J. **208**, 873.

Lindblom, L. (1977), "Mirror planes in Newtonian stars with stratified flows," J. Math. Phys. **18**, 2352.

Lindblom, L. (1978), Ph.D. thesis (University of Maryland at College Park), available in `http://www.tapir.caltech.edu/~lindblom/Content/Publications1970.html`.

Lindblom, L. (1980), "Some properties of static general relativistic stellar models," J. Math. Phys. **21**, 1455.

Lindblom, L. (1981), "Some properties of static general relativistic stellar models. II," J. Math. Phys. **22**, 1324.

Lindblom, L. (1988), "Static uniform-density stars must be spherical in general relativity," J. Math. Phys. **29**, 436.

Lindblom, L. (1992), "On the symmetries of equilibrium stellar models," Philos. Trans. R. Soc. London, Ser. A **340** (1658), 353.

Lindblom, L., and A. K. M. Masood-ul Alam (1994), "On the spherical symmetry of static stellar models," Comm. Math. Phys. **162** (1), 123.

Madsen, J. (2000), "Intermediate mass strangelets are positively charged," Phys. Rev. Lett. **85** (22), 4687.

Madsen, J. (2001), "Color-flavor locked strangelets," Phys. Rev. Lett. **87** (17), 172003.

Maison, D. (1978), "Are the stationary, axially symmetric Einstein equations completely integrable?" Phys. Rev. Lett. **41**, 521.

Maison, D. (1979), "On the complete integrability of the stationary, axially symmetric Einstein equations," J. Math. Phys. **20**, 871.

Majczyna, A., and J. Madej (2005), "Mass and radius determination for the neutron star in X-ray burst source 4U/MXB 1728-34," Acta Astron. **55**, 1.

Manchester, R. N., G. B. Hobbs, A. Teoh, and M. Hobbs (2005), "The Australia Telescope National Facility pulsar catalogue," Astrophys. J. **129** (4), 1993.

Manko, V. S., J. Martin, and E. Ruiz (1995), "Six-parameter solution of the Einstein–Maxwell equations possessing equatorial symmetry," J. Math. Phys. **36**, 3063.

Manko, V. S., J. D. Sanabria-Gomez, and O. V. Manko (2000), "Nine-parameter electrovac metric involving rational functions," Phys. Rev. D **62** (4), 44048.

Mars, M., F. C. Mena, and R. Vera (2007), "Linear perturbations of matched spacetimes: the gauge problem and background symmetries," Class. Quant. Grav. **24**, 3673.

Mars, M., and J. M. M. Senovilla (1998), "On the construction of global models describing rotating bodies; uniqueness of the exterior gravitational field," Mod. Phys. Lett. A **13** (19), 1509.

Martín, J. (2006), Private communication.

Martín, J., A. Molina, and E. Ruiz (2008), "Can rigidly rotating polytropes be sources of the Kerr metric?" Class. Quant. Grav. **25**, 105019.

Meinel, R., M. Ansorg, A. Kleinwächter, G. Neugebauer, and D. Petroff (2008), *Relativistic figures of equilibrium* (Cambridge University Press).

Milgrom, M. (1983), "A modification of the Newtonian dynamics as a possible alternative to the hidden mass hypothesis," Astrophys. J. **270**, 365.

Miller, J. C. (1977), "Quasi-stationary gravitational collapse of slowly rotating bodies in general relativity," Mon. Not. R. Astron. Soc. **179**, 483.

Miller, M. C. (2010), "QPO constraints on neutron stars," New Astron. Rev. **54** (3), 128.

Miller, M. C., F. K. Lamb, and G. B. Cook (1998), "Effects of rapid stellar rotation on equation-of-state constraints derived from quasi-periodic brightness oscillations," Astrophys. J. **509**, 793.

Müller, H., and B. D. Serot (1995), "Phase transitions in warm, asymmetric nuclear matter," Phys. Rev. C **52** (4), 2072.

Nakamura, K. (2003), "Gauge invariant variables in two-parameter nonlinear perturbations," Prog. Theor. Phys **110**, 723.

Nakamura, K. (2005), "Second-order gauge invariant perturbation theory," Prog. Theor. Phys **113** (3), 481.

Nakamura, K. (2007), "Second-order gauge invariant cosmological perturbation theory—Einstein equations in terms of gauge invariant variables—," Prog. Theor. Phys **117**, 17.

Nauenberg, M., and G. Chapline (1973), "Determination of properties of cold stars in General Relativity by a variational method," Astrophys. J. **179**, 277.

Neugebauer, G., and R. Meinel (1995), "General relativistic gravitational field of a rigidly rotating disk of dust: Solution in terms of ultraelliptic functions," Phys. Rev. Lett. **75** (17), 3046.

Nozawa, T., N. Stergioulas, E. Gourgoulhon, and Y. Eriguchi (1998), "Construction of highly accurate models of rotating neutron stars–comparison of three different numerical schemes," Astron. & Astrophys. Suppl. Ser. **132** (3), 431.

Oscoz, A., E. Mediavilla, and M. Serra-Ricart, Eds. (2008), *Spanish Relativity Meeting 2007. Relativistic Astrophysics and Cosmology*, Vol. 30 (EAS Publications Series).

Ostriker, J. P., and J. W. K. Mark (1968), "Rapidly rotating stars. I. The self-consistent-field method," Astrophys. J. **151**, 1075.

Papapetrou, A. (1966), "Champs gravitationnels stationnaires à symetrie axiale," Ann. Inst. Henri Poincaré, A **4** (2), 83.

Pappas, G., and T. A. Apostolatos (2013), "An all-purpose metric for the exterior of any kind of rotating neutron star," Mon. Not. R. Astron. Soc. **429** (4), 3007.

Pfister, H. (2011), "A new and quite general existence proof for static and spherically symmetric perfect fluid stars in general relativity," Class. Quant. Grav. **28**, 075006.

Poutanen, J., and M. Gierliński (2003), "On the nature of the X-ray emission from the accreting millisecond pulsar SAX J1808.4–3658," Mon. Not. R. Astron. Soc. **343** (4), 1301.

Rajagopal, K., and F. Wilczek (2001), "Enforced electrical neutrality of the color-flavor locked phase," Phys. Rev. Lett. **86** (16).

Read, J. S., B. D. Lackey, B. J. Owen, and J. L. Friedman (2009), "Constraints on a phenomenologically parametrized neutron-star equation of state," Phys. Rev. D **79** (12), 124032.

Rendall, A. D., and B. G. Schmidt (1991), "Existence and properties of spherically symmetric static fluid bodies with a given equation of state," Class. Quant. Grav. **8**, 985.

Rubin, V. C., W. K. Ford Jr, and N. Thonnard (1980), "Rotational properties of 21 SC galaxies with a large range of luminosities and radii, from NGC 4605 (R= 4kpc) to UGC 2885 (R= 122 kpc)," Astrophys. J. **238**, 471.

Sachs, R. K. (1964), "Gravitational radiation relativity," Groups and Topology (Les Houches 1963) eds DeWitt C and DeWitt B (New York: Gordon and Breach) .

Sanabria-Gómez, J. D., J. L. Hernández-Pastora, and F. Dubeibe (2010), "Innermost stable circular orbits around magnetized rotating massive stars," Phys. Rev. D **82** (12), 124014.

Sarnobat, P., and C. A. Hoenselaers (2006), "The Wahlquist exterior: second-order analysis," Class. Quant. Grav. **23** (18), 5603.

Schaab, C., and M. K. Weigel (1999), "Quasi-periodic oscillations in low-mass X-ray binaries and constraints on the equation of state of neutron star matter," Mon. Not. R. Astron. Soc. **308** (3), 718.

Schoen, R., and S. T. Yau (1979), "On the proof of the positive mass conjecture in general relativity," Comm. Math. Phys. **65** (1), 45.

Senovilla, J. M. M. (1987), "Stationary axisymmetric perfect-fluid metrics with $q + 3p = const$," Phys. Lett. A **123** (5), 211.

Senovilla, J. M. M. (1993), "Stationary and axisymmetric perfect-fluid solutions to Einstein's equations," in *El Escorial Summer School on Gravitation and General Relativity 1992: Rotating Objects and Relativistic Physics*, edited by F. J. Chinea and L. M. González-Romero (Springer-Verlag, Berlin-New York).

Shapiro, S. T., and A. P. Lightman (1976), "Rapidly rotating, post-Newtonian neutron stars," Astrophys. J. **207**, 263.

Shapiro, I. I. (1964), "Fourth test of General Relativity," Phys. Rev. Lett. **13**, 789.

Shapiro, S. L. (2000), "Differential rotation in neutron stars: Magnetic braking and viscous damping," Astrophys. J. **544** (1), 397.

Shaposhnikov, N., L. Titarchuk, and F. Haberl (2003), "The bursting behavior of 4U 1728–34: The parameters of a neutron star and the geometry of a neutron star-disk system," Astrophys. J. Lett. **593** (1), L35.

Sharma, R., and S. D. Maharaj (2007), "A class of relativistic stars with a linear equation of state," Mon. Not. R. Astron. Soc. **375** (4), 1265.

Shibata, M., Y. T. Liu, S. L. Shapiro, and B. C. Stephens (2006), "Magnetorotational collapse of massive stellar cores to neutron stars: Simulations in full general relativity," Phys. Rev. D **74** (10), 104026.

Shibata, M., and M. Sasaki (1998), "Innermost stable circular orbits around relativistic rotating stars," Phys. Rev. D **58** (10), 104011.

Simon, W. (1993), "On journeys to the Moon by balloon," Class. Quant. Grav. **10**, 177.

Sonego, S., and M. Bruni (1998), "Gauge dependence in the theory of non-linear spacetime perturbations," Comm. Math. Phys. **193** (1), 209.

Sotiriou, T. P., and V. Faraoni (2010), "f(r) theories of gravity," Rev. Mod. Phys. **82** (1), 451.

Stephani, H., D. Kramer, M. MacCallum, C. Hoenselaers, and E. Herlt (2003), *Exact solutions of Einstein's field equations* (Cambridge Univ. Press).

Stergioulas, N. (2003), "Rotating stars in Relativity," Living Reviews in Relativity **6** (3), Version: `lrr-2003-3`.

Stergioulas, N., and J. L. Friedman (1995), "Comparing models of rapidly rotating relativistic stars constructed by two numerical methods," Astrophys. J. **444**, 306.

Stergioulas, N., W. Kluzniak, and T. Bulik (1999), "Keplerian frequencies and innermost stable circular orbits of rapidly rotating strange stars," Astron. & Astrophys. **352**, L116.

Stewart, J. M. (1990), "Perturbations of Friedmann-Robertson-Walker cosmological models," Class. Quant. Grav. **7**, 1169.

Stewart, J. M., and M. Walker (1974), "Perturbations of space-times in general relativity," Proc. R. Soc. London, Ser. A **341** (1624), 49.

Strohmayer, T. E., W. Zhang, J. H. Swank, A. Smale, L. Titarchuk, C. Day, and U. Lee (1996), "Millisecond X-ray variability from an accreting neutron star system," Astrophys. J. Lett. **469** (1), L9.

Taylor, J. H., and J. M. Weisberg (1989), "Further experimental tests of relativistic gravity using the binary pulsar PSR 1913+16," Astrophys. J. **345**, 434.

Teichmüller, C., M. Fröb, and F. Maucher (2011), "Analytical approximation of the exterior gravitational field of rotating neutron stars," Class. Quant. Grav. **28** (15), 155015.

Thampan, A. V., D. Bhattacharya, and B. Datta (1999), "Implications of kHz quasi-periodic brightness oscillations in X-ray binaries for neutron star structure," Mon. Not. R. Astron. Soc. **302** (4), L69.

Thorne, K. S. (1980), "Multipole expansions of gravitational radiation," Rev. Mod. Phys. **52** (2), 299.

Trümper, J. E. (2011), "Observations of neutron stars and the equation of state of matter at high densities," Prog. Part. Nucl. Phys. **66** (3), 674.

Turolla, R., S. Zane, and J. J. Drake (2008), "Bare quark stars or naked neutron stars? The case of RX J1856. 5-3754," Astrophys. J. **603** (1), 265.

Usov, V. V. (2004), "Electric fields at the quark surface of strange stars in the color-flavor locked phase," Phys. Rev. D **70** (6), 067301.

Wahlquist, H. D. (1968), "Interior solution for a finite rotating body of perfect fluid," Phys. Rev. **172** (5), 1291.

Wahlquist, H. D. (1992), "The problem of exact interior solutions for rotating rigid bodies in general relativity," J. Math. Phys. **33**, 304.

Wald, R. (1984), *General relativity* (University of Chicago press).

Weber, E., and N. K. Glendenning (1991), "Exact versus approximate solution of Einstein's equations for rotating neutron stars," Phys. Lett. B **265** (1), 1.

Weber, F. (2005), "Strange quark matter and compact stars," Prog. Part. Nucl. Phys. **54** (1), 193.

Weber, F., and N. K. Glendenning (1992), "Application of the improved Hartle method for the construction of general relativistic rotating neutron star models," Astrophys. J. **390**, 541.

Weber, F., N. K. Glendenning, and M. K. Weigel (1991), "Structure and stability of rotating relativistic neutron stars," Astrophys. J. **373**, 579.

Weissenborn, S., I. Sagert, G. Pagliara, M. Hempel, and J. Schaffner-Bielich (2011), "Quark matter in massive compact stars," Astrophys. J. **740**, L14.

Whittaker, J. M. (1968), "An interior solution in general relativity," Proc. R. Soc. London, Ser. A **306** (1484), 1.

Will, C. M. (2006), "The confrontation between General Relativity and Experiment," Living Reviews in Relativity **9** (3), 10.12942/lrr-2006-3.

Wilson, J. R. (1972), "Models of differentially rotating stars." Astrophys. J. **176**, 195.

Wiltshire, R. J. (2012), "A rotating three component perfect fluid source and its junction with empty space-time," Gen. Relativ. Gravit. **44** (4), 941.

Witten, E. (1984), "Cosmic separation of phases," Phys. Rev. D **30**, 272.

Zdunik, J. L. (2000), "Strange stars-linear approximation of the EOS and maximum QPO frequency," Astron. & Astrophys. **359**, 311.

Zdunik, J. L., P. Haensel, D. Gondek-Rosinska, and E. Gourgoulhon (2000), "Innermost stable circular orbits around strange stars and kHz QPOs in low-mass X-ray binaries," Astron. & Astrophys. **356**, 612.

Zdunik, J. L., P. Haensel, and E. Gourgoulhon (2001), "The crust of rotating strange quark stars," Astron. & Astrophys. **372**, 535.

Zel'dovich, I. B., and I. D. Novikov (1971), *Relativistic Astrophysics*, Vol. 2 (University of Chicago Press).

Zhang, W., T. E. Strohmayer, and J. H. Swank (1998), "Discovery of two simultaneous kilohertz quasi-periodic oscillations in the persistent flux of GX 349+2," Astrophys. J. Lett. **500**, L167.